

THE JOURNAL OF PHYSICAL CHEMISTRY

(Registered in U. S. Patent Office)

CONTENTS

30TH NATIONAL COLLOID SYMPOSIUM, MADISON, WISCONSIN, June 18-20, 1952

Donald Graham and Robert S. Hansen: The Structures of Adsorbed Monolayers. I. Normal Aliphatic Alcohols and Carboxylic Acids Adsorbed from Aqueous Solutions on Graphon	1153
J. R. Zimmerman, B. G. Holmes and J. A. Lasater: A Study of Adsorbed Water on Silica Gel by Nuclear Resonance Techniques	1157
J. L. Shereshefsky and C. E. Weir: Adsorption of Gases and Vapors on Glass Spheres. Two-Dimensional Condensation of Oxygen	1162
J. L. Shereshefsky and E. R. Russell: Activated Adsorption of Oxygen on Glass	1164
John W. Ross and Robert J. Good: Adsorption and Surface Diffusion of <i>n</i> -Butane on Spheron 6 (2700°) Carbon Black	1167
L. H. Reyerson and Lowell E. Peterson: The Sorption of Gases by Solid Polymers. I. The Sorption of Ammonia by Nylon. II. The Sorption of Hydrogen Chloride by Nylon	1172
H. L. Friach: Gas Permeation through Membranes Due to Simultaneous Diffusion and Convection	1177
J. J. Chessick and A. C. Zettlemoyer: Studies of the Surface Chemistry of Silicate Minerals. IV. Adsorption and Heat of Wetting Measurements of Attapulgit	1181
Robert S. Hansen, Robert E. Minturn and Donald A. Hickson: The Inference of Adsorption from Differential Double-Layer Capacitance Measurements	1185
Henry L. Crespi, Robert A. Uphaus and J. J. Katz: The Ultracentrifugal Behavior of Some Proteins in Non-aqueous Solvents	1190
B. Roger Ray and Leroy G. Augenstine: Trypsin Monolayers at the Water-Air Interface. I. Film Characteristics and the Recovery of Enzymatic Activity	1193
Harold Van Kley and Mark A. Stammann: Electrophoresis of Polypeptidyl Proteins	1200
Masatami Takeda and Rynichi Endo: Viscosity of Dilute Polyvinyl Chloride Solution	1202
John G. Buzzell and Charles Tanford: The Effect of Charge and Ionic Strength on the Viscosity of Ribonuclease	1204
Wilfred H. Ward and John J. Bartulovich: Molecular Kinetic and Chemical Properties of Wool Cortical Cell Fractions	1208
Rodes Trautman: Operating and Comparing Procedures Facilitating Schlieren Pattern Analysis in Analytical Ultracentrifugation	1211
Fred L. Pundsack and George Reimschuessel: The Properties of Asbestos. III. Basicity of Chrysotile Suspensions	1218
James T. Richardson and W. O. Milligan: Magnetic Susceptibility Studies in the System NiO-Al ₂ O ₃	1223
R. G. Craig, J. J. Van Voorhis and F. E. Bartell: Free Energy of Immersion of Compressed Powders with Different Liquids. I. Graphite Powders	1225
L. S. Bartell and R. J. Ruch: The Wetting of Incomplete Monomolecular Layers	1231
W. M. Sawyer and F. M. Fowkes: Monolayers in Equilibrium with Lenses of Oil on Water. I. Octadecanol and Tetradecanoic Acid in White Oil	1235
David B. Ludlum: Micelle Formation in Solutions of Some Isomeric Detergents	1240
H. B. Klevens and C. W. Carr: Equilibrium Dialysis of Soap and Detergent Solutions	1245
B. M. E. van der Hoff: On the Mechanism of Emulsion Polymerization of Styrene	1250
Sydney Ross and J. N. Butler: The Inhibition of Foaming. VII. Effects of Antifoaming Agents on Surface-Plastic Solutions	1255
<hr/>	
Enzo Ferroni and Gabriella Gabrielli: Determination of the Equilibrium Constant by Means of Surface Tension Measurements	1258
Gideon Gelernter, Luther C. Browning, Samuel R. Harris and Charles M. Mason: The Slow Thermal Decomposition of Cellulose Nitrate	1260
C. W. Hoerr and H. J. Harwood: The Solubility of Tristearin in Organic Solvents	1265
Keihei Ueno and Arthur E. Martell: Infrared Studies on Synthetic Oxygen Carriers	1270
A. Zalkin, W. J. Ramsey and D. H. Templeton: Intermetallic Compounds between Lithium and Lead. II. The Crystal Structure of Li ₂ Pb	1275
M. L. Hunt, S. Newman, H. A. Scheraga and P. J. Flory: Dimensions and Hydrodynamic Properties of Cellulose Trinitrate Molecules in Dilute Solution	1278
I. A. Ammar and S. A. Awad: Hydrogen Overpotential on Silver in Sodium Hydroxide Solutions	1290
Richard P. Smith: The Relationship of Force Constant and Bond Length	1293
Donald G. Miller: On the Stokes-Robinson Hydration Model for Solutions	1296
Jake Bello, Helene C. A. Riese and Jerome R. Vinograd: Mechanism of Gelation of Gelatin. Influence of Certain Electrolytes on the Melting Points of Gels of Gelatin and Chemically Modified Gelatins	1299
Leo A. Wall, Mary R. Harvey and Max Tryon: Oxidative Degradation of Styrene and α -Deuterostyrene Polymers	1306
Charles M. Huggins, George C. Pimentel and James N. Shoolery: Proton Magnetic Resonance Studies of the Hydrogen Bonding of Phenol, Substituted Phenols and Acetic Acid	1311
C. A. Heller and Alvin S. Gordon: Isopropyl Radical Reactions. I. Photolysis of Diisopropyl Ketone	1315
Constantine A. Neugebauer and John L. Margrave: The Heats of Formation of Tetrafluoroethylene, Tetrafluoromethane and 1,1-Difluoroethylene	1318
J. O. Bockris and G. W. Mellors: Electric Transport in Liquid Lead Silicates and Borates	1321
NOTES: Glenn V. Elmore and Howard A. Tanner: The Photochemical Properties of Zinc Oxide	1328
G. Boocock and H. O. Pritchard: Some Kinetic Studies with <i>para</i> -Hydrogen	1329
F. P. Dwyer and A. M. Sargeon: Resolution of Tris-oxalato Metal Complexes	1331
Joseph H. Flynn: A Method for Determining Rate Equations for Reactions in which the Concentration of the Reactant is Unknown	1332
Paul W. Gilles and John L. Margrave: The Heats of Formation of Na ₂ O ₃ , NaO ₃ and KO ₃	1333
Robert P. Langguth, R. K. Osterheld and E. Karl-Kroupa: Verification by Chromatography of the Thermal Formation of Barium and Lead Tetrapolyphosphates	1335
George K. Estok: Obviation of Solution Density Measurements in Electric Moment Determinations	1336
Max J. Katz: Some Adsorption Data of Acetylene on Black	1338

THE JOURNAL OF PHYSICAL CHEMISTRY

(Registered in U. S. Patent Office)

W. ALBERT NOYES, JR., EDITOR

ALLEN D. BLISS

ASSISTANT EDITORS

ARTHUR C. BOND

EDITORIAL BOARD

R. P. BELL

JOHN D. FERRY

S. C. LIND

R. E. CONNICK

G. D. HALSEY, JR.

H. W. MELVILLE

R. W. DODSON

J. W. KENNEDY

E. A. MOELWYN-HUGHES

PAUL M. DOTY

R. G. W. NORRISH

Published monthly by the American Chemical Society at 20th and Northampton Sts., Easton, Pa.

Entered as second-class matter at the Post Office at Easton, Pennsylvania.

The *Journal of Physical Chemistry* is devoted to the publication of selected symposia in the broad field of physical chemistry and to other contributed papers.

Manuscripts originating in the British Isles, Europe and Africa should be sent to F. C. Tompkins, The Faraday Society, 6 Gray's Inn Square, London W. C. 1, England.

Manuscripts originating elsewhere should be sent to W. Albert Noyes, Jr., Department of Chemistry, University of Rochester, Rochester 20, N. Y.

Correspondence regarding accepted copy, proofs and reprints should be directed to Assistant Editor, Allen D. Bliss, Department of Chemistry, Simmons College, 300 The Fenway, Boston 15, Mass.

Business Office: Alden H. Emery, Executive Secretary, American Chemical Society, 1155 Sixteenth St., N. W., Washington 6, D. C.

Advertising Office: Reinhold Publishing Corporation, 430 Park Avenue, New York 22, N. Y.

Articles must be submitted in duplicate, typed and double spaced. They should have at the beginning a brief Abstract, in no case exceeding 300 words. Original drawings should accompany the manuscript. Lettering at the sides of graphs (black on white or blue) may be pencilled in and will be typeset. Figures and tables should be held to a minimum consistent with adequate presentation of information. Photographs will not be printed on glossy paper except by special arrangement. All footnotes and references to the literature should be numbered consecutively and placed in the manuscript at the proper places. Initials of authors referred to in citations should be given. Nomenclature should conform to that used in *Chemical Abstracts*, mathematical characters marked for italic, Greek letters carefully made or annotated, and subscripts and superscripts clearly shown. Articles should be written as briefly as possible consistent with clarity and should avoid historical background unnecessary for specialists.

Notes describe fragmentary or less complete studies but do not otherwise differ fundamentally from articles. They are subjected to the same editorial appraisal as are Articles. In their preparation particular attention should be paid to brevity and conciseness.

Communications to the Editor are designed to afford prompt preliminary publication of observations or discoveries whose

value to science is so great that immediate publication is imperative. The appearance of related work from other laboratories is in itself not considered sufficient justification for the publication of a Communication, which must in addition meet special requirements of timeliness and significance. Their total length may in no case exceed 500 words or their equivalent. They differ from Articles and Notes in that their subject matter may be republished.

Symposium papers should be sent in all cases to Secretaries of Divisions sponsoring the symposium, who will be responsible for their transmittal to the Editor. The Secretary of the Division by agreement with the Editor will specify a time after which symposium papers cannot be accepted. The Editor reserves the right to refuse to publish symposium articles, for valid scientific reasons. Each symposium paper may not exceed four printed pages (about sixteen double spaced typewritten pages) in length except by prior arrangement with the Editor.

Remittances and orders for subscriptions and for single copies, notices of changes of address and new professional connections, and claims for missing numbers should be sent to the American Chemical Society, 1155 Sixteenth St., N. W., Washington 6, D. C. Changes of address for the *Journal of Physical Chemistry* must be received on or before the 30th of the preceding month.

Claims for missing numbers will not be allowed (1) if received more than sixty days from date of issue (because of delivery hazards, no claims can be honored from subscribers in Central Europe, Asia, or Pacific Islands other than Hawaii), (2) if loss was due to failure of notice of change of address to be received before the date specified in the preceding paragraph, or (3) if the reason for the claim is "missing from files."

Subscription Rates (1956): members of American Chemical Society, \$8.00 for 1 year; to non-members, \$16.00 for 1 year. Postage free to countries in the Pan American Union; Canada, \$0.40; all other countries, \$1.20. \$12.50 per volume, foreign postage \$1.20, Canadian postage \$0.40; special rates for A.C.S. members supplied on request. Single copies, current volume, \$1.35; foreign postage, \$0.15; Canadian postage \$0.05. Back issue rates (starting with Vol. 56): \$15.00 per volume, foreign postage \$1.20, Canadian, \$0.40; \$1.50 per issue, foreign postage \$0.15, Canadian postage \$0.05.

The American Chemical Society and the Editors of the *Journal of Physical Chemistry* assume no responsibility for the statements and opinions advanced by contributors to THIS JOURNAL.

The American Chemical Society also publishes *Journal of the American Chemical Society*, *Chemical Abstracts*, *Industrial and Engineering Chemistry*, *Chemical and Engineering News*, *Analytical Chemistry*, *Journal of Agricultural and Food Chemistry* and *Journal of Organic Chemistry*. Rates on request.



(Continued from first page of cover)

Andrew J. Chadwell, Jr., and Hilton A. Smith: Studies with Rare Earth Catalysts	1339
Louis Watta Clark: The Kinetics of the Decomposition of Malonic Acid in Aromatic Amines	1340
Jake Bello: The Protonation of N-Methylacetamide	1341
Ignacio Tinoco, Jr., and P. A. Lyons: Diffusion of Isoionic Salt-free Bovine Serum Albumin	1342
COMMUNICATIONS TO THE EDITOR: Edward P. Egan, Jr. Extrapolation of Cooling Curves in Measurements of Heat Capacity	1344
Alvin S. Gordon and R. H. Knipe: Second Explosion Limits of Carbon Monoxide-Oxygen Mixtures	1344

THE JOURNAL OF PHYSICAL CHEMISTRY

(Registered in U. S. Patent Office) (© Copyright, 1956, by the American Chemical Society)

VOLUME 60

SEPTEMBER 24, 1956

NUMBER 8

THE STRUCTURES OF ADSORBED MONOLAYERS.

I. NORMAL ALIPHATIC ALCOHOLS AND CARBOXYLIC ACIDS ADSORBED FROM AQUEOUS SOLUTIONS ON GRAPHON

BY DONALD GRAHAM* AND ROBERT S. HANSEN**

Received February 24, 1956

Adsorption data indicate that normal aliphatic alcohols are adsorbed from aqueous solutions by Graphon without hydration and with only part of the carbon chains in contact with the adsorbent. The higher members show evidence of a transition at about 90% coverage in which the area occupied by a single molecule on the adsorbent surface is reduced by an amount approximately equal to that covered by one $-\text{CH}_2-$ group. The normal aliphatic carboxylic acids, on the other hand, appear to be adsorbed as monohydrates. At low coverage (at least in the cases of acetic and propionic acids) they tend to lie flat on the Graphon surface. At higher coverage only part of the carbon chain is directly bound to the solid.

Discussion

The properties of a monolayer at a solid-liquid interface are largely determined by the solvation, conformation and orientation, of the adsorbed molecules. Although some information is available regarding the air-water interface, most of the solid-liquid systems studied have been too complex for structural analysis.

Comprehensive data for the adsorption of normal aliphatic alcohols and carboxylic acids from aqueous solution on Graphon at 25° have recently been reported.¹

Since Graphon is a very uniform adsorbent and since appreciable interaction between adsorbed molecules is not observed in aqueous systems, these results provide for the first time a suitable starting point for development of the desired information.

The Hansen-Craig isotherms were reported in terms of $V\Delta C/m$ (the original solution volume per gram of adsorbent times the change in concentration during adsorption, quantities actually measured). From these data, the required values of X/m or the amount adsorbed per unit mass of adsorbent have been obtained by use of the expression

$$\frac{X}{m} = \frac{V\Delta C}{m} \left(1 + X_a \left[\frac{n + \frac{V_a}{V_b}}{X_b - nX_a} \right] \right) \quad (1)$$

(*) Jackson Laboratory, E. I. du Pont de Nemours and Company, Inc., Wilmington, Delaware.

(**) Institute for Atomic Research and Department of Chemistry, Iowa State College, Ames, Iowa.

(1) R. S. Hansen and R. P. Craig, *THIS JOURNAL*, **58**, 211 (1954).

in which

X = amount of adsorbate in mmoles
 m = mass of adsorbent in g.
 V = initial vol. of soln. in ml.
 ΔC = change in concn. during adsorption
 X_a = mole fraction of adsorptive compound in soln.
 X_b = mole fraction of water in soln.
 V_a = partial molal vol. of adsorptive compound in soln.
 V_b = partial molal vol. of water in soln.
 n = no. of mols of water associated with one mol. of adsorbate

If the adsorbate is not hydrated, the equation is reduced to the more familiar form

$$\frac{X}{m} = \frac{V\Delta C}{m} \left(1 + \frac{X_a V_a}{X_b V_b} \right) \quad (2)$$

To add convenience to our calculations and clarity to our results, the mass of the adsorbent, m , was replaced by its surface area A in units of 100 sq. meters. Thus by reference to the previously reported² Graphon surface area (78.7 sq. meters per g.), $V\Delta C/m$ was converted to $V\Delta C/A$, and X/A , the quantity adsorbed per 100 sq. meters of adsorbent surface, was calculated.

Activities for the three lower alcohols and acids were obtained from the literature.² The solutions of the higher members were sufficiently dilute to justify direct use of relative concentrations (the ratios of the measured concentrations to the saturation values at the same temperature, 25°).

Determination of the degree of hydration was based on three assumptions.

(2) (a) R. S. Hansen and F. A. Miller, *ibid.*, **58**, 193 (1954); (b) R. S. Hansen, F. A. Miller and S. D. Christian, *ibid.*, **59**, 391 (1955).

(1) The isotherm for the first monolayer approaches ideality (constant equilibrium function³).

(2) Hydration is approximately stoichiometric, one adsorbed molecule bearing 0, 1, 2, or 3, etc., molecules of water.

(3) The degree of hydration of all homologs is the same.

In determining the degree of hydration, greatest weight was given the data for the lowest homolog in each case because its wider solution concentration range accentuated any hydration effect.

Isotherms calculated for different degrees of hydration were compared with an ideal isotherm. This ideal isotherm was based on values of the equilibrium function and of $(X/A)_m$, the content in millimoles of 100 sq. meters of filled monolayer. The equilibrium function was derived from data over a range of coverage sufficiently low to avoid the effects of hydration. The value of $(X/A)_m$ was obtained from the intercept of a reciprocal plot, A/X vs. $1/\text{solute activity}$, a different value being obtained for each degree of hydration considered. The isotherm representing the correct degree of hydration approximates the ideal over a wide coverage range while those based on incorrect values of the degree of hydration deviate from the ideal with increasing coverage.

The same information can be obtained by comparing the experimental values of

$$\frac{V\Delta C}{m} \left(\text{corrected to } \frac{V\Delta C}{A} \right)$$

with corresponding calculated values representing different degrees of hydration. Equation 1 is used for this calculation with X/A obtained as before from the ideal $(X/A)_m$ (content of the first filled monolayer) and the equilibrium function.

Aliphatic Alcohols.—In the adsorption of ethanol on Graphon at 25°, the calculation of X/A for different degrees of hydration is illustrated in Table I. The results are plotted in Fig. 1. The dashed line

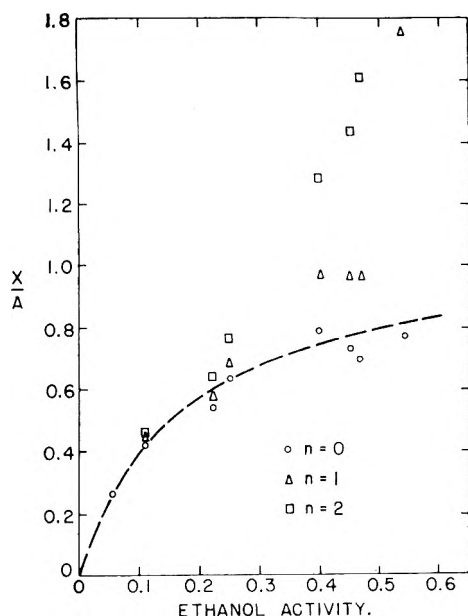


Fig. 1.—Calculated ethanol isotherms for different degrees of hydration.

(3) D. Graham, THIS JOURNAL, 57, 665 (1953).

represents an ideal isotherm calculated from a content of the first monolayer $(X/A)_m = 1.10$ mmoles/100 m.² and an equilibrium function $E.F. = 5.4$. (These values were obtained from the reciprocal plot shown in Fig. 2.)

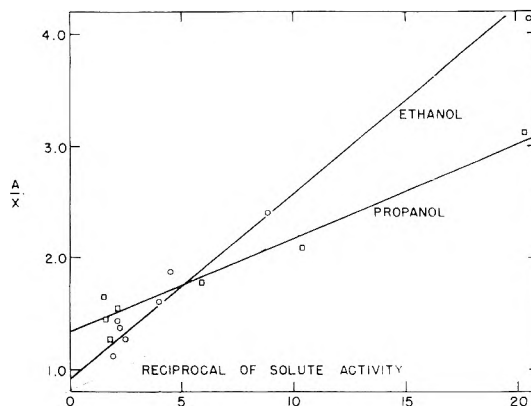


Fig. 2.—Reciprocal plots for adsorption of ethanol and propanol on Graphon.

The ideal isotherm is closely approximated by the points representing adsorption with no hydration of the ethanol while the others deviate markedly. The data for the other alcohols also fit ideal isotherms for adsorption without hydration, up to a point of transition to be discussed later. It is therefore concluded that the alcohols are adsorbed by Graphon from aqueous solution without hydration and that equation 2 may be used for calculation of the X/A values for the alcohols.

TABLE I

THE ADSORPTION OF ETHANOL FROM AQUEOUS SOLUTION ON GRAPHON AT 25°

Mole fraction ethanol	Activity ethanol	$\frac{V\Delta C}{m}$	$\frac{V\Delta C}{A}$	X/A		
				$n = 0$	$n = 1$	$n = 2$
0.0031	0.0115	0.048	0.061	0.062	0.062	0.062
.0071	.0261	.081	.103	.105	.106	.107
.0133	.0484	.183	.233	.242	.246	.249
.0324	.113	.299	.380	.417	.432	.446
.0694	.222	.345	.439	.535	.577	.641
.0805	.249	.394	.501	.630	.691	.764
.1612	.401	.390	.496	.791	.978	1.285
.1976	.452	.324	.412	.730	.970	1.44
.2217	.467	.290	.369	.700	.978	1.62

The reciprocal plot of the 1-propanol data (included with that of ethanol in Fig. 2) indicates that 1-propanol molecules occupy a larger area and are more strongly adsorbed but that the adsorption is in other respects similar to that of ethanol. However, reciprocal plots for the next three members of the series (see Fig. 3) include a break at $\theta \sim 0.9$ with a reduction in molecular area at higher coverage. This decrease in molecular area is approximately equal to the area increment representing one $-\text{CH}_2-$ group. The 1-heptanol data were too scattered to show this transition clearly but were not inconsistent with the assumption that a similar change occurred. It was therefore concluded that at coverages above $\theta \sim 0.9$, alcohols above C_3 tend to approach, by one step, the configuration of long chain normal aliphatic alcohols in a compressed film.

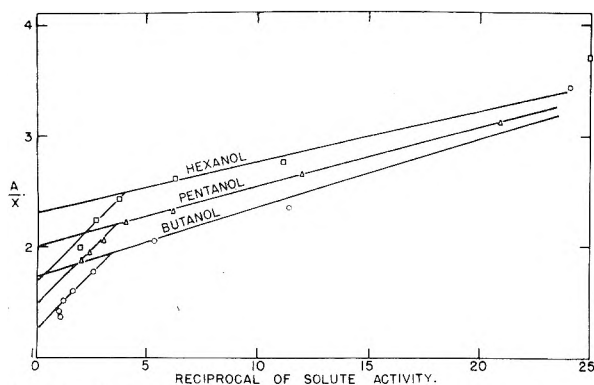


Fig. 3.—Reciprocal plots showing transitions in monolayers of alcohols adsorbed on Graphon.

The calculated molecular areas are listed in Table II. Molecular areas of the corresponding normal paraffins, which increase linearly with chain length, are included to provide a scale for comparison. These results show a conflict between two tendencies. The first is for all of the carbon atoms to be bound to the adsorbent surface as in the case of the normal paraffins. The second is for the portion of the alcohol molecule bearing the hydroxyl group to enter the aqueous phase. In the final compromise, ethanol is adsorbed with only one carbon atom bound to the adsorbent while in the case of 1-propanol, there are two. 1-Butanol, 1-pentanol and 1-hexanol are adsorbed at low coverage with 3-4 carbon atoms bound but at high coverage, only 2-3 remain on the Graphon surface. Detailed study of higher homologs probably would not be fruitful due to complexities resulting from chain interactions.

TABLE II

AREAS OCCUPIED BY INDIVIDUAL MOLECULES OF NORMAL ALIPHATIC ALCOHOLS ADSORBED ON A GRAPHON SURFACE

No. carbon atoms	Mol. area paraffin, Å. ²	Mol. area alcohol in dilute monolayer, Å. ²	Coverage θ at transition	Mol. area alcohol in concd. monolayer, Å. ²
1	15.5			
2	23.5	15
3	31.5	22
4	39.5	29	0.90	21
5	47.5	33	0.91	25
6	55.5	38	0.92	28
7	63.5	38

Aliphatic Acids.—Data for the adsorption of normal aliphatic acids on Graphon were treated as described for the alcohols. In this case, the reciprocal plots of the acetic acid data for $n = 0$ and $n = 2$ showed the deviations at high activities characteristic of low and high values of n . For $n = 1$, the reciprocal plot (Fig. 4) yields not one straight line but two, indicating a transition analogous to those observed with the alcohols of 4, 5 and 6 carbon atoms. At a coverage below $\theta = 0.78$, the indicated molecular area was 38 Å.² or about the same as butane. This suggests that the molecules lie flat on the surface with the two oxygen atoms occupying about the same area as —CH₂— groups. At higher coverages, the molecular area drops to 22 Å.² or approximately that of ethane. This is

interpreted as meaning that only one carbon atom is bound to the surface, the limiting cross section being that of the carboxy group which under these conditions (high coverage) projects out from the solid toward the aqueous phase. In each case, the molecule of water of hydration requires no space on the solid but probably lies between the carboxy group of the adsorbed acid and the mobile aqueous phase.

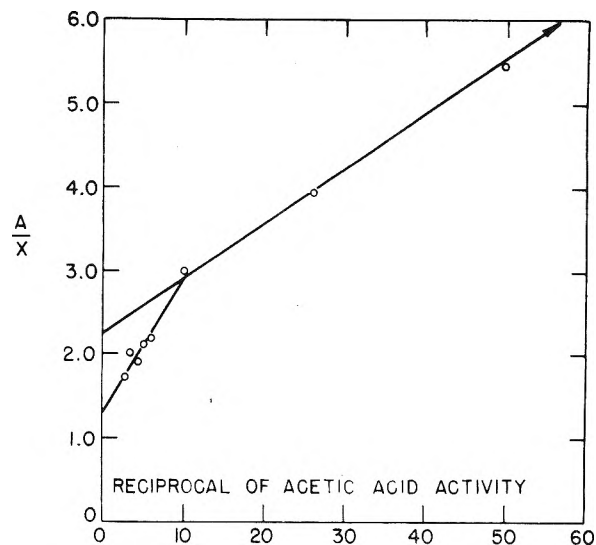


Fig. 4.—Reciprocal plot for the adsorption of acetic acid monohydrate on Graphon.

The data for the adsorption of propionic acid on Graphon suggests a behavior analogous to that of acetic acid but unfortunately it includes only one point in the low coverage region. The intercept of the high coverage line of the reciprocal plot (Fig. 5) indicates a molecular area of 23 Å.² which in this

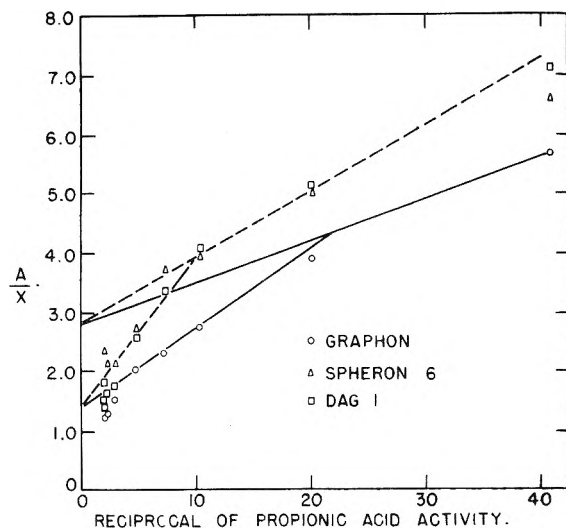


Fig. 5.—Reciprocal plot for adsorption of propionic acid as monohydrate on Graphon, Spheron 6 and DAG 1.

case can only be explained by assuming two carbon atoms of the propionic acid bound to the adsorbent surface. (If only the first were in contact with the solid the bond angles would result in an appreciably greater area as is readily demonstrated with molecular models.) The greater contact area tends to

reduce the effect of heterogeneity of the other carbons reported in reference (2), Dag 1 and Spheron 6, to the point where their high coverage reciprocal plots are sufficiently linear for determination of molecular areas from the intercepts. The reciprocal plots of the data for the adsorption of propionic acid on both Dag 1 and Spheron 6 fall on the same two straight lines. These lines were above (weaker adsorption) those for adsorption on Graphon but the intercepts for the high coverage line were the same. It was therefore assumed that the low coverage lines would also have the same intercept and a low coverage line for the Graphon system was drawn from the single experimental point to the low coverage intercept established from the Dag 1 and Spheron 6 data. The results of this treatment (see Fig. 5) indicate that propionic acid is adsorbed on carbon at low coverage with a molecular area of 46 \AA^2 and that on Graphon when the coverage $\theta = 0.64$ is passed, the molecular area drops to 23 \AA^2 . It is concluded that at low coverage, all carbon and oxygen atoms are bound to the surface but that at high coverage, contact with the solid is limited to the two carbons not bearing the oxygen atoms.

Data for the other acids, reported in reference (2), butyric, valeric, caproic and heptylic acids, include no points in the low coverage region and only a few at coverage sufficiently low to avoid the complica-

TABLE III
MOLECULAR AREAS OF NORMAL ALIPHATIC CARBOXYLIC ACIDS ADSORBED FROM AQUEOUS SOLUTION ON GRAPHON

No. carbon atoms	Mol. area paraffin, \AA^2	Mol. area acid in dilute monolayer, \AA^2	Coverage θ at transition	Mol. area acid in coned. monolayer, \AA^2
1	15.5
2	23.5	38	0.78	22
3	31.5	46	0.64	23
4	39.5	23
5	47.5	35
6	55.5	36
7	63.5	35

tion of multilayer adsorption. However, high coverage reciprocal plots of reasonable linearity were obtained.

The molecular area of butyric acid was approximately the same as that of propionic acid, indicating that at sufficiently high coverage, butyric acid is adsorbed with only two carbon atoms in contact with the solid. The indicated molecular areas of the three higher acids were all $35\text{-}36 \text{ \AA}^2$. They are apparently adsorbed with three carbon atoms bound to the solid, the slightly larger areas being explained by overhang.

The molecular areas of the aliphatic acids are summarized in Table III.

A STUDY OF ADSORBED WATER ON SILICA GEL BY NUCLEAR RESONANCE TECHNIQUES

BY J. R. ZIMMERMAN, B. G. HOLMES AND J. A. LASATER

Magnolia Petroleum Company, Field Research Laboratories, Dallas, Texas

Received February 24, 1956

Nuclear magnetic resonance measurements have been obtained from the hydrogen nuclei of H_2O adsorbed on silica gel by means of pulsed radio frequency techniques. The experimental data are values of T_2 , the inverse line width parameter, as a function of adsorbed water vapor coverage on the silica gel. Insofar as nuclear relaxation time (T_2) is concerned, a twofold phase system is observed at large surface coverage which presumably distinguishes between protons in the water adsorbed in and adsorbed on the monomolecular layer. At low surface coverages, $\theta < 0.5$, the measurements point out the existence of two discrete adsorption energy sites. The relaxation data pertaining to the lower energy sites at this low surface coverage strongly suggest that the relaxation effects due to interactions between adsorbed water molecules have been directly observed. A qualitative comparison of these experimental results is made with dielectric measurements obtained by Kurosaki. Where two-phase systems exist, some sample quantitative measurements of the relative number of water molecules associated with each adsorption phase are given.

Introduction

In recent years a number of new techniques have been applied in the study of adsorption phenomena, including the studies of the kinetics of adsorption, of accommodation coefficients of materials with varying amounts of adsorbed material, of infrared, ultraviolet and visible light adsorption spectra of the adsorbed material, and of dielectric behavior of adsorbed polar molecules. The spectroscopic techniques are all limited severely by experimental difficulties peculiar to adsorption systems. In all of these techniques for studying adsorption phenomena, the measurements are such as not to permit distinct identification of individual components contributing to the multi-phase adsorbing system; but rather such measurements represent an unresolved composite of the individual components.

The use of nuclear magnetic resonance pulse techniques¹ may, in some instances, be able to resolve these different adsorbing components for certain types of adsorbate. Nuclear relaxation processes^{2,3} arise from the magnetic interactions between the nucleus under study and its local field. The high frequency components of the local field determine the spin-lattice (T_1) relaxation time; the line width parameter ($1/T_2$) arises from the interactions with the low frequency spectrum of the local field and from a broadening associated with the life time of the spin state. If the nuclei of a system do not all enjoy the same average local field interactions during the time of relaxation measurements, then such a system might be defined as a multi-phase nuclear system. The i -th phase can then be described in terms of a set of relaxation times T_{1i} and T_{2i} . In a two-phase system, if either T_{1i} and T_{1j} or T_{2i} and T_{2j} can be accurately evaluated, then certain aspects of the two phases are subject to independent study by nuclear magnetic resonance techniques.

The multiple phase nuclear system technique has been used extensively in the determination of moisture content in proteins and starches.⁴ In this instance the resonance line width of the hydrogens of the solid chemical structure is extremely broad, while the line width of the adsorbed water is,

in comparison, very narrow. Wilson and Pake⁵ have observed this multi-phase system behavior in the study of quasi-crystalline polymers. Norberg and co-workers⁶ have recently extended the earlier work by Pake by measuring several distinct T_2 's for the protons in solid polyethylene. Tanaka⁷ has reported the observation of a multi-phase system in adsorbed water on carbon. In this instance a distinction was made between water adsorbed in and above the mono-molecular layer by observing a sharp resonance line superposed on a broad resonance line. The relaxation data which are described in the following pages have been obtained from nuclear magnetic resonance pulse (spin-echo) techniques.¹ In view of the excellent treatises now available, no general mathematical introduction to the field of nuclear resonance and the related spin-echo technique is presented. Arguments relating adsorption phenomena to nuclear relaxation phenomena are intentionally presented on a qualitative basis.

Experimental

Adsorption Apparatus.—A sample of 10.5582 g. of Davison⁸ commercial silica gel was weighed into a special sample holder equipped with a valve arrangement so that it could be attached or unattached to a high vacuum adsorption system without changing the pressure on the silica gel. The silica gel sample and holder were dried under vacuum (10^{-5} mm.) at a temperature of approximately 300° for six days. It was found that the silica gel sample had decreased in weight by 0.4473 g. during this treatment. It is believed that the silica gel was now dry and the dry weight of silica gel was taken as 10.1109 g.

The dried, evacuated silica gel and the vacuum pump were isolated; and water vapor was introduced into the manifold. The sample bulb was opened to the manifold and water vapor was adsorbed on the silica gel. An oil (Octoil) manometer was used to determine the water vapor pressure; however, the amount of water adsorbed by the silica gel was determined by direct weighing of the sample (bulb). This procedure was repeated for each nuclear magnetic resonance relaxation time measurement. Each measurement was performed at 25° .

Once the silica gel was saturated, a reverse procedure was used to desorb the adsorbed water. The amount of water desorbed at each step was also determined by weighing the sample. No obvious hysteresis effects were observed

(5) C. Wilson and G. Pake, *J. Polymer Sci.*, **10**, 503 (1953).

(6) I. Lowe, L. Bowen and R. Norberg, *Bull. Am. Phys. Soc.*, **30**, 16 (1955).

(7) K. Tanaka and K. Yamagata, *Bull. Chem. Soc. Japan*, **28**, 90 (1955).

(8) A chemical analysis of this gel has been made. The alumina content is approximately 0.2% by weight.

(1) E. Hahn, *Phys. Rev.*, **80**, 580 (1950).

(2) N. Bloembergen, E. Purcell and R. Pound, *ibid.*, **73**, 679 (1948).

(3) F. Bloch, *ibid.*, **70**, 460 (1946).

(4) T. Shaw and R. Elsken, *J. Chem. Phys.*, **21**, 565 (1953).

insofar as relaxation data are concerned over the range of coverages described in this paper.

The surface area measurements of the silica gel were obtained by a standard B.E.T. apparatus. Nitrogen was adsorbed at liquid air temperatures. An oxygen vapor pressure thermometer was used to measure these temperatures. Helium was used to determine the dead space. The sample was outgassed 24 hr. at 110° before each adsorption run for area measurement. The average surface area was found to be 625 m.²/g.

Nuclear Relaxation Measurements.—In order to obtain relaxation data from a two-pulse spin-echo system (see Fig. 1) the magnitude of two types of signals are obtained:

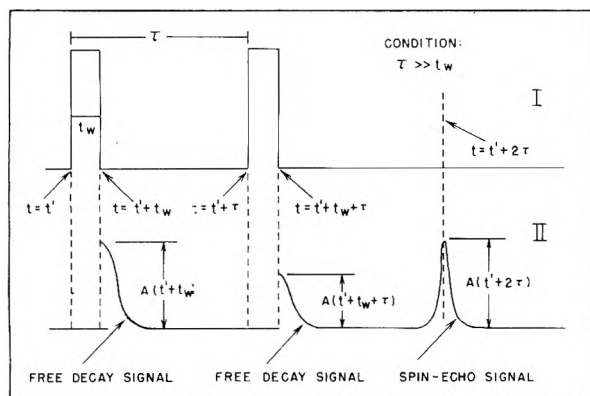


Fig. 1.—A N.M.R. schematic for two r.f. pulses: I, a plot of R.F. signal amplitude with time; II, a plot of nuclear signal amplitude with time.

(1) the spin-echo signal which occurs at time 2τ after the first r.f. pulse, where τ is the time between pulses; and (2) the free decay signals which arise immediately after each of the r.f. pulses. These signal amplitudes are measured as a function of τ . The relaxation times (T_2) are obtained from spin-echo signal amplitudes, whereas the spin-lattice relaxation times (T_1) are determined from free decay signal amplitudes. A typical plot of data for determining the relaxation times (T_2) for a water vapor adsorption of $(x/m) = 0.571$ is shown in Fig. 2 (curve II). If this adsorbed system were of a single phase, such a plot of spin-echo amplitude, $A(2\tau)$ vs. τ would be a simple straight line. The resulting slope of curve II at large τ corresponds to one phase of the system, while curve I, which is a plot of the difference between curve II and the extrapolated slope of curve II, corresponds to a second phase of the adsorbing system. In addition to the availability of relaxation time values, it is also possible, under suitable conditions as in Fig. 2 (see ratio A_{01}/A_{02}), to obtain the relative amounts of water molecules in the two adsorbing phases. For clarifying purposes, measurements in this paper relate only to T_2 relaxation data.

Generally, the experimental data are not sufficient for an accurate graphical analysis of a two-phase system. In order to extend the region of accurate evaluations, numerical analyses of the data by means of the Field Research Laboratories' Datatron⁹ computer have been made. No further discussion of the evaluation of relaxation data will be given at this time. However, a theoretical analysis of two-phase nuclear systems and appropriate numerical procedures will be submitted for publication in the near future.

Results

Relaxation (T_2) Data.—Relaxation (T_2) data were obtained over the water vapor adsorption range of $0.0434 \leq (x/m) \leq 0.571$. A plot of T_2 vs. (x/m) is shown in Fig. 3. θ is the fraction of monomolecular coverage, where the cross-sectional area of the water molecule was taken to be 10.6 Å.². For convenience of explanation, the curves of Fig. 3 may be divided into regions of three different

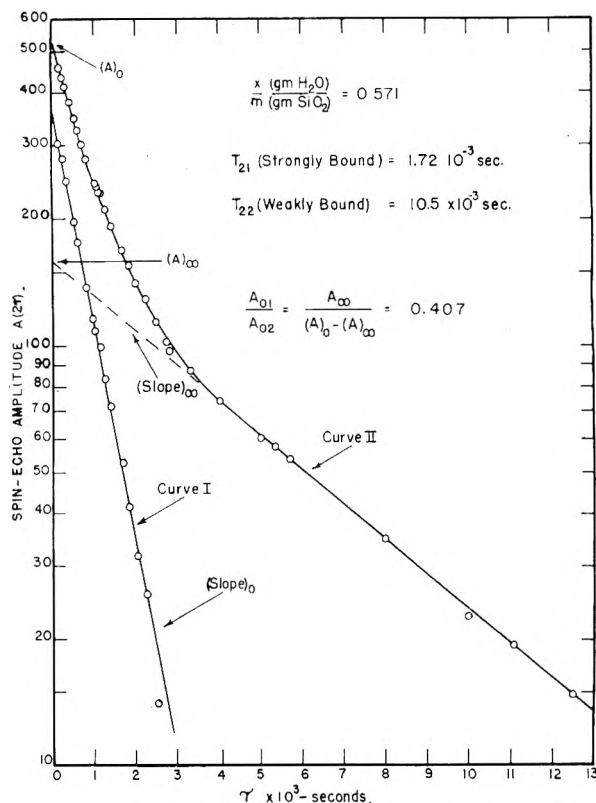


Fig. 2.—Transverse relaxation times for H₂O adsorbed on silica gel.

stages of adsorption corresponding to coverages of (a) $\theta > 2$, (b) $2 > \theta > 0.5$, (c) $\theta < 0.5$.

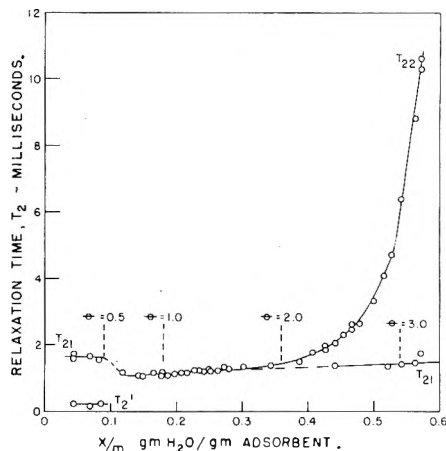


Fig. 3.—Transverse relaxation time for protons of H₂O adsorbed on silica gel.

(a) $\theta > 2$.—For vapor coverage $\theta > 2$, above approximately two monomolecular layers, a distinct resolution of two groups of water molecules is obtained, the groups corresponding to relaxation times T_{22} and T_{21} (Fig. 3). This two-phase system distinguishes between protons in the water adsorbed in and adsorbed on the monomolecular layer; i.e., the group corresponding to the relaxation time T_{21} is to be considered as having closer association with the silica gel surface than the other group corresponding to the relaxation time T_{22} . In a qualitative sense, the degrees of freedom of the more tightly bound group of water molecules would be expected

⁽⁹⁾ Manufactured by ElectroData Corporation of Pasadena, California.

to be restricted more than the degrees of freedom of the less tightly bound group and, therefore, $T_{21} < T_{22}$. Of particular interest is the fact that the T_{21} group at high coverage has a relaxation time not much different from that of the water molecules in the monomolecular layer region, $\theta = 1$. The fact that T_{21} does increase slowly toward higher coverage is due to the supposition that, as the number of molecules in the outer layers is increased, the random motion of the molecules in the monomolecular layer is increased appreciably. The observed increase in T_{21} as water vapor coverage is increased is expected on the basis that such an increase in random molecular motions would tend to average out some of the local field interactions which are responsible for relaxing the hydrogen nuclei; namely, the intra- and inter-molecular magnetic interactions between the hydrogen nuclei of the water molecules.

(b) $2 > \theta > 0.5$.—In the neighborhood of $\theta = 2$, as the quantity (x/m) decreases, the T_{22} and T_{21} data converge into a single phase system; *i.e.*, it is impossible to resolve different phases. For (x/m) in the region of approximately $0.12 < (x/m) < 0.20$ ($\theta \sim .75$), the hydrogen nuclei of the water molecules tend to enjoy the same average local magnetic field interactions during the time of the nuclear relaxation measurements.

(c) $\theta < 0.5$.—As water vapor coverage is reduced below a monomolecular layer, the adsorbed system continues to behave as a single phase system. However, in the region of $\theta = 0.5$, this single phase system shows a sharp increase in T_2 with further decrease in (x/m) . The most dominant local field interaction insofar as T_2 values of adsorbed water vapor on silica gel will arise from the nuclear spin-spin interactions between hydrogen nuclei of the same molecule. However, another, though smaller, contribution to local field will arise from spin-spin interactions between hydrogen nuclei of different molecules. This interaction can be effective if there is sufficient proximity between the molecules, *e.g.*, during collision or when molecules are adsorbed on adjacent sites. With the logical assumption that the adsorbed phase can be defined as a mobile film, the rather sudden increase in T_{21} as coverage is decreased in the neighborhood of $\theta = 0.5$ can be qualitatively interpreted as due to a decrease in effective inter-molecular interactions of the adsorbed molecules. Below $\theta = 0.5$ no appreciable change in T_{21} is observed; hence, the average local field interactions responsible for nuclear relaxation remains approximately constant at low coverage. This increase in T_{21} is observed both in the process of desorption and in the process of adsorption.

In addition to the system described by T_{21} , it is possible to resolve a second adsorbing phase at low water vapor coverages. The water molecules associated with this particular phase described by T_2' in Fig. 3 are not a part of any of the other adsorption phases hereto discussed. Because of the short relaxation time, $T_2' \sim 0.020$ second, and the relatively small number of water molecules associated with this phase, it is only at low coverage that this particular phase is subject to relaxation

measurements. The molecules associated with this phase are bound considerably more tightly to the surface than are any of the other phases described previously ($T_2' \ll T_{21}$). These adsorption sites may possibly be due to impurities in the silica gel. Adsorption measurements at this Laboratory not reported in this paper indicate that these adsorption sites very likely arise from the presence of the alumina impurity mentioned previously.

Comparison with Dielectric Measurements.—In the theory of nuclear relaxation applied to hydrogen nuclei in water molecules, Bloembergen, *et al.*,² pointed out the close parallelism between the nuclear correlation time τ_c and the Debye correlation time τ_D encountered in dielectric dispersion in polar liquids. Both the nuclear and Debye correlation times are a measure of the time during which molecular orientation persists. However, in the nuclear case, orientation is with respect to the direction of the H—H line, whereas in the dielectric case orientation is with respect to the electric dipole axis of the molecule. For a qualitative comparison, however, this difference is relatively unimportant; the nuclear and Debye correlation times may be assumed to be of the same order of magnitude.

A single phase nuclear spin system has a certain distribution of nuclear precessional frequencies due to the average local field interactions. If this system of spins is initially precessing in phase, then the time necessary for the spins to become out of phase is the classical definition of the inverse line width parameter, T_2 . T_2 is a function of both the interaction energies encountered in the local field environment and the nuclear correlation time, τ_c , which one defines as the time during which the particular interaction energies are effective.

Likewise, in dielectric measurements of a molecular system any variations in specific polarization of the molecule because of differences in molecular bonding to a surface or in interaction energies between molecules are related to the distribution of correlation times, τ_D , associated with the system. Hence, in the case of vapor adsorbed on a solid, distinct molecular phases can arise due to different degrees of polarization. It is possible, in some instances, to predict the existence of such phases by a measurement of the apparent dielectric constant as a function of coverage of the adsorbed vapor on the adsorbate.

Kurosaki¹⁰ has recently obtained such dielectric measurements for adsorbed water in silica gel (also Davison commercial gel). Because of the expected parallelism between nuclear and Debye correlation times with respect to persistence of orientation, a qualitative comparison of Kurosaki's dielectric measurements and our nuclear relaxation (T_2) measurements might be both interesting and worthwhile to other investigators in the adsorption field. In Fig. 4, (x/ms) , in milligrams of H₂O per square meter of adsorbate, is plotted both as a function of the apparent dielectric constant ϵ' (dotted line) and as a function of the relaxation time T_2 (solid lines).

In the adsorption stage $\theta > 2$, as mentioned pre-

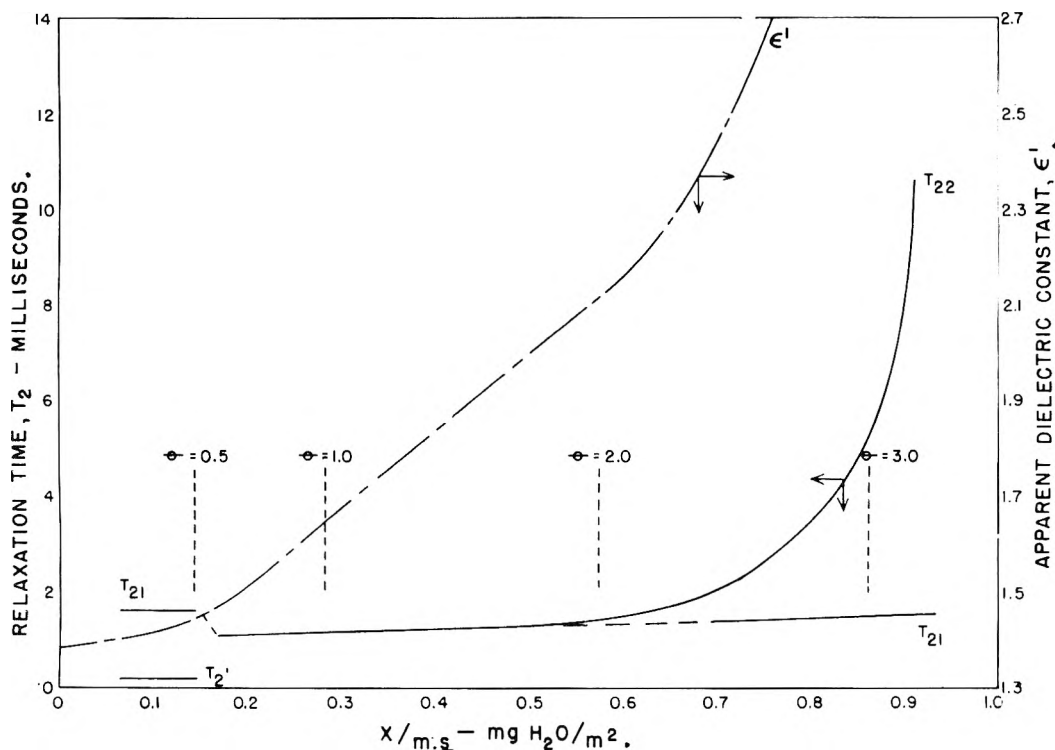


Fig. 4.—A comparison between dielectric and nuclear relaxation measurements.

viously, T_{22} and T_{21} data point out the existence of two-phase molecular behavior insofar as nuclear relaxation measurements are concerned. A change of slope of the apparent dielectric plot also appears in the same region of coverage ($\theta \sim 2$). Kurosaki has interpreted this change in slope as the development of a new adsorbing phase. Of particular significance is the fact that Debye dielectric dispersion was also observed in this region of coverage. This dispersion indicates that the sorbed water possesses a fixed Debye correlation time for a particular coverage. However, in view of the nuclear relaxation (T_2) data, it would appear that there exists in the adsorption stage $\theta > 2$ two distinct groups of water molecules identified by different specific polarizations, only one group exhibiting dielectric dispersive phenomena. Kurosaki¹⁰ realized the need for this conclusion in his comparison of experimental and theoretical calculations of apparent dielectric loss constant ϵ'' . Nuclear resonance techniques now point out this two phase behavior directly.

In the adsorption stage $0.5 < \theta < 2$, the slope of ϵ' vs. (x/ms) in Fig. 4 is less than the corresponding slope at higher vapor coverage; the specific polarization, of course, is less. The conclusions are that the water molecules in this region are more tightly adsorbed and perhaps have considerably less intermolecular interactions than do the molecules in the region $\theta > 2$. The nuclear relaxation (T_2) measurements are in qualitative agreement with these conclusions. In addition, the nuclear relaxation measurements show that the adsorption phase in this stage is quite like that of the tightly adsorbed phase (T_{21} data) at coverages of $\theta > 2$.

In the adsorption stage $\theta < 0.5$, the dielectric plot in Fig. 4 shows that the adsorbed water vapor

has a comparatively low specific polarization [small $\Delta\epsilon'/\Delta(x/ms)$]. Kurosaki concludes that the water molecules are more tightly bound in this region on the basis of the fact that the dielectric loss factor is nearly zero throughout the entire frequency range. The nuclear relaxation (T_{21}) data support these conclusions, if one means by a "more tightly bound" molecule as one free from intermolecular interactions with its neighboring adsorbed molecules.

Quantitative Analyses of Two-phase Systems.— In addition to relaxation time values, the relative number of hydrogen nuclei contributing to a two-phase adsorption system may be obtained under sufficiently favorable conditions. In Fig. 1, such a quantitative evaluation (A_{o1}/A_{o2}) is obtained for the adsorption of water vapor on silica gel with an $(x/m) = 0.571$. From Fig. 3, it is observed that such an (x/m) value corresponds to a coverage in excess of three monomolecular layers. For this value of (x/m) it is found that the ratio of the number of strongly bound and the number of weakly adsorbed molecules is $(A_{o1}/A_{o2}) = 0.407$. It follows that the (x/m) corresponding only to the strongly adsorbed group (T_{21} data) is approximately 0.17. This result is remarkably close to the monomolecular layer coverage $\theta = 1$ (see Fig. 3 for comparison).

Two similar measurements have been made at low coverage, $\theta < 0.5$. Since the T_2' data in Fig. 3 correspond to sites of very low potential (high energy sites), it is logical to assume that such a system will have considerable priority in the filling of its sites. For a value of $(x/m) = 0.0845$, machine calculations of the nuclear relaxation data yield a value of $(x/m) = 0.023$ for the high energy sites (T_2' data) and $(x/m) = 0.061$ for the remaining ad-

sorption sites (T_{21} data). For a value of $(x/m) = 0.0681$, nuclear relaxation data yield a value of $(x/m) = 0.028$ for the high energy sites. Thus, to a rough approximation, the coverage of the high energy sites remains unchanged in this region.

Conclusion

The co-existence of two adsorbing phases of water vapor on silica gel at a surface coverage region of $\theta > 2$ has been directly observed by nuclear magnetic relaxation measurements. A measure of the future importance of nuclear resonance techniques in certain fields of adsorption phenomena is borne out by the excellent qualitative correlation between the dielectric measurements and interpretations by Kurosaki and the nuclear relaxation (T_2) data pertaining to the existence of two-phase behavior.

In multilayer adsorption theories, arguments arise regarding the interaction effects imposed on the monolayer by molecules external to the monomolecular layer. The fact that T_{21} (Fig. 3) does increase slowly toward higher coverage is observed presumably because the random motion of the water molecules in the monolayer is increased.

Milligan¹¹ has observed from susceptibility measurements of water vapor adsorbed on silica gel that the monomolecular layer molecules "do not regain the susceptibility of bulk water even after the formation of several layers." The nuclear relaxation data corroborate this evidence directly by showing that T_{21} at high coverage ($\theta > 2$) is only slightly higher than T_{21} in the neighborhood of $\theta = 1$.

In specific instances where two adsorbing phases have been observed to exist, it has been possible to evaluate the relative number of molecules associated with each adsorbing phase. A sample

calculation for an adsorption of $(x/m) = 0.571$ shows that the number of water molecules associated with the stronger adsorbing phase (T_{21} data, Fig. 3) is remarkably close to the theoretical monomolecular coverage of $\theta = 1$.

Lateral interaction effects of adsorbed molecules is a well recognized problem; and for a mobile adsorbed system, these interaction effects rapidly become negligible in the region of $\theta = 0.5$. From the nuclear relaxation data, a rather sharp increase in T_{21} is observed (Fig. 3) in this critical region. It is impossible at this time to say whether such an increase is due to an intra-molecular averaging of the local field between hydrogen nuclei (more random freedom at the adsorbing site), or whether such an increase is due to a decrease in effective local field interactions between nuclei in separate adsorbing molecules.

The presence and associated effects of impurities on a surface often present formidable problems in adsorption experiments at low coverage. In this particular sample of silica gel, direct observation of the existence of such an adsorbing phase system is obtained (see Fig. 3, T_2' data). Calculations show that the number of water molecules associated with this adsorbing phase remains approximately constant in the region $0.25 > \theta < 0.5$. In comparison to the adsorbing phase (T_{21}) the adsorbing phase (T_2') corresponds to a greater heat of adsorption.

Acknowledgment.—The authors are especially indebted to Professor N. H. Hackerman of The University of Texas and to Dr. S. R. Faris of the Field Research Laboratories for their many stimulating discussions and suggestions pertaining to the phenomena of adsorption and its relation to nuclear resonance experiments during the various stages of this investigation.

(11) W. Milligan and H. Whitehurst, *THIS JOURNAL*, **56**, 1073 (1952).

ADSORPTION OF GASES AND VAPORS ON GLASS SPHERES. II. TWO-DIMENSIONAL CONDENSATION OF OXYGEN¹

By J. L. SHERESHEFSKY AND C. E. WEIR

Chemistry Department, Howard University, Washington, D. C.

Received February 24, 1956

Two-dimensional phase formation is described for oxygen on glass spheres at liquid air temperature. This phase formation was found absent at -78° . A supersaturated adsorbed phase is also described. The pressure of two-dimensional condensation is discussed in relation to surface activation and the van der Waals equation of state for surfaces.

In connection with studies in this Laboratory on the relationship of porosity of the adsorbent to adsorption the phenomenon of two-dimensional condensation was observed for nitrogen and oxygen. Also, it was found that supersaturation of the adsorbed phase may precede the formation of the two-dimensional two-phase system. In recent years, after the work on nitrogen² was published, a considerable amount of research has been done on this subject and a great deal more is known of the phenomenon.³ It is our object to present the research on the two-phase formation of the adsorbed phase of oxygen on glass spheres.

Experimental Details

Apparatus.—The adsorption system was of the volumetric type, and because of experimental low pressure requirements, the different parts of the system were separated by mercury cut-offs, and stopcocks were used only in the least sensitive areas.

One branch of the system included an adsorption vessel, a low temperature trap, a manometer, a buret and a McLeod gage. The adsorption vessel was a Pyrex flask of known volume with a graduated neck. The volume occupied by the adsorbent under different packings was measured by its position in the neck. The buret was used for calibrating the volumes of the different parts of the systems and for precise measurements of quantities of gas. Another part of the system was the evacuation branch. It included a vapor diffusion pump and a Hyvac oil pump connected in series. A third branch consisted of a vessel for storing the purified gas, a dosing stopcock for delivering approximate quantities of gas, and a purification train.

Materials.—Five thousand glass spheres which constituted the adsorbent and were approximately 3 mm. in diameter were cleaned with chromic and nitric acids, washed with distilled water and dried in an oven. Glass spheres treated in this manner showed by methylene blue⁴ adsorption to possess a real surface which was 54.5 times as large as the geometrical surface.

The oxygen was prepared by heating potassium permanganate in an evacuated system, and purified by passage through glass wool and potassium hydroxide. It was stored over phosphorus pentoxide. The helium used for calibration was purified by passage through activated charcoal at liquid air temperature.

Activation of Adsorbent.—The spheres were activated for adsorption measurements by heating and pumping at 250° in a high vacuum until a pressure less than 10^{-5} mm. of mercury was reached. The length of time that was required to attain this varied from 24 to 60 hours.

Thermal Flow Corrections.—The liquid air temperature and low experimental pressures required that the equilibrium pressures be corrected for transpiration. These corrections were made in accordance with the calibrations reported elsewhere.² No corrections were necessary in the isotherms at the temperature of carbon dioxide snow and ether.

Procedure.—A desired quantity of oxygen was introduced into the fore-chamber of the adsorption branch of the apparatus and its pressure determined on the manometer by means of a cathetometer reading to 0.01 mm. It was allowed to expand into the adsorption chamber by lowering the mercury cut-off separating these two parts of the adsorption branch. The pressure was measured at brief intervals on the McLeod gage until no further decrease in pressure occurred. This gage was of three stages, allowing the measuring of pressures in the ranges of from 10^{-5} to 10^{-3} , from 10^{-4} to 10^{-2} , and from 10^{-3} to 10^{-2} mm. of mercury. In making further additions of gas to the adsorbent, the mercury in the cut-off was raised to separate the adsorption vessel from the fore-chamber, a quantity of gas was introduced into the fore-chamber, its pressure measured, and allowed to expand into the adsorption chamber. The adsorption at any point n is given by the equation

$$A = \frac{V_1}{RT_1} (P_n - P_n^1) - \frac{V_2}{RT_2} P_n^1 \quad (1)$$

where V_1 and V_2 are the volumes of the fore-chamber and the adsorption vessel, respectively; P and P^1 are the pressures in the fore-chamber before expansion and at equilibrium after expansion, respectively; P_n^1 is the pressure in the cold adsorption chamber as corrected for transpiration; T_1 and T_2 are the absolute temperatures of the room and cold adsorption vessel, respectively.

Experimental Results

The isotherms obtained at liquid air temperature are shown in Fig. 1. Each isotherm was obtained on newly activated glass spheres packed at a different porosity and a different average number of contacts per sphere.⁵

Every isotherm in this figure, as in the case of nitrogen,² shows a sudden drop in pressure and a corresponding increase in adsorption, after a period of low linear adsorption that follows Henry's law. This behavior is strikingly illustrated in Fig. 2, where the equilibrium pressure is plotted as abscissa and, as the ordinate, is plotted the pressure that would prevail were the gas not adsorbed. In this plot the points of the initial linear adsorption process almost coincide with a linear curve representing the adsorption isotherm carried out at the same temperature in a blank vessel of volume equal to the void space in the adsorption flask.

The adsorption isotherms at the temperature of carbon dioxide snow and ether are given in Fig. 3. The number of contacts per sphere for the isotherms is different. These isotherms coincide, follow a linear course, and show no sudden pressure drop and no sudden adsorption increase.

The process following the sudden pressure drop in the low temperature isotherms was found to proceed slowly, in distinction to the rapid attainment of equilibrium at adsorption higher than that corresponding to the minimum pressure point.

(1) Based on a M.S. thesis of Charles E. Weir.

(2) J. L. Shereshefsky and C. E. Weir, *J. Am. Chem. Soc.*, **58**, 2022 (1936).

(3) S. Ross and W. Winkler, *ibid.*, **76**, 2637 (1954); *J. Colloid Sci.*, **10**, 330 (1955).

(4) F. Paneth and A. Radu, *Ber.*, **57B**, 1221 (1924).

(5) W. O. Smith, P. D. Foote and P. F. Busang, *Phys. Rev.*, **34**, 1271 (1929).

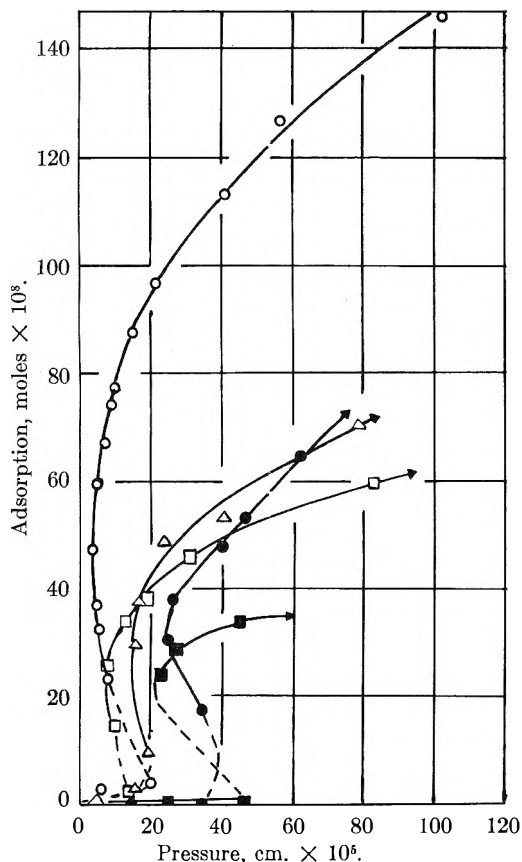


Fig. 1.—Adsorption of oxygen on glass spheres at liquid air temperature: ●, 8.5; ○, 9.3; ■, 8.0; □, 8.8; △, 9.0; contacts per sphere.

The pressure-time curves obtained in the broken line sections followed the equation

$$\ln(P/P_0) = kt \quad (2)$$

where P is the pressure at time t and P_0 is the initial pressure at $t = 0$. The value of the rate constant k for oxygen was found to equal that for nitrogen.²

Discussion

The phenomenon observed in this and the nitrogen studies, of a sudden drop in pressure accompanied by a rapid rise in adsorption, is considered by us to be due to the formation of a condensed two-dimensional phase. The sudden appearance of this phase is preceded by a labile supersaturated adsorbed phase, in which the adsorption varies linearly with pressure, in accordance with Henry's law. This interpretation is now amply corroborated.^{3,6} The transition of the labile adsorbed gas phase to the stable condensed phase is a slow process, taking place in accordance with equation 2 and following the paths indicated by the broken lines in Fig. 1.

According to the van der Waals type equation 3 for an adsorbed phase derived independently by DeBoer⁷ and Hill,⁸ condensation and the

$$P/P_0 = K_2 \theta / (1 - \theta) \exp(\theta / (1 - \theta)) \exp(-K_1 \theta) \quad (3)$$

pressure at which it takes place are dependent on

(6) E. Weingaertner, *Z. Elektrochem.*, **42**, 599 (1936).
 (7) J. H. DeBoer, "The Dynamical Character of Adsorption," Oxford, 1953, p. 170.
 (8) Terrell L. Hill, *J. Chem. Phys.*, **14**, 441 (1946).

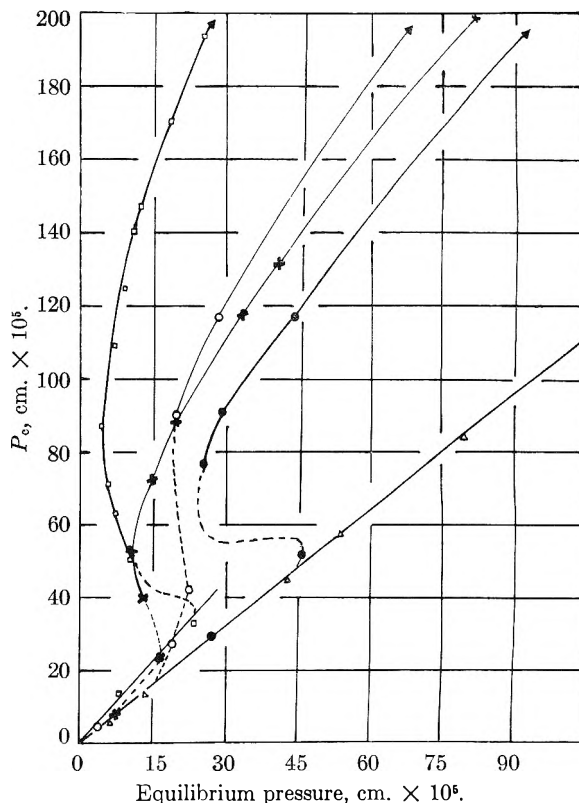


Fig. 2.—Transition of adsorbed oxygen phase: △, blank.

the values of the constants K_1 and K_2 . In this equation P/P_0 is the relative pressure and θ is the degree of surface population. The constant K_1 depends on temperature and the van der Waals

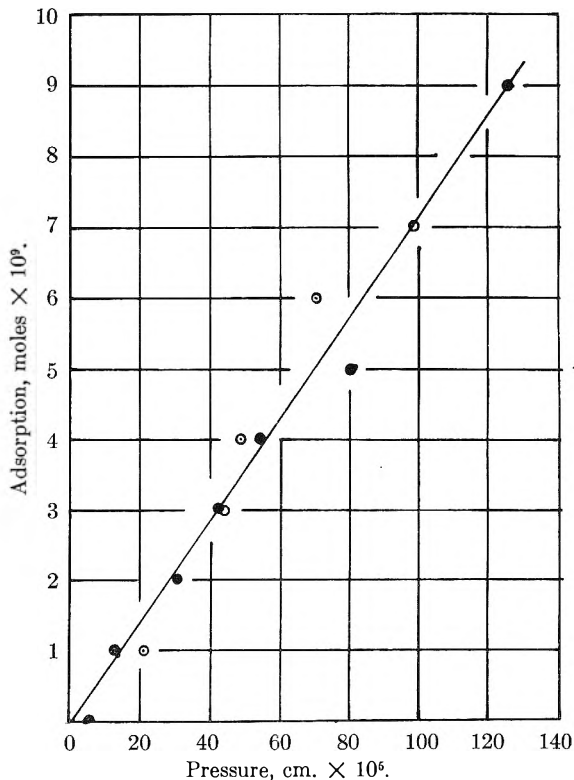


Fig. 3.—Adsorption of oxygen on glass spheres at -78° : ●, 8.8; ○, 9.3 contacts per sphere.

two-dimensional constants a and b . This constant depends only on the properties of the molecules of the adsorbate, which was the same in the several isotherms shown in Fig. 1. The constant K_2 , on the other hand, is related to the heat of adsorption, and measures mainly the strength with which the molecules are adsorbed on the surface. It appears therefore that the different minimum equilibrium pressures at which condensation takes place in the several isotherms are given rise by the variation in the energetic factors of the surface, and hence the variations in the constant K_2 .

The several isotherms presented here were obtained with the same spheres, but at different pack-

ings. In this connection, it is of interest to point out that there appears to be a correspondence between the amount of adsorption, the condensation pressure and the number of contacts per sphere. Since the sequence of obtaining the isotherms, and hence of the activation, was other than that of obtaining the different packings, the observed correspondence in the above properties cannot be ascribed to a successive change in activation of the adsorbent. It seems to us, therefore, that this relationship between the amount of adsorption, condensation pressure and the number of contacts per sphere is indicative of a greater probability of surface activity in the area of contact between two spheres.

ACTIVATED ADSORPTION OF OXYGEN ON GLASS¹

BY J. L. SHERESHEFSKY AND E. R. RUSSELL

Chemistry Department, Howard University, Washington, D. C.

Received February 24, 1956

Oxygen was adsorbed by glass spheres at pressures of 0.25, 0.5 and 0.75 atmosphere and at nine different temperatures, ranging from 0 to 300°. It appears that in this temperature range oxygen adsorption is of two types with characteristic activation energies and heats of adsorption. The maximum rate of adsorption appears to occur at about 155°. The heats of activation in the low temperature interval range from 2800 to 5000 cal./mole, in the high temperature interval from 3700 to 9200 cal./mole. The heat of adsorption is not greatly different in these two temperature intervals, and is calculated from 1230 to 2500 cal./mole, depending on the degree of surface coverage.

The present research is an outgrowth of the studies conducted in this Laboratory of two-dimensional condensation of nitrogen² and oxygen³ on glass. In view of the abnormal isotherms for these gases at low temperature and pressure, it was considered desirable to investigate the adsorption characteristics of these gases on glass at higher temperatures and pressures, in particular the energetic factors involved in the interaction of oxygen with glass surfaces. To this end, it was undertaken to study the rate of adsorption of oxygen on glass spheres at different pressures and temperatures.

Experimental

Apparatus.—The adsorptions were measured in an apparatus which included a Pyrex vessel to hold the adsorbent and connected through suitable mercury seal stopcocks to a gas reservoir and a gas buret, an evacuation system, a pressure control and a purification train.

The evacuation system consisted of a mercury vapor diffusion pump in series with a Hyvac oil pump and a McLeod gage. The pressure control was similar to that of Taylor and Strother⁴ and was enclosed in an air thermostat.

Materials.—The glass spheres, approximately 1900, with a total geometric surface of about 540 sq. cm. were cleaned in a 10% nitric acid solution, washed with distilled water and dried in a desiccator and steam heated oven.

The helium used in the calibration of the different parts of the apparatus, and also in the determination of the pre-expansion pressures, was purified by passing over hot copper, soda lime and anhydrous calcium chloride. The oxygen used as the adsorbate, was purified in a similar manner, except that it was first passed over hot copper oxide.

Calibrations.—The buret was calibrated with mercury prior to the assembly of the apparatus. A division on the buret was equivalent to 0.123 cc.

The part of the apparatus in which the gas was measured prior to its being introduced into the adsorption flask, hereafter referred to as the pre-expansion volume, was calibrated with helium and with the aid of the buret. Similarly was calibrated the volume of the adsorption vessel. The zero point on the buret at the experimental pressures and temperatures also was determined with helium. An appropriate quantity of helium was introduced into the pre-expansion volume, its pressure noted, and allowed to expand into the adsorption vessel to give the desired pressure at a given temperature. The position of the mercury in the buret after attainment of equilibrium was taken as the zero point. In the adsorption measurements, the difference of the height of the mercury from this point was considered as the amount adsorbed. The relative volumes of the pre-expansion and adsorption vessels were such as to insure that the pre-expansion pressure was not greatly different from the desired experimental pressure.

Procedure.—The temperature of the air thermostat enclosing the buret and manometer was maintained constant at a temperature slightly above that of the room. The temperature of the adsorption vessel with adsorbent was controlled by an electrically heated oil-bath, regulated by a De Khotinsky thermoregulator. The dry glass spheres after being introduced into the adsorption vessel were first evacuated for several hours at room temperature, then heated to 200° in an oil-bath and evacuated for 2.5 hours.

Upon completing the activation of the adsorbent, oxygen was introduced into the pre-expansion vessel at the pre-expansion pressure determined in the calibration. By manipulating the appropriate stopcocks, the oxygen was allowed to expand into the adsorption chamber. The rate of decrease of volume was noted by reading at definite intervals the position of the mercury in the buret. The pressure of the oxygen was maintained constant by the automatic pressure control.

Experimental Results

The rate of adsorption of oxygen on glass spheres was measured at 0.25, 0.5 and 0.75 atmosphere pressure and at nine different temperatures, between 0 and 300°. The type of rate curve obtained is shown in Fig. 1. The rates of adsorption at the lower pressures changed with time in the

(1) This paper is based on a M.S. thesis of E. R. Russell.

(2) J. L. Shereshefsky and C. E. Weir, *J. Am. Chem. Soc.*, **58**, 2022 (1936).

(3) J. L. Shereshefsky and C. E. Weir, *This Journal*, **60**, 1162 (1956).

(4) H. S. Taylor and C. O. Strother, *J. Am. Chem. Soc.*, **56**, 586 (1934).

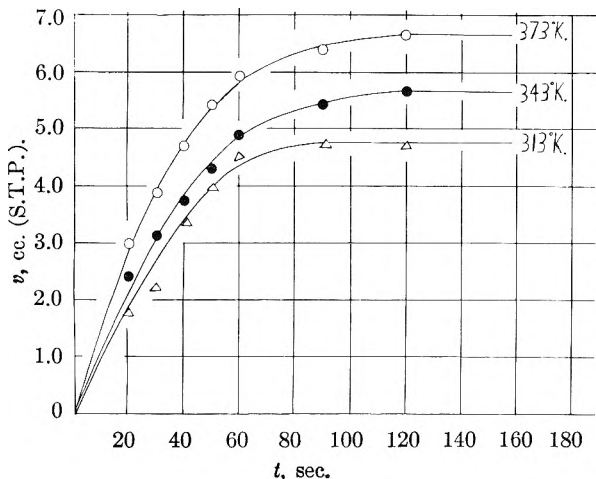


Fig. 1.—Rate of adsorption of oxygen at 0.75 atm. pressure.

same manner but were considerably slower. The rates seem to decrease exponentially with increase of the amount adsorbed, and are presented in a semi-logarithmic form of amount adsorbed v vs. the logarithm of the time t in Figs. 2, 3, 4 and 5. In Table I are given the final or equilibrium amounts adsorbed, which together with the rates given in the plots present the obtained data.

These semi-logarithmic plots are in accordance with the Elovich⁵ equation

$$dv/dt = ae^{-\alpha v} \quad (1)$$

of which the integrated form is

$$v = \frac{1}{\alpha} \ln(t + t_0) - \frac{1}{\alpha} \ln t_0 \quad (2)$$

$$\text{with } t_0 = 1/\alpha a \quad (3)$$

where v is cc. of oxygen adsorbed at time t , α and a are constants. These plots show that the amounts adsorbed and also the rates vary with temperature. The fact that t_0 is zero, that is, that v vs. $\ln t$ gives a straight line is evidence of the absence of an instantaneous process which precedes the slow process of adsorption. The break in the plot for 0.25 atm. and 0° is evidence of surface heterogeneity. The absence of breaks in the Elovich plots at the higher temperatures is perhaps indicative of the decreasing importance of structural heterogeneity at these temperatures.

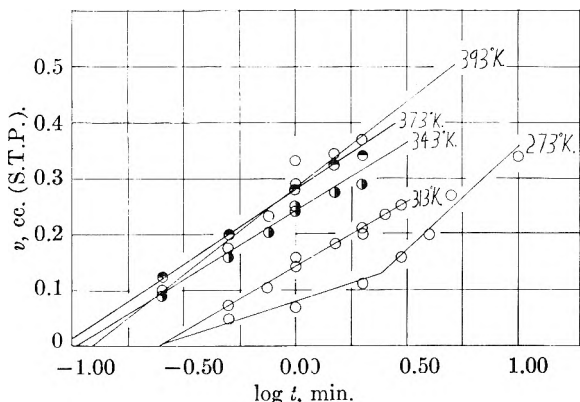


Fig. 2.—Rate of adsorption of oxygen at 0.25 atm. pressure.

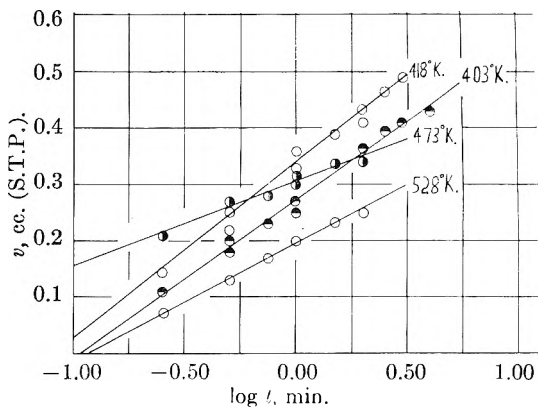


Fig. 3.—Rate of adsorption of oxygen at 0.25 atm. pressure.

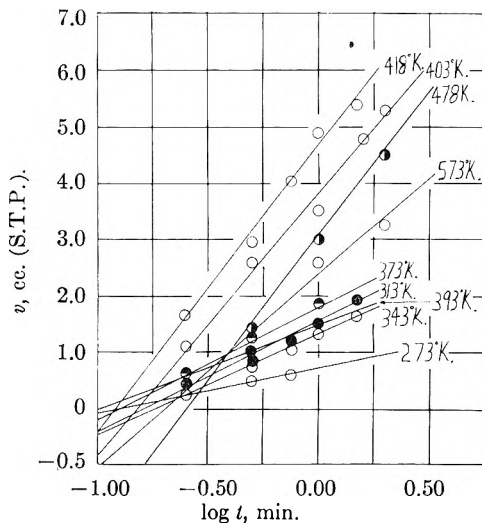


Fig. 4.—Rate of adsorption of oxygen at 0.5 atm. pressure.

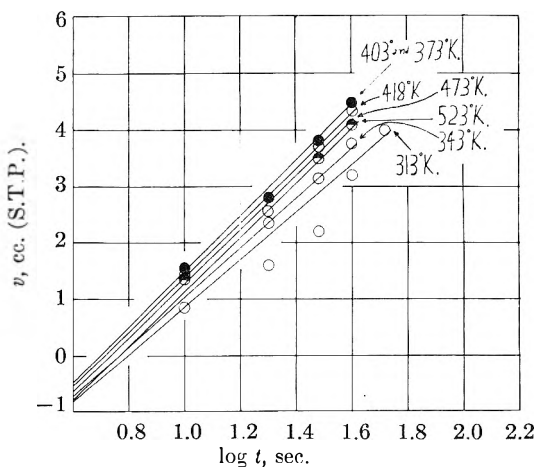


Fig. 5.—Rate of adsorption of oxygen at 0.75 atm. pressure.

TABLE I
Cc. (S.T.P.) O₂ AT EQUILIBRIUM

P _{atm}	Temperature, ° C.								
	0	40	70	100	120	130	145	200	300
0.25	0.34	0.25	0.29	0.34	0.37	0.43	0.49	0.34	0.25 ^a
.50	.97	2.22	1.77	2.11	1.34	5.32	5.50	4.54	3.93
.75	..	4.75	5.69	6.73	..	6.10	5.62	4.83	4.27 ^b

^a At 255°. ^b At 250°.

Calculations and Discussion

The activation energy of the adsorption process involved in these measurements may be calculated

(5) H. A. Taylor and N. Thon, *J. Am. Chem. Soc.*, **74**, 4169 (1952).

from the α -values of the Elovich plots for two or more temperatures. The slope of these plots is given by

$$dv/d \log t = 2.3/\alpha \quad (4)$$

from which is obtained the expression for the rate R at time t

$$R = dv/dt = 2.3/\alpha t \quad (5)$$

Combining (5) with the Arrhenius equation gives

$$2.3/\alpha t = Ae^{-E/RT} \quad (6)$$

Plotting the $\log \alpha t$ vs. the reciprocal of the absolute temperature gives straight lines, of which the slopes are equal to $E/2.3R$, from which the activation energy, E , may be obtained. Plots of this type for the different pressures and at $v = 0.2$ cc. (S.T.P.) are given in Fig. 6.

Besides allowing the evaluation of the activation energy, these plots also show that the rates of adsorption first increase with temperature, reach a maximum, and then decrease with rising temperature, which is indicative of two distinct adsorption processes, one increasing and the other decreasing with temperature. The temperature of the maximum rate is given by the intersection of the two straight lines. The maximum in the present studies corresponds approximately to 155° .

In Table II are given the activation energies obtained in the above manner at the pressures investigated and at various degrees of saturation of the surface. It is to be noted that for a given pressure and surface coverage there are two values of energy of activation, one for the temperature range of 0 to 155° and one for 155 to 300° . Furthermore, in each temperature range the activation energy progressively increases with increasing degree of surface coverage. The activation energy in the higher temperature range is greater than in the lower. These energies designated as I and II are given in Table II. They are comparable to those for oxygen on copper and nickel chromites.⁷

TABLE II

ENERGY OF ACTIVATION IN CALORIES PER MOLE							
V, cc. (S.T.P.) P (atm.)	0.25		0.5		0.75		II
	I	II	I	II	I	II	
0.15	4400	7650
.20	5000	8400	4000	6070	2800	..	3700
.25	5000	9200
2.0	8150	6550

The heats of adsorption may be calculated from the v_0 -values, the amounts adsorbed at equilibrium, and the corresponding temperatures, in accordance with the equation of Taylor and Sickman⁶

$$v_0 = Ke^{\lambda/RT} \quad (7)$$

where λ is the heat of adsorption. The values given in Table III were obtained from the slopes of plots of $\log v_0$ vs. $1/T$. It will be observed that also the heat of adsorption is different in the two temperature ranges, although the differences are not great. The heat of adsorption also, as it is to be expected, appears to decrease with increasing degree of coverage of the surface. These values

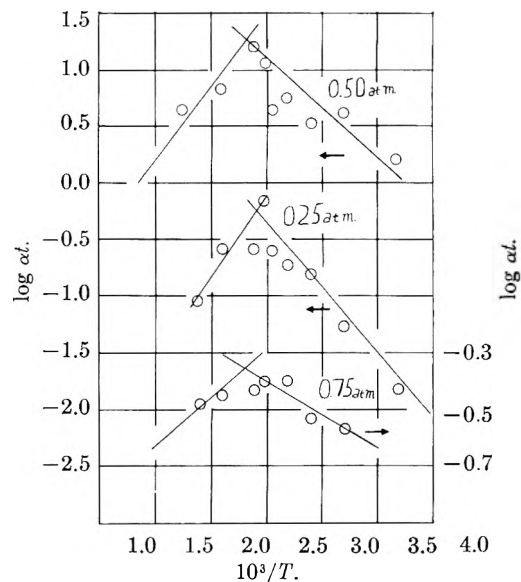


Fig. 6.—Energy of activation of oxygen adsorption at $v = 0.20$ cc.

are in good agreement with 2314 cal./mole obtained by van Itterbeek and van Dingenen⁸ at low temperatures and low pressures.

TABLE III

HEAT OF ADSORPTION OF O ₂ AT DIFFERENT PRESSURES			
P (atm.)	0.25	0.50	0.75
λ_I (cal./mole)	2300	2500	1330
λ_{II} (cal./mole)	2160	1900	1230

(6) H. S. Taylor and D. V. Sickman, *J. Am. Chem. Soc.*, **54**, 602 (1932).

(7) J. C. W. Frazer and L. Heard, *This Journal*, **42**, 865 (1939).

(8) A. van Itterbeek and W. van Dingenen, *Physica*, **4**, 631 (1937).

ADSORPTION AND SURFACE DIFFUSION OF *n*-BUTANE ON SPHERON 6 (2700°) CARBON BLACK

By JOHN W. ROSS¹ AND ROBERT J. GOOD

Applied Science Research Laboratory, University of Cincinnati, Cincinnati 21, Ohio

Received February 24, 1956

The adsorption and surface diffusion of *n*-butane on Spheron 6 (2700°) carbon black have been investigated. Entropies of adsorption were calculated and compared with entropy changes predicted from various models of the adsorbed phase. Both the model of a two-dimensional gas and the model of localized oscillators are compatible with the observed entropy of adsorption. The magnitude of the experimental apparent energy of activation for surface diffusion, however, makes the localized oscillator model appear to be the more reasonable. The dependence of the surface diffusion coefficient on the amount adsorbed was similar to that found by Carman and Raal. Their explanation of this dependence, however, is applicable only to heterogeneous surfaces and could not be applied here. An alternative explanation of the variation of the surface diffusion coefficient with coverage was arrived at through a consideration of the energy and entropy of activation for surface diffusion. The observed simultaneous increase in the energy of activation and the surface diffusion coefficient led to the conclusion that the entropy of activation increases rapidly enough to more than compensate for the increase in the activation energy.

Introduction

The degree of mobility possessed by molecules adsorbed on the surfaces of solids has recently received considerable attention. Two approaches have been utilized to study the surface migration of adsorbed molecules. In the first method, employed by Everett,² Kemball,³ and de Boer and Kruyer,⁴ experimental entropies of adsorption were compared with theoretical entropy changes based on different models for the adsorbed phase. In the second method, "surface diffusion coefficients" were calculated from measurements of the flow of adsorbed gases through porous media. This method has been used by Barrer and Barrie,⁵ Carman and Raal,⁶ and Haul.⁷ In several cases, the conclusions from these two different approaches appear to be contradictory.

The purpose of this work was to examine the adsorption of *n*-butane on Spheron 6 (2700°) carbon black, using both of the methods mentioned above, in an attempt to establish the degree of mobility of the adsorbed *n*-butane molecules.

Experimental

The carbon black employed in this study was obtained through the courtesy of W. D. Schaeffer of Godfrey L. Cabot, Inc. It is produced by heating Spheron 6, a medium processing channel black, for 2 hours at 2700°. It has been designated as Spheron 6 (2700°) by Polley, Schaeffer and Smith.⁸ This black has been reported to possess a highly homogeneous surface.⁹⁻¹⁰ Polley, Schaeffer and Smith⁸ have given a value of the surface area of 84.1 m.²/g. The density was found to be 1.99 ± 0.03 g./cc., as measured by means of helium displacement. Samples for ad-

sorption and flow measurements were outgassed at 200° for about eight hours to a pressure of less than one micron of mercury.

Instrument Grade *n*-butane was obtained from the Matheson Company. The purity was stated to be 99.9%.

The adsorption isotherms were measured by the volumetric method,¹¹ modified by the use of fixed expansion volumes instead of a gas buret. Measurements were made at 30.0 ± 0.05 and 41.7 ± 0.05°.

The apparatus used for the measurement of surface diffusion (Fig. 1) consisted essentially of a four-liter reservoir R, connected through the porous plug C to a buret B on the outlet side. The inlet pressure, measured on the mercury manometer M, was essentially constant owing to the relatively large volume. Constant pressure on the outlet side was maintained automatically. As the pressure in buret B rose, the mercury in the control differential manometer also rose. When the mercury touched the contact wire, the relay activated the electric motor which pulled down the leveling bulb attached to the buret. The pressure in the buret system was thus decreased until it was again just below the pre-set pressure. Small pressure drops in the range 0.3 to 3.8 cm. were used to ensure the validity of the diffusion coefficient.⁶

In operation the system was completely evacuated and flushed at least once. Stopcocks no. 4 and 6 were closed and gas admitted through no. 1 until the desired outlet pressure was reached. Then stopcocks 5 and 7 were closed and gas admitted through no. 1, until the chosen pressure drop was obtained. Fine adjustment of the pressure differential was made by raising or lowering the mercury level in the buret. Next, stopcock 7 was opened and, after allowing time for steady state to be attained, readings of time vs. height of mercury in the buret were taken. At the end of the run, the pressures were measured.

The flow rates for the *n*-butane varied from approximately 0.05–0.8 ml./min. Readings of volume vs. time were taken about 0.5 ml. apart until a total of nine or ten values were obtained. The flow rate was calculated from these by means of a least-squares fit. The precision of the flow rate determinations was approximately 1%, based on a standard deviation calculated from the least squares fit.

At the lower pressure differentials (0.3–1.5 cm.) the decrease in the pressure drop across the porous plug, caused by "over-shoot" in the control system, could not be detected. For pressure differences of 1.5 to 3.8 cm., the decrease in the differential pressure ranged from 0.01 to 0.03 cm. The effects of this variation in pressure on the flow rate were minimized by reading the buret at the moment the relay was activated. The pressure drop also was measured in the same manner.

The Spheron 6 (2700°) carbon black was packed in small increments into a precision bore Pyrex glass tube utilizing a modified pellet press and a torque wrench to ensure uniformity of packing. Various parameters of the porous plug were: length, 0.886 ± 0.008 cm.; area, 0.7126 cm.²; weight of powder, 0.5790 g.; porosity, 0.540.

(1) Part of a Thesis submitted by J. W. Ross to the Graduate School of the University of Cincinnati in partial fulfillment of the requirements for the degree of Doctor of Philosophy, August, 1955.

(2) D. H. Everett, *Trans. Faraday Soc.*, **46**, 453 (1950); **46**, 942 (1950); **46**, 957 (1950).

(3) C. Kemball, "Advances in Catalysis," Vol. II, Academic Press Inc., New York, N. Y., 1950, p. 233.

(4) J. H. de Boer and S. Kruyer, *Proc. Kon. Akad. v. Wet.*, **B55**, 451 (1952); **B56**, 67 (1953); **B56**, 236 (1953); **B56**, 415 (1953); **B57**, 92 (1953).

(5) R. M. Barrer and J. A. Barrie, *Proc. Royal Soc. (London)*, **213A**, 250 (1952).

(6) P. C. Carman and F. A. Raal, *ibid.*, **209A**, 38 (1951).

(7) R. A. W. Haul, *Nature*, **171**, 519 (1953); *Z. physik. Chem.*, **1**, 153 (1954).

(8) M. H. Polley, W. D. Schaeffer and W. K. Smith, *THIS JOURNAL*, **57**, 469 (1953).

(9) W. D. Schaeffer, W. K. Smith, and M. H. Polley, *Ind. Eng. Chem.*, **45**, 1721 (1953).

(10) C. Pierce and R. N. Smith, *THIS JOURNAL*, **54**, 354 (1950).

(11) S. Brunauer, "The Adsorption of Gases and Vapors," Princeton University Press, Princeton, N. J., 1943.

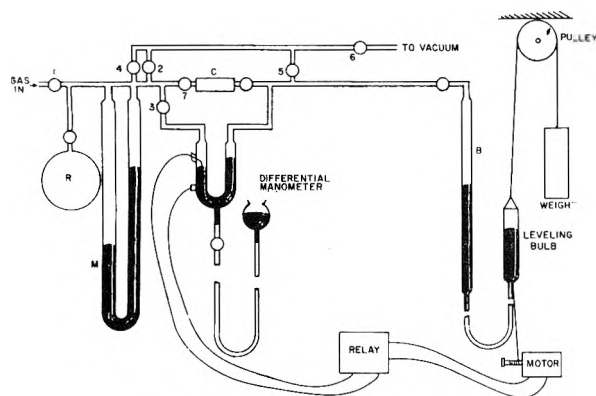
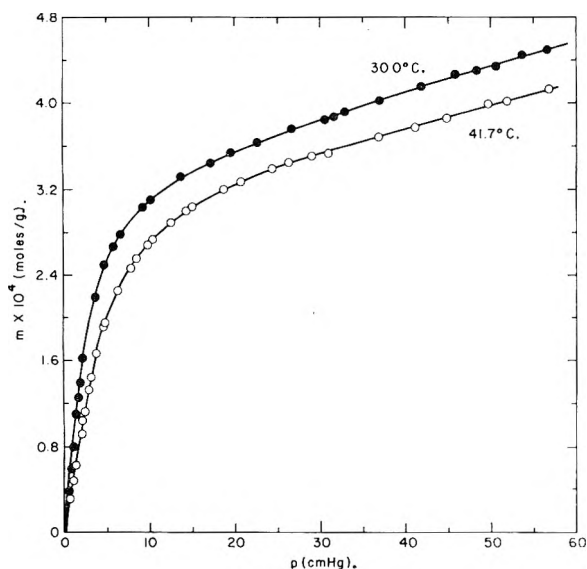


Fig. 1.—Surface flow apparatus.

In all calculations corrections were applied for the non-ideality of the *n*-butane vapor.

Results and Discussion

A. Adsorption.—Adsorption isotherms at 30.0 and 41.7° for *n*-butane on Spheron 6 (2700°) carbon black are shown in Fig. 2. The low pressure portions of both isotherms are linear to approximately $m = 0.9 \times 10^{-4}$ mole/g. The monolayer capacities, evaluated by means of the BET method, are 3.375×10^{-4} mole/g. at 30.0° and 3.458×10^{-4} mole/g. at 41.7°. The mean value of 3.417×10^{-4} mole/g. has been used for plotting various quantities against degree of coverage.

Fig. 2.—Adsorption isotherms, *n*-butane on Spheron 6 (2700°) carbon black.

The isosteric heat of adsorption ($H_L - \bar{H}_s$) and the equilibrium heat of adsorption ($H_L - H_s$)¹² have been plotted against fractional coverage θ , in Fig. 3. The constant heat values at low coverages is indicative of surface homogeneity and the rise in the heat curves has been explained as caused by attractive interactions between adsorbed molecules.¹³⁻¹⁵

- (12) T. L. Hill, *J. Chem. Phys.*, **17**, 520 (1949).
 (13) T. L. Hill, P. H. Emmett and L. G. Joyner, *J. Am. Chem. Soc.*, **73**, 5102 (1951).
 (14) C. Pierce and R. N. Smith, *ibid.*, **76**, 846 (1953).
 (15) J. Mooi, C. Pierce and R. N. Smith, *THIS JOURNAL*, **57**, 657 (1953).

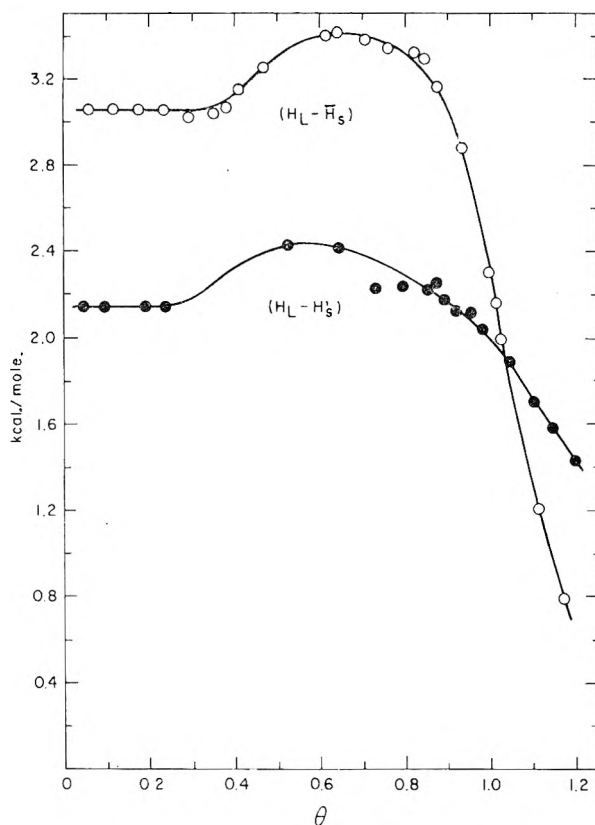
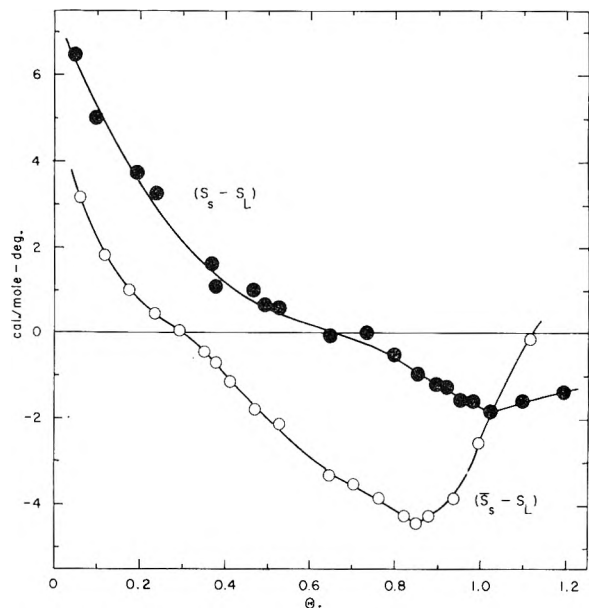
Fig. 3.—Heats of adsorption: ($H_L - \bar{H}_s$), isosteric; ($H_L - H_s'$), equilibrium.

Figure 4 shows plots of the differential and molar entropies of adsorption, relative to the liquid at the mean temperature, as a function of coverage.

Fig. 4.—Entropies of adsorption: ($S_s - S_L$), molar; ($\bar{S}_s - S_L$), differential molar.

Similar results have been reported for the adsorption of ethyl chloride on Spheron 6 (2700°)¹⁵ and for nitrogen on Graphon carbon black.¹² The fact that the molar entropy curve has a minimum close to $\theta = 1.0$ has been suggested as a possible device

for calculating monolayer capacities and thus, surface areas.¹³ It is interesting to note that even when the BET equation is not applicable, this minimum can lead to values for the surface area.¹⁵

In Table I, values of the molar entropies of adsorption, ΔS_m and ΔS_{loc}^o , calculated from the experimental data, are listed. For comparison, ap-

number of steps,¹² while computation of the differential entropies is more direct. In both tables, the agreement between columns 4 and 5 is much better than that between columns 2 and 3. A preliminary qualitative conclusion is that the adsorbed molecules can be described as mobile. The discrepancy between columns 4 and 5, in each case, can be attributed to restricted freedom of movement over the surface. This restriction increases as the degree of coverage becomes larger (which is to be expected) and becomes rather severe at the higher degrees of coverage.

Before a final conclusion can be reached, however, the models should be examined more closely. In particular, allowance should be made in the model of localized adsorption by permitting the molecules to vibrate in various directions.

Kemball⁹ has calculated the entropy associated with a one-dimensional oscillator, vibrating with a frequency ν at temperature T , from the relation

$$S_{vib} = R \left[\frac{h\nu}{kT} (e^{h\nu/kT} - 1)^{-1} - \ln(1 - e^{-h\nu/kT}) \right]$$

which assumes that the vibrations are simple harmonic.

The model of localized adsorption should be liberalized to include contributions to the entropy from vibrations of the adsorbed molecules, both perpendicular and parallel to the surface. For low coverages, the oscillations of the adsorbed molecules will be independent of one another and the entropy of vibration, ${}_{vib}S_s$, may be assumed to be independent of coverage. As the number of molecules on the surface increases, interactions among molecules will come into the picture, and the entropy of the system as a whole would be expected to decrease. Then, for the experimental entropy, ΔS_{loc}^o , the corresponding theoretical entropy change will be $({}_{tr}S_g^o - {}_{vib}S_s)$.

Using the model of a localized, three-dimensional oscillator, and assuming that the frequencies of the vibration in all three directions are the same, the experimental and theoretical entropy changes may be brought into agreement by choosing a frequency of vibration equal to 7.6×10^{11} sec.⁻¹, from which $({}_{tr}S_g^o - {}_{vib}S_s) = 20.0$ e.u. However, the vibration normal to the surface should have a higher frequency than vibrations parallel to the surface. A choice of $\nu = 1.5 \times 10^{12}$ sec.⁻¹ for vibrations perpendicular to the surface and $\nu = 6.1 \times 10^{11}$ sec.⁻¹ for vibrations parallel to the surface also leads to agreement between experimental and theoretical entropy changes: $({}_{tr}S_g^o - {}_{vib}S_s) = 20.3$ e.u. (A choice of frequencies a great deal higher than these would, of course, lead to a negligible contribution to the entropy.)

The object of the above qualitative calculations is not to prove that the molecules of the adsorbed *n*-butane are to be physically identified with localized, two- or three-dimensional oscillators. The purpose is to point out that, in this case, an alternative to the "mobile" model also yields entropy changes in agreement with those calculated from adsorption isotherms.

B. Diffusion.—The specific flow rate of helium through the packed plug of Spheron 6 (2700°),

TABLE I

STANDARD MOLAR ENTROPIES OF ADSORPTION: EXPERIMENTAL AND THEORETICAL, BASED ON IDEAL MOBILE AND LOCALIZED MODELS OF ADSORPTION

θ	$-\Delta S_{loc}^o{}^a$ (exptl.)	$({}_{tr}S_g^o - 2R \ln 2)^a$ (theor.)	$-\Delta S_m^b$ (exptl.)	$({}_{tr}S_g^o - {}_{tr}S_s^o)^b$ (theor.)
0.048	19.7	36.5	11.0	12.0
.096	18.5	36.5	11.0	12.0
.191	18.6	36.5	11.0	12.0
.377	20.6	36.5	12.2	12.0
.527	20.2	36.5	12.1	12.0
.647	20.3	36.5	12.3	12.0
.731	19.8	36.5	12.0	12.0
.796	20.0	36.5	12.4	12.0
.851	20.1	36.5	12.6	12.0
.892	20.1	36.5	12.8	12.0
.920	20.1	36.5	12.8	12.0
.982	20.1	36.5	13.0	12.0

^a Localized model; standard state of monolayer: $\theta = 0.500$. Vibrational degrees of freedom about adsorption sites ignored. ^b Two-dimensional gas model; standard state of monolayer: area per molecule = 1260×10^{-16} cm.²

propriate entropies computed from the models of ideal mobile adsorption and ideal localized adsorption are given.⁴ A similar comparison of the differential molar entropies is given in Table II. The differential molar quantities are probably more accurate than the molar quantities, since calculation of the latter involves a rather large

TABLE II

STANDARD DIFFERENTIAL MOLAR ENTROPIES OF ADSORPTION: EXPERIMENTAL AND THEORETICAL, BASED ON IDEAL MOBILE AND LOCALIZED MODELS OF ADSORPTION

θ	$-\Delta S_{loc}^o{}^a$ (exptl.)	${}_{tr}S_g^o{}^a$ (theor.)	$-\Delta S_m^b$ (exptl.)	$({}_{tr}S_g^o - {}_{tr}S_s^o)^b$ (theor.)
0.049	20.5	38.3	13.9	12.0
.117	20.6	38.3	13.9	12.0
.176	20.3	38.3	13.9	12.0
.234	20.1	38.3	13.3	12.0
.293	19.9	38.3	13.8	12.0
.351	19.9	38.3	13.9	12.0
.410	20.1	38.3	14.3	12.0
.468	20.2	38.3	14.7	12.0
.527	20.1	38.3	14.8	12.0
.585	19.9	38.3	14.8	12.0
.644	20.3	38.3	15.6	12.0
.702	20.1	38.3	15.7	12.0
.761	19.8	38.3	15.8	12.0
.820	19.4	38.3	16.0	12.0
.878	19.5	38.3	15.9	12.0
.937	16.7	38.3	15.4	12.0

^a Localized model; standard state of monolayer: $\theta = 0.500$. Vibrational degrees of freedom about adsorption sites ignored. ^b Two-dimensional gas model; standard state of monolayer: area per molecule = 1260×10^{-16} cm.²

calculated from a least squares fit of the flow data (at 30.0°), gave

$B_{He} = (1/\Delta p)(dn/dt) = 1.411 \times 10^{-12} + 0.0008 \times 10^{-12}\bar{p}$ where the units of B_{He} are (cm.²/dyne)(moles/sec.) and \bar{p} is in cm. The standard deviation of the slope was 0.0002×10^{-12} and that of the intercept was 0.007×10^{-12} . The small dependence of the specific flow rate on the mean pressure leads to the conclusion that the flow occurred almost entirely by the Knudsen mechanism.

Calculation of the surface area by the gas flow method described by Kraus, Ross and Girifalco¹⁶ gave a value of 84.1 m.²/g., in agreement with that obtained by the adsorption method.⁸

The flow rate for *n*-butane through the same plug was measured, and calculation of surface diffusion coefficients for butane was carried out by the method of Carman and Raal.⁶

In Fig. 5, the logarithms of the surface diffusion coefficients D_s have been plotted against the

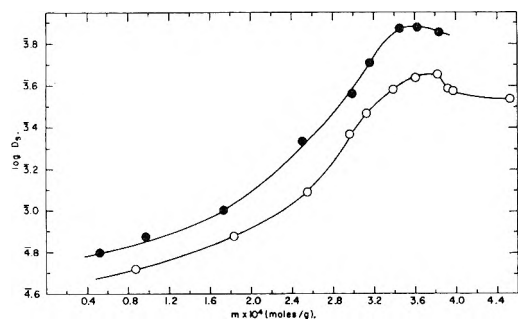


Fig. 5.—Surface diffusion coefficient as a function of amount adsorbed.

amount adsorbed. The vertical distance between the curves is proportional to the apparent activation energy for surface migration, E^* , which is shown as a function of coverage in Fig. 6.

A possible explanation will now be given of the data of the surface diffusion measurements. It must be stated first, however, that it would be very difficult to reconcile the energy of activation for surface migration, 4 to 10 kcal. per mole, with the two-dimensional gas model. Hence we base this discussion on the localized oscillator model.

As shown in Fig. 3, above $\theta = 0.35$, the isosteric heat of adsorption increases a little with increasing coverage, to a maximum at about $\theta = 0.65$, and then decreases. This increase, no doubt, is caused by attractive lateral interactions among the adsorbed molecules; the effects are sometimes referred to as "coöperative condensation" effects¹⁷ which are analogous to phase changes.¹⁸ In the case of adsorption on heterogeneous surfaces this effect is obscured by the concomitant decrease in adsorption energy. For adsorption on homogeneous surfaces, at low temperatures and with simple molecules, these lateral interactions have been reported to lead to "steps" in the isotherm.¹⁵

As the contribution of lateral interactions increases, it would be expected that the activation

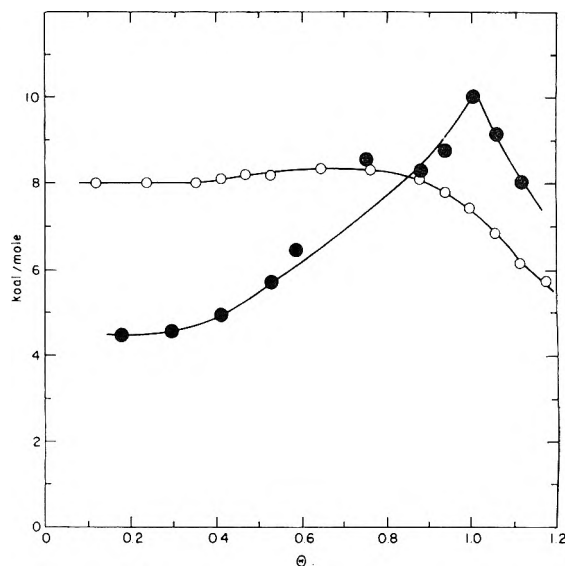


Fig. 6.—Apparent activation energy for surface diffusion (●) and isosteric heat of adsorption (○).

energy for surface migration would also increase. At very low coverages, the molecules are independent of one another, but as the coverage is increased, lateral interactions come into play and in order to move over the surface, the molecules require an additional amount of energy to overcome this interaction. The surface diffusion will then begin to resemble the self-diffusion of molecules in a liquid.

A consideration of the surface area available to an adsorbed molecule also leads to the conclusion that the activation energy for surface migration should rise with increasing amount adsorbed. The mean distance between adsorbed molecules decreases very rapidly with θ at low coverages. This is illustrated in Fig. 7, where the square root of the area available to a *n*-butane molecule has been plotted against fractional monolayer coverage. Two important qualitative conclusions can be reached from an examination of this figure. First, it would be predicted that the effect of lateral interactions among the adsorbed molecules might be expected to become noticeable at coverages above about $\theta = 0.3$ to 0.4. From an examination of Fig. 6, such apparently is the case. The second conclusion is that the model of a two-dimensional gas for the adsorbed phase is not applicable at the higher coverages. At a very low coverage (about $\theta = 0.03$) the mean distance between adsorbed molecules is equal to the mean distance between molecules of an ideal gas at S.T.P. As more molecules are adsorbed, the mean distance between molecules decreases rapidly to values which are more characteristic of the liquid state.

From the above discussion, it seems plausible (using the model of localized adsorption) that at low coverages the activation energy for surface migration may be independent of coverage, since once a molecule has gained sufficient energy to travel over the surface, it can move over relatively long distances with little interference from the other adsorbed molecules. At higher coverages, even though "activated" with respect to the sur-

(16) G. Kraus, J. W. Ross and L. A. Girifalco, *THIS JOURNAL*, **57**, 330 (1953).

(17) G. D. Halsey, *J. Chem. Phys.*, **16**, 931 (1948).

(18) W. D. Harkins, "The Physical Chemistry of Surface Films," Reinhold Publ. Corp., New York, N. Y., 1952.

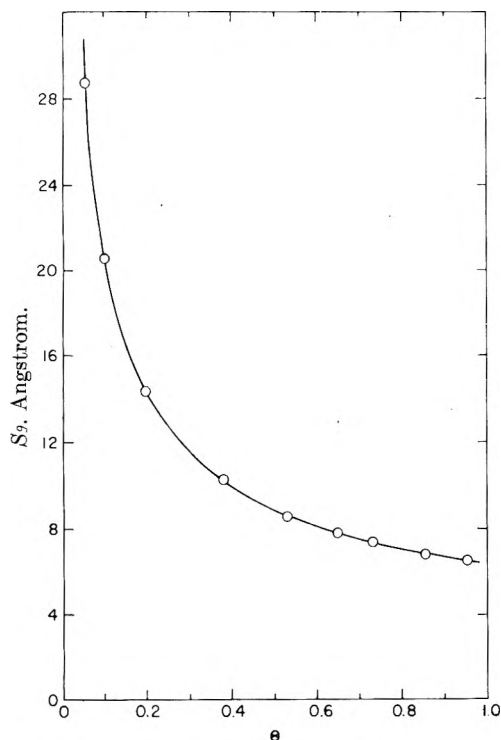


Fig. 7.—Available area for an adsorbed *n*-butane molecule.

face, the movement of one molecule is restricted by its neighboring molecules. In order to travel any appreciable distance the molecule will require additional activation energy to overcome this interference. As the density of the adsorbed film increases, *i.e.*, as the coverage increases, this activation energy will also increase and will lead to a rise in the total activation energy for surface migration.

From Figs. 5 and 6, it is readily apparent that the surface diffusion coefficients and the energy of activation both increase at the same time. This is essentially the same situation that Carman and Raal⁶ explained by assuming that various adsorbed molecules have different energies due to the heterogeneity of the surface. This explanation cannot be applied to the *n*-butane-Spheron 6 (2700°) system, however, since the surface in this case is homogeneous.

The description of energy changes involved in an activated process is incomplete if only the activation energy is given, since, in general, an entropy of activation will also be associated with the process. The Arrhenius equation, from which experimental energies of activation are calculated, "hides" the activation entropy term in the "constant" coefficient. A more complete equation is

$$D_s = D_0' e^{\Delta S^*/R} e^{-\Delta H^*/RT}$$

where ΔS^* is the entropy of activation and ΔH^* is the heat of activation. It is evident from this equation that a concomitant increase in D_s and the energy of activation, such as that observed in the present case, could be caused by an increase in the entropy of activation with increasing coverage. We may conclude that this is probably the case for *n*-butane adsorbed on Spheron 6 (2700°) carbon black.

This is not a particularly surprising conclusion in view of the fact that the entropy of the adsorbed phase has been shown to decrease as the coverage increases, and, in fact, becomes less than that of the liquid state. Furthermore, the increase in the apparent activation energy for surface diffusion is evidently caused by an increasing degree of interaction among the adsorbed molecules, and it is just in that case that the entropy of activation would be expected to increase.

A conclusion can now be drawn as to the localized *vs.* mobile adsorption models, for this system. The entropy of adsorption leads to no definite conclusion, since when the entropy of oscillation of the localized molecules is included it is found that both models are compatible with the data. The diffusion measurements, however, point strongly to the localized model, for the magnitude of the energy of activation for surface diffusion is much too great for the mobile model. The observed variation of energy of activation, and the trend of an increase in entropy of activation with coverage, are also consistent with the localized model.

Acknowledgment.—This investigation was supported, in part, by the Office of Ordnance Research, U. S. Army, under Contract No. DA 33-008 ord 123.

THE SORPTION OF GASES BY SOLID POLYMERS.¹ I. THE SORPTION OF AMMONIA BY NYLON. II. THE SORPTION OF HYDROGEN CHLORIDE BY NYLON

BY L. H. REYERSON AND LOWELL E. PETERSON²

Contribution from the School of Chemistry, University of Minnesota, Minneapolis, Minn.

Received February 24, 1956

The sorption isotherms of NH_3 on undrawn nylon were determined at 30.4 and -31.3° . The results are much like those for H_2O on nylon and indicate that the sorption sites are the carbonyl groups which are not hydrogen bonded to the imido groups in adjacent molecules. The sorption of HCl showed very different behavior. At -78.9° two molecules of HCl were taken up for every amide group in the nylon before the isotherm departed much from the zero pressure axis. At 0 and 20° one molecule of HCl was sorbed per amide group at almost zero pressure. The nylon fibers would shrink in length and swell in cross section during the early part of the HCl sorption process and then slightly elongate at higher relative pressures. The HCl bound at the amide groups was difficult to remove except at higher temperatures. After complete removal the nylon showed a greater crystallinity than before sorption. Thus it appears that hydrogen chloride penetrates the nylon, breaking all hydrogen bonds between adjacent chains and permitting a more perfect alignment on desorption.

The interaction of Nylon with acids and bases has been the subject of a number of investigations in recent years. However most of these studies have been done using aqueous solutions. Wall and his co-workers³ measured the sorption of small amounts of NaOH from solution and concluded that the terminal carbonyl groups bound the NaOH . Elod and Frolich⁴ studied the sorption of HCl and NaOH from more concentrated solutions and concluded that the sorption takes place without degradation of the Nylon with the imido groups acting as proton acceptors. They also believed that the carbonyl groups were responsible for the NaOH binding.

Sorptions of water vapor, nitrogen and one or two acidic gases have been studied on Nylon. Rowen and Blaine⁵ compared the sorption of water vapor and nitrogen and found that the surface area calculated from the water isotherm by applying B.E.T. theory was much greater than that found from the nitrogen isotherm. They concluded that polar water molecules were able to penetrate the nylon where nitrogen cannot go. Several other investigators found that water vapor was sorbed strongly by nylon and that the isotherms were sigmoidal in character. The mode of attachment of water to nylon has usually been considered as hydrogen bonding between water and the carbonyl groups of the peptide linkage. Pauling⁶ interpreted the results of Bull⁷ for water vapor sorption on nylon, by assuming that the B.E.T. monolayer point corresponds to the sorption of one water molecule on every carbonyl group which is not already saturated through hydrogen bonding with an imido group in an adjacent chain. The water sorbed at the monolayer point would indicate that only about 6% of the carbonyl and imide groups fail to meet each other in ad-

acent chains. Dolc⁸ points out that a high degree of crystallinity is responsible for the fact that only about 10% of the peptide groups could adsorb water in his experiments. Recently Benson and Seehof⁹ studied the sorption of BF_3 on nylon. They found that on desorption some of the gas remained permanently bound and the amount depended on the pressure of the gas to which the polymer had been exposed. As a result of the above studies it seemed desirable to carefully investigate the sorption of NH_3 and HCl on undrawn nylon fibers.

Experimental

Undrawn bright 66 nylon yarn of about 5 denier-per-filament kindly supplied by the du Pont Company, was used in this work. It contained 0.02% TiO_2 . Before use, the anti-static coating was removed by immersing the samples in successive portions of reagent grade CCl_4 for from three to six days. The sorbed solvent was removed *in vacuo*, and any water vapor was desorbed just before sorption isotherms were begun, by heating *in vacuo* to 95° for three days.

Synthetic ammonia 99.9% pure was distilled into a flask surrounded by a Dry Ice-acetone mixture. A small piece of sodium metal was admitted to the frozen ammonia, and the flask was warmed to just beyond its melting point. After the sodium had reacted with the trace water, the ammonia was frozen again and any liberated hydrogen pumped off. Then with due precaution the ammonia was distilled into receiving tubes holding 4 cc. of the liquid. These were then sealed off and stored in Dry Ice.

Pure hydrogen chloride was prepared by dropping reagent grade hydrochloric acid into a flask containing reagent grade sulfuric acid. The flask was connected to a vacuum line with a trap cooled by liquid nitrogen and all stopcocks were lubricated with a fluorocarbon grease. The hydrochloric acid was allowed to flow slowly into the sulfuric acid. The dehydrated HCl gas distilled into the trap after passing through phosphorus pentoxide on glass wool. When sufficient HCl had collected in the trap, the dehydration part of the system was sealed off and the liquid HCl distilled from the trap into the sample bulbs, holding 8-10 g. each of HCl . These bulbs were stored in a Dry Ice-acetone bath. When needed the tubes of both ammonia and HCl could be attached to the sorption system through break-offskys and by proper manipulation the liquids could be drawn for the actual sorption studies. The apparatus was a modification of the system reported by Reyerson and Honig¹⁰ having a very sensitive quartz spiral balance of the McBain type. The tube section of the system holding the quartz spiral was thermostated by pumping water at a constant temperature through a surrounding jacket. The

(1) This material was part of a thesis submitted to the Graduate School of the University of Minnesota in partial fulfillment of the requirements for the Ph.D. degree.

(2) General Mills Research Laboratories, Minneapolis, Minnesota.

(3) F. Wall and T. Swoboda, *THIS JOURNAL*, **56**, 650 (1952); F. Wall and P. Saxton, *ibid.*, **57**, 370 (1953).

(4) E. Elod and H. Frolich, *Melliand Textilber*, **30**, 239, 405 (1949).

(5) J. W. Rowen and R. L. Blaine, *Ind. Eng. Chem.*, **39**, 1659 (1947).

(6) L. Pauling, *J. Am. Chem. Soc.*, **67**, 555 (1945).

(7) H. Bull, *ibid.*, **66**, 1499 (1944).

(8) M. Dolc, *Ann. N. Y. Acad. Sci.*, **51**, 705 (1949).

(9) S. Benson and J. Seehof, *J. Am. Chem. Soc.*, **75**, 5925 (1953).

(10) L. H. Reyerson and J. M. Honig, *ibid.*, **75**, 3917 (1953).

lower portion of the same tube surrounding the nylon sample was immersed in a low temperature thermostat (cryostat). The cryostats described in the previous work could be adjusted for the temperatures required, and they would then maintain this temperature for long periods of time. The force constant of the spiral was found to be 59.83 ± 0.01 mg./cm. under a total load of 1.3 g. A microscope mounted on a heavy steel frame was used to measure the extensions of the spiral during sorption.

The vapor pressure of the ammonia was maintained constant for a given adsorption point by keeping the U tube holding the liquid ammonia immersed in the cryostat at a constant temperature. From this measured temperature, the vapor pressure of the liquid ammonia in the closed sorption system could be determined from the data of Overstreet and Giaque.¹¹ In a given run the temperature of the cryostat controlling the vapor pressure of the ammonia was adjusted to give the desired pressure, and the nylon was allowed to sorb the ammonia until equilibrium was reached. This required 24 hours or less for each point at the higher temperature but at the lower temperature a much longer time was needed. The vapor pressures of ammonia varied from 0 to 986 mm. for the isotherm measured at 30.4° and from 0 to 747 mm. for the one at -31.3° . Even at the highest ammonia pressure the nylon sorbed less than 6 mg./g. Each isotherm was obtained by measuring adsorption points up to the maximum pressure followed by desorption points down to zero pressure.

It was found impossible to measure the pressures of HCl by the same method as for ammonia so that a direct manometric method was adopted. Successive increments of HCl gas were admitted to the system from a reservoir of liquid HCl which had a vapor pressure of about 1.5 atmospheres. Because large volumes of HCl were sorbed on nylon, provision had to be made for varying the volume of the system. This was done by varying the level of Hg in a large volume side tube. The actual pressures of HCl at equilibrium were read to ± 0.01 cm. on a wide bore manometer. In the low pressure range equilibrium was established very slowly, sometimes taking a week, while at higher pressures from one to four days were required. Desorption points required only about a day each until low pressures were reached. Several unusual happenings were observed during HCl sorptions and they will be discussed later.

Results

The sorption isotherms of ammonia on nylon at 30.4 and -31.3° are shown in Figs. 1 and 2. The amounts adsorbed are plotted against the relative pressures of the gas. In each case a hysteresis loop was observed on desorption but the loop always closed at zero pressure indicating that no ammonia was permanently bound on the nylon. The sorption of HCl on nylon at -78.9° is shown in Fig. 3 while the measurements at 0 and 20° are given in Fig. 4. Adsorption at -78.9° was very slow sometimes taking a week before equilibrium was reached. Desorption at this temperature proceeded more rapidly until the low pressure range had been reached. This isotherm shows unusual characteristics in that the nylon takes up two moles of HCl per mole of amide linkage before the isotherm departs from the zero pressure axis. Following this a rather normal sigmoidal isotherm with a small hysteresis loop is found. Desorption occurs more rapidly than adsorption until two molecules of HCl remain on each amide link. The loss of this bound HCl in a high vacuum is exceedingly slow. At the end of ten days of pumping 1.95 moles of HCl still remained bound to each mole of amide link. If the sample was allowed to warm to room temperature one mole of the gas came off rather rapidly but the remainder again was re-

moved at a very slow rate. This retention of one molecule of HCl per amide link seems to check the isotherms at 0 and 20° shown in Fig. 4. Here the uptake of HCl follows the zero pressure axis until one molecule is adsorbed per amide link after which an isotherm was obtained which showed almost no hysteresis on desorption. In one case a sample which still contained some HCl was removed from the gas line and examined. It had lost its tensile strength and felt sticky to the touch. The fibers broke on slight drawing. When observed under a microscope the untreated nylon was transparent and had a filament diameter of $26.1 \pm 0.5 \mu$. The nylon filaments after sorbing HCl were still transparent but they had swelled to a diameter of $30.1 \pm 0.8 \mu$ which was a 14% increase. While the untreated fibers remained clear on contact with water, the treated one turned white and became opaque. This swelling of the nylon was accompanied by a corresponding shrinkage in length. The shrinkage was sufficiently great to cause the crushing of one of the glass frames on which the nylon was wound. The remaining bound HCl could be removed easily by heating the evacuated system to about 90° for three hours. The sample returned to its original weight and no longer was sticky to the touch. The tensile strength and other properties seemed to be comparable to that of the original nylon. However, the nylon had permanently assumed whatever shape it had during the sorption-desorption process. For example, if it had been coiled on a glass rod it became permanently coiled. Since two moles of HCl was sorbed per mole of amide links at -78.9° and only one mole at 0 and 20° it was deemed desirable to measure an isobar between these temperature extremes. Figure 5 gives the results obtained at 1 cm. pressure over this temperature range. About a week's time was necessary to reach equilibrium at each point. The isobar shows no sharp break in the capacity of the nylon to sorb HCl under constant pressure at the several temperatures but a rather smooth transition.

An interesting phenomenon occurred during the measurement of the rate of approach to equilibrium in the high pressure region at the different temperatures. Here the nylon initially sorbed a larger amount of HCl than was retained at equilibrium. Figure 6 illustrates the unusual rate of approach to equilibrium together with the corresponding pressure changes in the closed system. Figure 7 illustrates the dependence of fiber length and diameter on the uptake of HCl.

These experiments suggested that basic structural changes might have occurred during the sorption-desorption process. X-Ray diffraction studies were carried out on nylon before sorption, during sorption and after complete desorption. Four X-ray diffraction photographs are shown in Fig. 8. They were taken using copper $K\alpha$ radiation. Picture A was obtained by radiating untreated nylon; B was from nylon having less than one mole of HCl per mole of peptide group; the nylon for C held less than half a mole of HCl per mole of peptide and D was from completely desorbed nylon. The diffuse inner ring showing in pictures

(11) R. Overstreet and W. F. Giaque, *J. Am. Chem. Soc.*, **59**, 254 (1937).

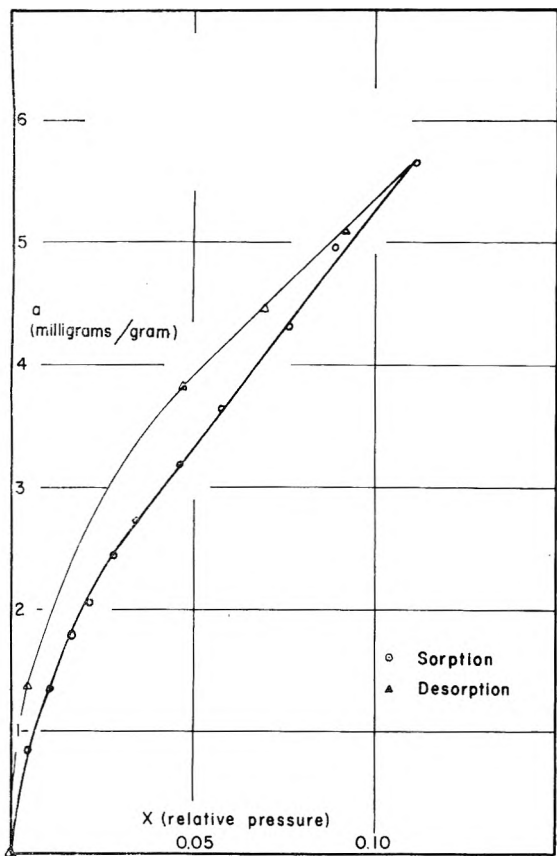


Fig. 1.—Sorption isotherm ammonia on nylon at 30.4°.

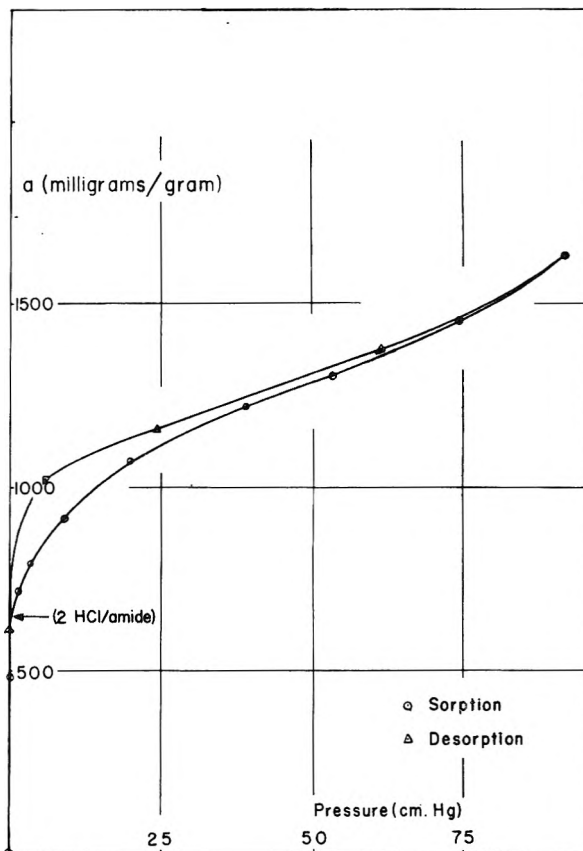


Fig. 3.—Sorption isotherm hydrogen chloride on nylon at -78.9°.

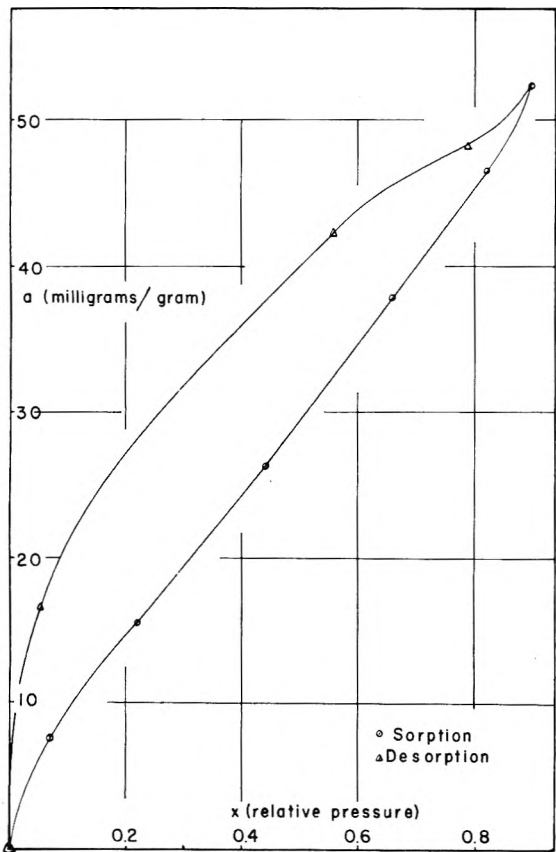


Fig. 2.—Sorption isotherm ammonia on nylon at -31.3°.

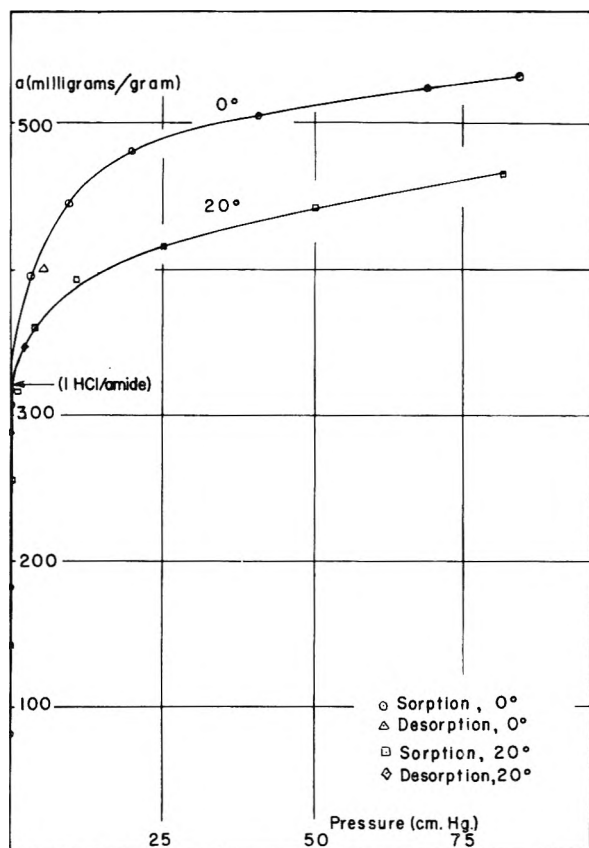


Fig. 4.—Sorption isotherms HCl on nylon at 0 and 20°.

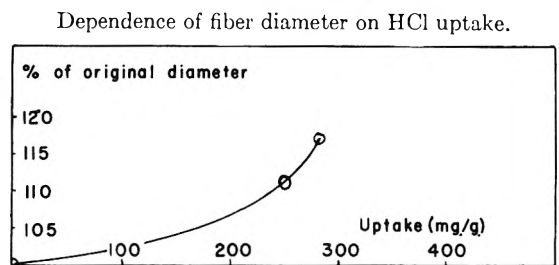
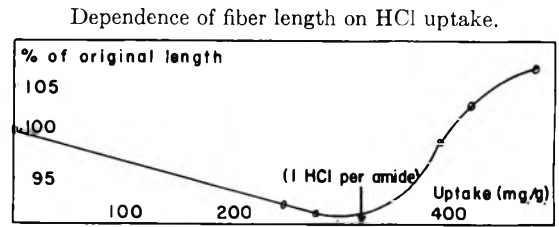
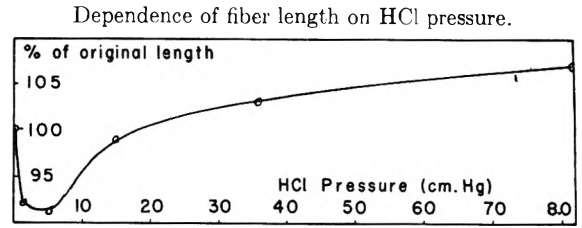
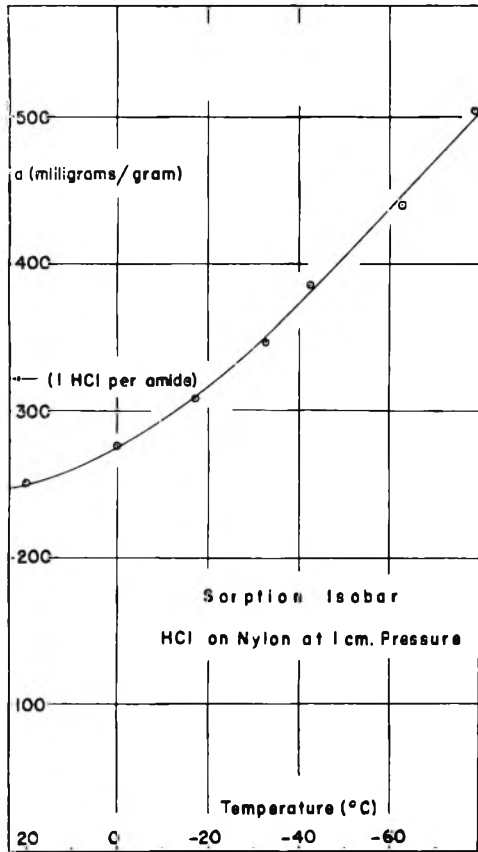


Fig. 7.

Fig. 5.—Sorption isobar HCl on nylon at 1 cm. pressure.

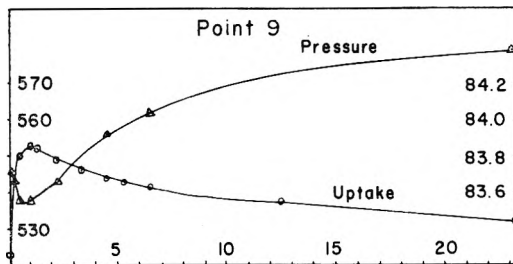
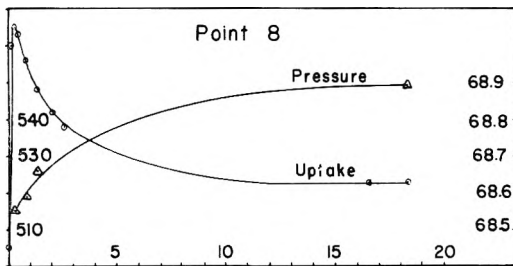
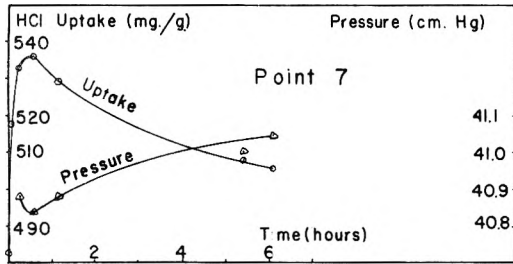


Fig. 6.—Rate of sorption and pressure of HCl on approach to equilibrium.

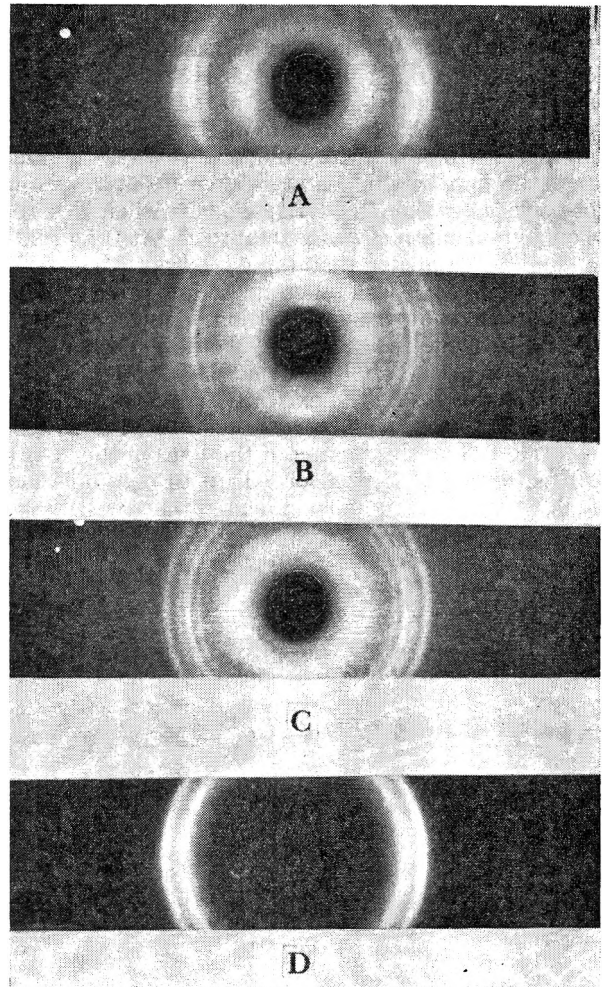


Fig. 8.

A, B and C appeared only when a nickel filter was used to remove β -radiation and was attributed to its use. It is evident from these studies that the sorption-desorption of HCl on nylon permits the re-orientation of the long chain molecules. This re-orientation permits the nylon system to permanently assume the shape it held during a sorption-desorption run.

Discussion

This investigation revealed two very different types of sorption for the gases studied. Nylon showed no marked affinity for ammonia. At 30.4° less than 0.05 mmole was sorbed per gram in contrast to 2 mmoles of water sorbed under the same pressure at 25° as observed by Bull. The second isotherm was measured at -31.3° in order to reach higher relative pressures. Here there was marked similarity to the results Bull obtained for water at the same relative pressures. From B.E.T. plots Bull reported a monolayer point corresponding to an uptake of 1.07 mmoles of H₂O per gram of nylon, while in this work the monolayer point indicated that 0.95 mmole of NH₃ was sorbed per gram nylon. Thus a similar interpretation seemed logical, namely, that the ammonia molecules were sorbed on those sites where the carbonyl groups had not hydrogen bonded with amide links. The case of complete removal of the sorbed ammonia indicated that the energies of binding were weak.

On the other hand nylon showed a remarkable capacity for taking up gaseous HCl. At -78.9° nylon sorbed about 5 moles of HCl per mole of peptide groups at a pressure of 919 mm. (relative pressure = 0.86). More unusual yet was the fact that the first two moles was taken up at very low pressure and then held tenaciously when desorption by evacuation was attempted. At 0 and 20° a similar situation maintained except that only one mole of HCl was taken up at low pressure and tightly held during evacuation. Such behavior strongly suggested that all of the polymer was accessible to the HCl and that in penetrating the solid the gas broke the existing hydrogen bonds at the amide groups and probably formed a hydrochloride. The sharpening of the lines in the X-ray diffraction as HCl was sorbed up to one mole per mole of amide group also indicated that these mole-

cules were located at definite intervals in the structure. In the light of the low solubility of HCl in hydrocarbons such as hexane it did not seem probable that there was much of any HCl sorption on the hydrocarbon chains at low pressure, but this should not prevent diffusion between them. The rather exact stoichiometric ratios at low pressure sorption seemed to be good evidence for the view that the HCl was taken up at the peptide groups. The observed swelling of the fibers with corresponding shrinkage in length, followed by relaxation at higher partial pressures, also suggested localized strong uptake at the low pressures followed by more general surface sorption. On the assumption that the HCl breaks the hydrogen bonds at the amide links, the improved crystallization, as observed in the X-ray studies, seemed reasonable. The long chain molecules would be freer to assume lower energy levels so that upon removal of the HCl by heating the molecules could hydrogen bond but in a more ordered fashion. Simple dipole-dipole interactions between HCl and the polar groups of the polymer might also play a considerable role because of the low dielectric constant of the polymer. It is interesting to consider that HCl molecules might act as a lubricant for the straightening of the long polymer molecules. This could be happening in the cases where the curl or shape was permanently put into the polymer.

Equilibria between nylon and HCl were reached slowly. This could be attributed to chemisorption having a considerable energy of activation but a slow rate of diffusion into the polymer might well be a factor. Structural changes in the nylon during the sorption process were thought to produce changes in uptake following each increase in the pressure of the gas as shown in Fig. 5. Since it was proved that no foreign gas was given off during the sorption process it was felt that structural changes accounted for the slight decrease in the amount sorbed as equilibrium was approached.

This investigation has suggested that the same technique be used to study other polymers having similar hydrogen bonding. One crystalline protein, insulin already has been investigated¹² and other studies are under way in this Laboratory.

(12) L. H. Reyerson and L. E. Peterson. *THIS JOURNAL*, **59**, 1117 (1955).

GAS PERMEATION THROUGH MEMBRANES DUE TO SIMULTANEOUS DIFFUSION AND CONVECTION

By H. L. FRISCH

Department of Chemistry, University of Southern California, Los Angeles 7, California

Received February 24, 1956

The theory of gas permeation by simultaneous diffusion and convection through membranes possessing pores or channels is developed particularly in reference to gas transmission measurements through polymer films. Considerable simplification is obtained when the gas dissolved in the membrane matrix is in equilibrium across an interface with the gas in the channels (solution equilibrium). This state is generally attained rapidly. Measurements of the rate of gas transmission, particularly the time lag, under various applied pressure gradients can be shown to yield, besides the value of the diffusion constant, the gas solubility, the specific convection velocity of the gas as well as other parameters, characteristic of the permeation mechanism, information concerning the membrane porosity (and thus something of the structure). The effect of the absence of solution equilibrium is investigated and the magnitude of such an effect is estimated. The temperature dependence of the convective contribution to the permeability coefficient is derived.

I. Introduction

In the absence of stress or thermal gradients within a membrane, the transmission of gases or vapors through membranes (polymer or otherwise) takes place as a result of diffusion and/or convection. In polymer membranes diffusion controlled permeation is apparently the principal mechanism. The gas dissolves at the high pressure side of the membrane, passes through by an activated diffusion process and evaporates at the opposite surface.¹ Above the second-order transition temperature of the polymer composing the membrane the diffusion is Fickian with a concentration dependent diffusion coefficient.²

Membranes containing small channels, cracks or flaws in the long-range structure of the membrane permit the convection of the gas or vapor through such channels. In principle, many types of convective mechanisms are possible.¹ Structural and experimental considerations present some limitations on the variety; for example, the small pressure gradients across the membranes used in studying them prevent the establishment of turbulent flow. When the gas pressure applied to the membrane is small and the channel-radius is small in comparison with the free path of the gas, the gas flow is of the Knudsen type with ϵ convection velocity v_k satisfying³

$$v_k = \frac{k'_k}{\sqrt{\rho p}} \times \frac{\partial p}{\partial x}; \quad k'_k = \frac{r}{6} \quad (1)$$

where r is the average channel radius, p is the gas pressure, $\partial p/\partial x$ the pressure gradient across the membrane and ρ the gas density. For larger channels (roughly 0.1 μ or larger in diameter for ordinary diatomic gases at N.T.P.) or higher pressures the flow changes to viscous, compressible capillary flow satisfying Poiseuille's Law for fairly straight channels or Darcy's Law for very tortuous channels. The velocity v satisfies

$$v = \frac{k'}{\eta_g} \times \frac{\partial p}{\partial x} \quad (2)$$

with η_g the gas viscosity (in the gaseous phase), where k' for Poiseuille flow is given by $k' = r^2/8$

and k' for Darcy flow is generally taken as an empirically determined constant.⁴ These relations have been used to interpret gas permeation through papers, glassine, certain cellulosic membranes, etc.⁵ as well as other types of membranes.¹ Further modifications which have to be introduced as a result of gas adsorption, capillarity, the effect of the channel orifice, etc., are discussed in the literature.^{1,3}

The simultaneous transmission of gases through membranes by both diffusion and convection has in the past received little (if any) attention. The present communication is an attempt at some elementary considerations bearing on the theory of this type of transport. We will find that measurements of the rate of gas transmission through such "porous" membranes can be used to study structural characteristics of the membrane as well as details of the mechanism of gas flow.

II. Gas Permeation due to Both Diffusion and Convection.—Consider a membrane possessing small channels whose radius does not fluctuate too widely, so that the gas pressure in each channel does not differ markedly from the average gas pressure $p(x, t)$ at a thickness x of the membrane. We assume that flow in the perpendicular y and z directions can be neglected (*i.e.*, we are dealing with a relatively thin membrane). Let $c(x, t)$ be the concentration of dissolved, diffusing gas and $C_g(x, t)$ the average total gas concentration at x in all channels where

$$C_g(x, t) = p(x, t)/RTg \quad (3)$$

with R the gas constant, T the absolute temperature and g a constant factor which is inversely proportional to the total channel volume and whose magnitude depends on the concentration units employed. We neglect small deviations from ideal behavior of the gas. Gas present in the channels may dissolve in the polymer matrix adjoining at a rate given by $K_1^{(s)}p(x, t)$. Similarly gas dissolved in polymer may evaporate at the channel surface with a rate given by $K_1^{(e)}c(x, t)$. The K_1 's may be functions of both c and C_g , although when the concentrations are small we will neglect this variation in the partition constants. The internal

(1) R. M. Barrer, "Diffusion In and Through Solids," Cambridge, 1951, p. 382 ff., etc.

(2) R. J. Kokes and F. A. Long, *J. Am. Chem. Soc.*, **75**, 6142 (1953).

(3) C. Zwikker, "Physical Properties of Solid Materials," Interscience Publishers, Inc., New York, N. Y., 1954.

(4) S. Tsakonas and R. Skalak, "Laminar Flow through Granular Media," Technical Report No. 2 CU 2-53-ONR-266(10)-CE, Columbia Univ., New York, N. Y., 1953.

(5) J. P. Casey, "Pulp and Paper," Vol. II, Interscience Publishers Inc., New York, N. Y., 1952, p. 846 ff.

solubility coefficient, $S_i = K_i^{(s)}/K_i^{(e)}$, will equal the external solubility coefficient S , unless the average channel radius r is so small that a correction due to activity effects has to be applied.

Applying the principle of conservation of mass to a small volume element ($x, x + dx$) of unit area of the membrane we see that the change of $c(x, t)$ with time is due to three effects: (a) diffusion, (b) loss due to evaporation, and (c) gain due to solution of gas in the channels, *i.e.*

$$\frac{\partial c}{\partial t} = \frac{\partial}{\partial x} \left\{ \mathfrak{D}(c) \frac{\partial c}{\partial x} \right\} + K_i^{(s)} C_g RT g - K_i^{(e)} c \quad (4a)$$

with $\mathfrak{D}(c)$ the differential diffusion coefficient which is in turn related to the integral diffusion coefficient by

$$D(c) = \frac{1}{c} \int_0^c \mathfrak{D}(c') dc'$$

Similarly the change of $C_g(x, t)$ with time is due to: (a) convection of gas in the channels, (b) gain due to evaporation of dissolved gas and (c) loss due to solution of the gas in the polymer, *i.e.*

$$\frac{\partial C_g}{\partial t} = \frac{\partial}{\partial x} \{ v(C_g) C_g \} - K_i^{(s)} C_g RT g + K_i^{(e)} c \quad (4b)$$

where $v(C_g)$ is the convection velocity given by eq. 1 or 2. Equation 4 together with boundary conditions at the exterior surfaces of the membrane completely specify the transport process given the concentration of gas free in channels and dissolved in the membrane matrix at some initial instant.

If the process of solution of the gas in the membrane proceeds at a faster rate than either convection or diffusion of the gas, then one may assume that local solution equilibrium has been attained

$$K_i^{(s)} C_g(x, t) RT g = K_i^{(e)} c(x, t) \quad (5)$$

or

$$C_g(x, t) = \phi c(x, t)$$

where

$$\phi = K_i^{(e)}/K_i^{(s)} RT g = 1/SRTg$$

This type of behavior is generally exhibited by membranes composed of synthetic polymers with only a few notable exceptions.⁶ For membranes satisfying eq. 5 the transport is found, on adding eq. 4, to satisfy a single modified Smoluchowski equation in the total gas concentration, $n(x, t) = c(x, t) + C_g(x, t) = (1 + \phi) c(x, t)$

$$\frac{\partial n}{\partial t} = \frac{\partial}{\partial x} \left\{ \mathfrak{D} \times \frac{\partial}{\partial x} \left(\frac{n}{1 + \phi} \right) + v \times \frac{n}{1 + \phi} \right\} \quad (6)$$

where $\mathfrak{D} = \mathfrak{D}(n/(1 + \phi))$ and $v = v(n/(1 + \phi))$. The ratio of gas carried by diffusion to that carried by convection is $1/\phi$. Since solution equilibrium has been attained the boundary conditions are also greatly simplified. They depend of course on the experimental arrangement chosen to study the gas transmission. In particular, if the membrane surfaces are in contact with gas reservoirs maintained at constant pressures, then the boundary conditions are of the Nernst type; the concentration of gas at the boundary $n = n_B$ is a constant determined by the pressure of the adjoining gas reservoir p_B by the relation

$$n_B = S(1 + \phi)p_B \quad (7)$$

An arrangement which frequently is used¹ is one for which the gas reservoir at $x = l$ is maintained at $p_B = p_2$ and the other membrane surface at $x = 0$ is in contact with a vacuum, *i.e.*, $p_1 = 0$. This leads to particularly simple formulas and affords no real loss in generality and will henceforth be used wherever eq. 7 applies.

We shall consider first membranes for which solution equilibrium applies before discussing the complications which arise when eq. 5 fails.

III. The Steady-state Permeation of Gas through a Membrane in Solution Equilibrium.— At steady state ($\partial n/\partial t = 0$) we find on integrating eq. 6 that the steady-state flux of gas, q , is given by

$$q = \mathfrak{D} \frac{\partial}{\partial x} \left(\frac{n}{1 + \phi} \right) + v \times \frac{\phi n}{1 + \phi} \quad (8)$$

Two cases immediately arise depending on whether v is given by eq. 1 or 2. In the case of Knudsen flow, *i.e.*, for very small channels, a direct integration of eq. 8 leads to

$$ql = \frac{n(l)}{1 + \phi} [D + k_K \phi]$$

which by virtue of eq. 7 becomes

$$ql = p_2 \{ DS + k_K/RTg \} \quad (9)$$

where the constant k_K is given by

$$k_K = k_K' \sqrt{\frac{p}{\rho}} = \frac{k_K' c_s}{\sqrt{C_P/C_V}}$$

with c_s the local velocity of sound and C_P and C_V the heat capacities at constant pressure and volume respectively. The permeability coefficient, as measured experimentally, is thus found⁷ to be

$$P = ql/p_2 = DS + k_K/RTg \quad (10)$$

which is independent of the pressure p_2 and consists of the usual diffusion dependent term DS and a convective contribution k_K/RTg .

More important is the case when the convection velocity is given by eq. 2. We shall be concerned with this case in the remainder of this paper and shall make use of the results derived in this section.

Integrating eq. 8 and from 0 to l , we find,⁷ on using eq. 2 with $\gamma = k'/\eta_g$

$$\begin{aligned} ql &= D \left[c(l) + \frac{\phi^2 \gamma}{2D} c^2(l) \right] \\ &= DS \left[p_2 + \frac{\phi^2 \gamma S}{2D} p_2^2 \right] \end{aligned} \quad (11)$$

or

$$\begin{aligned} P &= ql/p_2 = P_2 DS + \pi p_2 \\ \pi &= \phi^2 \gamma S^2/2 \end{aligned} \quad (12)$$

Thus by plotting P versus p_2 we expect to find a straight line whose ordinate intercept gives the diffusion dependent term DS while the slope gives the parameter π . While the steady state, which is attained after a sufficiently long wait, allows one to determine P , it does not yield any information concerning the desired values of D , S , ϕ , g and γ separately. To obtain these parameters it is necessary to make measurements in the transient portion of

(7) M. Swarc, V. T. Stannett, H. L. Frisch, R. Waack and N. H. Alex, "The Evaluation of Gas Transmission Rates of Flexible Packaging Material," Final Report, Contract DA 44-109-qm-1445, (1954).

(6) A. E. Korvezee and E. A. J. Mol, *J. Polymer Sci.* **2**, 371 (1947).

the gas transmission process and in particular it will be shown that it suffices to measure the time lag L of attainment of the stationary state in analogy with ordinary diffusion controlled permeation.¹

IV. The Time Lag in Gas Permeation through a Membrane in Solution Equilibrium.—The exact solution of eq. 6 offers considerable difficulty in view of the non-linearity of the equation. Again two cases can be distinguished according to whether diffusion or convection of gas is the more important mode of transport. In polymer membranes and even glassine membranes of certain types, it is molecular diffusion which is predominant in view of the smallness and rarity of channels or cracks in the membrane. In view of this predominance eq. 6 may be linearized⁸ but before we carry this out we introduce dimensionless quantities throughout by the substitution, assuming $\mathfrak{D} = D$ a constant

$$\frac{n}{1+\phi} = c; u = \frac{c}{c_2}; c_2 = Sp_2; y = \frac{x}{l}; 1 \gg a = \frac{\phi^2 \gamma c_2}{2D}; \tau = \frac{tD}{l^2(1+\phi)} \quad (13)$$

which carries eq. 6 into

$$\frac{\partial u}{\partial \tau} = \frac{\partial^2}{\partial y^2} \{u + au^2\} \quad (14)$$

with

$$\begin{array}{lll} u \rightarrow 0 & \text{as } y \rightarrow 0; & \tau > 0; \\ u \rightarrow 1 & \text{as } y \rightarrow 1; & \tau > 0; \\ u \rightarrow 0 & \text{as } \tau \rightarrow 0 & 0 < y < 1 \end{array}$$

The effects due to convection increase in magnitude as we approach the membrane surface $y = 0$ from $y = 1$. Hence, let

$$\begin{aligned} w &= 1 - u \\ u^2 &= 1 - 2w + w^2 \\ &\approx 1 - 2w \end{aligned}$$

so that

$$\begin{aligned} \frac{\partial w}{\partial \vartheta} &= \frac{\partial^2 w}{\partial y^2} - O\left(a \frac{\partial^2 w^2}{\partial y^2}\right) \\ &\approx \frac{\partial^2 w}{\partial y^2} \text{ with } \vartheta = \tau(1+2a) \end{aligned} \quad (15)$$

The linearized eq. 15 has to be solved under the conditions

$$\begin{array}{lll} w \rightarrow 1 & \text{as } y \rightarrow 0, & 0 < y < 1 \\ w \rightarrow 1 & \text{as } y \rightarrow 0, & \vartheta < 0 \\ w \rightarrow 0 & \text{as } y \rightarrow 1, & \vartheta < 0 \end{array}$$

The desired solution is well known¹

$$\begin{aligned} w &= 1 - y - \frac{2}{\pi} \sum_{n=1}^{\infty} \frac{1}{n} \sin n\pi y \exp[-n^2\pi\vartheta] + \\ &\frac{4}{\pi} \sum_{m=0}^{\infty} \frac{1}{(2m+1)} \sin(2m+1)\pi y \exp[-(2m+1)^2\pi 2\vartheta] \approx \\ &1 - u \end{aligned} \quad (16a)$$

and the steady-state value of w is found to be given by

$$(w)_s = 1 - y \quad (16b)$$

Thus for large ϑ the term $-a(\partial^2 w / \partial y^2)$ neglected in this treatment does not exceed $2a^2$ and may thus be neglected in comparison with the other terms in eq. 15.

(8) This procedure is preferred *in lieu* of perturbation expansion since the latter must be carried out in the highest order derivative term of eq. 6.

Following Barrer¹ the time lag L in the permeation is found by plotting the flow of gas (per unit volume) through the membrane, which is directly experimentally measured, *versus* the time. This flow is given by

$$\begin{aligned} Q(t) &= \int_0^t q(0, t) dt = \int_0^t \left\{ \frac{D}{1+\phi} \frac{\partial n}{\partial x} + \frac{v\phi n}{1+\phi} \right\} dt = \\ &\frac{c_2 D}{l^2} \int_0^t \left[\frac{\partial}{\partial y} \{u + au^2\} \right]_{y=0} dt = \frac{c_2 D(1+2a)}{l} \\ &\left\{ t + 2 \sum_{n=1}^{\infty} \int_0^t \exp \left[-\frac{n^2 \pi^2 D(i+2a)t}{l^2(1+\phi)} \right] dt - \right. \\ &\left. 4 \sum_{m=0}^{\infty} \int_0^t \exp \left[-\frac{(2m+1)^2 \pi^2 D(1+2a)t}{l^2(1+\phi)} \right] dt \right\} \end{aligned}$$

by virtue of eq. 8 and 16a. As $t \rightarrow \infty$, $Q(t)$ approaches the straight line.

$$[Q(t)]_{t \rightarrow \infty} = \frac{c_2 D(1+2a)}{l^2} \left\{ t + \frac{l^2(1+\phi)}{3D(1+2a)} - \frac{l^2(1+\phi)}{2D(1+2a)} \right\} = \frac{Q_s}{l} \{t - L\}$$

where Q_s is the steady-state flow (per unit volume)

$$Q_s = \frac{c_2 D(1+2a)}{l^2} l$$

and L is the time lag

$$L = \left(\frac{l^2}{6D} \right) \left[\frac{1+\phi}{1+2a} \right] \approx (1+\phi-2a) \left(\frac{l^2}{6D} \right) \quad (17)$$

or

$$\frac{L}{L_0} = 1 + \phi - \frac{\phi^2 \gamma c^2}{D}$$

where $L_0 = l^2/6D$ is the time lag in the absence of convection.¹ Since $\phi = (SRTg)^{-1}$, $c_2 = Sp_2$ and $\pi = \phi^2 \gamma S^2/2 = \gamma/2(RTg)^2$ we have

$$L = L[p_2] = \frac{l^2}{6} \left[\frac{1}{D} + \frac{1}{(DS)(RTg)} - \frac{2\pi p^2}{DS D} \right]$$

Hence a plot of L *versus* p_2 should give a straight line whose slope is $-(2\pi/DS)(1/D)(l^2/6)$. By combining these measurements with the steady-state results [which give separately π and DS , cf. eq. 12 and hence $2\pi/DS$] we can solve for $1/D$ since the thickness, l , of the membrane is known by direct measurement. From the value of D thus obtained and the value of DS (from the steady-state ordinate intercept), S can be calculated. From the ordinate intercept in the L *versus* p_2 plot we find

$$\frac{l^2}{6} [D^{-1} + (DS)^{-1}(RTg)^{-1}]$$

RTg can be determined since l , D and DS are known. Thus ϕ may be evaluated, the ratio of gas carried by diffusion to that carried by convection, since $\phi = (RTg)^{-1}S^{-1}$, where both factors are now known. Finally, γ can be found by substituting the now known values of RTg in the formula for π and solving for $\gamma = 2\pi(RTg)^2$. Thus g , S , D , ϕ and γ are obtained from a number of permeation runs at various values of the applied pressure p_2 .⁹

V. Gas Permeation in a Membrane without Solution Equilibrium.—We again consider the case that the convection velocity of the gas is given by eq. 2 and that $a \ll 1$. Substituting eq. 2

(9) The time lag for Knudsen flow is easily shown to be $L = l^2/6[D + k_k\phi]$.

in eq. 4 one obtains the simultaneous non-linear equations

$$\frac{\partial c}{\partial t} = D \frac{\partial^2 c}{\partial x^2} + K_1^{(s)} C_g R T g - K_1^{(e)} c \quad (19)$$

$$\frac{\partial C_g}{\partial t} = \frac{\gamma}{2} \frac{\partial^2 C_g}{\partial x^2} = K_1^{(s)} C_g R T g + K_1^{(e)} c$$

with D the diffusion constant. Since solution equilibrium no longer applies, eq. 19 must be solved under boundary conditions which differ considerably from the simple Nernst type. The appropriate boundary conditions can be found by considering the net flow of gas through the polymer interface per unit volume. Since gas does not concentrate at the interface in unlimited quantity, the excess of gas dissolving in the matrix of the membrane at the interface must be immediately available for diffusion, *i.e.*

$$-\frac{D}{l} \left(\frac{\partial c}{\partial x} \right)_B = K_1^{(e)} [S p - c]_B \quad (20)$$

Since the pressure of the gas in the channels must be a continuous function, *cf.* eq. 3

$$(C_g)_B = p_B / R T g \quad (21)$$

An approximate solution of eq. 19 can be obtained by assuming that in first approximation deviations from the concentrations at solution equilibrium are small, *i.e.*

$$C_x = c\phi + \xi(x, t) \quad (22)$$

where terms $O(\xi^2)$ can be neglected. On substitution of eq. 22 in eq. 19 and adding the resulting equations, one finds that

$$(1 + \phi) \frac{\partial c}{\partial t} - D \frac{\partial^2}{\partial x^2} \left[c + \frac{\phi^2 \gamma}{2D} c^2 \right] = \gamma \phi \frac{\partial^2 (c \xi)}{\partial x^2} - \frac{\partial \xi}{\partial t}$$

Let c_0 be the value of c when solution equilibrium is reached, *i.e.*, *cf.* eq. 14

$$(1 + \phi) \frac{\partial c_0}{\partial t} - D \frac{\partial^2}{\partial x^2} \left[c_0 + \frac{\phi^2 \gamma}{2D} c_0^2 \right] = 0 \quad (23)$$

then a first approximation to ξ is given by $\xi_0(x, t)$ satisfying

$$\frac{\partial \xi_0}{\partial t} - \gamma \phi \frac{\partial^2}{\partial x^2} [c_0 \xi_0] = 0 \quad (24)$$

Equations 23 and 24 have to be solved under the boundary condition given by eq. 20 for c_0 and

$$(\xi_0)_B = -\frac{D \phi}{l K_1^{(e)}} \left(\frac{\partial c_0}{\partial x} \right)_B \quad (25)$$

From a physical point of view we see that the principal difference in the permeation behavior in the absence of solution equilibrium from that attained in a membrane with solution equilibrium lies in (a) the variation in position and time of $\Phi(x, t)$ the ratio of gas carried by convection to that carried by diffusion and (b) the different type of boundary condition satisfied by the flow. We will estimate the variation of Φ with x in a special case when the rate of transport is primarily determined by retardation at the boundary surfaces.⁶ In the absence of convective transport, membranes of cellulose triacetate have been reported⁶ to exhibit this type of behavior. Thus assuming that a stationary state with respect to diffusion and convection has been attained

$$\frac{\partial c_0}{\partial t} = \frac{\partial \xi_0}{\partial t} = 0$$

we have to solve

$$\frac{\partial^2}{\partial x^2} \left\{ c_0 + \frac{\phi^2 \gamma}{2D} c_0^2 \right\} = 0 \quad (26)$$

$$\frac{\partial^2}{\partial x^2} [c_0 \xi_0] = 0$$

Letting $\lambda = D/\phi^2 \gamma$ we find on integrating eq. 26 that

$$\xi_0(x) = \frac{\alpha x + \beta}{c_0(x)} \quad (27)$$

$$c_0(x) = -\lambda + [\lambda^2 + Ax + B]^{1/2}$$

where α , β , A and B are constants of integration. To simplify the mathematics of evaluating these constants from the boundary condition, we write

$$c_0(x) \approx [\lambda^2 + B]^{1/2} - \lambda + \frac{Ax}{2[\lambda^2 + B]^{1/2}}$$

obtained by expanding the square root in eq. 27, taking $Ax \ll \lambda^2 + B$, with

$$A = \frac{2K_1^{(e)} l}{D} \left\{ \left[\frac{S p_2 D}{l^2 K_1^{(e)}} \right]^2 + \lambda \left[\frac{S p_2 D}{l^2 K_1^{(e)}} \right] + \lambda^2 \right\}$$

$$B = \left[\frac{S p_2 D}{l^2 K_1^{(e)}} \right]^2 + 2\lambda \left[\frac{S p_2 D}{l^2 K_1^{(e)}} \right]$$

Thus

$$c_0(x) \approx \frac{S p_2 D}{l^2 K_1^{(e)}} \left[1 + \frac{K_1^{(e)} l}{D} x \right] \quad (28)$$

$$\xi_0(x) \approx -\frac{\phi S p_2 D}{l^2 K_1^{(e)}}$$

The desired ratio $\Phi_0(x)$ is then given by virtue of eq. 28 and 22 as

$$\left[\frac{C g(x)}{c(x)} \right]_0 = \Phi_0(x) = \phi \left[\frac{K_1^{(e)} \times l^2 \left(\frac{x}{l} \right)}{D + K_1^{(e)} \times l^2 \left(\frac{x}{l} \right)} \right]$$

$$\Phi_0(x) = \phi \left(\frac{\beta y}{1 + \beta y} \right) \quad (29)$$

$$\beta = K_1^{(e)} l^2 / D \text{ and } y = x/l$$

From the foregoing it is clear that the approximations made are justified as long as $\beta \ll 1$. At the high pressure side of the membrane the fraction of the gas carried by convection is much larger than near the vacuum side as would be intuitively expected. The absence of any reference to the parameter λ in eq. 29 is due to the approximation made in going from eq. 27 to 28 which only applies if λ is very large. From an experimental point of view a simple test for the absence of solution equilibrium is the dependence of the observed permeability coefficient on the thickness of the membrane l . This is partially apparent in eq. 28. In the absence of convection it has been shown⁶ that when eq. 5 fails

$$P = \frac{DS}{1 + \left(\frac{2DS}{K_1^{(e)} l} \right)} \quad (30)$$

VI. Temperature Dependence of the Permeability Coefficient.—In the absence of convection the diffusion-controlled permeability coefficient, $P = DS$, possesses the temperature dependence shown below¹

$$P = P_0 \exp(-E_p/RT) \quad (31)$$

where the activation energy for permeation, E_p , is the sum of the activation energy for diffusion,

E_D , and the heat of solution of the gas in the polymer, ΔH , and P_0 is independent of temperature. We have seen that in the presence of convection the permeability coefficient P could be written as a sum of a contribution due to diffusion, DS , and a term due to convection P_{conv} , cf. eq. 10 and 12. For Knudsen flow we can rewrite eq. 10, as long as the gas does not depart too strongly from ideality

$$P_{\text{conv}} = P - DS = \frac{r}{6} c_s / (C_p / C_v)^{1/2} RTg \approx \frac{r}{6} (MRT)^{1/2} g \quad (32)$$

where M is the molecular weight of the gas. The dependence of P_{conv} on the square-root of the temperature implies that the importance of this term becomes smaller with increasing temperature while the diffusion contribution, DS , is generally found to increase with temperature.¹

For capillary flow one finds from eq. 12 P_{conv} or rather π the pressure coefficient of that quantity the relation

$$\pi = \frac{k^1}{g^2} (RT)^{-2} \eta_g^{-1} = \frac{\partial P_{\text{conv}}}{\partial p_2}$$

If in first approximation the gas behaves as if composed of hard spheres then the kinetic theory of gases shows that η_g is directly proportional to the square root of the temperature and thus

$$\pi = \pi_0 (T_0/T)^{2.5} \quad (33)$$

where π_0 is the constant pressure coefficient at the temperature T_0 . Thus again the temperature dependence of P_{conv} is much less pronounced than that of DS with P_{conv} decreasing with increasing temperature. For sufficiently precise permeation data over an extended temperature interval eq. 32 and 33 could be used as a test for both the presence and type of convection mechanism operative in a given membrane.

In conclusion the author wishes to thank Prof. V. T. Stannett and M. Szwarc of the Chemistry Department, College of Forestry of the State University of New York, for helpful discussions in the course of this work.

STUDIES OF THE SURFACE CHEMISTRY OF SILICATE MINERALS. IV. ADSORPTION AND HEAT OF WETTING MEASUREMENTS OF ATTAPULGITE

By J. J. CHESSICK AND A. C. ZETTLEMOYER

A Contribution from the Surface Chemistry Laboratory, Lehigh University, Bethlehem, Penna.

Received February 24, 1956

Nitrogen and water adsorption isotherms were measured for samples of the clay mineral attapulgite outgassed at 25, 100, 190 and 500°. Heats of immersion in water were also obtained including those for samples equilibrated at continuously increasing water vapor pressures. Samples outgassed at 25° adsorbed water physically, principally on the external surface. As increasing amounts of water were adsorbed, an accompanying loss of surface area as measured by the Harkins-Jura Absolute Method, occurred. This decrease appeared to be due to the filling up of inter-particle channels between primary fibers. Evacuation at 100° removed a small additional amount of water, but decreased the external area only slightly. The excess water driven off is believed to have been external surface water associated with exchange ion or other active sites. The attapulgite was completely regenerated by treatment with water vapor at 25° and moderate relative pressures. More water was removed and a large decrease in external area occurred after evacuation at 190°. Part of this water came from within the intracrystalline channels present in the primary attapulgite fibers. The sample was almost completely regenerated by exposure to water at its saturation pressure at 25°. Much more water was lost during evacuation at 500°, the major portion irreversibly. There is evidence that most of the irreversibly desorbed water came from within the intracrystalline channels. The entrance to these channels evidently became blocked during activation at 500°. Water taken up at 25° by this activated sample was adsorbed primarily on external sites.

Introduction

The previous studies in this field dealt with the surface chemistry of chrysotile asbestos^{1,2} and a sample of Wyoming bentonite³ as revealed by gas adsorption and heat of wetting measurements. In the present work a similar study of attapulgite clay is described.

Barrer and co-worker^{4,5} have made an extensive study of attapulgite primarily using adsorption techniques. This work has been supplemented and extended here with an immersions calorimetric study including samples exposed to increasing water vapor pressures. A combination of adsorp-

tion and calorimetric techniques are particularly useful in distinguishing the amounts of water held to the surface by different binding energies.

Experimental

Attapulgite clay is an acicular hydrated magnesium silicate. The primary clay fibers contain channels which run parallel to the crystal length and which contain water molecules. In addition electron photomicrographs have shown that the needle-like fibers are in loose, somewhat parallel aggregation. The sample used in this work was especially purified by the producer to make it grit free.⁶ The material was washed well with distilled water to remove soluble materials, dried at about 50° in air, crushed in an agate mortar, then stored at 25° and 0.2 relative pressure to ensure a uniform water content before use. The major impurity is sepiolite; small amounts of montmorillonite are also present.

Successive water vapor isotherms were measured at 25° for a single sample outgassed at 25° for 14 days; at 100°

(1) G. J. Young and F. H. Healey, *THIS JOURNAL*, **58**, 881 (1954).

(2) F. H. Healey and G. J. Young, *ibid.*, **58**, 885 (1954).

(3) A. C. Zettlemoyer, G. J. Young and J. J. Chessick, *ibid.*, **59**, 962 (1955).

(4) R. M. Barrer and N. Mackenzie, *ibid.*, **58**, 560 (1954).

(5) R. M. Barrer, N. Mackenzie and D. M. Macleod, *ibid.*, **58**, 568 (1954).

(6) The sample was supplied through the courtesy of Dr. C. G. Albert, Minerals and Chemicals Corporation of America.

TABLE I
 ADSORPTION AND HEAT OF WETTING MEASUREMENTS OF ATTAPULGITE

Sample treatment	Wt. loss ^a % initial wt.	B.E.T. areas, m. ² /g. N ₂ H ₂ O	Wt. gain ^b % initial wt.	h(SL) cal./g.
Outgassed 1½ days, 25° Ads. of H ₂ O, 25°	7.80	217 243	7.73	-26.2
Outgassed 2½ hr., 100° Ads. of H ₂ O, 25°	9.10	200 286	8.80	-37.2
Outgassed 2½ hr., 190° Ads. of H ₂ O, 25°	12.02	160 279	8.54	-41.1
Saturate with H ₂ O, Evacuate 2 wk. at 25°		204		-27.2
Outgassed 4 hr., 500° Ads. of H ₂ O, 25°	16.84	135 154	4.11	-21.6
Saturate with H ₂ O, Evacuate 2 wk. at 25°		140		

^a Wt. loss; initial state at 25° and 0.2 relative pressure. ^b Wt. gain on adsorption of water at 25° and 0.2 relative pressure.

for 24 hours; at 190° for 24 hours and finally at 500° for 4 hours. Equilibrium pressures were read on an oil manometer filled with Apiezon "B" oil. Equilibrium was attained within 24 hours for relative pressures up to about 0.4; beyond this relative pressure much longer equilibrium times were required. However, no isotherms were measured beyond 0.7 relative pressure. A conventional volumetric adsorption apparatus was employed for nitrogen measurements at liquid nitrogen temperature. Mathieson pure grade nitrogen was further purified by passing through fine copper gauze heated to 500° and dried with anhydrous calcium sulfate.

The calorimeter used in the heat of immersion studies has been described.⁷ Values for the heats of immersion were obtained for outgassed attapulgite samples and for samples equilibrated at continuously increasing amounts of adsorbed water. The samples for heat of adsorption measurements that were exposed to water vapor were prepared on an adsorption apparatus and sealed off after the desired equilibrium pressure was attained. The same outgassing conditions were used in the wetting studies as for the adsorption measurements.

Because of the large water content of attapulgite and its variation with changes in relative humidity during storage it was necessary to establish that the initial water content of all the samples was the same. A standard initial state was obtained by storing the clay at 25° and 20% R.H. before use. Weight losses on evacuation were calculated from this initial state and are tabulated as per cent. initial weight. In addition because the external surface as well as the weight of the sample was found to be a function both of the activation temperature and of the relative pressure of water over the sample, it was also necessary to define a dry weight of sample for use in calculating heat of immersion and adsorption values. For samples evacuated at 25°, the dry weight after evacuation to constant weight was used. This same dry weight was also used for samples activated at 100 and 190° since these samples could be regenerated to their original condition by treatment with water vapor. Additional water driven off at 100 and 190° was thus considered a constituent part of the clay compared to that removed by the 25° activation; the latter was shown to be principally physically adsorbed water. To be consistent, the dry weight after the 25° evacuation was also used for samples evacuated at 500°.

Results

Studies of Attapulgite Evacuated at 25°.—The 4-g. sample used in the gravimetric adsorption studies required 10 days evacuation at 25° at a final vacuum of 10⁻⁵ mm. before a constant weight was reached. Barrer⁴ showed that the surface of an attapulgite sample, measured by nitrogen adsorption, also increased with activation time although area changes were small after 80 hours

outgassing. A similar increase in surface area was noted here, although no systematic study was made. The significant results for attapulgite outgassed at 25° are listed in Table I. In column 2 and 5 of Table I, the weight loss by evacuation from the initial state at 25° and 0.2 relative pressure is shown to equal the weight gain by adsorption under these same conditions. These results show the reversibility of water adsorption at 25°. The area calculated from water adsorption is about 12% larger than the value from nitrogen adsorption.

The heat of immersion curve for attapulgite outgassed at 25° is plotted in Fig. 1. The heat values are shown as a function of the relative pressure at which the samples were equilibrated with water vapor before heat measurements were made. These values were plotted on a per gram basis rather than on the more usual per unit area basis because of the complication caused by the change in surface area during evacuation or adsorption of water. A plot of the heat curve on a per unit area basis was also made and was similar in shape to the curves in Fig. 1. The high heat values at low coverages declined rapidly at first then more slowly toward a value of about -55 ergs/cm.² near saturation.

Studies of Attapulgite Evacuated at 100°.—Pertinent results for attapulgite studied after evacuation at 100° are also included in Table I. Comparison of these results with that obtained for samples evacuated at 25° revealed: 1. The additional water desorbed at 100° amounted to 0.0152 g./g. clay. 2. The nitrogen area decreased slightly from 217 to 200 m.²/g. 3. The calculated water area increased from 243 to 286 m.²/g. 4. The heat of immersion in water increased from -26.2 to -37.2 cal./g.

The heat of immersion curve for attapulgite outgassed at 100° is also plotted in Fig. 1. An inspection of this heat of immersion curve reveals higher heats at low coverages for attapulgite evacuated at the higher temperature. That the curves merge near 0.6 relative pressure appears significant. Apparently, complete regeneration of the outgassed sample occurred as the water vapor pressure was increased. It can also be seen from the weight gain columns of Table I that nearly all the water

(7) A. C. Zettlemoyer, G. J. Young, J. J. Chessick and F. H. Healey, *This Journal*, **57**, 649 (1953).

desorbed at 100° resorbs at 25° and 0.2 relative pressure.

Attapulgitte Outgassed at 190°.—Data for attapulgitte outgassed at 190° are included in Table I. A sample outgassed at 190° suffered a 12% wt. loss from the initial state condition. In addition, the external area decreased to 160 m.²/g. probably due to mild sintering. The weight gain on adsorption of water at 25° and 0.2 relative pressure was only 8.5% showing that the sample was far from regenerated by water vapor at this low relative pressure. Furthermore, only a portion of this water was reversibly adsorbed on the external surface at 25°. Adsorption-desorption measurements showed this amount of water to be equivalent to that necessary to cover an area of about 160 m.²/g., the nitrogen surface area. The remainder of the water adsorbed irreversibly into the intracrystalline channels present in the primary fibers of the clay. Although more water was removed by the 190° activation, this could not be returned to the sample at relative pressures up to 0.7, the highest relative pressure used in the adsorption isotherm measurements.

Attapulgitte Outgassed at 500°.—There is little doubt that irreversible changes occurred in the structure of attapulgitte outgassed at 500°. The nitrogen area decreased, but not markedly, from that obtained after the 190° activation. However, the calculated water area was only slightly greater than that obtained from nitrogen adsorption measurements. It is obvious that water driven off at 500°, principally from the intracrystalline channels, was not returned by the adsorption process which was carried up to about 0.7 relative pressure. Irreversible sintering also occurred since no regeneration of external area was found possible by exposure of the sample to water at its saturation pressure at 25° for 24 hours. The irreversible structural change after the 500° activation is best shown by the large decrease in heat of wetting which fell to -21.6 cal./g., compared to -41.1 cal./g. for the activation at 190°. Obviously, water removed at 500° was not replaced on immersion in water which was the most efficient method for regeneration for other activation temperatures.

Discussion

Samples outgassed at 25° adsorbed water vapor physically. This adsorption most likely occurred entirely on the external surface even though the calculated water area was somewhat larger than that obtained from nitrogen adsorption. This increased water adsorption could be due to a limited access of water molecules to the intracrystalline channels present in the ultimate fibers of the clay. Barrer⁴ has already shown that these channels, even though emptied by high temperature activation, are not accessible to nitrogen or other non-polar molecules. More likely, however, this increased water adsorption found under these conditions resulted from the physical nature of the sample itself. Electron photo-micrographs have shown this clay to consist principally of needle-like fibers in loose, somewhat parallel aggregation; hence wedge-shaped capillaries are common. The smaller water molecules can either be accommodated in the narrower intercrystalline channels

or can penetrate further into the tapered channels than can the larger nitrogen molecules.

The heat of immersion curve for attapulgitte was shown to fall rapidly and approach a value of about -55 ergs/cm.² near saturation. Usually

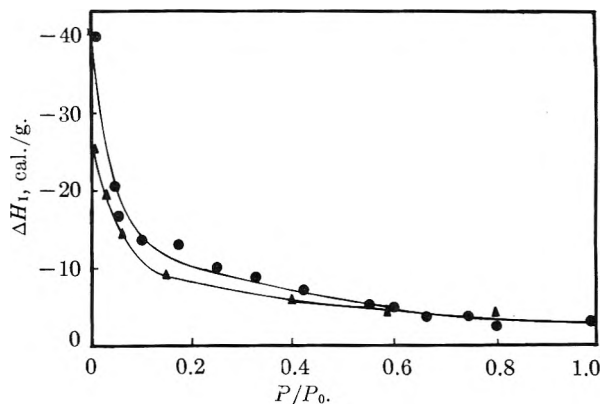


Fig. 1.—Heats of immersion of attapulgitte in water: ▲, outgassed at 25° for 14 days; ●, outgassed at 100° for 24 hours.

with typically hydrophilic, non-porous solids, the heat values near saturation approach -118 ergs/cm.², the heat liberated when one square centimeter of a water-water vapor interface is destroyed. The low heat value found for attapulgitte saturated with water vapor is equivalent to that for the immersion of a solid covered with a duplex film and having an area of 75 m.²/g. rather than the 217 m.²/g. measured for the outgassed attapulgitte. Thus it becomes apparent that area available to nitrogen begins to disappear before the second adsorbed water layer is completed due to the filling of capillaries between primary fibers of the clay agglomerates.

The difference in the heat of immersion for attapulgitte freed of adsorbed water by evacuation at 25° and that for a sample covered with a monolayer of adsorbed water amounts to about -300 ergs/cm.² (about -4 kcal./mole H₂O). This magnitude is often found where physical adsorption alone occurs on the surface of polar solids. This same difference for a sample of bentonite⁸ evacuated under similar conditions amounted to -575 ergs/cm.². Surface heterogeneity is the most likely explanation for the higher heats on bentonite. Heat of desorption values calculated from heat of immersion and adsorption data clearly illustrated the marked heterogeneity of the bentonite surface to water adsorption.⁸

Heat of desorption values for attapulgitte are shown plotted in Fig. 2 as a function of the volume of water adsorbed. The low values and the linearity of the curves are indicative of a homogeneous attapulgitte surface. In sharp contrast, the heats of desorption values for bentonite are nearly double at the lowest coverages measured and decline rapidly with increasing coverages although the heat values are still above those for attapulgitte at monolayer coverages.

After the 100° evacuation the small decrease in nitrogen area could result from sintering or from a

(8) A. C. Zettlemoyer, G. J. Young and J. J. Chessick, *THIS JOURNAL*, **59**, 962 (1955).

closer packing of the primary fibers on removal of some additional water. The ease with which the sample was regenerated by treatment with water vapor suggested that sintering did not occur at this temperature.

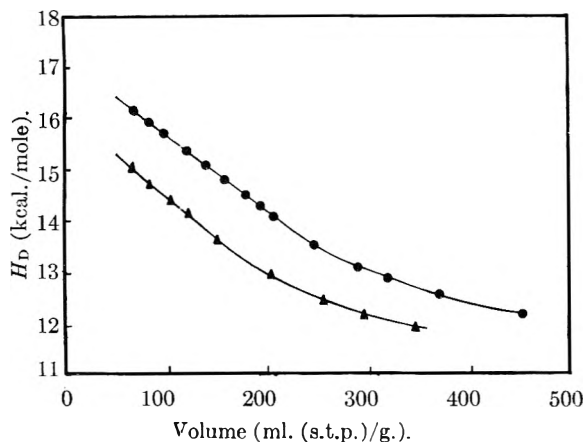


Fig. 2.—Heats of desorption of water from attapulgite at 25°: ▲, outgassed at 25° for 14 days; ●, outgassed at 100° for 24 hours.

The difference in the initial heat of immersion values for the two evacuation temperatures, 25 and 100°, represents the wetting of additional sites freed of adsorbed water by the 100° activation. Since the sample can be regenerated easily, the water is reabsorbed on immersion and the heat effect for reabsorbing amounts to -13.2 kcal./mole H_2O . This value compares favorably to -12.3 kcal./mole H_2O found for bentonite evacuated in a similar manner.⁸ Energy-wise, the additional water removed from both samples at 100° appears about the same, unlike the water removed at 25°. This high heat value found for bentonite was thought to result from the wetting of high energy sites which might be hydratable, that is, exchange ions or surface hydroxyl groups uncovered by activation at 100°. It is likely that a similar situation pertains to attapulgite. In addition, since the sample was very nearly regenerated by treatment with water vapor at 25° and 0.2 relative pressure, the parallelism of the heat of desorption curves shown in Fig. 1 reflects the similarity of the adsorption process thereafter to that for a 25° evacuated sample.

More drastic changes occurred after the 100° evacuation. Although the sample could again be regenerated, exposure to water-vapor near saturation pressure at 25° was necessary. Such treatment caused the external area to increase to 204 $m^2/g.$ as measured by nitrogen adsorption after

suitable evacuation; this final area is close to the 217 $m^2/g.$ found for the original sample. More evidence that the sample is regenerated after treatment with water vapor comes from heat of immersion measurements. A sample activated at 190°, then exposed to water near its saturation vapor pressure at 25°, and finally evacuated 14 days at 25° gave a heat of immersion of -27.2 cal./g. This value agrees well with the -26.2 cal./g. found for an original sample which had only been evacuated at 25°.

It is of interest also to consider the magnitude of the differences in energies of adsorption of water for the two activation conditions, 100 and 190°. Again, the differences in the initial heats of immersion values represent the heat of wetting of the new sites produced by the 190° activation. Evidence will be presented to show that the excess water removed at 190° is reabsorbed during the immersion process. The heat for the reabsorption of this water was calculated to be -2.3 kcal./mole H_2O ; this value is surprisingly low compared to the -13.2 kcal./mole found for the reabsorption of the excess water removed at 100°. The additional water removed by activation at 190° came principally from the intracrystalline channels in the primary fibrils, although some of this water is apparently associated with the decrease in area on activation. The low heat of -2.3 kcal./mole H_2O could result from distortion of narrow intracrystalline channels during adsorption, so that the endothermic nature of this distortion is just exceeded by the exothermic nature of the adsorption process.⁴ Although the attapulgite channels are large enough to accommodate small non-polar molecules, Barrer found that polarity rather than molecular dimensions governs entry of those smaller molecules into the channels, and the low heat of hydration by water must result from high energy barriers to diffusion and adsorption. These might be imperfections in the crystals.

The largest amount of water, nearly 17.0 wt. %, was desorbed during evacuation at 500°; the major portion came off irreversibly. The evidence presented in Table I suggests that most of the irreversibly desorbed water came from within the intracrystalline channels. The entrance to these channels evidently became blocked during activation at 500°. Treatment with water vapor or immersion in water did not regenerate this activated sample to any significant extent.

Acknowledgment.—This work was carried out under contract N8onr-74300 with the Office of Naval Research whose support is gratefully acknowledged.

THE INFERENCE OF ADSORPTION FROM DIFFERENTIAL DOUBLE LAYER CAPACITANCE MEASUREMENTS^{1,2}

BY ROBERT S. HANSEN, ROBERT E. MINTURN AND DONALD A. HICKSON

Institute for Atomic Research and Department of Chemistry, Iowa State College, Ames, Iowa

Received February 24, 1956

Frumkin's theory of the dependence of surface tension on polarization and solute activity is modified and extended to establish the dependence of differential capacitance on polarization and adsorption. The resulting equation is applied to experimental capacitances in the system mercury-0.1 *M* perchloric acid-pentanoic acid. Variations of both actual and apparent adsorption with polarization are emphasized, and the relevance of these variations to the capacitance determination of adsorption is discussed.

Introduction

A recent paper from this Laboratory emphasized the desirability of establishing methods for measurement of adsorption from solution at low specific area metal surfaces, and surveyed the application of hydrogen overvoltage phenomena to this problem.³ Preliminary work on inference of adsorption from double layer capacitance measurements was also included.

Grahame⁴ has published an extensive review of work on the electrical double layer, including work on double layer capacitance. The large part of such work has involved the use of mercury electrodes, and Grahame and his co-workers have attained a high degree of reproducibility and precision in measurement of double layer capacity in systems involving mercury. Because of the availability of a considerable amount of information on the character of the mercury-aqueous electrolytic solution double layer, and especially because of the possibility of varying electrode polarizations over a considerable range, mercury was selected as well suited to a study of the effect of adsorbable components on the double layer capacitance.

Barclay and Butler⁵ included a brief study of the effect of *t*-amyl alcohol concentration on the double layer capacitance at the mercury surface in a general paper on double layer capacitance, but did not attempt to correlate observed effects quantitatively with adsorption, nor did they investigate the dependence of these effects on polarization. Frumkin⁶ has published an extensive theoretical treatment of the effect of adsorbable components on the electrocapillary curve; we shall extend his results to differential capacitance curves in the present work. The Russian physical chemists have maintained an active interest in the application of differential capacitance measurements to adsorption problems; notable contributions include work by Frumkin and Melik-Gaikazyan⁷ on inference of adsorption kinetics from double layer capacitance frequency dependence and a

study by Melik-Gaikazyan⁸ in which formation of polymolecular layers adsorbed at the mercury surface was inferred from capacitance results.⁹

Theoretical

The dependence of boundary tension on boundary polarization and activity of a single adsorbable component is given by

$$d\gamma = -Q dV - RT\Gamma d \ln a \quad (1)$$

in which γ is the boundary tension, Q the charge per unit area on the electrode side of the double layer, V the potential of the electrode of interest with respect to a reference electrode (in the discussion to follow we shall for convenience refer V to the electrocapillary maximum) and Γ is the surface excess of the adsorbable component per unit area. From eq. 1 it follows that

$$\left(\frac{\partial \ln a}{\partial V}\right)_{\Gamma} = -\frac{1}{RT} \left(\frac{\partial Q}{\partial \Gamma}\right)_V \quad (2)$$

If the functions $Q(\Gamma, V)$ and $\Gamma(a, V = 0)$ are known eq. 2 can be used to establish the function $\Gamma(a, V)$. Frumkin⁶ assumes

$$Q(\Gamma, V) = Q_w(1 - \theta) + C'(V - V_N)\theta \quad (3)$$

and

$$\frac{\theta}{1 - \theta} = B_0 a e^{-2\alpha\theta} \quad (4)$$

in which θ is the fraction of the surface covered by adsorbate ($\theta = \Gamma S$, where S is the molar area of the adsorbate), Q_w is the boundary charge per unit area at polarization V in absence of adsorbate, C' is the differential capacitance (assumed constant) of the double layer when $\theta = 1$, and V_N is the potential (referred to the potential at the electrocapillary maximum in the absence of adsorbate) at which there is no charge on the double layer when this double layer contains adsorbate at $\theta = 1$. B_0 and α are constants. The assumptions as to the character of the functions $Q(\theta, V)$ and $\theta(a, V = 0)$ contained in eq. 3 and 4 lead, using eq. 2, to the general dependence of θ on V and a , thus

$$\frac{\theta}{1 - \theta} = B a e^{-2\alpha\theta} = B_0 e^{-S\Phi/RT} a e^{-2\alpha\theta} \quad (5)$$

where

$$\Phi = \int_0^V [Q_w - C'(V - V_N)] dV \quad (6)$$

The preceding development is a slight modification (to account for the known variation of the differ-

(8) V. I. Melik-Gaikazyan, *ibid.*, **26**, 1184 (1952).

(9) We are indebted to Dr. David C. Grahame for making available to us translations of references 7 and 8.

(1) Based in part upon a dissertation submitted by Robert E. Minturn to the Graduate School, Iowa State College, in partial fulfillment of the requirements for the degree of Doctor of Philosophy, 1955.

(2) Work was performed in the Ames Laboratory of the Atomic Energy Commission.

(3) R. S. Hansen and B. H. Clappitt, *THIS JOURNAL*, **58**, 908 (1954).

(4) D. C. Grahame, *Chem. Revs.*, **41**, 441 (1947).

(5) I. M. Barclay and J. A. V. Butler, *Trans. Faraday Soc.*, **36**, 128 (1940).

(6) A. Frumkin, *Z. Physik*, **35**, 752 (1926).

(7) (a) A. Frumkin and V. I. Melik-Gaikazyan, *Doklady Akad. Nauk. U.S.S.R.*, **77**, 855 (1951); (b) V. I. Melik-Gaikazyan, *Zhur. Fiz. Khim.*, **26**, 560 (1952).

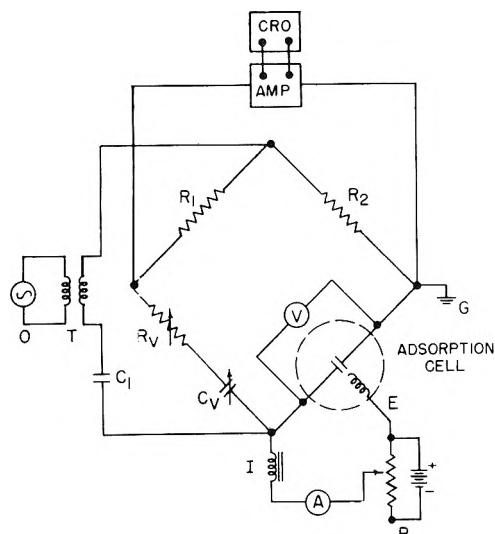


Fig. 1.—Circuit diagram for capacitance bridge.

ential capacitance C_w of the mercury-aqueous electrolytic solution double layer with polarization (2) of one given in detail by Frumkin,⁶ who also emphasizes that the physical significance of eq. 5 and 6 is that, at high polarizations and hence, at high fields in the double layer, material of low dielectric constant will be displaced by material of high dielectric constant in a manner analogous to the "salting out" effect.

The depression of boundary tension at coverage θ and polarization V is given by

$$\gamma_0 - \gamma = \int_0^V Q_w dV = \frac{RT}{S} [\ln(1 - \theta) + \alpha \theta^2] \quad (7)$$

Since the differential capacitances must satisfy

$$C = \frac{\partial Q}{\partial V} = - \frac{\partial^2 \gamma}{\partial V^2} \quad (8a)$$

$$C_w = \frac{\partial Q_w}{\partial V} = - \frac{\partial^2 \gamma_0}{\partial V^2} \quad (8b)$$

Equation 7 implies the dependence of differential double layer capacitance C on polarization and adsorbate activity; the result, after moderate algebraic manipulation, can be expressed in the form

$$C = C_w - \theta \left\{ (C_w - C') - \frac{S}{RT} \frac{1 - \theta}{1 - 2\alpha\theta(1 - \theta)} [Q_w - C'(V - V_N)]^2 \right\} \quad (9)$$

The terms $C_w - \theta(C_w - C')$ represent the capacitance of an adsorbate-filled capacitor of area θ and a water filled capacitor of area $(1 - \theta)$ connected in parallel, and would be the total differential capacitance according to eq. 3, if θ did not change with V ; the remaining terms on the right side of eq. 9 arise from the change in θ with V , and could be considered ϵ pseudo-capacitance in the sense that no set of invariant capacitors could be arranged to give rise to such a term.

An apparent fractional surface coverage θ_{app} can now be defined by

$$\theta_{app} = \frac{C_w - C}{C_w - C'} = \theta \left\{ 1 - \frac{S}{RT} \frac{(1 - \theta)}{1 - 2\alpha\theta(1 - \theta)} \frac{[Q_w - C'(V - V_N)]^2}{C_w - C'} \right\} \quad (10)$$

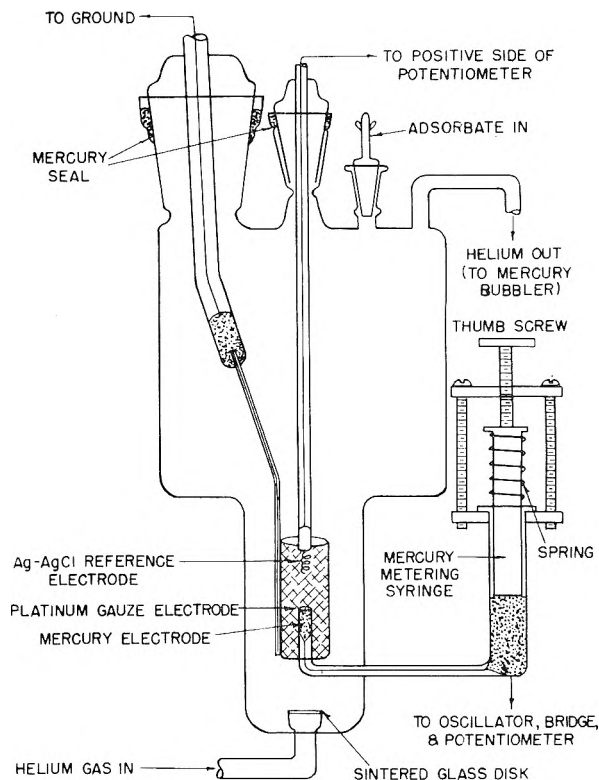


Fig. 2.—Adsorption-capacitance cell.

This is the quantity measured by Hansen and Clampitt; the term C' was neglected by them. In eq. 10, C and C_w are measurable, C' is in principle best obtained by extrapolation of $C(a, V = V_N)$ to infinite a from low activity results, since its inference from measurements in pure liquid solute would involve tenuous assumptions as to similarity of orientation in the compact double layer and character of the diffuse double layer in the pure solute case, B_0 , S/RT , α and V_N remain as adjustable parameters; V_N is best established by setting $Q_w = C'(V - V_N)$ at the average maximum in several plots of θ_{app} against V at several activities, B_0 and α are best established from dependence of θ on V at the potential of maximum θ_{app} , and S/RT is then chosen for best representation of the dependence of θ_{app} on V .

The following reservations as to the validity of eq. 10 should be made explicit.

(1) Equation 3 is probably most nearly valid if the diffuse double layer contribution to capacitance can be ignored, and hence eq. 10 should be applied to solutions with at least moderate electrolyte concentrations.

(2) Equation 4 limits application to unimolecular adsorption. Modification to permit application to multimolecular adsorption would involve introduction of an isotherm equation valid for such adsorption at this point, and probably a more complex variation of eq. 3.

(3) C' and V_N are here treated as constants; since C_w varies with polarization C' may also vary; further V_N would change if the orientation of a dipolar adsorbate changes, and hence might be expected to change somewhat with coverage.

Experimental

The impedance bridge used for capacitance measurements is shown in Fig. 1, and is similar to one designed by Grahame.¹⁰

R_1 and R_2 are small temperature coefficient wire-wound Nobleloy resistors of resistance 1004.5 ohms each. R_v is a Leeds and Northrup a.c.-d.c. decade resistor, catalogue No. 4755, with resistance variable in 0.10 ohm steps from 0 to 11,000 ohms. C_v is a Freed Transformer Co. Decade Capacitor Model 1350 with capacitance continuously variable from 0 to 11 microfarads. It was calibrated against a Beco Model 250-C impedance bridge. The power source O , a Hulett-Packard wide-range oscillator model 200 CD, fed a 1000 cycle a.c. current into the 10:1 transformer T and was adjusted to maintain an a.c. signal of approximately 4 millivolts, as measured by the meter V , across the cell terminals. The unbalanced signal across the bridge was amplified by the 1000 cycle high gain amplifier AMP and detected on the Du Mont type 323 cathode ray oscilloscope CRO. The potentiometer P was adjusted to apply the desired polarizing voltage to the test electrode using the Ag-AgCl electrode E as reference. The microammeter A measured d.c. current through the cell. AC signal was eliminated from the potentiometer circuit by the 3 henry inductance I , and direct current was eliminated from the transformer circuit by the 2 μ f. condenser C .

The Pyrex adsorption cell is shown in Fig. 2. Helium, purified by passage through an activated uranium train at 240° and a charcoal trap maintained at liquid nitrogen temperature, stirred the solution and provided an inert atmosphere. The mercury bubbler and mercury seals prevented contaminating gases from entering the cell. The positive pressure in the cell minimized oxygen contamination when adsorbate was added through the appropriate taper. The mercury surface was renewed when desired by turning the thumb screw controlling the plunger in the mercury metering syringe, causing the mercury to overflow and the mercury surface to renew. There was no contact between solution or vapor and stopcock grease. The reference electrode was a Ag-AgCl electrode prepared by the thermal-electric method of Harned.¹¹

The mercury electrode was formed in a 2.5 mm. i.d. Pyrex tube section, so that the top of the mercury meniscus was approximately tangent to the plane of the top of the tube. A platinum screen cylinder surrounded the mercury electrode, and was in series with the mercury electrode in the a.c. circuit; its area, and hence its capacitance, was large compared to that of the mercury drop, so that its effect on cell impedance should have been negligible.

Dry, clean air was bubbled through Goldsmith Bros. triple-distilled mercury for two days, after which the mercury was filtered, washed thoroughly with 50% concentrated nitric acid by volume, followed by washing with distilled water, dried and distilled three times *in vacuo*. Water

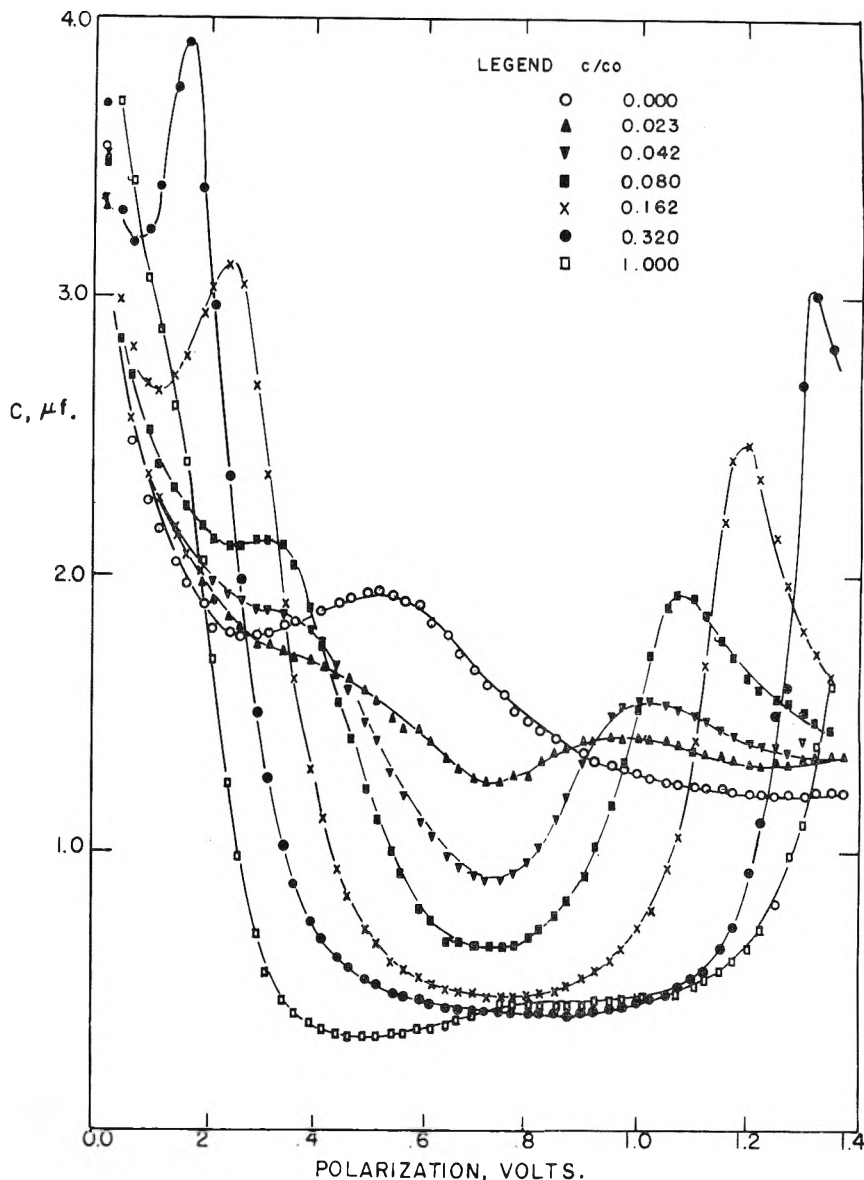


Fig. 3.—Dependence of differential capacitance on polarization and adsorbate activity, system mercury-0.100M aqueous perchloric acid-pentanoic acid. C/C_0 is reduced concentration of pentanoic acid. Capacitances can be converted to capacitances per unit area by division by the electrode area of approximately 0.074 cm.² Potentials are referred to Ag-AgCl electrode in 0.001 KCl.

used was redistilled from alkaline permanganate solution. Eastman Kodak Co. best grade *n*-valeric acid was distilled in a 30-plate Oldershaw column at reflux ratio 10 to 1; the fraction used had a boiling range of 186.5 to 186.8° corrected to 760 mm.

The electrolytic solution was 0.100 M HClO₄ and 0.0010 M KCl; approximately 400 ml. of this solution was added to the adsorption cell. An anode compartment with a fine pore fritted glass plate was inserted through the standard taper joint provided by the "ground" exit in Fig. 2, and the solution pre-electrolyzed 12 hours at 5×10^{-3} amp. with a stream of hydrogen bubbling through the solution, using a platinum flag electrode inserted through the central standard taper joint as cathode.

The anode compartment and flag electrode were then replaced by platinum screen electrode and Ag-AgCl electrode as shown in Fig. 2. The hydrogen stream was replaced by a purified helium stream which was allowed to bubble through the solution for at least two hours to remove any dissolved non-inert gas. Adsorbate was added through the "adsorbate in" standard taper joint using a pipet or micropipet depending on amount, helium being passed through the solution for at least one hour after each addition.

(10) D. C. Grahame, *J. Am. Chem. Soc.*, **71**, 2975 (1949); (*b*) *Rec. Chem. Prog.*, **11**, 93 (1950).

(11) H. S. Harned, *J. Am. Chem. Soc.*, **51**, 416 (1929).

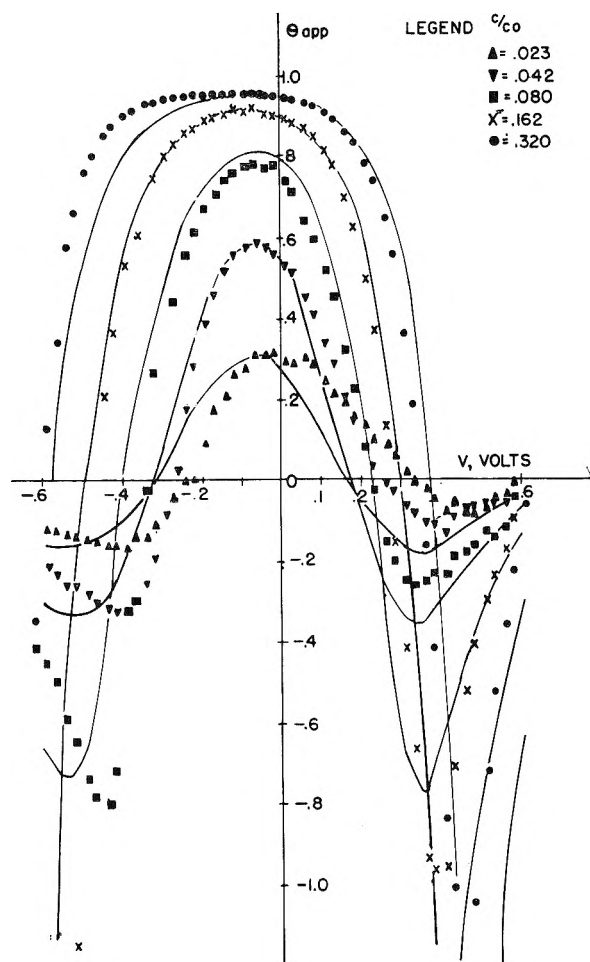


Fig. 4.—Dependence of apparent fractional surface coverage on polarization and adsorbate reduced concentration. Points are experimental, curves are calculated from eq. 10. Potentials are referred to the electrocapillary maximum, taken as -0.6 volt relative to $N/1000$ Ag—AgCl electrode.

If the mercury meniscus had been accurately hemispherical, its area, computed from the diameter of the tube in which it was formed, would have been 0.098 cm^2 . Actually, the drop diameter is rather large for the meniscus to be considered a spherical segment and the interfacial contact angle is somewhat less than 180° and depends somewhat on the manner of formation. Both of these effects tend to cause an electrode area less than $2\pi r^2$, and the latter effect causes this area to be imperfectly reproducible. Therefore, when the electrode was renewed it was adjusted to give the same capacitance as the previous electrode at the polarization at which formed; with this adjustment the capacitance-potential curve could be reproduced to within a fraction of a per cent. at all but the most anodic polarizations investigated.

Results

Results in the form of differential capacitance-potential data for six different reduced concentrations (concentration divided by saturation concentration) of pentanoic acid varying from 0.02 to 1.00 are presented graphically in Fig. 3. Observed capacitances can be converted to capacitances per unit area by division by electrode area; as previously indicated, this area should be rather less than 0.098 cm^2 , and an area of 0.074 cm^2 was used in calculations as leading to capacitances per unit area closely parallel to those reported for a similar electrolyte by Crahame.⁴ An error in assignment

of electrode area will lead to the same relative error in the parameter S and in the same direction but will not affect values of other parameters used in the treatment of apparent adsorption.

In Fig. 4 experimental values of θ_{app} are compared with curves calculated for the corresponding activities using the following values of parameters

$$\begin{aligned} B_0 &= 10.5 \\ C' &= 5.21 \mu\text{f./cm}^2 & \alpha &= 1.00 \\ V_N &= 0.24 \text{ volt} & S/RT &= 0.81 \text{ cm}^2/\mu\text{j.} \end{aligned}$$

Integrals $Q_w = \int_0^V C_w dV$ and $\int_0^V Q_w dV$ needed for calculations were evaluated graphically. It will be seen that eq. 10 gives an excellent representation of the general dependence of θ_{app} on V , differences between theory and experiment certainly being of such an order of magnitude as to be ascribed to minor variations in C' and V_N not accounted for in the theory. Values of parameters are physically reasonable. A value of $0.81 \text{ cm}^2/\mu\text{j.}$ corresponds to a molecular area of 33.5 \AA^2 approximately sufficient to accommodate a methyl and two methylene groups but not the entire molecule in a "lying down" configuration. The parameter α accounts for attractive interaction between adsorbed molecules, and it should be possible to estimate its magnitude from comparable interactions in solution. The quantity $RT \ln f_0$ represents the change in interaction free energy per mole when pentanoic acid is transferred from pure pentanoic acid to a state of infinite dilution in water. f_0 is the activity coefficient of pentanoic acid at infinite dilution in water. The corresponding interaction free energy change in the adsorbed layer is represented by $2\alpha RT$, except that molecules in the film are always bounded on one side by the adsorbent, on the other side by (essentially) water. Hence, we should expect $2\alpha \approx \frac{1}{2} \ln f_0$. The value of 2α thus estimated from solution activity coefficient is 2.5 compared to 2.0 used. The value of V_N , 0.24 volt or 0.805×10^{-3} e.s.u., coupled with the value of 33 \AA^2 for S , is interpretable tentatively as corresponding to an oriented dipole layer with normal component of the dipole moment 0.21ϵ debye units, where ϵ is the effective dielectric constant within the dipole. One might expect $1 < \epsilon < 2$, so that the normal component of the dipole would be small. This is in the order of magnitude to be expected if part of the alkyl chain were adsorbed and the carboxyl group extended away from the surface into the aqueous medium.

An important conclusion illustrated by Fig. 4 and eq. 10 is that actual and apparent surface coverages coincide only in the neighborhood of the maximum in the θ_{app} vs. V curve, so that, in estimating adsorption from double layer capacitance measurements, it is essential that the variation of capacitance with potential be sufficiently investigated to establish the polarization at this maximum, and that isotherms be determined at this polarization. More extensive conclusions can be reached from fairly complete capacitance-polarization-activity data. In this case, not only fractional coverage but actual amounts adsorbed can be established, since molecular areas (S) can be obtained from curvatures of the θ_{app} vs. V plots. Finally, it

is to be emphasized that the actual adsorption of a solute by a metal depends on its polarization. Dipolar molecules normally adsorbed with positive end of the dipole toward the metal will be most strongly adsorbed somewhat on the cathodic side of the electrocapillary maximum. Those adsorbed with negative end of the dipole toward the metal will be most strongly adsorbed somewhat on the anodic side of the electrocapillary maximum, and that at sufficient polarizations, either anodic or cathodic, organic molecules will be almost completely desorbed in the presence of aqueous electrolytes.

The dependence of capacitance on polarization in 0.100 M HClO_4 saturated with pentanoic acid is shown in Fig. 3, but no corresponding curve is shown in Fig. 4 because this curve illustrates the effect of multimolecular adsorption on capacitance, as was first shown by Melik-Gaikazyan.^{5b} The pronounced dip below the apparent convergence limit is interpreted by Melik-Gaikazyan as due to an increase in thickness of the compact double layer accompanying multi-molecular adsorption, and the stepwise rise above this limit due to a "pseudocapacitance" accompanying the desorption of the second layer.

THE ULTRACENTRIFUGAL BEHAVIOR OF SOME PROTEINS IN NON-AQUEOUS SOLVENTS¹

BY HENRY L. CRESPI, ROBERT A. UPHAUS AND J. J. KATZ

Argonne National Laboratory, Lemont, Illinois

Received February 24, 1956

Data obtained from ultracentrifugal and light scattering experiments indicate that proteins dissolved in trifluoroacetic acid and in trifluoroacetic acid-diethyl ether mixtures may be studied by methods standard for aqueous solutions. Ultracentrifugal analysis of several proteins in 3:1 trifluoroacetic acid-diethyl ether mixtures yielded the following experimental sedimentation constants: Silk fibroin, 2.25S; rattail tendon, 1.94S and 2.3S (two components); insulin, 1.80S. Bovine plasma albumin in a 4:1 trifluoroacetic acid-diethyl ether mixture gave an experimental sedimentation constant of 1.5S. Preliminary light scattering work indicated the following approximate molecular weights: silk fibroin, 60,000; rattail tendon collagen, 70,000; insulin, 6,000.

Introduction

Recently, attention has been directed to the observation that certain strong anhydrous acids are solvents for proteins. Hydrogen fluoride^{2a} and trifluoroacetic acid^{2b} have received attention in this regard.

It is the purpose of this paper to serve as the introduction to a concerted, quantitative study of the behavior of certain proteins in one of these solvents, *i.e.*, trifluoroacetic acid. This acid boils at 71° melts at -15.6° and has a density at 20° of 1.4890 g./cc.³ It is completely miscible at room temperature with ether, acetone, benzene and water. Its dielectric constant at 30° is 8.22.⁴

It has been shown previously^{2b} that bovine plasma albumin recovered from trifluoroacetic acid yields the same ultracentrifugal pattern as the starting material. In further experiments using trifluoroacetic acid-ethyl ether mixtures as the protein solvent, bovine plasma albumin was recovered, in about 80 to 90% yield, essentially unchanged in ultracentrifugal characteristics. With these indications that the fundamental protein linkage is not destroyed, a study of silk fibroin, collagen and insulin has been initiated.

Experimental

A. Preparation of Materials. Trifluoroacetic Acid.—The commercially available material (Minnesota Mining and Manufacturing Co.) was slowly distilled *in vacuo* into a reservoir, the last third of the original material being discarded. The acid was distilled as needed from the reservoir into a closed pipet and from the pipet into the protein container. Except for a few experiments in which the trifluoroacetic acid was distilled from P₂O₅, no drying agents were used because of the danger of contamination with trifluoroacetic acid anhydride.

Diethyl Ether.—Anhydrous, reagent ethyl ether was distilled *in vacuo* into a reservoir from a small amount of anhydrous MgSO₄. The ether was distilled out as needed and kept at -78° during storage.

Sodium Trifluoroacetate.—This salt was prepared from trifluoroacetic acid and sodium carbonate according to the method of Hara and Cady.⁵ *Anal.* Calcd.: Na, 16.91. Found: Na, 16.79.

Silk Fibroin.—Commercially available material (Nutritional Biochemicals Corp.) was dewaxed by extracting with a 1:1 solution of ethanol and ether for 25 hours. The mate-

rial was then placed on the vacuum line and pumped to remove water and solvents. Failure to dewax in this way resulted in a small quantity of undissolved material after dissolution of the silk in trifluoroacetic acid.

Rattail Tendon.—Tendons were removed from the tails of freshly killed normal adult white rat, washed several times with distilled water and lyophilized. They were kept under vacuum until used.

Insulin.—Commercially available material (Sharpe and Dohme⁶) originally rated at 28 units/mg. (March, 1954) was used directly as received.

B. Preparation of Solutions.—All solutions were prepared on a high-vacuum line. A weighed amount of protein was placed in a test-tube fitted with a ground glass joint and fixed to the vacuum line. The appropriate amount of sodium trifluoroacetate and a magnetic stirrer were also introduced into the vessel. The sample was then dried in a high vacuum (<10⁻⁵ mm.) for at least 12 hours to remove moisture. With bovine plasma albumin and insulin, it was judged sufficient to dry for two hours at 60° in a high vacuum. Solvent was then distilled into a serological pipet which was fitted with a male joint and sealed at the tip and which served as the measuring vessel. After allowing the liquid in the pipet to come to thermal equilibrium with the surroundings, the volume was read. Following distillation into the sample tube, the residual volume was again read. All transfers were effected on the vacuum line by distillation with liquid nitrogen.

The protein was first dissolved in the trifluoroacetic acid whether pure trifluoroacetic acid or a mixed solvent was used. The frozen solvent was melted quickly and allowed to run down onto the protein. Stirring was initiated as soon as the liquid began to form and continued until complete solution or, in the case of the rattail tendon, for several minutes after reaching room temperature. While the other proteins dissolve rapidly, collagen requires many hours before dissolving. At room temperature, about 12 hours are required to dissolve the rattail tendon. If a mixed solvent was needed, the solution in trifluoroacetic acid was refrozen and the required volume of the ether solvent distilled in from another pipet on the line. The mixture was then melted with constant stirring. By effecting the dissolution in this way, the heat of mixing of organic solvents in trifluoroacetic acid was easily dissipated. In all cases, the final solution was frozen and removed from the line by sealing the sample tube with a hand torch. Solutions were thus stored in the complete absence of atmospheric oxygen and water. Protein concentrations are expressed in grams per milliliter of solvent.

C. Ultracentrifugal Procedure.—All analyses were conducted using the Spinco Model E Ultracentrifuge. Standard 12 mm., 4° cell assemblies with Kel-F centerpieces and screw plug gaskets were used throughout. The cells were filled and plugged in a nitrogen-filled dry box. Unless otherwise noted, all runs were made at 59,780 r.p.m. with a bar angle setting of 70°. The illustrations presented are to be read from left to right and sedimentation is proceeding from left to right. No abnormal trouble with cell leakage was experienced. It was found advisable to rinse the cells with water before disassembling in order to make sure that all of the trifluoroacetic acid is removed.

(1) Based on work performed under the auspices of the U. S. Atomic Energy Commission.

(2) (a) J. J. Katz, *Nature*, **173**, 265 (1954); *Arch. Biochem. Biophys.*, **51**, 293 (1952); (b) J. J. Katz, *Nature*, **174**, 509 (1954).

(3) Booklet, "Trifluoroacetic Acid," Minnesota Mining and Manufacturing Co., 1949.

(4) W. Dannhauser and R. H. Cole, *J. Am. Chem. Soc.*, **74**, 6105 (1952).

(5) R. Hara and George H. Cady, *ibid.*, **76**, 4285 (1954).

(6) We wish to express our gratitude to the Sharpe and Dohme Company for their generosity in making this material available to us.

Since trifluoroacetic acid is not a good ionizing solvent,⁷ one would not expect a charge effect of the order of magnitude of that observed for proteins in aqueous solution. Measurements on 1% solutions of silk fibroin and of highly purified mercaptalbumin (Pentex Incorporated) showed both solutions to have conductivities of the order of 1×10^{-5} mho. Conductivity measurements made on 0.1 *M* sodium trifluoroacetate in trifluoroacetic acid and on a similar solution containing 1% silk fibroin indicate the possibility of some charge effect, as the conductivity of the protein plus salt solution was greater than that containing salt alone (5×10^{-5} mho against 3×10^{-5} mho). Accordingly, ultracentrifugal analyses were made of 0.3% silk fibroin solutions dissolved in trifluoroacetic acid only and in trifluoroacetic acid with varying concentrations of sodium trifluoroacetate. Because of the present lack of sufficient data for obtaining corrected sedimentation constants, precise calculations are not yet available. One would expect from the properties of trifluoroacetic acid, to find the primary charge effect, if such an effect is indeed found, to be quite small. A secondary charge effect might also be induced by the use of sodium trifluoroacetate. However, the choice of buffer salt is limited due to interaction with the solvent.⁵

Since trifluoroacetic acid-ethyl ether mixtures are conducting, it was judged that any charge effect would be sufficiently minimized by the further addition of sodium trifluoroacetate. All analyses reported were therefore performed in 0.1 *M* sodium trifluoroacetate solutions.

Reference patterns obtained by centrifuging trifluoroacetic acid and trifluoroacetic-diethyl ether mixtures indicated a considerable gradient due, presumably, to the compression of the solvent in the centrifugal field. In an analysis of 0.5% bovine plasma albumin in trifluoroacetic acid, the protein was found to both sediment and float at the same time. The rates of movement were both quite low, less than 0.5 *S*, but the experiment served to highlight the fact that a considerable density gradient existed in the centrifugal field.

This experiment is shown in Fig. 1B. Plots of $\log x$ vs. time generally showed some curvature. The experimental sedimentation constants reported were calculated on the basis of the slope of the best straight line obtainable from the first four points of the $\log x$ vs. time plot.

Results and Discussion

At the present writing, four different proteins have been analyzed ultracentrifugally. These are bovine plasma albumin, silk fibroin, rattail tendon collagen and insulin. A 0.5% solution of bovine plasma albumin in 4 volumes trifluoroacetic acid and 1 volume ether, with no salt added, sedimented at an experimental rate of 1.5 *S*. The boundary region did not spread as rapidly as in aqueous solutions. This lack of spreading could be the result of a self-sharpening effect due to the density and viscosity gradient in the solvent. A trace of faster moving material, visible upon analysis of aqueous solutions of this protein, was also present in the acid-ether solution. Figure 2C, shows the ultracentrifugal pattern obtained from this material.

Many analyses in trifluoroacetic acid-diethyl ether solutions of varying compositions were consistent in indicating that silk fibroin dissolved in these solvents yields a monodisperse system. The boundaries were sharp and symmetrical. Figure 2D shows a pattern obtained from a 0.5% solution of silk fibroin in 3 volumes trifluoroacetic acid:1 volume ether. The experimental sedimentation rate was 2.25 *S*.

Solutions of rattail tendon in 3 volumes trifluoroacetic acid:1 volume ether exhibited two components. The main component, which amounted to

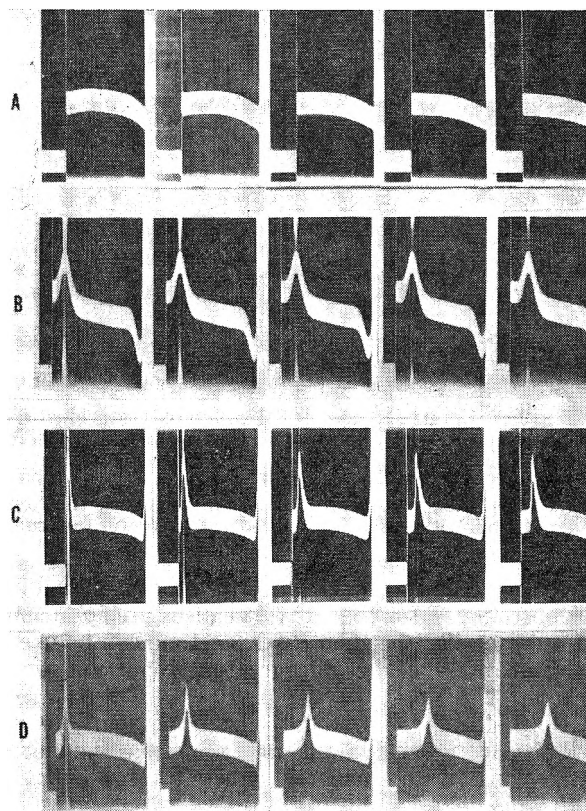


Fig. 1.—A, reference line obtained from a mixture of 3 volumes trifluoroacetic acid and 1 volume ethyl ether. Exposures are at 32-min. intervals, the first taken 38 min. after reaching speed; temperature of run, 19.0°. B, bovine plasma albumin in trifluoroacetic acid. Exposures are at 32-min. intervals, the first taken 210 min. after reaching speed; temperature of run, 20.3°.

Fig. 2a.—C, bovine plasma albumin in 4:1 trifluoroacetic acid-ethyl ether. Exposures are at 32-min. intervals, the first taken 18 min. after reaching speed; temperature of run, 22.0°. D, Silk fibroin in 3:1 trifluoroacetic acid-ethyl ether. Exposures are at 32-min. intervals, the first taken 38 min. after reaching speed; temperature of run, 19.4°.

90–95% of the observed material, sedimented at the rate of 1.94 *S*, while the second, less concentrated component moved at the rate of 2.3 *S*. Figure 2E, shows the result of analysis of a 0.5% solution of rattail tendon.

Fairly satisfactory results were obtained from analysis of insulin dissolved in a mixture of 1 volume trifluoroacetic acid and 1 volume ether. Although the boundary region spread rapidly, it became separated from the meniscus rapidly enough to permit calculation of a sedimentation constant. A 0.6% solution of insulin gave an experimental sedimentation rate of 1.8 *S*, as illustrated in Fig. 2F. It is anticipated that more rapid sedimentation will be obtained using trifluoroacetic acid-acetone mixtures of very low density.

The use of diethyl ether as a diluent in ultracentrifugation has been found beneficial for a variety of reasons. It reduces the medium density and permits more rapid sedimentation. Proteins containing tryptophan are very sensitive to air oxidation when in trifluoroacetic acid solution; the solutions turn pink even in the presence of very small amounts of oxygen. The addition of diethyl ether in some unspecified way minimizes the production

(7) J. H. Simons and K. E. Lorentzen, *J. Am. Chem. Soc.*, **74**, 4756 (1952).

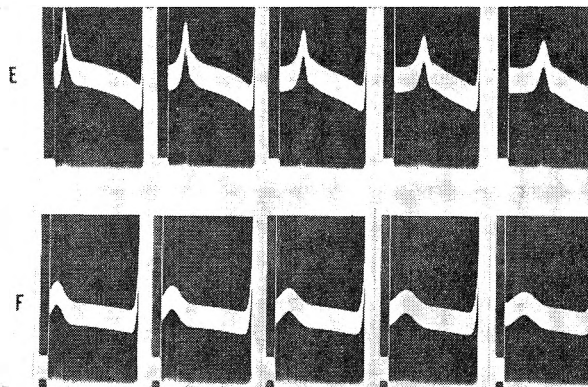


Fig. 2b.—E, rattail tendon in 3:1 trifluoroacetic acid-ethyl ether. Exposures are at 32-min. intervals, the first exposure taken at 45 min. after reaching speed; temperature of run, 20.1°, bar angle, 60°. F, insulin in 1:1 trifluoroacetic acid-ethyl ether. Exposures are at 16-min. intervals, the first taken 40 min. after reaching speed; temperature of run, 17.0°.

of colored solutions. However, if ether is added in proportion greater than 1:1, it causes precipitation of the protein. In such cases, acetone can be used as diluent in considerably greater proportion than 1:1.

Both silk fibroin and rattail tendon solutions in trifluoroacetic acid alone or trifluoroacetic acid-ether yield water insoluble precipitates if poured into large volumes of water.

Preliminary Results of Light Scattering Experiments

Before initiating a more comprehensive study of the molecular weights of various proteins in trifluoroacetic acid by means of light scattering, a brief survey was made. It must be emphasized that the

figures reported herein may be subject to later revision as techniques are refined and more extensive measurements made. Light scattering measurements were made in a photometer based on Brice's design. Ninety degree readings were taken in a square cell and the instrument calibrated with Ludox in the usual way.

Measurements indicate that the molecular weight of silk fibroin in trifluoroacetic acid is about 60,000. This figure is to be compared with the value of 84,000, based on the histidine, lysine and arginine content⁸ and the values 60,000-150,000 obtained by ultracentrifuge studies of fibroin solubilized with copper-ethylenediamine complexes.⁹

A preliminary determination of the molecular weight of insulin indicates that the fundamental unit has a molecular weight of around 6,000. Using only ninety degree measurements, the molecular weight of collagen appeared to be 70,000; since no angular measurements have yet been made this figure may later be revised.

Conclusion

From the evidence at hand, it appears that a new solvent system is available for the quantitative study of proteins, especially the fibrous proteins. Although the use of trifluoroacetic acid results in certain manipulative inconveniences, there appears to be no great obstacle to the performance of standard protein chemistry with this solvent. Particularly interesting, of course, is the prospect of studying water-insoluble proteins such as collagen and silk fibroin by techniques which are standard for aqueous solutions.

(8) M. C. Corfield, F. O. Howitt and R. Rolson, *Nature*, **174**, 603 (1954).

(9) F. H. Holmes and D. I. Smith, *ibid.*, **169**, 193 (1952).

TRYPSIN MONOLAYERS AT THE WATER-AIR INTERFACE. I. FILM CHARACTERISTICS AND THE RECOVERY OF ENZYMATIC ACTIVITY¹

By B. ROGER RAY AND LEROY G. AUGENSTINE

Contribution from the Department of Chemistry and Chemical Engineering, University of Illinois, Urbana, Ill.

Received February 24, 1956

Trypsin films spread over a limited surface area of ammonium sulfate were studied as to film pressure-area and film pressure-concentration characteristics and the amount of recoverable enzymatic activity. A Wilhelmy type balance employing electromagnetic control was used. A method for recovering films was developed which permitted a sensitive enzymatic assay. It was found that film pressure and recoverable activity were very dependent upon the past history (manipulations) and the age of the film. No activity could be recovered from films which had previously existed at surface concentrations below 6 γ /100 cm.² In more concentrated films, spread for 5 min., the recoverable activity corresponded to the amount of enzyme spread in excess of 10 γ /100 cm.² The recoverable activity decreased, independently of surface concentration, with increasing film age. The data suggest that the unfolded trypsin molecule has lost all activity and that a compressed film is composed of definite fractions of enzyme in globular and unfolded configurations.

Introduction

In recent years considerable interest has developed in the physico-chemical properties of proteins adsorbed at interfaces, principally the air-solid and air-water interfaces. An excellent review is that of Bull.² Another direction of study has been into the effects of adsorption upon biological activity. Most of this work has been concerned with either proteolytic or antigen-antibody reactions carried out at the interface. Rothen³ has summarized the research in this field.

A number of reports have been made on the recovery of protein from a film followed by a determination of the effect that spreading had on the biological activity—in particular, enzymatic activity. The lack of experimental details in most of the published work is to be deplored. Gorter⁴ reported 80% recovery of activity from pepsin and trypsin films. However, no other quantitative data were given, so that the state of the films is unknown. Rothen,³ who was successful in recovering active insulin but not metakentrin and gonadotropic hormone, suggests that it is probably impossible to recover activity from a completely unfolded molecule. Langmuir and Schaefer⁵ recovered 80% of the activity of pepsin films after deposition on a slide. Several investigators⁶ have compressed mixed films of pepsin and albumin into threads and have measured the proteolytic activity of the threads. The recent work of Cheesman and Schuller⁷ is noteworthy for the care taken and, in addition, for the details that are furnished. Using pepsin they recovered up to 50% activity.

The evidence is, then, that activity can be recovered from monolayers of several different enzymes. But there is little known as to the critical conditions, *i.e.*, factors such as the manner and extent of spreading, age of film and method of recovery. The first objective of the present work

was to study these factors as they apply to trypsin.

The behavior of proteins at interfaces is obviously part of the general problem of elucidation of protein structure. There has been proposed already a "weak-link" hypothesis relating to protein reactivity^{1,8}; this has been utilized to interpret certain radiation effects upon proteins⁹ in bulk. It is our feeling that additional information of value may be gained from investigation of the effects of radiation upon adsorbed protein. In particular, the effects of radiation upon film pressure and upon recoverable enzymatic activity seemed worthy of study. To this end, X-ray and ultraviolet irradiations of trypsin monolayers have been carried out.

The present contribution forms the first of a series of three. Here we describe the physical characteristics of compressed monolayers of trypsin and the recovery of enzymatic activity. The second contribution presents the results of the irradiation studies; the last paper discusses the results and attempts an interpretation in terms of the "weak-link" concept.

Film Pressure Characteristics

A. Experimental Methods

1. **Measurement of Film Pressure.**—The apparatus was a modification of a Wilhelmy-type balance described by Bull.² The novel features were the electromagnetic balancing and the photoelectric determination of the end-point.¹ Characteristics of this film balance are that readings are readily reproducible to 0.01 dyne/cm., it is capable of operation from a distance (useful in radiation experiments), the determination of the "end-point" is reduced to the simple observation of the deflection of a microammeter, and the complete operation can be made automatic.

Film troughs and barriers were made of Lucite and were heavily paraffined before use. The experiments were carried out inside a glass case which retarded evaporation and reduced contamination and thermal changes. In experiments extending over long periods of time the film trough was enclosed by close-fitting Lucite covers to eliminate evaporation. The work was done in an isolated basement room relatively free of organic vapors and dust, and constant as to temperature over intervals of a day or so. Temperature variation was less than $\pm 0.5^\circ$ for any one experiment, and all experiments were between 22 and 24° except where noted.

2. **Preparation of Solutions.**—The support solution was 15% ammonium sulfate to which 10 ml. of saturated sodium barbiturate (Veronal) had been added per liter of

(1) In part from a thesis by Leroy G. Augenstine submitted to the Graduate College of the University of Illinois in partial fulfillment of the requirements for the Ph.D. Degree in Physico-Chemical Biology, 1955. Additional experimental details can be found in the thesis.

(2) H. Bull, *Advances in Protein Chem.*, **3**, 95 (1947).

(3) A. Rothen, *ibid.*, **3**, 122 (1947).

(4) E. Gorter, *Proc. Roy. Soc. (London)*, **155**, 707 (1936).

(5) I. Langmuir and V. Schaefer, *J. Am. Chem. Soc.*, **60**, 1351 (1938).

(6) (a) D. Mazia and G. Blumenthal, *J. Cell. Comp. Physiol.*, **35**, Suppl. 1, 171 (1950); (b) T. Hayashi and G. Edison, *J. Coll. Sci.*, **5**, 437 (1950); (c) J. Kaplan, *ibid.*, **7**, 382 (1952).

(7) D. Cheesman and H. Schuller, *ibid.*, **9**, 113 (1954).

(8) L. Augenstine, "Information Theory in Biology," ed. H. Quastler, Univ. of Illinois Press, Urbana, Ill., 1953, pp. 119-122.

(9) E. Pollard, "Biochemical Aspects of Basic Mechanisms in Radiobiology," National Research Council, No. 367, 1954, p. 1-29.

solution to control the pH at 7.6. Merck Analytical Grade chemicals and conductivity water from a tin-lined still were used. After considerable investigation, the following standard purification procedure was adopted to remove surface-active contaminants from the support solution. After standing 6 hours, activated charcoal (Darco G-60) was added in the amount of 10 g./l. After 15 minutes the solution was twice vacuum filtered through medium and extremely fine filter papers. This charcoal treatment was repeated after 30 hours. The solution was then allowed to stand for at least 12 hours and was again vacuum filtered through fine filter paper just before being placed in the film trough. Well-washed, acid treated, analytical grade filter papers were employed.

Prior to the spreading of enzyme, the support solution was swept two or more times. (The only exceptions are the data in Fig. 1.) First, excess solution was swept off with a

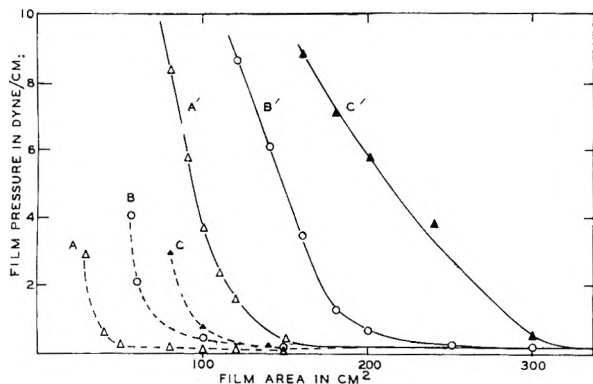


Fig. 1.—The effect of surface contamination on film pressure-area plots of trypsin. The dashed curves, A, B, C, show the compression characteristics of three support solutions without enzyme. The solid curves, A', B', C', refer to the same solutions with 10% of trypsin spread on each. The initial area was 400 cm.² in all cases.

barrier; then small amounts of support solution were added and the surface reswept. This filtering and sweeping procedure gave a support solution which showed, on the average, a 0.25 dyne/cm. decrease in surface tension upon a 5:1 compression. A 5:1 compression means that a barrier was slowly moved from the end of the trough opposite the Wilhelmy plate toward the plate to decrease the area fivefold. Our criterion of not more than 0.25 dyne/cm. surface pressure upon a 5:1 compression is less exacting than that of 0.15 dyne/cm. upon 8:1 compression recommended by Bull² for force-area determinations. However, the present experiments were concerned with measurements of film pressure of relatively compressed films rather than with force-area relations initiated at very large areas.

The trypsin solutions were prepared in Pyrex which had been surface treated with a silicone (Desicote). Twice recrystallized, salt-free trypsin (Worthington Biochemical Co.) was sprinkled on the surface of 1×10^{-5} M HCl. Without stirring the solution was kept in the refrigerator for 12 hours. The pH was then adjusted to 7.6 with Veronal and the volume made up to give a 0.01% solution of enzyme. Ten-ml. portions of this solution were frozen in polyethylene vials and thawed as needed. The crystalline trypsin supply was stored at -7° , and no loss in activity was observed during the course of the work.

In the pressure-area determinations a fixed amount of protein solution was carefully placed dropwise on the surface using a Blodgett pipet delivering 0.0752 ml. In the pressure-concentration measurements variable amounts of protein solution were deposited from a 0.1-ml. graduated pipet. The enzyme concentrations were adjusted so that either one Blodgett pipet or 0.1 ml. contained 10% of enzyme. Both pipets were Desicote-treated.

B. Results

1. Effect of Surface Contamination on Pressure-Area Curves.—It is, of course, essential that the support solution be sufficiently free of contamination. Particularly, we were interested that a low degree of contamination be retained over the periods of time involved in the experiments.

Repeated sweeping of the support solution was found to be inadequate by itself, perhaps partly due to slow diffusion effects. Extended treatment with activated charcoal plus sweeping was the most successful. Our experience with polyethylene bottles as containers for the solution has been that some were inert but that others introduced surface-active contaminants.

The compression characteristics of surfaces possessing different degrees of contamination are shown in Fig. 1. Since the initial area in each case was 400 cm.², the 5:1 compression point is at 80 cm.². Dashed curve A is typical of the characteristics obtained with the standard procedure described above; dashed curves B and C resulted from inadequate charcoal treatment and either limited or no sweeping of the surface prior to the measurements. The solid curves are the result of spreading trypsin on these three surfaces at an area and for periods of time corresponding to maximal spreading.

As Bull² has pointed out, an important check is whether pressure-area behavior is independent of the amount of protein. It was found that $F-A$ plots for both trypsin and pepsin were independent over twofold increments in concentration whenever the initial spreading area exceeded 1.5 m.²/mg. and the time prior to compression was of the order of 20 minutes. We define these conditions as being compatible with maximal spreading. The results were in excellent agreement with those reported by other investigators.^{7,10} The solid curve A' in Fig. 1 is a portion of a representative $F-A$ curve obtained with the regular procedures.

2. Films Spread Over a Limited Area.—We found that films spread at large areas and then compressed had permanently lost all enzymatic activity. (The shortest length of time between spreading and compression studied was one minute). Therefore, our interest was directed to films spread over limited rather than essentially infinite areas. The film pressure, measured 5 minutes after spreading a given aliquot of protein over the fixed area of 100 cm.², is plotted against surface concentration in each of the solid curves in Fig. 2. (The reciprocal function of surface concentration—film area—is given at the top.) Although film area is the traditional measure used by surface chemists, the surface concentration is the convenient measure in the present investigation.

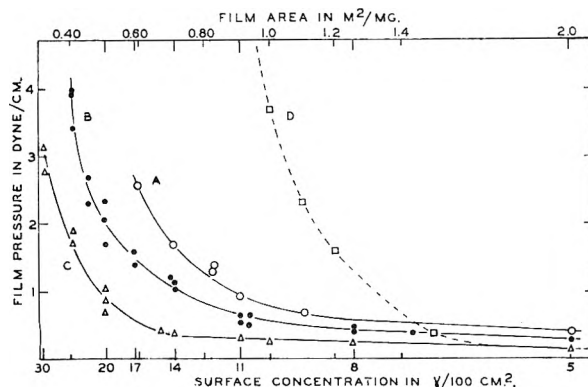


Fig. 2.—The effect of various preparation procedures on film pressure-concentration plots of trypsin. Curves A, B and C refer to enzyme on support solutions which had been adequately treated with charcoal and filtered 2 hours before use, 10 hours before use, and 48 hours before use, respectively. Solutions were refiltered just prior to use. Curve D is a typical $F-A$ curve obtained by spreading trypsin at an area greater than 1.5 m.²/mg. for 20 min., or more, before compression.

Such curves will be designated as $F-C$ plots, as opposed to $F-A$ plots. The difference lies in the conditions leading to the data: in $F-A$ plots the amount of protein is held constant and the film area is varied; in $F-C$ plots the area is held constant and the amount of protein varied. Very different film characteristics result. For example, the dashed curve D in Fig. 2 is an $F-A$ plot, being the middle portion of curve A' from Fig. 1.

(10) E. Mishuck and F. Eirich, "Monomolecular Layers," ed. H. Sobotka, A.A.A.S., 1954, pp. 14-32.

Pressure-concentration ($F-C$) plots were found to depend to an important extent upon the temperature of the support solution, age of the film, and the elapsed time from the final charcoal treatment of the support solution. The effect of elapsed time from the final charcoal treatment is demonstrated in Fig. 2. The preparation procedure adopted was the one found to minimize the film pressure for a given surface concentration (curve C). Replicate $F-C$ determinations had standard deviations as high as 10-15%. Since spreading involved the deposition of from 3 to 15 drops onto the surface and required 15-45 sec., some of this variability was no doubt due to the difficulty of reproducing the "dropwise" sequence.

3. Transitions between $F-C$ and $F-A$ Curves.—The film pressure at any given area is, in many situations, dependent upon both the spreading conditions and subsequent manipulations (expansions or compressions) made prior to the measurement. To illustrate, the behavior of a typical film of trypsin carried through a series of compressions and expansions is summarized in Table I. Step 1 consisted of spreading 22 γ of enzyme upon an area of 40 cm.². After two minutes the film was expanded (step 2) to 60 cm.² and the film pressure measured 2 minutes later. The film was then expanded (step 3) to 80 cm.² and allowed to age for 21 min. during which the pressure increased from 9.1 to 12.0 dyne/cm.

TABLE I
THE EFFECTS OF FILM MANIPULATION AND AGE ON THE FORCE-AREA CHARACTERISTICS OF A TRYPSIN MONOLAYER

Step no.	Type of manipulation	Age of film since last previous manipulation	Film area, cm. ²	Film pressure, dyne/cm.
1	Spreading		40	>16.0
2	Expansion	2	60	10.0
3	Expansion	3	80	9.1
		5	80	10.8
		10	80	11.7
		15	80	12.0
4	Compression	21	80	12.0
5	Expansion	2	70	19.5
6	Expansion	2	80	9.2
		4	100	4.0
		4	100	4.4
		8	100	4.8
7	Expansion	2	120	1.8
		4	120	1.9
		7	120	2.1
8	Expansion	2	160	0.2
		4	160	0.2
9	Compression	1	100	7.2
		2	100	7.1
		6	100	6.8
10	Expansion	2	160	0.1
		4	160	0.1
11	Compression	3	100	6.7
12	Expansion	2	300	<0.1
13	Compression	2	200	0.2
14	Compression	1	180	0.3
15	Compression	2	160	0.5
16	Compression	2	140	0.6
17	Compression	2	120	4.4
18	Compression	3	100	8.3
19	Compression	3	80	14.8
		6	80	13.8
		9	80	13.6

Additional data regarding the importance of manipulative steps are shown in Fig. 3. The data were obtained early in the study and film pressures at corresponding areas were not always measured at the same elapsed time after spreading. There is undoubtedly a very significant difference between films spread and maintained at a constant area

(open circles) and those compressed to that area (curves). There is qualitative indication that expansion to a given area from a more limited area of initial spreading (dashed curves) is not equivalent to initial spreading at the given area (solid curves).

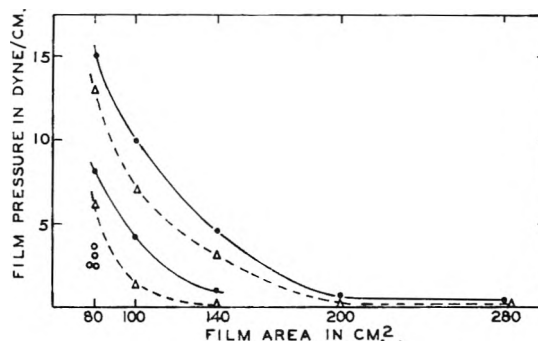


Fig. 3.—The effect on the film pressure of different film manipulations. The solid curves are for films spread and maintained for 3 min. at the maximum area shown before being compressed. The dashed curves refer to films spread for 30 sec. at 80 cm.² and then expanded to, and maintained for 3 min., at the maximum area shown before being compressed. The open circles are for 4 films spread and held at the fixed area of 80 cm.² for 5 min. In each case 15 γ of trypsin was spread.

4. Variation of Film Pressure with Time and Temperature.—Films at areas less than that required for maximal spreading show pronounced aging effects. This is demonstrated in Fig. 4. The film pressure of a film 60 min. after formation is roughly twice that of a film after 5 min. For film ages up to 100 min. the per cent. increase in F was essentially the same for all surface concentrations studied. As the film area exceeds 1.5 m.²/mg., that necessary for maximal spreading, film pressure equilibrium is quickly reached.

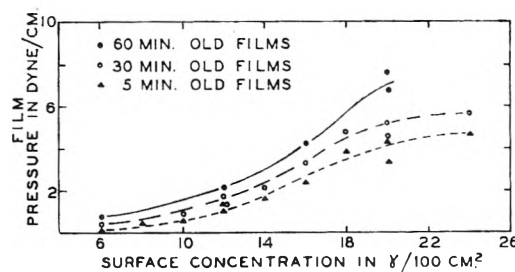


Fig. 4.—The effect of film age on film pressure-concentration plots.

It was always found that the film pressure increased for a film allowed to age at a constant area, following either spreading or expansion, and that it decreased following compression. In one series of experiments, films were allowed to age up to 75 hours to determine whether a constant film pressure would be reached. These results are presented in Fig. 5 and indicate that none of the films reached an equilibrium following either spreading or expansion within the 75-hour period, although the slopes of the aging curves became small, as shown in Curves B and C. The influence of temperature and of variations in temperature can be seen in curves A and C.

The Recovery of Enzymatic Activity

A. Experimental Methods

1. Recovery Procedures.—A successful method should permit recovery of all the film, should induce a minimum of changes in the protein entity, and should permit a quantitative determination of the enzyme activity. These several requirements are not easy to satisfy. For instance, if the film is allowed to expand during the recovery, enzyme activity will be lost; too much support solution prevents an accurate assay. Adaptations of seven methods were investigated with varying degrees of success. Thin layers of methylene blue solution were found helpful in studying the flow patterns.

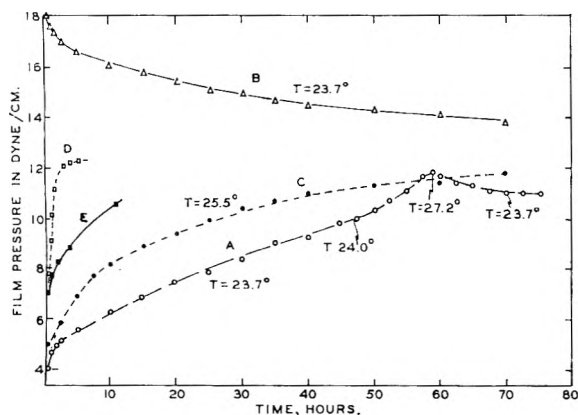


Fig. 5.—The effect of film age and temperature on the film pressure of films spread over limited areas. (A) 20γ spread and maintained at 100 cm.^2 for 75 hours under varying temperature conditions. (B) film A compressed after 75 hours to 80 cm.^2 and maintained for 70 additional hours. (C) 20γ spread and maintained at 100 cm.^2 (D) 20γ spread and maintained at 80 cm.^2 (E) film D expanded after 5 hours to 100 cm.^2 and maintained for an additional 12 hours. Curves D and E were determined at $22\text{--}23^\circ$ and the other curves at the temperatures indicated.

In Method I the film plus about 20 ml. of support solution were swept off by a barrier into a drain which ran around three sides of the trough. This method was abandoned when less than 5% of the enzymatic activity could be recovered. The film becomes partially crumpled before the overflow begins and this may be responsible.

In Method II, Gorter's⁴ silk-net procedure was modified. We used a piece of 51 denier nylon stocking stretched over a paraffined glass frame. Recovery was effected by lifting the submerged net up through the surface. It was found that at best only 20% of the activity could be recovered. Cheesman and Schuller⁷ were successful with pepsin when they substituted filter paper for a net and drained the solution down through the paper.

Method III was a modification of Rothen's ring method.³ A 60 cm.² meshwork of Chromel #22 wire was dipped horizontally into the surface of the film and then carefully withdrawn. The film enclosed by the ring was removed in a manner analogous to that used by children with soap bubbles. Variable results were obtained, probably because of turbulence.

In Method IV a 30° polyethylene funnel fitted with a drain and pinch clamp was used as a trough. The support solution partially filled the funnel. After spreading the trypsin, 10 ml. of water were carefully layered on the surface of the solution. The funnel was slowly drained with the last 25 ml. of the volume being diluted to 100 ml. with water. When 14γ of trypsin were spread on 100 cm.^2 for three minutes, up to 50% of the activity could be recovered. However, the variability for six samples ran about 30%. There were difficulties in sweeping and in carrying out manipulations of the film in the funnel.

The principle of Method V was to transfer the insoluble protein film over onto the surface of a second solution in which the film was soluble. One basin of the trough held the collecting solution and was separated by a paraffined, knife-edge barrier from the spreading basin. To recover the film, paraffined covers were slid on so as to raise the level of the film-covered solution and to cause the two solutions to coalesce. Then, upon sliding the barrier the film was transferred over onto the collecting solution, dissolving as it did so. When 14γ of trypsin was spread on 80 cm.^2 for 2 to 4 minutes and was swept into 23% sucrose (if the densities of the two solutions were different, strong convection currents occurred over the edge of the knife-edge) it was possible to recover from 40 to 67% of the activity. This method was eventually abandoned because, in the final step of the recovery, variable concentrations of sulfate were collected and these adversely affected the assays.

The idea in Method VI was to transfer the film and a thin layer of support solution over onto a flat paraffined surface using movable barriers which were latched together to keep

the area constant. The film and the 40 ml. of accompanying support solution were then diluted and collected for assay. When 14γ was spread over 80 cm.^2 for three minutes it was found that $60 \pm 3\%$ of the activity was recoverable. Occasionally, trouble was encountered due to an incomplete seal between the solution isolated on the catch shelf and that in the spreading basin.

In Method VII the surface concentration was controlled in most of the experiments by varying the amount of protein spread on a fixed area of 100 cm.^2 . The spreading basin was $10 \times 10 \times 0.43\text{ cm.}$ Starting with 60 ml. of support solution, a double sweeping reduced the volume to 43 ml. (This was the minimum amount which would always cover 100 cm.^2 of paraffined surface without drawing into islands.) After the protein had been spread, a $10 \times 10\text{ cm.}$ framework was placed on the trough to convert the spreading basin into a 2 cm. deep recovery basin. Then 100 ml. of water were added; draining, rinsing, and assay followed. When 17.5γ was spread for three minutes, $52 \pm 5\%$ of the activity was recovered. This method was adopted because of the following desirable features: (1) the whole film is unequivocally recovered without having undergone additional compression or expansion effects; (2) danger of film leakage around a movable barrier is eliminated; (3) chance contamination or dilution of the support solution is avoided; (4) the reproducibility of the procedure, as evidenced by the assay results, is good; (5) the operations are simple; (6) a sufficiently small amount of support solution is carried along to permit sensitive assay; (7) no adsorptive material, such as filter paper, is introduced.

2. Assay.—This is complicated by several factors. A very small amount of enzyme is present in a monomolecular film and only a part of that can be recovered in active form. Also, the test conditions for producing and recovering a film yield the recovered enzyme in the presence of support solution which reduces its proteolytic rate. Of assay methods described in the literature, five seemed applicable¹¹⁻¹⁴ and were tested. We found a modification of the casein turbidometric method of Chow and Peticolas¹³ satisfactory for the low specific activities being assayed.

The diluted sample from the film trough was run directly into a polyethylene bottle and further diluted with water to reduce sulfate concentration to a set tolerable level. (The digestion rate increased 8-fold when the ammonium sulfate concentration was reduced from 6 to 0.5%.) Casein-Veronal solution was added to bring the casein concentration in the final solution to 0.2% and the pH to 7.9. The casein-Veronal stock solution was a mixture of 5% casein solution, saturated Veronal, and distilled water plus a trace of phenylmercuric acetate. The casein solution was kept frozen and samples were thawed as needed. Before use the casein-Veronal solution was shaken at least three times vigorously enough to produce a large amount of surface foam, followed by vacuum filtration.

The enzyme-substrate solution was allowed to stand for 15 minutes after which the nephelos was determined. This was designated as the zero reading, N_0 . At least two subsequent readings were made on each sample some 3-4 hours apart and somewhere between 12 and 24 hours after the zero reading. The value of $-\log N/N_0$ is used as the index of digestion (in plotting, $100 \log N_0/N$ is used for convenience). For the turbidity determinations, 5-ml. aliquots of the solution and 5 ml. of 5% trichloroacetic acid were mixed. After 10 minutes the reading was taken on a Coleman nephelometer.

The amount of digestion was converted into the per cent. of the activity recovered from the film as compared to the same amount of enzyme which had not been spread. To accomplish this it was necessary to determine the relationship between the amount of digestion and quantity of original (unspread) protein by assaying, concurrently with the recovered samples, a series of dilutions of the stock enzyme solution. The two series of solutions, that is from the film trough and from stock, were similar in all possible respects, such as time, temperature and composition of the solutions. The only difference was that the one had been

(11) D. Mazia and G. Blumenthal, *J. Cell. Comp. Physiol.*, **35**, suppl. 1, 171 (1950).

(12) R. Tomarelli, J. Charney and M. Harding, *J. Lab. Clin. Med.*, **34**, 428 (1949).

(13) B. Chow and M. Peticolas, *J. Gen. Physiol.*, **32**, 17 (1949).

(14) M. Anson, *ibid.*, **22**, 79 (1939).

spread, while the other stood in solution nearby. In each set of experiments both series were run.

For assaying low levels of activity it is imperative that a container be used whose walls will not absorb the enzyme. For instance, we let 50 ml. of 0.001% trypsin solution stand in a Pyrex flask for 15 min. and then rinsed four times with distilled water. A residual activity corresponding to 9 γ of trypsin was found, *i.e.*, if a blank assay was run in the flask, casein was digested as if 9 γ of trypsin was present.¹⁵ The residual activity could be removed with fuming nitric acid. On the other hand, a container which was not wet by the enzyme solution had a residual activity, following quadruple rinsing with distilled water, of about 0.2 γ . Two such containers were tested, a Pyrex bottle treated with Desicote and a polyethylene bottle.

Although the residual activities following rinsing were the same for the silicone-treated glass and polyethylene bottles, the reaction rates of identical solutions in these containers were not. Relative rates found for bottles with different surfaces were

Untreated Pyrex	1.
Silicone-treated Pyrex	1
Polyethylene	1/3 to 1/5
Paraffined Pyrex	1/6
Paraffined polyethylene	1/6

B. Results on Recovery of Activity

1. **Effect of Surface Concentration and Film Pressure.**—In Fig. 6 are presented typical data on recovery. In both A and B, films were spread for 5 min. It can be seen that

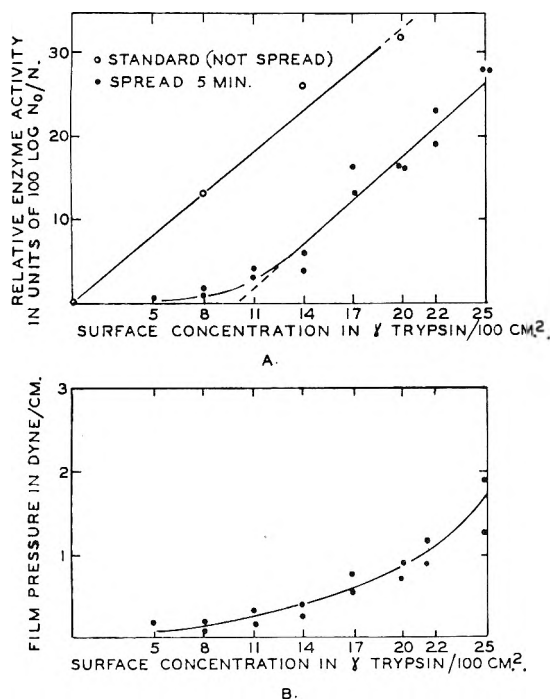


Fig. 6.—A, relation of surface concentration to the amount of recoverable activity; B, force-concentration characteristics of films shown in A.

the amount of activity which can be recovered after 5 min. is very small when the surface concentration is 10 γ /100 cm.² (1.0 m.²/mg.) or less. However, apparently the amount of protein spread in excess of 10 γ is all recoverable providing recovery occurs soon after spreading. The film pressure associated with 10 γ /100 cm.² is seen, in Fig. 6B, to be 0.25 dyne/cm. These results have been repeated in

(15) Nine micrograms adsorbed uniformly over the glass area of 52 cm.² in contact with 50 ml. of solution would correspond to close-packed spheres of 22.0 Å. diameter. This value is midway between the thickness of an extended polypeptide chain and the diameter of 43.2 Å. given by Moelwyn-Hughes¹⁶ for the trypsin molecule.

(16) E. Moelwyn-Hughes, "The Enzymes," Vol. I, Part I, ed. J. B. Sumner and K. Myrback, Academic Press, New York, N. Y., 1950, p. 34.

several experiments with the two parameters, 10 γ /100 cm.² and 0.25 dyne/cm., varying 10 and 30%, respectively.

2. **Effect of Film Age.**—The results presented in Fig. 6 were obtained when the film was recovered precisely 5 minutes after spreading began. One of the two studies on the effect of the age of the film on the recoverable activity is shown in Fig. 7. The activity is seen to decrease as the

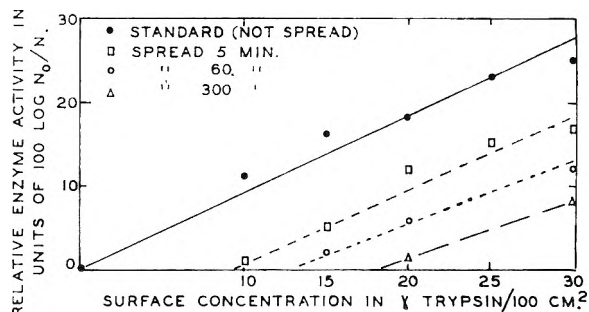


Fig. 7.—Effect of age of film on recoverable activity.

age of the film increases. Further, this decrease is nearly independent of surface concentration (and thus film pressure), so long as the concentration is higher than the minimum amount required for the maintenance of activity. It appears that a given amount of enzyme has become inactivated after any particular spread time. Actually there is slightly less absolute loss at high concentrations than at low, but the difference is small. The data from Figs. 6 and 7, plus comparable data from other experiments have been pooled in Fig. 8 to show the limits of the rela-

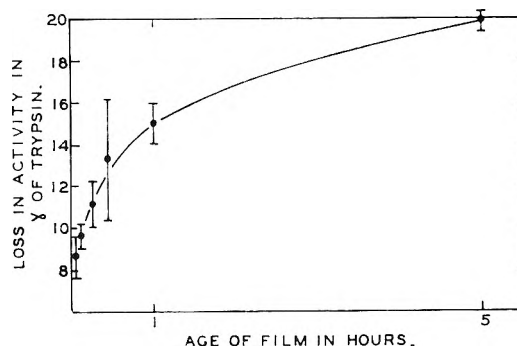


Fig. 8.—Loss of trypsin activity as a function of the age of the film.

tionship between film age and loss of activity. For example, if 40 γ /100 cm.² is spread for 5 minutes, about 30.5 γ of active enzyme can be recovered, whereas, if it is spread for 5 hours about 20 γ of active enzyme can be recovered. Since the data shown in Fig. 8 were obtained at temperatures ranging from 22.2–25.6°, it appears that the loss of activity with time is relatively insensitive to differences in temperature in this range.

Discussion

The results presented on surface contamination may serve to emphasize some of the complications in film studies while furnishing a quantitative basis for the present work. It can be seen from Fig. 1, that as the total amount of surface contamination increases relative to the amount of spread material, both the area of spreading and the shape of the *F-A* curves change. This means that the contaminants react in such a manner as to increase the total amount of material in the film and that the compression characteristics of the contaminants are different from those of the protein. The time dependence associated with the charcoal treatment of the support solution (Fig. 2) remains unexplained. It was readily reproducible and was

apparently some aging process which did not change the pH by more than 5% or the amount of measurable surface contamination by more than 20% (as determined by compression measurements.)

Factors like the above have significance in monomolecular film work and it is, therefore, desirable that workers give information on the condition or characteristics of their "clean" surfaces. Such information is very valuable; at the least it serves to establish the degree of refinement of the work being reported.

Several methods are available for the recovery of protein films. Of those compatible with retention of enzymatic activity, we feel that Method VII has certain distinct merits. Since the entire film is collected, variability, which might result from recovery of certain portions of non-homogeneous films, is avoided. For example, a ring method^{3,5} might give non-representative samples in case the activity was not uniformly distributed over the surface or, again, if the adhesional probabilities of active and inactive portions were different for the glass or metal surfaces used in the collection procedures.¹⁷⁻¹⁹

The method of recovery based upon compression of mixed enzyme-substrate films^{6b,6c,11} has a number of undesirable features. First, thread formation involves a very drastic manipulation of the film. Second, the assay is based upon autolysis of the thread so that only mixed enzyme-substrate films are suitable. However, the most serious objection is that the threads can only be formed by proceeding through the sequence of film steps and thus the absolute amounts of activity lost in spreading and manipulation cannot be determined.

In the net method^{4,7} there is the possibility that enzyme will pass through. Also Cheesman and Schuller found that it was not possible to redissolve pepsin from the filter paper—this complicated the assay kinetics and the interpretation of the results. The net method has the advantage that the assay requires an hour or so instead of a day as in our method.

Mention has been made of wall induced effects. Trypsin undergoes strong adsorption onto glass and the proteolytic activity was found to be very difficult to remove. Silicone treatment appeared to minimize this direct adsorption. However, surprisingly, differences in digestion rates were observed which were not affected by silicone treatment. Possible explanations for the differences between polyethylene bottles were considered: the reaction rate might be affected by the total area of the interface between solution and polyethylene or the reaction could be light sensitive since the rate seemed to drop in relation to the opacity of the container wall. However, both the interfacial area and the ambient light were varied by factors of two with no significant change. The only known difference between polyethylene bottles was the period of usage—perhaps impurities or low molecular weight components leach out.

(17) F. Hutchinson, *Rad. Research*, **1**, 43 (1954).

(18) I. Langmuir and V. Schaefer, *Chem. Revs.*, **24**, 181 (1939).

(19) H. Sobotka and E. Bloch, *J. Phys. Chem.*, **45**, 9 (1941).

There is general agreement that protein molecules spread at areas greater than 1.5 m.²/mg. completely unfold and yield so-called gaseous films which in most cases reach equilibrium within a few minutes.² Here, our results with trypsin are in good agreement with those of Mishuck and Eirich.¹⁰

On the other hand, compressed, or limited area, films behave in a different and more complex manner.^{2,20} Comparison of *F-A* and *F-C* plots, curves C and D of Fig. 2, illustrates the two types of trypsin films. The dependence of the film pressure upon film manipulation and time are brought out in Table I. A series of compressions and expansions between two fixed areas (steps 8-9-10-11) yielded film pressures which appeared to be quite reproducible from cycle to cycle. However, when the film was expanded to a greater area (step 12), a new set of higher film pressures was found upon recompression (steps 13 through 18). Once the film was expanded and allowed to stand at an area exceeding 1.5 m.²/mg. for 20-30 minutes, the typical *F-A* plot was obtained (steps 13 through 19). The importance of prior manipulation is demonstrated in Fig. 3. All these data are consistent with the view that each new increment of area permits an additional fraction of protein to unfold in a manner that is irreversible within the limits of these experiments.

We have pointed out that there is a transition between the two types of films. We interpret this to involve a shifting ratio of folded to unfolded molecules. In the *F-A* type film the initial spreading at essentially infinite area allows all the molecules in the film to unfold completely. However, in spreading at a limited area we believe that the first molecules deposited unfold and provide a protective film pressure so that additional protein does not unfold, but rather remains in its globular configuration and retains enzymatic activity. Any subsequent expansion to a larger area allows more of the globular molecules to unfold.

The possibility that unfolding is not instantaneous, but rather requires considerable time, would account for the aging effects following spreading or expansion. Bull² suggests that following compression a dehydration of the film and a change in the orientation of the amino acid residues occur which would produce a gradual decrease in pressure.

Cheesman and Schuller⁷ have reported *F-C* and *F-A* plots and also aging effects for pepsin films. Our results with trypsin are in general agreement. These workers felt that only unfolded protein exists in the topmost layer of the surface and that a native molecule which moves into this surface from the bulk solution unfolds in the process and loses its activity. We do not feel this to be the case; rather we believe that globular and unfolded species coexist in the plane of the film. However, a discussion of this will be deferred to the third paper of this series.

A surface concentration of 10 γ /100 cm.² produces a film pressure of about 0.25 dyne/cm. This appears to be the approximate value of the protective pressure necessary for the maintenance of

(20) M. Joly, *Biochim. Biophys. Acta*, **2**, 624 (1948); *J. Phys. Radium*, **11**, 171 (1950).

trypsin enzymatic activity since essentially no activity can be recovered from films having a lesser concentration, whereas the protein spread in excess of 10γ is all recoverable from films which have been spread briefly. However, this pressure is not completely effective in maintaining activity since the recoverable activity decreases with film age. This decrease is nearly independent of surface concentration (and thus film pressure). It appears that a characteristic amount of enzyme becomes inactivated during a given time interval. Bull²¹ has suggested that microscopic ripples may be produced in the film from building vibration. Since these ripples might be points at which expansion could occur under non-equilibrium conditions, there might result an unfolding that was independent of film pressure.

DISCUSSION

HENRY L. CRESPI (Argonne National Laboratory).—Have you considered the possibility that the loss of activity with increasing film age may be due to autolysis?

B. ROGER RAY.—Yes, in fact acetylated trypsin has been obtained from Worthington Biochemical Co. to determine whether trypsin which has been modified to prevent autolysis²² still loses activity with increasing film age. Although this possibility is being investigated it is doubtful whether it is an important factor. If it were, the autolytic rate should be a function of the concentration of active material and thus the loss in activity should be proportional to the surface concentration. This was not observed.

(21) Personal communication.

(22) Worthington Biochemical Co., Descriptive Manual No. 8.

F. HAUROWITZ.—In my experiments involving liquid-liquid systems, I came to the conclusion that most of the proteins tested remained globular in the high-pressure range when adsorbed at a water-xylene interface. What evidence do you have that your films were a mosaic of unfolded and globular protein rather than a film of globular molecules, each of them coated by an expanded protein film?

B. R. RAY.—The main evidence indicating that our viscous films were a mosaic of globular and unfolded protein in the plane of the surface, as opposed to the type of film you suggest or some form of duplex film,⁷ is obtained from a comparison of F-C and F-A plots. Such an analysis will be presented in detail in paper III of this series but can be summarized as follows: In a completely expanded film (F-A type) an increase in film pressure is produced when the surface concentration is increased by mechanical compression of completely unfolded molecules; whereas, an increase in the film pressure of our viscous films (F-C type) is produced when the surface concentration is increased by the addition of more protein. According to our interpretation, protein added above a critical amount remains globular and in the plane of the surface. Since the surface area (and thus the "compression efficiency") of a spherical molecule of molecular weight 36,000 is $\frac{1}{4}$ that of the same molecule completely unfolded and having the thickness of an extended polypeptide chain, one would predict that it should require four times as many globular molecules as unfolded molecules to produce equal increments in the film pressure. Using the data between 1.0 and 3.0 dyne per cm., presented by Cheesman and Schuller,⁷ a ratio of 3.1:1 is found. Using plots C and D in Fig. 2 a ratio of 4.4:1 is found. (Plot C was chosen since most of our data were collected under conditions comparable to those leading to C—although the data presented in Fig. 4 were obtained under conditions more compatible with B.) Since a number of factors, such as non-spherical molecules or unequal compressibilities for spherical and completely unfolded molecules, would yield ratios different than 4:1, those of 3.1:1 and 4.4:1 seem to be reasonably consistent with our model of a mosaic film.

ELECTROPHORESIS OF POLYPEPTIDYL PROTEINS¹

BY HAROLD VAN KLEY AND MARK A. STAHMANN

*Department of Biochemistry, University of Wisconsin, Madison, Wisconsin**Received February 24, 1956*

Changes in the electrophoretic mobility of bovine albumin and rabbit albumin after modification by the chemical attachment of polypeptides of leucine, phenylalanine, lysine and glutamic acid are reported. Some interpretations of the results and possible application of polypeptidyl proteins to physical chemical studies are discussed.

Electrophoresis provides a convenient tool for studies which concern changes in the ionic groups of a protein. This study will report changes in the electrophoretic mobility of proteins caused by the addition of amino acid residues in the form of polypeptides to the protein.

The preparation of soluble polypeptidyl proteins was developed by Stahmann and Becker² who ran reactions of N-carboxyamino acid anhydrides with proteins in buffered aqueous solution. Several other preparations of polypeptidyl proteins and viruses have been reported.³⁻⁷ This reaction yields a protein containing new amino acid residues attached through peptide bonds to the α and ϵ -amino groups of the original protein.^{2,3}

Many methods are available for modification of proteins,⁸ most of which result in a change in the functional groups of the protein. A desirable modification for biological and electrophoretic studies would be the addition of charged groups without the introduction of a foreign constituent or a type of bonding not found in the native protein. Green and Stahmann⁴ prepared polyglutamyl bovine albumin by mild alkaline hydrolysis of poly- γ -ethylglutamyl bovine albumin; however, electrophoretic analysis of a control sample of bovine albumin after exposure to the conditions used in the hydrolysis showed about 90% of the protein migrated at a changed mobility so that interpretation of their results is uncertain. A recent development⁷ has made possible the preparation of proteins modified by the addition of the ionic amino acids, glutamic acid and lysine, under such mild conditions that all changes in the properties of the modified protein may be attributed to the added amino acids.

Electrophoretic studies were made on bovine and rabbit serum albumins modified with polypeptides of the neutral amino acids L-leucine and DL-phenylalanine, and with the ionic amino acids L-lysine and L-glutamic acid. Preliminary observations on the electrophoretic behavior of the latter materials have been reported.⁷ This communication will present in more detail the electrophoretic results

and some interpretations which may be derived from them.

Experimental

Preparation of Polypeptidyl Proteins.—The polypeptidyl proteins were prepared by treating the protein with the N-carboxyamino acid anhydrides in bicarbonate buffer at 4° as described by Tsuyuki, Van Kley and Stahmann.⁷

Preparation of Samples for Electrophoresis.—An approximately 1% (w./v.) solution of the lyophilized protein was dissolved in 0.1 ionic strength buffer and dialyzed overnight with agitation against two changes of the same buffer.

Electrophoretic Analysis.—Electrophoresis measurements were made with a Spinco Model H Electrophoresis-Diffusion Apparatus. The experiments were conducted in a 1.8-ml. capacity quartz micro Tiselius cell equipped with Alberty electrodes at a bath temperature of 2.0°. Conductivity measurements were made at 0° in a No. 033-0081 electrolytic conductivity cell (Perkin-Elmer Corp., Norwalk, Conn.) using a L. and N. Portable Conductivity Bridge.

Calculation of Mobility.—Measurements of the distance of migration were made on the descending limb,⁹ measuring the distance moved by the first moment of the boundary curve. The first moment was the maximum gradient for symmetrical boundaries; the method of Alberty¹⁰ was employed for non-symmetrical boundaries. The mobility was calculated from the plot of distance migrated in cm. vs. time in seconds; the slope, which is the product of the mobility (u) and the field strength (E), was calculated by the method of least squares.¹¹ From the known field strength the mobility was calculated.

Results and Discussion

Electrophoresis experiments on each protein preparation were carried out at the pH expected to give the most significant mobility change. The results of some of the electrophoretic studies are summarized in Table I.

Proteins modified with polypeptides of neutral amino acids were studied at pH 8.6 where the substitution of an α -amino group for the ϵ -amino group of lysine would be most apparent. The intrinsic pK of the α -amino group in bovine albumin is reported to be 7.75¹² while that of the ϵ -amino group is given as 9.8. A pH intermediate between these values would produce a decreased number of ionized amino groups in a polypeptidyl protein compared to the original protein where all the ϵ -amino groups are free. The native protein migrates as an anion at this pH; a decrease in the number of positively charged amino groups was reflected in an increase in the mobility as an anion. Poly- γ -ethylglutamyl bovine albumin showed a 9% increase in mobility over the unmodified albumin at pH 8.6 in sodium veronal buffer,⁴ a similar

(1) Published with the approval of the Director of the Wisconsin Agricultural Experiment Station. Supported in part by a research grant (No. E-101) from the National Microbiological Institute of the National Institutes of Health, United States Public Health Service, and the Herman Frasch Foundation.

(2) M. A. Stahmann and R. R. Becker, *J. Am. Chem. Soc.*, **74**, 2695 (1952).

(3) R. R. Becker and M. A. Stahmann, *J. Biol. Chem.*, **204**, 745 (1953).

(4) M. Green and M. A. Stahmann, *ibid.*, **213**, 259 (1955).

(5) H. Fraenkel-Conrat, *Biochem. Biophys. Acta*, **10**, 180 (1953).

(6) M. Sela, *Bull. Res. Council of Israel*, **4**, 109 (1954).

(7) H. Tsuyuki, H. Van Kley and M. A. Stahmann, *J. Am. Chem. Soc.*, **78**, 764 (1956).

(8) F. W. Putnam in H. Neurath and K. Bailey, "The Proteins," Vol. I. Part B, Academic Press, Inc., New York, N. Y., 1953.

(9) R. A. Alberty in H. Neurath and K. Bailey, "The Proteins," Vol. I, Part A, Academic Press, Inc., New York, N. Y., 1953.

(10) R. A. Alberty, *J. Chem. Education*, **25**, 426 (1948).

(11) K. Mather, "Statistical Analysis in Biology," Methuen and Co., Ltd., London, 2nd. Ed., 1946.

(12) C. Tanford, S. A. Swanson and W. S. Shore, *J. Am. Chem. Soc.*, **77**, 6414 (1955).

TABLE I
ELECTROPHORETIC MOBILITY OF POLYPEPTIDYL PROTEINS^a

Protein	Moles amino acid added per mole protein	% increase in amino acid content	pH	Buffer	Mobility $\times 10^5$ cm. ² v. ⁻¹ sec. ⁻¹ in	% change in mobility
Bovine albumin	5.3	Acetate	-2.10	..
Bovine albumin	6.3	Cacodylate	-2.51	..
Bovine albumin	7.5	Tris chloride	-4.80	..
Bovine albumin	8.6	Veronal	-6.37	..
Rabbit albumin	5.3	Acetate	-1.68	..
Rabbit albumin	8.6	Veronal	-6.56	..
Poly-L-leucyl bovine albumin	49	75	8.6	Veronal	-6.92	9
Poly-L-leucyl rabbit albumin	..	59	8.6	Veronal	-7.22	10
Poly-DL-phenylalanyl bovine albumin	42	175	8.6	Veronal	-7.71	21
Poly-DL-phenylalanyl rabbit albumin	..	184	8.6	Veronal	-7.81	19
Poly-L-lysyl bovine albumin	14	23	7.5	Tris chloride	-4.79 ^b	0
Poly-L-lysyl bovine albumin	14	23	7.5	Tris chloride	-4.32 ^c	10
Poly-L-glutamyl bovine albumin	74	95	5.3	Acetate	-4.87	132
Poly-L-glutamyl bovine albumin	277	355	5.3	Acetate	-8.90 ^c	324
Poly-L-glutamyl bovine albumin	277	355	6.3	Cacodylate	-9.79	290
Poly-L-glutamyl rabbit albumin	..	282	5.3	Acetate	-6.88	314

^a Ionic strength = 0.1 in all cases. ^b Mobility of maximum gradient of the curve. ^c Mobility of the first moment of the curve.

mobility change was noted for poly-L-leucyl albumin in these studies. A much greater mobility increase (21%) was noted for poly-DL-phenylalanyl bovine albumin although the number of moles of amino acid added per mole of protein was approximately the same as in the poly-L-leucyl albumin. Rabbit serum albumin modified with these same two amino acids showed a similar difference. The abnormal mobility change for poly-DL-phenylalanyl bovine albumin is being investigated further.

All of the polypeptidyl proteins prepared by the addition of neutral amino acids migrated with a single symmetrical boundary under the conditions tested. Immuno-electrophoresis¹³ gave a single arc of precipitate indicating a high degree of homogeneity in the modified proteins.¹⁴

Electrophoretic patterns for polylysyl proteins showed a tailing of the moving boundary indicating that the addition of lysine residues was not uniform among all the protein molecules modified. The reaction with the anhydride is initiated by the nucleophilic amino groups; the addition of new ϵ -amino groups to the protein would introduce more such groups so that further reaction with the protein molecules which initially react is favored. The heterogeneity of the polylysyl proteins precludes their application in studies where uniformity of the samples is a major criterion.

A quite uniform product was indicated for the polyglutamyl proteins suggesting that these products may be excellent experimental material for a variety of applications. The spreading of the moving boundary was a little greater than for the unmodified protein but the boundary remained quite symmetrical. Immuno-electrophoresis confirmed these observations. The sample with a 95% increase in glutamic acid content gave a symmetri-

cal boundary in pH 5.3 acetate buffer while the sample with a 355% increase did not give a symmetrical boundary at pH 5.3. However, at pH 6.3 a symmetrical boundary was obtained. This may be due to a non-uniform ionization at pH 5.3 of a part of the large number of glutamic acid residues in the latter preparation.

The polyglutamyl proteins appear to be excellent materials for studies on the relationship between charge and electrophoretic mobility. It is possible to determine the number of added carboxyl groups by an independent analysis for the glutamic acid content of the modified proteins and to then estimate the contribution of each added carboxyl group to the mobility increase under identical conditions of pH, buffer and ionic strength. The mobility increase observed for the polyglutamyl bovine albumin was much lower than that which would follow from the relationship of charge to mobility reported by Longworth and Jacobsen¹⁵ which was based on titration data. These results would suggest that this relationship is not applicable to such large changes in mobility or to such highly charged proteins where the initial ionization of some of the ionic groups may suppress subsequent ionization.

Proteins modified with ionic amino acid residues are a unique type of polyelectrolyte which may be useful for many physical chemical studies. A small or a large net charge may be added to the protein and the change in physical properties observed and compared to those of the unmodified protein under the same conditions. These polypeptidyl proteins may also be used for comparison with proteins which normally carry a high net charge and exhibit abnormalities in behavior due to this charge.

Acknowledgment.—The materials used in this study were made available through the cooperation of Dr. H. Tsuyuki.

(13) P. Grabar and C. A. Williams, Jr., *Biochim. Biophys. Acta*, **17**, 67 (1955).

(14) M. A. Stahmann, H. Tsuyuki, K. Weinke, C. Lapresle and P. Grabar, *Compt. rend. l'acad. sci. (France)*, **241**, 1528 (1955).

(15) L. G. Longworth and C. F. Jacobsen, *THIS JOURNAL*, **53**, 126 (1949).

VISCOSITY OF DILUTE POLYVINYL CHLORIDE SOLUTION

BY MASATAMI TAKEDA¹ AND RYUICHI ENDO

Tokyo College of Science, Tokyo, Japan

Received March 5, 1956

It is shown that η_{sp}/c for a polyvinyl chloride fraction in cyclohexanone decreases linearly as the concentration is lowered from 4 to 1 g./l. and then increases as the concentration is lowered further. This increase in η_{sp}/c is well explained by the theory of Öhrn which proposes the adsorption of polymer to the wall of the capillary of the viscometer. The equation for analysis of this phenomenon is derived and using this equation the dependence of the minimum concentration of η_{sp}/c , C_{crit} , with molecular weight and temperature is discussed.

Introduction

In our previous report² some experimental results were reported in which an upturn in η_{sp}/c with decreasing concentration of polyvinyl chloride was indicated. We carried out further experimental study of this unexpected phenomenon in viscometric behavior of dilute solutions of the non-electrolyte polymer. In the course of our study, Streeter and Boyer³ reported the same tendency on the curve of η_{sp}/c vs. concentration of polystyrene and they ascribed this phenomenon to an expansion of the individual coil in very dilute solution. However, recently Öhrn⁴ showed that the anomalous dilute solution data are well explained by an adsorption of polymer on the wall of the capillary. In this paper several experimental results in the viscometric behavior of polyvinyl chloride solution are reported and some considerations are given according to Öhrn's point of view.

Experimental Part

We used Ubbelohde's viscometer with a capillary of 0.27 mm. in radius and 12.15 cm. in length. Flow time for cyclohexanone was 824 ± 0.1 second at 30°.

We also used the double capillary viscometer according to Öhrn and it has radii of 0.22 and 0.6 mm.

The constant temperature bath was kept within the deviation of $\pm 0.002^\circ$ at 15–30° and $\pm 0.01^\circ$ at 50–60°.

The solutions were made by two different methods. In method A all solutions are prepared by dissolving weighed polyvinyl chloride in cyclohexanone at 90° for 3 hr. The volume change during this time due to evaporation of the solvent from closed flask was corrected by adding new solvent to that flask in a constant temperature bath of 20°. In method B concentrated solutions which were made by method A are diluted by pipetting this solution into pure solvent.

Fractions of polyvinyl chloride used in this experiment are fractionated from industrial polymer. Fractions I and II were fractionated from C-46 of Mitui Chemical Co. Fractions III, IV and V were fractionated from Geon 101 of Japan Geon Co. One per cent. polymer solution in cyclohexanone was fractionated with the addition of purified methanol. Solutions of fraction I and II were made by method A and solutions of fraction III, IV and V were made by method B for measurement.

Approximate molecular weights are estimated from $[\eta]$ using the following equation

$$[\eta] = KM^\alpha \quad (1)$$

where $[\eta]$ is the intrinsic viscosity and M is the osmotic molecular weight. The values of the constants which were determined from the work of Staudinger and Härberle⁵ are $K = 7.2 \times 10^{-6}$, $\alpha = 0.925$.

(1) Fulbright and Smith-Mundt Exchange Research Scholar, 1955. Department of Chemistry and Chemical Engineering, University of Illinois.

(2) M. Takeda and E. Turuta, *Bull. Chem. Soc. Japan*, **25**, 80 (1952).

(3) D. J. Streeter and R. F. Boyer, *J. Polymer Sci.*, **14**, 5 (1954).

(4) O. E. Öhrn, *ibid.*, **17**, 137 (1955).

(5) H. Staudinger and M. Härberle, *Makromol. Chem.*, **9**, 35 (1953).

Experimental Results and Discussion

Typical results of the experiment are shown in Fig. 1.

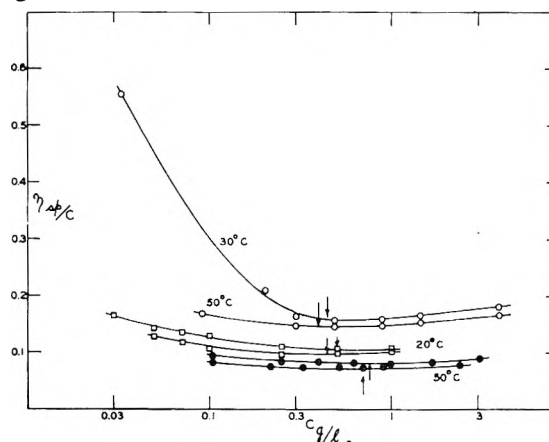


Fig. 1.—Typical results showing tendency for the upturn in η_{sp}/c plots at low concentration of polyvinyl chloride fractions in cyclohexanone. Fraction I (○); II, (●); III, (□); C_{crit} (→).

Upturn of η_{sp}/c curve increases with increasing molecular weight and decreases with increasing temperature. The minimum of η_{sp}/c curve which is called the critical concentration, C_{crit} , in Boyer and Streeter's paper⁶ is determined from the curve where η_{sp}/c is the ordinate and c is the abscissa. The values of C_{crit} are shown in Table I and on Fig. 1. C_{crit} decreases with increasing molecular weight and decreases with increasing temperature.

TABLE I
CRITICAL CONCENTRATION, C_{crit} AND THICKNESS OF THE ADSORBED LAYER OF POLYMER IN C_{crit} , $a(C_{crit})$ OF POLYVINYL CHLORIDE FRACTIONS

Fraction	Mol. wt. 10^4	Temp. of measurement, °C	$[\eta]$, l./g.	C_{crit} , g./l.	$a(C_{crit}) \times 10^3$, Å.
I	4.9	50	0.071	0.7	0.9
		20	.076	.7 ₅	1.1
III	6.6	30	.094	.5 ₅	0.9
		15	.100	.6	1.3
IV	7.0 ^{a,b}	30	.100	.8	1.9
		30	.100	.5	2.5
V	8.0 ^{a,b}	30	.115	.8	2.4
		30	.115	.5 ₅	3.1
I	10.4	50	.136	.4	1.1
		30	.145	.4 ₅	1.5

^a From the measurement of 0.22 mm. capillary. ^b From the measurement of 0.60 mm. capillary.

(6) R. F. Boyer and D. J. Streeter, *J. Polymer Sci.*, **17**, 154 (1955).

The results of experiments using the viscometer which has two different capillaries are shown in Fig. 2. It is seen that the dependence of the phe-

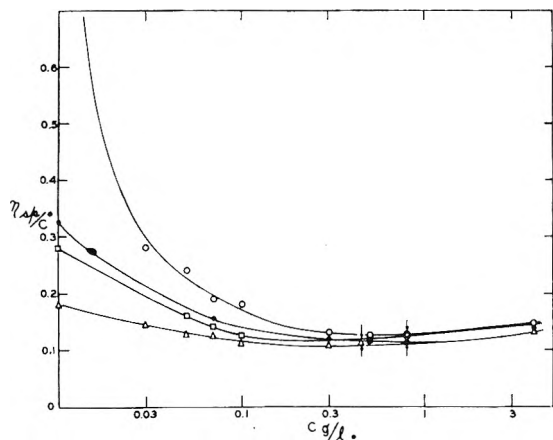


Fig. 2.—Experimental results of double capillary viscometer showing the effect of capillary size. Fraction IV, radius of capillary 0.22 mm. (●); 0.6 mm. (Δ). Fraction V, radius of capillary 0.22 mm. (○); 0.6 mm. (□). C_{crit} (→), 30°.

nomena on capillary size is very striking and these results are very similar to Öhrn's experimental results. Considering the adsorption of polymer, Öhrn derived the following equation.

$$\eta_{sp}^*/c = \eta_{sp}/c + 4a(c)(\eta_{sp}/c + 1/c)/r \quad (2)$$

where η_{sp}/c is the true value, η_{sp}^*/c is the observed value, $a(c)$ is the thickness of the adsorbed polymer at some concentration and r is the radius of the capillary.

If η_{sp}/c is negligible to $1/c$, equation 2 becomes

$$\eta_{sp}^*/c = \eta_{sp}/c + 4a(c)/cr \quad (3)$$

In Fig. 3 the agreement of experimental results with equation 3 is shown. In Table II we give the

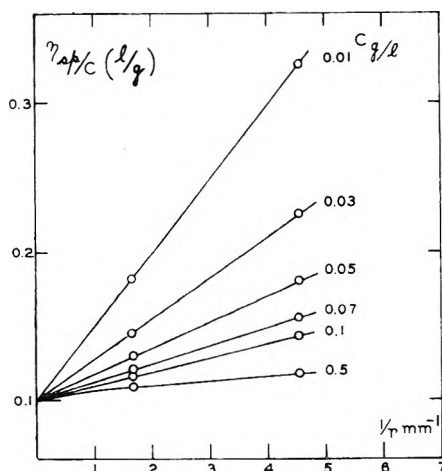


Fig. 3.—Relation of observed η_{sp}/c to $1/r$ at various concentration; fraction IV, 30°.

values of $a(c)$ calculated from the slope of the line in Fig. 3 and $a(c)$ of fraction V which are obtained by the same analysis.

These results suggest that the general applicability of adsorption correction for the treatment of

TABLE II
THICKNESS OF THE ADSORBED LAYER OF POLYMER, $a(c)$ AT VARIOUS CONCENTRATION

Concn., g./l.	Fraction IV, $a(c) \times 10^3, \text{Å.}$	Fraction V, $a(c) \times 10^3, \text{Å.}$
0.01	1.40	1.84
.03	2.06	2.65
.05	2.20	3.20
.07	2.11	3.19
.1	2.31	3.31
.5	1.92	2.20

viscosity of dilute polyvinyl chloride solution. Huggins⁷ presented the following equation

$$\eta_{sp}/c = [\eta] + k' [\eta]^2 c \quad (4)$$

where $[\eta]$ is intrinsic viscosity and k' is an independent constant from molecular weight.

When this equation is combined with equation 2, we obtain

$$\eta_{sp}^*/c = ([\eta] + k' [\eta]^2 c) (1 + 4a(c)/r) + 4a(c)/rc \quad (5)$$

From this equation we can derive the relation between C_{crit} and other quantities. From the definition of C_{crit} , it is clear that

$$(\partial \eta_{sp}^*/c / \partial c)_{c \rightarrow C_{crit}} = 0 \quad (6)$$

If we combine equation 5 with 6, and assume that $a(c)$ is a constant $a(C_{crit})$ near C_{crit} for simplicity, we obtain

$$k' [\eta]^2 (1 + 4a(C_{crit})/r) - 4a(C_{crit})/rc^2 = 0 \text{ at } c = C_{crit} \quad (7)$$

Now we consider $1 \gg 4a(c)/r$, equation 7 becomes

$$a(C_{crit}) \doteq 1/4 k' [\eta]^2 C_{crit}^2 \quad (8)$$

From equation 8 we can estimate the thickness of adsorption at C_{crit} , $a(C_{crit})$ from the observed value of C_{crit} and $[\eta]$. Using this method $a(C_{crit})$ are calculated and shown in Table I. The agreement of $a(C_{crit})$ for sample IV and V with the value of $a(c)$ near C_{crit} in Table II is not bad. In this calculation we used the value of 0.52 as k' from Breitenbach, Forster and Renner's work.⁸ It is seen that equation 8 can cover the observed dependence of C_{crit} with molecular weight and temperature, if we assume reasonable $a(C_{crit})$ values. However, $a(C_{crit})$ value for sample I is about $1/3$ of $a(c)$ value in lower concentration which was roughly estimated from experimental value of η_{sp}/c in Fig. 1. Even if we consider the tendency of slight decrease of $a(c)$ in higher concentration which is seen in Table II, this disagreement is too large and it might be due to too simple assumption of $a(C_{crit}) = \text{const.}$

Boyer and Streeter⁶ suggested that C_{crit} might be increasing with increasing molecular weight, if $a(C_{crit})$ increases with increasing molecular weight. However, this is not always true, from equation 8

$$C_{crit}^2 \propto a(C_{crit}) / [\eta]^2$$

and from equation 1

$$[\eta] \propto M^\alpha$$

(7) M. L. Huggins, *J. Am. Chem. Soc.*, **64**, 2716 (1942).

(8) J. W. Breitenbach, E. L. Forster and A. J. Renner, *Kolloid Z.*, **127**, 1 (1952).

Therefore C_{crit} might increase with increasing molecular weight when

$$\alpha(C_{\text{crit}}) \propto M^{\beta} \quad 2\alpha < \beta$$

When $2\alpha > \beta$, we might have the decrease of C_{crit} with increasing molecular weight which is the case observed in this experiment.

Batzer⁹ found that branched polyvinyl chloride showed a maximum in η_{sp}/c at low concentration, whereas less branched polyvinyl chlorides have a

(9) H. Batzer, *Makromol. Chem.*, **12**, 145 (1954).

straight line plot in η_{sp}/c and c curve. This experiment may be explained by assuming different adsorption character of samples.

We can conclude that the adsorption theory of Öhrn is the most reliable explanation for present anomalous viscometric behavior of dilute polyvinyl chloride solutions. It is also noted that equation 5 might be useful for exact determination of $[\eta]$ from viscosity data, when the correction term due to adsorption is not negligible in higher concentrations like 1 g. \sim 2 g./l.

THE EFFECT OF CHARGE AND IONIC STRENGTH ON THE VISCOSITY OF RIBONUCLEASE¹

By JOHN G. BUZZELL² AND CHARLES TANFORD

Contribution from the Department of Chemistry, State University of Iowa, Iowa City, Iowa

Received February 24, 1956

The intrinsic viscosity of ribonuclease near its isoionic point is 3.30 cm.³/g., i.e., 0.033 dl./g. This is one of the lowest values reported for any protein, indicating that the ribonuclease molecule is very compactly folded. When the molecule acquires a charge there is only a small increase in intrinsic viscosity: the maximum values observed over the range of pH 1 to 11 lying between 3.5 and 3.6. Thus the ribonuclease particle appears to undergo no appreciable deformation when charged. The observed changes in $[\eta]$ are, however, slightly greater than those predicted by Booth for the pure electroviscous effect in solutions of charged spheres. The slopes, $d(\eta_{\text{sp}}/c)/dc$, of viscosity plots increase sharply with increasing charge (Z) and decreasing ionic strength (μ). Empirically, the equation $\eta_{\text{sp}}/c = [\eta] + (K_1 + K_2 Z^2/\mu^{3/2}) [\eta]^2 c$ fits the present data, as well as those previously reported for serum albumin, with K_1 equal to 1.9 in both cases. This value is close to that predicted by Guth and Gold for uncharged spheres.

This paper reports a study of the viscosity of aqueous solutions of the protein ribonuclease between pH 1 and pH 11, essentially the entire pH range over which this protein is stable. As in a previous similar study of bovine serum albumin,³ our major interest lies in the effect of charge and ionic strength, both on intrinsic viscosity and on the further increase in specific viscosity with concentration. The principal difference between ribonuclease and serum albumin is that the former behaves as an essentially undeformable solid particle throughout its range of stability, whereas serum albumin does so only between pH 4.3 and 10.5.

Experimental

Ribonuclease.—Crystalline ribonuclease, of bovine origin, lots 381-059 and 381-062, was obtained from Armour and Co. The two lots used differ in the relative content of the two major chromatographic components. The difference between these components, however, is only the substitution of a free carboxyl group for an amide group⁴ and the physical properties appear to be unaffected by this difference, except that there is a small difference in the charge-pH relationship. No experimentally significant difference between the two lots used could be detected in the present study.

The protein was dissolved in water and the solutions were passed down an ion-exchange column of the type designed by Dintzis⁵ for serum albumins. The resulting stock solutions were assumed salt-free and isoionic. Their protein

content was determined by drying to constant weight at 107°.

The more concentrated solutions used for viscosity measurement were prepared from such stock solutions by addition of appropriate amounts of standard HCl, KOH, KCl and conductivity water. The more dilute solutions were usually prepared by weight dilution of more concentrated solutions. All solutions were filtered through fritted Pyrex glass funnels immediately before determination of their viscosities.

Measurement of Density and Viscometer Flow Time.—The viscosity is determined from measurements of flow time in a capillary viscometer and of density in a pycnometer. All measurements were made at 25.0°. The apparatus used and the procedure for measurement were the same as previously described for serum albumin.³ Two modifications of the procedure were found desirable. (1) It was found that viscometers were more difficult to clean after use with ribonuclease than they had been after use with serum albumin. Hot concentrated HNO₃ was found to be the most effective cleaning agent, and was used in place of the sulfuric acid-dichromate solution employed in the work with serum albumin. (2) It was found that smooth curves of η_{sp}/c versus concentration, for isoionic ribonuclease solutions, could not be obtained when Cannon-Fenske viscometers were used. Instead a break appeared, at a protein concentration about 1.5 g./100 ml., very similar to that observed for ovalbumin by Bull.⁶ Bull ascribed this effect to a difference in the wetting of the glass surface (below a critical concentration) by the falling and rising menisci of the liquid. We did not attempt to confirm this explanation directly. However, the effect was completely eliminated by use of Ubbelohde "suspended level" viscometers,⁷ in which surface tension plays a less important role than it does in the Cannon-Fenske viscometers. Accordingly, virtually all the results reported, including all of those at the isoionic point, were obtained using Ubbelohde viscometers. The effect here described did not occur in acid solutions, and a few of the results reported for acid solutions were obtained using Cannon-Fenske viscometers.

Units of Concentration and of Viscosity.—It has been customary in viscosity experiments to express concentration

(1) Presented at the 30th National Colloid Symposium, Madison, Wisconsin, June 18-20, 1956.

(2) Abstracted in part from the Ph.D. Thesis of John G. Buzzell, State University of Iowa, August, 1955.

(3) (a) C. Tanford and J. G. Buzzell, *THIS JOURNAL*, **60**, 225 (1956);

(b) C. Tanford, J. G. Buzzell, D. G. Rands and S. A. Swanson, *J. Am. Chem. Soc.*, **77**, 6421 (1955).

(4) C. Tanford and J. D. Hauenstein, *Biochim. Biophys. Acta*, **19**, 535 (1956).

(5) H. M. Dintzis, Ph.D. Thesis, Harvard University, 1952.

(6) H. B. Bull, *J. Biol. Chem.*, **133**, 39 (1940).

(7) L. Ubbelohde, *Ind. Eng. Chem., Anal. Ed.*, **9**, 85 (1937).

in g./100 ml. As a result, the *intrinsic viscosity*, which is the limit at zero concentration of $(\eta - \eta_0)/\eta_0 c$, where η_0 is the solvent viscosity, is obtained in the units deciliters/gram. Since our previous paper, and especially in making theoretical calculations based upon viscosity, we have found it increasingly cumbersome to employ these particular units. Accordingly, in the present paper, we have used g./cc. as the unit of concentration, with the result that intrinsic viscosity is expressed in c.g.s. units, cc./g. This not only simplifies calculations, but also gives more convenient numbers: values of $[\eta]$ for proteins fall between 3 and 50, instead of between 0.03 and 0.50, as they do in the units of dl./g.

Extrapolation Procedure, Ionic Strength, Definition of Components.—These topics were discussed in the preceding paper on serum albumin,^{3a} and apply equally to the present study.

Results

Figure 1 shows typical experimental data. The intercepts and slopes of the straight lines through these data were determined by the method of least squares. The intercepts are the intrinsic viscosities, the slopes represent concentration dependence.

Table I shows all intrinsic viscosities obtained in this way. Most entries in Table I represent duplicate determinations, and some represent the averages of two sets of duplicates. Table I also shows the slopes obtained from all experiments. The slopes given are not always those obtained from the original least-squares calculation. Since no significant difference in intrinsic viscosity was observed at any pH between pH 5.9 and 11, at $\mu = 0.01$ or above, the slopes in this range were recomputed by a least-squares calculation assum-

ing a common intercept for all of the linear plots. This procedure caused a significant change in the slope only in one or two isolated determinations, in which the deviation of $[\eta]$ from the average value was large. In these cases the corrected slope was in better agreement with the slopes in other experiments.

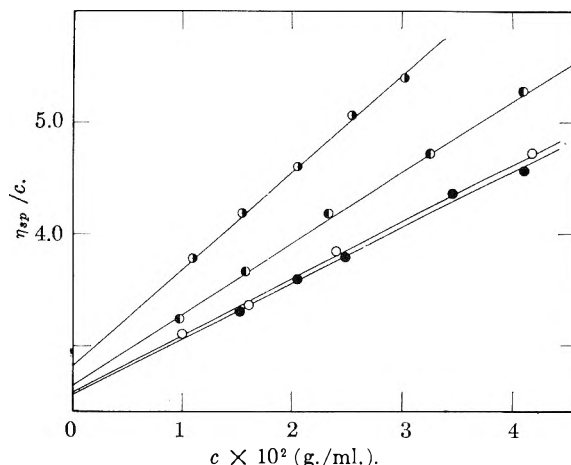


Fig. 1.—Representative experimental data: reading from top to bottom the curves represent, respectively, pH 4.4 and $\mu = 0.02$, pH 5.9 and $\mu = 0.02$, pH 7.5 and $\mu = 0.05$, pH 9.6 and $\mu = 0.05$.

Table I also shows the mean charge, \bar{Z} , per protein molecule at each pH used. This was calculated from titration curves of ribonuclease obtained in this Laboratory.⁸

One experiment is not included in Table I, that at pH 1.0 and $\mu = 0.15$, which resulted in a higher value of $[\eta]$ (4.5), and a smaller slope (23) than the other results in the acid region would lead one to expect. In view of the fact that free HCl and protein charges made up the major part of the ionic strength in this experiment, whereas everywhere else at least half the ionic strength is made up of KCl, no attempt has been made to interpret this result at present.

Between pH 5.9 and 11, *i.e.*, between $\bar{Z} = +6$ and -7 , at $\mu = 0.01$ or above, there is no significant variation in $[\eta]$. The mean value for all determinations in this range, with its root mean square deviation, is 3.30 ± 0.04 . Beyond this region of charge and ionic strength there is a significant but small increase in $[\eta]$. Values are tabulated in Table II, and compared with values pre-

TABLE I
INTRINSIC VISCOSITIES AND SLOPES

pH	Ionic strength	\bar{Z}	$[\eta]$, cm. ³ /g. ^a	$d(\eta_{sp}/c)/$ dc, cm. ³ /g. ¹⁰
1.0	0.25	19	3.49	35
2.8	.05	16	3.58	39
	.15	16.5	3.50	18
4.4	.02	9.5	3.41	43
	.05	10	3.35	26
	.15	10.5	3.40	19
5.9	.02	6	3.32	32
6.5	.05	5	3.28	25
	.15	5	3.25	21
7.5	.02	3.5	3.31	28
	.05	3.5	3.29	26
	.15	3.5	3.32	22
9.6	0	..	3.36	37
(isoionic)	.001	..	3.39	34
	.01	..	3.24	27
	.02	..	3.30	26
	.05	..	3.27	25
	.15	..	3.25	21
10.6	.02	-4.5	3.33	23
	.05	-4.5	3.36	22
10.7	.02	-5	3.36	26
	.05	-5	3.34	21
11.0	.02	-6.5	3.35	32
	.05	-7	3.35	25

^a To convert $[\eta]$ to the more conventional units of deciliters/g. divide by 100; to obtain the slopes in the corresponding units divide by 10^4 .

TABLE II
ELECTROVISCOUS EFFECT

pH	μ	\bar{Z}	Increase in $[\eta]$ over value of 3.30		
			Obsd.	Booth's eq.	Excess unaccounted for
1.0	0.25	19	0.1 ₉	0.03	0.1 ₆
2.8	.05	16	.2 ₈	.09	.1 ₉
	.15	16.5	.2 ₀	.04	.1 ₆
4.4	.02	9.5	.1 ₁	.07	.0 ₄
9.6	zero	..	.0 ₆	.03 ^a	.0 ₃

^a Although Z is zero, Z^2 is not zero at the isoionic point. The calculated value is based on $Z^2 = 3$, with the ionic strength calculated as half the hydroxyl ion concentration. For all other values listed in the table, the difference between Z^2 and $(Z)^2$ is negligible.

(8) C. Tanford and J. D. Hauenstein, in preparation.

dicted as electroviscous effect by the equation of Booth.⁹ It should be noted that the experimental uncertainty in $[\eta]$ is of the order of 0.1, so that the experimental values given are barely outside the experimental error.

Figure 2 shows a plot of the observed slopes as a function of charge and ionic strength. As in the

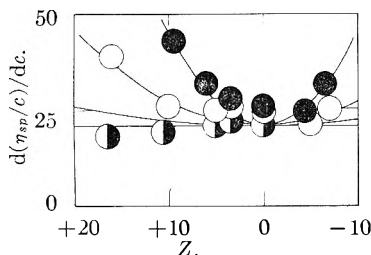


Fig. 2.—Slopes of viscosity plots as a function of charge at constant ionic strength: $\mu = 0.02$ (●), $\mu = 0.05$ (○), and $\mu = 0.15$ (◐). The solid lines are parabolas according to equation 2, with K_1 and K_2 given in Table IV.

case of serum albumin, the slopes approach a limiting value at high ionic strength and zero charge. The limiting slope is about 21 cm.⁶/g.², compared to the value of 26 cm.⁶/g.² found for serum albumin. The ratio of the limiting slope to $[\eta]^2$, however, has the same value, 1.9, for both proteins.

From the density data used in connection with the viscosity measurements a partial specific volume was calculated: $\bar{v} = 0.728$. This value is considerably higher than that measured by Rothen (0.709),¹⁰ and somewhat lower than the approximate value (0.73–0.74) reported by Vilbrandt, *et al.*¹¹ The technique used was exactly the same as for serum albumin. For that protein our figure for \bar{v} agreed within 0.001 with the most precise determination in the literature.

Discussion

The Size and Shape of the Equivalent Hydrodynamic Particle.—The intrinsic viscosity of ribonuclease is the lowest reported for any protein, with the exception of myoglobin, for which a slightly lower value of 3.1 has been found.¹² It may thus be concluded that ribonuclease is one of the most compactly-folded of all proteins.

As in the preceding paper,^{3a} one may calculate the dimensions of rigid particles whose hydrodynamic behavior would be equivalent to that found for ribonuclease. The equations of the preceding paper, with $[\eta]$ in c.g.s. units, are

$$[\eta] = \nu(\bar{v} + \delta_1 v_1^0) = 10\pi NR_e^3/3M \quad (1)$$

where \bar{v} is the protein partial specific volume, v_1^0 is the specific volume of pure solvent, δ_1 is the number of grams of solvent incorporated in the hydrodynamic particle per gram of dry protein, M is the dry molecular weight of the protein,¹³ N is Avogadro's number, ν is the Einstein–Simha constant, equal to 2.5 for spheres, and increasing for more asymmetric shapes, and R_e is the radius of an equivalent solid sphere.

(9) F. Booth, *Proc. Roy. Soc. (London)*, **A203**, 533 (1950). The form of the equation here used is equation 9 of ref. 3a.

(10) A. Rothen, *J. Gen. Physiol.*, **24**, 203 (1940).

(11) C. F. Vilbrandt, *et al.*, quoted by J. T. Edsall, in H. Neurath and K. Bailey, ed., "The Proteins," Vol. 1B, Academic Press, Inc., New York, N. Y., 1953.

(12) J. Wyman and E. N. Ingalls, *J. Biol. Chem.*, **147**, 297 (1943).

(13) The amino acid content and partial amino acid sequence have been determined by C. H. W. Hirs, S. Moore and W. H. Stein, *J. Biol. Chem.*, in press. Their data lead to $M = 13,683$. This figure has been used wherever necessary in the subsequent calculations. (We are indebted to Dr. Stein for making his results available to us in advance of publication.)

If one were to assume that the hydrodynamic particle has perfect spherical symmetry and is completely anhydrous, then, setting $\nu = 2.5$ and $\delta_1 = 0$, $[\eta]$ would become equal to 1.82. The difference between the value of 3.30 observed over much of the pH range and this figure may be ascribed to deviation from spherical symmetry ($\nu > 2.5$), to hydration ($\delta_1 > 0$), or to a combination of both. One cannot distinguish between these effects, but it is certain that both must be quite small.

Thus, placing $\nu = 2.5$, one obtains a maximum value of 0.59 for δ_1 . The corresponding equivalent sphere has a radius, $R_e = 19.3$ Å. Placing $\delta_1 = 0$, one obtains for ν the maximum value of 4.53, which corresponds, by the equation of Simha,¹⁴ to a prolate ellipsoid of axial ratio 3.9, or to an oblate ellipsoid of axial ratio about 4.7.

It is not likely that the hydrodynamic particle has perfect spherical symmetry and it is impossible for it to be anhydrous. A compromise equivalent hydrodynamic particle may be obtained by assuming an intermediate value for δ_1 , say 0.2. This leads to $\nu = 3.56$, or an axial ratio of 2.8 for an equivalent prolate ellipsoid.

These same figures may also be computed from other hydrodynamic measurements, and some values so obtained are shown in Table III. It is clear that the values of sedimentation and diffusion constants obtained by different investigators are in very poor agreement, a fact which is reflected in the molecular weights which they calculate from them, which range from 12,700 to 17,000. Within the large limits of error implicit in the mutual disagreement between the separate diffusion and sedimentation constants, the results agree with those obtained in the present study. The large probable error in the diffusion and sedimentation constants means that it is not worth while to calculate a value for the Scheraga and Mandelkern shape factor β , as was done with interesting results for serum albumin.^{3a}

Table III: EQUIVALENT HYDRODYNAMIC PARTICLES. The table compares data from 'This paper' with other studies (Rothen, Vilbrandt, Anfinson) for equivalent sphere radius (Å) and prolate ellipsoid parameters (viscosity, diffusion, sedimentation) assuming $\delta_1 = 0.2$.

	Equiv. sphere (radius Å)			Equiv. prolate ellipsoid; assuming $\delta_1 = 0.2$		
	Viscosity	Diffusion	Sedimentation	Viscosity	Diffusion	Sedimentation
This paper	19.3	2.8
Rothen ^b	..	18.0	19.9	..	2.4	3.7
Vilbrandt, <i>et al.</i> ^c	..	21.0	15.2	..	4.6	^a
Anfinson, <i>et al.</i> ^d	..	21.6	17.4	..	5.1	1.5

^a This sedimentation constant does not allow a value of δ_1 as high as 0.2 for a molecular weight of 13,683. ^b Ref. 10. ^c Ref. 11. ^d C. B. Anfinson, R. R. Redfield, W. L. Choate, J. Page and W. R. Carroll, *J. Biol. Chem.*, **207**, 201 (1954).

Effect of Charge and Ionic Strength on Intrinsic Viscosity.—There are two ways in which charge and ionic strength may influence intrinsic viscosity.

(14) R. Simha, *THIS JOURNAL*, **44**, 25 (1940); J. W. Mehl, J. L. Oncley and R. Simha, *Science*, **92**, 132 (1940).

(1) The necessity of maintaining an ion atmosphere about the macro-ion may result in additional dissipation of energy and a corresponding increase in viscosity, without any deformation of the macro-ion itself. This effect is known as the *electroviscous effect*. (2) The mutual repulsion between like charges may cause an expansion of the macro-ion, either isotropic, producing an increase in solvation, or lateral producing an increase in asymmetry. The intrinsic viscosity would then increase by an amount calculable by equation 1.

For many years there was considerable question as to which of these effects caused the sizable viscosity increase observed with increasing charge or decreasing ionic strength for many colloidal particles. Partly responsible for this was the fact that equations derived by Smoluchowski¹⁵ and by Krasny-Ergen¹⁶ predicted a very large electroviscous effect. A re-examination of this question by Booth,⁹ in 1950, indicated, however, that the Smoluchowski and Krasny-Ergen equations were in error, and that the electroviscous effect should, in fact, be small. The observations made by us, both for serum albumin and ribonuclease, confirm Booth's prediction. For serum albumin³ there was excellent agreement between the observed excess intrinsic viscosity and Booth's equation between pH 4.3 and 10.5. Very much larger changes in intrinsic viscosity were found to occur outside this pH region, but these are accompanied by corresponding changes in other physical parameters, all of which point unequivocally to the fact that a considerable expansion of the albumin ion is taking place.

As Table II shows, the excess intrinsic viscosity observed for ribonuclease is barely outside the limits of experimental error, and of the order of magnitude predicted by Booth's equation, throughout the range of stability of the protein. The observed values appear to be uniformly higher than those predicted, which may be due to the fact that Booth's equation was derived for spheres, whereas we have seen that the particles in ribonuclease solutions are not quite as compact as spheres. Alternatively, the difference may indicate that there is actually a slight expansion of the molecule, at least in the most acid solutions. This could be caused, perhaps, by a slight stiffening of lysine and arginine side chains as a result of mutual repulsion. It should be noted that, if the effect is due to expansion, it represents an increase in the

radius of an equivalent sphere from 19.3 Å. to only 19.6 Å., *i.e.*, it is trivial compared to the marked expansion which occurs in serum albumin below pH 4.3, and which must represent a pronounced configurational change.

It is worthwhile to note again, as was already concluded from the work on serum albumin alone,^{3b} that whether or not expansion of a protein molecule occurs as its charge is increased is not primarily a function of the charge density attained, but that it depends on the intrinsic internal bonding of the protein molecule. In serum albumin ($R_e \sim 33$ Å.), expansion sets in on the acid side when the net charge becomes approximately +10; in the much smaller ribonuclease molecule a charge of +19 is reached without expansion. In ovalbumin ($R_e \sim 30$ Å.) a charge of +40 is reached without appreciable increase in intrinsic viscosity.¹⁷

Effect of Charge and Ionic Strength on the Slope of Viscosity Plots.—With rising concentration η_{sp}/c increases above its limiting value owing to interaction between the protein molecules. Within the concentration range here covered the increase is approximately linear. There is no theory available for the effect of charge and ionic strength on this increase, but a theoretical equation exists for the viscosity increase to be expected for uncharged spheres.¹⁸ We have found (*cf.* Fig. 2) that an empirical equation of the form

$$\eta_{sp}/c = [\eta] + (K_1 + K_2 \bar{Z}^2/\mu^{3/2}) [\eta]^2 c \quad (2)$$

fits the data for both serum albumin and ribonuclease. For uncharged molecules this equation would reduce to the form of the equation of Guth and Gold.¹⁸ Moreover, the value of K_1 observed by us, both for serum albumin and for ribonuclease, agrees closely with that predicted by the equation of Guth and Gold, as Table IV shows.

TABLE IV
EMPIRICAL CONSTANTS FOR EQUATION 2

	K_1	K_2
Serum albumin ^{3a}	1.9	6.4×10^{-5}
Ribonuclease	1.9	2.0×10^{-5}
Eq. of Guth and Gold ¹⁸	2.26	..

Acknowledgment.—This investigation was supported by research grants NSF-G326 and NSF-G 1805 from the National Science Foundation and by research grant H-1619 from the National Heart Institute, of the National Institutes of Health, Public Health Service.

(15) M. Smoluchowski, *Kolloid Z.*, **18**, 190 (1916).

(16) W. Krasny-Ergen, *ibid.*, **74**, 172 (1936).

(17) H. B. Bull, *Trans. Faraday Soc.*, **36**, 80 (1940).

(18) E. Guth and O. Gold, *Phys. Rev.*, **53**, 322 (1938).

MOLECULAR KINETIC AND CHEMICAL PROPERTIES OF WOOL CORTICAL CELL FRACTIONS

BY WILFRED H. WARD AND JOHN J. BARTULOVICH

Western Utilization Research Branch, Agricultural Research Service, United States Department of Agriculture, Albany 10, California

Received February 24, 1956

Wool corticals cells prepared by acid treatment have been resolved into two main fractions differing in density and composition. Proteins made soluble by reduction of wool exposed 96 hours to 6 *N* HCl at 26° were measured in 0.2 *N* NaCl plus 0.5 *M* mercaptoethanol at pH 8. The molecular weight of protein from both fractions is about 40,000 and the molar frictional ratio 1.8 as calculated from the sedimentation constant 2.5 *S* and average intrinsic viscosity 0.19 deciliter per gram using the anhydro is prolate ellipsoid model. The relative ease with which the light fraction is released from the fiber, its lower sulfur content and lower density relate this fraction to the less consolidated "ortho" segment of the wool fiber. The heavy fraction then corresponds to the "para" segment. The sulfur content, yield and intrinsic viscosity of separated cortical cell fractions change with time of treatment. The results indicate that differences in composition and physical properties are due to differences existing in the original wool although modified by acid treatment. The acid removes protein material relatively poor in sulfur and of low intrinsic viscosity from both cell fractions in such a way that the resistant residues approach similarity in sulfur content and increase in intrinsic viscosity. These results indicate that both wool fiber segments include resistant components of high sulfur content but differ in the proportion of components more readily dissolved by acid.

Introduction

This paper is a report of research characterizing products of acid degradation of wool in order to understand and control degradation during processing. The cortex making up the interior of an ordinary unmedullated wool fiber is its largest histological fraction, about 90% of the whole. A considerable variety of hydrolytic treatments has been found to break it up into spindle-shaped "cells" about 5 to 7 μ wide and 80 μ long. These have a fibrous structure. The surfaces have fine ridges parallel to the long dimension and are covered with a chemically resistant layer. Reagents reported to break up wool into spindle cells include concentrated aqueous ammonia, dilute potassium hydroxide, concentrated sulfuric acid, dilute cetyl-sulfonic acid, pancreatin, trypsin and papain. Spindle cells have also been prepared by bacterial action. Binkley¹ has prepared spindle cells by the action of 6 *N* hydrochloric acid near room temperature. The last reagent has been chosen for special study in this research.

Much evidence shows that the process by which the cells are consolidated into a fiber is not uniform, so that one side of the fiber normally differs from the other to a greater or lesser degree in chemical and mechanical responses to environment. For example, a wool fiber cross-section commonly shows bilateral differences in dye absorption, in natural pigmentation, in relative swelling by bases or acids, and in resistance to attack by enzymes and other chemicals including fresh bromine water and aqueous urea solutions with reducing agents. It has even been reported that wool-destroying insects prefer one side over the other. The bilateral asymmetry is closely related to fiber crimp. Since crimp and chemical stability are of the greatest importance in processing and use of wool, bilateral differences are of practical as well as fundamental interest.

Preparation of Cell Fractions for Molecular Kinetic Comparison.—An Idaho medium wool (WC-5)² was used

for a molecular kinetic comparison of light and heavy cell proteins. The wool was Soxhlet-extracted with benzene and rinsed with hot water. A clean portion was soaked 96 hours at room temperature, about 26°, in 6 *N* hydrochloric acid. The acid:wool ratio was 20:1. The wool was drained, rinsed carefully in distilled water, and beaten with water in a Waring Blender.³ The separated cells were recovered by filtering on a hardened paper, washed until the washings gave no turbidity with silver nitrate, and kept in ethyl alcohol. On the basis of similar experiments the total yield of undissolved wool components is estimated to have been between 60 and 70%.

The cells were fractionated in aqueous chloral hydrate density gradient columns⁴ and washed with water. The sulfur and nitrogen contents are given in Table I. The sulfur analyses indicate that the light fraction composed 43% of this preparation.

TABLE I

SULFUR AND NITROGEN CONTENTS OF MEDIUM WOOL, SPINDLE CELL PREPARATION AND FRACTIONS USED FOR MOLECULAR KINETIC STUDIES

Material	Sulfur, %	Nitrogen, %
Original wool	3.64	16.8
Spindle cell preparation	4.48	15.9
Light fraction	3.53	16.0
Heavy fraction	5.20	15.6

In view of the probable interaction between chloral hydrate and wool protein,⁵ chlorine contents of the cells are of interest. Typical preparations have been found to contain from less than 0.1 to 1.0% chlorine before fractionation and from 0.2 to 2.0% chlorine after contact with chloral hydrate. The latter figures correspond to 0.24 to 2.4% chloral not removed by washing. The higher values were observed with heavy fractions as noted in Table III.

For molecular kinetic studies reported here the cells were dissolved in 0.5 *M* mercaptoethanol containing 0.2 *M* sodium chloride and adjusted to pH 8. An undissolved membranous residue amounted to 1 to 2% of the spindle cell weight. The amount of undissolved residue decreased with increasing time of exposure to acid. The heavy fraction gave about 10% more residue than the light. Each cell protein solution was dialyzed in commercial cellulose tubing against six times its volume of solvent. Tests of similar preparations showed about 40% of the total nitrogen diffusible through the membrane. This proportion increased with longer exposure to acid but was not consistently different for the two cell fractions. The following measure-

(3) Mention of specific commercial products does not imply recommendation by the Department of Agriculture.

(4) W. H. Ward and J. J. Bartulovich, *Text. Research J.*, **25**, 888 (1955).

(5) J. M. Preston and M. V. Nimkar, *J. Textile Inst.*, **41**, T446 (1950).

(1) C. H. Binkley, unpublished results from this Laboratory.

(2) This wool has been the object of other studies, for example, W. H. Ward, C. H. Binkley and N. S. Snell, *Text. Research J.*, **24**, 314 (1955), which records its chemical composition.

ments of intrinsic viscosity and sedimentation constant of the dialyzed solutions then apply to material representing 35 to 40% of the original wool fiber, distributed roughly equally between light and heavy fractions.

Molecular Kinetic Comparison of Cortical Cell Fractions.

—Viscosities of the two solutions of cortical cell protein relative to the dialysates were measured at 30° at concentrations from 0.2 to 1.2%. Ubbelohde viscometers giving flow times of 300 to 500 seconds were used. The kinetic energy correction was negligible. Concentrations were found by difference from nitrogen analyses of the solution and dialysate. Measured densities of the solutions and dialysates were taken into account.

Ultracentrifugal sedimentation constants were found for the same solutions by means of a Spinco Model E centrifuge, using the synthetic boundary cell. Measurements were made at the ambient temperature and referred to water at 20° in the usual way.

The intrinsic viscosity of the light fraction was 0.20 deciliter per gram and the slope $d(\eta_{sp}/c)/dc$ 0.039 deciliter² gram⁻². The intrinsic viscosity of the heavy fraction was 0.18 deciliter per gram and its slope 0.035 deciliter² gram⁻². These are least-squares values. The sedimentation results showed no clear difference between the two preparations. The combined sedimentation results gave $1/s = 0.40 + 0.036c$, where s is Svedberg units referred to water at 20° and c is in grams of protein per 100 ml. The standard sedimentation constant at zero concentration is then 2.5 S .

TABLE II

MOLECULAR PROPERTIES OF REDUCED SPINDLE CELL PROTEIN FROM VISCOSITY AND SEDIMENTATION

Basis of determination	f/f_0	M
Solute taken as unsolvated hard spheres	1	17,500
Prolate ellipsoids of revolution, unsolvated	1.81	42,600
Oblate ellipsoids of revolution, unsolvated	2.16	55,600
Solvated sphere, the bound solvent equal in composition and density to the original solvent	2.19	56,900
Solvated sphere, water alone bound, with density of normal water	3.47	113,000

TABLE III

PROPERTIES OF CORTICAL CELL PREPARATIONS FRACTIONATED AFTER VARIOUS TIMES OF ACID TREATMENT AT 30°

Time of treatment, hr.	28		48		66		90	
	Light	Heavy	Light	Heavy	Light ^a	Heavy	Light ^a	Heavy
Fraction								
Yield, % original wool	38.2	25.5	27.9	11.9	14.4	6.8	1.2	10.8
Yield, % cortical cell preparation	60	40	70	30	68	32	10	90
Total sulfur, %	4.19	5.24	6.46	7.35	6.34	6.27	6.80	6.68
Cystine sulfur, %	4.0	4.8	4.8	5.3	5.8	5.9	6.5	5.9
Nitrogen, %	15.6	15.3	15.3	15.2	14.7	14.5	14.4	14.5
Chlorine, %	0.51	2.04	0.25	0.40	0.32	0.36	0.28	0.22
Density ^b , g. cm. ⁻³								
Range ^c					1.482-1.515		1.489-1.500	
Separate layers	1.450-2	1.476-9 ^d	1.452	1.475-9				
Intrinsic viscosity, dl./g.	0.147	0.115	0.228	0.158				

^a Note that these "light" fractions do not correspond in density or sulfur content to those isolated after shorter treatments. ^b Densities were measured in aqueous chloral hydrate gradients at 30° by comparing positions of cortical cell material with those of standardized floats. ^c The 66 and 90 hour preparations did not give separate layers in gravity separation, but were fractionated in the centrifuge in the usual way. ^d An intermediate layer of density 1.468-1.475 can be distinguished just above this heavy fraction.

Molecular Weight and Molar Frictional Ratio.—Estimates of the molecular weight and molar frictional ratio of the reduced spindle cell protein not diffusing through cellulose membrane were made from the mean intrinsic viscosity 0.19₂ deciliter per gram, the standard sedimentation constant 2.4₃ S and the assumed value of the partial specific volume 0.72, estimated from the amino acid composition of whole wool. The sedimentation constant and partial specific volume permit calculation of a minimum possible molecular weight, 17,500 taking the molar frictional ratio to be unity. The actual molecular weight is this minimum value multiplied by the 3/2's power of the molar frictional ratio, which is found from the intrinsic viscosity and partial specific volume. Several different models may be assumed

in translating the intrinsic viscosity into the molar frictional ratio. Results calculated from some of these assumptions are given in Table II.

In the case of wool protein not exposed to acid but reduced and dissolved in aqueous urea, the prolate ellipsoidal model gives results most clearly agreeing with measurement of free diffusion. Provisional acceptance of the molecular weight and shape indicated by this model suggests the following conclusions. The molecular kinetic units of reduced protein from acid-prepared spindle cells are appreciably larger than those from the original wool reduced in aqueous urea. The spindle-cell protein forms a relatively elongated unit, but less so than the proteins solubilized in urea. The mean molecular weights of proteins from the different spindle cell fractions may differ slightly, but probably not more than 10 to 15%. Such a difference would permit an actual difference of as much as 0.4 S in the sedimentation constants or 0.05 deciliter per gram in the intrinsic viscosities. Such differences approximate the greatest observed in these studies.

Electrophoretic Analysis of Cortical Cell Protein.—The portion of the wool fiber more resistant to chemical attack has been found repeatedly (for example by Lindley,⁶ by Binkley,⁷ and by Mercer and colleagues^{7,8}) to differ in composition from the less resistant part. In several instances the resistant part has been identified with the *para*-cortex. The composition of the *ortho* segment has been estimated from the difference in composition of the whole wool and its resistant portion.⁸ Thus, evident differences in the contents of acid and amino acids have been ascribed directly to the different segments. This inference may be invalid because of the presence of other wool fiber components in the dissolved portion, including material from the resistant segment. However, if the two cortical segments do differ in their contents of ionizable groups this fact should be readily shown by electrophoresis.

Whole and fractionated cortical cell preparations were therefore tested by electrophoresis on paper (Whatman no. 3), with xylose and Armour bovine plasma albumin as reference substances. An unfractionated cell preparation from Idaho Rambouillet (WC-4) wool exposed to 6 N hydrochloric acid for 110 hours at room temperature was used for exploratory work, supplemented by tests with light and heavy fractions from the same wool treated 66 hours at 30°.

The properties of these fractions are included in Table III. Analyses in 0.1 M mercaptoethanol with 0.05 M Na₂HPO₄ (pH 8.1) or 0.1 N NaCl (pH adjusted to 8.6) or in 0.05 M Na₂SO₃ (pH 9.38) in each instance showed a single component moving slightly faster than the plasma albumin. The components were located by oven-drying in the presence of aniline vapor (to show the xylose) followed by staining with 0.1% brom phenol blue in 5% mercuric chloride and 5%

(6) H. Lindley, *Nature*, **160**, 190 (1947).

(7) E. H. Mercer, R. L. Golden and E. B. Jeffries, *Text. Research J.*, **24**, 615 (1954).

(8) R. L. Golden, J. C. Whitwell and E. H. Mercer, *ibid.*, **25**, 334 (1955).

acetic acid. Part of the unfractionated sample was treated with 1.6% peracetic acid, freshly diluted from Becco 40% acid, for 20 minutes at room temperature, washed free of oxidant, and extracted with 0.05 *N* ammonia. This extract showed a single component slightly *slower* than the unoxidized material.

These tests give no indication of any differences in electrophoretic properties of different spindle cell fractions. The different fractions of this preparation, therefore, do not differ appreciably in their net amounts of groups ionized at pH 8 to 9. Results to be summarized in the next section suggest that one fraction disappears or merges its identity with the other as the time of treatment is extended. It is therefore possible that further study of fractions from wool given the shortest possible treatment might show additional electrophoretic components.

Changes in the Insoluble Wool Residue with Time of Exposure to Acid.—In order to clarify the relations of the light and heavy cortical cell fractions to the original fiber, preparations were made with different times of acid treatment. Trends in relative and absolute yield, density and sulfur, cystine and nitrogen contents were established. For this series Idaho Rambouillet (WC-4) wool was treated with 6.1 *N* hydrochloric acid at 30.0°. The wool disintegrated appreciably more quickly than at room temperature. The minimum time for substantial disintegration at 30° was about 30 hours as opposed to about 90 hours at room temperature. The results are given in Table III.

From these results, the light cortical fraction is estimated to amount to about 60% of this original wool. This figure is indicated both by the relative yields as isolated and by extrapolating backward to zero time of treatment. In addition, the disappearance of the less dense fraction with extended treatment, the increase in the density of the material isolated, the over-all increase in sulfur and cystine content confirming observations of Lindley,⁶ the increases in intrinsic viscosity of the reduced protein fraction, and the failure to find appreciable differences in electrophoretic properties and ultracentrifugal sedimentation of these protein fractions suggest very strongly that both cortical cell fractions include protein components of high sulfur content that are considerably more resistant to degradation by acid than the rest of the fiber. The difference between the two cortical segments then includes differences in proportions of components with lower sulfur that are more readily dissolved by acid.

Acknowledgments.—Elementary analyses reported are the work of L. M. White, G. E. Secor and A. M. Mylne. Cystine was determined by J. E. Moore. J. W. Pence helped us in carrying out paper electrophoresis. We are likewise indebted to H. P. Lundgren and other co-workers both in this Laboratory and elsewhere for many useful suggestions for this and further research.

OPERATING AND COMPARATING PROCEDURES FACILITATING SCHLIEREN PATTERN ANALYSIS IN ANALYTICAL ULTRACENTRIFUGATION

BY RODES TRAUTMAN

The Rockefeller Institute for Medical Research, New York, New York

Received March 12, 1956

The simultaneous introduction of several alterations in ultracentrifuge operation and in measuring the photographic plate are described which enable an over-all improvement and simplification of the analysis. The alterations are: (a) centrifuging at a predetermined temperature; (b) using a double sector centerpiece; (c) using a combination phaseplate-wire schlieren diaphragm; (d) photographing at predetermined integral values (in minutes) of the true sedimentation time without measuring or requiring reproducibility of acceleration time; (e) equipping a two-dimensional micrometer comparator with a 5X projector and revolution counter reading directly to 0.01 mm. on the plate; (f) replacing the schlieren pattern with a tabulation of a significant number of its two dimensional coordinates; (g) selecting the measured points of the schlieren pattern so that they occur at equal intervals of the cube of the radius; and (h) using a printing calculator to record these coordinates. A special tabulation of squares and cubes of the radius is described for use with a comparator. A summary is given of the formulas for: (a) the concentration at any level; (b) the molecular weight determined in sedimentation velocity by the Archibald principle; (c) the true boundary position; (d) the sedimentation rate; (e) the initial concentrations in paucidisperse systems; and (f) the distribution of sedimentation rates in polydisperse systems.

The theory and equipment for analytical ultracentrifugation¹⁻³ recently have been developed sufficiently to warrant complex analysis of the entire refractive index gradient patterns obtained from solutions of biochemical interest. In particular, it is now possible to determine: (a) the molecular weight over a broad range of weight averages without obtaining sedimentation equilibrium for every level in the cell; (b) the sedimentation rate of skew boundaries; (c) the relative composition with respect to the paucidisperse components in concentrated solutions; and (d) the distribution of sedimentation rates in the polydisperse components even with significant diffusion in the boundary region. It is the purpose of this paper to describe operating and comparing equipment, procedures and formulas found useful in performing the above analyses. Especial attention is given to the selection of ordinates of the schlieren pattern spaced equally on a radius-cubed scale instead of uniformly on the radius scale, or at random. The reason for this choice is that an increment of r^3 corresponds to an increment of $r^2 dr$ since $d(r^3) = 3r^2 dr$. The integral $\int r^2(\partial n/\partial r) dr$, where $\partial n/\partial r$ is the index of refraction gradient, can then be evaluated as a summation of ordinates each chosen at the center of successive equal increments on this radius-cubed scale.⁴ Only $\int r^2(\partial n/\partial r) dr$ appears in the determination of the initial concentrations in paucidisperse systems,⁴ or of the molecular weight before loss of the plateau solution.⁵ Both integrals $\int r^2(\partial n/\partial r) dr$ and $\int (\partial n/\partial r) dr$ are needed to obtain the true boundary position⁶ or the concentration at any intermediate level in the approach to sedimentation equilibrium^{5,7} and spacing of ordinates uniformly on a linear scale or a radius-cubed scale will be equally convenient.

In the determination of the concentration at any level in a velocity ultracentrifuge experiment only $\int (\partial n/\partial r) dr$ appears, in which case the radius-cubed scale is inconvenient. But this calculation is rarely needed, since concentrations corrected to zero time are generally of more interest. The radius-cubed scale is also useful in calculating the apparent distribution function⁸ from the concentration gradient since each ordinate must be multiplied by r^3 .

Ultracentrifugation Equipment and Procedures

The sedimentation analysis is simplified if experiments in a given series are all made at the same temperature, if the true sedimentation time is accurately and conveniently known, and if the base line is simultaneously on the photographic plate with the schlieren pattern from the solution. The following are modifications of the Spinco Model E ultracentrifuge and operating procedure.²

(a) Whenever practicable the experiment is performed at 20.0°. To do this, the rotor is precooled in a refrigerator to a temperature below 20° and then brought to the desired value, as measured with the thermocouple in contact with the suspended rotor, with the aid of a 250 watt infrared lamp before closing the vacuum chamber. Such a lamp, about 10 cm. away from the rotor, heats the rotor about 20°/hour. The adiabatic cooling of the rotor on acceleration must be considered.⁹ The refrigeration for the vacuum chamber is set empirically such that the rotor temperature at the completion of the experiment is within $\pm 0.1^\circ$ of the initial temperature.

(b) Correction for the sedimentation that occurs during acceleration is made by maintaining the drive current constant during this period and starting the automatic camera when the speed is two-thirds of its final value.³ This procedure is simplified by the use of a mechanical stop¹⁰ which prevents the "exposure time adjustment dial" from rotating until the desired speed is reached. A micro-switch under the mechanical stop also starts a running time meter¹² reading in 0.01 minute, permanently installed between the vacuum gage and the viewing window and wired in parallel with the synchronous motor. The dial is held at a position corresponding to half way between the shutter microswitches, so that the true sedimentation time of any exposure taken automatically is accurately an

(1) J. W. Williams, *J. Polymer Sci.*, **12**, 351 (1954).

(2) Technical Manual for Spinco Model E Ultracentrifuge, Spinco Division, Beckman Instruments, Inc., Belmont, California.

(3) E. G. Pickels, in "Methods of Medical Research," Vol. 5, A. C. Corcoran, ed., Year Book Publishers, 1953.

(4) R. Trautman and V. N. Schumaker, *J. Chem. Phys.*, **22**, 551 (1954).

(5) S. M. Klainer and G. Kegeles, *This Journal*, **59**, 952 (1955).

(6) R. Goldberg, *ibid.*, **57**, 194 (1953).

(7) W. J. Archibald, *ibid.*, **51**, 1204 (1947).

(8) R. L. Baldwin, *ibid.*, **58**, 1081 (1954).

(9) D. F. Waugh and D. A. Yphantis, *Rev. Sci. Instr.*, **23**, 609 (1952).

(10) Identical with the timing latch used in the Gofman lipoprotein procedure¹¹ to start the camera, in that case, when acceleration is completed.

(11) O. de Lalla and J. W. Gofman, in "Methods of Biochemical Analysis," D. Glick, ed., Interscience Publishers, New York, N. Y., 1954.

(12) R. W. Craemer Company, Inc., Centerbrook, Connecticut.

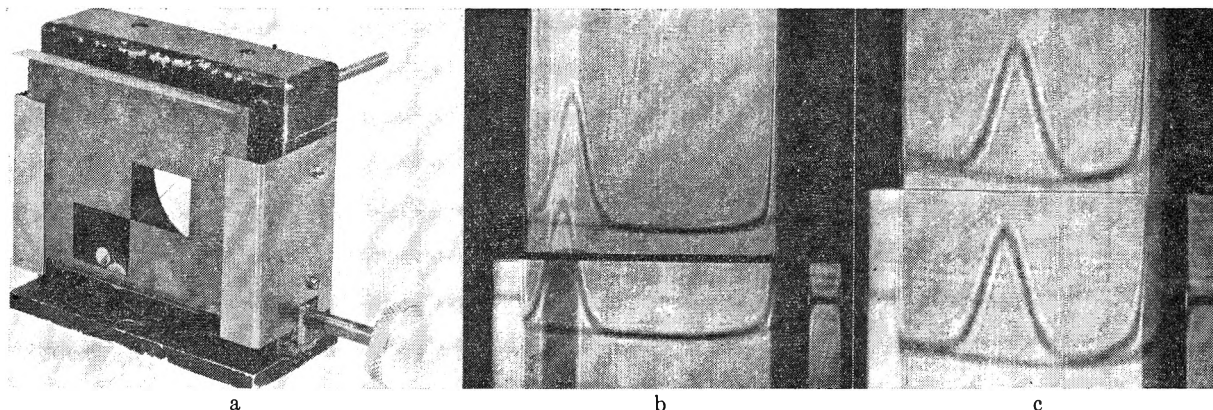


Fig. 1.—Modified schlieren diaphragm mount: (a) Mount as seen from the direction of light travel. Vertical centering of pattern on plate is accomplished by thumb screw at lower right. Diagonal wire is on border of phaseplate. Mask can be positioned in oversized friction guides. This mask is used only in special cases of two cells used simultaneously. (b) Schlieren pattern with mask in place. The same protein, pepsin at 8.4 mg./ml. concentration, is in both cells. The lower pattern is displaced downwards due to a 1° quartz prism as the upper window of the double sector centerpiece. The right hand reference is from the reference in the AN-D rotor. The position and width of the horizontal band across the pattern depend upon the vertical position and alignment, respectively, of the mask; speed 59,780 r.p.m., $t = 52$ min., $\theta = 60^\circ$. (c) Schlieren pattern at $t = 128$ min. and $\theta = 45^\circ$.

integral multiple of 2 minutes. The running time meter aids in recording the time of each exposure and in visual interpretation of the pattern during the experiment.

(c) A Wolter phaseplate¹³ modified by addition of 0.003" diameter wire along the edge of the MgF_2 coating on half of a polished plate glass¹⁴ is used as a schlieren diaphragm.

(d) The double sector centerpiece of Beams and Dixon¹⁵ and Milch¹⁶ is used with solution in one side and solvent in the other. The loss in contrast due to the superposition of two schlieren patterns is minimized with the phaseplate and is more than compensated for by the gain in accurate, convenient registration of the baseline. For sedimentation, a wedge quartz² is used for the upper quartz window of the cell, oriented to deflect the light toward the center of rotation, thus displacing the pattern downward on the photographic plate relative to the baseline in the image of the reference holes.¹⁷ To further enable greater utilization of the vertical space on the photographic plate, even when only one cell is used, the schlieren diaphragm mount has been modified as shown in Fig. 1a. The two screws allowing cross motion to the optical track formerly at the lower right, have been replaced by a single screw and knob extending outside the dust cover, so that the pattern may be centered at will during the experiment. In using two cells, when the pattern from the plain and the wedge cells do not overlap, the original contrast for each pattern may be restored by insertion of the "checkboard" mask shown in place in Fig. 1a. The entire group of deflected and undeflected rays from the wedge cell is displaced to the right on this mount (for a cell giving downward displacement on the screen) and interrupts the schlieren diaphragm edge as a group above the intersections of the rays from the plain cell. The upper part of the light source image contributing to the background from the plain cell is thus masked out, as is the lower part of the light source image from the wedge cell. This optional procedure is for experiments with two cells, not for two sectors in one cell. An example is shown in Fig. 1b in which two double sector cells are used. Note the change in contrast in different parts of the pattern arising from overlap of various combinations of the light from the 4 sector openings. Later in the experiment, Fig. 1c, the maximum gradient in the lower pattern is less than the separation of the patterns brought about by the wedge quartz and the quality of the optical registration is the same as if each cell were used alone.

(13) H. Wolter, *Ann. Physik*, **7**, 182 (1950).

(14) R. Trautman and V. W. Burns, *Biochim. Biophys. Acta*, **14**, 26 (1954).

(15) J. W. Beams and H. M. Dixon, III, *Rev. Sci. Instr.*, **24**, 228 (1953).

(16) L. J. Milch, *Lab. Invest.*, **2**, 441 (1953).

(17) This procedure is identical to that of Gofman.¹¹ One chooses a plain cell or one displacing the pattern upward or downward on the screen depending upon whether flotation or sedimentation patterns are to be viewed.

Comparison Equipment and Procedures

Two-dimensional Micrometer Comparator.—A photograph of the comparator used is shown in Fig. 2, rather than a schematic drawing giving the details of construction. It is intended to illustrate some features that can be added to existing comparators, not to suggest duplication in entirety. The image of a portion of the schlieren pattern is projected onto a vertical white cardboard at the top, back by means of a camera lens and front surface mirror. This 5X image can be shielded with an oscilloscope viewing hood (not shown) so that it can be clearly seen in a room of normal illumination without eyestrain or loss of contrast. The quality of this optical system is not critical since only those pencils of light are used which reach the fiducial mark, chosen here to be a small circle. Each axis has a 1 mm. pitch screw. The axis of abscissas x , running left and right, and corresponding to the radial axis r in the cell, has been equipped with a revolution counter geared up 1 to 10 so that it reads directly in 0.01 mm. The cross axis of ordinates y is also calibrated in 0.01 mm. on the handwheel. Because of the curved nature of the centrifuge baseline on a schlieren pattern, it is in general necessary to make the subtraction of the ordinate of the baseline y_{soln} from the ordinate of the solution pattern y_{soln} . This difference will be denoted as Δy . A printing calculator¹⁸ has been found to be extremely well suited for the direct transcription and arithmetic operations of the coordinates.

Comparison Procedure.—The key simplifying procedure in using the comparator is to set the abscissa scale so that its origin, $x = 0$, occurs at the location of the center of rotation on the plate. Thus, the plate is positioned left or right so that the abscissa counter (or scale or handwheel) reads $M_0 r_{\text{inner}}$ when the inner, and/or $M_0 r_{\text{outer}}$ when the outer reference edge is on the comparator fiducial mark, where M_0 is the camera magnification. A tabulation can be made of these settings as a function of speed for the various ultracentrifuges and counter balances used. It is possible to set the plate to within ± 0.005 cm. (on the rotor) of its true position.

Rather than using the actual values of x^3 , it will be convenient to index the radius-cubed scale by at most three digit integers proportional to x^3 . Thus define for the comparator a fixed scale

$$Z \equiv (10x/x_r)^3 \quad (1)$$

from which

$$x^2 dx = (x_r^3/3000) dZ \quad (2)$$

Z can be called the "cubed-scale index number." The Z scale reference x_r is a fixed number chosen to be just radially beyond the bottom of the cell when a plate from the ultracentrifuge with the largest M_0 is aligned on the comparator. For M_0 less than 2.20, the value of $x_r = 160.00$ mm. is convenient and is chosen here. It would be ideal to have

(18) Olivetti Corporation of America, New York, New York.

an additional counter on the comparator of Fig. 2, giving $(x/16)^3$ directly. Since this is not available, the radius-cubed scale is represented by a tabulation, an abbreviation of which is given in columns 1 and 4 of Table I. Whatever the choice of x , the tabulation must cover a factor of 2 in Z since the cube of the ratio of the radii of the bottom and the top of a standard Spinco cell is 2.0. The choice of $Z = 1000$ near the bottom permits the x position of 500 intermediate points to be calculated, without interpolation, from standard tables of squares, cubes and roots. Three such intermediate points are given as 686, 687 and 688 in Table I.

TABLE I

Z ($10x/x_r$) ³	$Z^{1/3}/10$ x/x_r	$100Z^{-2/3}$ $(x_r/x)^2$	$x_r = 160.00$ mm. x (mm.)	$\log(x/100)$
500	0.793701	1.5874	126.99	0.10378
20	.804145	1.5464	128.66	.10945
40	.814325	1.5080	130.29	.11492
60	.824257	1.4719	131.88	.12018
80	.833955	1.4379	133.43	.12526
600	.843433	1.4057	134.95	.13017
20	.852702	1.3753	136.43	.13492
40	.861774	1.3465	137.88	.13951
60	.870659	1.3192	139.31	.14397
80	.879366	1.2932	140.70	.14829
686	.881516	1.2856	141.11	.14956
687	.882373	1.2844	141.18	.14977
688	.882801	1.2831	141.25	.14998
700	.887904	1.2684	142.07	.15249
20	.896281	1.2448	143.41	.15656
40	.904504	1.2223	144.72	.16053
60	.912581	1.2008	146.01	.16439
80	.920516	1.1801	147.28	.16815
800	.928318	1.1604	148.53	.17182
20	.935990	1.1415	149.76	.17539
40	.943539	1.1233	150.97	.17888
60	.950969	1.1058	152.16	.18229
80	.958284	1.0890	153.33	.18561
900	.965489	1.0728	154.48	.18887
20	.972589	1.0572	155.61	.19205
40	.979586	1.0421	156.73	.19516
60	.986485	1.0276	157.84	.19821
80	.993288	1.0136	158.93	.20120
1000	1.000000	1.0000	160.00	.20412

In making a reading of the ordinate Δy at a particular Z , say 600, the x axis handwheel is turned, moving the aligned plate until the counter reads the corresponding x value,

TABLE II

Z	Δy (mm.)	Z	Δy (mm.)
600	0.53	700	11.94
20	2.49	20	7.41
40	3.98	40	3.49
60	9.13	60	1.63
80	13.16	80	0.70
		800	0.36

$$\begin{aligned} \Sigma \Delta y_i &= 54.82 \\ \Delta Z \tan \theta \Sigma \Delta y_i &= 1096 \\ W &= 8.44 \text{ mg./ml.} \\ \Sigma (x_r/x_i)^2 \Delta y_i &= 70.43 \\ \Delta Z \tan \theta \Sigma (x_r/x_i)^2 \Delta y_i &= 1409 \\ A &= 7.12 \text{ mg./ml.} \\ (x_r/\bar{x})^2 &= 1.2847 \\ \bar{x} &= 141.16 \text{ mm.} \\ x_{\text{max. ordinate}} &= 141.06 \text{ mm.} \end{aligned}$$

Comparator readings and calculations for the lower pattern of Fig. 1c.

$$\begin{aligned} F_x F_y &= 5.05 \times 10^{-3} (\text{mg./ml.})/\text{mm} \\ F_a &= 9.79 \times 10^3 (\text{S min.}) \\ x_a &= 129.56 \text{ mm.} \end{aligned}$$

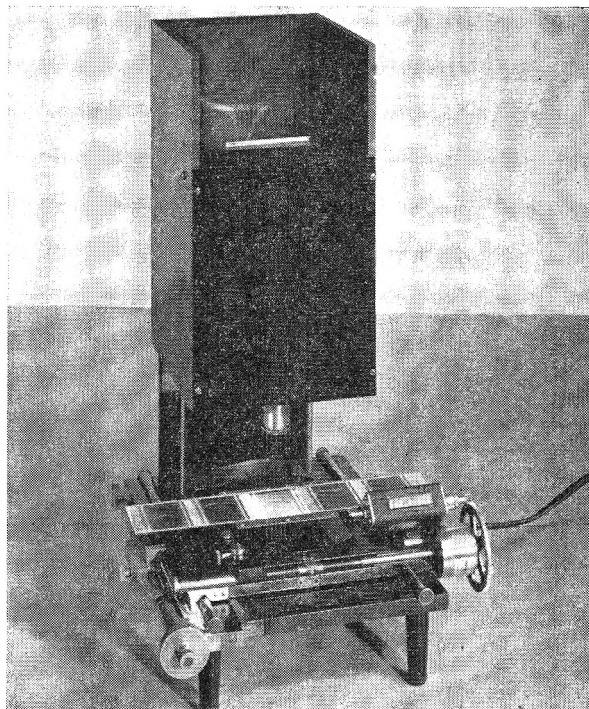


Fig. 2.—Precision screw two-dimensional comparator. An ultracentrifuge plate is shown on the bakelite holder which can be aligned by means of a small thumb screw just in front of the second frame from the left. The holder travels on two pairs of drill rods placed at right angles with a three-point suspension on each pair. The handwheel at lower right moves the plate left and right and is equipped with a counter reading directly in 0.01 mm. Rapid scanning is done by sliding the plate in its holder. The handwheel at lower left moves the plate front and back and is calibrated in 0.01 mm. The screw in the center left just under the end of the plate releases the plate holder for rapid scanning front and back. Not shown is an oscilloscope viewing hood which fits into the top of the black box housing the projector.

namely, 134.95 mm. This value of Z and/or x can be indexed on the calculator tape using the non-add operation. The y -axis handwheel is then turned until the solution schlieren pattern is on the fiducial mark. The reading is entered as a plus then, correspondingly, the reading when the solvent schlieren pattern is moved to the fiducial mark is entered as a minus, and the difference, Δy , is taken. If the spacing $\Delta Z = 20$ were chosen, then the counter would be advanced to 136.43 mm. corresponding to $Z = 620$, and the ordinates at this location measured. The readings taken on the lower pattern of Fig. 1c are given in Table II.

Since ordinates are measured only at tabulated x values, which are actual distances from the center of rotation, the accessory relations of r^3 , r^2 and $\ln r$ involved in the theory can also be tabulated. These are given in Table I in the more useful form of $Z = (10 x/x_r)^3$, column 1; $(x_r/x)^2$, column 3; and $\log x$, column 5. The first 3 columns are universal, and the fifth differs only by a constant, for any choice of x_r . The fourth column is calculated from column 2 merely by multiplying by the chosen value of x_r for the comparator at hand. All values in Table I are also independent of the magnification M_0 . This special tabulation is a convenient complement to the two dimensional comparator. The necessity for cubes, squares and logarithms is strictly a geometrical consequence of the sector shaped cell in a centrifugal field and does not depend upon the position of the meniscus, bottom of the cell, or whether flotation or sedimentation is taking place.

Notation.—The two-dimensional coördinates actually measured on the plate at any particular time t will be denoted by x and y . Their respective counterparts in the rotor are the radius r and the difference in the refractive index gradient between solution and solvent $\partial n/\partial r$. The difference

in refractive index $\Delta n \equiv n_{\text{soln}} - n_{\text{solv}}$ will be taken as a measure of the concentration. Both x and r are zero at the center of rotation and are not considered functions of the time. The radial distance measured on the x scale of an identifiable moving point will be denoted by \bar{x} on the plate and \bar{r} in the cell. Here \bar{r} and \bar{x} are functions of the time. An asterisk (*) will be used to denote quantities calculated as though diffusion and concentration dependence were negligible. The superscript zero (0) when applied to an s rate indicates infinite dilution of the sedimenting solute, but when applied to a concentration means the initial value in the cell. Let M_0 be the magnification of the schlieren camera lens; M_c the magnification of the cylindrical lens; a' , the optical path of the cell; b' , the optical lever arm; θ , the angle the schlieren diaphragm makes with the light source; ω , the angular velocity of rotation; s , the sedimentation coefficient ("s rate") in svedbergs S (10^{-13} sec.); t , the true centrifugation time in minutes; in a conventional cell, r_a , the meniscus position for sedimentation or the bottom of the cell for flotation and r_b , the bottom of the cell for sedimentation and the meniscus for flotation; and, in a synthetic boundary cell,¹⁹ r_0 , the meniscus, and r_a , the initial position of the synthetic boundary. Three apparatus constants will be given special symbols

$$\begin{aligned} F_x &\equiv x_r/(3000M_0), \\ F_y &\equiv 1/(a'b'M_c), \\ F_s &\equiv 10^{13} \ln 10/(60\omega^2) \end{aligned} \quad (3)$$

Using these notations the following functions of r and $\partial n/\partial r$ can be calculated directly from the coordinates measured on the comparator.^{1,2,3,20} Calculable from x or Z

$$r = x/M_0 = 300F_x Z^{1/2} \quad (4)$$

$$s^* \equiv \frac{10^{13} \ln r/r_a}{60 \omega^2 t} = \frac{F_s}{t} \log \frac{x}{x_a} = \frac{F_s}{3t} \log \frac{Z}{Z_a} \quad (5)$$

Calculable from \bar{x}

$$\bar{r} = \bar{x}/M_0 \quad (6)$$

$$s \equiv \frac{10^{13}}{60 \omega^2 \bar{r}} \frac{d\bar{r}}{dt} = F_s \frac{d \log \bar{x}}{dt} \quad (7)$$

$$\bar{s}^* \equiv \frac{1}{t} \int_0^t s dt = \frac{F_s}{t} \log \frac{\bar{x}}{x_a} \quad (8)$$

Here s^* is the combination of the coordinate x with the time t of the exposure to make an "s rate scale" (equation 5), while \bar{s}^* is the time average of the instantaneous sedimentation coefficient s of a particular moving point (equation 8).

Calculable from y

$$\frac{\partial \Delta n}{\partial r} = \frac{\tan \theta}{a'b'M_c} (y_{\text{soln}} - y_{\text{solv}}) = F_y \tan \theta \Delta y \quad (9)$$

Calculable from Z and y

$$\begin{aligned} \int_{r_1}^{r_2} \frac{\partial \Delta n}{\partial r} dr &= \frac{\tan \theta}{a'b'M_c M_0} \int_{x_1}^{x_2} \Delta y dx \\ &= F_x F_y \tan \theta \int_{z_1}^{z_2} (x_r/x_a)^2 \Delta y dZ \\ &\equiv A(Z_1, Z_2) \end{aligned} \quad (10)$$

$$\begin{aligned} \int_{r_1}^{r_2} \left(\frac{r}{r_a}\right)^2 \frac{\partial \Delta n}{\partial r} dr &= \frac{\tan \theta}{a'b'M_c M_0} \int_{x_1}^{x_2} \left(\frac{x}{x_a}\right)^2 \Delta y dx \\ &= F_x F_y \tan \theta (x_r/x_a)^2 \int_{z_1}^{z_2} \Delta y dZ \\ &\equiv W(Z_1, Z_2) \end{aligned} \quad (11)$$

The notations $A(Z_1, Z_2)$ and $W(Z_1, Z_2)$ have been introduced for brevity in listing the formulas in the following sections. A corresponds to the area of the schlieren pattern on the linear x scale, and W to the "area" on the x^3 or "warped scale."⁴ If $Z_2 - Z_1$ is divided into m equal intervals ΔZ , and the ordinate Δy_j is measured at the center of each of these intervals on the cubed-scale, then A and W can be evaluated as

$$A(Z_1, Z_2) = F_x F_y \tan \theta \Delta Z \sum_{j=1}^m (x_r/x_j)^2 \Delta y_j \quad (12)$$

$$W(Z_1, Z_2) = F_x F_y (x_r/x_a)^2 \tan \theta \Delta Z \sum_{j=1}^m \Delta y_j \quad (13)$$

W is a simple summation, whereas A is the accumulated sum of the products obtained by multiplying each ordinate by the appropriate $(x_r/x)^2$ from column 3 of Table I. If this factor varies only in the last 3 places over the range from Z_1 to Z_2 , then it may be more convenient to subtract a number B from each value and use the following form for calculation

$$\sum_{j=1}^m (x_r/x_j)^2 \Delta y_j = B \sum_{j=1}^m \Delta y_j + \sum_{j=1}^m [(x_r/x_j)^2 - B] \Delta y_j$$

The integrals A and W are independent of the particular value of the limits when they are in plateau regions where $\Delta y = 0$. Typically ΔZ and the location Z_3 of the first ordinate to be measured are chosen using tabulated values of Table I. Then $Z_1 = Z_3 - \Delta Z/2$ and $Z_2 = [Z_3 + (m-1)\Delta Z] + \Delta Z/2$. The summation from Z_1 to Z_2 may be appropriately divided into two or more parts at different spacings. This is indicated when the continuation of a very close spacing, chosen to give about 10 points on a narrow peak, would be unnecessarily time consuming in reading a region containing a broad pattern. If the last ordinate reading were taken at Z_j for a series with spacing ΔZ_1 , then the next reading should be taken at $Z_{j+1} = Z_j + \Delta Z_1/2 + \Delta Z_2/2$, and then at $Z_{j+2} = Z_{j+1} + \Delta Z_2, \dots$, for the new series at a spacing of ΔZ_2 .

Velocity Sedimentation Analysis

The equations of velocity ultracentrifugation to be considered assume the existence of an all-component-plateau, a region of limited radial extent containing all the initial components but with no concentration gradients. The subscript p refers to any point selected in this plateau. It is no longer necessary to further assume that there are no concentration gradients at the meniscus nor that sedimentation coefficients are constant with concentration or time during an experiment. Complete derivations, interpretations or limitations are not given, instead the appropriate formulas are collected and converted to the notation of the two dimensional comparator. The equations are applicable for flotation as well as sedimentation.

(19) E. G. Pickels, W. F. Harrington and H. K. Schachman, *Proc. Natl. Acad. Sci., U.S.A.*, **38**, 943 (1952).

(20) T. Svedberg and K. O. Pedersen, "The Ultracentrifuge," Clarendon Press, Oxford, 1940.

The Concentration at Any Level in the Cell.—Klainer and Kegeles⁵ indicate, in effect, that the concentration at any level r in the cell can be expressed in terms of the initial concentration and the concentration gradient pattern for $r_a \leq r \leq r_p$ as

$$\begin{aligned} \Delta n &= \Delta n^0 - \int_{r_a}^{r_p} \left(\frac{r}{r_a}\right)^2 \frac{\partial \Delta n}{\partial r} dr + \int_{r_a}^r \frac{\partial \Delta n}{\partial r} dr \\ &= \Delta n^0 - W(Z_a, Z_p) + A(Z_a, Z) \end{aligned} \quad (14)$$

and for $r_p \leq r \leq r_b$ as

$$\begin{aligned} \Delta n &= \Delta n^0 + \int_{r_p}^{r_b} \left(\frac{r}{r_b}\right)^2 \frac{\partial \Delta n}{\partial r} dr - \int_r^{r_b} \frac{\partial \Delta n}{\partial r} dr \\ &= \Delta n^0 + (r_a/r_b)^2 W(Z_p, Z_b) - A(Z, Z_b) \end{aligned} \quad (15)$$

where Δn^0 is the initial concentration. In calculating the concentration at the starting level Z_a and the bottom of the cell Z_b , the A term in equations 14 and 15, respectively, is zero.

At sufficiently high speeds the concentration gradient at r_a drops to zero as the sedimentation overcomes the back diffusion. In this case the concentration at any level Z is

$$\Delta n = \int_{r_a}^r \frac{\partial \Delta n}{\partial r} dr = A(Z_a, Z) \quad (16)$$

and equation 14 then yields the initial concentration⁴

$$\Delta n^0 = \int_{r_a}^{r_p} \left(\frac{r}{r_a}\right)^2 \frac{\partial \Delta n}{\partial r} dr = W(Z_a, Z_p) \quad (17)$$

The left-hand side of equation 17 is also given by the index of refraction difference, $n_{\text{soln}} - n_{\text{solvent}}$, measured on a differential refractometer.²¹ If the synthetic boundary cell¹⁹ is used in the ultracentrifuge as a differential refractometer, the boundary will diffuse back toward the meniscus r_0 from the starting position r_a . To include all the gradients the integration should start at r_0 , and $\Delta n^0 = W(Z_0, Z_p)$. If the displacement of the boundary is negligible due to sedimentation, then Δn^0 is also given⁵ by $A(Z_0, Z_p)$.

Molecular Weight Analysis.—Archibald⁷ proposed to utilize the approach to sedimentation equilibrium in a sector cell in order to obtain the weight average molecular weight. Klainer and Kegeles⁵ developed the theory for use with schlieren optics and have shown that sufficient precision can be obtained in the very early part of the experiment before disappearance of the plateau solution, using the known position of the meniscus and/or bottom of the cell. The condition that no solute flow out of the cell either at the meniscus r_a or the bottom r_b implies from the flow equation⁷ for these two levels for all time and any speed that

$$\left(\frac{s}{D}\right)_a \omega^2 \Delta n_a - \frac{1}{r_a} \left(\frac{\partial \Delta n}{\partial r}\right)_a = 0 \quad (18)$$

$$\left(\frac{s}{D}\right)_b \omega^2 \Delta n_b - \frac{1}{r_b} \left(\frac{\partial \Delta n}{\partial r}\right)_b = 0 \quad (19)$$

where D is the diffusion coefficient. The subscript a or b has been added to (s/D) since s and D both represent weight average values of the composition in the neighborhood of a and b , respectively. In a heterogeneous system this composition changes with time. It is desired to obtain the best value

of s/D from the experiment, or series of experiments at several speeds, so that the weight average molecular weight M_w of the solute can be computed from^{7,20} $M_w (1 - \bar{V}\rho) = RTs/D$, where \bar{V} is the partial specific volume of the solute, ρ the solution density, T the absolute temperature, and R the gas constant. Substitute equation 14, evaluated at Z_a into equation 18 and equation 15, evaluated at Z_b into equation 19, using also equations 3 and 9

$$\left[\frac{F_a F_y x_r \tan \theta \Delta y_a}{5 \times 10^{14} \ln 10 F_x x_a}\right] = - \left(\frac{s}{D}\right)_a [W(Z_a, Z_p)] + \left(\frac{s}{D}\right)_a \Delta n^0 \quad (20)$$

$$\left[\frac{F_a F_y x_r \tan \theta \Delta y_b}{5 \times 10^{14} \ln 10 F_x x_b}\right] = \left(\frac{s}{D}\right)_b \left[\left(\frac{x_a}{x_b}\right)^2 W(Z_p, Z_b)\right] + \left(\frac{s}{D}\right)_b \Delta n^0 \quad (21)$$

These are of the form $q \equiv \pm (s/D)p + (s/D)\Delta n^0$ and a plot of q vs. p will yield s/D as slope and $p^0 = \Delta n^0$ as intercept on the p axis. The type of plot obtained is indicated in Fig. 3 where the various

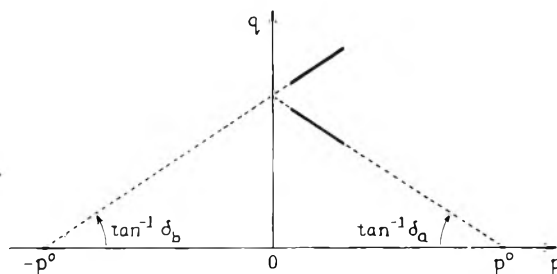


Fig. 3.—Molecular weight determination before sedimentation equilibrium. Data from successive frames from experiments at several speeds fall in solid portion of line. Extrapolation is made to determine slope $\delta = s/D$ and intercept p^0 . (See text for explanation of variables p and q .)

points in the solid lines are to be obtained from successive times in one experiment and/or all the experiments at several speeds. Since initially in the experiment $(s/D)_a = (s/D)_b$, deviations of the two slopes from equality, and/or non-linearity can be used to ascertain limitations of the particular experiment such as heterogeneity or concentration dependence. The initial concentration Δn^0 can be determined from the intercept p^0 , or if Δn^0 is known from refractometer measurements or a high speed experiment where equation 17 is applicable, p^0 can be used as an additional point.

Sedimentation Rate and Boundary Position.—The equation of continuity states for the plateau concentration Δn_p that $d\Delta n_p/dt = -120(10^{-13})\omega^2 s\Delta n_p$ where s is the weight average sedimentation rate of the solute. Expressed for s , this relation is

$$s = - \frac{10^{13}}{120\omega^2} \frac{d \ln \Delta n_p}{dt} = \frac{10^{13}}{6C\omega^2} \frac{d \ln \bar{r}}{dt} = F_s \frac{d \log \bar{x}}{dt} \quad (22)$$

The identity sign indicates the specification that the s rate of a moving boundary be the same as the s rate of the solute in the plateau. This has been used by Goldberg⁶ to define the boundary position \bar{r} . The integration of equation 22 gives⁴

$$(r_a/\bar{r})^2 = \Delta n_p/\Delta n^0 \quad (23)$$

Calculating from the boundary region between Z_a and Z_p , equation 14 in 23 yields

$$(x_a/\bar{x})^2 = 1 - [W(Z_a, Z_p) - A(Z_a, Z_p)]/\Delta n^0 \quad (24)$$

while utilization of the region between Z_p and Z_b gives from equation 15

$$(x_a/\bar{x})^2 = 1 + [(x_a/x_b)^2 W(Z_p, Z_b) - A(Z_p, Z_b)]/\Delta n^0 \quad (25)$$

If the concentration gradient is reduced to zero at the starting level, or the synthetic boundary cell is used, equation 23, employing equation 17, reduces to⁶

$$\bar{r} = \left[\frac{\int_{r_a}^{r_p} r^2 (\partial \Delta n / \partial r) dr}{\int_{r_a}^{r_p} (\partial \Delta n / \partial r) dr} \right]^{1/2} \quad (26)$$

This square root of the second moment of the refractive index gradient distribution, in engineering terms, is equivalent to the radius of gyration of the schlieren pattern about the center of rotation and also the location of the step in the plateau concentration resulting from a hypothetical rearrangement of solute to give an infinitely sharp boundary.⁶ Using equations 10 and 11, or 24 and 17, equation 26 yields not only the interrelationship of A and W but the formula for calculation of \bar{x} to within 0.01 mm. on the comparator

$$\left(\frac{x_r}{\bar{x}}\right)^2 = \left(\frac{x_r}{x_a}\right)^2 \frac{A(Z_a, Z_p)}{W(Z_a, Z_p)} = \frac{\sum_{j=1}^m (x_r/x_j)^2 \Delta y_j}{\sum_{j=1}^m \Delta y_j} \quad (27)$$

It is essential that the same ordinates be used in both integrals so that an error in one x_j or Δy_j will have a lesser effect on the ratio.

An example of this calculation is given in Table II for the pattern of Fig. 1c. The value of \bar{x} or $\log \bar{x}$ is obtained by interpolation in Table I, entering column 3 with the calculated value of $(x_r/\bar{x})^2 = 1.2847$. For this apparently symmetrical pattern the difference between the position of the maximum ordinate 141.06 and the boundary position 141.16 is only 0.10 mm. on the plate, which corresponds to about 0.05 mm. in the cell.

Whether \bar{x} is obtained as a close approximation as the position of a maximum ordinate, or from equations 24, 25 or 27, its s rate is determined from a plot of $\log \bar{x}$ against the time t . The s rate is then calculated from the slope of the line in accordance with equation 7 or 22. In special cases, initial slopes can be obtained by the chord method.²² Alternately, \bar{s}^* can be calculated and the initial s rates determined by extrapolation of \bar{s}^* to zero time as described by Alberty.²³

Paucidisparity Relations.—For several components, possibly measured in different photographs, equation 17 can be expanded to^{4,22}

$$\Delta n_1^0 + \Delta n_2^0 + \dots = \Delta n_1^* + \Delta n_2^* + \dots \quad (28)$$

where the terms on the left refer to the initial concentration of the components, numbered from the slowest in s rate, and the terms on the right to $(r/r_a)^2 (\partial n / \partial r)$ integrated over each (resolved)

(22) R. Trautman, V. N. Schumaker, W. F. Harrington and H. K. Schachman, *J. Chem. Phys.*, **22**, 555 (1954).

(23) R. A. Alberty, *J. Am. Chem. Soc.*, **76**, 3733 (1954).

peak, and also numbered from the slowest in s rate. Each term on the right of equation 28 is not necessarily equal to the corresponding true concentration term on the left. This is due to a fundamental property of moving boundary analysis referred to for the velocity ultracentrifuge as the Johnston-Ogston²⁴ effect. Shown in the insert in Fig. 4 is the notation for describing this effect. Let the subscript f represent the fastest component present, the appearing component, and s represent any slower component at any boundary under consideration. Let s_s' be the sedimentation rate of the slow component ahead of the boundary and \bar{r}_s' the boundary position (not visible as a peak) corresponding to this s rate in accordance with equation 22

$$(\bar{r}_s'/r_a) = (\bar{r}_f/r_a)^{s_s'/s_f^0} \quad (29)$$

if²²

$$s_s'/s_f = s_s^0/s_f^0 \quad (30)$$

Using these terms, the general solution for the Johnston-Ogston effect considering the interplay of the radial dilution and the concentration dependence is²²

$$\frac{\Delta n_{sf}^*}{\Delta n_s^*} = \frac{(1/\bar{r}_s')^2 - (1/\bar{r}_f)^2}{(1/\bar{r}_s')^2 - (1/\bar{r}_f)^2} = \frac{(x_r/\bar{x}_s')^2 - (x_r/\bar{x}_f)^2}{(x_r/\bar{x}_s')^2 - (x_r/\bar{x}_f)^2} = \frac{W_{sf}}{W_s} \quad (31)$$

where equations 6 and 17 have been used, and the correction Δn_{sf} and W_{sf} are defined such that

$$\begin{aligned} \Delta n_s^0 &= \Delta n_s^* - \Delta n_{sf}^* = W_s - W_{sf} \\ \Delta n_f^0 &= \Delta n_f^* + \Delta n_{sf}^* = W_f + W_{sf} \end{aligned} \quad (32)$$

If $(\bar{r}/r_a)^2 \approx 1 + 2 \ln(\bar{r}/r_a)$, then this equation can be written, using equations 5, 22, 29 and 30 as²²

$$\frac{\Delta n_{sf}^*}{\Delta n_s^*} = \frac{s_s^*/s_f^* - s_s^0/s_f^0}{1 - s_s^0/s_f^0} = \frac{W_{sf}}{W_s} \quad (33)$$

This relationship is shown graphically in Fig. 4. Enter with the observed s_s^*/s_f^* , proceed vertically to the correct s_s^0/s_f^0 line and then read off the correction at the left. If both components alone exhibit approximately the same concentration dependence k_f , and s_s' is also given approximately by

$$s_s' = s_s^*(1 - k_f c_f) \quad (34)$$

where c_f is the change in total concentration at the fast boundary, then elimination of s_s' in equation 30 gives

$$s_s^*/s_f^* = (s_s^0/s_f^0)/(1 - k_f c_f) \quad (35)$$

This equation is also plotted in Fig. 4 for $k_f c_f = 0.1$ and 0.2 , corresponding to a 10% and a 20% change, respectively, in s rate of the slow component across the fast boundary.

De Lalla and Gofman¹¹ and Baldwin²⁵ solve the paucidisparity system by successive reapplication of the two component formula. The slowest component is considered first. The corrections to apply to the area of the slowest boundary are calculated at each faster boundary in order. Then the next faster component is considered, and all the corrections to apply to the area of the second

(24) J. P. Johnston and A. G. Ogston, *Trans. Faraday Soc.*, **42**, 789 (1946).

(25) R. L. Baldwin, *J. Am. Chem. Soc.*, **76**, 402 (1954).

boundary are calculated successively across each faster boundary, This reapplication of equation 32 yields

$$\begin{aligned} \Delta n_1^0 &= \overset{(1)}{W_1} - \overset{(3)}{W_{12}} - \overset{(6)}{W_{13}} - \dots \\ \Delta n_2^0 &= \overset{(2)}{W_2} + \overset{(4)}{W_{12}} - \overset{(8)}{W_{23}} - \dots \\ \Delta n_3^0 &= \overset{(5)}{W_3} + \overset{(7)}{W_{13}} + \overset{(9)}{W_{23}} - \dots \end{aligned} \quad (36)$$

where the numbers above the terms indicate the order the calculations are to be made. In calculating W_{13} , for example, $s_1^* = s_3^*$, $s_3^* = (s_1^0/s_2^0)s_2^*$ from equation 30.

Polydispersity Relations.—In addition to containing a paucidisperse system of peaks, the schlieren pattern may represent polydispersity or a continuum of sedimentation components in each peak. To ascertain this, the schlieren pattern is converted to an apparent distribution function¹ with respect to s^* and then extrapolated to infinite time to remove diffusion effects.⁸ The relationship has been given as

$$\begin{aligned} g^*(s^*) &= \frac{60 \omega^2 r l}{10^{13} \Delta n^0} \left(\frac{r}{r_a} \right)^2 \frac{\partial \Delta n}{\partial r} \\ &= \left(\frac{3l \ln 10}{F_a} \right) \left[\frac{(x_r/x_a)^2 F_x F_y \tan \theta}{\Delta n^0} \right] Z \Delta y \quad (37) \end{aligned}$$

where s^* is to be obtained from equation 5, and Δn^0 may be determined from a differential refractometer or from equation 17. The tabulation of (x_r/x) is useful in making the extrapolation of g^* for each selected s^* against $1/(xl)$ to infinite time.²⁶

(26) L. J. Gosting, *J. Am. Chem. Soc.*, **74**, 1542 (1952).

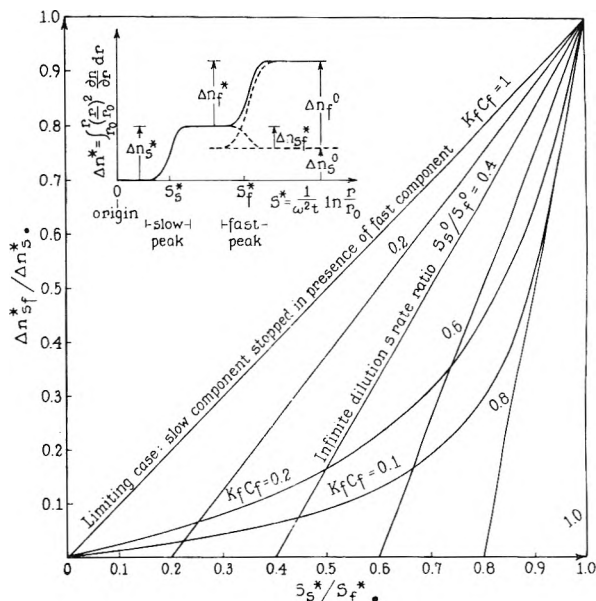


Fig. 4.—Johnston-Ogston correction for two-sedimenting components. Insert in upper left gives the notation for the correction Δn_{sf}^* , a superimposed concentration change of the slow component at the fast boundary. The ratio of the correction, Δn_{sf}^* , to the observed slow boundary initial time area, Δn_s^* , is read from the vertical scale, entering with the observed ratio of boundary s rates, s_s^*/s_f^* . Either the ratio of the infinite dilution s rates, s_s^0/s_f^0 , or the concentration dependence, $k_f C_f$, must be known.

Acknowledgment.—The author wishes to express appreciation to Dr. L. G. Longworth for making available the basic two-dimensional movement of the comparator and for very many helpful discussions and criticisms of this paper.

THE PROPERTIES OF ASBESTOS. III. BASICITY OF CHRYSOTILE SUSPENSIONS¹

BY FRED L. PUNDSACK AND GEORGE REIMSCHUSSEL

Contribution from the Johns-Manville Research Center, Manville, New Jersey

Received February 24, 1956

It is shown by means of conductivity and colorimetric analyses data that in aqueous suspensions hydroxyl and magnesium ions dissociate from the surface of chrysotile. Provided enough fiber surface is presented to the solution, an equilibrium comparable to that attained by magnesium hydroxide is reached. The saturation concentration of magnesium hydroxide in equilibrium with eight different chrysotile specimens is determined as well as the solubility product constant for the fiber surface. The total basicity of chrysotile is evaluated, and the material is titrated stepwise with hydrochloric acid. The titration data are interpreted in terms of the structure of chrysotile.

Introduction

It has been pointed out that in aqueous suspensions the hydrated magnesium silicate mineral chrysotile ($Mg_6(OH)_8Si_4O_{10}$) bears a marked resemblance to magnesium hydroxide.² One purpose of the work reported here was to determine quantitatively by means of conductivity measurements the degree to which magnesium and hydroxyl ions dissociated from the surface of chrysotile and to demonstrate the manner in which this effect was dependent upon the exposed surfaces. While this study has been limited to chrysotile, many of the arguments and conclusions apply to certain of the kaolin clay mineral group ($Al_2O_3 \cdot 2SiO_2 \cdot 2H_2O$) which has been described as the aluminum analog of chrysotile.³

In common with most minerals, the composition of chrysotile varies from the ideal to a greater or lesser extent depending upon the source of the sample. This is reflected by the fact that at least three different varieties of chrysotile known as soft, semi-harsh and harsh are recognized. Although the terms are somewhat ambiguous in that they refer to the "feel" of the fiber when touched, in general, a soft fiber has a higher tensile strength and greater flexibility than a harsh fiber. It has been reported that the harsh fiber varieties have lower combined water contents than do the soft varieties.⁴ In the current study it was felt that these differences in the properties of various varieties of chrysotile might be reflected by the degrees of dissociation of hydroxyl and magnesium ions from the surfaces of the fibers. With this in mind chrysotile specimens from eight localities were examined for degree of surface dissociation to see if significant differences did occur.

The basicity of chrysotile is demonstrated by the fact that the fiber reacts with acids, and if the acid is strong the fiber will react completely to form a hydrated silica residue. This has been recognized for a long time,⁵⁻⁷ but no detailed study of the course of the reaction appears to have been made. This same type of reaction occurs to differing extents with many members of the clay minerals

group⁸⁻¹⁰ and a number of other silicate compounds containing an appreciable number of hydroxyl groups (*e.g.*, certain calcium silicate hydrates). In view of the prevalence of this reaction, and its direct relationship to the structure of chrysotile it was studied in some detail. Chrysotile suspensions were "titrated" with a strong acid, and it will be shown that the results give some insight into the number and distribution of hydroxyl groups in the crystal structure.

Experimental

Materials.—The following specimens of chrysotile were used in this work: (1) Danville from Asbestos, Quebec; (2) Arizona Soft from Gila County, Arizona; (3) Arizona Harsh from Gila County, Arizona; (4) Munro from near Matheson, Ontario; (5) Vimy from Vimy Ridge Mine near Black Lake, Quebec; (6) Normandie from near Black Lake, Quebec; (7) Shabani from Shabani district, Southern Rhodesia; (8) Transvaal from Carolina district, Transvaal. Samples 1, 2, 7 and 8 are usually classified as the soft variety of chrysotile whereas samples 3, 4, 5 and 6 exhibit varying degrees of "harshness." The fiber samples selected for study were carefully separated by hand from native ore specimens, and then they were examined to ensure that the fiber was free of all gross impurities. Portions of the selected samples were pulverized by passing them through a Laboratory Wiley Mill fitted with a 60-mesh screen.

The water used in the conductivity measurements was carefully distilled, but probably it was not free of carbon dioxide. The water had a uniform conductivity of 3×10^{-6} ohms⁻¹ cm.⁻¹.

The hydrochloric acid employed in the titration of chrysotile was of reagent grade.

Conductivity Measurements.—The conductivity of a series of suspensions of each fiber sample containing various concentrations of solids was determined. The procedure consisted of adding the desired amount of pulverized fiber to 50 ml. of distilled water in a 125-ml. Erlenmeyer flask, and then the mixture was agitated at $25 \pm 1^\circ$ for 16 hours. This period of time was sufficient to establish equilibrium. The suspensions were centrifuged, and the conductivity of the supernatant liquid was determined in a constant temperature bath regulated at $25.00 \pm 0.02^\circ$. A Model RCIB Conductivity Bridge manufactured by Industrial Instruments, Inc., was used for the measurements. The conductivity cell was a dip type fitted with platinum black electrodes. It had a cell constant of 1.0242 determined with a standard 0.02 *N* potassium chloride solution.

In addition to the pulverized fiber samples, a series of measurements were made on the Danville fiber in various degrees of openness to establish the relationship between exposed surface and the release of ions into the solution.

Titration.—The total basicity of chrysotile was established by making a suspension of 0.5868 g. of the Danville fiber in 200 ml. of 0.1471 *N* hydrochloric acid. The mixture was refluxed overnight, and then it was allowed to cool

(1) Preceding paper in this series, F. L. Pundsack, *THIS JOURNAL*, **60**, 361 (1956).

(2) F. L. Pundsack, *ibid.*, **59**, 892 (1955).

(3) G. W. Brindley, "X-Ray Identification and Crystal Structure of Clay Minerals," The Mineralogical Society, London, 1951.

(4) M. S. Badollet, *Trans. Can. Inst. Mining Met.*, **54**, 151 (1951).

(5) Anon., *Gummi-Z.*, **41**, 1861 (1927).

(6) D. Wolochow, Canadian Patent 340,901 (April 1934).

(7) L. M. Pidgeon, *Can. J. Research*, **12**, 41 (1935).

(8) L. Wolf, *Ber.*, **14**, 393 (1933).

(9) P. G. Nutting, U. S. Geol. Survey, *Profess. Paper* 197 F, pp. 219-235 (1943).

(10) J. A. Pask and B. Davies, U. S. Bur. Mines Tech. Paper 664, pp. 56-78 (1945).

before it was filtered. The residue was washed to remove any occluded solution, and the total acidity of the combined filtrates was determined by titration with a standard sodium hydroxide solution. A blank run showed that no acid was lost during the refluxing operation so the difference between the initial and final acidity of the solution could be attributed to reaction with the fiber. Several samples were run and the method gave very reproducible results (*i.e.*, $\pm 1\%$).

The "titrations" were carried out by placing an accurately weighed 0.5-g. sample of pulverized Danville fiber in 150 ml. of distilled water. Small increments of 0.5150 *N* hydrochloric acid were added to the suspension, and the system was refluxed overnight between each addition of acid. After each refluxing cycle and before the addition of the next increment of acid, the suspension was cooled to room temperature. A small portion of the mixture was withdrawn and the *pH* was determined with a Beckman Model G *pH* meter. The portion withdrawn was replaced in the system, and the cycle of adding acid and refluxing was continued. In this way a point by point plot of *pH* versus ml. of acid added was obtained. Three samples titrated with this method yielded the same results.

Analyses for Magnesium and Soluble Silica.—The amount of magnesium ion in equilibrium with the different asbestos suspensions was determined colorimetrically with a method described by Harvey, Komarmy and Wyatt.¹¹ The procedure consists of measuring the absorption of a complex formed between magnesium ions and the reagent Eriochrome Black T. The reagent was manufactured by the Hach Chemical Company.

Soluble silica in equilibrium with the asbestos suspension was determined with a molybdenum blue method described by Bunting.¹² In this procedure the yellow silicomolybdic acid complex¹³ is formed first, and after 7–10 minutes it is reduced to form molybdenum blue. The absorption due to this latter material is then related to the silica concentration. Several workers have demonstrated recently that in the formation of the yellow silicomolybdic acid complex only low molecular weight species of silica react, and in this sense, the formation of the complex is a real measure of "soluble silica."^{14–15}

Results

Conductivity.—The data for the conductivity of pulverized chrysotile asbestos suspensions are summarized in Table I. It is apparent from these results that all the fibers contain a soluble electrolyte or electrolytes¹⁶ in addition to the magnesium and hydroxyl ions dissociated from the fiber

surface. Based on conductivity measurements the excess soluble electrolyte content is expressed arbitrarily as equivalent sodium chloride in Table I. The nature of the conductivity values can be seen in Fig. 1 which is a plot of data for representative samples. The experimental conductivity curves are made up of two distinct components. One of the components is due to the contribution of the relatively insoluble ions released by the fiber (*i.e.*, magnesium and hydroxyl ions¹⁷), and the other component is due to a soluble electrolyte present in the fiber. The contribution of the former to the conductivity of the system reaches a maximum at a point corresponding to saturation of the solution with magnesium and hydroxyl ions, but the contribution of the latter increases uniformly as the amount of solid fiber in suspension is increased. However, extrapolation of the upper straight line portion of the experimental conductivity curve to zero concentration will give an intercept which corresponds to the conductivity at saturation of the relatively insoluble ions dissociated from the fiber surface. With this intercept value the approximate concentration of magnesium and hydroxyl ions present at saturation can be calculated in theory from the standard expression^{18,19}

$$C = \frac{L_s 10^3}{\Lambda_0} \quad (1)$$

where

C = gram equivalents per liter

L_s = total specific conductance of the ions (*i.e.*, zero intercept value)

Λ_0 = equiv. conductance of Mg(OH)₂ at infinite diln.

The zero intercept values were corrected for the conductivity of the water (*i.e.*, 3×10^{-6} ohms⁻¹ cm.⁻¹), and a Λ_0 value of 251 ohms⁻¹ cm.² was used²⁰ in calculating the saturation concentration values shown in Table II. The use of Λ_0 is an approximation, but at the low ionic concentrations which exist in the saturated suspension the approximation appears valid.

The direct application of the saturation concentration values to a calculation of the "solubility product constant" for the fiber surface as shown in equation 2 is valid only if the fiber structure is the sole source of equivalent concentrations of magnesium and hydroxyl ions. Analyses of the chrysotile suspensions indicate that these conditions are not satisfied. In all the fiber samples magnesium

$$K_s = [\text{Mg}^{++}] [\text{OH}^-]^2 \quad (2)$$

ions enter the solution from two sources: the fiber

(17) Probably the surface of the chrysotile fiber is in equilibrium with dissociated magnesium and hydroxyl ions and some monomeric or low molecular weight ionic silicic acid species. Analyses of the suspensions, however, has shown that the concentration of soluble silica in solution is of the order of 0.4 p.p.m. or about 6.7×10^{-5} molar with respect to SiO₂. The equivalent conductivity of the soluble silica species is not known, but the contribution of these species to the conductivity of the system is small compared to the combined conductivities of the magnesium and hydroxyl ions. Thus, to a first approximation the simplifying assumption has been made that the fiber surface is in equilibrium with magnesium and hydroxyl ions only.

(18) F. Daniels, J. H. Mathews, J. W. Williams and staff, "Experimental Physical Chemistry," McGraw-Hill Book Co., New York, N. Y., 1949.

(19) S. Glasstone, "Textbook of Physical Chemistry," D. Van Nostrand Co., New York, N. Y., Ed. 2, 1946.

(20) D. A. MacInnes, "The Principles of Electrochemistry," Reinhold Publ. Corp., New York, N. Y., 1939.

TABLE I

SPECIFIC CONDUCTIVITY OF CHRYSOTILE ASBESTOS SUSPENSIONS (Ohms⁻¹ cm.⁻¹ × 10⁶)

Sample	% Chrysotile in suspension				% equiv. NaCl ^d
	0.20	1.00	2.00	2.90	
Danville ^a	..	12.5	17.5	23.4	0.24
Arizona Soft ^b	6.0	10.9	17.1	22.2	.27
Arizona Harsh	5.3	7.4	9.7	11.9	.10
Munro	3.5	5.4	6.4	7.7	.05
Vimy	4.8	7.8	10.9	13.5	.13
Normandie ^c	5.0	9.8	13.9	17.8	.19
Shabani	4.8	10.5	16.3	20.6	.24
Transvaal	6.1	11.3	17.0	21.8	.25

^a Additional points: 0.07% = 3.0×10^{-5} ; 0.13% = 4.7×10^{-5} ; 0.40% = 8.4×10^{-5} . ^b 0.3% = 6.7×10^{-5} . ^c 0.5% = 6.7×10^{-5} . ^d Hypothetical NaCl in the sample required to account for that portion of the conductivity not due to Mg(OH)₂ ionized from the fiber surface.

(11) A. E. Harvey, J., J. M. Komarmy and G. M. Wyatt, *Anal. Chem.*, **25**, 498 (1953).

(12) W. E. Bunting, *Ind. Eng. Chem., Anal. Ed.*, **16**, 612 (1944).

(13) J. D. H. Strickland, *J. Am. Chem. Soc.*, **74**, 872 (1952).

(14) E. Weitz, H. Francke and M. Schuchard, *Chem. Z.*, **74**, 256 (1950).

(15) G. B. Alexander, *J. Am. Chem. Soc.*, **75**, 5655 (1953).

(16) Soluble electrolyte is used here in the sense that the electrolyte is relatively more soluble than magnesium hydroxide.

TABLE II
SOLUBILITY AND DISSOCIATION DATA FOR CHRYSOTILE IN WATER

Sample	Extrapolated ordinate intercept (ohms ⁻¹ cm. ⁻¹ × 10 ⁶)	Mg(OH) ₂ at satn. × 10 ⁴ (moles/l.)	% Chrysotile at satn.	Mg ⁺⁺ at satn. × 10 ⁴ (g. ions/l.)	K _S = [Mg ⁺⁺][OH] ⁻
Danville	6.8	1.4	0.7	2.9	2.3 × 10 ⁻¹¹
Arizona soft	4.6	0.9	.3	1.2	4 × 10 ⁻¹²
Arizona harsh	4.6	0.9	.2	0.9	3 × 10 ⁻¹²
Munro	3.9	0.8	.8	1.1	3 × 10 ⁻¹²
Vimy	4.6	0.9	.6	1.6	5 × 10 ⁻¹²
Normandie	5.2	1.0	.9	2.6	1.0 × 10 ⁻¹¹
Shabani	5.2	1.0	.7	2.6	1.0 × 10 ⁻¹¹
Transvaal	5.6	1.1	.6	1.9	9 × 10 ⁻¹²

structure and as a component of the soluble electrolytes. This is shown by the fact that in all the suspensions the concentration of magnesium in solution increases as the per cent. solid fiber increases. Beyond the saturation point the increase in magnesium ion concentration is a direct function of the amount of fiber added to the system, which indicates that magnesium ions are entering the solution in the form of a soluble electrolyte. On the other hand, the fiber structure appears to be the only source of hydroxyl ions. Therefore, at the saturation point magnesium and hydroxyl ions will not be present in equivalent quantities. In order to evaluate K_S it is necessary to determine directly the magnesium ion concentration in a solution exactly saturated with respect to magnesium hydroxide. The hydroxyl ion concentration at this point is given by the concentration of magnesium hydroxide as shown in Table II. The magnesium ion concentration can be determined colorimetrically by analysis of a suspension at the saturation point. This latter point may be established approximately since it corresponds to the deviation of a plot of the conductivity data from the upper straight line portion of the curve. For example, in Fig. 1 a saturated suspension of Danville fiber is obtained at about a 0.7% solids concentration, and a Munro fiber yields a saturated suspension at about 0.8% solids concentration. Even though these points are approximate, a deviation of $\pm 0.1\%$ does not alter the magnesium ion concentration appreciably. Therefore, suspensions corresponding to these approximate saturation points were prepared and analyzed for magnesium ions. In some cases the concentrations were obtained by extrapolation of magnesium concentration values obtained at higher suspension concentrations. The data are summarized in Table II.

In the case of a relatively insoluble silicate such as chrysotile in which the dissociation of ions into solution is limited almost entirely to surface groups, the concentration of ions in a given fiber-water system will be dependent upon the amount of fiber surface exposed to the free solution. This is supported by the observation that a 1-g. block of unopened fiber agitated with 50 ml. of water for 24 hours yielded a solution with a conductivity of 1.4×10^{-5} ohms⁻¹ cm.⁻¹. This compares with a value of 6.8×10^{-5} ohms⁻¹ cm.⁻¹ for 1 g. of the same fiber pulled apart with tweezers and treated in the same fashion. Both the preceding values are con-

siderably lower than the 17.5×10^{-5} ohms⁻¹ cm.⁻¹ value recorded for the fiber in a pulverized state. These observations also indicate that the "soluble electrolytes" within a block of fiber do not have ready access to free solution until the fiber bundles are separated and opened.

Total Basicity of Chrysotile.—It was found that 0.5868 g. of the Danville fiber reacted with 12.63 meq. of hydrochloric acid. If the unit cell composition of chrysotile, $Mg_6(OH)_8Si_4O_{10}$ with a mass of 554.2, is taken as a convenient expression for a "molecule" of chrysotile, the acid reaction corresponds to 11.92 equivalents of base per mole of chrysotile. This is in good agreement with the value of 12.00 equivalents which would be expected on the basis of the empirical composition of a unit cell of chrysotile, $6MgO \cdot 4SiO_2 \cdot 4H_2O$, in which the magnesium oxide is treated as the only basic constituent.

Acid Titration of Chrysotile.—The titration curve for a 0.5360-g. sample of pulverized Danville fiber reacted with 0.5150 *N* hydrochloric acid at 100° exhibits several inflections. The first increments of acid up to an addition of 1 ml. cause a sharp decrease in *pH* from an initial value of 10 to about 6.8. This point corresponds to the addition of 0.515 meq. of acid which is enough acid to react with about 4.5% of the fiber. After this first inflection point the titration curve exhibits a plateau until a second pronounced change in the slope of the curve occurs beyond the addition of about 12 ml. of acid. The curve exhibits a definite inflection point corresponding to the addition of 15 ml. of acid (*i.e.*, 67% complete reaction), and then it tails off at a *pH* of about 2.3 as the titration is completed.

Discussion

Solubility and Dissociation of Chrysotile.—The conductivity and colorimetric analyses data indicate that all the varieties of chrysotile examined dissociate magnesium and hydroxyl ions from their surfaces and eventually reach an equilibrium comparable to that attained by magnesium hydroxide.²¹ The individual samples vary by a factor of 10 with respect to the degree of surface dissociation, although the variations are moderate when the wide range of sample sources is considered. The degree of surface dissociation exhibited by the samples cannot be correlated directly with physical properties such as tensile strength or flexibility.

(21) J. W. Ryznar, J. Green and M. G. Winterstein, *Ind. Eng. Chem.*, **38**, 1057 (1946).

However, the degree of dissociation probably does affect the chemical behavior and reactivity of the fiber.

The saturation concentration of magnesium hydroxide in equilibrium with the chrysotile surface as determined with conductivity measurements gives calculated hydroxyl ion concentrations which are in good agreement with concentration values determined from pH measurements. For example, the hydroxyl ion concentration in equilibrium with the Danville fiber is 2.8×10^{-4} g. ions per liter on the basis of the extrapolated conductivity data. This is equivalent to a pH of 10.45 which compares well with an experimental pH value of 10.33. However, the measurement of pH with a glass and calomel electrode in chrysotile-water systems is subject to a "suspension effect" which has often been observed in clay suspensions.^{22,23} This effect with chrysotile has been described earlier,² but it was not recognized as a relatively common phenomenon. Jenny and his co-workers suggest that the effect is caused by abnormal junction potentials at the calomel electrode in certain colloidal systems or suspensions.²⁴ In any event, the determination of pH values in chrysotile suspensions must be made with due regard for the suspension effect.

All the chrysotile samples contain soluble electrolytes in varying quantities although the amount is very small in some cases. These electrolytes are associated intimately with the fiber bundles and probably are homogeneously distributed throughout the fiber veins in the deposit. Conductivity measurements on the massive serpentine associated with one of the fiber samples indicates that the serpentine contains a soluble electrolyte in about the same quantity as does the fiber. This may mean that soluble electrolyte is more or less homogeneously distributed throughout the entire ore body. There appears to be some correlation between the "softness" of the fiber and a relatively high electrolyte content. The nature of the soluble electrolytes has not been established, but in some of the suspensions chloride ions are present in appreciable amounts along with magnesium and potassium cations. However, the nature of the soluble electrolytes appears to vary depending upon the source of the specimen. Due to a common ion effect the presence of magnesium ions in the form of a soluble electrolyte can be expected to repress the hydroxyl ion concentration in chrysotile suspensions as the solids content is increased beyond the saturation point. However, in the concentration range investigated in this work, the conductivity measurements did not have enough precision to reflect the repression of the hydroxyl ion

Acid Titrations.—It is possible that the sharp, pronounced drop in the pH of a chrysotile suspension when the first increments of acid are added is due to the reaction of the hydroxyl groups on the surface of the fundamental fibrils. It would be logical to expect these groups to be most readily accessible to acid attack. If the validity of this assumption is granted then the data show that es-

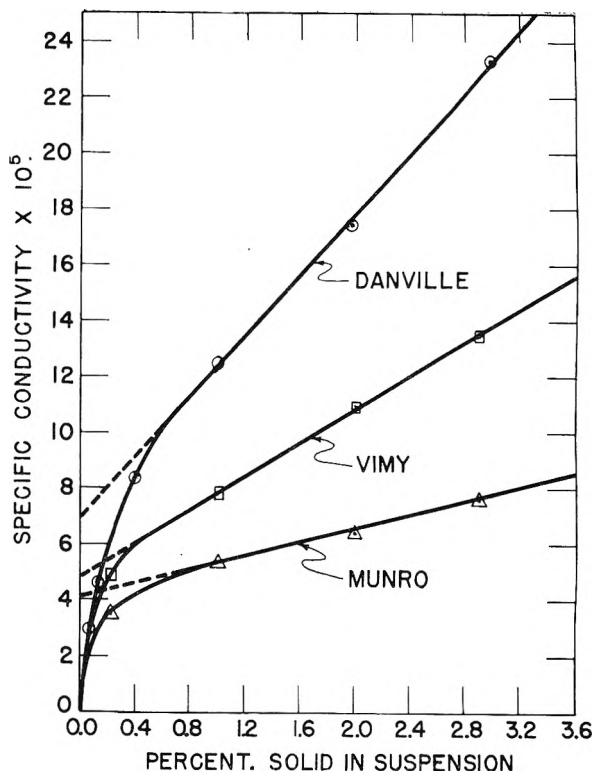


Fig. 1.—Typical plots of the conductivity data for different chrysotile samples.

entially all the surface hydroxyl groups have reacted when about 4.5% of the total fiber basicity has reacted. Since the hydroxyl groups in the chrysotile structure (*i.e.*, $Mg_6(OH)_8Si_4O_{10}$) comprise two-thirds of the total basicity of the composition, this result implies that about 7% of the total hydroxyl groups in the structure exist on the surface of fundamental fibrils.

The second break in the titration curve with an inflection point corresponding to 67% complete reaction probably represents the completion of the acid reaction with all the remaining structural hydroxyl groups. The inflection point occurs at a position corresponding to the reaction of 8 of the total of 12 equivalents of base in the composition $Mg_6(OH)_8Si_4O_{10}$.

The remainder of the acid-base reaction is most likely associated with the hydration of the silica from the original chrysotile structure to form the relatively high surface area hydrated silica residue which is observed as the final reaction product. Thus, the complete acid titration of chrysotile proceeds in at least three distinguishable steps: (1) the reaction of the surface hydroxyl groups; (2) the reaction of the remaining structural hydroxyl groups; (3) the reaction to form a hydrated silica residue.

In connection with the behavior of chrysotile in acid systems it is of interest to note that a single sample of massive serpentine²⁵ from Balmat, N. Y., was ground to -200 mesh and titrated with the

(22) H. Pallmann, *Kolloidchem. Beih.*, **30**, 334 (1930).

(23) G. Weigner, *J. Soc. Chem. Ind., (London)*, **50**, 103T (1931).

(24) H. Jenny, T. R. Nielsen, N. T. Coleman and D. E. Williams, *Science*, **112**, 164 (1950).

(25) Serpentine ($3MgO \cdot 2SiO_2 \cdot 2H_2O$) occurs in both massive and fibrous (*i.e.*, chrysotile) forms. In most chrysotile deposits the fiber is found in the form of veins distributed throughout a massive serpentine matrix, although in some instances the fiber occurs in limestone and dolomite bodies (*e.g.*, the Arizona and Transvaal fibers).

procedure outlined for chrysotile. The massive serpentine, which is usually described in terms of the same composition as chrysotile (*i.e.*, $Mg_6(OH)_3Si_4O_{10}$ or a multiple thereof), yielded a titration curve unlike that of chrysotile. After an initial drop in pH with the first additions of acid, the pH remained steady at about 6.0–6.2 until complete reaction was attained when the pH dropped abruptly to less than 3.0. The difference in titration behavior between chrysotile and massive serpentine probably is a reflection of differences in the arrangement of the ions within the individual crystalline lattices. The validity of the observation on massive serpentine tends to be substantiated by the report that massive serpentine is less subject to attack by acids than is chrysotile.²⁵

There appear to be few comparative data in the literature on the acid titration of kaolinite ($Al_2(OH)_4Si_2O_7$) or related clay minerals,²⁷ although the

(26) T. F. Bates and B. Nagy, *Am. Mineralogist*, **37**, 1055 (1952).

(27) R. E. Grim, "Clay Mineralogy," McGraw-Hill Book Co., Inc., New York, N. Y., 1953.

acid solubility of these materials has been reported,²⁸ and there is a considerable literature on the titration of clay acids.²⁹ On the basis of the limited amount of comparative data available with respect to reactions with acids, the mineral halloysite³⁰ probably is more nearly the aluminum analog of chrysotile than is kaolinite.

Acknowledgment.—We wish to thank Dr. Julie Yang who set up the analytical procedures for the magnesium and soluble silica analyses. Mr. Marion Badollet and Mr. William Streib contributed helpful discussions on the varieties and physical properties of chrysotile, and Dr. A. B. Cummins made several useful suggestions concerning the selection of samples.

(28) J. A. Pask and B. Davies, U. S. Bur. Mines Tech. Paper 664, pp. 56–78 (1945).

(29) C. E. Marshall, "The Colloid Chemistry of the Silicate Minerals," Academic Press, Inc., New York, N. Y., 1949.

(30) Halloysite and kaolinite are usually described with the same composition, but they are believed to differ in their structural arrangements.²⁷ For a recent discussion of the terminology of this group of minerals see G. T. Faust, *Am. Mineralogist*, **40**, 1110 (1955).

MAGNETIC SUSCEPTIBILITY STUDIES IN THE SYSTEM NiO-Al₂O₃BY JAMES T. RICHARDSON¹ AND W. O. MILLIGAN*The Rice Institute, Houston, Texas**Received February 24, 1956*

Magnetic susceptibility measurements on a series of NiO-Al₂O₃ samples, prepared by the heat treatment of the dual hydroxide gels at 700 and 1000°, lead to the conclusion that, for the 1000° samples, the Weiss constant, θ , (a) varies linearly with decreasing NiO concentration to about 60 mole % NiO, (b) remains constant over the range 40-60 mole % NiO, and (c) decreases linearly to zero at infinite dilutions of NiO. For the 700° samples, the Weiss constant varies linearly with the molar ratio over the complete concentration range. These results agree with X-ray evidence that, at the 1000° level of heat treatment, the nickel spinel, detected at equimolar ratios, forms solid solutions with excess nickel or aluminum oxide. The magnetic moments of the 700 and 1000° samples remain constant at 3.20 bohr magnetons until about 60 mole % NiO, where they show an increase and pass through a maximum returning to 3.2 for infinitely dilute nickel oxide. This increase in magnetic moment has been associated with a shift in the order-disorder cation distribution in the NiO-Al₂O₃ samples.

Introduction

In a previous report from this Laboratory,² the authors have presented the results of magnetic susceptibility measurements at room temperature on a series of NiO-Al₂O₃ samples, prepared at every 5 mole % NiO and heat treated at temperature levels of 300, 400, 500, 600 and 700°. Variations in the susceptibility-concentration curves due to the size and morphology of the original hydroxide particles and to the occurrence of zones of mutual protection³ were observed.

X-Ray diffraction studies on this system, reported by Milligan and Merten,⁴ show that equimolar mixtures of nickel and aluminum oxides react at 1000° to form nickel spinel NiO·Al₂O₃. This compound has the spinel structure and forms solid solutions with excess of each of the pure oxides. The diffraction lines of NiO·Al₂O₃, observed at heat treatments of 1000°, are not present at heat treatments of 700°.

It is the purpose of this paper to report the results of magnetic susceptibility measurements over a wide range of temperatures on NiO-Al₂O₃ samples prepared at 1000 and 700°.

Experimental

The preparation of the samples and the method of magnetic measurement have been reported elsewhere.² The susceptibility was measured in the temperature range from -196 to 600°. The field strength was varied from 0 to 4 kilogauss. No field dependence of the susceptibility was found.

Discussion

After correction for the diamagnetism of the alumina, the magnetic susceptibilities, χ , per gram of NiO for each sample follow a Curie-Weiss law

$$\chi = C/(T + \theta) \quad (1)$$

where θ is the Weiss constant, C is the Curie constant and is related to the magnetic moment, μ_{eff} , by

$$\mu_{\text{eff}} = 2.84\sqrt{C_M} \quad (2)$$

The Weiss constants are plotted in Fig. 1 as a function of concentration. In the case of the samples heat treated at 1000°, the Weiss constant decreases linearly to an approximately constant value at about 40-60 mole % NiO, and then decreases more slowly to zero at infinite dilution of NiO. This be-

havior suggests that the spinel, NiAl₂O₄, formed in the equimolar region, forms solid solutions with the pure oxides. These results are in complete agreement with X-ray studies previously reported.⁴ The samples heat treated at 700°, however, show the existence of a solid solution over the complete concentration range, confirming the X-ray evidence that the ordered spinel is not formed at this temperature level of heat treatment.

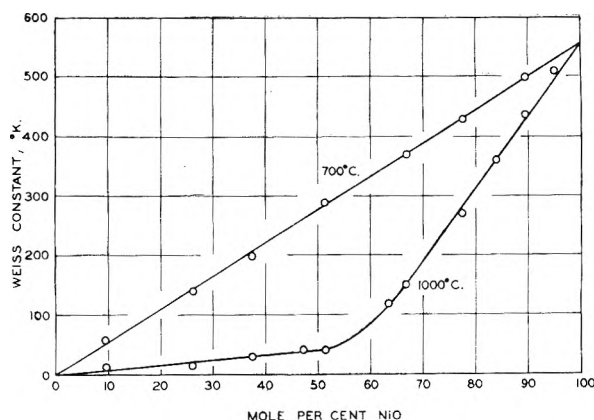


Fig. 1.—Weiss constants as a function of composition for NiO-Al₂O₃ gels heat treated at 700 and 1000°.

The magnetic moments of the nickel ion are plotted in Fig. 2 for the two series of heat treatments. The moments of the samples prepared at 1000 and 700° remain constant at a value of 3.20 bohr magnetons from 100 to about 60 mole % NiO and then increase, both curves passing through a maximum and returning to 3.20 bohr magnetons at 100 mole % Al₂O₃. The increase in the magnetic moment is accompanied by a change in color of the samples from green to blue.

These results agree with those reported previously² for the magnetic moments of the 700° series. However, in the absence of measured values of θ it had been assumed previously that the data followed an ideal Curie law. The correction for the Weiss constant accounts for the difference in the slope of the magnetic moment vs. concentration curves in reference (2) and Fig. 2. There is no evidence of "induced valency" in these samples.

In the nickel aluminate spinel structure, the Ni⁺⁺ ions may occupy tetrahedral sites (A sites) to give a normal spinel or octahedral sites (B sites) to give an inverse spinel. The physical properties and crystal structures of spinels have been discussed re-

(1) Humble Oil and Refining Co. Fellow 1952-1955.

(2) W. O. Milligan and J. T. Richardson, *THIS JOURNAL*, **59**, 831 (1955).

(3) W. O. Milligan, *ibid.*, **55**, 497 (1951).

(4) W. O. Milligan and L. Merten, *ibid.*, **50**, 465 (1946).

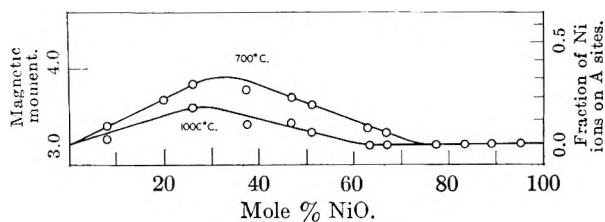


Fig. 2.—Magnetic moment in bohr magnetons as a function of composition for NiO-Al₂O₃ gels heat treated at 700 and 1000°.

cently by Romeijn⁵ and Gorter.⁶ X-Ray diffraction measurements reported by Romeijn⁵ and Greenwald, *et al.*,⁷ have shown NiAl₂O₄ to possess a partially inverted spinel structure, *i.e.*, Ni²⁺ ions on both A and B sites. The value of x , the fraction of Ni²⁺ ions on A sites, is given by Romeijn⁵ as 0.24 and by Greenwald, *et al.*,⁶ as 0.15. The magnetic susceptibility measurements reported above for NiO-Al₂O₃ are in fair agreement with those reported by Greenwald, *et al.*,⁷ for their annealed sample.

Smart^{8a} and Wangness^{8b} have suggested that Ni²⁺ ions on A and B sites have a different magnetic moment due to difference in the "quenching" by the crystalline fields. This quenching produces, for Ni²⁺ on a B site, a singlet level with lowest energy. The Landé factor, g_B , has a "spin only" value which is found experimentally to be 2.3. For Ni²⁺ ions on A sites, the lowest level is a triplet, with a higher g value. As the cation distribution changes the net magnetic moment will vary, due to the different g values for the two sites. Using the relationship

$$\mu_{\text{eff}}^2 = x g_A^2 [S(S+1)] + (1-x) g_B^2 [S(S+1)] \quad (3)$$

where g_A , g_B are the Landé factors for A and B sites, respectively, and S is the spin quantum number, Greenwald, *et al.*,^{8a} have calculated from measured x and μ_{eff} values a value for g_A of about 3.6 for the annealed sample.

If it is assumed that the above ideas are applicable to the NiO-Al₂O₃ system heat treated at 1000°, the following deductions can be made. Using equation 3 and the known values of g_A and g_B , the values of x can be calculated from the measured

(5) F. C. Romeijn, *Philips Res. Rep.*, **8**, 304 (1953).

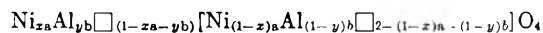
(6) E. W. Gorter, *ibid.*, **9**, 295 (1954).

(7) S. Greenwald, S. J. Pickart and F. H. Grannis, *J. Chem. Phys.*, **9**, 1597 (1954).

(8) (a) J. S. Smart, *Phys. Rev.*, **94**, 847 (1954); (b) R. K. Wangness, *ibid.*, **91**, 1085 (1953).

magnetic moments. This is illustrated in Fig. 2 by the scale on the right. From 100–60 mole % NiO the value of x remains constant at zero. This result indicates that the Ni²⁺ ions occupy octahedral sites in this composition range. This is in agreement with the green color which is usually associated with Ni²⁺ ions with octahedral symmetry. As the concentration of NiO is further decreased, x increases approaching a value of 0.20 at approximately 25% NiO. The increase is associated with a change in color from green to blue.

If it is assumed that the pure γ -alumina has the spinel structure Al_{1/2}□_{1/2}O₄, where □ is a lattice vacancy, then the mixture of NiO and NiAl₂O₄ has the composition



where x is the fraction of Ni ions on A sites, y the fraction of Al ions on A sites, a and b the number of Ni and Al ions, respectively, such that a corresponds to twice the mole % of NiO. It will be noted in Fig. 2 that the value of x approaches a maximum which, in the 700° series, is close to the value of 1/3 for a random distribution.

The small value of x for the NiAl₂O₄ sample prepared at 1000° suggests that it is almost completely inverted. It is expected that a higher heat treatment at 1300° would give the inverted form. Furthermore, for a series of samples heat treated at 1300° the increase of x through a maximum would be expected to greatly decrease, if a more perfectly ordered spinel is formed.

The interpretation given above would probably not apply to samples prepared at lower heat treatments, inasmuch as particle size and surface effects would produce complex results.

The results reported for the NiO-Al₂O₃ system heat treated at 700° and 1000° indicate that atomic dispersion exists within the samples. It is expected that an extension of these measurements to lower heat treatments will indicate either the presence of atomic dispersion or "islands" of NiO, since homogeneous samples will all show Curie-Weiss effects whereas inhomogeneous samples containing small aggregates of NiO will display complex effects.⁹

The authors are indebted to Humble Oil and Refining Company for making possible this work by the establishment of a fellowship program at The Rice Institute.

(9) J. T. Richardson and W. O. Milligan, *Phys. Rev.*, in press.

FREE ENERGY OF IMMERSION OF COMPRESSED POWDERS WITH DIFFERENT LIQUIDS. I. GRAPHITE POWDERS¹

R. G. CRAIG,² J. J. VAN VOORHIS AND F. E. BARTELL

University of Michigan, Ann Arbor, Michigan

Received February 24, 1956

A method is described for the determination of the energy of wetting, *i.e.*, the free energy of immersion, of finely divided solid material by a liquid. The method consists of obtaining complete vapor adsorption isotherms for a liquid adsorbate with an adsorbent comprised of a finely divided solid material which has been highly compressed into the form of plugs. These plugs are porous and possess capillary systems which give adsorption effects similar to those obtained with solid porous gels. The free energy of immersion can therefore be calculated from the adsorption data by application of the Gibbs adsorption equation as used by Dobay, Fu and Bartell in their study of silica gel.³ The free energies of immersion of each of a series of different graphite powders with the liquids toluene, carbon tetrachloride, *n*-heptane, cyclohexane and *n*-propyl alcohol were determined. The values obtained show that the free energy of immersion (expressed in free energy per unit area) is independent of surface, *i.e.*, of the particle size of the powdered material and of pressures used in compressing the plugs; it is dependent only on the nature of the surface of the powdered material. The surface areas, average pore volumes, average dry pore radii and porosities were determined for each of the graphite plugs used. The molecular cross sectional areas of the adsorbed molecules and the heats of adsorption of the first layer were determined for the various systems from the B.E.T. plots of the adsorption data. Standard free energies of adsorption were calculated in order to evaluate the relative strengths of the adsorptive bonds.

Introduction

It is generally recognized that knowledge of the magnitude of free surface energy changes which occur when solids are wetted by liquids is of great importance in the field of surface chemistry. Unfortunately owing to uncertainties or difficulties attendant to known methods such data have seldom been made available. Since publication of the work of Bangham and Razouk⁴ showing that the Gibbs adsorption equation is applicable to the determination of free surface energy changes which occur on solids during adsorption of vapors upon them, investigators have made use of this method for the determination of free surface energy changes with such systems. For non-porous solids, Boyd and Livingston⁵ and Harkins and co-workers,^{6,7} used a formulation for the free surface energy lowering at relative pressures from zero to one, as

$$-\phi_{SO/SL} = (\gamma_{SO} - \gamma_{SL}) = \frac{RT}{M a_s} \int_{p/p_0=0}^{p/p_0=1} x/m \, d \ln p/p_0 + \gamma_{LV}^0 \quad (1)$$

where $\phi_{SO/SL}$ is the free surface energy lowering which occurs when unit area of solid-vacuum interface is replaced by unit area of solid-liquid interface; γ represents any free surface energy, surface tension or interfacial tension value; subscripts SO, SL and LV⁰ represent a solid-vacuum, a solid-liquid and a liquid-saturated vapor interface, respectively; M is the molecular weight of the adsorbate; a_s is the surface area of the solid; x/m is the

weight adsorbed per weight of sample and p/p_0 is the relative pressure. The expression $(\gamma_{SO} - \gamma_{SL})$ will be referred to in this paper as representing the free energy of immersion of the solid in the liquid.

By making appropriate changes in the method and the theory, the above described treatment was extended by Dobay, Fu and Bartell,³ and by Fu and Bartell⁸ to include porous solids. The main difference in behavior between porous and non-porous solids is that during adsorption of a vapor on a porous solid, the solid-vacuum interface is replaced by a solid-liquid interface and a liquid-vapor interface, and at $p/p_0 = 1$ because of the filling of the pores the liquid-vapor interface is completely destroyed; while in the case of adsorption of a vapor on a non-porous solid the area of the liquid vapor interface at $p/p_0 = 1$ is not destroyed and the area is considered to be essentially equal to that of the solid-vacuum interface. The following formulation was developed for the evaluation of the free surface energy lowering at $p/p_0 = 1$ on porous solids

$$-\phi_{SO/SL} = (\gamma_{SO} - \gamma_{SL}) = \frac{RT}{M a_s} \int_{p/p_0=0}^{p/p_0=1} x/m \, d \ln p/p_0 \quad (2)$$

During the adsorption of an adsorbate on a porous solid the surface area available for adsorption decreases continuously to a zero value at $p/p_0 = 1$, and therefore in order to evaluate the above integral it would seem that a knowledge of the film thickness at various p/p_0 values must be known. This is true if the free surface energy change is desired from $p/p_0 = 0$ to $p/p_0 = b$, where $0 < b < 1$. Fu and Bartell⁸ have shown, however, that if the free surface energy change from $p/p_0 = 0$ to $p/p_0 = 1$ only is desired, a hypothetical process can be substituted for the real process where the initial and final states of each are the same. This method makes more certain the evaluation of the integral and the subsequent calculation of the free energy of immersion $(\gamma_{SO} - \gamma_{SL})$, the work of adhesion $W_a = (\gamma_{SO} - \gamma_{SL} + \gamma_{LV}^0)$ and the work of spreading or the initial spreading coefficient $W_s = (\gamma_{SO} - \gamma_{SL} - \gamma_{LV}^0)$.

(8) Y. Fu and F. E. Bartell, *THIS JOURNAL*, **55**, 662 (1951).

(1) Presented before the 30th National Colloid Symposium which was held under the auspices of the Division of Colloid Chemistry of the American Chemical Society in Madison, Wisconsin, June 18-20, 1956.

(2) A portion of this work received financial aid from E. I. du Pont de Nemours Company and is from the thesis of Robert G. Craig, submitted in partial fulfillment of the requirements of the Degree of Doctor of Philosophy at the University of Michigan, Ann Arbor, Michigan.

(3) D. G. Dobay, Y. Fu and F. E. Bartell, *J. Am. Chem. Soc.*, **73**, 308 (1951).

(4) D. H. Bangham, *Trans. Faraday Soc.*, **33**, 805 (1937); D. H. Bangham and R. I. Razouk, *ibid.*, **33**, 1459 (1937); *Proc. Roy. Soc. (London)*, **A166**, 572 (1938).

(5) G. E. Boyd and H. K. Livingston, *J. Am. Chem. Soc.*, **64**, 2383 (1942).

(6) G. Jura and W. D. Harkins, *ibid.*, **66**, 1356 (1944).

(7) E. H. Loeser, W. D. Harkins, and S. B. Twiss, *THIS JOURNAL*, **7**, 251, 591 (1953).

In the determination of the free energy of immersion from the complete adsorption isotherm of non-porous powder several factors leading to difficulties are involved: (1) it is difficult to determine equilibrium values near $p/p_0 = 1$, (2) it is not possible to extrapolate the adsorption isotherm to a definite limiting value at $p/p_0 = 1$, and (3) the "non-porous" powder functions partially as a porous solid during the process of adsorption because in a free flowing non-porous solid the particles are sufficiently close together so that large numbers of capillary spaces actually are formed. Of the three factors mentioned the last usually constitutes the greatest source of error when high area solids are used. If, however, porous solids are used these difficulties are avoided.

The adsorption isotherms of organic vapors on Linde silica powders were shown by Carman and Raal⁹ to give type II isotherms, while if the powders were held under compression, type IV isotherms, characteristic of a silica gel, were obtained. This indicated to us that if powdered non-porous solids could be highly compressed into plugs having capillary type systems they should function as rigid porous solids, thus making possible the calculation of the free energy of immersion, the work of adhesion and the work of spreading from the complete adsorption isotherm of an adsorbate on these porous plugs. This method would avoid the difficulties which are encountered when the free flowing, non-porous powders as such are used, but still would permit the determination of the free surface energy changes which actually occur on these finely divided solids.

The present investigation consisted of taking a series of finely divided graphite powders, compressing them into rigid porous plugs, determining the complete adsorption isotherms with a series of adsorbates, and calculating the free surface energy changes which occurred during adsorption.³

Experimental

Materials. Graphites.—In the following description of the graphite powders a "purified graphite" will indicate that the powder was treated with hot 1-1 HCl, filtered, thoroughly washed, dried, powdered, heated in an evacuated quartz tube at 1000° until a high vacuum was obtained, cooled and stored in a helium atmosphere. All graphites were furnished by the Acheson Colloids Company and have the following designations and surface areas.¹⁰

Graphite	Acheson code	Area, m. ² /g.	Treatment
A	EC-753-96A	386	Purified
B	EC-753-96A	382	Unpurified
B-T	EC-753-96A	383	Unpurified evacuated and heated at 1000° in a quartz tube until high vacuum obtained
C	EC-753-72A	323	Purified
D	EC-603A	247	Unpurified
E	EC-753-23A	136	Purified
F	EC-753-144A	472	Purified

Adsorbates.—Toluene, reagent grade was shaken with successive portions of concentrated sulfuric acid, washed with distilled water, washed with dilute sodium carbonate

solution and again with distilled water, dried over calcium chloride and activated silica gel, refluxed over mercury, and run through an alumina column. The liquid was fractionated using a thirty-six stage Snyder column, the middle fraction collected and finally dried using freshly extruded sodium ribbon. Carbon tetrachloride, reagent grade, was purified in the same manner as was toluene except that only alumina and silica gel were used for drying. Cyclohexane, reagent grade, was purified by the same procedure used for toluene except that refluxing over mercury was omitted. *n*-Propyl alcohol, reagent grade, was dried by the method of Lund and Bjerrum¹¹ and the liquid was fractionated directly from this mixture. After purification, all adsorbates were distilled into break-off vials, degassed, frozen, evacuated, sealed off and stored until used.

Apparatus.—The volumetric adsorption apparatus and method used to determine the surface areas of the solids were similar to those described by Emmett.¹²

The gravimetric adsorption isotherms were determined by using a multiple (six unit) modified McBain-Baker¹³ quartz spring balance. Temperature control of the adsorption tubes was accomplished by using a water thermostated bath, the temperatures of which could be regulated to $\pm 0.03^\circ$. Each adsorption tube was connected through a mercury stock valve to a manifold; the adsorbate tube and a mercury manometer were also connected to this manifold. When the mercury was raised in the manometer the adsorption system was completely isolated and contamination of the adsorbate by stopcock grease was eliminated. The vapor pressure of the adsorbate was controlled by the temperature of an adsorbate thermostated bath. With the multiple (six unit) adsorption balance the vapor adsorption isotherms of a single adsorbate on six different adsorbents were determined simultaneously. The techniques used to obtain these isotherms were similar to those described by Bartell and Dobay.¹⁴ Probably the most serious experimental difficulty was condensation of mercury on the quartz springs at very low pressures. Corrections were made for this by determining the zero readings of the quartz springs just prior to starting the adsorption run; after the vapor of the adsorbate had been admitted to the adsorption system this condensation ceased.

The apparatus used to prepare the compressed porous plugs consisted of a steel cylinder, 1.25" thick and 2.5" in diameter with a $3/8$ " hole drilled through its axis. A $3/8$ " steel plunger, machined to give a sliding fit, and a polished steel base plate, which could be fastened to the base of the cylinder by three Allen screws, completed the apparatus. The porous plugs were prepared by placing the graphite powder into the hole in the cylinder and then applying pressure to the plunger by an hydraulic press. Usually the pressure was applied for a period of 10 minutes. The pressure used in preparing a porous plug is given in thousands of pounds upon the ram and is shown by the number following the graphite designation. For example, graphite A-4 indicates that graphite A powder was subjected to a pressure of 4000 p.s.i. on the ram during the plug formation. The actual pressure on the $3/8$ " plug was 36,216 p.s.i. (ratio, pressure on ram to pressure on plug = 1 to 9.054).

Results and Discussion

The difference in shape of the adsorption isotherms of cyclohexane with a graphite powder and with a porous plug prepared from this powder is shown in Fig. 1. The weights adsorbed in the initial portions of the isotherms are nearly identical, but at higher p/p_0 values, because of the greater exposed surface area of the graphite B powder, the weight adsorbed by it becomes greater than that adsorbed by the graphite B-4 plug. With the plug, as $p/p_0 \rightarrow 1$, the capillary spaces in the porous plug became filled with liquid, thus the weight adsorbed

(11) H. Lund and J. Bjerrum, *Ber.*, **64A**, 210 (1931).

(12) P. H. Emmett, "Advances in Colloid Science," Vol. I, Interscience Publishers, Inc., New York, N. Y., 1942, pp. 1-36.

(13) J. W. McBain and A. M. Bakr, *J. Am. Chem. Soc.*, **48**, 690 (1926).

(14) F. E. Bartell and D. G. Dobay, *J. Am. Chem. Soc.*, **72**, 4388 (1950).

(9) P. C. Carman and F. A. Raal, *Nature*, **167**, 112 (1951).

(10) In the determination of the B.E.T. surface areas the nitrogen area was assumed to be 16.2 Å.²

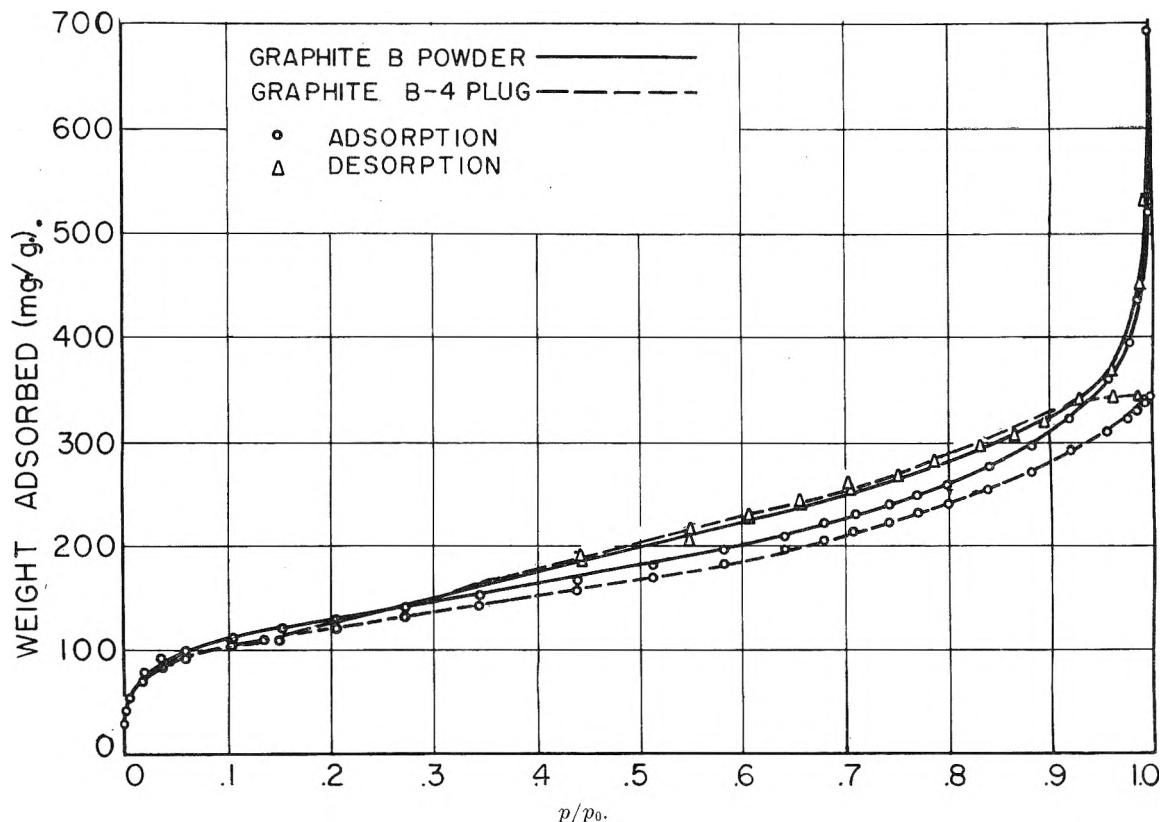


Fig. 1.—Adsorption-desorption isotherms of cyclohexane on graphite B powder and graphite B-4 plugs at 26°.

reached a limiting value. In contrast, the weight adsorbed by the graphite B powder increased rapidly as $p/p_0 \rightarrow 1$ and appeared not to reach a limiting value. Hysteresis was observed on desorption for both graphite B powder and the graphite B-4 plug. The fact that graphite B powder showed hysteresis on desorption is, we believe, due to the capillary spaces formed by particle approach or contact and to irregularities in the solid particles. The hysteresis loop, as should be expected, was much larger and extended over a wider p/p_0 range for the graphite B-4 plug, than for graphite B powder.

Figure 2 shows the difference in shape of the adsorption isotherms of toluene on a purified and on an unpurified graphite plug. This difference in shape is presumably due to the difference in the average pore radius and to the pore radii distribution. Adsorption of cyclohexane on unpurified heat treated graphite B-4T plug gives an isotherm typical and nearly identical to that with a purified graphite A-4 plug, while the isotherm of cyclohexane on graphite B-4 plug is typical of one for an unpurified graphite plug. Graphite B-T was prepared by heating graphite B in a vacuum until a high vacuum was obtained, which procedure removed surface oxides and adsorbed gases. Thus, the surface condition of the graphite powders must be one of the main factors in controlling the average pore radius and the pore radii distribution.

Adsorption isotherms of carbon tetrachloride, *n*-propyl alcohol and *n*-heptane on graphite B-4 are shown in Fig. 3. These isotherms of organic adsorbates on porous plugs are isotherms typical of porous solids. They show hysteresis and permit

extrapolation to a limiting value for the amount adsorbed at saturation.

After complete adsorption and desorption curves had been obtained, the same porous plugs were again used and second run adsorption and desorption points determined for all isotherms. Second run adsorption points agreed with the first run adsorption points up to $p/p_0 \sim 0.1$. From $p/p_0 \sim 0.1$ to 0.5, second run adsorption points were 0–2 mg./g. higher than the first run adsorption points and from $p/p_0 \sim 0.5$ to 1 were 2–5 mg./g. higher, with the exception of *n*-heptane on unpurified graphites, where at $p/p_0 = 0.9$ the second run adsorption points were approximately 10 mg./g. higher. Second run desorption points always agreed with first run desorption points. This indicates that little swelling of the porous plugs occurred during adsorption and that the porous plugs could be treated as rigid solids permitting the calculation of the free energies of immersion from the complete adsorption isotherms of the various vapors on these plugs. Also, since the second run adsorption points agree with the first in the low pressure region and very nearly agree up to $p/p_0 = 0.5$ any slight swelling of the plugs would not materially change the calculated free energy of immersion values because the low pressure points are of the most importance in the energy change calculations. Thus, the integral in equation 2 can be evaluated without difficulty.

The values obtained for a variety of graphites with a series of adsorbates are listed in Table I. Inspection of the table shows that within experimental error the free energy of immersion is independent of the pore size, the pore size distribution and the surface area of the solid. Also, the non-

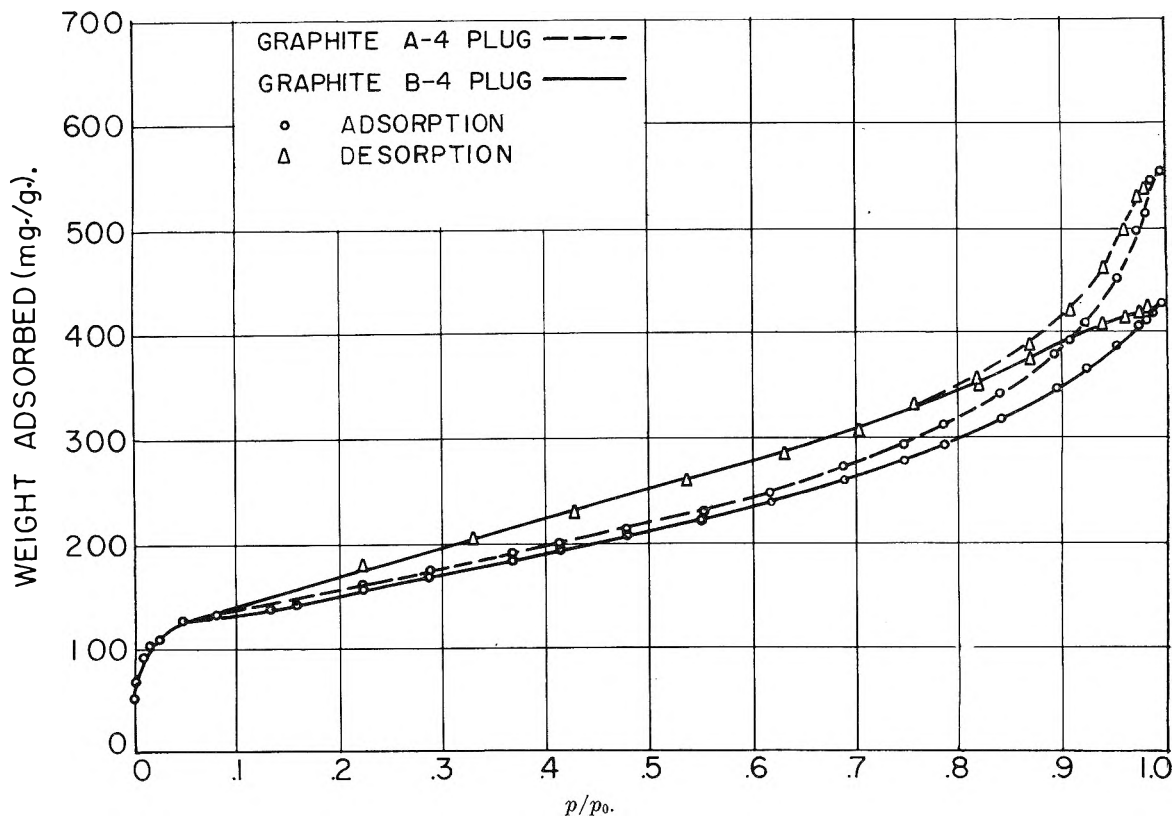


Fig. 2.—Adsorption-desorption isotherms of toluene on graphite A-4 and B-4 plugs at 26°.

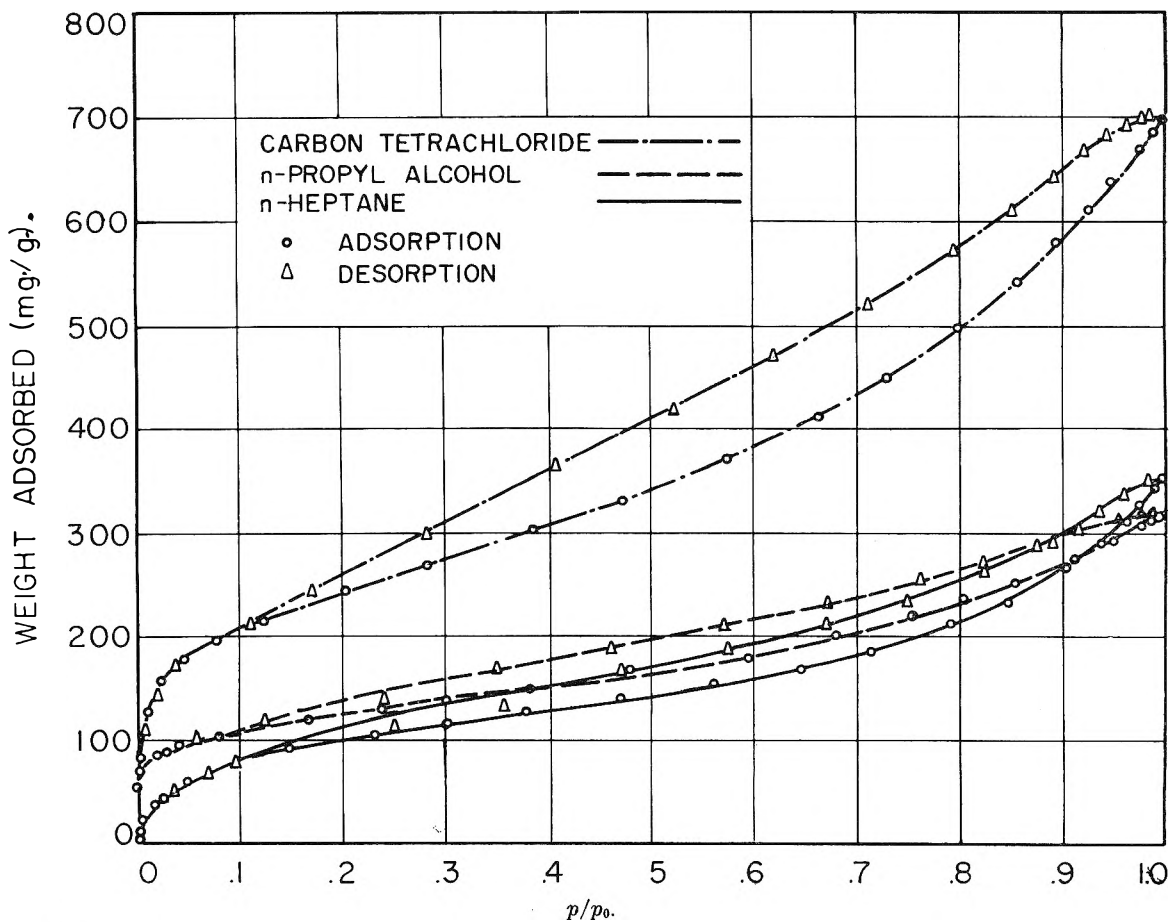


Fig. 3.—Adsorption-desorption isotherms of carbon tetrachloride, *n*-propyl alcohol and *n*-heptane on graphite B-4 plugs at 26°.

TABLE I

Graphite	FREE ENERGY OF IMMERSION ($\gamma_{so} - \gamma_{sL}$) OF GRAPHITES WITH VARIOUS LIQUIDS (ergs/cm. ²) AT 26°				
	Toluene	Carbon tetrachloride	n-Heptane	Cyclohexane	n-Propyl alcohol
A-2	69.2 ± 0.7				
A-4	71.0	60.1 ± 0.5	54.5 ± 1.2	55.8 ± 0.6	68.9 ± 0.5
A-6			50.1		
A-10		59.8			
B-4 ^a	71.6	59.2	55.0	54.1	57.7 ± 0.9
B-4T				55.7	
C-4	70.8	59.7	52.4		68.3
D-4 ^a	70.4				59.6
E-4			54.0		
E-6		61.1	52.3		
E-10		60.9			
F-4	72.4				
Av.	70.9 ± 0.3	60.1 ± 0.2	53.1 ± 0.5	55.2 ± 0.4	68.6 ± 0.2
					58.6 ± 0.6 ^a

^a Unpurified graphite.

polar adsorbates, toluene, carbon tetrachloride, *n*-heptane and cyclohexane, show no significant difference between the purified and unpurified graphites. The probable reason for the free energy of immersion being ~ 10 ergs/cm.² higher for *n*-propyl alcohol on the purified graphites is that the unpurified graphites (B-4 and D-4) still have some surface oxides present when adsorption starts. Since the *n*-propyl alcohol molecules tend to orient themselves with the non-polar end toward the clean graphite surface and the polar end toward the oxide surface, the disorder and following interaction of the molecules tends to decrease the free surface energy change during adsorption on the unpurified graphite surface. This is substantiated by the calculated apparent molecular cross sectional area of *n*-propyl alcohol on the unpurified graphite surface, 43 Å.², compared with 37 Å.² on the purified graphite surface. The apparent cross sectional areas of the remaining liquid adsorbates were substantially the same on both purified and unpurified graphites.

Comparison of free energy of immersion values on graphites with literature values is somewhat futile since there are very few such data reported in the literature. The values that are available were determined on non-porous powdered solids and, therefore, are not strictly comparable. Heats of immersion and heats of wetting values of comparable liquids on graphites should, however, be in the same order as the free energy of immersion values. The data of Harkins and Boyd,¹⁵ of Bartell and Suggitt,¹⁶ and of Healey, *et al.*,¹⁷ show this to be the case. One of the most difficult problems in comparing the free surface energy change for graphites is the lack of knowledge of the previous history and treatment of the graphites prior to adsorption.

The average pore volumes of the purified graphite plugs A, C, E and F, listed in Table II, are in the same order as their surface areas. This is also true of the unpurified graphite plugs if they are considered separately. Porous plugs prepared from the high area purified graphites A, B-T, C and F have approximately the same average dry radius (calcu-

lated from twice the volume to surface ratio), while the low area graphite E plugs have, as expected, a larger average dry pore radius. The average dry radius of high area unpurified graphites B and D plugs are low, the average dry radius of the lower area graphite D plug being less than that of the graphite B plug.

TABLE II

PHYSICAL PROPERTIES OF GRAPHITE PLUGS

Graphite	Surface area, m. ² /g.	Pore vol., cc./g.	Av. dry pore radius (Å).	Porosity
A-2	381	0.66	34	
A-4	383	.66	34	0.70
A-6	380	.59	31	
A-10	380	.61	32	
B-4 ^a	371	.46	25	.60
B-4T	362	.68	38	
C-4	316	.58	36	.70
D-4 ^a	217	.33	31	.53
E-4	129	.33	51	.53
E-6	127	.32	50	
E-10	127	.31	49	
F-4	471	.84	36	.72

^a Unpurified graphite.

The % porosity was calculated from the relation

$$\text{porosity} = (\rho - \rho_a)/\rho \quad (3)$$

where ρ is the density of graphite and ρ_a the apparent density of the porous plug. Graphite E-4 and D-4 plugs have the same porosities and the same average pore volumes but graphite E-4 has a much higher average dry radius due to its lower surface area. Unpurified graphites B and D have good packing characteristics as is indicated by the relatively low porosities, average pore volumes and average dry pore radii of the unpurified graphite B-4 and D-4 plugs. The purified graphite plugs A-4, C-4 and F-4, with areas between 316 and 471 m.²/g., have nearly the same porosities and average dry pore radii but have average pore volumes in the order of their areas. The pore radius range, calculated from the desorption isotherms, by use of the Kelvin equation, is from 15 to 1500 Å. The saturation values of the adsorption isotherms of water on the porous plugs indicated that the plugs consisted of approximately 80% micro pores and 20% macro pores.

(15) W. D. Harkins and G. E. Boyd, *J. Am. Chem. Soc.*, **64**, 1195 (1942).

(16) F. E. Bartell and R. M. Suggitt, *This Journal*, **58**, 36 (1954).

(17) F. H. Healey, J. J. Chessick, A. C. Zettlemoyer and G. J. Young, *ibid.*, **58**, 887 (1954).

The gravimetric adsorption data of the organic adsorbates on graphites A-4 and B-4 plugs were plotted according to the simple, linear B.E.T. equation and straight line plots were obtained in all cases in the region from $p/p_0 = 0.05$ to 0.2. Values for the volumes adsorbed at monolayer coverage, V_m , obtained from the B.E.T. plots are listed in Table III. If the B.E.T. nitrogen areas are assumed to be valid, the apparent molecular cross-sectional areas of the adsorbed molecules can be calculated. The value of 37 \AA^2 listed is for *n*-propyl alcohol on graphite A-4, while a value of 43 \AA^2 was obtained on graphite B-4. As had previously been observed^{18,19} the cross sectional areas obtained from the B.E.T. plots are approximately 30% greater than those obtained by assuming that the adsorbed molecules correspond to the plane of closest packing in the liquified gas.

TABLE III

CHARACTERISTICS OF ADSORBED FILMS ON GRAPHITE PLUGS

Adsorbate	V_m , cc./g.	Apparent mol. cross sectional area, 26° (\AA^2)	E_1 (B.E.T.) kcal./ mole	$-\Delta F^0$, kcal./ mole
Toluene	29.7	47	15.4	5.5
Carbon tetrachloride	29.7	47	11.8	4.2
<i>n</i> -Heptane	23.1	62	15.1	5.0
Cyclohexane	26.7	52	12.5	4.6
<i>n</i> -Propyl alcohol ^a	38.9	37	15.0	4.0

^a With unpurified graphite *n*-propyl alcohol gave a molecular cross sectional area of 43 \AA^2 .

The heat of adsorption of the first layer, E_1 , was also calculated from the B.E.T. plots and the values listed in Table III show reasonable agreement with experimentally determined heats of adsorption and with the generalization that E_1 values of various adsorbates on a single adsorbent are usually in the same order as the boiling points of the liquids.

(18) H. K. Livingston, *J. Colloid Sci.*, **4**, 447 (1949).

(19) J. E. Bower, Thesis, University of Michigan, 1951.

Plots of the equilibrium function *versus* surface coverage were made for each system according to the method suggested by Graham.²⁰ For each system the initial decrease in the equilibrium function at the lowest measured surface coverage indicated that the surface of the graphite was heterogeneous with several kinds of adsorption sites. Values for the standard free energies of adsorption, calculated from the extrapolated values of equilibrium functions are listed in Table III. Although these values are only relative values they indicate the relative strength of the adsorption bond. The order of the $-\Delta F^0$ values can be explained in the following manner. Toluene has the highest value since the ring is planar and the methyl group is free to rotate so that the molecule can lie flat on the surface with seven hydrogens contributing to the binding. Similarity of the molecule with the structure of the graphite could also have some effect. *n*-Heptane is next in order and the high $-\Delta F^0$ value together with its high heat of adsorption has been interpreted²¹ to mean that the molecule lies flat on the surface with each $-\text{CH}_2-$ contributing to the binding. Cyclohexane is next, which has been explained²² by the distortion of the molecule at the surface so that six hydrogens are in contact with the surface rather than three. Carbon tetrachloride is next, which can be explained since only three chlorine atoms per molecule can be in contact with the surface. *n*-Propyl alcohols is last which is presumably due to the effect of a polar molecule on a non-polar surface. The order of the $-\Delta F^0$ values is not the same as that for the $(\gamma_{SO} - \gamma_{SL})$ values. This is not so surprising, however, since the former is a measure of the strength of the adsorption bond at low surface coverages, while the latter is the free surface energy change for all layers up to saturation of the solid.

(20) D. Graham, *THIS JOURNAL*, **57**, 665 (1953).(21) R. A. Beebe, C. L. Kington, M. H. Polley and W. R. Smith, *J. Am. Chem. Soc.*, **72**, 40 (1950).(22) R. N. Smith, C. Pierce and H. Cordes, *ibid.*, **72**, 5595 (1950).

THE WETTING OF INCOMPLETE MONOMOLECULAR LAYERS

By L. S. BARTELL AND R. J. RUCH

Department of Chemistry, Iowa State College, Ames, Iowa

Received February 24, 1956

The composition and wetting properties of films formed on polished metal surfaces by adsorption from solutions of *n*-octadecylamine in *n*-hexadecane were studied. The surface concentration of adsorbed molecules was measured by an optical method due to Drude. Fresh films were found to contain very nearly the same amount of amine as conventional Langmuir-Blodgett monolayers and, in addition, appreciable amounts of solvent. Films with included solvent were not more readily wetted by pure solvent than were dry monolayers. Contact angles of water and hexadecane were not strongly affected by depletion of monolayers until more than half of the adsorbed molecules were removed. Rough estimates were made of the activation energy of desorption as a function of depletion.

Introduction

It is well known that a single layer of molecules adsorbed on a surface may profoundly alter the wetting properties of the surface. It is of special interest, therefore, to examine the wetting of surfaces only partially covered by adsorbed molecules in order to determine the degree to which an already minuscule surface phase must be diluted before its effects are no longer felt. The experimental difficulty involved in measuring the amount of material adsorbed on a small area of a well defined surface has greatly restricted studies of incomplete layers in the past. A modification of an optical method developed by Drude,¹ Tronstad,² and Rothen³ was found to be suitable for measuring fractional surface coverages by the molecules selected for the present study even on areas smaller than one square centimeter. The adsorbed films reported upon below are of the type first studied extensively by Zisman, *et al.*,^{4,5} and consist of long chain hydrocarbon molecules with polar groups adsorbed on metal slides. Zisman discovered that such films, when formed by adsorption from solution in hydrocarbon solvents like *n*-hexadecane, were so poorly wetted by the solvent that they could be withdrawn from the solvent, apparently as dry monolayers. Experiments in which solutions of *n*-octadecylamine⁴ and perfluorodecanoic acid⁶ were depleted by adsorption on polished platinum surfaces of known geometric areas indicated that the amount of solute adsorbed corresponded roughly to that which would be present in a fairly close-packed monolayer. The structure of such films after standing in a high vacuum was found by electron diffraction⁷⁻⁹ to resemble that of Langmuir-Blodgett monolayers. No estimate has been available for the extent of solvent inclusion in the film, a factor which has turned out to be of some interest.

The present investigation is concerned with two problems: (a) the further characterization of adsorbed films of long-chain polar molecules on metal slides, and (b) the variation of wetting properties accompanying the gradual removal of the films.

(1) P. Drude, *Ann. physik. Chem.*, **36**, 532 (1889); **36**, 865 (1889); **39**, 481 (1890).

(2) L. Tronstad, *Trans. Faraday Soc.*, **29**, 502 (1933).

(3) A. Rothen, *Rev. Sci. Instr.*, **16**, 26 (1945).

(4) W. C. Bigelow, D. L. Pickett and W. A. Zisman, *J. Colloid Sci.*, **1**, 513 (1946).

(5) W. C. Bigelow, E. Glass and W. A. Zisman, *ibid.*, **2**, 563 (1947).

(6) F. Schulman and W. A. Zisman, *ibid.*, **7**, 465 (1952).

(7) L. O. Brockway and J. Karle, *ibid.*, **2**, 277 (1947).

(8) W. C. Bigelow and L. O. Brockway, *ibid.*, **11**, 60 (1956).

(9) E. F. Ilare, E. G. Shafrin and W. A. Zisman, *This Journal*, **58**, 236 (1954).

Experimental

Unless it is otherwise stated, all of the observations described below pertain to films of *n*-octadecylamine. The films were formed by deposition by the Langmuir-Blodgett technique and by adsorption from solution in hexadecane with concentrations ranging from 0.02 to 0.1% by weight. A few comparison films of stearic acid were formed by adsorption from solution in hexadecane.

The *n*-hexadecane used as a solvent and in contact angle measurements was obtained from the Eastman Kodak Company and was percolated through alumina and silica gel to remove any polar impurities. Normal octadecylamine, obtained from Armour and Company, was contaminated by carbon dioxide adsorbed from the air in the initial experiments. In later work the carbon dioxide was removed as described by Zisman, *et al.*,⁵ but it was not observed to have a very marked effect on the adsorbed films.

It was originally expected that platinum surfaces would be particularly well suited to the present study because of the ease with which organic contaminants could be removed by flaming. Platinum slides 1 mm. thick were polished by several techniques. Surface characteristics varied erratically and no platinum surfaces have yet been obtained that can be regarded as completely satisfactory for the present research. One slide repeatedly adsorbed amines but not acids on one area, and acids but not amines on another. Investigation revealed no trace of inorganic polishing agents to account for preferential adsorption.

A reasonably satisfactory alternative was found in chromium plated steel slides cut from large commercial ferrotype plates. Although the slides were far from being perfect optically, they gave satisfactory performance with the optical method. A variety of procedures was tried in order to obtain surfaces sufficiently clean for adsorption to take place. Any grease present was removed with pure benzene. Extraction in an all-glass Soxhlet extractor with carbon tetrachloride or methanol for periods up to 15 hours proved to be ineffective in removing contaminants which interfered with satisfactory adsorption. Simple steaming for short periods was of little avail. Several methods which were successful in the preparation of surfaces exhibiting reasonably rapid adsorption of amine from hexadecane were: (a) cleaning with chromic acid cleaning solution, rinsing with water and drying with clean filter paper; (b) gentle flaming; (c) moderately strong flaming to a dull red glow; (d) polishing with alumina, rubbing with filter paper under flowing distilled water to remove the tenaciously adhering alumina, and drying with filter paper.

The grease-free surfaces obtained before treatments (a)-(d) were examined by electron diffraction. The patterns found were diffuse rings showing some preferred orientation. They were tentatively identified as being due to chromic oxide and chromium metal. Treatment (b) did not seem to cause further oxidation, as indicated by optical measurements, unless the flaming was prolonged. Prolonged flaming occasionally resulted in large and erratic jumps of perhaps 40-80 Å. in film thickness. Diffraction patterns following treatment (b) were indistinguishable from those of unflamed slides. Treatment (c) resulted in the formation of easily visible films of oxide 1000 Å. or more in thickness. Treatment (d) removed surface oxide and chromium metal asperities to a large degree and, with prolonged polishing, led to diffraction patterns showing only the diffuse halos characteristic of polished metals.

Subjective though method (b) is, it has the advantage of

great simplicity and generally results in a surface which remains completely wettable by water for periods up to or longer than 0.5 hour in air. The surface following treatment (d) is difficult to reproduce and appears to be much more susceptible to contamination. Method (b) was used in most experiments to be described.

The properties of adsorbed films of amine were not observed to depend upon the time allowed for adsorption to take place provided the time was at least one minute. No attempt was made to control the temperature during experiments and it varied from 22 to 25°.

The instrument used to measure the amount adsorbed was similar in optical arrangement to the ellipsometer described by Rothen³ except for the half-shade device. Rothen's method of depositing a split Langmuir-Blodgett film on the slide to obtain half-fields was, of course, impracticable for the present study and a phase shifting plate mounted close to the specimen was used instead.

The technique of making readings was essentially the same as that of Rothen, and it was assumed that, for the very thin films studied, the ellipsometer readings were a linear function of the average amount of adsorbed material per area. It is believed that the readings indicate the material on smooth flat regions of the surface and do not include the possibly appreciable amount of material in cracks and other irregularities. Experiments are under way to test the above hypotheses.

The instrument was calibrated primarily by comparing the adsorbed films with Langmuir-Blodgett monolayers of *n*-octadecylamine but comparisons were also made with similar layers of *n*-octadecyl alcohol and of barium stearate. The area per molecule in the comparison films deposited under moderately high piston oil pressures is known to be very nearly the same as the easily measured area per molecule on water at the same surface pressure.^{10,11} Comparison of films of different composition but of similar refractive index can be made by utilizing Drude's simplified formulas.¹

The sensitivity and reproducibility of the optical method appeared to be approximately 0.03 monolayer or better when moderately good slides were used. Even with relatively poor slides and unfavorable conditions readings seemed significant to 0.1 monolayer or so. The sodium-D lines were used for illumination.

Results and Discussion

Thickness of Adsorbed Films.—The thickness of films adsorbed from solutions of octadecylamine on flamed platinum varied and, immediately after withdrawal from the solvent, was sometimes found to be much greater than that of a true monolayer. Films that were initially thick were observed to evaporate slowly in air until, after an hour or so, they reached and remained at the thickness of an amine monolayer. There is little doubt that appreciable amounts of solvent are carried along with solute in the adsorption process with such films. The incomplete wetting by the solvent of these thick films of hydrocarbon tails liberally mixed with normal hydrocarbon solvent molecules is rather surprising and is being investigated further. It is probable that the adsorbed solvent molecules are highly oriented. It is possible that the effect is closely related to cybotaxy.

Results on chromium plated slides were more uniform. Occasionally, perhaps because of imperfect preparation of surfaces, adsorbed films were obtained which were thinner than Langmuir-Blodgett monolayers. Most of the films, however, were about 20% thicker than a monolayer when first removed from the solvent. These latter films evaporated slowly in air or pumped down in a few

minutes in a vacuum to a stable thickness corresponding to a fairly close-packed monolayer. Advancing and receding angles for hexadecane were the same on the solvent-rich films as they were on the dried films.

The area per molecule of amine adsorbed from 0.02 to 0.1% solutions in *n*-hexadecane was estimated to be approximately 23 Å.², which is somewhat larger than the area in close-packed films. The value of 30 Å.² obtained by Zisman, *et al.*,⁴ using the "multiple dip" method with octadecylamine on platinum is possibly to be regarded as an average value corresponding to adsorption from very dilute solutions.

Depletion of Monolayers.—It proved to be unexpectedly difficult to remove the adsorbed monolayers completely. The first two-thirds or so of a layer was readily removed by gentle flaming or by dissolution in pure benzene, but the remainder of the layer showed astonishing resistance to removal, even by flaming. Boiling for several minutes in mesitylene (170°) or for an hour in benzene removed only a small fraction of the last third of an amine layer. The layer was very rapidly removed by polishing with alumina.

It was possible to get an estimate of the activation energy of desorption of the molecules from chromium slides by comparing the rates of dissolution in benzene at different temperatures. The results of the preliminary studies are not very accurate because the initial rates of solution were too fast and the rates at intermediate coverage too slow to permit precision. A further complication which arises is that activation energies vary with surface coverage and appear to be sensitive to surface preparation.

The results indicate that the desorption energy of the molecules first leaving the film is very much smaller than the heat of adsorption of 14.5 kcal./mole found by Zisman⁵ on platinum. The desorption energy increases with depletion to a value comparable to or larger than Zisman's result. It should be noted that Zisman's measurements refer to the coverage corresponding to complete wetting by the solvent and, according to the present study, complete wetting occurs only at fairly extensive depletion. A low initial desorption energy was also obtained by Karle¹² who gave an estimate of 6 kcal./mole for the initial evaporation from layers of crotonic acid on glass slides.

The Wetting of Incomplete Monolayers.—All work with depleted layers was done on chromium plated slides. The method of depletion of monolayers selected as a standard procedure in this study was dissolution in pure benzene. Tests indicated that analytical reagent benzene contained no adsorbable impurities to contaminate the depleted layers. It is not certain that the benzene itself played a completely negligible part in the wetting experiments beyond the removal of amine molecules.

Contact angles of pure *n*-hexadecane and of water were measured on films formed by adsorption

(10) L. Denard, *J. chim. phys.*, **36**, 210 (1939).

(11) I. Langmuir, V. J. Schaefer and H. Sobotka, *J. Am. Chem. Soc.*, **59**, 1751 (1937).

(12) J. Karle, *J. Chem. Phys.*, **17**, 500 (1949).

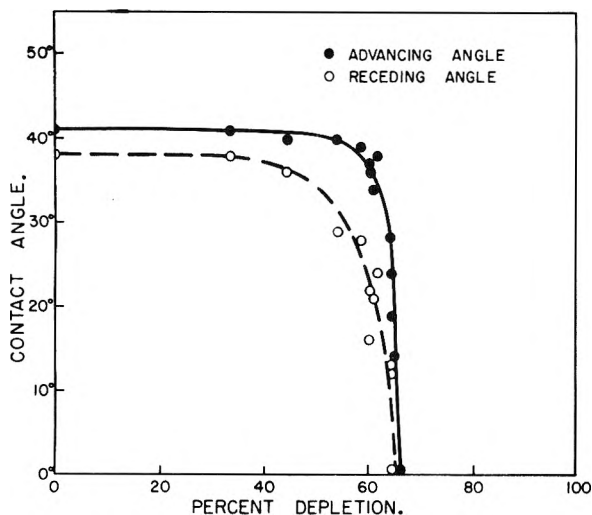


Fig. 1.—Contact angles of *n*-hexadecane on Langmuir-Blodgett monolayer depleted by benzene.

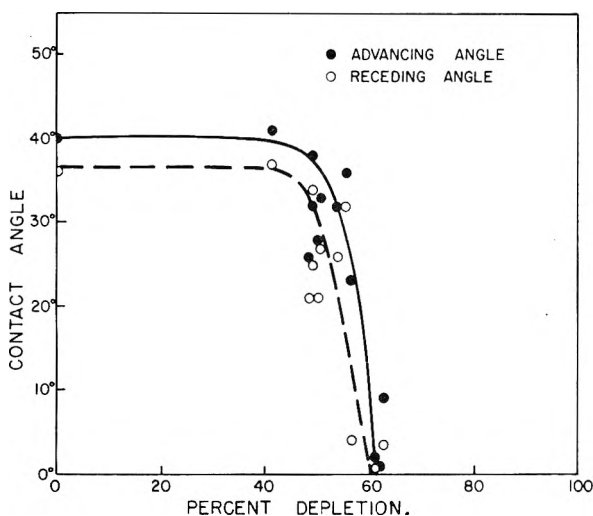


Fig. 2.—Contact angles of *n*-hexadecane on adsorbed monolayer depleted by benzene.

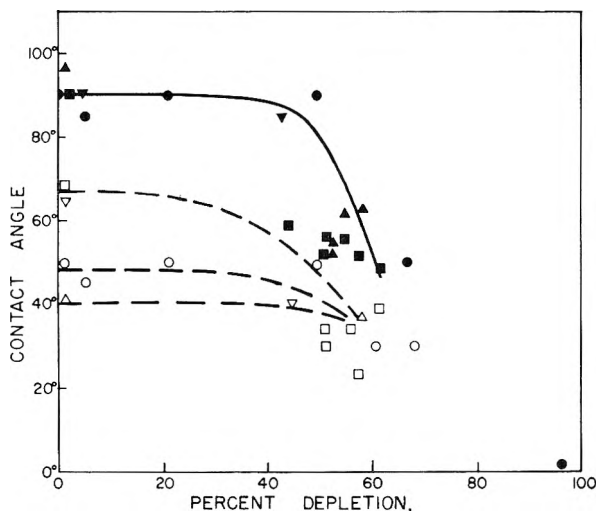


Fig. 3.—Contact angles of water on several different depleted films. Solid line represents advancing angles, dashed lines represent receding angles on different films.

from hexadecane, and angles of hexadecane were measured on films formed by the Langmuir-Blodgett technique. The results of typical runs of contact angle *vs.* per cent. depletion are plotted in Figs. 1-3. Characteristic of the results is the small change in contact angle until about half of the amine layer is removed. Beyond this point the contact angle falls rapidly, with the advancing angle lagging slightly behind the receding angle in responding to depletion. While the coverage corresponding to wetting is less than that originally predicted by Zisman⁵ who conjectured that monolayers are only oleophobic when the coverage is not much less than unity, it is in harmony with the later finding by Bigelow⁸ that wetting begins only when electron diffraction patterns of the layers are distinctly weaker than those of complete layers.

In several dozen experiments with octadecylamine, the advancing angle with hexadecane started out at $39 \pm 2^\circ$ and fell to 0° when about 60% of the amine molecules had been removed. Approximately the same values were obtained for Langmuir-Blodgett monolayers and for layers adsorbed from solution. There was some evidence that advancing angles fell somewhat sooner and less abruptly on slides cleaned by very gentle flaming than on slides flamed more vigorously. Whereas the advancing angle on undepleted films was virtually independent of the method of preparation of the surface, the receding angle was quite sensitive to differences. It ranged from only 1° to more than 20° below the advancing angle depending upon whether the slides had been fairly well flamed or only very gently flamed. The coverage at which the advancing angle fell to zero was never observed to be more than a few hundredths of a monolayer from that at which the receding angle fell to zero.

Films of stearic acid did not require as severe depletion as amine films to give complete wetting. Observations of volatility and solubility showed that the acid molecules were less firmly anchored to the slides than amine molecules.

The receding angle of water on amine films was very much more dependent than the advancing angle upon the preparation of the surface. Depletions great enough for complete wetting by water have only been made so far by fairly vigorous flaming. Unfortunately, the lack of control associated with this method has prevented the study of depletions in the range of 75 to 95% removal. The contact angle of water falls to zero somewhere within this range. Breath figures on slides depleted by flaming show that the coverage is irregular.

The optical technique permits a remarkably intimate examination of the wetting of depleted layers and shows graphically how freely solvent molecules interact with adsorbed molecules even when wetting is poor. If a drop of pure hexadecane is advanced over a complete monolayer of octadecylamine and then receded it is observed that the region once covered by the drop is partially depleted by solvent action. On the other hand, if a drop of hexadecane is advanced and receded over a layer that has already been depleted by about 35%, it is observed that the region once covered is somewhat more densely populated than the surrounding regions.

Apparently the solvent molecules enter some of the holes in the incomplete layers and play a role similar to that of the hydrocarbon tails around them. The solvent slowly evaporates over a period of minutes until the region that was in contact with the solvent recovers its original (depleted) population. By way of comparison, evaporation of the same amount of hexadecane from a liquid hexadecane surface under otherwise similar conditions takes place in a fraction of a second. Drops of water advanced over the surface and receded fairly promptly have produced no perceptible changes in the films studied.

Zisman, *et al.*,¹³ showed in a series of experiments on halogenated surfaces of varying halogen content, that contact angles respond smoothly to changes in free surface energy. Zisman also demonstrated, however, that while wetting properties of a surface can be predicted up to a point from consideration of the free surface energies of the liquid and solid before wetting, that contact angles depend significantly on the detailed molecular interactions occurring during wetting. The abrupt change in contact angle observed in the present investigation during the gradual removal of mono-

(13) A. H. Ellison and W. A. Zisman, *THIS JOURNAL*, **58**, 260 (1954).

layers is certainly not simply describable in terms of a smooth variation in free energy of the surface.

Attempts to follow the structure of the depleted films by electron diffraction were not definitive due to the masking of the pattern of the amine by the pattern of the underlying oxide film. Previous diffraction studies of monolayers on glass⁸ have indicated that there is no discernible difference between the orientation of the highly elongated molecules in complete and in depleted films. The implication of the diffraction results is that molecules hold each other upright in clusters at all coverages studied so far. It is doubtful, however, whether the above diffraction experiments would have been able to detect molecules lying flat and occupying the area between clusters at coverages down to 0.3 of a layer. Neither is it known to what extent the underlying surface is exposed at severe depletions.

It is clear that the explanation of the wetting properties of films requires a more complete knowledge of the structure of depleted layers than is available at present. Discussion of models of the process of wetting that are suggested by the above preliminary results will be deferred until after further investigation by refined techniques.

MONOLAYERS IN EQUILIBRIUM WITH LENSES OF OIL ON WATER. I. OCTADECANOL AND TETRADECANOIC ACID IN WHITE OIL

BY W. M. SAWYER AND F. M. FOWKES

Shell Development Company, Emeryville, California

Received February 24, 1956

The equilibrium conditions established when lenses of white oil containing octadecanol or tetradecanoic acid are placed on a clean water substrate have been examined. For all concentrations the final spreading coefficient of these systems is negative. Above a certain concentration of solute in the oil lenses, the monolayers formed by adsorption at the oil-water interface are in equilibrium with the monolayers formed at the air-water interface by shedding solute from the lenses. Under these conditions there exists a constant difference in film pressures at the oil-water interface and at the air-water interface which is independent of solute concentration. A little known method described by Langmuir has been used to measure this difference directly. For octadecanol solutions this difference is zero and for tetradecanoic acid solutions on 0.01 *N* HCl it is 5.8 dynes/cm. The molecular area in the octadecanol films is $20 \pm 1 \text{ \AA}^2$ /molecule at each interface. A continuous close-packed monolayer therefore exists over the entire water surface. For the tetradecanoic acid solutions on 0.01 *N* HCl, the situation is slightly different in that the area per molecule in the interfacial films is somewhat greater than that in the monolayers at the air-water interface. The monolayers may be considered in the manner of Langmuir as having independent upper and lower boundary tensions. For octadecanol the equilibrium is then a lens of oil resting on the closed-packed hydrocarbon tails; for tetradecanoic acid this is only approximately correct. For dilute solutions of octadecanol solute does not escape from the oil lenses and no film pressure was detected at the air-water interface, although the film pressure at the oil-water interface was several dynes/cm. The absence of a detectable film pressure may be due to a kinetic limitation on the transfer of solute across the linear periphery of the lens.

The behavior of lenses of oil on water has been examined by a number of investigators.¹⁻⁹ However, relatively few lens-monolayer studies with solutions have been reported. Langmuir, in a monumental paper on lenses,^{3a} extended a derivation given by Hardy¹ to include a relation between the dimensions of large lenses on water and the three relevant boundary tensions. This was only applied experimentally to non-spreading oils in the absence of a solute. Experimental observations for solutions were largely restricted to systems which form relatively stable thin films. In a subsequent paper^{3b} Langmuir recognized that these "duplex" films were unstable but that changes occurred relatively slowly so that measurements of the metastable condition were possible. Harkins⁹ also considered duplex films unstable. The shedding of solute molecules from lenses was observed by Langmuir^{3b} and a critical concentration for this activity noted. Zisman⁴ has described the phenomenon of shedding solute (edge diffusion) for a variety of solutes, although this process occurs only slowly in appropriate ranges of concentration. Heymann and Yoffe^{6b} have measured directly the film pressure of solutions of oleic acid in paraffin oil. The study presented here is an extension of previous work in that it is concerned with an experimental description of the equilibrium state attained between relatively thick, stable lenses of mineral oil containing octadecanol or tetradecanoic acid and aqueous substrates. This equilibrium, achieved in the absence of auxiliary "piston oils," is described in terms of molecular packing of solute

and two directly measured film pressures: π_{ow} for the adsorbed solute and π_w for the solute shed to the air-water interface.

Experimental

Methods.—Interfacial tensions were calculated from photographic negatives obtained by the pendant drop technique.¹⁰⁻¹³ Oil was delivered from a hypodermic syringe through a stainless steel tip to form drops in the aqueous phase contained in a Pyrex cell. The Pyrex cell had optically plane windows and it and the syringe were jacketed. The cell and syringe fit together with a ground glass joint to make an essentially closed system. Water was rapidly circulated through the jackets to keep the cell contents at 25.0°. The horizontal position of the cell and syringe combination was adjusted in the optical path of the camera with a mechanical stage. The light source was a 2-watt Concentrated Arc Lamp¹⁴ housed in a microscope lamp mounting equipped with a mechanical iris, Wratten 61-N green filter and aspheric lens. This combination gave a parallel light beam. In the camera, a magnification of $4 \times$ to $30 \times$ was obtained with extension tubes and bellows and with two interchangeably mounted camera lenses: a 35 mm. *f* 3.5 Wollensak Movie Camera lens used backwards and a 105 mm. *f* 4.5 Zeiss Tessar lens. Since the cell was mounted on an adjustable platform, the fine focusing was done by moving the cell rather than by changing the magnification of the camera. This arrangement allowed the taking of several pictures at the same magnification and permitted precise determination of the magnification by photographing a ruled slide with undisturbed camera adjustment. Eastman Super Panchro Press B 4×5 cut film was used. The whole apparatus was mounted on an optical bench of $3/4$ " steel rods under tension.

All glass apparatus was cleaned with solvent, warm chromic acid, and rinsed with distilled water before use. The stainless steel dropping tips were cleaned with solvent and boiling, redistilled acetone. Values of the interfacial tension were calculated from measurements made directly on the film by means of the tables of Fordham.¹⁵ Duplicate measurements of the same negative agreed to 0.1%.

The spreading pressures and force-area curves were obtained with a Dervichian-Wilhelmy type surface balance arranged for automatic recording. The balance was a

(1) (a) W. B. Hardy, *Proc. Roy. Soc. (London)*, **A86**, 610 (1911); (b) **A88**, 313 (1913).

(2) C. G. Lyons, *J. Chem. Soc.*, 623 (1930).

(3) (a) I. Langmuir, *J. Chem. Phys.*, **1**, 756 (1933); (b) *J. Franklin Institute*, **218**, 143 (1934).

(4) (a) W. A. Zisman, *J. Chem. Phys.*, **9**, 534 (1941); (b) **9**, 729 (1941); (c) **9**, 789 (1941).

(5) R. S. Bradley, *Trans. Faraday Soc.*, **36**, 999 (1940).

(6) (a) E. Heymann and A. Yoffe, *Trans. Faraday Soc.*, **38**, 408 (1942); (b) **39**, 217 (1943).

(7) N. F. Miller, *THIS JOURNAL*, **45**, 289 (1941).

(8) N. F. Miller, **45**, 1025 (1941).

(9) W. D. Harkins, *J. Chem. Phys.*, **9**, 552 (1941).

(10) J. M. Andreas, E. A. Hauser and W. B. Tucker, *THIS JOURNAL*, **42**, 1001 (1938).

(11) G. W. Smith and L. V. Sorg, *ibid.*, **45**, 671 (1941).

(12) G. L. Mack, J. K. Davis and F. E. Bartell, *ibid.*, **45**, 846 (1941).

(13) G. W. Smith, *ibid.*, **48**, 163 (1944).

(14) Sylvania Electric Products, Inc., New York.

(15) S. Fordham, *Proc. Roy. Soc. (London)*, **A194**, 1 (1948).

Heusser¹⁶ assay balance equipped with a prism and mirror to translate the motion of the balance beam into motion of a light beam. The movement of the light beam was recorded directly on the strip chart of a Photo-Pen Recorder.¹⁷⁻¹⁸ The trough (24 × 64 × 1 cm.) was located in an air thermostat. Water from a constant temperature reservoir was rapidly circulated through all sides of the thermostat and the false bottom of the trough. The trough and barriers were 18-8 stainless steel and waxed with high melting paraffin (92°) before each use. The enclosed air was rapidly saturated with water by a small fan blowing across a reservoir in the bottom of the box. Temperature was maintained constant to less than 0.05°. The barriers could be driven at various speeds by means of a gear-reduction box; total time for force-area curves varied from 1 min. to 1 hour. Combinations of paper speed on the Photo-Pen chart and barrier speed could compress or expand the area axis on the chart. By using slides of various dimensions the sensitivity on the vertical axis of the chart paper could be varied from 0.005 to 0.1 dyne/cm.

Compounds for force-area curves were added as solutions in hexane by means of a calibrated, micrometer-driven hypodermic syringe. In all measurements of the equilibrium spreading pressure of oil solutions, sufficient solution was added so that the loss of spreading molecules from the oil lens did not significantly alter the bulk concentration in the lens. Equilibrium was considered to have been established when additional drops of solution caused only a momentary increase in surface pressure followed by a rapid return to the previous value. For these measurements film pressures as low as 0.09 dyne/cm. could easily be detected.

The diameter of large floating lenses of known volume was measured while simultaneously observing the film pressure at the air-water interface by means of a small Wilhelmy balance. The experimental arrangement consisted of a 20 cm. watch glass containing the aqueous substrate which rested on edges of a rectangular glass dish full of water. These were located in a waxed box with a flat glass top and bottom. The water in the glass dish maintained a constant temperature within 1° during several hours. Water-soaked cleaning tissues maintained high humidity. A lens was formed on the substrate in the watch glass by adding solution from a buret through a hole in the upper glass plate. An essentially parallel light beam was directed upward from below the box so as to form an image of the lens on a piece of tracing paper placed on the upper glass plate. Provided the space between the outer glass dish and the glass bottom of the box was full of water, this image was sharp and of the same diameter as the lens. A Wilhelmy plate was suspended in the substrate, through a hole in the glass top, from one arm of a torsion balance. This balance was equipped with a prism-mirror combination and an optical lever permitted measurements of the film pressure simultaneously with measurements of the lens diameter.

The lens diameters were found to be extremely sensitive to adventitious contamination and to film pressures on the water surface. When a given lens-monolayer system was near equilibrium the addition of oil solution to the lens caused a perceptible increase in film pressure and consequently a smaller diameter than the equilibrium value. As the film pressure decreased to its equilibrium value the lens expanded to its equilibrium diameter, which was used for calculation.

Materials.—The oil was a highly refined, naphthenic white oil with the following properties at 25.0°: density 0.8323 g./ml., n_D^{25} 1.4583, surface tension (ring method, corrected) 28.85 dynes/cm. Its molecular weight was 290. The density of the solutions did not differ by more than 0.0002 from the solvent. In order to remove adsorbable impurities, the oil was passed through a column of dry silica gel and the first 5% and last 20% were rejected. After thorough sweeping with nitrogen, the oil could be stored in the dark for several days before surface-active contamination became detectable. Octadecanol D was a center cut from a low pressure distillation. Its freezing point (modified Rossini) was 57.46°. The force-area curve indicated some impurities were present. Octadecanol P was prepared by recrystallization of D from ethanol at 0°. Its freezing point

was 57.95°. The value given by Ralston¹⁹ is 57.98°. The force-area curve for octadecanol P was perceptibly different from D and agreed closely with that reported by Copeland.²⁰ The film pressure in equilibrium with the solid was 33.7 dynes/cm. at 25.0°. The absence of ionizable impurities was indicated by film pressures of a concentrated solution which did not vary by more than 0.15 dyne/cm. on substrates of pH 1 and 11.5. The tetradecanoic acid was recrystallized after distillation and had a freezing point of 54.15° compared with 54.4° given by Ralston.¹⁹ The film pressure in equilibrium with the solid acid at 25° was 20.4 dynes/cm. The water was redistilled from alkaline permanganate and condensed in a block tin condenser. It was stored in Pyrex bottles. The surface tension of water was taken as 72.00²¹ dynes/cm. at 25.0° and its density as 0.9971 g./ml. The *n*-hexane used as solvent for spreading monolayers was Phillips 99 mole % pure *n*-hexane, which was freshly distilled to remove surface-active impurities which otherwise contaminated the surface.

Results

An oil with a negative spreading coefficient, $F = \gamma_w - (\gamma_o + \gamma_{ow})$ will not spread on water but will remain as a stable lens; its equilibrium configuration is dictated by the boundary tensions, the gravitational potential energy of the elements of volume, and the pressure differences across the curved surfaces. A similar definition of the spreading coefficient applies for an oil containing a surface-active solute which alters the oil-air (γ'_o) or oil-water (γ'_{ow}) interfacial tension. In cases of interest here $\gamma_o = \gamma'_o$ and the spreading coefficient of the solution becomes $\gamma_w - (\gamma_o + \gamma'_{ow})$. This is identical with the initial spreading coefficient of Harkins⁹ and may be calculated from known values of γ_w and γ_o and a measured value of γ'_{ow} . When γ'_{ow} becomes sufficiently small the spreading coefficient becomes positive and a drop of solution will spread to a thin but unstable film on water. When a drop of such solution is placed on the clean water substrate of a film balance, the film pressure increases nearly instantaneously and on addition of more solution continues to rise to an equilibrium value. Accompanying this spreading is the formation of a monolayer of solute molecules at the air-water interface. The equilibrium film pressure in this monolayer is designed π_w . The spreading coefficient under these conditions achieves a final value $F' = \gamma'_w - (\gamma_o + \gamma'_{ow})$ and is not in general accessible by measures of γ'_{ow} ($= \gamma_{ow} - \pi_{ow}$) or π_w alone. In terms of equilibrium film pressures $F' = F + \pi_{ow} - \pi$.

The equilibrium state of the films formed in spreading pressure experiments with solutions of octadecanol is shown in Figs. 1 and 2. In Fig. 1 the film pressure attained at A was not influenced by additional drops of solution, the usual criterion of equilibrium. At B the film was compressed causing a nearly instantaneous increase in film pressure followed by a rapid decrease. At C the film was expanded with accompanying decrease in film pressure and a slower increase to the equilibrium value attained at A. In the experiment shown as curve ABCF in Fig. 2, a film of octadecanol (laid down from hexane) was compressed

(19) A. W. Ralston, "Fatty Acids and their Derivatives," John Wiley and Sons, Inc., New York, N. Y.

(20) L. L. Copeland, W. D. Harkins and G. E. Boyd, *J. Chem. Phys.*, **10**, 272 (1942).

(21) "International Critical Tables," Vol. IV, McGraw-Hill Book Co., New York, N. Y., p. 447.

(16) Heusser Instrument Mfg. Co., Salt Lake City, Utah.

(17) Beckman Instruments, Inc., Belmont, California.

(18) D. J. Pompec and C. J. Penner, *Rev. Sci. Instr.*, **13**, 218 (1942).

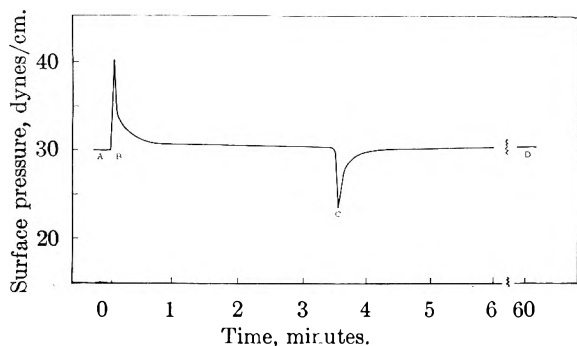


Fig. 1.—Effect of small changes in trough area on the film pressure of a spread monolayer in equilibrium with lenses of octadecanol solution in white oil: A, equilibrium film pressure; B, compression; C, expansion; film pressure at D equals that at A.

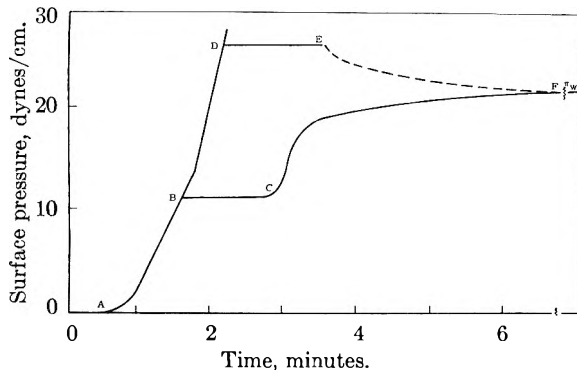


Fig. 2.—Equilibrium film pressure for a solution of octadecanol in white oil on pre-existing octadecanol monolayers at two different pressures at 25.0°: π_w , equilibrium pressure with no pre-existing monolayer; solution addition at C and E; lines at the left are the force-area curve for pure octadecanol.

along AB to 11.52 dynes/cm. and stopped. Drops of a solution of octadecanol of previously determined $\pi_w = 21.7$ were added at C. The initial spreading coefficient for this system was +1.9 dynes/cm. The film pressure increased rapidly and an equilibrium value of 21.9 dynes/cm. recorded. The curve ABDEF indicates a similar experiment made with the initial film pressure 3.5 dynes/cm. above the equilibrium value. In this case the initial spreading coefficient was -11.7 dynes/cm. An equilibrium value of 21.83 dynes/cm. was recorded. The above values are equal within experimental error. In these experiments the concentration of octadecanol in the oil lens is not significantly altered. Since the same final π_w is obtained with initial film pressure greater or less than the equilibrium value, the monolayers are demonstrated to be in equilibrium with the oil lenses. The establishment of equilibrium in a matter of minutes during the manipulation of the monolayers shown in Fig. 1 indicates that octadecanol molecules are rapidly transferred from the air-water interface to the oil-water interface and vice versa.

The time dependence of the interfacial tension of octadecanol solutions is shown in Table I. The pure sample, octadecanol P, shows no significant time dependence. The interfacial tension of dilute solutions of octadecanol D decreased several dynes/cm. in the first 10 minutes but

remained constant for the subsequent 80 minutes. Since there is no extended time dependence of the interfacial tension of octadecanol solution, the surface and interfacial monolayers can rapidly reach equilibrium with the bulk oil of the lenses.

TABLE I
EFFECT OF TIME ON THE INTERFACIAL TENSION OF SOLUTIONS OF OCTADECANOL P IN WHITE OIL vs. WATER AT 25.0°

0.089 % wt.	0.124 % wt.	0.194 % wt.	0.292 % wt.
Time, min.	Time, min.	Time, min.	Time, min.
γ'_{ow}	γ'_{ow}	γ'_{ow}	γ'_{ow}
0.6	1	2	1
47.78	45.52	38.29	30.64
5	7	5	5
46.96	45.50	38.27	30.24
10	15	11	10
46.50	45.37	37.90	30.00
15	30	15	15
45.96	44.9=	38.17	30.04
21	45	20	20
46.66	45.11	38.07	29.78
34	60	30	30
46.49	45.00	38.04	29.82
40	75	40	61
46.51	45.23	38.04	29.92
62	93	50	91
46.21	45.34	37.99	29.90
80	120	60	120
46.47	45.39	37.88	29.74
100	135	95	151
46.73	45.31	37.68	29.45
		157	37.68

The relation between the equilibrium values of the film pressures π_w and the interfacial film pressure π_{ow} for solutions of octadecanol in white oil is shown in Table II. It is evident that these film pressures are equal, provided the solutions are sufficiently concentrated. Thus, the lens-monolayer equilibrium described above is characterized by an equality of film pressures which does not depend on concentration of octadecanol in the bulk oil. More dilute solutions apparently do not form a surface film at the air-water interface, although an interfacial pressure of several dynes/cm. may exist at the oil-water interface of a lens on the substrate. The zero value of π_w of the 0.089% wt. octadecanol solution was obtained after observation in constant environment for 21 hours. In this experiment sufficient oil solution was added to give fourteen times the number of molecules of octadecanol required to produce a readily detectable film pressure of 0.09 dyne/cm. The absence of an observable film pressure for dilute solutions suggests that pure oil should completely dissolve a monolayer of octadecanol provided a sufficiently dilute solution was formed in the oil lenses. The results presented in Fig. 3 suggest

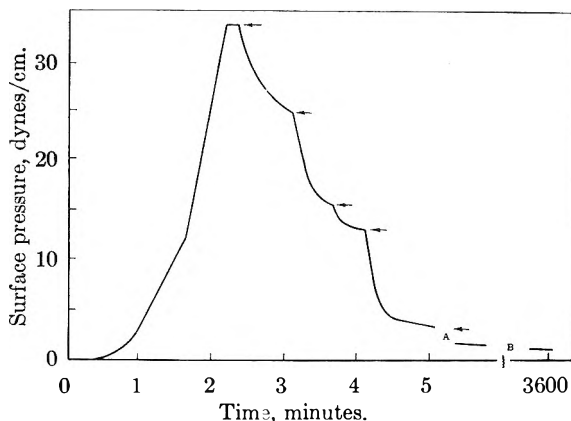


Fig. 3.—Dissolution of a pre-existing octadecanol monolayer by white oil. The addition of pure oil is indicated by arrows; intervals A and B are 13 min. and 60 hr.

this to be the case. A monolayer of octadecanol (deposited from hexane solution) was compressed to 32 dynes/cm. and drops of oil added at points indicated by arrows. The recorded film pressure decreased rapidly and after 60 hours was recorded as 1.7 dynes/cm. However, reducing the trough area did not result in a detectable increase in film pressure. The recorded value of 1.7 dynes/cm. was apparently due to the lack of reversibility of the Wilhelmy balance, and the water surface was effectively void of octadecanol.

TABLE II

VARIATION OF FILM PRESSURES OF OCTADECANOL SOLUTIONS AT THE OIL/WATER AND AIR-WATER INTERFACE AT 25.0°

Concn.	π_w - Wilhelmy balance π_{ow} - pendant drop		
	Equil. film pressure π_w , dynes/cm.	Interfacial Pressure π_{ow} , dynes/cm. $\pi_{ow} = 51.32 - \gamma'_{ow}$	Spreading coefficient $F' = \gamma'_{ow} - (\gamma_o + \gamma'_{ow})$
Sample P			
0.089	0	4.85	-3.6
0.124	0	6.07	-2.1
0.194	13.8	13.55	-8.0
0.292	21.7	21.57	-8.1
0.518	34.3
Sample D			
0.08	0	5.3	-2.9
0.28	20.0	19.9	-8.1
0.32	24.1	23.6	-7.5

The equality of film pressures shown in Table II indicates the final spreading coefficient of the solution to be equal to that for the solvent. This was demonstrated independently by the lens-diameter technique described by Langmuir.^{3a} The spreading coefficient of an oil on water is related to the thickness of a lens of infinite radius by

$$F = -(1/2)qt^2_{\infty}(\rho_1 - \rho_2)\rho_2/\rho_1 \quad (1)$$

where ρ_2 and ρ_1 are the densities of the oil and water. For large lenses of radius R and known volume V , $V/\pi R^2 = t_{\infty} - A/R + B/R^2$ where A and B are constants depending in a complicated manner on the densities and boundary tensions. For sufficiently large lenses ($R > 2.5$ cm.) B/R^2 is negligible and t_{∞} is obtained as the intercept on a linear plot of $V/\pi R^2$ vs. $1/R$. Values of t_{∞} can also be obtained from measurements of the thickness of large lenses.⁵ The results of a series of measurements on pure white oil are shown in Table III as obtained from curves corresponding to B in Fig. 4. Since γ_c and γ_w are accurately established quantities, the accuracy of this method was assessed by comparing values of γ_{ow} obtained from values of F , as calculated by equation 1 and the definition of F , with values of γ_{ow} determined by the pendant drop method. The excellent agreement between the two methods is shown in Table III. The lens diameter method is well suited for measuring γ_{ow} , since t_{∞} is accurately obtained and its value is a small fraction of γ_{ow} .

Provided an adequate criterion for lens-monolayer equilibrium is included in the measurements, the lens-diameter technique can be applied to

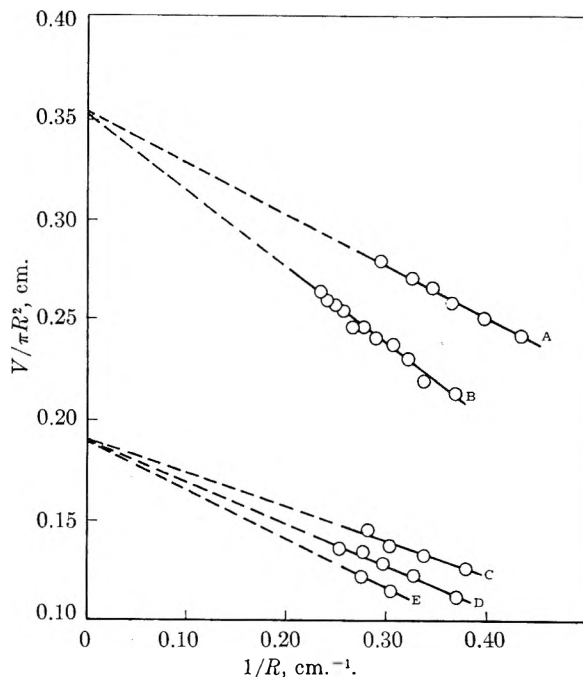


Fig. 4.—Lens-diameter method for obtaining the thickness of a lens of infinite radius. Solutions in white oil: (A), 0.32% wt. octadecanol; B, pure white oil; C, D, and E, 0.35%, 0.67%, 1.37% wt. tetradecanoic acid on 0.01 *N* HCl substrate.

solutions. In this case F' is calculated from t_{∞} . Lens-diameter measurements were made on an octadecanol solution at equilibrium values of π_w as indicated by a Wilhelmy balance present in the trough at the same time. Curve A in Fig. 1 shows the results. The equality of the intercept with that for the pure oil confirms directly the equality

TABLE III

REPRODUCIBILITY OF DIAMETER-VOLUME AND PENDANT DROP METHODS OF MEASURING γ_{ow} FOR WHITE OIL AT 25°

t_{∞}	$\gamma_w = 72.00$, $\gamma_o = 28.85$		
	Lens-diameter method F	γ_{ow}	Pendant drop method γ_{ow}
0.344	-7.98	51.13	51.94 51.86
.351	-8.30	51.45	51.46 50.92
.348	-8.16	51.31	51.05 50.71
.350	-8.25	51.40	51.10 51.48
			51.61 51.00
Av.	-8.17	51.32	51.31

of π_w and π_{ow} . Measurements of t_{∞} were obtained for solutions of tetradecanoic acid on 0.01 *N* HCl as shown in curves C-E of Fig. 4. The final spreading coefficient for the three solutions is -2.4 dynes/cm. The simultaneously measured values of π_w are 7.9, 9.7 and 12.5 dynes/cm. These are related to the interfacial film pressures π_{ow} by the equation $-2.4 = -8.2 + \pi_{ow} - \pi_w$. Thus, as in the case of the octadecanol solutions, the difference in film pressures at the air-water interface is a concentration independent quantity. The equilibrium state for these films differs from that for octadecanol film in that π_{ow} always exceeds π_w by 5.8 dynes/cm. A similar result has been obtained by Heymann and Yoffe^{6b} for solutions of oleic acid in a paraffin oil. They found that for

sufficiently concentrated solutions, $\pi_{ow} - \pi_w = 10.3$ dynes/cm. For more dilute solutions, however, their results show π_{ow} to exceed π_w by such an amount that the final spreading coefficient was positive. It is unlikely that these dilute solutions are in equilibrium with the monolayers.

Discussion

The results presented here and those of Heymann and Yoffe⁶ indicate that, when lenses of solutions of simple, water-insoluble surface active solutes in mineral oil are placed on a clean water substrate, the film pressures measured at the air-water interface are related to the film pressures of the adsorbed solute at the oil-water interface by an additive constant. These results have been obtained in the absence of auxiliary "piston oils." In the presence of a truly insoluble piston oil similar results might also be obtained. However, the rapid solubility of an octadecanol monolayer in pure mineral oil suggests that mixed films of the piston oil and solute might readily form.

Application of the Gibbs adsorption equation to the interfacial tensions for octadecanol solutions indicates an average value for the molecular area at the oil-water interface (σ_{ow}) of $21 \text{ \AA}^2/\text{molecule}$ for concentrations above about 0.14% wt. The force-area curve for octadecanol shows that pure octadecanol molecules under film pressure of 8.2 dynes/cm. have $\sigma_{aw} = 20.78 \text{ \AA}^2/\text{molecule}$; under a film pressure 30 dynes/cm. this value is decreased to $19.64 \text{ \AA}^2/\text{molecule}$. Thus, the equilibrium surface and interfacial films of octadecanol are not only under the same pressure but are at the same surface concentration. The equilibrium state is therefore a continuous, tightly packed monolayer of octadecanol molecules over the entire water surface with a lens of oil solution resting on, and in equilibrium with, this monolayer. If this monolayer is considered in the sense of having independent boundary tension³ at the upper and lower surfaces, a value for the interfacial tension of the oil solution against its monolayer may be derived. For each film the upper boundary tension "tails-in-air" (γ_{ta}) plus the lower boundary tension "heads-in-water" (γ_{hw}) is equal to the observed boundary tension γ_w . Similarly at the oil-water interface the observed γ'_{ow} is equal to γ_{hw} plus γ_{to} (tails-in-oil). The spreading coefficient is now $F' = \gamma_{ta} - \gamma_o - \gamma_{to}$. The value γ_{ta} should be approximately constant for tightly packed films and value will differ from γ_o by some small value ϵ . Since the final spreading coefficient does not depend on octadecanol concentration, the value of γ_{to} for white oil against the close-packed methyl groups of the octadecanol monolayers is approximately 8.2 dynes/cm.

Applying the Gibbs adsorption equation to the film pressures of non-ionized tetradecanoic acid films and considering the acid as monomer in the oil solutions gives $\sigma_{ow} = 85 \text{ \AA}^2/\text{molecule}$. The force-area curve^{3a} for tetradecanoic acid films on 0.01 N HCl indicates a σ_{aw} of $39 \text{ \AA}^2/\text{molecules}$ at a film pressure of 8 dynes/cm. and $35 \text{ \AA}^2/\text{molecule}$ at 12.5 dynes/cm. The values of σ_{aw} for tetra-

decanoic acid are therefore appreciably less than values of σ_{ow} . If, as suggested by Langmuir,^{3b} the Gibbs equation gives areas in the interfacial film which are twice too large due to dimer formation, values of σ_{ow} still exceed somewhat those of σ_{aw} . The concept of independent boundary tensions can apply only roughly to tetradecanoic acid monolayers. Since these are not as tightly packed the approximations that $\gamma_{ta} = \gamma_o$ and that γ_{hw} is the same in each interface may be seriously in error. However, such calculation gives $\gamma_{to} = 2.4$ dynes/cm.

The critical concentration below which a surface-active solute does not escape to the air-water interface was suggested by Langmuir^{3b} as the concentration of solute in a non-spreading oil which just makes $\pi_{ow} = -F$. At, and above, this concentration, the initial value of F' is positive and the free energy change favors the formation of a thin film rather than lenses. For octadecanol solutions this occurs at a concentration of about 0.14% wt. The shedding and retraction of oil lenses from their monolayers noted by Langmuir^{3b} was described in detail by Zisman.^{4a} These phenomena were observed for octadecanol solutions which shed monolayers to the air-water interface by examining the lens periphery with a microscope. Even at very slow rates of shedding the edge of the lens retracts from the newly shed surface film in a discontinuous fashion. Very sudden retractions of small sections of the periphery occurred at irregular intervals and unpredicted places along the periphery. The retractions were always violent and minute lenses were expelled from the large lens. For solutions below the critical concentration for shedding, the periphery was quiescent. Although no film pressures have been detected for solutions more dilute than 0.14% wt. and pure oil would appear to dissolve completely a pre-existing monolayer, it is unlikely that this concentration represents a true equilibrium limitation. The suggestion of Langmuir^{3a} that such a thermodynamic equilibrium exists is based on vapor adsorption of stearic acid and on the observations of Cary and Rideal²² that crystals of fatty acids do not form monolayer on 0.01 N HCl below a particular temperature depending on the fatty acid. These authors consider that this results from a kinetic limitation on the rate of transfer from crystals. It appears likely then that the apparent critical concentration represents a concentration at which an abrupt transition in the mechanism of shedding occurs. Above this value rapid pulsations of the lens can establish equilibrium rapidly, while below it these pulsations are impossible. In this case and in the corresponding case of Cary and Rideal, there must exist a large energy barrier for escape of solute. This may be related to the passage of molecules through the linear periphery of the lens as suggested by Zisman.^{4a} For more concentrated solutions, the transfer of solute molecules demonstrated in Fig. 1 takes place relatively uninhibited by kinetic restrictions.

(22) A. Cary and E. Rideal, *Proc. Roy. Soc. (London)*, **A109**, 301, 318, 331 (1925).

MICELLE FORMATION IN SOLUTIONS OF SOME ISOMERIC DETERGENTS¹BY DAVID B. LUDLUM²*Contribution from the Department of Chemistry, University of Wisconsin, Madison, Wisconsin**Received February 24, 1956*

Measurements of electrical conductivity and of optical turbidity are reported for solutions of three isomeric dodecylbenzene sulfonates in water solution. The conductance behavior of these solutions is similar to that which has been reported for other detergents, while the light scattering behavior is typical of solutions of highly charged particles. Critical concentrations and micelle sizes have been determined from these measurements, and the conclusion has been drawn that an increase in hydrophobic nature lowers the critical micelle concentration and increases the micelle size in agreement with the predictions of recent theories of micelle formation.

Introduction

Micelles are formed in solutions of ionic detergents when the energy gained by bringing the hydrophobic parts of the monomers together is sufficient to overcome the opposing repulsive forces. This study was undertaken to determine the effect of varying the hydrophobic nature of an anionic detergent on the critical micelle concentration and on the properties of the micelles themselves. Three isomeric sodium dodecylbenzene sulfonates, differing from each other in the point of attachment of the benzene ring to the dodecyl chain and exhibiting a varying hydrophobic nature resulting from differences in the effective length of the hydrocarbon side chain, were chosen to investigate any such effects.

Debye³ has studied a series of cationic detergents and has found that an increase in hydrocarbon chain length leads to the formation of larger micelles at lower concentrations. Because of the importance of such studies to recent theories of micelle formation, they have been extended here to a series of anionic detergents which show similar behavior, modified somewhat by the high charge on the micelle. Dodecylbenzene sulfonates were selected because they are strong electrolytes not hydrolyzed in solution, and because they are relatively soluble. Critical micelle concentrations were determined from measurements of electrical conductivity, and micelle sizes were obtained from light scattering measurements.

Theory

The theory of micelle formation has been discussed in recent articles by other authors.^{4,5} Briefly, micelles are formed when the energy released by the aggregation of the hydrocarbon parts of the monomers is sufficient to overcome the electrical repulsion among the ionic groups and to balance the decrease in entropy accompanying the formation of micelles. A balance of these opposing forces leads to the formation of micelles of a definite size at and above the critical micelle concentration.

Theories of micelle formation express the total free energy of the system in terms of the molec-

ular characteristics of the monomer and the micelle. Free energy is then minimized with respect to micelle size and critical concentration yielding expressions relating these two quantities to the characteristic properties of the detergent.

The detergent monomer may be characterized in part by a parameter, W_n , which measures its hydrophobic nature. This parameter is related to the area of hydrocarbon exposed to water in solution and to the attractive forces which exist between the hydrocarbon parts of different monomers. The higher dependence of the electrical energy on the number of monomers in a micelle leads to the prediction that an increase in W_n , or an increase in the hydrophobic nature of the monomer, will result in an increase in micelle size and a decrease in critical concentration if all other properties of the detergent remain the same. This condition is most nearly met in isomeric detergents where only the hydrocarbon part of the monomer is varied.

In order to determine values of n , the number of monomers in a micelle, and C_0 , the critical concentration, from experimental conductivity and light scattering measurements, it is necessary to investigate the equilibrium which exists between monomers and micelles. For the formation of a micelle containing n anions and p gegenions in an anionic detergent, we may write approximately, substituting molar concentrations for activities: $C_M/C_A^n C_B^p = K$, where K is an equilibrium constant, C_M is the concentration of the micelle $A_n B_p^{-(n-p)}$, C_A is the concentration of monomer A^- , and C_B is the concentration of gegenion B^+ . Using Debye's notation, we take C_0 to be an arbitrary constant which is later identified with the critical micelle concentration, and set $K = C_0^{1-n-p}$, $\gamma_M = C_M/C_0$, $\gamma_A = C_A/C_0$, and $\gamma_B = C_B/C_0$. Finally, we introduce the quantity $\gamma = C/C_0$, where C is the molar concentration of anion or gegenion we would have if there were no association, and add two equations representing the conservation of mass in micelle formation. We then have the following system of equations describing the monomer-micelle equilibrium

$$\begin{aligned} \gamma_M &= \gamma_A^n \gamma_B^p \\ n \gamma_M + \gamma_A &= \gamma \\ p \gamma_M + \gamma_B &= \gamma \end{aligned} \quad (1)$$

Equations 1 may be solved numerically (for particular values of n and p) to give γ_A , γ_B and γ_M as functions of γ . The results of one such calculation, with n equal to 70 and p equal to 50, are shown in Fig. 1. Similar results are obtained for other values of n and p if n is sufficiently large;

(1) This paper is based on a thesis submitted by David B. Ludlum to the Faculty of the University of Wisconsin in partial fulfillment of the requirements for the degree of Doctor of Philosophy, August, 1954.

(2) E. I. du Pont de Nemours and Co., Polychemicals Department, Experimental Station, Wilmington, Delaware.

(3) P. Debye, *Ann. N. Y. Acad. Sci.*, **51**, 575 (1949).

(4) Y. Ooshika, *J. Colloid Sci.*, **9**, 254 (1954).

(5) I. Reich, *THIS JOURNAL*, **60**, 257 (1956).

the conclusions which follow have been verified for n greater than 20, the range of values experimentally encountered.

We note from Fig. 1 that micelles first appear at γ approximately equal to 1, or $C = C_0$; this is the justification for identifying C_0 , defined by the equation $K = C_0^{1-n-p}$, with the experimentally observed critical micelle concentration. For values of γ greater than one, it is also clear that γ_M is a nearly linear function of γ with a slope, $\Delta\gamma_M/\Delta\gamma$, of $1/70$. It has been established by direct calculation that $\Delta\gamma_M/\Delta\gamma$ may in general be closely approximated by $1/n$, independent of the value of p . Thus, for n equal to 70, $\Delta\gamma_M/\Delta\gamma$ is at most 3.8% different from $1/n$, where p varies from 0 to 70. Accordingly, we may to a good approximation express C_M as a linear function of C

$$C_M = (C - C_0)/n \quad (2)$$

This equation is useful in the treatment of the light scattering data.

It is not necessary to develop a detailed theory of conductivity in detergent solution to determine critical concentrations from conductivity data. If we plot specific conductance *versus* concentration for a detergent solution, we obtain a graph consisting of two intersecting straight lines. Below the critical concentration, the conductance increases as the concentration of detergent monomers and gegenions increases; above the critical concentration, highly charged micelles are also present, and conductance increases at a different rate. The critical concentration may, therefore, be determined from the point at which the slope of the specific conductance *versus* concentration curve changes.

Ionic interactions contribute to slight deviations from linearity in each region and, in addition, make it difficult to relate micellar mobilities to the molecular characteristics of the micelles. Nevertheless, some information on the relative micelle size and charge may be obtained by comparing the conductivity data for related detergents above the critical concentration.

The theory of the scattering of light from solutions of highly charged particles has been treated in a number of recent articles.^{6,7} The equation relating amount of light scattered to the concentration of ions in solution is given by Prins and Hermans as

$$\frac{Kc_2}{R_{90}} = \frac{1}{M} \left\{ 1 + \frac{1000(n-p)^2(c_2/M)}{2C_A + 1000(n-p)(c_2/M)} \right\} \quad (3)$$

where n , p and C_A are defined above, c_2 is the concentration of micelle in g./ml., M is the molecular weight of the micelle, R_{90} is Rayleigh's ratio, and K is the scattering constant: $2\pi^2 n_0^2 (dn/dc_2)^2 / N\lambda_0^4$. Here, n_0 is the refractive index of solvent, dn/dc_2 is the change in refractive index with concentration of micelle (taken equal to dn/dc), N is Avogadro's number and λ_0 is the wave length of incident light.

Equation 3 may be simplified if we refer to Fig. 1 and consider C_A to be an approximately linear function of C_M and hence of C_2 above the critical

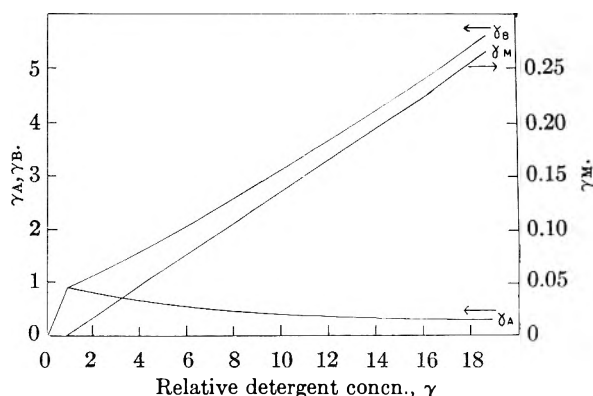


Fig. 1.—Relative concentrations in a detergent solution: γ_A , relative monomer concentration; γ_B , relative gegenion concentration; γ_M , relative micelle concentration.

concentration. Then, equation 3 may be written in the form

$$\frac{Kc_2}{R_{90}} (1 + D_1 c_2) = \frac{1}{M} + D_2 c_2 \quad (4)$$

Here, D_1 and D_2 are constants which could be evaluated in terms of n , p , C_0 and M . However, no precise significance has been attached to these constants here and equation 4 has been used in this form simply to guide the extrapolation of the quantity Kc_2/R_{90} to zero concentration.

If we neglect the slight difference between the molecular weight of the micelle, and n times the molecular weight of the detergent monomer and gegenion, equation 2 gives c_2 in terms of the experimental quantity "c", the total detergent concentration. Thus, $c_2 = c - c_0$, where all concentrations are expressed in g./ml.

From the extrapolated value of Kc_2/R_{90} , we may obtain a value for the molecular weight, M , of the micelle and thus for the aggregation number, n .

Experimental

Highly purified samples of the three isomeric dodecyl benzene sulfonates studied here were supplied by Dr. D. G. Kolp, Procter and Gamble Company, Cincinnati, Ohio. These compounds were designated sodium 2-dodecylbenzene sulfonate (Na 2-DBS), sodium 3-dodecylbenzene sulfonate (Na 3-DBS) and sodium 4-dodecylbenzene sulfonate (Na 4-DBS), corresponding to the sodium salts of monosulfonated 2-phenyldodecane, 3-phenyldodecane and 4-phenyldodecane, respectively. According to Dr. Kolp, the position of the benzene ring on the side chain was known definitely from the method of synthesis. The compounds were carefully extracted with petroleum ether to remove unsulfonated hydrocarbon and recrystallized from isopropyl alcohol to remove other electrolytes. Infrared absorption data indicated, however, that some of the *meta* as well as the *para* isomer may have been present; steric effects apparently prevented the formation of very much of the *ortho* isomer.

In making up solutions for conductivity and light scattering measurements, considerable care had to be exercised to obtain the true dry weights of the detergents since these compounds are hygroscopic. The dilute solutions required for conductivity measurements were made by adding conductivity water from a calibrated pipet to a known weight of dried detergent. Concentrations on a volume basis were calculated from the known weight of solution by assuming that the density was not significantly different from that of water; for the low concentrations used, about 0.001 molar, this is a reasonable assumption. More concentrated solutions for light scattering studies were made up in volumetric flasks.

The Leeds and Northrup equipment used to measure the conductivities of the detergent solutions has been described

(6) P. Doty and R. F. Steiner, *J. Chem. Phys.*, **20**, 85 (1952).

(7) W. Prins and J. J. Hermans, *THIS JOURNAL*, **59**, 576 (1955).

adequately elsewhere.^{8,9} A water thermostat, in which the conductivity cell could be submerged, was used to control the temperature to within $\pm 0.005^\circ$ at 25° and at 30° .

The conductivity cell itself was of the vertical type and had a capacity of about 19 ml. and a cell constant of 0.834. It was used with bright platinum electrodes because detergents are strongly absorbed from solution by spongy platinum. The fact that the resistance did not change appreciably with time or frequency of signal indicates that this procedure did not introduce any error from polarization. All conductivities were determined at 1000 cycles per second and checked occasionally at 500 and 2000 c.p.s.

Light scattering measurements were carried out in a commercial photometer manufactured by the Phoenix Precision Instrument Company, and described in a paper by Brice, Halwer and Speiser.¹⁰ This instrument was used essentially as received from the manufacturer, except that two heating elements consisting of a large number of copper fins soldered onto $3/8$ -inch copper tubing were installed inside the photometer. By circulating water through the tubing from a large external thermostat, the temperature inside the instrument could be held constant to within about 1° , at temperatures between 25 and 35° .

The instrument came supplied with an opal glass diffuser which served as a standard to relate galvanometer readings to reduced intensity of scattered light. The accuracy of this calibration was checked by determining the reduced intensity from solutions of standard polystyrene received from Professor Debye's laboratory; for these solutions, the value of R_{90} based on the opal glass calibration agreed to within 1% of the accepted value.

Two important experimental difficulties were encountered in determining values of R_{90} for detergent solutions. One of these, the removal of dust from the solutions, is common to all detergents. The other problem, fluorescence resulting from minor impurities in these particular detergents, was important only when blue incident light was used, and was avoided by employing green ($546\text{ m}\mu$) light.

Although pressure filtration through an ultra-fine sintered glass filter proved to be quite an effective means of removing dust from pure water, it was soon evident from the inconsistent results obtained that it was not satisfactory for detergent solutions. Examination of solutions which had been treated in this manner indicated that fine particles of glass were being removed from the filter by the detergent. A Selas micro-porous (0.3 porosity) porcelain filter showed the same difficulty.

Since the ultra-fine glass filter appeared to remove the ordinary particles quite well, the procedure finally adopted was to filter the solutions into dust-free centrifuge tubes and centrifuge out the heavier glass particles. For this purpose, a Model SS 1-a Servall centrifuge, capable of developing fields of the order of 20,000 times gravity, was employed. After 3 hours of centrifugation, 25 ml. of solution was

withdrawn carefully from each of two centrifuge tubes and transferred to a commercial semi-octagonal dissymmetry cell. This technique resulted in highly consistent data, an apparent lack of dust as determined by visual examination, and low values of the dissymmetry ratio.

Since repeated filtration followed by centrifugation did not change the values of R_{90} , it was apparent that neither process was affecting the concentrations of the solutions. Direct confirmation of this was obtained by checking the refractive index of a solution which had been filtered to make sure that the concentration had not changed.

The other experimental quantity needed to interpret the light scattering data was a value of dn/dc , the specific refractive index increment for the detergent. This quantity was measured on a differential refractometer which has been described by Dismukes and Alberty.¹¹ Green light for measurements was isolated from an AH 4 mercury lamp with a Wratten 77a filter, and solutions of sucrose were used for calibration. Refractive index measurements were made at 25° , but it was found that $(n - n_0)/c$ is not sensitive to small variations in temperature.

Results

Conductivity Measurements.—Data from conductivity measurements are presented in Fig. 2 where specific conductance of the solute (specific conductance of the solution minus specific conductance of the solvent) is plotted against detergent concentration. Specific conductances at 25° are read from the vertical axis at the right-hand side of the figure; specific conductances at 30° , from the vertical axis at the left-hand side of the figure. The critical concentrations determined from this graph are listed in Table I.

TABLE I

Detergent	G./ml.	Critical concn. in Mole/l.
Na 2-DBS	4.15×10^{-4}	1.19×10^{-3}
Na 3-DBS	5.10×10^{-4}	1.46×10^{-3}
Na 4-DBS	5.53×10^{-4}	1.59×10^{-3}

These values are for either 25 or 30° ; there was no appreciable change of critical concentration with temperature.

It is interesting to note that the conductivities of all three detergents fall on the same straight line in the monomer region. This implies that the equivalent conductance of the detergent monomer, γ_A^- , is nearly the same for all three isomers and that the differences in conductivity appearing in the micelle region are due to differences in the micelles themselves. It is clear from Fig. 2 that the micelles formed from Na 4-DBS are more efficient in transporting electrical charge than the micelles formed from Na 3-DBS and these micelles, in turn, are more efficient than the ones formed from Na 2-DBS. These are, however, only net results which may arise from differences in shape as well as differences in size and charge on the micelles. Further interpretation of these results must, therefore, await the development of a more detailed theory which will, in addition, take into account interionic effects between these highly charged particles.

The effects of a change in temperature were studied primarily because it was difficult to control exactly the temperature at which light scattering measurements were made. However, it appears that a small change in temperature does not have

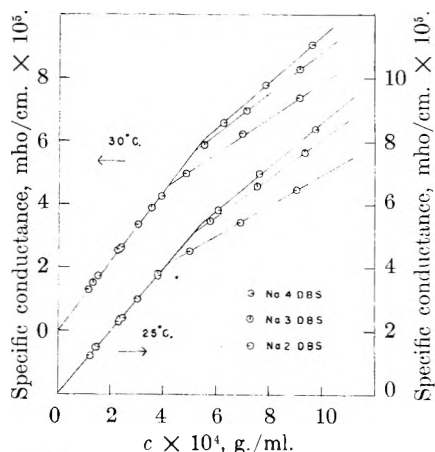


Fig. 2.—Conductivity of sodium dodecylbenzenesulfonates.

(8) "Direction Books No. 1296 and 11208," Leeds and Northrup Company, Philadelphia, Pa.

(9) P. H. Dike, *Rev. Sci. Instr.*, **2**, 379 (1931).

(10) B. A. Brice, N. Halwer and R. Speiser, *J. Opt. Soc. Am.*, **40**, 768 (1950).

(11) E. B. Dismukes and R. A. Alberty, *J. Am. Chem. Soc.*, **75**, 809 (1953).

much effect on the properties of the micelles. It has already been noted that the critical concentrations are not measurably different at 25 and 30°; it is clear that the conductivities themselves do change, but this may be accounted for by the change in the viscosity of the solvent. Thus, the slope of the graph of specific conductance *versus* concentration in the monomer region increases by exactly the same factor that the solvent viscosity decreases and, within experimental error, this is also true in the micelle region. It seems probable, therefore, that the micelles formed at 30° are not appreciably different from those formed at 25°, a conclusion borne out by the light scattering data.

Refractive Index Measurements.—The results of refractive index measurements at 25° are given by the equation, $n - n_0 = 0.1724c$, with an average deviation for the experimental data of 0.8%. This equation applies only to solutions of Na 3-DBS and Na 4-DBS; the other detergent, Na 2-DBS, was too insoluble for light scattering and refractive index measurements at these temperatures.

Although a break in graphs of the quantity $n - n_0$ *versus* c has been reported at the critical micelle concentration for a number of other detergents, careful measurements with blue light carried out by the author at the Procter and Gamble Co. Miami Valley Research Laboratories have not indicated any departure from a linear relationship for these detergents. Substituting the value, 0.1724 cm.³/g., for $(n - n_0)/c$ in the definition of the light scattering constant, K , we obtain $K = 1.951 \times 10^{-7}$ mole cm.²/g.² for experiments with green light.

Light Scattering Measurements.—The light scattering data for solutions of Na 3-DBS are presented in Fig. 3, and similar data for Na 4-DBS, in Fig. 4. For each of these detergents we have plotted the usual light scattering parameter, c_2/R_{90} , (read from the left hand vertical axis) *versus* c_2 , the weight concentration of micelle. For uncharged particles, such a graph is usually a straight line and the y -intercept leads to a value for the molecular weight of the scattering unit. Here, marked curvature is evident and, although the intercept at $c_2 = 0$ is still proportional to the reciprocal of the molecular weight, some guide to the extrapolation is clearly necessary; this has been supplied by equation 4 which predicts that, for the appropriate value of D_1 , a graph of $c_2/R_{90} (1 + D_1c_2)$ *versus* c_2 would be a straight line.

Actually, it was found that fair approximations to straight lines were obtained for a range of values of D_1 , and that all of these graphs had nearly the same intercept, or value of $1/KM$. It was decided, therefore, to determine the best fitting straight line in the sense that the following sum, taken over all the experimental points for a given detergent, would be a minimum

$$\sum_i \left\{ \frac{c_{2i}}{R_{90i}} (1 + D_1c_{2i}) - \frac{1}{KM} - \frac{D_2c_{2i}}{K} \right\}^2$$

By differentiating this expression with respect to $1/KM$, D_2/K and D_1 , and setting these derivatives equal to zero, we obtained equations for these constants in terms of certain averages of c_{2i} and R_{90i} . These equations are given in the Appendix to this paper.

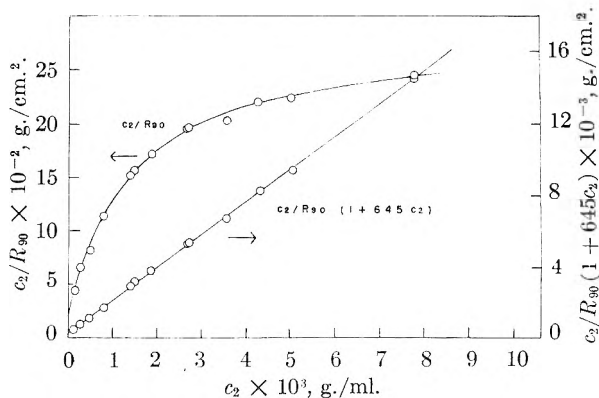


Fig. 3.—Light scattering from solutions of sodium 3-dodecylbenzenesulfonate.

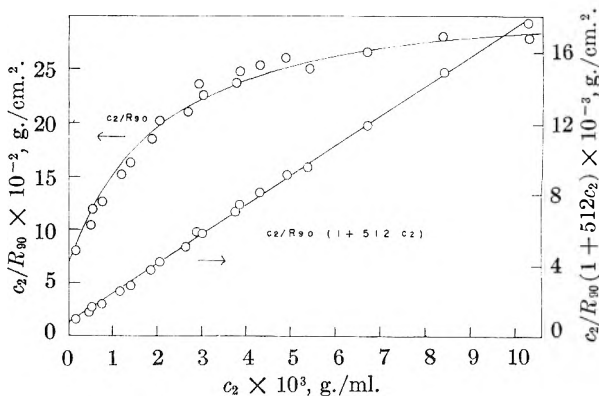


Fig. 4.—Light scattering from solutions of sodium 4-dodecylbenzenesulfonate.

Evaluation of these averages led to the following values for the constants

	Na 3-DBS	Na 4-DBS
$1/KM$	258	622
D_2/K	1.87×10^6	1.68×10^6
D_1	645	512

Thus, according to equation 4, a graph of $c_2/R_{90} (1 + 645c_2)$ against c_2 for Na 3-DBS should be a straight line with an intercept of 258 and a slope of 1.87×10^6 , whereas the corresponding graph for Na 4-DBS of $c_2/R_{90} (1 + 512c_2)$ against c_2 should be a straight line with an intercept of 622 and a slope of 1.68×10^6 . These quantities have been plotted in Figs. 3 and 4, where values of $c_2/R_{90} (1 + D_1c_2)$ are read from the vertical axis on the right hand side of each figure.

It is evident that the data are fitted very well by equation 4. No further interpretation has, however, been given to the values of D_1 and D_2 here; this expression is used simply to guide the extrapolation of values of c_2/R_{90} to zero concentration. The curves in Figs. 3 and 4 have been drawn through the values of c_2/R_{90} in agreement with these best fitting straight lines.

Values of M and n for the two detergents have been calculated from the y -intercepts, and the results are presented here in tabular form

	$1/KM$	M	n
Na 3-DBS	258	19.9×10^3	57
Na 4-DBS	622	8.2×10^3	24

From these data, it is at once evident that the more hydrophobic of these detergents, Na 3-DBS, forms larger micelles than Na 4-DBS.

The large charge effects which have been noted here are probably associated with the low critical concentrations of these detergents. Detergents having higher critical concentrations, and hence higher concentrations of free electrolyte, show little or no departure from linearity¹² when c_2/R_{90} is graphed against c_2 .

One additional qualitative observation on the light scattering behavior of these solutions may be mentioned. By means of the thermostat installed in the photometer, it was possible to vary the temperature at which the light scattering measurements were made. When a carefully prepared stock solution was sealed into a light scattering cell and values of R_{90} determined over a temperature range of 25 to 35°, no detectable variation in scattering was observed. This seems to indicate that small changes in temperature do not affect greatly the properties of the detergent micelles. For this reason, no further attempt was made to control the exact temperature at which light scattering measurements were performed.

We have thus been able to conclude that more hydrophobic detergents tend to form larger micelles at lower concentrations than similar, but less hydrophobic, detergents. This is in agreement with the effect of a change in W_n , representing the hydrophobic nature of the detergent, indicated in the section on theory of micelle formation. It should be noted that both the change in critical concentration and the change in size of micelle with hydrophobic nature result from the higher dependence of the electrical energy of interaction on the number of units in a micelle; the conclusions are, therefore, not dependent on the detailed structure assumed for the micelle.

Acknowledgment.—The author takes particular pleasure in acknowledging the generous help of Professor J. W. Williams during the course of this

(12) H. V. Tartar and A. L. M. Lelong, *THIS JOURNAL*, **59**, 1185 (1955).

research. He is indebted to the Procter and Gamble Company for supplying the purified detergents he has studied, and to the Wisconsin Alumni Research Foundation and the National Science Foundation for financial assistance.

Appendix

Equations for the constants $1/KM$, D_2/K and D_1

$$\frac{1}{KM} = \frac{\begin{vmatrix} \sum_i \frac{c_{2i}}{R_{90i}} & \sum_i c_{2i} & \sum_i \frac{c_{2i}^2}{R_{90i}} \\ \sum_i \frac{c_{2i}^2}{R_{90i}} & \sum_i c_{2i}^2 & \sum_i \frac{c_{2i}^3}{R_{90i}} \\ \sum_i \frac{c_{2i}^3}{R_{90i}^2} & \sum_i \frac{c_{2i}^3}{R_{90i}} & \sum_i \frac{c_{2i}^4}{R_{90i}^2} \end{vmatrix}}{\Delta}$$

$$\frac{D_2}{K} = \frac{\begin{vmatrix} N & \sum_i \frac{c_{2i}}{R_{90i}} & \sum_i \frac{c_{2i}^2}{R_{90i}} \\ \sum_i c_{2i} & \sum_i \frac{c_{2i}^2}{R_{90i}} & \sum_i \frac{c_{2i}^3}{R_{90i}} \\ \sum_i \frac{c_{2i}^2}{R_{90i}^2} & \sum_i \frac{c_{2i}^3}{R_{90i}^2} & \sum_i \frac{c_{2i}^4}{R_{90i}^2} \end{vmatrix}}{\Delta}$$

$$D_1 = - \frac{\begin{vmatrix} N & \sum_i c_{2i} & \sum_i \frac{c_{2i}}{R_{90i}} \\ \sum_i c_{2i} & \sum_i c_{2i}^2 & \sum_i \frac{c_{2i}^2}{R_{90i}} \\ \sum_i \frac{c_{2i}^2}{R_{90i}} & \sum_i \frac{c_{2i}^3}{R_{90i}} & \sum_i \frac{c_{2i}^3}{R_{90i}^2} \end{vmatrix}}{\Delta}$$

Here, N is the number of measurements, and Δ is the determinant

$$\begin{vmatrix} N & \sum_i c_{2i} & \sum_i \frac{c_{2i}^2}{R_{90i}} \\ \sum_i c_{2i} & \sum_i c_{2i}^2 & \sum_i \frac{c_{2i}^3}{R_{90i}} \\ \sum_i \frac{c_{2i}^2}{R_{90i}} & \sum_i \frac{c_{2i}^3}{R_{90i}} & \sum_i \frac{c_{2i}^4}{R_{90i}^2} \end{vmatrix}$$

EQUILIBRIUM DIALYSIS OF SOAP AND DETERGENT SOLUTIONS¹BY H. B. KLEVENS^{2a} AND C. W. CARR^{2b}

Received February 24, 1956

Equilibrium dialysis measurements have been made on a series of anionic and cationic soaps and detergents. Contrary to previously published reports, equilibration across cellophane membranes was observed in all cases for salt-free and polar hydrocarbon-free detergent solutions. The addition of dissolved hydrocarbon changed little and long chain alcohols and amine additives increased markedly the time necessary for equilibration. A change in the ionic strength of the solvent by the addition of KCl resulted in even greater times necessary for transport across the cellophane membranes and, where the solvent was between 0.5–1.0 *N* KCl, equilibration had not been obtained in 100 days. However, in these latter cases, there was always a gradual approach to equilibrium. These data indicate that earlier measurements and all interpretations as to critical micelle concentrations, micelle formation, etc., based on these measurements must be reconsidered in the light of the new findings. These interpretations are markedly clarified by a series of experiments using graded collodion membranes of varying porosities.

Recently Yang and Foster³ have shown that the ions of various buffered and unbuffered detergent preparations do not distribute themselves uniformly across a cellophane membrane except at concentrations below the critical micelle concentration (CMC). It was further proposed by these authors that these measurements would give some indication of a CMC. These results were obtained with relatively non-homogeneous commercial preparations, Santomerse No. 3, principally sodium dodecylbenzene sulfonate, and a technical alkyl dimethylbenzylammonium chloride, a major constituent of which was the dodecyl salt.

Subsequent discussion⁴ of this paper led to the suggestion that polar and apolar impurities in the detergent preparations could explain some of these results. A further impurity, the buffer salts, as well as the low molecular weight paraffin chain salts might also account for non-equilibration. More recently, an attempt has been made to explain the findings of Yang and Foster by postulating diffusion of micelles through the cellophane membranes.⁵ With increase in ionic strength of the solvent (and a corresponding increase in micellar size), there is a supposed lack of equilibration on both sides of the membrane. In the two reports mentioned above, 24–48 hours were allowed for equilibration. According to Yang and Foster,³ longer times produced no further changes in the system, even up to one month. To clarify further the matter concerning the diffusion or non-diffusion of micellized substances through membranes, the present work has been carried out with "pure" soaps and detergents in the presence and absence of added polar and apolar compounds and electrolytes. Measurements have been extended to 60–90 days to obtain equilibration, and the porosities of the membranes have been estimated by studying the diffusion of various proteins through these membranes. Finally, a series of equilibration measurements with dodecylammonium chloride and graded collodion membranes were completed and these latter data appear to reconcile some of

the apparent inconsistencies in the published literature.

Experimental

Materials.—Perfluorohexanoic acid and perfluorooctanoic acid were research samples supplied by the Minnesota Mining and Manufacturing Company.

Aerosol MA, sodium dihexylsulfosuccinate, was a highly purified research sample supplied by Dr. J. K. Dixon of the American Cyanamid Company.

Two samples of sodium dodecyl sulfate, foam fractionated and free of dodecanol and inorganic impurities, were supplied by Dr. Leo Shedlovsky of Colgate-Palmolive Peet Company and by Dr. J. Bolle of the Centre National des Recherches Scientifiques in Paris.

Potassium dodecanoate and potassium tetradecanoate were prepared by saponification of carefully fractionated esters of the corresponding acids followed by repeated recrystallizations.

Sodium octyl- and decylbenzene sulfonates were carefully purified samples prepared by Dr. M. Pallansch in a manner similar to that used by Paquette, Lingafelter and Tartar⁶ except that the reduction of the ketone was carried out by the Wolf-Kishner method in place of the Clemmensen method in order to produce compounds essentially free of possible isomers.

Dodecylammonium chloride was prepared from a carefully fractionated dodecylamine in the usual manner, followed by repeated recrystallizations.

Sodium glycocholate, a bile salt, was a commercial preparation and was included in this study because of our current interest in these bile salts and to show the effect of undetermined impurities on equilibrium studies across membranes.

The solvent used for the various detergents was distilled water. For the fatty acid soaps, the solvent was potassium hydroxide solutions at pH 10 or higher, used in order to minimize hydrolysis. For those experiments in which the ionic strength of the solvent was varied potassium chloride solutions were used.

Dialysis.—Visking cellophane casings, 20/32 inches in diameter, were previously boiled in either distilled water or in soap solutions at least three times for periods of from 3–12 hours to remove any residual soluble components. After thorough rinsing, no difference in time necessary for dialysis equilibration was noted for those membranes boiled in water or in soap solutions.

Graded collodion membranes were prepared using 90–96% ethanol solutions as solvents according to a method developed recently by C. W. C. Detailed procedures will be published shortly, but it has been determined that these membranes are reproducible, have an apparent narrow range of pore sizes and are stable over extended periods in solutions of low pH.

Ten ml. portions were added to the liquid-tight casing and these were placed in a tube containing ten ml. of the solvent. The tubes were stored and shaken in a constant temperature water-bath (36.7°). These casings were tightly tied to minimize the possible increase in total volume in the casing. All data in these series were corrected for small volume changes. At all times, an essentially equal liquid level inside and outside the membrane was main-

(1) A portion of this work was done in Paris while H. B. K. was an advanced research scholar under the Fulbright program (1951–52).

(2) (a) Mellon Institute, University of Pittsburgh, Pittsburgh, Pennsylvania. (b) Department of Physiological Chemistry, University of Minnesota, Minneapolis, Minnesota.

(3) Y. T. Yang and J. F. Foster, *THIS JOURNAL*, **57**, 628 (1953).

(4) Discussion by J. Th. G. Overbeek, by H. B. Klevens, by K. Mysels and by J. F. Foster at the Colloid Symposium held at Ames, Iowa, June 25–27, 1953; *THIS JOURNAL*, **57**, 633 (1953).

(5) B. S. Harrap and I. J. O'Donnell, *ibid.*, **58**, 1097 (1954).

(6) R. G. Paquette, E. C. Lingafelter and H. V. Tartar, *J. Am. Chem. Soc.*, **66**, 686 (1943).

tained, in order to present as large a surface as possible for dialysis. A number of membranes were tested before and after dialysis studies for possible changes in porosity due to the high osmotic pressures within the casing. No differences in ovalbumin (molecular weight 44,000) transport were observed.

Analysis.—Concentrations of soap and detergent on both sides of the membrane were determined by the spectral dye method^{7,8} using pinacyanol chloride with the anionics and acidified phenolindophenol with the cationics. In a few cases, equilibration was followed by conductivity measurements. When the concentrations were below the CMC, titrations were made with dye solutions containing amounts of the detergent above the CMC. In addition, for amine concentrations below the CMC, we used titrations with NaOH with thymolphthalein as an indicator.

By the use of suitable optical techniques as well as of a standard reference end-point (indicative of the CMC), it is quite simple to obtain CMC or concentration values which are reproducible to within 3–4%. Equilibration across a membrane is assumed to occur when agreement within this range is found for concentrations of surfactant on both sides of the membrane.

Critical micelle concentrations were determined by the spectral dye method^{7,8} and, in a few cases, by conductivity measurements and are in all cases in agreement with published data using this or a similar method. The number, N , of molecules per micelle was determined by light scattering measurements in the case of the detergents and by ultracentrifugation for the fatty acid salts. Comments regarding the character of the X-ray pattern for the dodecylammonium chloride and the fatty acid salts were obtained from Dr. R. W. Mattoon. Repeated efforts to obtain a pattern for the two layer array in the perfluoro acids and Aerosol MA, using techniques similar to those of Dr. Mattoon, were not successful. This could be due to the small size of these micelles and to the extremely gaseous nature of these aggregates.

At all times the solvent for the dye solutions was identical with that used for the detergent solutions. Dye solutions were about $5 \times 10^{-6} M$, were usually freshly prepared and, if not, were stored in the dark until used. Due to the low solubility of cyanine dye solutions at high ionic strength, it was necessary to dissolve the dye first in small amounts of water and then to dilute them with appropriate salt solutions.

Results

For all the systems reported here, two perfluoro acids, sodium salt of dihexyl sulfosuccinate (Aerosol MA), sodium dodecyl sulfate, dodecylammonium chloride, sodium *n*-octyl- and *n*-decylbenzene sulfonate, potassium dodecanoate, potassium tetradecanoate and sodium glycocholate, in which the solvent was either water or $10^{-3} N$ KOH, there was no evidence of non-uniform distribution of surfactant on both sides of a membrane. These results appear to be at variance with those reported by Yang and Foster.³

These differences are seen in Fig. 1 where equilibrium dialysis results with pure detergents, sodium octyl- and sodium decylbenzene sulfonate, are compared with dialysis results³ in which a commercial preparation, Santomerse No. 3 (principally sodium dodecylbenzene sulfonate) has been used. The data with the commercial Santomerse show a definite break at a concentration which is approximately equivalent to its CMC; no break or discontinuity is observed with the pure alkyl benzene sulfonates. Similarly with the other purified detergent and soap preparations, we could not observe a break in the curve. Although our data in Fig. 1 involve the use of water as a solvent, a

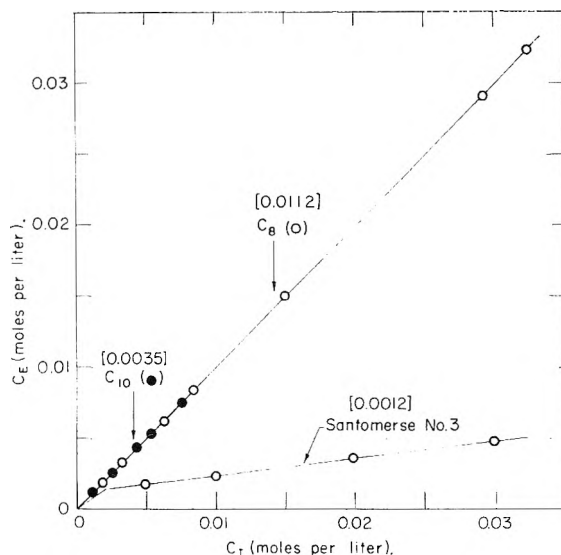


Fig. 1.—Equilibrium dialysis of sodium alkylbenzene sulfonates: C_E , concentration outside membrane; C_I , concentration inside membrane; C_8 (octyl) and C_{10} (decyl) benzene sulfonates (this report). Santomerse No. 3 (mixed alkylbenzene sulfonate): data of Yang and Foster. Numbers in brackets are the CMC values in moles per liter.

change in solvent from water to buffer had no such marked effect as the occurrence of a break in the curve of the previous data.³

With increase in concentration, there was in all cases an increase in the time necessary for equilibration. Below the CMC, for all systems studied, equilibration was obtained in about two hours; above the CMC, for a particular membrane, this time appeared to be a function of both concentration and of type of detergent used. For a series of detergent solutions, where the initial concentrations were about $10 \times$ CMC, it is seen from the data in Table I that there is no definite correlation between equilibration times and CMC and only a small one between these times and micellar weight. There appears to be a somewhat better correlation between these times and the diffuseness of X-ray patterns indicative of the two-layer micelles. However, as these data show, there is definite equilibration in all cases.

Effect of Change in Solvent.—When the solvent was changed from water to one containing various hydrocarbon and polar hydrocarbon additives as well as by increases in ionic strength, a number of very interesting findings were observed. The addition of a solubilized hydrocarbon, such as *n*-heptane, had very little effect on the time necessary for equilibration. This is as expected, since the addition of hydrocarbons has been shown to have little effect on the CMC and on the size of micelles.⁹ Recent experiments using benzene and naphthalene as solubilized hydrocarbons show that the hydrocarbons diffuse through the membranes. When equilibration of the surfactant was reached, spectral measurements showed that the aromatic hydrocarbons had equal concentrations on both sides of the cellophane casing. The addition of solubilized polar hydrocarbons to various soap and detergent solutions results in marked decreases in

(7) M. L. Corrin, H. B. Klevens and W. D. Harkins, *J. Chem. Phys.*, **14**, 216, 480 (1946).

(8) H. B. Klevens, *This Journal*, **51**, 114 (1947).

(9) H. B. Klevens, *ibid.*, **54**, 1012 (1950).

TABLE I
TIME (*t*) NECESSARY FOR EQUILIBRATION OF DETERGENT SOLUTIONS AGAINST WATER USING CELLOPHANE CASINGS AS MEMBRANES

(Initial concentration = $10 \times \text{CMC}$; 37°)

Detergent	CMC (moles/l.)	<i>t</i> , hr.	<i>N</i> , no. of molecules/micelle	Character of X-ray pattern for two-layer array
C ₉ F ₁₁ COOH	0.050	2-4	...	Not observable
C ₇ F ₁₅ COOH	.0051	2-4	<10	Not observable
Aerosol MA	.038	2-4	8-20	Not observable
C ₁₂ H ₂₅ NH ₂ Cl	.014	50	50	Very diffuse
C ₁₁ H ₂₃ COOK	.025	60	30-50	Diffuse
C ₁₂ H ₂₅ COOK	.0070	75	50-70	Diffuse
C ₁₂ H ₂₅ OSO ₃ Na	.0051	50	65-70	...
C ₈ H ₁₇ C ₆ H ₄ SO ₃ Na	.0112	50
C ₁₀ H ₂₁ C ₆ H ₄ SO ₃ Na	.0035	50-75
Na Glycocholate ^a	.02	250

^a The CMC of this surfactant was found to be 1% or about 0.02 *M* based on the premise that only the glycocholate was present. A 5% solution was placed in a cellophane bag and immersed in an equal volume of water. At 4 hours, there were no detectable micelles outside; at 24 hours, the outside concentration was 1.3%; and at 150 hours, it was 1.8%, or about 75% of equilibrium concentration. All values have been corrected for small volume changes.

the CMC,¹⁰ as our measurements in Table II also show, but few data are available to show whether there is a corresponding increase in micellar weight. The results collected in Table II indicate that the addition of solubilized *n*-octanol increases the equilibration time from 50 to as many as 350 hours. Somewhat less time is required for equimolar concentrations of a shorter chain alcohol, *n*-hexanol, when it is solubilized in sodium dodecyl sulfate. There is an increase in the equilibration time when *n*-hexylamine is solubilized. No information is

available as to the transport of these solubilized materials through the membrane. It is interesting to note that these results are in complete accord with the increase in solubilizing power of various detergents in which polar hydrocarbons are used as additives.¹¹ It is indeed unfortunate that we do not know more about the actual micellar sizes of these detergent-polar hydrocarbon mixed micelles, but preliminary ultracentrifuge data indicate at least a twofold increase in micellar weight from about 15,000-20,000 for the dodecyl sulfate to about 50,000 for the mixed micelle.¹²

However, we do know that there is a marked increase in micellar weights (and a corresponding decrease in CMC) upon the addition of various electrolytes to soap and detergent solutions. As the data in Table II show, there is also a very definite increase in the time of equilibration of potassium tetradecanoate solutions with increase in the ionic strength of the solvent. For the highest electrolyte concentrations, 0.5 and 1.0 *N* KCl, equilibration had not as yet been reached in 90-100 days, but, for each successive determination, equilibration was definitely being approached. All available samples of the latter two systems were utilized before absolute equilibration had been accomplished, and it was considered not necessary to re-run these latter measurements since they would have involved at least another 4-5 months.

Porosity of Membranes.—Various proteins of known molecular weights were used in these experiments which were performed in a manner similar to those with soaps and detergents listed above. Equal portions of buffered protein solution and buffer were placed in and outside the cellophane bag, respectively. The data in Table III represent the per cent. of the equilibrium concentration that is measured in the outside (originally protein-free) solution. For example, if the original

TABLE II

THE EFFECT OF VARIOUS ADDITIVES ON THE TIME (*t*) NECESSARY FOR EQUILIBRATION OF POTASSIUM TETRADECANOATE AND SODIUM DODECYL SULFATE SOLUTIONS AGAINST 10^{-3} *N* KOH USING CELLOPHANE CASINGS AS MEMBRANES

(Initial concentration = $10 \times \text{CMC}$; 36.7°)

Solvent	CMC (moles/l.)	<i>t</i> (hours)
K tetradecanoate		
0.001 <i>N</i> KOH	0.007	75
0.01 <i>N</i> KOH	.006	100
0.10 <i>N</i> KOH	.0045	450
0.001 <i>N</i> KOH plus		
0.05 <i>N</i> KCl	.0055	300-400
0.10 <i>N</i> KCl	.0045	600
0.20 <i>N</i> KCl	.003	1000
0.50 <i>N</i> KCl ^a	.0015	>2000
1.0 <i>N</i> KCl ^b	.0008	>2500
Na dodecyl sulfate		
0.001 <i>N</i> KOH	0.005	50
0.001 <i>N</i> KOH plus		
<i>n</i> -heptane ($1/2$ satd.)	.0045	55
0.007 <i>M</i> pentanol	.004	85
0.025 <i>M</i> pentanol	.0025	175
0.025 <i>M</i> pentamine	.0018	275
0.003 <i>M</i> octanol	.0025	150
0.005 <i>M</i> octanol	.0015	250
0.007 <i>M</i> octanol	.0006	370

^a Solutions viscous. ^b Solutions very viscous.

(10) A. F. H. Ward, *Proc. Roy. Soc. (London)*, **A176**, 412 (1940); A. W. Ralston and D. N. Eggenberger, *J. Am. Chem. Soc.*, **70**, 983 (1948); K. Shinoda, *This Journal*, **58**, 1136 (1954).

(11) H. B. Klevens, *J. Chem. Phys.*, **17**, 1004 (1949); *J. Am. Chem. Soc.*, **72**, 3581 (1950).

(12) Recently Mysels (*J. Colloid Sci.*, **10**, 507 (1953)) has indicated that the micellar weight of the sodium dodecyl sulfate may actually be about 30,000 to 35,000, at least as determined from light scattering measurements.

inside solution is 2% and the measured outside concentration at 4 hours is 0.5%, the calculated value would be 50%.

TABLE III
DIFFUSION OF PROTEINS THROUGH CELLOPHANE TUBING

Protein	Mol. wt.	Time, hr.	% of equilibrium concn.
Serum albumin	70,000	4	2
		26	2
		200	10
Ovalbumin	44,000	24	2
		150	15
Phosvitin	21,000	4	25
		24	74
Lysozyme	14,500	4.5	34
		28	84
Salmine	8,000	4	41
		26	93

These results would tend to indicate that molecules in aggregates of 15,000 to about 25,000 molecular weight could diffuse through these membranes. It is not known whether the small amounts of proteinaceous material which diffused through in 6-8 days was the original intact molecule or whether this was some breakdown product from denaturation and/or hydrolysis.

Equilibration through Graded Membranes.—Initially, 8.0 cc. of 0.2 M dodecylammonium chloride was placed in a series of collodion sacs which had been prepared so as to have different porosities. The numbers 90-96 on Figs. 2 and 3 correspond to the amount of ethanol used as a swelling agent for the collodion. With increase in alcohol concentration, there is an increase in average pore size. An estimate of the porosities of these collodion membranes can be gleaned from the following. The 96% membranes just prevent serum albumin from passing. The 93% membranes just prevent salmine (mol. wt. = 8000) from passing. The 90% membranes just prevent sucrose (mol. wt. = 342) from passing, and as can be seen in Fig. 2, the passage of dodecylammonium chloride (mol. wt. = 221) through these membranes is not very rapid.

These membranes, containing the 8 cc. of solution, were placed in vials containing 20 cc. of water. These membranes were not tied off, as was done in the case of the cellophane casings, because of the stiffness of the collodion sacs.

Figure 2 is a comparison of membranes of various porosities. For the inside solutions, the initial decrease in concentration is always much more than the increase in concentration of the outside solutions. This is due to osmotic dilution of the inner solution; *i.e.*, water diffuses in from the outside. Duplicate points were obtained for all data in Fig. 2 and 3. In addition, the curves for the 93% and the 95% membranes were determined in two separate experiments, the same curve being obtained each time.

Figure 3 is a comparison of two different concentrations with the 93% membranes. 0.2 M dodecylammonium chloride is used for one curve

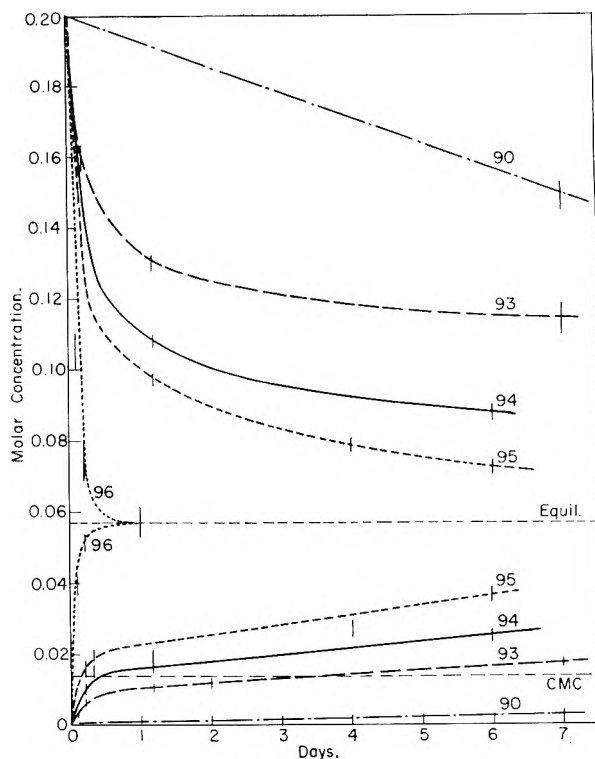


Fig. 2.—The effect of membrane porosity on the diffusion of dodecylammonium chloride through collodion membranes. The numbers 90-96% are concentrations of ethanol in water used as solvents for collodion in the preparation of the membranes.

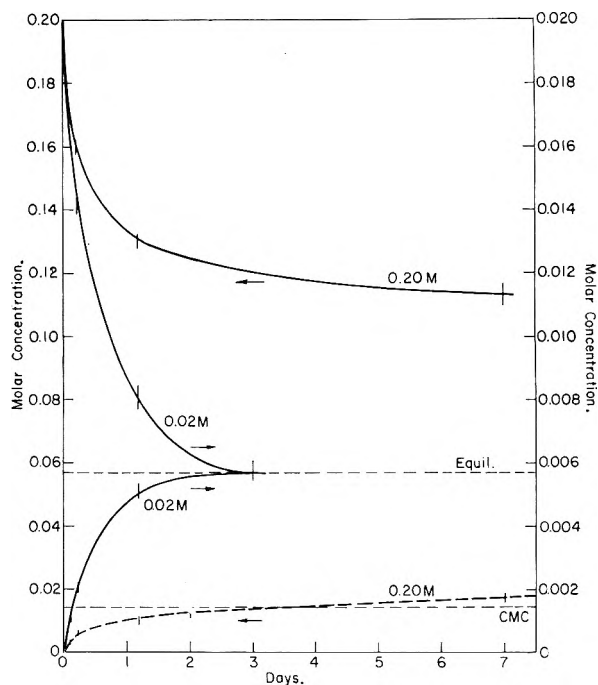


Fig. 3.—Comparison of two different concentrations of dodecylammonium chloride on the rates of diffusion through collodion membranes (prepared from 93% ethanol in water as the solvent).

and 0.02 M amine for the other. For this latter curve, the concentration scale is $\frac{1}{10}$ of that for the 0.2 M curve. For the 0.02 M solution, true equilibrium is reached in less than two days (at

about 0.0057 M), which is the time for the outside solution to reach the CMC when the 0.2 M solution is used.

Discussion

The discussion⁴ of the paper of Yang and Foster³ tended to explain the results of these latter authors as being anomalous and due primarily to the presence of various impurities in the commercial preparations they used. Somewhat purified, salt-free, polar hydrocarbon-free soaps and detergents have been shown above to equilibrate readily across cellophane membranes, which are themselves permeable to aggregates or molecules of 15,000–20,000 molecular weight. This has also been shown to be true for a purified preparation of sodium dodecyl sulfate.⁵ Further, the data in this report indicate that there is also equilibration even when quite large micelles are present, as when long chain alcohols and electrolytes are added. These results are in contrast to the results of previous authors,^{3,5} who reported that in systems in which there were large micelles, there was little or no diffusion of the material through cellophane, even after one month. It is true that in many of the systems we have studied, there were often very small quantities of detergent diffused through in the first 24–48 hours, particularly when the CMC was of the order of 10^{-3} to 10^{-4} , and the micellar weights about 10^6 . However, in all but two cases, diffusion continued until equal concentrations were reached on both sides, this sometimes requiring as much as 1000 hours. Even in the two cases where equal concentrations were not observed in 90–100 days, there was still an increasing approach to equilibration.

On the basis of their non-diffusion of micellized material across cellophane, Yang and Foster suggested that equilibrium dialysis could be used as a method for determining CMC. Our results, however, show quite conclusively that there are many systems in which there is diffusion of micellized material through cellophane. Thus it would appear that equilibrium dialysis with cellophane membranes could not be generally applied for the measurement of CMC.

Whether micelles diffuse through membranes as readily as free ions possibly can be answered now. We prepared some collodion membranes which were capable of retaining salmine (molecular weight of 8,000) but would pass molecules of molecular weight of 3,000 according to unpublished results found by C. W. C. These were not stable in solutions of anionic detergents and broke apart after 3–4 days of shaking, but the data obtained previous to their rupture indicated a slowing down of equilibration of sodium dodecyl sulfate. The very rapid equilibration of the perfluoro acids and Aerosol MA could be due to the fact that these surfactants form very small micelles, but could also be explainable on the basis that these compounds form very gaseous films as shown by various surface studies. It is to be expected that any solutions of these compounds would exhibit little tendency to form stable micelles.

However, the data covering diffusion and equilibration through the graded membranes tends

to reconcile, in part, our results and those of Yang and Foster.³ These can be summarized briefly as follows

(1) The average pore size of the membrane relative to the micelle size and even to the size of the single surfactant ion is an important factor in all these equilibration studies.

(2) When the pore size is much larger than the micelle size, true equilibrium is reached rapidly due probably to the diffusion through the membranes of micellar as well as the single surfactant ions.

(3) When the pore size is about the same or smaller than the micelles, true equilibrium is approached only very slowly.

(4) When the concentration of detergent is below the CMC, true equilibrium is reached rapidly, the rate depending on the size of pores relative to the size of the detergent molecule.

(5) Even when the concentration is above the CMC, equilibration of the free ions (up to concentrations equivalent to the CMC) proceeds fairly rapidly.

(6) The original point of Yang and Foster concerning the slow build-up of micelles in the dialyzate is confirmed. Micelles definitely form in the dialyzate but at a very slow rate, so that the approach to equilibrium can be extremely slow in many cases. However, the slow rate of micelle formation in the dialyzate does not necessarily mean, as has been suggested by Yang and Foster, that micelles form slowly from the monomers present in concentrations above the CMC.

(7) The method of equilibrium dialysis possibly could be used for determining the CMC, only if it is known that the micelle size is considerably greater than the pore size of the membrane.

It is extremely difficult at the moment to reconcile our concepts of micelle formation being a very rapid process in soap and detergent solution with the extremely long times necessary for equilibration when the concentrations of free ions are very low and the size of the micelles quite large. These results suggest that the diffusion of free ions through the membranes is not a very slow process and that the formation of micelles may be the limiting factor. The small differences in osmotic pressure on both sides of the membrane in those systems with low CMC and micelles of high molecular weight must be important in our consideration of equilibration, but this factor we cannot now assess accurately.

However, there now appears to be little validity for the previously published reports that surfactant solutions would not equilibrate across membranes and that this non-equilibration could be used as a new method for the determination of the presence of micelles, as has been suggested by Yang and Foster.³ Further, since we have observed that, for any particular system, the time of equilibration increases with increase in detergent concentration, it would appear not at all unreasonable to expect equilibration data obtained at the end of some arbitrary time (48 hours as picked by Harrap and O'Donnell⁵), to show one, two or even more discontinuities as was actually observed by these latter two authors.

ON THE MECHANISM OF EMULSION POLYMERIZATION OF STYRENE

BY B. M. E. VAN DER HOFF

Polymer Corporation Limited, Research and Development Division, Sarnia, Ontario, Canada

Received February 24, 1966

Some kinetic aspects of the emulsion polymerization of styrene were investigated to test the validity of the Smith-Ewart theory for latices containing more than 10^{14} particles per ml. water. Polymerizations were carried out with a variety of potassium fatty acids soaps and cumene hydroperoxide. The conversion-time curves consisted mainly of two essentially straight lines. At about 55% conversion there was a transition to a lower rate of polymerization. Swelling ratios of the latex particles, measured during polymerization, demonstrated that the disappearance of the monomer droplets coincided with the change in reaction rate. From rate data and electron micrograph analyses it was deduced that the rate of polymerization per particle, R_p , and the particle concentration, N , in the range $N = 5 \times 10^{14}$ to 5×10^{15} /ml., are related by $R_p = cN^{-0.83}$. The constant c depends on the concentration and the nature of the soap. Molecular weight data were also interpreted to indicate that the emulsifier plays a role in the polymerization process after the disappearance of micelles. These results which cannot be explained by the Smith-Ewart theory were compared with data obtained in similar systems by other authors.

Introduction

The quantitative aspects of the rate of emulsion polymerization and the number of particles in the resulting latex have been worked out theoretically by Smith and Ewart¹ on the basis of a number of assumptions. These authors distinguish three cases in which the number of free radicals in a latex particle is, respectively, much less than unity, about unity (case 2), and much more than unity. Subsequently Smith² and several other authors reported results of experiments which supported the theory, especially for case 2. The agreement between theory and experiments, however, was not very satisfactory until recently when Bartholomé, Gerrens, Herbeck and Weitz³ published the results of experiments designed to test the Smith-Ewart theory. These workers conclusively proved the validity of this theory for emulsion polymerization of styrene under the conditions of their experiments.

There are, however, other reports of experimental results which cannot be accommodated within the framework of the Smith-Ewart theory. Morton, Salatiello and Landfield,⁴ for example, made an attempt to calculate the rate constant for the propagation step in the polymerization of butadiene and found that, contrary to theory, the rate of polymerization per particle was not constant. Kolthoff, Meehan and Carr⁵ reported that increasing the soap concentration during the copolymerization of butadiene and styrene in such a way that no new particles are formed, results in an increase in the over-all rate of reaction and thus in the rate per particle. Smith² found, in experiments with seed latex, that the polymerization rate per particle was essentially constant only below a certain particle concentration. Bovey and Kolthoff⁶ established that the rate of reaction per particle in a particular set of seeded polymerizations was proportional to the -0.28 power of the number of particles.

(1) W. V. Smith and R. H. Ewart, *J. Chem. Phys.*, **16**, 592 (1948).(2) W. V. Smith, *J. Am. Chem. Soc.*, **70**, 3695 (1948).(3) E. Bartholomé, H. Gerrens, R. Herbeck and R. M. Weitz, paper presented at the discussion meeting of the German Bunsen Society, Hoechst, Germany, *Z. Elektrochem.*, **60**, 334 (1956).(4) M. Morton, P. P. Salatiello and H. Landfield, *J. Polymer Sci.*, **8**, 111 (1952).(5) I. M. Kolthoff, E. J. Meehan and C. W. Carr, *ibid.*, **7**, 577 (1951).

(6) F. A. Bovey and I. M. Kolthoff in F. A. Bovey, I. M. Kolthoff, A. J. Medalia and E. J. Meehan, "Emulsion Polymerization," Interscience Publishers, Inc., New York, N. Y., 1955, p. 194.

It appears that the Smith-Ewart theory readily accounts for the results obtained at particle concentrations lower than about 10^{14} particles per ml. aqueous phase. Near constancy of the polymerization rate per particle was found by Smith² at these concentrations. The similar results of Bartholomé, *et al.*,³ were also obtained at concentrations lower than about 2×10^{14} particles per ml. water.

It was considered of interest to investigate the kinetics of polymerization in a somewhat higher particle concentration range. This study was also motivated by practical considerations, since some commercial polymerizations yield high solids latices. Polymerization experiments were, therefore, carried out to obtain high particle concentrations, the results of which are reported here.

Experimental

Procedure.—Emulsion polymerizations of styrene were carried out in a 400-ml. thin walled brass vessel. An aqueous solution of soap and electrolyte, a solution of initiator in styrene, and a stirrer magnet enclosed in Teflon were transferred to the vessel and nitrogen was bubbled through the contents for 5 minutes. The vessel was closed and more nitrogen was introduced to a pressure of about 5 p.s.i. to avoid formation of a partial vacuum on withdrawal of samples. The total volume of a charge was usually 120 ml. The filled vessel was immersed in a water-bath, which was maintained at $50 \pm 0.05^\circ$, and the magnetic stirrer and stopwatch were started simultaneously. The vessel contents rapidly reached equilibrium temperature; after 100 seconds the temperature of the charge was 45° and after 4 minutes, 49° . Through the wall of the vessel four copper capillary tubes reached from near the bottom to above the surface of the water-bath. Samples of the reaction mixture were withdrawn with a syringe at regular time intervals *via* these tubes. The solids content of a latex was determined by precipitation of the polymer with 0.01% solution of quinone in acetone and evaporation of the volatile components for 5 to 8 hours on a hotplate.

The polymerizations were carried to high conversions, usually > 0.9 .

Chemicals.—*Styrene* was obtained by distillation under vacuum of a technical product (99.8%). A middle fraction was collected and stored at -10° for periods not longer than a month. No polystyrene was formed under these conditions.

The potassium salts of saturated and unsaturated fatty acids were used as *emulsifiers*. The soaps were prepared from acids with melting points not more than 3 deg. below the melting points reported in the literature. The acids were allowed to react in aqueous alcoholic solution with carbonate-free analytical grade potassium hydroxide. A 3% excess of the alkali was used. The soaps were recrystallized 2 or 3 times from alcohol or appropriate alcohol-acetone mixtures. Potassium production soap is a technical grade potassium stearate. It was used as received.

Cumene hydroperoxide was prepared from a commercial

68% solution according to a simplified version of the purification described by Fordham and Williams.⁷ The resulting product was analyzed by a procedure recorded in the same publication; the content of active material was 98% or higher. No loss of activity was noted during storage for several months at -10° .

Potassium chloride was a reagent grade product.

Nomenclature.—For the sake of brevity each recipe is indicated by a symbol. The following is the standard recipe: 4.00 g. of potassium stearate, 0.100 g. of potassium chloride, 0.300 g. of cumene hydroperoxide, 200 g. of 0.001 *N* potassium hydroxide in water, and 100 g. of styrene.

Other soaps were used in molecularly equivalent amounts. Each recipe is designated by three numbers: the first is the factor by which the standard amount of soap is multiplied, the last is a similar factor for the initiator, and the middle number indicates the number of carbon atoms in the soap molecule. For example recipe $1/4$ -16-2 indicates that 0.913 g. of potassium palmitate and 0.600 g. of cumene hydroperoxide were used. Potassium oleate, elaidate and production soap are designated by the letter O, E and P, respectively.

Particle Size Measurements.—Electron micrographs of the particles were made for each latex. The negatives were projected onto a transparent screen and the diameters of the images measured to the nearest half millimeter. On the screen 1 millimeter corresponded to 100 Å. A polystyrene latex (run 15 N-7, av. particle diam. 3330 Å., standard deviation 70 Å.), supplied by Dow Chemical Company through the courtesy of Dr. E. B. Bradford, was used for calibration. The number of particles measured was 150-300 depending on the width of the distribution of diameters. The coefficient of variation of this distribution ranged from 0.05 to 0.12. The number of particles was calculated from the average volume of the particles.

Molecular Weight Determination.—Latex was dissolved in a mixture of 80 parts of toluene to 20 parts of isopropyl alcohol and further diluted with toluene. The flow times of these solutions were measured as a function of concentration in a viscometer described by Craig and Henderson.⁸ Viscosity numbers obtained from these data were used to calculate the molecular weight according to a relation developed by Palit.⁹

Results

The progress of polymerization was followed by taking samples at regular time intervals. The results of an experiment with charge 1-12-1, are depicted in Fig. 1. There is an induction period, attributed to small amounts of oxygen present in the technical grade nitrogen used to rinse vessel and ingredients, after which the rate of reaction increases to a value which is constant from about 0.2 to 0.5-0.6 conversion (region I). The rate then decreases rather sharply to a constant value (region II) between $1/2$ and $3/4$ that of the previous rate. A more gradual decrease in reaction rate (beginning of region III) occurs at a conversion of about 0.88.

The point on the conversion-time curve where the rate begins to deviate from the value of region I corresponds to the conversion at which the monomer droplets disappear. This is demonstrated in Table I where the swelling ratio of the polymer particles is given as a function of conversion for a typical polymerization. It is to be noted that this ratio is almost constant after 20% conversion. These data were obtained from experiments in which about 10 ml. of latex was withdrawn from the polymerization vessel, quickly transferred to a centrifuge tube and spun. For the polymerization

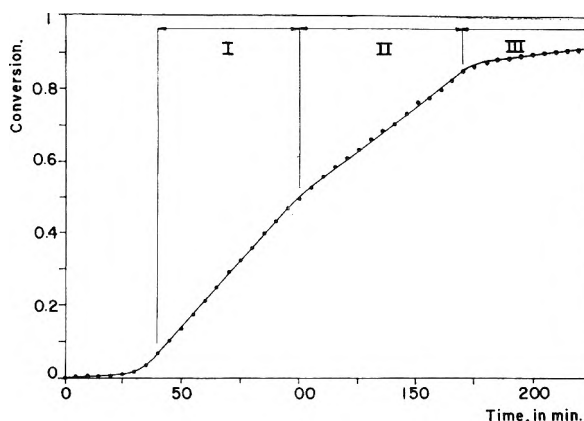


Fig. 1.—The degree of conversion as a function of the reaction time. Polymerization according to recipe 1-12-1.

referred to in Table I the transition from region I to region II occurred at 52 to 58% conversion. On the basis that the transition occurs at the moment of disappearance of the monomer droplets it can be calculated that the swelling ratio in the transition region is 1.92 to 1.72. The first of these values is in good agreement with the measured value for the swelling ratio at 52% conversion.

TABLE I

THE RELATION BETWEEN THE SWELLING RATIO OF THE POLYMER PARTICLES AND THE DEGREE OF CONVERSION
RECIPE 1-14-1

Conversion	Swelling ratio (g. monomer + g. polymer)/ g. polymer	Conversion	Swelling ratio (g. monomer + g. polymer)/ g. polymer
0.100	2.64	0.325	2.15
.136	2.45	.362	2.15
.175	2.37	.400	2.04
.212	2.13	.436	2.12
.250	2.22	.474	2.05
.288	2.14	.510	(1.94) ^a

^a This value is rather inaccurate due to the small amount of styrene obtained.

From the swelling ratio of the particles, the monomer concentration $[M]$ in the particles can be calculated. For the example given above it is found that $[M] = 4.5$ mol./l. As has already been indicated the monomer concentration can be calculated from the conversion at which the rate of polymerization starts to diminish. This "break," unfortunately, cannot be determined with sufficient accuracy to permit calculations of reliable monomer concentrations. However, almost all the experiments reported here exhibit the break between 48 and 60% conversion, which corresponds to monomer concentrations between 4.8 and 3.8 mole/l.

It was also established, with a series of electron micrographs of samples taken at 5% conversion intervals between 15 and 70% conversion, that for the systems described here, the number of particles is constant after about 15% conversion.

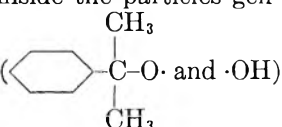
The unusual form of the conversion-time curve is attributed to the type of initiator used. When polymerization was initiated with potassium persulfate in similar recipes the well known S-shaped curves were obtained. It is envisioned that toward the end of region I the oil-soluble cumene hydro-

(7) J. W. L. Fordham and H. L. Williams, *Can. J. Research*, **27B**, 943 (1949).

(8) A. W. Craig and D. A. Henderson, *J. Polymer Sci.*, **19**, 215 (1956).

(9) S. R. Palit, *Indian J. Phys.*, **29**, 65 (1955).

peroxide diffuses with the styrene into the particles and that in region II this initiator decomposes inside the particles. This view is corroborated by the results of experiments in which additional cumene hydroperoxide was introduced at 35% conversion. The reaction rate in this case was constant from 20 to 84% conversion. In another experiment initiator was added at 65% conversion, *i.e.*, in region II. There the rate of polymerization was restored to that of region I. It was also found that when a relatively large amount of initiator is originally dispersed in soap solution the difference in rate of polymerization between region I and II is much less than when the initiator is originally dissolved in the styrene. In region II the initiator inside the particles gen-

erates free radicals in pairs ( and $\cdot\text{OH}$)

and it is envisioned that polymerization proceeds by virtue of the difference in terminating and initiating activity of these two radicals. Thus a rate of polymerization results lower than in region I, where the free radicals enter the particles one by one from the aqueous phase. As the polymerization proceeds in region II the monomer concentration inside the particles decreases and hence the rate of propagation diminishes but at the same time the viscosity of the reaction medium increases causing a decrease in the rate of mutual termination of radicals. These two opposing effects apparently result in a zero order of reaction.

For each experiment the over-all rate of polymerization in region I was measured and the number of particles per ml. aqueous phase (N) was obtained from electron micrographs. From these two quantities the rate of polymerization per particle (R_p , g./sec.) was calculated. For about half the number of experiments the molecular weight of the polymer was determined.

Some electrolyte is necessary to reduce the viscosity of the latices that contain small particles to permit adequate stirring at high conversions. Therefore, 0.1 g. of potassium chloride per 100 g. of styrene was included in the recipe. The addition of this small amount of electrolyte does not influence appreciably the number of particles initiated nor the rate of polymerization per particle (see Table II).

TABLE II

INFLUENCE OF ELECTROLYTE ON NUMBER OF PARTICLES AND RATE PER PARTICLE (Recipe 1-14-1)

KCl, g./100 g. styrene	0	0.1	0.3	1.0
$N \times 10^{-15}$	1.7	2.1	1.8	3.4
$R_p \times 10^{20}$	3.3	3.0	3.8	1.9

Two series of experiments were carried out in which the amount of initiator was varied. With increasing initiator charge, it was found that the number of particles increased and the rate of polymerization per particle diminished and that these two factors are related as is depicted in Fig. 2. The open circles refer to a series of polymerizations with the standard amount of potassium laurate as emulsifier and initiator charges varying from

$1/15$ th of, to 9 times, the standard amount. The solid circles represent experiments with $1/8$ th of the standard amount of potassium palmitate and with initiator levels from the standard charge to 9 times this amount. From the slope of the lines it is calculated that R_p is proportional to $N^{-0.83}$. It should be mentioned that there is some irreproducibility in the values of R_p and N obtained in identical experiments. Nevertheless the points representing each of these experiments all fall on the lines drawn in Fig. 2. This is interpreted to mean that the number of particles initiated is not fully controlled, but that once a certain particle concentration is formed the reaction proceeds with a rate which, for a given emulsifier system, is determined by N only.

The interdependence of R_p and N is not restricted to styrene systems initiated by cumene hydroperoxide. A. C. MacLeod of this Laboratory copolymerized butadiene and styrene at particle concentrations from 2 to 8×10^{14} /ml. using potassium persulfate as initiator. Analysis of the results of these experiments showed R_p to be proportional to $N^{-0.77}$.

Other experiments were carried out in which standard amounts of the following emulsifiers were used: potassium soaps of myristic, palmitic, margaric, stearic, oleic and elaidic acids. The results are also shown in Fig. 2. It can be concluded that small changes in the chemical structure of the soap and/or the presence of small amounts of impurities in the emulsifier causes a difference in rate per particle at a given particle concentration. There is, however, no difference between the soaps containing 12, 14 and 16 carbon atoms.

The amount of emulsifier was varied in two other series of experiments in which standard amounts of initiator were charged. The results are plotted in Fig. 3, which shows that the amount of soap affects the rate per particle apart from influencing the number of particles initiated: at a given particle concentration the higher the soap level the higher is R_p . The open circles represent a series of experiments carried out with from $1/4$ of, to twice the standard charge of potassium myristate. The experiments depicted by solid circles were run with different levels of potassium production soap corresponding to $1/16$ th of, to 4 times, the standard amount of soap.

Discussion

The evidence reported above conflicts with the Smith-Ewart theory (case 2) which was conclusively verified for the emulsion system used by Bartholomé, *et al.*³ This theory is based on the assumption that there is a polymer chain growing in each particle half the time, the chain being initiated and terminated by successive free radicals entering the particle. The rate per particle therefore depends only on the temperature and the local monomer concentration.

In Fig. 4 the data of different authors are assembled in schematic form. Smith² did not report the emulsifier used, and since his results show considerable scatter they are indicated as a rather wide band. Bartholomé, *et al.*,³ used the potassium salt of sulfated C_{18} olefins as emulsifier. They operated at 45° and their data have been recalculated to 50°

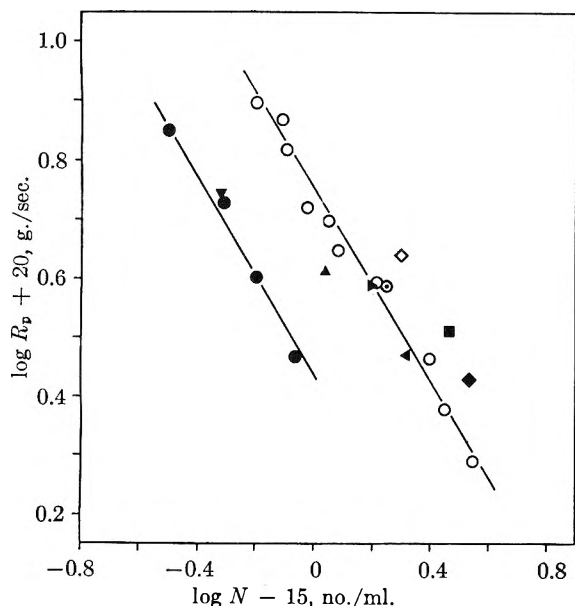


Fig. 2.—The relation between polymerization rate per particle, R_p , and particle concentration, N . Variation of amount of initiator (lines) and nature of emulsifier (symbols): O, 1-12-m; ●, 1/8-16-m; ▼, 1-20-1; ▲, 1-18-1; ▴, 1-16-1; ◀, 1-14-1; ·, 1-12-1; ◇, 1-17-1; ■, 1-E-1; ◆, 1-0-1.

using a value for the activation energy of 6.5 kcal. Bovey and Kolthoff⁶ found that R_p depends on the -0.28 power of N , at a particle concentration of about 10^{14} /ml.; they did not specify the soap used. The latter data determine only the slope of a line in a $\log R_p$ versus $\log N$ plot (Fig. 4).

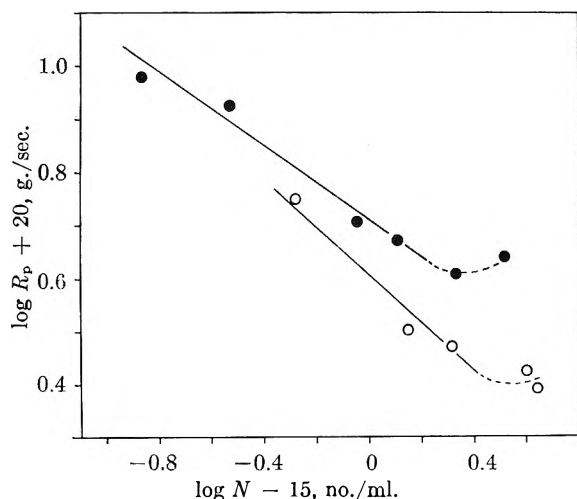


Fig. 3.—The relation between polymerization rate per particle, R_p , and particle concentration, N . Variation of amount of emulsifier: ●, n-P-1; O, n-14-1.

It seems, therefore, that above a minimum particle concentration, the rate per particle depends on particle concentration, and also on the nature of the emulsifier. Smith² has advanced the idea that diffusion of monomer cannot keep pace with the polymerization resulting in a decrease in rate. However, Flory¹⁰ concludes from theoretical considerations that "monomer is easily supplied to

(10) P. J. Flory, "Principles of Polymer Chemistry," Cornell University Press, Ithaca, N. Y., 1953, p. 210.

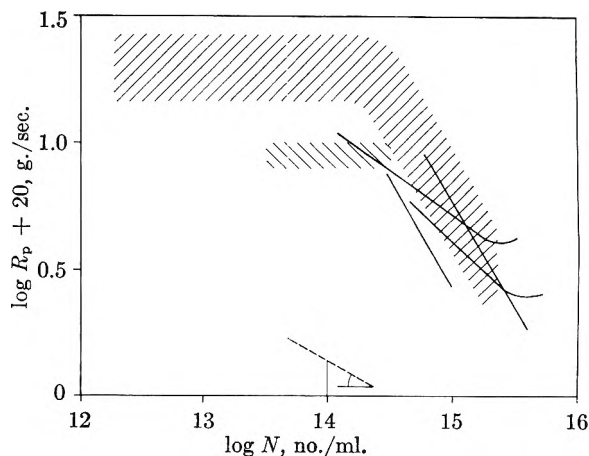


Fig. 4.—The relation between polymerization rate per particle, R_p , and particle concentration, N : // // //, ref. 2; \\\ \\\ \\\, ref. 3; - - -, ref. 6; —, this paper, Figs. 2 and 3.

the polymer particles at the required rate." This is substantiated by the measurements of the swelling ratio in the growing particles reported here. That the monomer concentration found here (3.8–4.8 mole/l.) is somewhat smaller than that reported by Bartholomé, *et al.*, (5.2–5.9 mole/l.) may be due to a different interfacial tension between the monomer-polymer particle and the serum (*cf.* reference 11).

It is seen in Fig. 4 that rates per particle have been found which are $1/10$ th of those measured by Smith.¹²

The data obtained here were also examined in the following way. Let us consider the quantity of A , defined by

$$A = \frac{\text{amount of initiator}}{\text{no. of particles}} \times \text{mol. wt.}$$

For the usual range of initiator concentration the fraction is proportional to the number of free radicals entering a particle in unit time and the second factor is a measure of the time a single polymer chain grows. Therefore, R_p should be proportional to A . For a number of experiments the ratio $R_p/A \equiv \alpha$ has been calculated in arbitrary units. Table III

TABLE III
VALUES OF α FOR DIFFERENT INITIATOR CHARGES IN THE RECIPES 1-12-m AND 1/8-16-m

Amt. of initiator $m \times \text{std. amt.}$	Recipe 1-12-m		Recipe 1/8-16-m	
	No. of exp.	α	No. of exp.	α
9	1	(1.8)	1	(0.6)
6	1	3.8	1	0.8
3	1	3.1	1	1.1
3/2	2	2.9		
1	4	3.8	2	1.1
3/4	1	2.6		
1/2	1	2.9		
1/4	1	3.5		
1/8	2	4.0		
1/15	2	(7.0)		

(11) M. Morton, S. Kaizerman and M. W. Altier, *J. Colloid Sci.*, **9**, 300 (1954).

(12) In other experiments rates per particle have been obtained up to 4 times the average value found by Smith, but these data have not been included here since it has not yet been established that for these systems, too, the number of particles is constant during the reaction. Coalescence of particles in the later stages of the reaction will cause calculated values of R_p to be too high.

lists values of α for different values of initiator charge; the soap concentration was constant.

The ratio α is substantially constant except for the extreme initiator levels.

In Table IV values of α are given for polymers formed at different emulsifier concentrations.

TABLE IV

VALUES OF α FOR DIFFERENT SOAP CHARGES IN THE RECIPES $n-14-1$, $n-16-1$ AND $n-P-1$

Amt. of soap $n \times$ std. amt.	Recipe $n-14-1$		Recipe $n-16-1$		Recipe $n-P-1$	
	No. of Exp.	α	No. of exp.	α	No. of exp.	α
4	1	(3.3)				
2	1	4.5			1	5.4
1	3	4.2	3	3.4	2	3.8
1/2	1	4.0	2	2.9	1	3.7
1/4	3	2.4	1	1.3	1	2.5
1/8			4	1.0	1	1.1
1/16					1	0.7

It is seen that α decreases as the soap concentration decreases.

Table V lists the values of α obtained in recipes with standard amounts of initiator and standard amounts of different soaps. Although the spread about the listed α values is $\pm 20\%$ it can nevertheless be concluded that α varies with the nature of the soap.

TABLE V

VALUES OF α FOR DIFFERENT SOAPS IN THE STANDARD RECIPE

Soap	12	14	16	17	18	20	O	E	P
α	3.5	4.2	3.4	5.0	1.9	0.7	5.3	5.7	3.8
Expt.	4	3	3	2	3	2	2	2	2

The data presented here are not sufficient to establish the mechanism of polymerization in the sys-

tems described. It is, however, concluded that the emulsifier takes part in the polymerization process. After the preparation of this paper had been completed this author learned of the "competitive growth" experiments carried out by Bradford, Vanderhoff and Alfrey,¹³ who further polymerized a seed consisting of a mixture of two monodisperse latices with different average particle sizes. With the help of electron micrographs it was then possible to determine the rate of growth of each group of particles. They established that the rate of polymerization per particle is proportional to the 0.83 power of the *volume* of the particle. This relation was found in the particle size range from 2600–16000 Å. and for a particle concentration of about 10^{13} /ml., and preliminary results indicate it to be valid from 10^{11} to 10^{14} /ml.¹⁴ These results conflict with those obtained by Bartholomé, *et al.*³

Since the styrene to water ratio was constant in our experiments the average *volume* of the particles is inversely proportional to the *number* of particles per ml. water. Thus the results of our experiments with constant soap charge also yield a proportionality between rate per particle and the 0.83 power of the *volume* of the particles.

Acknowledgments.—The author thanks Polymer Corporation Limited for permission to publish this paper. The assistance of Messrs. R. J. Lane and L. Morris is acknowledged. Thanks are due to Mr. W. Rupar for providing us with the electron micrographs and to Mr. W. A. Congdon for the viscosity measurements. The helpful criticism of Dr. L. Breitman is gratefully appreciated.

(13) E. B. Bradford, J. W. Vanderhoff and T. Alfrey, Jr., *J. Colloid Sci.*, **11**, 135 (1956), and J. W. Vanderhoff, J. F. Vitkuske, E. B. Bradford and T. Alfrey, Jr., *J. Polymer Sci.*, **20**, 225 (1956).

(14) J. W. Vanderhoff, private communication.

THE INHIBITION OF FOAMING. VII. EFFECTS OF ANTIFOAMING AGENTS ON SURFACE-PLASTIC SOLUTIONS

BY SYDNEY ROSS AND J. N. BUTLER

Department of Chemistry, Rensselaer Polytechnic Institute, Troy, N. Y.

Received February 24, 1956

Solutions of soaps, commercial synthetic detergents and proteins produce foams of outstanding stability by virtue of plastic surface films. Solutions of USP grade sodium lauryl sulfate are shown to form surface-plastic films. Aging the sodium lauryl sulfate solution, or changing the pH with sulfuric acid or with sodium hydroxide, or the addition of small amounts of antifoaming agents to the solution—each of these actions tends to retard or destroy the formation of the surface-plastic film. The addition of commercial antifoams to protein solutions is also shown to reduce or inhibit the normal surface plasticity of such solutions. The mechanism of antifoaming action in surface-plastic solutions is, therefore, related to the destruction of the surface-plastic film by the antifoam.

The surface of certain types of solution shows an enhanced viscosity compared to that of the underlying bulk liquid. The solutions themselves may be dilute and have normal, *i.e.*, Newtonian, flow behavior, yet the existence of a plastic film *at the surface* can be demonstrated readily. Focusing an ultramicroscope on the surface of a solution of sodium stearate that contained some finely-divided barium sulfate, Wilson and Ries¹ report: "At first the colloidal particles of barium sulfate were observed to be in violent Brownian motion, but in a few minutes after preparing the fresh surface this (motion) was replaced by a slower vibrational movement in which all the particles in the field moved in unison, as if suspended in a jelly." Gelation of the surface film was observed to build up for an hour after a fresh surface had been formed; the final thicknesses attained in different solutions varied from 10 to 40 μ .

The importance of surface plasticity in stabilizing foams has been amply demonstrated. Solutes that impart surface plasticity to aqueous solutions include proteins,² saponin,³ soaps⁴ and detergents⁵; precisely those solutes best known to produce stable and plastic foams, such as meringue, whipped cream, fire-fighting foams and shaving lather.

The sequent paper of the present series⁶ reported the experiments of J. N. Butler on the inhibitory effect of tributyl phosphate on the surface plasticity of aqueous sodium lauryl sulfate solution. To the same effect Criddle and Meader⁷ have recently reported the destruction of surface plasticity of an oil solution by the addition of dimethylsilicone. Tributyl phosphate is a well-known commercial antifoam for aqueous systems, and dimethylsilicone is an antifoam for hydrocarbons. An important part of the mechanism of their antifoaming action is, therefore, suspected to reside in their inhibition or destruction of the surface plasticity of the solution. The present paper reports the effects of a number of agents on the surface plasticity of sodium

lauryl sulfate solution and egg albumin solution. It is shown that antifoaming agents for these solutions all behave in a similar way in inhibiting the formation of surface plasticity.

Apparatus and Materials.—Surface viscosity was studied by means of a torsion-pendulum surface viscometer similar to that of Wilson and Ries.¹ A sharp-edge cylinder was used instead of a disc to reduce end-effects and disturbance of the liquid surface; a diagram of the apparatus was provided in reference 6. The amplitude of the oscillation was plotted on a logarithmic vertical scale *vs.* the swing number on a linear horizontal scale. When the movement of the pendulum is damped in a Newtonian fluid, the logarithmic decrement (d) can be calculated by

$$d = (1/n) \log A_1/A_2 \quad (1)$$

where A_1 and A_2 are the amplitudes at the beginning and end, respectively, of a set of n swings. This equation does not give a constant value of d for any but Newtonian fluids. For a plastic surface the decrease of apparent viscosity at greater amplitudes is reflected in the smaller slope of the curve of A *vs.* n . For purposes of comparison the relative steepness of the curve is measured as the slope of the chord between amplitudes 5 and 10. The "apparent surface viscosity" is defined as the value of d thus obtained.

Because of the small surface area of the cylinder edge, the shearing stress in these measurements is small, which accounts for the high value of d for non-Newtonian surfaces compared with that for the surface of pure water. The value of d for 0.10% sodium lauryl sulfate is 0.202; whereas the value of d for the water surface is 0.0071—a ratio of 28 to 1. The values obtained by this method are reproducible within a precision of 2% for any single determination and 6% for a set of determinations on different solutions. Errors caused by temperature variation were small, as the temperature was controlled to within 0.1°.

The materials used are listed below in Table I.

The solutions were prepared by dissolving a weighed amount of the surface active agent in a known volume of water in which the antifoam had previously been dissolved, or suspended in fine droplets by mixing in a Waring Blendor. The solutions were usually used for measurements of surface viscosity immediately after preparation.

Results

For most of the present investigation an aqueous solution of USP grade sodium lauryl sulfate was used, as this solute has already been the subject of an extensive study of surface viscosity by Brown, Thuman and McBain.⁵ These authors have shown that carefully purified sodium lauryl sulfate has a Newtonian surface viscosity little different from that of pure water; the addition of small amounts of lauryl alcohol or sodium octadecyl sulfate (less than 1% of the dry powder) causes the formation of plastic viscosity at the surface. Small quantities of these substances are almost certainly present in the USP grade of sodium lauryl sulfate.

(1) R. E. Wilson and E. D. Ries, "Colloid Symposium Monograph," Vol. 1, Williams and Wilkins, Baltimore, Md., 1923, p. 145.

(2) J. Plateau, *Mém. acad. roy. sci. belg.*, [8] **37**, 49, (1869).

(3) S. A. Shorter, *Phil. Mag.*, **71**, 560 (1909).

(4) E. J. Burcik, J. R. Sears and A. Tilotson, *J. Colloid Sci.*, **9**, 281 (1954).

(5) A. G. Brown, W. C. Thuman and J. W. McBain, *ibid.*, **8**, 491 (1953).

(6) S. Ross, Symposium on Foams and Their Applications, A. C. S. Meeting at Minneapolis, Minn., Sept. 16, 1955.

(7) D. W. Criddle and A. L. Meader, Jr., *J. Appl. Phys.*, **26**, 840 (1955).

TABLE I

MATERIALS USED, TRADE NAMES, COMPOSITION, COMMERCIAL SOURCE

Material	Trade Name	Source	Concn., wt./vol.
Sodium lauryl sulfate, USP	Fisher Sci. Co.	0.1%
Sodium alkyl aryl sulfonate	Nacconol NRSF	Natnl. Aniline Divn.	0.1%
Diocetyl sodium sulfosuccinate	Aerosol OT	Am. Cyanamid Co.	0.1%
Egg albumin, dry	Merck and Co.	0.1%
2-Ethylhexanol	Octyl alcohol	Carbide and Carbon Chemicals Corp.	
Methylisobutylcarbinol	Hexyl alcohol	Carbide and Carbon Chemicals Corp.	
Triocetyl phosphate	TOF Plasticizer	Carbide and Carbon Chemicals Corp.	
Tributyl phosphate	Commercial Solvents Corp.	
Sorbitan monolaurate	Span 20	Atlas Powder Co.	
Polyoxyethylene sorbitan monocölate	Tween 80	Atlas Powder Co.	

The type of measurement used in the present investigation permits the observation of the change of apparent surface viscosity as the surface ages. In Fig. 1 are reported the observations for the change of apparent surface viscosity with the age of the surface. Comparisons are made for the same solution immediately after its preparation and again after remaining in bottle for one day, two days and ten days. The older solutions take increasingly longer to build up plasticity at a newly-formed surface.

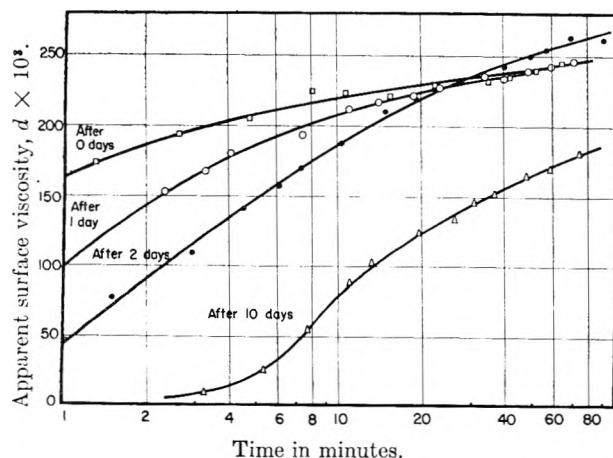


Fig. 1.—Aging of solutions of sodium lauryl sulfate: apparent surface viscosity *versus* age of the surface, for solutions of 0.10% sodium lauryl sulfate kept up to 10 days.

Rather similar effects to those obtained with older solutions were observed on fresh solutions by changing the pH, either with H_2SO_4 or $NaOH$. In Fig. 2 the effect of decreasing pH is reported, and in Fig. 3 the effect of increasing pH. From pH 7.0 to pH 2.45, adding acid lowers the initial value of the apparent surface viscosity, but raises the final value. Below pH 2.45, adding more acid increasingly re-

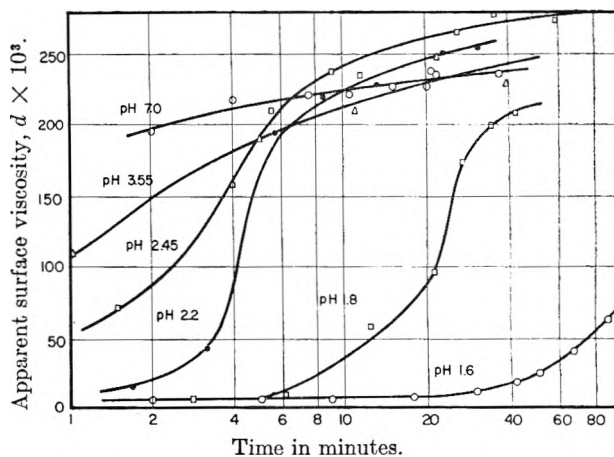


Fig. 2.—The effect of sulfuric acid on the apparent surface viscosity of 0.10% sodium lauryl sulfate solutions.

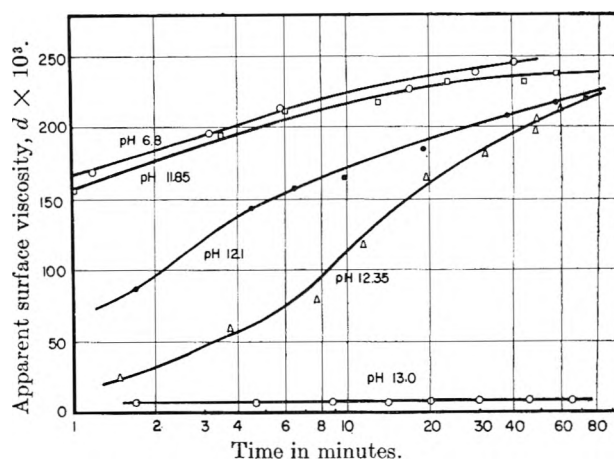


Fig. 3.—The effect of sodium hydroxide on the apparent surface viscosity of 0.10% sodium lauryl sulfate.

tards the formation of surface plasticity. The effect of addition of base is much less pronounced at first; there is hardly any change in the rate of surface aging from pH 7.0 to 11.85, but small additions of base beyond that point soon destroy completely all surface plasticity in the solution.

The effects of several commercial antifoams on the surface plasticity of freshly prepared solutions of sodium lauryl sulfate are twofold: first, the freshly formed surface of the solution containing the antifoam has a Newtonian viscosity, close to or identical with that of water itself; second, after an induction period, whose extent depends on the concentration of antifoam present, there is a sudden increase of the apparent surface viscosity, accompanied with increasingly greater deviation from Newtonian toward plastic behavior of the surface. Typical of the results obtained are Figs. 4 and 5, which report, respectively, the effects of 2-ethylhexanol and methylisobutylcarbinol. A comparison of the inhibitory action of antifoaming agents can be made by measuring the number of minutes, designated $T_{1/2}$, required for the apparent surface viscosity to reach half of its ultimate maximum value. Table II reports $T_{1/2}$ for a number of agents that have been found to inhibit the foaming of 0.10% sodium lauryl sulfate solution. The range of concentrations found effective for foam inhibition

is reported in column 2 of Table II; the information is derived from a report by S. Ross⁸ and from unpublished results obtained in this Laboratory by P. Seipel. There is a significant parallelism between the concentration ranges for effective foam inhibition and those in which the agents show a marked inhibitory or destructive action on the formation of a plastic surface film.

TABLE II

THE INHIBITION OF SURFACE PLASTICITY IN 0.10% SODIUM LAURYL SULFATE SOLUTIONS BY ANTIFOAMING AGENTS

Antifoaming agent	Concn. for foam inhibition (%)	Concn. used (%)	$T_{1/2}$ (min.)
2-Ethylhexanol	0.005 to 1.0	0.01	< 1
		.05	2.5
		.07	5.0
		.10	18
		.15	> 100
Methylisobutylcarbinol	0.10 to 1.0	0.10	< 1
		.50	2.7
		.75	9.2
		1.00	> 100
Tributyl phosphate	0.01 to 0.1	0.01	1.2
		.03	5.5
		.04	46
		.05	> 100
50% Methylisobutylcarbinol plus 50% tributyl phosphate	approx. 0.01	0.005	< 1
		.02	1.2
		.05	10.0
		.10	> 100

The apparent surface viscosity of solutions of egg albumin increased linearly with time; no sign of leveling off was observed. The higher concentration (0.10%) formed a plastic surface film more rapidly than the lower concentration (0.01%). Addition of tributyl phosphate to the 0.10% solution decreased the rate of formation of the plastic surface; tributyl phosphate (0.05%) added to the more dilute (0.01%) albumin solution caused an induction period of about ten minutes before the plastic surface commenced to form, which it then did slightly more rapidly than before. The mechanism for the formation of a plastic surface film in proteins is probably a surface polymerization; denaturation of the protein at the solution-air interface is also known to take place.

Span 20 (Atlas Powder Co) is the agent used commercially to prevent foaming of egg white during dehydration.⁸ The addition of as little as 0.001% of Span 20 to a 0.01% egg albumin solution completely inhibited the formation of a plastic surface film. The surface viscosity of the system remained Newtonian and indistinguishable from that of water.

The general mechanism of antifoaming action is only partly elucidated by these findings. It has been demonstrated before⁵ that not all foaming solutes develop surface-plastic solutions. In the present investigation Nacconol NRSF, Triton X-100, hexadecyldimethylbenzylammonium chloride and Aerosol OT, all solutes that produce stable foams in aqueous solution, were tested, and all were found to have Newtonian surface viscosities only

(8) S. Ross, "The Inhibition of Foaming," Rens. Polytech. Inst. Bull., Eng. Sci. Series, 63 (1950).

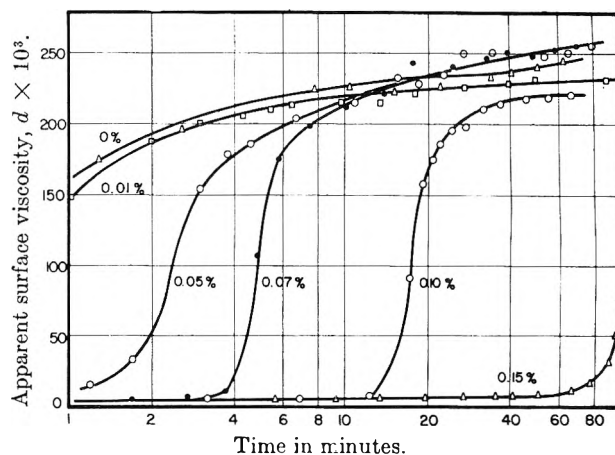


Fig. 4.—The effect of 2-ethylhexanol, a commercial antifoam, on the apparent surface viscosity of 0.10% sodium lauryl sulfate.

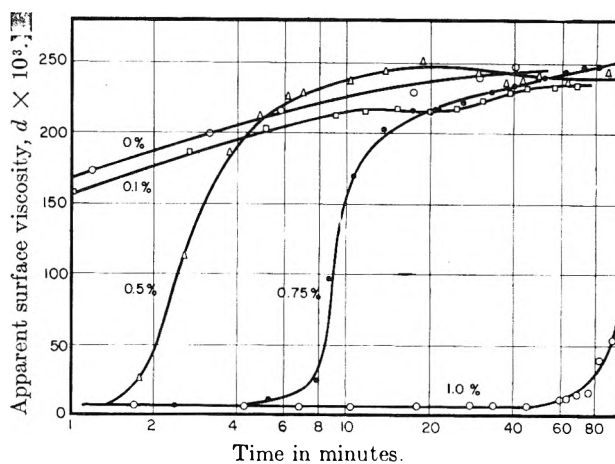
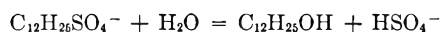


Fig. 5.—The effect of methylisobutylcarbinol, a commercial antifoam, on the apparent surface viscosity of 0.10% sodium lauryl sulfate.

slightly different from water. The addition of antifoams to these solutions suppressed the foam, and was usually accompanied with a small decrease in the surface viscosity. All the surfaces were Newtonian, and none of the systems showed any change of the surface viscosity with the age of the surface, as had been observed in the sodium lauryl sulfate solutions. The action of antifoams cannot therefore be ascribed in every system to the destruction of the plastic surface films of the foam. A discussion of other mechanisms of antifoaming action will be found in reference 6.

Discussion

The production of plastic surfaces in solutions of synthetic detergents and soaps is usually ascribed to hydrolysis products, such as fatty alcohols⁶ or acid soaps.⁴ In the present study of sodium lauryl sulfate the dependence of the surface plasticity on pH suggests the formation of lauryl alcohol by the reaction



It is now well recognized that reactions that occur slowly in the bulk solution may take place rapidly at the solution-air interface. The relatively slow production of a plastic surface film in solutions

where bulk hydrolysis is negligible can be well accounted for by the formation of hydrolysis products taking place only at the surface.

The apparent depletion of 10-day old solutions of sodium lauryl sulfate (see Fig. 1) can be traced to another cause. Solutions kept even for one day developed a slight haze; on standing for ten days, a definite precipitate formed; the aging process was accelerated by allowing a larger surface to be ex-

posed to the air. These facts suggest that atmospheric oxidation may be taking place, changing the lauryl alcohol at the surface to insoluble lauric acid.

The bearing of the present findings on the mechanism of antifoaming action, at least for solutions in which the stability of the foam can be directly traced to the presence of plastic surface films, needs no further comment.

DETERMINATION OF THE EQUILIBRIUM CONSTANT BY MEANS OF SURFACE TENSION MEASUREMENTS

By ENZO FERRONI AND GABRIELLA GABRIELLI

Instituto di Chimica Fisica, Dell'Universita di Firenze, Firenze, Italy

Received June 24, 1955

For the system $I_2 + C_2H_5OH + CCl_4$, the surface tension shows a minimum corresponding to a molar ratio 1:1 *i.e.*, corresponding to the complex $I_2-C_2H_5OH$. The correlation between concentration of the complex and decrease of surface tension (evaluated as a difference between the mean of the surface tensions of the single components and the measured surface tension) is studied. This correlation appears to be linear in the range 0.0120–0.011 *M*. A general method of calculation for the determination of the apparent equilibrium constant of the complex is proposed. The average value of the constant is found to be 1.239, practically coincident with those obtained by other workers using different methods.

The correlation between surface tension minima and complex formation in solution has been mentioned by several workers.¹ We have previously studied the formation of molecular compounds (antipyrine-chloral hydrate)² and of complex ions (halides of cadmium and halides of potassium).³

In this work it has been emphasized that any correlation between surface tension minima and molarity ratio of the components of the complex could only be deduced after a study of the surface tension behavior of the single components.

It is known that many salt solutions display surface tension minima at low concentrations. These minima have been described by Jones and Ray.⁴ Such minima can be present in ternary systems too, and therefore it would be wrong to relate these minima to a possible complex (or molecular association). Surface-active substances, moreover, can have surface tension minima at very low concentrations. It is known, for example, that sodium oleate shows three minima at concentrations of 7.5×10^{-5} , 12.2×10^{-5} , 13.9×10^{-5} , respectively, corresponding to the formation of unimolecular films.⁵ Minima of surface tension can also be caused by the partition of a surface-active solute between the interface liquid-gas and another interlayer (which may already exist or may be formed in the liquid at a certain concentration), as for instance for a micelle "solution."

It is known, moreover, that the surface tension shows a minimum value corresponding to the criti-

cal micellar concentration.⁶ It is obvious that all these minima are completely independent of the formation of a hypothetical complex.

Except where minima are found in the surface tension-activity curves of the single components or are due to the formation of unimolecular films or correspond to the critical micellar concentration, it may be inferred that minima in surface tension, as measured by the ring method, will only be found where ionic or molecular complexes are formed. To study the correlation between surface tension activity and complex concentration, the system of two components forming a single complex in inert solvent has been chosen as particularly suitable. The system $C_2H_5OH + I_2$ in CCl_4 seems to satisfy this condition.

Experimental

The surface tensions have been measured with the tensiometer used in our institute.⁷ The given values have been read directly on the tensiometer, without the Harkins and Jordan corrections. It follows that greater values are obtained with respect to those corrected or obtained by other methods.

The temperature during the experiments was kept constant at $25 \pm 0.1^\circ$ using a jacketed container around which the liquid from a thermostat was circulated. Ethanol, iodine and carbon tetrachloride were of highest grade Merck quality and were further purified by the usual methods.

System $C_2H_5OH-CCl_4$.—The capillary activity of C_2H_5OH in CCl_4 has been studied in the concentration range 0.0025–0.05 *M*. The values of the surface tension for the different concentrations are given in Table I, each being the average of five measurements.

Except in the range 0.0025–0.0078 *M*, the surface tension decreases as the molarity of the solution increases until, after a certain point, it remains constant. This is the normal behavior.

System I_2-CCl_4 .—The variations in the value of surface tension with concentration, for the range 0.0025–0.05 *M*, are reported in Table II.

(6) J. L. Moilliet and B. Collie, "Surface Activity," Spon Ltd., London, 1951, p. 14.

(7) G. Piccardi, Brevetto Italiano No. 462316, February 1950–March 1951.

(1) M. R. Nayar, L. N. Srivastava and K. V. Nayar, *J. Indian Chem. Soc.*, **29**, 241 (1952).

(2) E. Ferroni, G. Gabrielli and M. Giarfuglia, *Ric. Sci.*, **25**, 539 (1955).

(3) E. Ferroni and G. Gabrielli, *Ann. Chim.*, in press.

(4) G. Jones and W. A. Ray, *J. Am. Chem. Soc.*, **59**, 187 (1937); **63**, 288 (1941); I. Langmuir, *Science*, **88**, 430 (1937); *J. Chem. Phys.*, **6**, 873 (1938).

(5) P. Lecomte Du Nouy, "Equilibres Superficiels des Solution Colloïdales," Ed. Masson, 1929, p. 98.

TABLE I
C₂H₅OH-CCl₄

Molarity	Surface tension (dynes/cm.)	Molarity	Surface tension (dynes/cm.)	
0.0025-0.0078	28.69	.01390	28.49	
.00860	28.66	.01510	28.47	
.00875	28.65	.01660	28.43	
.00920	28.64	.01750	28.42	
.01040	28.61	.01800	28.41	
.01130	28.55	.02000	28.40	
.01250	28.54	.02100	28.35	
.01350	28.52	0.0220	.05	28.33

TABLE II
I₂ + CCl₄

Molarity	Surface tension (dynes/cm.)	Molarity	Surface tension (dynes/cm.)	
0.0025-0.033	28.33	0.0400	28.63	
.0344	28.37	.0416	28.64	
.0357	28.47	.0435	28.67	
.0370	28.54	0.045-	.05	28.68
.0384	28.61			

The capillary activity of I₂ in CCl₄ is undoubtedly anomalous, because it is inactive up the molarity 0.033 *M*, after which the surface tension increases. No hypothesis is suggested here for this phenomenon, which, however, seems well worthy of an accurate, independent study.

In the present research no surface tension minima are present.

System I₂-C₂H₅OH in CCl₄.—In Table III the molarities of the two components are given in columns 1 and 2 and the corresponding surface tensions in column 3. The total molarity in every solution is constant and equals 0.025 *M*.

TABLE III

I ₁	C ₂ H ₅ OH	Surface tension (dynes/cm.)	I ₂	C ₂ H ₅ OH	Surface tension (dynes/cm.)
0.02250	0.00250	28.33	0.01125	0.01375	28.11
.02125	.00375	28.30	.01300	.01500	28.14
.02000	.00500	28.27	.00875	.01625	28.165
.01875	.00625	28.24	.00750	.01750	28.19
.01750	.00750	28.22	.00325	.01875	28.22
.01625	.00875	28.182	.00500	.02000	28.255
.01500	.01000	28.15	.00375	.02125	28.255
.01375	.01125	28.11	.00250	.02250	28.31
.01250	.01250	28.09			

When the surface tension is plotted against the corresponding molarity: it can be seen that (a) there is a single minimum; as there are no collateral phenomena in the curve for the single components, the minimum would confirm the existence of a single complex; (b) the minimum of the surface tension corresponds to the molarity ratio 1:1. This result has been confirmed by several experiments.

Correlation between the Decrease in Surface Tension and the Complex Concentration.—It has been decided to measure the decrease ($\Delta\sigma$) by subtracting the surface tensions of the solutions I₂-C₂H₅OH in CCl₄, in molarity ratio 1:1, from the mean of the surface tensions of the solutions, I₂ in CCl₄ and C₂H₅OH in CCl₄ at the same molarity (as the molarity ratio corresponding to the complex formation is 1:1). That is, it is supposed that the mean of the surface tensions of the single components in CCl₄ represents the surface tension of a hypothetical solution of I₂ and C₂H₅OH in CCl₄,

without the interaction which forms the complex. In Table IV are reported the values of the surface tension decreases ($\Delta\sigma$) for the different molarities.

TABLE IV

I ₁ , <i>M</i>	C ₂ H ₅ OH, <i>M</i>	$\Delta\sigma$	I ₂ , <i>M</i>	C ₂ H ₅ OH, <i>M</i>	$\Delta\sigma$
0.0120	0.0120	0.29	0.0160	0.0160	0.67
.0125	.0125	.34	.0175	.0175	0.86
.0140	.0140	.48	.0200	.0200	1.22
.0150	.0150	.56	.0225	.0225	1.51

Plotting $\Delta\sigma$ against molarity it can be seen that in the interval 0.0120–0.016 *M* there is a linear relation between the two variables. We attribute a conditional value to this relationship in order to calculate the equilibrium constant analogously to the application of the spectrographic method using Beer's law.

Determination of the Equilibrium Constant.—From the experiments reported above it is possible to conclude: (a) the minimum of the surface tension is due to one complex; (b) The "depth" of the minimum increases in proportion to the molarity of the complex in the range 0.012–0.016 *M*. From this it can be said that where two solutions show the same decrease of surface tension they have the same complex concentration.

Let C_1 and C_2 be the concentrations of the two components and C_{AB} the complex concentration (in moles/l). For a solution which shows a decrease $\Delta\sigma_1$

$$C_{AB} = K\Delta\sigma_1$$

In the same way for a solution showing the decrease $\Delta\sigma_2$, where C_1^1 and C_2^1 are the concentrations of the components and C_{AB}^1 the complex concentration, in moles/l.

$$C_{AB}^1 = K\Delta\sigma_2$$

If $\Delta\sigma_1 = \Delta\sigma_2$, $C_{AB} = C_{AB}^1$. Then for solution 1

$$K = \frac{C_{AB}}{(C_1 - C_{AB})(C_2 - C_{AB})}$$

and for solution 2

$$K = \frac{C_{AB}}{(C_1^1 - C_{AB})(C_2^1 - C_{AB})}$$

From these two expressions it is possible to calculate C_{AB} and then the equilibrium constant.

In columns 1 and 2 of Table V are reported the molarities of the I₂ and of the C₂H₅OH in CCl₄ (the sum of the molarities is constant and equals 0.03 *M*) and in column 3 the mean of the surface tensions of I₂ in CCl₄ and C₂H₅OH in CCl₄ at the corresponding molarities is given. Column 4 shows the measured surface tensions of the I₂ + C₂H₅OH-CCl₄ solutions and 5 the decrease $\Delta\sigma$ *i.e.*, the difference between the values given in columns 3 and 4.

The values reported in Table III are completed in Table VI. In column 1 and 2 are again listed the molarities of I₂ and C₂H₅OH in CCl₄; in column 3 the average of the surface tensions (calculated as above) and in 4 the values of $\Delta\sigma$, *i.e.*, the difference between the figures of column 3 and those reported in Table III.

TABLE V

I_2 , M in CCl_4	C_2H_5OH , M in CCl_4	Mean s.t.	Obsd. s.t.	$\Delta\sigma$
0.0270	0.0030	28.51	28.30	0.21
.0255	.0045	28.51	28.25	.26
.0240	.0060	28.51	28.10	.31
.0225	.0075	28.51	28.16	.35
.0210	.0090	28.485	28.075	.41
.0195	.0105	28.47	28.00	.47
.0180	.0120	28.44	27.93	.51
.0165	.0135	28.42	27.88	.54
.0150	.0150	28.40	27.83	.57
.0135	.0165	28.38	27.84	.54
.0120	.0180	28.37	27.85	.52
.0105	.0195	28.36	27.87	.49
.0090	.0210	28.34	27.88	.46
.0075	.0225	28.33	27.91	.42
.0060	.0240	28.33	28.11	.22
.0045	.0255	28.33	28.19	.14
.0030	.0270	28.33	28.25	.08

TABLE VI

I_2 , M in CCl_4	C_2H_5OH , M in CCl_4	Mean s.t.	$\Delta\sigma$
0.02250	0.00250	28.51	0.18
.02125	.00375	28.51	.21
.02000	.00500	28.51	.24
.01875	.00625	28.51	.265
.01750	.00750	28.51	.29
.01625	.00875	28.49	.308
.01500	.01000	28.47	.32
.01375	.01125	28.44	.33
.01250	.01250	28.43	.34
.01125	.01375	28.41	.30
.01000	.01500	28.40	.26
.00875	.01625	28.38	.215
.00750	.01750	28.37	.18
.00625	.01875	28.365	.145
.00500	.02000	28.365	.11
.00375	.02125	28.335	.08
.00250	.02250	28.33	.02

We now have the data necessary to calculate the equilibrium constant.

Let (1) be the solutions for which the sum of the partial molarities is 0.030 M (Table V) and let (11) be the solutions for which the sum of the partial molarities is 0.025 M (Table VI). By interpolation of the values given in these tables it is possible to see that different solutions show the same decrease $\Delta\sigma$. From this it is possible, as has been shown, to calculate the equilibrium constant. In Table VII are given some of the pairs of solutions of (1) and (11), both of which show the same decrease $\Delta\sigma$ and the corresponding calculated value of the equilibrium constant.

TABLE VII

I_2 , M	C_2H_5OH , M	I_2 , M	C_2H_5OH , M	K , inst.
0.0240000	0.0060000	0.016125	0.008875	1.445
.0255000	.0045000	.019000	.006000	1.27
.0233250	.0066750	.011250	.013750	1.336
.0270375	.0029625	.021250	.003750	1.29
.0232500	.0067500	.012500	.012500	0.916
.0236250	.0063750	.015000	.010000	0.836
.0246375	.0053625	.017500	.007500	1.58

The average value of the apparent equilibrium constant of the complex $C_2H_5OH + I_2$ at $25 \pm 0.1^\circ$ is hence 1.239. This value is in good agreement with those obtained by other workers using different methods.⁸ The method which we have used can therefore be regarded as applicable, at least in this case, to the determination of the equilibrium constant, although the intervention of other phenomena may limit the application of this method.

The authors wish to express their gratitude to Prof. Piccardi, Director of the Institute, for his very valuable advice.

(8) J. H. Hildebrand and R. L. Glascock, *J. Am. Chem. Soc.*, **31**, 26 (1909); J. Groh, *Z. anorg. Chem.*, **162**, 299 (1927); J. Kleinberg and A. W. Davidson, *Chem. Revs.*, **42**, 606 (1948).

THE SLOW THERMAL DECOMPOSITION OF CELLULOSE NITRATE¹

By GIDEON GELERNTER, LUTHER C. BROWNING, SAMUEL R. HARRIS AND CHARLES M. MASON

Contribution from the Physical Research Section, United States Bureau of Mines, Bruceton, Pa.

Received October 25, 1955

Studies on the slow thermal degradation of cellulose nitrate in a current of inert gas and the decomposition at low pressures of cellulose nitrate tagged with isotopic N^{15} on the sixth carbon atom are described. The lower thermal stability of the nitrate groups in the second and third positions of the glucoside unit was established by the thermal decomposition studies with isotopic nitrogen and a chemical reaction sequence postulating early cleavage between the second and third carbon atoms formulated on the basis of the total experimental data obtained.

The decomposition of cellulose nitrate must proceed through a sequence of reactive intermediates or possibly several competing sequences. This study was made in an attempt to trace the main sequence of the decomposition and consisted of two distinct sets of experimental data: one involves the slow decomposition under low pressure of cellulose nitrate tagged with N^{15} on the sixth carbon atom of the glucoside unit; the other one

involves samples of high nitrogen cellulose nitrate which were heated in a current of inert gas and a study made of the gaseous products of decomposition.

Experimental

I. Slow Thermal Decomposition of N^{15} -Tagged Cellulose Nitrate.— $6-N^{15}$ -Tagged cellulose nitrate was prepared according to Grassie and Purves,² by nitration in two separate stages, using N^{15} -enriched nitric acid for the first step. Three samples of tagged cellulose nitrate (No. 1, 2 and 3)

(1) This work was supported by the Office of the Chief of Ordnance under Army Project 503-02-001, Ordnance Project TB3-0110.

(2) V. R. Grassie and C. B. Purves, private communication.

were prepared. The N^{15} -enrichment of the preparations and residues of decomposition was determined by mass spectrometer analysis of the nitric oxide collected in the nitrometer (Table I).

TABLE I
ANALYTICAL DATA ON SAMPLES USED AND RESIDUES OBTAINED

Sample	Nitrogen, %	% N^{15} (of total N)
Untagged cellulose nitrate	11.6	0.38
High-nitrogen cellulose nitrate	14.0	0.38
Cellulose 6-mono-nitrate		
1st preparation	..	21.1
2nd preparation	6.12	21.6
3rd preparation	6.88	21.69
Cellulose nitrate		
No. 1	10.8	13.0
No. 2	10.95	10.5
No. 3	11.79	9.39
Residue from		
run 25	8.55	14.0
run 26	9.17	13.9
run 27	8.44	14.0

In these experiments, small charges of cellulose nitrate were heated in a vacuum system and the gaseous products collected with a Toepler pump. The system was arranged so that the decomposition product could be collected in successive fractions, some corresponding to very short periods of time. The gas samples were analyzed on the mass spectrograph for N^{15} -enrichment and composition. The procedure was as follows: A weighed sample was placed in a small tube and connected to the vacuum system. The tube was enclosed by the thermostat (157–157.7°) and the pressure allowed to rise to 1 mm. where it was maintained automatically by a "thermccap" relay,³ dibutyl phthalate manometer and Toepler pump arrangement which pumped the excess gaseous products into the gas collecting system. When successive fractions were required, the system was evacuated between each fraction. After each run, the solid residue was weighed and analyzed for total and isotopic nitrogen. No attempt was made to freeze out NO_2 prior to contact with the mercury in the Toepler pump. Although there was some reaction between the mercury and NO_2 , it was felt that the main interest lay in the relative amount of N^{15} in the gaseous products and that this would be affected only slightly, if at all.

To test and standardize the procedure, trial runs were made on untagged cellulose nitrate synthesized by the same method as the N^{15} -tagged material, and on samples of high nitrogen cellulose nitrate similar to the material used in the other experiments.

II. Slow Thermal Decomposition of Cellulose Nitrate in a Current of Inert Gas.—The apparatus for this study consisted of a rigid glass and metal train, mounted on a movable frame which could be lowered to immerse the reaction chamber and a heat-exchange coil into an oil thermostat. The reaction chamber was a straight cylindrical glass tube connected by ground-glass joints to the heat-exchange coil on the one side and to the lead-off tube and analytical train on the other.

Samples of highly nitrated cellulose nitrate (14.0% N) were dried for several hours at 70° and weighed into the reaction tube where they were supported by a glass-wool plug. The system was swept out thoroughly with argon which was first passed through the heat-exchange coil. It was then lowered into the thermostat and heated for the desired length of time. Volatile products of decomposition were swept into the analytical absorption train and determined subsequently. The degraded solid residue was weighed to determine total loss of weight. Fractions of the solid residue were used for various analytical determinations (nitrogen, carbonyl, carboxyl, infrared absorption spectra).

(3) Made by Niagara Electron Laboratories, Andover, New York.

Carbonyl was determined by a modification of the Bryant and Smith⁴ method which employed small samples and corrected for the acidity originating from possible hydrolysis of unchanged residual products by means of blank titrations made with and without reagent on an undegraded cellulose nitrate sample. Titrations were performed with a pH meter to a pH 5.00.

Carboxyl determinations were performed by the method of Unruh, McGee, Fowler and Kenyon.⁵

Infrared absorption spectra were taken on dispersions of the residual material in Nujol. For this purpose, a small amount of the sample (about 0.01 g.) was dispersed on a rock salt window with a few drop of Nujol.

An analytical train adapted from Milligan⁶ was used to determine mixtures of NO_2 , NO , CO_2 , CO and H_2 . Amounts of H_2O and volatile organic products such as CH_2O , $HC-OOH$, etc., were not determined. In the presence of organic materials, the possibility of reaction within the train itself did arise. This train consisted of a series of absorption flasks and absorption tubes. The first flask contained concentrated H_2SO_4 , the second concentrated $H_2SO_4-HNO_3$ (50:1). This was followed by a tube containing ascarite, a tube filled with CuO kept at 350°, a tube with dehydrite, and finally another ascarite tube. The first H_2SO_4 solution absorbed NO_2 and any NO up to equimolar with NO_2 . The $H_2SO_4-HNO_3$ solution absorbed any excess NO . CO_2 was retained in the ascarite tube, whereas H_2 and CO were oxidized by CuO to H_2O and CO_2 and absorbed in the two final tubes. The tubes were weighed to determine the amount absorbed directly. Aliquots were pipetted out from the absorption flasks and titrated with excess $KMnO_4$ and thereafter $FeSO_4$ solution. A second aliquot of the H_2SO_4 solution was treated in a nitrometer. NO_2 and NO were computed from the two analyses on this absorbent.

The nitrometer consisted of a micro-size nitrometer tube sealed to a straight 10-cc. pipet and mounted vertically on a wooden board. The board was clamped to a horizontal steel rod in such a manner that it oscillated freely by action of a steel lever arm from a mechanical shaker (160 oscillations per minute). Leveling bulbs, connected to the nitrometer by thick-walled flexible rubber tubing, rested on separate adjustable stands. With this device, samples of very small size and of a wide range of nitrogen content could be analyzed.

Results

I. Slow Thermal Decomposition of N^{15} -Tagged Cellulose Nitrate.—Seven decomposition runs were made on the first two preparations of cellulose nitrate tagged with N^{15} . The results of these runs are given in Table II where runs 25, 26 and 27 are duplicate experiments on the decomposition of preparation no. 1, all at 157.0 to 157.7°. Run 28 is a duplicate of 25, 26 and 27, except that preparation no. 2 was used. Several successive fractions are listed for each run.

Preparation no. 3 was used in one run to verify the results obtained with the earlier samples. Analysis was performed only to determine the per cent. N^{15} . The three gaseous fractions collected with the preparation no. 3 corresponded to 1.7, 1.7 and 4.2% loss of weight, respectively. Their N^{15} -content was 6.60, 6.67 and 6.95% N^{15} of the total nitrogen in each fraction, respectively. The conditions were identical to those described in connection with run 31.

The test procedure was modified in run 29 by mixing ("diluting") the charge with cellulose, in runs 30 and 31 by the use of a lower temperature of decomposition, namely, 152.1 to 152.7°, and in run 31 also by continuous removal of gaseous de-

(4) W. M. D. Bryant and D. M. Smith, *J. Am. Chem. Soc.*, **57**, 57 (1935).

(5) C. C. Unruh, P. A. McGee, W. F. Fowler and W. L. Kenyon, *ibid.*, **69**, 349 (1947).

(6) L. H. Milligan, *THIS JOURNAL*, **28**, 544 (1924).

TABLE II
 COMPOSITION OF GASEOUS PRODUCTS OF DECOMPOSITION OF TAGGED CELLULOSE NITRATE

Run	Fraction	Sample wt., g.	% decomposition	N ¹⁵ , %	NO ₂	N ₂ O	CO ₂	Mole % in product NO	CO	H ₂ O	HCHO
Prep. 1											
25	1	0.0806	4.6	9.6	1.5	0.6	13.5	64.2	14.0	2.5	3.7
	2		5.3	10.8	0.1	0.4	12.2	51.0	19.6	14.9	1.8
	3		6.6	12.2	.2	2.8	17.6	33.4	25.4	18.2	2.4
26	1	0.1047	2.7	9.8	0.9	4.0	13.0	59.1	10.5	9.4	3.1
	2		4.7	10.6	.1	2.5	10.0	54.4	17.9	13.2	1.9
	3		5.7	11.3	37.1	24.8	..	38.1	..
27	1	0.1007	0.8	9.7	1.5	..	18.1	56.5	9.1	8.0	6.8
	2		.7	9.7	0.3	0.4	12.4	59.3	14.8	11.3	1.5
	3		3.3	10.6	.2	.7	10.7	53.4	19.6	13.3	2.1
	4		5.7	11.1	.2	.1	13.7	46.8	20.3	16.8	2.1
	5		6.3	12.6	.2	9.1	11.7	29.9	29.6	17.3	2.2
Prep. 2											
28	1	0.1001	0.67	6.93	0.6	..	14.9	58.1	8.3	15.1	3.0
	2		1.0	7.38	.3	..	12.5	55.8	11.3	19.7	0.4
	3		3.0	7.77	.2	..	10.0	51.3	13.6	21.9	2.0
	4		4.0	8.19	.2	0.6	10.8	50.3	17.4	18.7	2.0
29	1	0.0685	1.5	6.93	0.2	6.6	10.1	50.0	7.9	23.5	1.7
	2		4.0	7.78	0.2	..	11.1	51.5	11.0	24.6	1.6
30	1	0.0699	3.1	7.28	1.3	..	14.0	57.6	9.9	14.8	2.4
	2		3.75	7.85	1.5	..	10.7	54.1	12.6	18.9	2.2
	3		3.75	8.30	0.9	..	10.4	51.3	14.3	21.0	2.1
31	1	0.0748	1.34	7.09	0.3	2.1	10.9	31.3	7.0	44.9	2.0
	2		2.68	7.35	.2	..	10.4	35.9	8.7	43.3	1.5
	3		2.68	7.67	.4	..	10.7	40.9	12.7	33.4	1.9

composition products, that is, continuous operation of the Toepler pump.

In each run, the percentage of N¹⁵ of the total nitrogen in the gaseous products was well below the average percentage for the preparation used and there was a perceptible increase in the percentage of N¹⁵ in the products from successive fractions.

Results of these tests indicated a remarkable constancy of the initial N¹⁵-content of the gaseous products. Mixing with cellulose proved quite ineffective. The rather small, though apparently real, decrease of the total per cent. N¹⁵ in run 30 (lower temperature of decomposition) follows from the difference in stability itself. For, if the energy of activation of the 6-group is higher, the decrease of its independent rate of decomposition should be more marked at decreased temperatures. In run 31, the lower values of N¹⁵, fraction by fraction, indicate a strong effect of the decomposition products on the further course of reaction, but the rather constant initial N¹⁵ value makes it appear unlikely that initial values are much affected by induced decomposition. Evidence from these runs does not however go far enough to clarify these detailed aspects.

II. Slow Thermal Decomposition of Cellulose Nitrate in a Current of Inert Gas.—The series of experiments on decomposition in a current of inert gas, run on samples of 14% N-cellulose nitrate, produced both volatile products and solid residues. NO₂, NO, CO₂ and CO were determined for each run. The values obtained are given in Table III.

A number of tests were performed on the solid residues of decomposition. Nitrogen determina-

tions on the residues generally agreed with the amount of NO and NO₂ found in the volatile products. Some carbonyl values obtained are listed in Table IV. It also seemed interesting to compare moles of carbonyl found with moles of NO₂ obtained previously for the same runs. The values for carboxyl were negligibly low.

The absorption spectra obtained were in general much like cellulose nitrate spectra with the nitrate bands reduced in intensity and with two new bands, one at 2.9 μ due to OH, and one at 5.75 μ which, on the basis of the chemical tests described, must be due to carbonyl, although carboxyl might show up in this same region. In a special series, three charges of cellulose nitrate, each weighing about 0.8 g., were heated at 152° in a stream of argon for 4, 8 and 15 hours, respectively. The corresponding losses of weight were 4.59, 18.15 and 39.3%. Infrared spectra were taken on the residues. Portions of these were also subjected to the carbonyl and carboxyl tests discussed above. Carbonyl was found to be 0.45 mmole/gram of degraded material for the first charge, and in excess of 1.5 mmoles for the second and third. No carboxyl was present. The OH band at 2.9 μ appeared clearly even in the first sample, whereas the band at 5.75 μ developed from a very slight shoulder in the first to a pronounced peak in the third, indicating the gradual accumulation of carbonyl in the residue.

Discussion

Introduction of isotopic N¹⁵ into the nitrate group on the sixth carbon atom of cellulose nitrate seemed the most logical way to determine the relative initial stability of the nitrate groups on carbons two, three and six.

TABLE III

ANALYTICAL DATA OBTAINED IN THE SLOW THERMAL DECOMPOSITION OF CELLULOSE NITRATE (14.0% N)^a

Run	Size, g.	Temp., °C.	% loss of wt., P	% loss of total N, X	X/P	NO/NO ₂	CO ₂	% of volatiles	CO	% of unrecovered volatiles
3	0.67	146.4	3.45	6.68	1.94	0.83
4	1.03	146.4	6.37	10.38	1.63	1.21
5	1.04	149	5.54	8.78	1.58	1.06
6	1.03	152.4	5.33	8.80	1.65	1.33
7	1.04	152.4	6.78	9.54	1.41	1.28	14.3	15.6	23.3	23.3
8	1.08	152.4	8.14	12.40	1.52	1.43	12.4	16.4	21.5	21.5
9	0.30	152.4	7.9	12.10	1.54	1.32	11.4	12.7	23.3	23.3
10	1.05	152.4	7.02	8.79	1.25	1.33	12.9	14.5	31.6	31.6
11	0.52	152.4	..	9.56	..	1.21
12	.48	152.4	5.48	8.10	1.48	1.18
13	.46	152.4	10.37	14.62	1.41	1.57	12.1	16.9	25.8	25.8
14	.71	152.4	5.48	9.27	1.69	1.16	12.8	13.3	14.6	14.6
15	.49	152.4	7.35	11.0	1.49	1.22	11.8	..	24.0	24.0
16	.21	152.4	4.36	9.32	2.14	0.45
17	.25	152.4	4.20	9.32	2.22	0.62	8.5	2.8	1.9	1.9
18	.36	152.4	5.84	11.46	1.96	1.18	12.7	..	5.2	5.2
19	.52	150.0	6.48	10.7	1.65	1.25	14.3	19.2	12.3	12.3
20-a	.70	153.6	1.84	3.79	2.06	0.56	10.9	4.7	3.1	3.1
20-b	.70	153.6	2.71	3.89	1.43	1.25	10.1	13.2	28.0	28.0
20-c	.70	153.6	2.13	4.3	2.02	1.89	29.6	44.5
20-d	.70	153.6	3.96	4.73	1.20	2.63	14.1	19.5	32.6	32.6

^a All runs approximated four hours except no. 4 which was 10 hours and 20-a, b, c and d which were samples withdrawn at 1.5-hour intervals.

TABLE IV

MOLES OF CARBONYL DETERMINED IN DEGRADED NITROCELLULOSE

Run	Carbonyl (mmole/l g.)	Carbonyl/NO ₂ (mole ratio)
18	0.477	0.91
15	.562	1.14
14	.50	1.16
12	.407	1.10

Unfortunately, the number of nitrate groups introduced per glucoside unit in two-stage nitration by the method of Grassie and Purves² is limited to about 2. This fact has been established by Lemieux who considered it as due to "steric hindrance".⁷ The unnitrated group (mainly 2 or 3) apparently remains as hydroxyl. The N¹⁵-tagged test compound thus differs importantly from fully nitrated cellulose nitrate. However, as both hydroxyl and nitrate groups are electronegative, though admittedly of different magnitudes, it is believed that valid conclusions regarding the mechanism of decomposition may be drawn from the study of this material. As N¹⁵ occupies the sixth position in the glucoside unit, the fact that in each run the percentage of N¹⁵ of the total nitrogen in the gaseous products, as shown in Table II, was well below the average percentage for the preparation used, and that there was a perceptible increase in the percentage of N¹⁵ in the products from successive fractions, constitute clear-cut evidence for the lower thermal stability of the 2,3-nitrate groups and for the decrease of the stability of the 6-nitrate group in the course of decomposition.

Whereas a high degree of significance cannot be denied the N¹⁵ ratios obtained, data on chemical composition of the gas fractions have to be viewed

with caution. Many of the primary decomposition products undoubtedly are highly reactive and capable of further reaction at any subsequent stage. This explains the virtual absence of NO₂ in the gaseous products as well as the low concentration of formaldehyde. Similarly, values for CO₂, CO, H₂O and N₂O in Table II do not necessarily indicate the quantities of these compounds formed directly by decomposition.

The observed lower stability of the 2,3-nitrate groups and decreasing stability of the 6-nitrate group in the course of decomposition should be still more marked with fully nitrated cellulose nitrate.

The wide differences in composition of the volatile products obtained in the slow thermal decomposition of cellulose nitrate in a current of inert gas indicates an initial reaction followed in varying extent by successive secondary reactions. One means to study the extent of secondary reaction, or more particularly its onset, is to examine the ratio of the per cent. loss of total nitrogen, X, to the per cent. loss of total weight, P, since, if the initial reaction consisted—as has frequently been proposed—of the loss of NO₂ only, this ratio would reach a maximum value of 2.15. It is recognized that this applies only during the initial time lag between reaction at the 2,3-positions and of the 6-group. The ratios obtained are shown as X/P in Table III. In some of the runs where the duration of reaction was short or with very small samples, the ratio approaches the value of 2.15. One may conclude that the lower value of the ratio in other runs is attributed to secondary reactions.

The ratio of NO to NO₂ should be zero if NO₂ is the primary product and no secondary reaction has occurred. It is seen that the lowest values in Table III are given by those runs in which, accord-

(7) R. V. Lemieux, *Can. J. Research*, **25B**, 485 (1947).

ing to the ratio X/P , little secondary reaction has occurred.

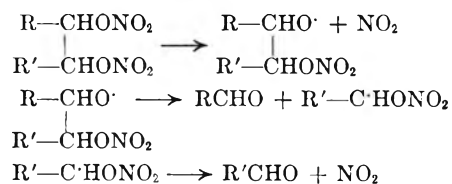
The presence of CO_2 and CO in the reaction products in themselves indicate secondary reaction beyond the initial splitting off of NO_2 . Again it is to be noted that the per cent. of unrecovered volatiles likewise seems to increase with the degree of secondary reaction.

The data in Table III may also be examined for the effect of charge size, temperature and time of treatment. Inasmuch as volatile products must pass through layers of solid, an increase in the size of charge should result in increased secondary reaction if the latter is a heterogeneous reaction between initial volatile products and solid residue. Comparison of runs no. 16 and 17 in Table III with other runs indicates a marked difference due to size, in both total amount of reaction, and in degree of secondary reaction. This, however, appears limited primarily to very small sizes. The effect of temperature on the degree of secondary reaction is not sufficiently clear within the narrow range used. The effect of time is shown by run No. 20 which consisted of a single charge heated in four successive 1.5-hour periods.

The changing composition of the products may be taken to indicate a whole sequence of decomposition steps. With very small charges or at an early stage, reaction appears to consist essentially in splitting off of NO_2 . Increase in either size of charge or duration of reaction leads to increased secondary reaction which is evidence for the strong effect of primary products on the further course of reaction.

The two series of experiments combine to show that decomposition of cellulose nitrate essentially begins by splitting off of nitrogen dioxide in the 2- and 3-positions followed by reaction of the NO_2 split off with the residue and reaction products with ultimate disruption of the molecule.

A general mechanism for the decomposition of the vicinal dinitrates may be written



Kuhn and DeAngelis,⁸ for example, found that this type of mechanism predominated in the decomposition of the vicinal dinitrites in the gaseous state. If it is considered that the limited mobility and low collision frequency in cellulose nitrate is comparable to the gaseous state, one may conclude from the experimental evidence presented showing

(8) L. P. Kuhn and L. DeAngelis, *J. Am. Chem. Soc.*, **76**, 328 (1954).

the initial splitting off of NO_2 from the second and third position on the cellulose nitrate, that the decomposition of the latter follows a mechanism similar to that proposed for the vicinal dinitrates. In general, this agrees with the mechanism discussed by Wolfrom.⁹ With this as the first stage in the decomposition, the second stage would be a heterogeneous solid-gas interaction of the newly formed nitrogen dioxide with equally new aldehyde groups. A third stage follows quickly with the decomposition of the 6-nitrate group which may have been initially proceeding at a slow rate but becomes accelerated by the likely exothermicity of stage 2. On the basis of experience with simpler nitrate esters,¹⁰ the decomposition of the 6-nitrate group should involve splitting off of NO_2 , followed by splitting off of formaldehyde, followed by further rearrangement of the residue with fission of the glucoside structure.

The presence of hydroxyl which was indicated in the infrared spectroscopic analysis of solid residues may point to some reaction beyond the stages considered or otherwise be evidence for the partial validity of an alternate mechanism, namely, abstraction of hydrogen by the intermediate alkoxy radical. Carbonyl, likewise observed, is used up in secondary reaction and can thus accumulate only slowly in the residue.

The following sequence of chemical reactions summarizes the main stages deduced which seem to represent at least the initiating sequence in an over-all process of decomposition which rapidly assumes further complexity: (1) decomposition of the 2,3-nitrate groups by the general mechanism of vicinal dinitrates; (2) reaction of NO_2 with the newly formed aldehyde groups at positions 2 and 3; (3) accelerated decomposition of the 6-nitrate groups to give NO_2 , formaldehyde and a further rearrangement of the residue involving rupture of the cellulose chain.

Acknowledgments.—The authors are especially indebted to R. A. Friedel, A. G. Sharkey and the staff of the Mass Spectrometer Section for their assistance and cooperation. The suggestion to use N^{15} in the 6-nitrate group as a means of studying the decomposition mechanism originated with Lester P. Kuhn of the Ballistic Research Laboratories, Aberdeen Proving Ground, Maryland. Ralph Klein and Morris Mentser participated in early discussions and the preliminary experimental work.

(9) M. L. Wolfrom, J. H. Frazer, L. P. Kuhn, E. E. Dickey, S. M. Olin, D. O. Hoffman, R. S. Bower, A. Chaney, Eloise Carpenter and P. McWain, *ibid.*, **77**, 6573 (1955).

(10) G. K. Adams and C. E. H. Bawn, *Trans. Faraday Soc.*, **45**, 494 (1949); L. Phillips, *Nature*, **160**, 753 (1947); **165**, 564 (1950); J. B. Levy, *J. Am. Chem. Soc.*, **76**, 3254, 3790 (1954); Peter Gray, *Trans. Faraday Soc.*, **51**, 1370 (1955).

THE SOLUBILITY OF TRISTEARIN IN ORGANIC SOLVENTS¹

BY C. W. HOERR AND H. J. HARWOOD

Contribution from the Research Division of Armour and Company, Chicago, Illinois

Received November 7, 1955

The solubility of tristearin has been determined quantitatively in hexane, benzene, carbon tetrachloride, chloroform, ethyl acetate, acetone and ordinary unhydrogenated cottonseed oil. The solubility of this triglyceride is decreased markedly by increased polarity of the solvents. In the presence of solvents, tristearin exhibits three distinct solubility curves corresponding to the three crystalline forms established previously by melting point determinations and X-ray measurements. The occurrence of a fourth crystalline form reportedly melting at 70° is not confirmed by the solubility studies.

The polymorphic behavior of the triglycerides has received more attention than all other aliphatic compounds. Probably because of differences in reported results, particular emphasis has been placed on investigation of the saturated, single-acid triglycerides. Malkin,²⁻³ Lutton⁴⁻⁶ and others^{7,8} have reported numerous attempts to characterize the several crystalline modifications of these triglycerides by correlating their observed melting points with the X-ray diffraction measurements of the respective crystal lattices. Until recently, there has been some question as to whether three or four basic configurations of triglycerides occur, and the various investigators have differed further over correlation of observed melting points with the respective crystal forms revealed by the X-ray diffraction studies. It now appears that three distinct crystal forms of the saturated, single-acid triglycerides have been established quite definitely.^{9,10}

With the exception of a report on solubilities in aceto- and butyroglycerides,¹¹ no solubility studies comparable to those on other aliphatic compounds have been reported for the triglycerides. This paper reports the solubility of tristearin in hexane, benzene, carbon tetrachloride, chloroform, ethyl acetate, acetone and ordinary unhydrogenated cottonseed oil. The observed polymorphic behavior is correlated with the known thermal characteristics and crystalline structure of tristearin.

Experimental

The tristearin used in this investigation was prepared by Dr. R. R. Allen by the interesterification of triacetin with highly purified methyl stearate using sodium methoxide as the catalyst. The product was recrystallized repeatedly from acetone.

Cooling and heating curves were obtained by the usual

(1) Presented before the Division of Paint, Plastics and Printing Ink Chemistry at the 128th Meeting of the American Chemical Society, Minneapolis, Minn., September, 1955.

(2) (a) T. Malkin, *J. Chem. Soc.*, 2796 (1931). (b) C. E. Clarkson and T. Malkin, *ibid.*, 985 (1948).

(3) T. Malkin, "Glyceride Polymorphism," "Progress in the Chemistry of Fats and Other Lipids," Vol. II, Academic Press, Inc., New York, N. Y., 1954.

(4) E. S. Lutton, *J. Am. Chem. Soc.*, **67**, 524 (1945).

(5) E. S. Lutton, *ibid.*, **70**, 248 (1948).

(6) E. S. Lutton, F. L. Jackson and O. T. Quimby, *ibid.*, **70**, 2441 (1948).

(7) A. E. Bailey, M. E. Jefferson, F. B. Krieger and S. T. Bauer, *Oil and Soap*, **22**, 10 (1945).

(8) L. J. Filer, Jr., S. S. Sidhu, B. F. Daubert and H. E. Longenecker, *J. Am. Chem. Soc.*, **68**, 167 (1946).

(9) O. T. Quimby, *ibid.*, **72**, 5064 (1950).

(10) E. S. Lutton, *ibid.*, **77**, 2646 (1955).

(11) T. L. Ward, A. T. Gros and R. O. Feuge, *J. Am. Oil Chemists' Soc.*, **32**, 316 (1955).

procedure used in this Laboratory.¹² Fifteen-gram samples of tristearin were placed in a jacketed Pyrex test-tube equipped with a mercury thermometer and Nichrome wire stirrer. The thermometer which was graduated in 0.1° intervals had been calibrated by the National Bureau of Standards. The stirrer was actuated uniformly by means of an oscillating device operated by an electric motor controlled by a Variac transformer. Samples were stirred during cooling only until crystals appeared; the samples were not stirred

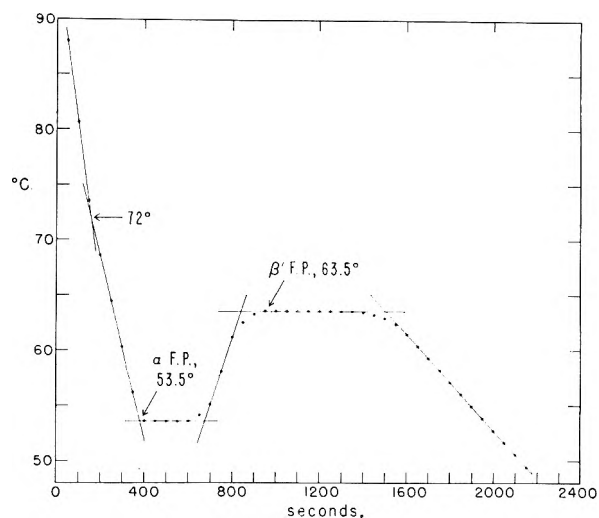


Fig. 1.—Cooling curve of tristearin showing plateaus at the α and β' freezing points.

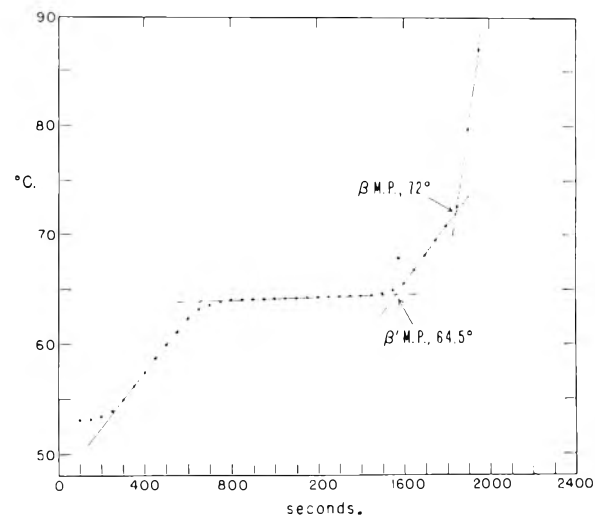


Fig. 2.—Heating curve of tristearin after minimum holding time showing a plateau at the β' melting point and a change of slope at the β melting point.

(12) C. W. Hoerr, R. A. Reck, G. B. Coreoran and H. J. Harwood, *This Journal*, **59**, 457 (1955).

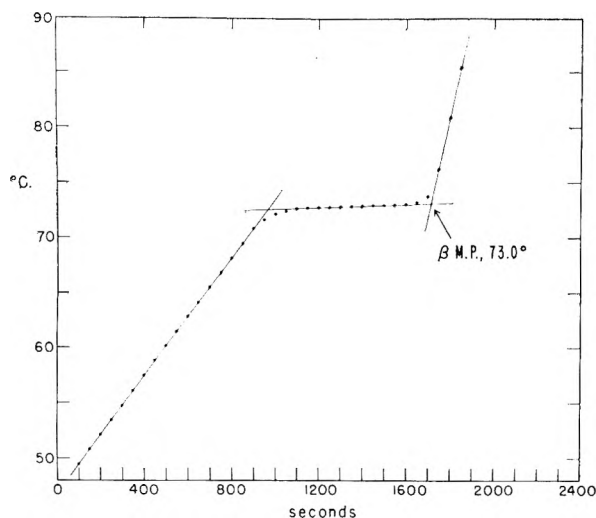


Fig. 3.—Heating curve of tristearin after extended holding time showing only a plateau at the β melting point.

during heating to avoid channeling. For cooling curve determinations the jacketed tubes were placed in a water-

curves the bath was held at about 90°. Time was measured by means of an electrical timer, and temperatures were recorded at 100 sec. intervals throughout the cooling and heating experiments. The time-temperature curves obtained by this procedure are shown in Figs. 1-3.

The solubility of tristearin was determined by the usual methods employed in this Laboratory.^{12,13} For solubilities in the higher temperature ranges, particularly near the boiling points of the solvents, weighed amounts of solute and solvent were sealed in small glass tubes which were rotated slowly in a 4-l. water-bath. Temperatures of the bath were increased gradually or held constant at desired levels by means of a special Glas-Col heating mantle.

For solubility measurements in the lower temperature ranges, weighed amounts of the components were put into jacketed test-tubes similar to those used for the cooling and heating curve determinations. The temperature of the samples was raised or lowered by the use of water-baths of appropriate temperatures.

In both solubility procedures, temperatures at which visible changes occurred in the samples were recorded. The solubility curves shown in Figs. 4-7 were obtained by plotting solution temperatures against weight per cent. of solute.

The solvents were similar to those used in the previous solubility studies. They were of the best grade commercially available and were freshly distilled through a Stedman-packed column before use. The cottonseed oil used was a

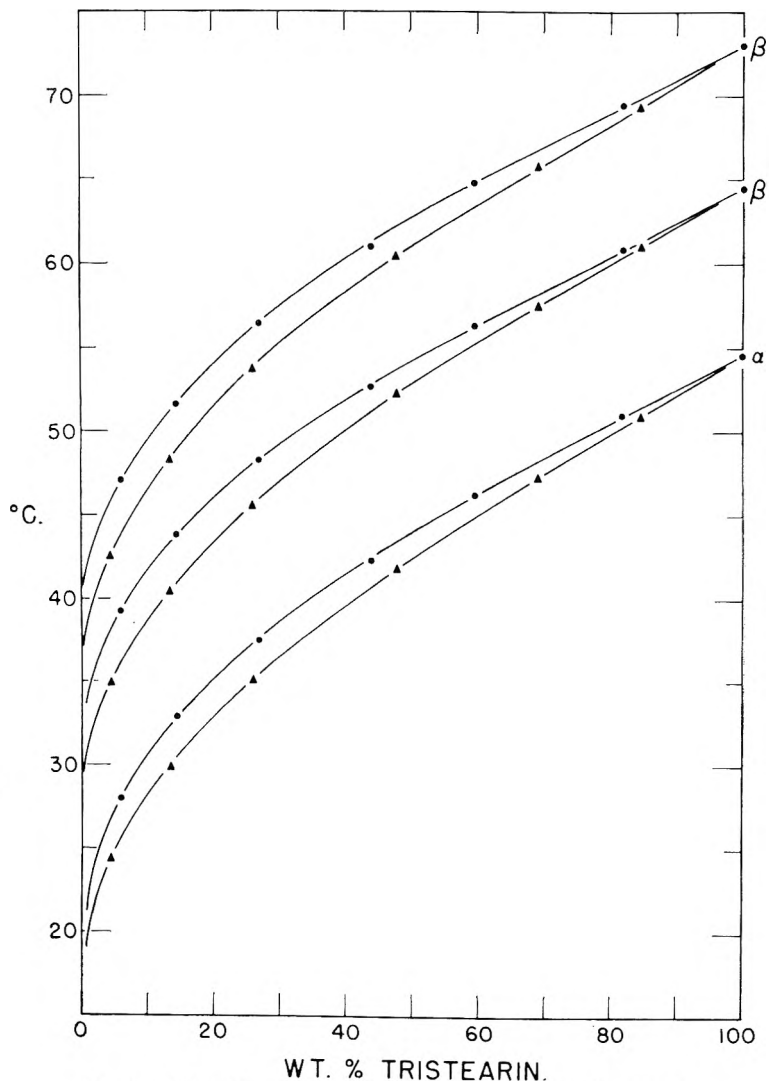


Fig. 4.—Solubility of tristearin in hexane ● and in benzene ▲.

bath maintained at about 40° after initially heating the samples to 100° to destroy all crystal nuclei.⁹ For heating

(13) P. L. DuBrow, C. W. Hoerr and H. J. Harwood, *J. Am. Chem. Soc.*, **74**, 6241 (1952).

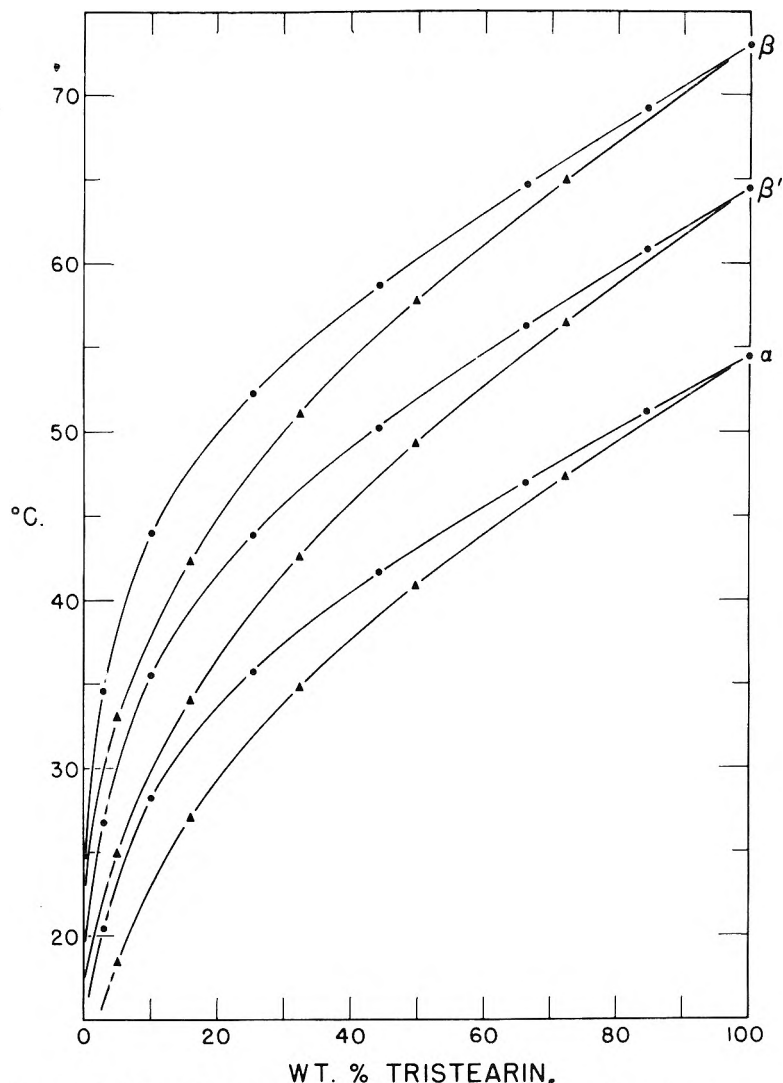


Fig. 5.—Solubility of tristearin in carbon tetrachloride ● and in chloroform ▲.

high-grade, refined, winterized, unhydrogenated oil obtained from regular plant production.

Results and Discussion

The behavior of tristearin during cooling and heating shown in Figs. 1-3 is generally typical of long-chain compounds which exhibit more than one crystalline form.¹⁴ The curves for tristearin are quite similar to those obtained for other triglycerides.⁶

The cooling curve in Fig. 1 shows that tristearin begins to crystallize from the liquid in the α-form. In a matter of minutes, transformation causes the temperature of the sample to rise to the β' freezing point and crystallization in this latter form continues until the sample has solidified.

If the sample is heated as soon as crystallization is essentially complete, behavior shown by the curve in Fig. 2 is observed. The initial portion of the curve below 64.5° represents melting of mixtures of the α- and β'-form; between 64.5 and 72° mixtures of β' and β are melting. Insufficient quantities of the β-form were present in this sample to produce a 72° plateau.

If, however, a sample is held for an hour or two at temperatures a few degrees below the β' freezing point (or overnight at room temperature), a curve like that in Fig. 3 is obtained upon heating. Under these conditions, transformation from the β'- to the β-form is complete, and only the melting of this latter form is observed.

It will be noted in Fig. 1 that there is an inflection in the cooling curve in the neighborhood of 72°. This inflection, which is reproducible, suggests that the energy of the system has been reduced to such an extent that there occurs some sort of preliminary orientation which restricts the free rotation of the molecules in the liquid state. No visible crystallization occurs during cooling until the α freezing point is reached.

The following freezing and melting points of the crystalline forms of tristearin were estimated from the cooling and heating curves:

Form	F.p., °C.	M.p., °C.	Lit. m.p., °C. ^{9,10}
α	53.5	..	54.0
β'	63.5	64.5	64.5
β	..	73.0	73.0

(14) E. J. Hoffman, C. W. Hoerr and A. W. Ralston, *J. Am. Chem. Soc.*, **67**, 1542 (1945).

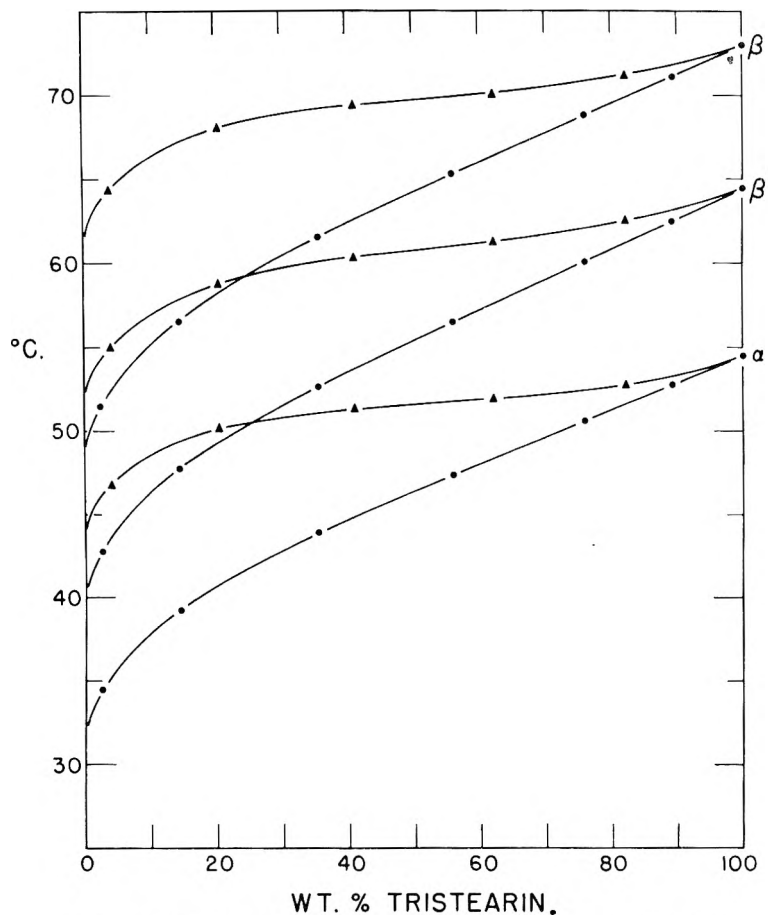


Fig. 6.—Solubility of tristearin in ethyl acetate ● and in acetone ▲.

The α freezing point determined by this method is about 0.5° lower than the reported α "cloud point."^{9,10} The other values indicate that the purity of the tristearin used in these experiments was equal to that reported elsewhere.^{9,10}

The solubility curves in Figs. 4-7 show that tristearin is more soluble in the non-polar solvents than in those of higher polarity. It is somewhat more soluble in the chlorinated hydrocarbons than in hexane or benzene. Its solubility in cottonseed oil corresponds quite closely to that in the simple ester, ethyl acetate. In the highly polar solvents, such as methanol and acetonitrile, the solubility of tristearin is so limited (determined approximately as 1-2% in boiling solvent) that its systems with these solvents exhibit immiscible liquid regions over most of the concentration range at temperatures above the β melting point.

The noteworthy feature of these solvent systems is the fact that tristearin exhibits a distinct solubility curve for each of its three crystalline forms in each of the solvents investigated. In every case, the triglyceride precipitated from isotropic solution at temperatures on the curve for the α -form. If the mixtures are heated slowly, the solute gradually dissolves until almost clear solution is obtained in the neighborhood of the β' curve. As temperatures on this curve are approximated, however, the material abruptly reprecipitates in its intermediate-melting form. As heating is continued this material gradually redissolves until

final solution is obtained at temperatures on the β curve.

The α or β' crystals which are precipitated upon cooling can be caused to dissolve to isotropic solution at temperatures on their respective solubility curves by placing the mixtures immediately in baths of appropriate temperatures. If the precipitated crystals are maintained for some time (a half-hour or more) at temperatures below the β' curve, no apparent solution occurs upon heating until temperatures of the β curve are attained.

Visible observation of the crystals during precipitation from solution seems to confirm reports that the α form is definitely crystalline^{9,10} rather than "vitreous".³ This lowest-melting form precipitates as transparent platelets which transform within a short time to a visibly more opaque form.

It was found that by seeding isotropic solutions which were maintained at appropriate predetermined temperatures, tristearin could be induced to precipitate in either the β' - or β -forms. As in the case of experiments in the absence of solvent,⁹ this proved to be a difficult and tedious procedure. In all cases, the higher-melting forms were obtained far more readily by transformation of the lower-melting forms.

As was observed in the cooling curve experiments, the crystalline transformations of tristearin in the presence of solvents always proceed irreversibly from α - to β' - to β -forms. The rate of transformation appears to be much the same in all

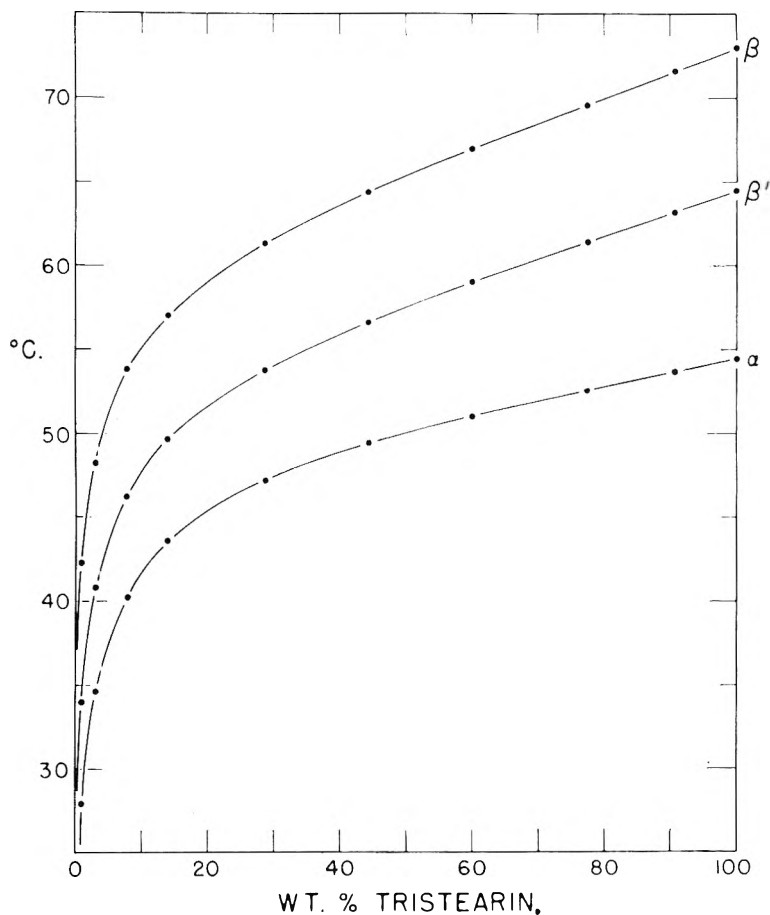


Fig. 7.—Solubility of tristearin in cottonseed oil.

the solvents, and does not seem to be altered appreciably by change of concentration of the solute.

The solubility studies confirm clearly that tristearin exhibits three distinct crystalline forms which have already been characterized by unique lattice spacings. The three forms evidenced by

the solubility determinations possess melting points which coincide with those which have been established by other methods.^{9,10} The occurrence of a form melting at 70°, designated β' by Malkin,³ is not confirmed. If this form exists, it is highly probable that the solubility studies would have evinced some indication of the fact.

INFRARED STUDIES ON SYNTHETIC OXYGEN CARRIERS¹

BY KEIHEI UENO² AND ARTHUR E. MARTELL

Contribution from the Chemical Laboratories of Clark University, Worcester, Mass.

Received December 15, 1955

Infrared absorption frequencies from 4000 to 400 cm^{-1} are reported for bis-salicylaldehydeethylenediimine and its Cu(II), Ni(II), VO(II) and Co(II) chelates. Frequencies are assigned in most cases to bond or group vibrations, and the change of spectra which accompanies coordination with a metal ion is discussed in connection with the structural change which occurs. The spectral changes of inactive, active and oxygenated samples of the Co(II) chelate are discussed. The following bands are tentatively assigned to the metal specific vibrations: a band at 1298 cm^{-1} of the vanadyl chelate to V-O stretching, four bands in the 636-500 cm^{-1} region of the metal chelates to metal-ligand bonds, and a band at 565 cm^{-1} of oxygenated Co(II) chelates to Co-O stretching.

As an extension of the study previously reported³ on the spectra of bisacetylacetonethylenediimine chelates as models of the oxygen carrying chelate compounds, it was decided to carry out a similar study on bis-salicylaldehydeethylenediimine-Co(II), which is known to be an oxygen carrier. The reversible oxygen absorption property of this chelate compound was discovered first by Tsumaki.⁴ Calvin and co-workers later investigated the kinetics of oxygenation,⁵ polarographic reduction potentials,⁶ and the X-ray crystallography⁷ of this substance and related metal chelates. Diehl and co-workers⁸ have investigated reversible oxygenation of this and many related compounds. Tsumaki⁴ has also studied the change of absorption spectra in the visible and ultraviolet regions before and after the oxygenation. No infrared absorption studies of this or related compounds have been reported thus far. The purpose of the present work is to study the infrared absorption spectra of bis-salicylaldehydeethylenediimine-Co(II) during the course of oxygenation, along with the infrared spectra of the ligand and its Ni(II), Cu(II) and VO(II) chelates.

It is known that the cobalt(II) chelate exists in several forms, some of which are capable of reversible oxygen absorption, and some of which are inactive toward oxygen.⁹ All of these modifications were prepared for infrared study. Although the Ni(II) and Cu(II) chelates are devoid of reversible oxygen carrying property, all these chelates including the Co(II) chelate are known to form square-planar coordination compounds, and were also studied to provide information on the structure of this type of metal chelate. The vanadyl chelate was also investigated since the vanadium-oxygen bond might provide an interesting comparison with the oxygenated form of bis-salicylaldehydeethylenediimine-Co(II).

Experimental

Preparation of Materials.—Bis-salicylaldehydeethylenedi-

(1) This research was supported by a grant from National Institute of Health, U. S. Public Health Service.

(2) Postdoctoral Research Fellow, Clark University, 1953-1955. Dojindo & Co., Kumamoto-shi, Japan.

(3) K. Ueno and A. E. Martell, *THIS JOURNAL*, **59**, 998 (1955).

(4) T. Tsumaki, *Bull. Chem. Soc., Japan*, **13**, 252 (1938).

(5) C. H. Barkeley and M. Calvin, *J. Am. Chem. Soc.*, **68**, 2257 (1946).

(6) A. E. Martell and M. Calvin, "Chemistry of the Metal Chelate Compounds," Prentice-Hall, Inc., New York, N. Y., 1952, p. 350.

(7) E. W. Hughes, C. H. Barkeley and M. Calvin, OEM Sr-279, March 15, 1944.

(8) H. Diehl, *et al.*, *Iowa State Coll. J. Sci.*, **22**, 165 (1948), and 13 papers preceding.

(9) R. H. Bailes and M. Calvin, *J. Am. Chem. Soc.*, **69**, 1886 (1947).

imine and its Ni(II) and Cu(II) chelates were kindly prepared by Miss H. Hyytiäinen of this Laboratory according to the method described by Pfeiffer.¹⁰ The corresponding vanadyl chelate was prepared according to Bielig and Bayer.¹¹ The inactive form of the Co(II) chelate was first prepared from ethylenediamine, salicylaldehyde and cobaltous acetate in ethanol according to the procedure described by Calvin.⁵ Two samples of active form were prepared from the red inactive crystals, one by heating the pyridinate and the other by heating the chloroformate of the Co chelates *in vacuo*. Bis-salicylaldehyde-1,2-propylenediimine-Co(II) was also prepared by an analogous method from 1,2-propylenediamine, salicylaldehyde and cobaltous acetate.

Reversible Oxygenation Process.—Oxygenation was carried out by passing purified dry oxygen into a small tube containing finely powdered active compound. Oxygenation was continued until the sample absorbed 4.94% of its weight,⁹ which corresponds to two moles of chelate to one mole of oxygen. The original brown color of the active compound changed to black after oxygenation. The removal of oxygen was accomplished by heating the sample at 100° under reduced pressure. Deoxygenation proceeded quite rapidly and was accompanied by the reverse color change. Of all the metal chelates prepared, only bis-salicylaldehydeethylenediimine-Co(II) was found to be capable of reversible oxygenation.

Measurement of Infrared Absorption Spectra.—Infrared absorption spectra were measured with a Perkin-Elmer Model 21 double beam recording infrared spectrophotometer. Sodium chloride optics were used in the region from 4000 to 650 cm^{-1} , and an interchangeable potassium bromide prism assembly was used in the region from 650 to 400 cm^{-1} . The potassium bromide pellet technique was used for the measurement of all samples. Although it was necessary to evacuate the die in order to obtain a transparent pellet, the evacuation during the short period of preparation was found to give no appreciable effect on the oxygenated sample. Inactive, active and active oxygenated forms of bis-salicylaldehydeethylenediimine-Co(II) were also studied in chloroform solution.

The significant spectral lines below 1700 cm^{-1} which were found for the compounds studied are reported in Table I, together with the assignments that were possible in each case.

Discussion

For purposes of discussion, the experimental results may be divided into two general classifications; 1, the change of infrared absorption spectra of bis-salicylaldehydeethylenediimine which occurs on metal chelation, and 2, the change of infrared absorption spectra of the active Co(II) chelate during the course of reversible oxygenation. These will be discussed separately.

Infrared Absorption Spectra of Bis-salicylaldehydeethylenediimine Chelates.—In accordance with the structure of the ligand I, one would expect to find a hydroxyl stretching vibration in the 3300 cm^{-1} region of the ligand, but not the spectra of

(10) P. Pfeiffer, E. Breith, E. Lubbe and T. Tsumaki, *Ann.*, **503**, 84 (1933).

(11) H. J. Bielig and E. Bayer, *ibid.*, **580**, 135 (1953).

TABLE I

INFRARED ABSORPTION SPECTRA OF BISALICYLALDEHYDEETHYLENEDIIMINE AND ITS METAL CHELATE COMPOUNDS

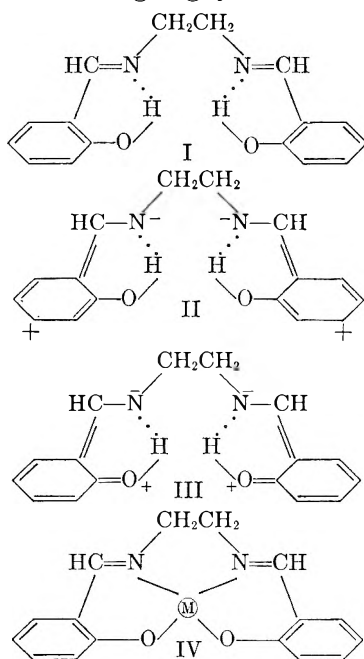
Ligand	Ni(II)	Cu(II)	Metal chelates			Co(II) Active	Active oxygenated	Assignments
			VO(II)	Inactive				
1633vs		1645vs	1631vs				} Phenyl ring. Conjugated phenyl ring	
1612s	1621vs	1629vs	1615vs	1628s	1625m ^a	1631s		
1579vs	1600s	1600s	1600vs	1608vs	1607vs	1604vs		
				1545m		1547m		
1526m	1536s	1532s	1541s	1532s	1533s	1534s	C:N stretching	
1499vs							Phenyl ring	
1461s	1465s	1469m	1470s	1472m	1471m	1471s	-CH ₂ - deformation	
	1451s	1449vs	1447vs	1452vs	1446vs	1452vs		
				1434m				
				1398vw				
	1384m	1388w	1391s	1386w	1384w	1386w		
1373m								
	1345m	1347m		1350m	1348m	1349m		
1340w								
	1330m	1333m	1336m	1328m	1333m	1329m		
1317m								
	1313m	1305m		1308w	1309s	1310w		
			1298s				V-O stretching	
1293m				1290m	1290m	1292w		
1282s							O-H . . . in H bonded rings	
						1274m		
				1258vw	1260vw			
				1249vw	1251vw	1257w		
1248m	1238w	1237m	1239w	1236m	1237m	1236m	} <i>o</i> -Disubstd. phenyl	
1220m				1221m	1221m	1220m		
				1206m		1207m		
1200m	1199m	1191s	1200m	1197m	1201m	1198m		
				1150w				
1149vs	1143m	1140m	1148m	1140m	1141m	1141m		
1113m	1125s	1125s	1128m	1126s	1127s	1127s	} <i>o</i> -Disubstd. phenyl	
1105m								
	1087m	1085m	1090m	1087m	1087m	1087m	} { C-O stretching in the chelate rings	
		1050m	1050w	1052m	1052w	1053m		
							<i>o</i> -Disubstd. phenyl	
1041vs								
1020s	1024m	1025m	1029w	1025w	1025w	1026w	} <i>o</i> -Disubstd. phenyl	
980m	987vw	976m	980s	974w	985w	970w		
971m				968w	974w			
	948vw	952w		952m	952w	953m		
				945w	945w	946w		
935w		930vw		922vw	941m			
898m	901m	903m	904m	903m	903m	904m		
855s ^b	850vw	852w	857m	851m	851m	851m		
	843vw	847w		845w	845w	845w		
					832w			
772s	798w	786w	798s	792w	798w	795w		
755vs	748m	747m	757s	757m	757m	757m	} <i>o</i> -Disubstd. phenyl	
				751s	752s			
749vs	741m	739m	741m	748s	745s	747s		
741vs				740m	740m	740m	} <i>o</i> -Disubstd. phenyl?	
	732m	732m		730s	730s	730s		
					725s			
					667w			
647m	665w	647w	646m	658w	658w	659w		
	630w	636w	628s	626w	627m	627m	} Metal chelate ring	
		617m		620w	606m	620m		
	598w	598w	597m	598w	598w	593m	} Metal chelate ring	
		578m	575w					
		570m						
						565w	Co-O stretching vibration	
562m								
558m								

TABLE I (Continued)

Ligand	Metal chelates			Assignments			
	Ni(II)	Cu(II)	VO(II)	Inactive	Co(II) Active	Active oxygenated	
	550vw	547vw		552vw	550vw	548vw	} Metal chelate ring
	520vw	500m		510vw	514w	515w	
486m	486vw	467m	475m	473w	480w		
473m	468w	463m	461m	465w	463m	465m	
433w	430w	440w				433vw	
418vw	418vw	418vw	412w	418vw	422w	413w	
	407w						

^a Shoulder. ^b H bonded out-of-plane OH bonding.

the metal chelates. No such an absorption band was found, but a broad band of intermediate intensity appeared at 2600 cm^{-1} . Since no corresponding band can be observed in the absorption spectra of metal chelates, this broad absorption is assigned to O-H stretching vibration. It is known that strong hydrogen bonding causes a shift of the O-H stretching band at the lower frequency and causes the broadening of the band.¹² This is especially true if the hydrogen bonding takes place as part of a resonating ring system.¹³



If one considers the resonance contributions of the polar structures II and III, it would be reasonable to expect strong hydrogen bonding in the ligand, and the assignment of the broad band at 2600 cm^{-1} to the hydrogen bonded O-H stretching vibration therefore seems reasonable.

Because of the resonance in the hydrogen-bonded ring systems, it is necessary that each six-membered ring including the replaceable hydrogen be planar and coplanar to the phenyl ring to which this ring system is fused. However, the two bicyclic ring systems cannot be in the same plane because of steric hindrance and the electrostatic repulsions of N...H-O groups. These considerations are analogous to those previously reported for bisacetylacetonediimine.³ In the

(12) L. J. Bellamy, "The Infrared Spectra of Complex Molecules," John Wiley and Sons, Inc., New York, N. Y., 1954, p. 86.

(13) R. S. Rasmussen, D. D. Tunnicliff and R. R. Brattain, *J. Am. Chem. Soc.*, **71**, 1068, 1073 (1949).

chelates of Cu(II), Ni(II) and Co(II), both rings can be fixed in the same plane without steric hindrance by the central metal, which provides square planar coordination bonds to the tetradentate ligand, as is shown in the formula IV. In the vanadyl chelate, similar coplanarity of the metal chelate is also necessary, with the exception of the oxygen-vanadium bond which is normal to the plane of the molecule, as will be discussed later. The coplanarity of metal chelates of bisacetylaldehydeethylenediimine is further supported by the fact that the cobalt(II) chelate was found to be coplanar through X-ray study.⁷

Several absorption bands between 2700 and 3200 cm^{-1} , which appear at the same position for both ligand and metal chelates, can be assigned to C-H stretching vibrations of CH, CH₂ and aromatic CH bonds.

No significant absorption can be found either in ligand or in the metal chelates below this region down to 1650 cm^{-1} , and the main absorption bands appear from 1650 to 450 cm^{-1} , the lower frequency limit of potassium bromide optics. The absorption bands in this region which are listed in Table I, can be classified roughly into three groups: the absorption bands which are common to both ligand and the metal chelates, the absorption bands which are characteristic of the ligand, and the absorption bands which are characteristic of the metal chelates.

As is clear from the formulas of the ligand I and of the metal chelates IV, absorptions resulting from the aromatic rings can be expected for all compounds. Three bands of very strong intensity in the ligand at 1633, 1612 and 1579 cm^{-1} , and the corresponding bands in the metal chelates with the exception of Ni and Co chelates (for which the first two bands are too close to be resolved), are assigned to the C=C stretching vibration of phenyl rings. The last band at 1579 cm^{-1} , which shifts to slightly higher frequency by metal chelation, is probably due to the vibration of phenyl rings conjugated with carbon-nitrogen double bonds. Another phenyl absorption band should occur near the 1500 cm^{-1} region, and a very strong band of the ligand at 1499 cm^{-1} can be assigned to this absorption. However, no corresponding band can be found in the metal chelates. Since the intensity of 1500 cm^{-1} absorption band of the phenyl ring was reported to fluctuate very widely,¹⁴ the corresponding band of metal chelates may be too weak to be observed.

Several additional bands in the lower frequency region also may be assigned to the phenyl ring

(14) Reference 12, p. 62.

vibrations. Two absorptions of intermediate intensity at 1248 cm^{-1} and at 1113 cm^{-1} in the ligand, and the corresponding bands in the metal chelates, are assigned to *o*-disubstituted phenyl rings. Similarly two bands at 1020 and 980 cm^{-1} in the ligand and the corresponding bands in the metal chelates are assigned to the same grouping. One more band in this region at 1050 cm^{-1} , which is too weak to be observed in the ligand and Ni chelate, is perhaps due to *o*-disubstituted phenyl rings.

The *o*-disubstituted aromatic ring is also known to give rise to absorptions corresponding to C-H out-of-the-plane deformation vibrations. The very strong bands of the ligand at 755, 749 and probably at 741 cm^{-1} , and the analogous two or three bands of the metal chelates can be assigned to this mode of vibration.

In the double bond region, there is an intermediate-intensity band common to all compounds which appears at 1526 cm^{-1} for the ligand and is shifted to slightly higher frequency with increasing intensity for the metal chelates. The absorption due to non-conjugated C=N stretching vibration is usually found in the region of 1690-1640 cm^{-1} , and it is known to shift to the lower frequency with conjugation. The difference of about 100 cm^{-1} cannot be considered as merely a conjugation effect, however, in view of the wide differences in bond strength and charge distribution between aromatic rings and the H-bonded ligand rings and metal-chelate rings being considered here. The hydrogen-bonded ring systems of the compounds under investigation are greatly stabilized by conjugation and the situation would thus be intermediate between simple conjugation and that which exists in aromatic ring systems. Therefore the 1526 cm^{-1} band is tentatively assigned to the absorption originating from C=N stretching vibration of the conjugated ring system.

Next to the double bond region, a band of strong or intermediate intensity which is fairly stable in position from the ligand to the metal chelates, is found in the region of 1461-1472 cm^{-1} . This band is assigned to the C-H deformation vibration of the ethylene bridge.

A strong ligand band at 1282 cm^{-1} , having no corresponding bands in the metal chelates, is assigned to hydrogen-bonded O-H in-plane bending vibration. This assignment is supported by disappearance of the band when the hydroxyl hydrogen is replaced by a metal, and by the fact that similar O-H absorptions were observed in the region of 1290-1280 cm^{-1} for bisacetylacetonethylenediimine and related compounds.³ An additional band of strong intensity at 855 cm^{-1} is similarly assigned to the hydrogen bonded out-of-the-plane O-H bending vibration, since the corresponding band is observed in 850-800 cm^{-1} region for bisacetylacetonethylenediimine and related compounds.³

Another characteristic absorption of intermediate intensity is found at 1105 cm^{-1} in the ligand, with a corresponding band of the metal chelates in the lower frequency region of 1090-1085 cm^{-1} . This absorption is assigned to the C-O stretching

vibration of the hydrogen-bonded ring system of the ligand. The shift to the lower frequencies in the metal chelates can be explained by the increased mass of metal linked to oxygen as well as to possible weakening of C-O linkage. It is interesting to note that the increasing order of shift from the original position follows the order of increasing mass of the metal, *i.e.*, V, Co, Ni and Cu, and parallels the order of decreasing basicity for the metals Co, Ni and Cu. Although there are no data on stability constants of these metal chelates, Pfeiffer¹⁵ found the relative stabilities of some metal chelates of this ligand to follow an order of $\text{Cu} > \text{Ni} > \text{Zn} > \text{Mg}$. In general, the stabilities of metal chelate compounds has been known to follow the general order $\text{Cu} > \text{Ni} > \text{Co}$.¹⁶ Therefore, if one assumes the shift of the C-O absorption band to follow the order of stabilities of the metal chelates, it can be seen that the strengthening of the metal-oxygen bonding will be accompanied by a decrease in C-O bond strength.

Several absorption bands were found to be characteristic of the metal chelates. It is to be expected that there would be a change in the spectra as the result of the influence of coordination on the nature of the ligand bonds not directly attached to the metal, as well as some additional bands arising from the metal-ligand vibrations. These metal-ligand absorptions should appear in the lower frequency region as was found in the case of bisacetylacetonethylenediimine-metal chelates,³ for which three metal-specific absorptions were observed in the region between 668 and 480 cm^{-1} . Thus two weak absorption bands of the metal chelates of bisalicylaldehydeethylenediimine at 636-626 cm^{-1} and 593-598 cm^{-1} are assigned to the metal-specific vibrations. Two additional absorptions at 547-552 cm^{-1} and at 520-500 cm^{-1} , which are usually very weak, are also assigned to metal-donor linkages. Since, however, there are no apparent relationships between the shift of metal-specific absorptions and the kind of metals, these bands must result from rather complicated modes of vibration and should be assigned to the vibrations of the central metal chelate rings rather than to specific metal-ligand bonds.

Some irregularities are found in the metal-specific absorptions of the vanadyl chelate. An absorption at 628 cm^{-1} is unusually strong and two bands at lower frequencies are missing, and are probably too weak to be observed. The irregularities in the absorption spectra of vanadyl chelate are found not only in the metal-specific absorptions, but also in the higher frequency regions. An ordinarily medium or weak metal chelate absorption at 1384-1391 cm^{-1} becomes very strong in the vanadyl chelate. A similar irregularity is observed in the absorption band at 1313-1298 cm^{-1} . This band is of intermediate intensity but becomes strong in the vanadyl chelate, and has the lowest frequency of this group of bands. This absorption band, however, may be the result of the

(15) P. Pfeiffer, H. Thielert and H. Glaser, *J. prakt. Chem.*, **152**, 145 (1939).

(16) D. P. Mellor and L. Maley, *Nature*, **159**, 370 (1947); **161**, 436 (1948).

superposition of two bands, a strong absorption band at 1298 cm.^{-1} , and a band of intermediate intensity which corresponds to the bands observed for the other metal chelates. It is interesting to note that a similar band, observed in the vanadyl chelates of tetraphenylporphine at 1337 cm.^{-1} , was assigned to the V-O stretching vibration.¹⁷

The central metal ion in the vanadyl chelates is known to have five coordinate bonds,¹⁸ four to the tetradentate ligand and one to the oxygen. Since the ligand has a planar structure, it is reasonable to assume that the direction of the vanadium-oxygen bond is normal to the plane of the ligand molecule, an arrangement which is shown schematically in Fig. 1. Since the steric configuration around van-

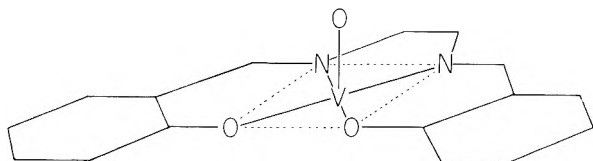


Fig. 1.—Steric configuration of bis(salicylaldehyde-ethylenediamine)-VO(IV).

adium is somewhat similar to that of the tetraphenylporphine vanadyl chelate,¹⁷ the absorption band of the vanadyl chelate at 1298 cm.^{-1} can reasonably be assigned to V-O stretching vibration. Taking this frequency value for this mode of vibration, one calculates the stretching force constant of this particular bond to be 12.0×10^5 dyne/cm. This value is about the same as that of the C=O stretching force constant ($k_{\text{C=O}}$ (acetone) = 12×10^5 dyne/cm.), and slightly lower than the value obtained for vanadyl tetraphenylporphine.¹⁷

Changes in Infrared Absorption Spectra in the Course of Reversible Oxygenation.—It has been shown already that not all crystalline forms of bis(salicylaldehyde)ethylenediamine-Co(II) are capable of reversible oxygenation, and that only special forms which are prepared by certain chemical process have well-developed oxygen carrying properties. Calvin and co-workers⁷ have attributed this property to the special arrangement of the metal chelate molecules in the crystal lattice.

The absorption spectra of inactive samples synthesized directly from salicylaldehyde, ethylenediamine and cobaltous acetate in ethanol, are different in some respects from the spectra of the active form. The most remarkable changes, illustrated in Fig. 2, were observed in the regions $1650\text{--}1600\text{ cm.}^{-1}$, $1350\text{--}1250\text{ cm.}^{-1}$, $975\text{--}925\text{ cm.}^{-1}$, $650\text{--}550\text{ cm.}^{-1}$ and $500\text{--}450\text{ cm.}^{-1}$. Since the active and inactive samples have the same chemical composition, and since there should be no difference in the structure of the chelate molecules, the difference of absorption spectra should be due to the different arrangements of molecules in the crystalline lattice.¹⁹

(17) K. Ueno and A. E. Martell (to be published elsewhere).

(18) M. M. Jones, *J. Am. Chem. Soc.*, **76**, 5995 (1954).

(19) It is known that differences in crystal structure may sometimes result in rather striking differences in the infrared spectra of otherwise identical substances, cf. H. Gilman "Organic Chemistry," Vol. 3, John Wiley and Sons, New York, N. Y., 1953, p. 139.

Two samples of active oxygen carriers prepared by different methods were also compared. When the spectra of bis(salicylaldehyde)ethylenediamine-Co(II) prepared from the pyridinate and that of the active form prepared from the chloroformate were compared, they were found to be identical.

A rather interesting finding is the difference of spectra of active and inactive forms in the $1650\text{--}1600\text{ cm.}^{-1}$ region. Two absorption bands of the inactive sample, with maxima at 1628 and 1608 cm.^{-1} , changed into single band in the active sample with a maximum at 1607 cm.^{-1} , with the first band submerged as a shoulder at around 1625 cm.^{-1} . However, in the case of bis(salicylaldehyde)-1,2-propylenediamine-Co(II), which is a homolog of the ethylenediamine derivative, and which has been known to be deficient of the oxygen carrying property, the spectra of the metal chelate synthesized directly from the components by the same method, and the spectra of sample prepared by heating the pyridinate *in vacuo*, are completely identical, with two absorption bands in the $1650\text{--}1600\text{ cm.}^{-1}$ region. Thus the additional methyl group attached to the ethylenediamine carbon bridge prevents the chelate molecules from forming the crystal lattice arrangement which is favorable for oxygenation. The difference in the absorption spectra of active and inactive chelates must therefore be due to a difference in crystal structure. This conclusion is further strengthened by comparison of the absorption spectra in chloroform solution. The spectra of both samples in $1650\text{--}1600\text{ cm.}^{-1}$ region were found to be exactly the same, with a single maximum at 1605 cm.^{-1} . Calvin⁷ also found polymorphism in the active and inactive forms through X-ray studies.

Remarkable changes in the absorption spectra resulting from oxygenation of active sample are illustrated in Fig. 2. These spectral changes may be due to the difference in the crystal structure before and after the oxygenation, as well as to the direct coordination of oxygen to cobalt and the secondary influences of oxygenation on the other bonds in the ligand.

It is noteworthy that the single band at 1607 cm.^{-1} with a shoulder at around 1625 cm.^{-1} , found in the active sample, splits again into two bands at 1631 and 1604 cm.^{-1} upon oxygenation. In general, the spectra of oxygenated samples are found to resemble more the spectra of the inactive chelates than those of the active unoxxygenated forms.

A few remarkable differences are observed in the regions $1350\text{--}1250\text{ cm.}^{-1}$ and $650\text{--}550\text{ cm.}^{-1}$. In the $1350\text{--}1250\text{ cm.}^{-1}$ region, a characteristic band of the active sample at 1309 cm.^{-1} decreases in intensity on oxygenation, remaining as a weak shoulder at the corresponding position and a new band of intermediate intensity appears at 1274 cm.^{-1} . In the $650\text{--}550\text{ cm.}^{-1}$ region, an additional band of weak intensity at 565 cm.^{-1} is observed in the oxygenated sample. Since the bonding between oxygen and cobalt cannot be very strong, and since the oxygen molecule is considered to bridge two cobalt atoms, the 565 cm.^{-1} band can reasonably be assigned to the stretching

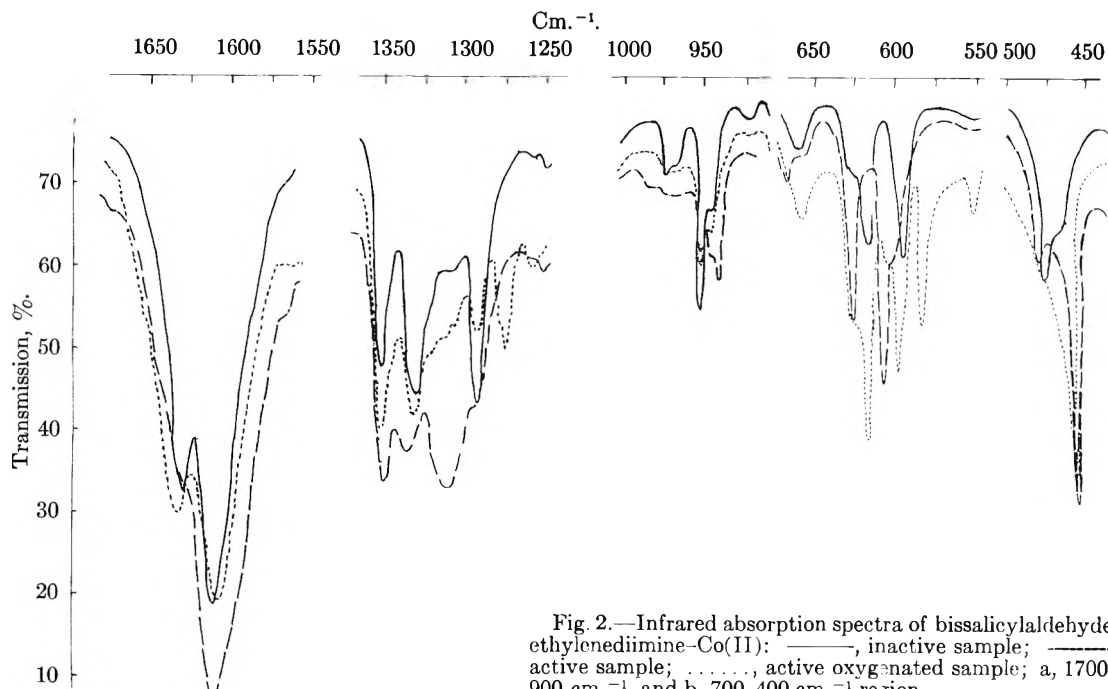


Fig. 2.—Infrared absorption spectra of bis(salicylaldehyde)ethylenediimine-Co(II): —, inactive sample; - - -, active sample;, active oxygenated sample; a, 1700-900 cm.^{-1} , and b, 700-400 cm.^{-1} region.

vibration of Co-O-O-Co linkages in the oxygenated crystals.

When the oxygenated sample was dissolved in chloroform, the evolution of oxygen was observed, and the resulting solution gave exactly the same spectra as those of inactive or active samples. The dissolution of an oxygenated sample results in the breakdown of the crystal lattice and preferential coordination of the chloroform molecule to the

cobalt(II) atom. As a result, the chloroform solution of the oxygenated form would be expected to have spectra identical to those of inactive or active samples.

The fact that the spectrum of the deoxygenated sample, which was prepared by heating the oxygenated sample in vacuum, was identical to that of the active sample, indicates the reversibility of the oxygenation process.

INTERMETALLIC COMPOUNDS BETWEEN LITHIUM AND LEAD. II. THE CRYSTAL STRUCTURE OF Li_8Pb_3 ¹

BY A. ZALKIN AND W. J. RAMSEY AND

University of California Radiation Laboratory, Livermore Site, Livermore, Cal.

D. H. TEMPLETON

Department of Chemistry and Radiation Laboratory, University of California, Berkeley, California

Received February 21, 1956

The compound Li_8Pb_3 has been characterized by single crystal and powder X-ray diffraction data. It is monoclinic, space group $C2/m$, with $a = 8.240$, $b = 4.757$, $c = 11.03$ Å., $\beta = 104^\circ 25'$, and $Z = 2$. There is a body centered cubic pseudocell with $a = 3.364$ Å. and containing two atoms. The structure consists of ordered substitution in these sites in such a way that one-third of the Pb atoms have 8 Li neighbors each and two-thirds have one Pb and 7 Li neighbors each.

Introduction

During a study of the compounds in the lithium-lead system, we investigated by X-ray diffraction techniques a phase with composition between LiPb and Li_3Pb . Some preliminary diffraction data for this phase along with a determination of the structures of Li_3Pb and Li_7Pb_2 have already been published.² Grube and Klaiber³ studied the phase

diagram for this system by means of thermal analysis and measurements of electrical resistivity as a function of temperature. The compound they referred to as Li_5Pb_2 ($\text{Li/Pb} = 2.50$), we have found to be Li_8Pb_3 ($\text{Li/Pb} = 2.67$) on the basis of the crystallographic investigations and also by chemical analysis ($\text{Li/Pb} = 2.68 \pm 0.01$). It will be noted that the difference in compositions between the stoichiometry we have determined and that given by Grube and Klaiber³ amounts to only 0.013 mole fraction unit.

(1) The work described in this paper was sponsored by the U. S. Atomic Energy Commission.

(2) A. Zalkin and W. J. Ramsey, *THIS JOURNAL*, **60**, 234 (1956).

(3) G. Grube and H. Klaiber, *Z. Electrochem.*, **40**, 754 (1934).

Experimental

The material was prepared by fusing the two metals together in an argon atmosphere in a manner described in a previous paper.² All samples were prepared in an argon-filled dry box to avoid reaction with the atmosphere. A small metallic chunk, which turned out to be a poor single crystal, was isolated in a thin-walled capillary of 0.3 mm. diameter. Single crystal patterns about the *a*-axis were photographed with the Weissenberg camera using $\text{CuK}\alpha$ radiation; a rotation pattern and layers zero, one and two were obtained. Powder diffraction patterns were photographed in a camera of 11.46 cm. diameter with samples mounted in capillaries.

Determination of Structure.—The single crystal photographs indicated a monoclinic cell with dimensions $a = 8.25 \text{ \AA.}$, $b = 4.75 \text{ \AA.}$, $c = 11.1 \text{ \AA.}$, $\beta = 106^\circ$. Because of the poor quality of these photographs, it is believed that the following results derived from the powder photograph as described below are more accurate: $a = 8.24 \text{ \AA.}$, $b = 4.76 \text{ \AA.}$, $c = 11.03 \text{ \AA.}$, $\beta = 104.5^\circ$. The systematic absences and Laue symmetry correspond to space groups C2, Cm or C2/m. A satisfactory structure was found in the higher symmetry, C2/m. The cell volume corresponds to about 22 atoms, judging from the atomic volumes in the other lithium lead alloys.² With the composition Li_5Pb_2 , the primitive unit would contain 3.15 lead atoms. With three lead atoms a structure was found which is in good agreement with the intensity data; therefore, the composition is Li_3Pb_3 with two formula units per unit cell. The density calculated from the cell dimensions is 5.37 g. cm.^{-2} ; that measured by argon displacement is $5.33 \pm 0.04 \text{ g. cm.}^{-3}$.

The atomic positions were first deduced in the following way. In Li_3Pb^2 and LiPb^4 the atoms have the body-centered cubic structure of metallic lithium,⁵ but with appropriate substitution of Li by Pb. Therefore a search was made for an arrangement by which eleven cubic cells could be fitted into the observed monoclinic cell. One such arrangement was easily found, with the monoclinic dimensions related to the cubic cell dimension a_0 and the cubic axes, \mathbf{a}_1 , \mathbf{a}_2 and \mathbf{a}_3 as

$$\begin{aligned} \mathbf{a} &= \mathbf{a}_1 + \mathbf{a}_2 - 2\mathbf{a}_3 & a &= \sqrt{6}a_0 \\ \mathbf{b} &= \mathbf{a}_1 - \mathbf{a}_2 & b &= \sqrt{2}a_0 \\ \mathbf{c} &= (3\mathbf{a}_1 + 3\mathbf{a}_2 + 5\mathbf{a}_3)/2 & c &= \sqrt{43}/2a_0 \\ \beta &= 104^\circ 25' = \sin^{-1}(11/\sqrt{120}) \end{aligned}$$

If the monoclinic cell fits this cubic net exactly, then the diffraction angles are given by the relation

$$\sin^2 \theta = (21.5h^2 + 60.5k^2 + 12l^2 + 8hl)\lambda^2/4(11a_0)^2 = N\lambda^2/4(11a_0)^2$$

It can be shown that N is always even if $h + k$ is even. The powder pattern was indexed according to this scheme, which is equivalent to taking a body centered cubic cell with dimension $11a_0$ and with many absences. The value obtained for a_0 was 3.364 \AA. , and from this the monoclinic dimensions were deduced by the equations given above. The fit of the powder pattern (Table I) is good but not perfect. These data suffer from absorption effects

which were not corrected for. The deviations between the observed and the calculated $\sin^2 \theta$ values are greater and more random than would be expected for absorption effects alone, showing that there is probably a slight deviation from this ideal shape.

In general, the lines of the powder pattern appear fairly sharp; however, toward the back reflection region some of the lines show multiplicity effects. Two sets of doublets ($N/2 = 363$ and 484) are clearly discernible but not well enough defined to separate out individual reflection planes.

A check of the deviations between observed and calculated $\sin^2 \theta$ indicates better agreement when the values of l in hkl run larger. This indicates that the a and b axes are probably shorter than indicated above by a few parts per thousand.

The atomic positions of the body-centered cubic structure can be described in space group C2/m as a twofold set and 5 fourfold sets of special positions:

$$\begin{aligned} 2(a): & (000) + (C) \\ 4(i): & \pm(x0z) + (C) \text{ with } x, z = 5/11, 4/11; 4/11, 1/11; \\ & 3/11, 9/11; 2/11, 6/11; \text{ and } 1/11, 3/11 \end{aligned}$$

Six lead atoms can be accommodated in the set 2(a) and one of the sets 4(i). The 00*l* data listed in Table II show that only the parameter $z = 4/11$ is acceptable among the above choices. Inspection of other rows of constant hk showed repetition at intervals of 11 in l of the same sequence of intensities, as would be expected for parameters which are integral multiples of $1/11$. Calculations showed that these sequences occurred as expected for $x, z = 5/11, 4/11$. Intensities were also calculated for the powder data, as listed in Table I, and again agreement was obtained. No deviation from the ideal parameters has been detected with the data. The value of z can be in error by no more than 0.002. The value of x is not determined precisely because of the lack of single crystal data for high values of h .

The lithium atomic positions are not determined by the intensity data, but since the cell dimensions and lead positions are in such good agreement with the hypothesis of the cubic arrangement, it is likely that lithium fills the remaining positions with the parameters listed above. Thus we give the structure

$$\begin{aligned} 2\text{Pb}_I \text{ in } 2(a): & (000) + (C) \\ 4\text{Pb}_{II} \text{ in } 4(i): & \pm(x0z) + (C) \text{ with } x = 5/11, z = 4/11 \\ 4\text{Li}_I \text{ in } 4(i) \text{ with } & x = 4/11, z = 1/11 \\ & 4\text{Li}_{II} \text{ in } 4(i) \text{ with } x = 3/11, z = 9/11 \\ & 4\text{Li}_{III} \text{ in } 4(i) \text{ with } x = 2/11, z = 6/11 \\ & 4\text{Li}_{IV} \text{ in } 4(i) \text{ with } x = 1/11, z = 3/11 \end{aligned}$$

The structure is illustrated in Fig. 1. This arrangement disperses the lead atoms as much as is possible in this unit cell and symmetry. Each Pb_I has 8 Li nearest neighbors. Each Pb_{II} has 7 Li and one Pb nearest neighbors. For the parameters listed above, the nearest neighbor distance is 2.91 \AA. Each Li has 8 nearest neighbors and 6 next nearest neighbors. The number of these which are Pb atoms are 4 and 0, 0 and 6, 3 and 3, and 4 and 0 for Li_I , Li_{II} , Li_{III} and Li_{IV} , respectively.

(4) H. Nowotny, *Z. Metallkunde*, **33**, 388 (1941).

(5) H. Perltz and E. Aruja, *Phil. Mag.*, **30**, 55 (1940).

TABLE I
POWDER DIFFRACTION DATA FOR Li_3Pb_3

$N/2$	hkl	I_o	I_o^a	Obsd.	$\sin^2 \theta^b$	Calcd.
6	001	<1				
24	002	3				
41	20 $\bar{1}$ 110	14	VW	0796		0786
43	200 11 $\bar{1}$	120	S	0833		0824
51	20 $\bar{2}$ 111	56	M	0988		0977
54	003	40	M	1051		1035
57	201 11 $\bar{2}$	9	W	1100		1092
73	20 $\bar{3}$ 112	56	S-	1406		1399
83	202 11 $\bar{3}$	2	VVW	1599		1591
96	004	5				1840
107	20 $\bar{4}$ 113	14	M-	2065		2051
121	203 020 11 $\bar{4}$ 31 $\bar{1}$	300	VS	2333		2319
127	021 31 $\bar{2}$	2				
145	022 311 31 $\bar{3}$	18	VW	2794		2779
150	005	19				
153	20 $\bar{5}$ 114	120	M	2939		2932
162	22 $\bar{1}$ 40 $\bar{1}$	14				
164	220 40 $\bar{2}$	41	M+	3164		3143
171	204 11 $\bar{5}$	2				
172	400 22 $\bar{2}$	56	W	3313		3296
175	023 312 31 $\bar{4}$	240	S	3366		3354
178	40 $\bar{3}$ 221	9				
194	401 22 $\bar{3}$	56	M-	3730		3718
204	222 40 $\bar{4}$	2				
211	20 $\bar{6}$ 115	9	W	4044		4044
216	006	19	W+	4139		4139
217	024 313 31 $\bar{5}$	27	W+	4173		4159
228	402 22 $\bar{4}$	14	W	4372		4369
233	205 11 $\bar{6}$	9				
242	40 $\bar{5}$ 223	150	M+	4641		4637
271	025 314 31 $\bar{6}$	111	M	5223		5193
274	403 22 $\bar{5}$	120	M	5290		5251
281	207 116	2				
283	421 51 $\bar{2}$ 130	23				
285	42 $\bar{2}$ 51 $\bar{1}$ 131	240	S-	5502		5462
292	40 $\bar{6}$ 224	2				
293	420 51 $\bar{3}$ 131	53	M-	5658		5615
294	007	5				
299	42 $\bar{3}$ 510 13 $\bar{2}$	15	VW-	5767		5730
307	206 117	120	M-	5904		5883
315	421 514 132	111	M-	6081		6037
325	42 $\bar{4}$ 511 13 $\bar{3}$	3				
332	404 22 $\bar{6}$	9				
337	026 315 31 $\bar{7}$	111	M+	6480		6458
349	422 51 $\bar{5}$ 133	27	VW	6713		6688
354	407 225	9				
363	{ 208 60 $\bar{2}$ 425 $\bar{5}$ 117 512 134 33 $\bar{1}$	600	VS	6989 ^c		6956
369	60 $\bar{3}$ 60 $\bar{1}$ 330 33 $\bar{2}$	3				
384	008	40				
387	500 604 331 33 $\bar{3}$	18				
393	207 118	14				
395	423 51 $\bar{6}$ 134	240	S-	7595		7570
402	405 227	2				
413	42 $\bar{6}$ 513 13 $\bar{5}$	3				
415	316 318 027	27				
417	601 605 332 33 $\bar{4}$	240	M+	8013		7991
428	40 $\bar{8}$ 226	120	M	8206		8202
453	424 517 135	18				
457	209 118	2				
459	60 $\bar{6}$ 333 33 $\bar{5}$ 427	27				
475	427 514 13 $\bar{6}$ 22 $\bar{8}$	18				
484	22 $\bar{8}$ 406 62 $\bar{2}$ 040	300	M+ W	9275 } ^c 9301 }		9275
486	009	3				
490	62 $\bar{1}$ 62 $\bar{3}$ 041	3				
491	208 119	56				
505	028 317 319	240	M	9676		9678
508	620 62 $\bar{4}$ 042	18				
513	607 603 334 33 $\bar{6}$	111	M	9850		9831
514	409 227	14				

^a S, strong; M, medium; W, weak; VW, very weak.
^b $\lambda(\text{CrK}\alpha) = 2.2909 \text{ \AA}$. ^c Doublets.

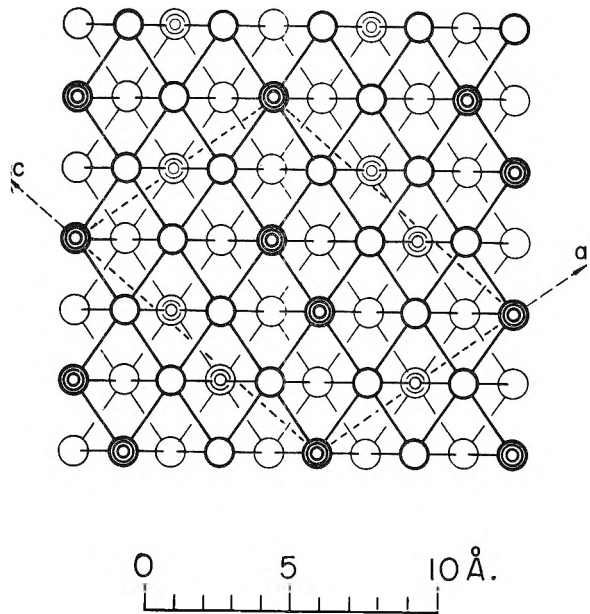


Fig. 1.—Structure of Li_3Pb_3 , projected on OL (010). The structure consists of alternate layers in the two positions indicated. The shaded circles represent Pb atoms.

TABLE II
CALCULATED STRUCTURE FACTORS AND OBSERVED INTENSITIES FOR 00*l* REFLECTIONS

l	$F/4 = 0.5 + \cos 2\pi lz$					Obsd. I
	5/11	4/11	$\frac{2}{3}/11$	2/11	1/11	
0	1.5	1.5	1.5	1.5	1.5	..
1	-0.5	-0.2	0.4	0.9	1.3	O
2	1.3	0.4	-0.5	-0.5	0.9	W
3	-0.2	1.3	0.9	-0.2	0.4	S
4	0.9	-0.5	1.3	0.4	-0.2	W+
5	0.4	0.9	-0.2	1.3	-0.5	M+
6	0.4	0.9	-0.2	1.3	-0.5	S
7	0.9	-0.5	1.3	0.4	-0.2	W
8	-0.2	1.3	0.9	-0.2	0.4	S-
9	1.3	0.4	-0.5	-0.5	0.9	W+
10	-0.5	-0.2	0.4	0.9	1.3	W
11	1.5	1.5	1.5	1.5	1.5	VS

Discussion

The arrangement and stacking of the atoms in this structure is similar to that found in Li_3Pb , Li_7Pb_2 and LiPb_2 ; this is as if an ordered replacement of lithium atoms by lead atoms has occurred in the body-centered cubic lattice of lithium metal. A novel feature in the Li_3Pb_3 structure is that the Pb_{II} atoms occur in pairs, since in the other lithium-lead arrangements no Pb has a Pb nearest neighbor; for this particular composition, however, this arrangement disperses the lead atoms as much as is possible in this unit cell and symmetry. From the lack of lead clusters in the other structures and for one third of the atoms in this structure, it is evident that the free energy advantage of a lead dimer is not substantial, and these pairs may have no significance other than a geometrical one.

Acknowledgment.—The authors extend their thanks to Mr. V. Silveira for photographing and measuring the powder patterns and for his aid in performing some of the computations.

DIMENSIONS AND HYDRODYNAMIC PROPERTIES OF CELLULOSE TRINITRATE MOLECULES IN DILUTE SOLUTIONS^{1a,b}

BY M. L. HUNT, S. NEWMAN, H. A. SCHERAGA AND P. J. FLORY

Contribution from the Department of Chemistry, Cornell University, Ithaca, N. Y., and the Allegany Ballistics Laboratory, Cumberland, Md.

Received February 27, 1956

Viscosity, sedimentation and light scattering measurements were carried out on six fractions of cellulose trinitrate (CTN) in ethyl acetate solution to obtain weight average molecular weights and configurational parameters. In addition, osmotic pressure measurements made on these same fractions in acetone or butanone solution provided information for the evaluation of molecular weight heterogeneity. The molecular weight range of these fractions was $\bar{M}_w = 40,000$ to 575,000 with heterogeneities corresponding to $\bar{M}_w/\bar{M}_n = 1.2$ to 2.2. Radii of gyration calculated from light scattering measurements confirm the observations of previous investigators indicating an unusual stiffness of the CTN chain. The persistence length required by the Porod-Kratky chain model corresponds to about 23 structural units; the segment for the Kuhn equivalent chain model is twice as great. The following empirical relations were obtained for the intrinsic viscosity $[\eta]$ and the sedimentation constant S_0 : $[\eta] = 2.50 \times 10^{-5} \bar{M}_w^{1.01}$ and $S_0 = 0.304 \times 10^{-16} \bar{M}_w^{0.29}$. The exponents in these equations differ significantly from those usually found for flexible polymers. Also, $[\eta]M/(\bar{s}^2)^{3/2}$ and $f_0/\eta_0(\bar{s}^2)^{1/2}$ differ from their asymptotic values Φ' and P' , respectively, where \bar{s}^2 is the mean square radius of gyration and f_0 is the frictional coefficient. It is shown that excluded volume and thermodynamic effects do not contribute significantly to this behavior. A small contribution to the exponents in the foregoing empirical equations arises from the chain stiffness. The latter manifests itself by a departure of the chain configuration from random flight behavior and a concomitant decrease in \bar{s}_0^2/M with decreasing \bar{M} , which can be accounted for by the Porod-Kratky chain model. While the remaining portions of these exponents could be accounted for by hydrodynamic effects considered in the Kirkwood-Riseman or Debye-Bueche theories, the parameters thereby deduced lead to erroneous asymptotic values for $[\eta]M/(\bar{s}^2)^{3/2}$ and $f_0/\eta_0(\bar{s}^2)^{1/2}$. In view of the failure of these theories to apply it is concluded that hydrodynamic permeation is not an important factor. Alternatively it is suggested that, because of chain stiffness, the configuration of CTN in ethyl acetate exhibits severe deviations from random flight statistics with a related deviation from spherical symmetry over the molecular weight range investigated. Presumably, if similar investigations could be carried out in a higher molecular weight range these anomalies would disappear, and the behavior of CTN at high molecular weight would be similar to that observed for more flexible polymers at much lower molecular weight. Finally, on the basis of the results obtained for the unusually stiff chains of CTN and also for flexible polymers, it appears unlikely that hydrodynamic permeation is ever of appreciable significance in the viscosity and sedimentation behavior of dilute polymer solutions.

Introduction

An unusually large molecular extension is indicated for typical cellulose derivatives, such as the nitrate, acetate, and butyrate, by the high viscosities of their dilute solutions and by light scattering dissymmetry measurements.²⁻⁴ This characteristic feature of the cellulosic chain, often referred to as chain stiffness, introduces effects which complicate the interpretation of molecular properties in dilute solution. In particular, the proportionality^{5,6} between the effective hydrodynamic radius and the radius of gyration $(\bar{s}^2)^{1/2}$ observed to hold almost universally for other polymers,⁷ even down to comparatively low molecular weights, should not be expected to hold for chains as stiff as those of the celluloses, except for chains of very great length. Thus, the intrinsic viscosity for highly extended chains cannot be taken to be proportional to

$(\bar{s}^2)^{3/2}/M$. Similarly, the translational frictional coefficient should not be proportional to $(\bar{s}^2)^{1/2}$. Even the customary proportionality between \bar{s}^2 and M , modified as required by long range interference and polymer-solvent interaction, must fail for stiff chains which are not very great in length.

The present investigation on the configuration and the frictional properties of cellulose trinitrate (hereafter designated CTN) was undertaken with the object of exploring the limitations of existing theories. Our results are in general agreement with those of the similar investigation published recently by Holtzer, Benoit and Doty.⁴ We have, however, attempted a more complete analysis of the importance of such factors as (a) deviations from spherical symmetry, (b) hydrodynamic permeation, and (c) aberrations in the configurational statistics at low chain lengths.

Experimental

Sample Preparation.—In order to obtain fractions having a wide range of molecular weight, two samples of cellulose (H and L) were nitrated and fractionated. The parent celluloses were a purified cotton linters (H) of D.P. ~ 1600 and a purified chemical cotton (L) of D.P. ~ 400 . These were nitrated in an identical manner under anhydrous conditions with a phosphoric acid-nitric acid mixture in the presence of excess phosphorus pentoxide. The method of preparation of the nitrating mixture and the procedure for nitration have been described previously by Alexander and Mitchell.⁸ The product was subjected to additional boiling in methanol for purposes of stabilization. Nitrogen determinations on the unfractionated cellulose nitrates by the FeCl₂-TiCl₃ titration method⁹ gave values of 13.54% N for the low D.P. material (L) and 13.49% N for the high (H).

(8) W. J. Alexander and R. L. Mitchell, *Anal. Chem.*, **21**, 1497 (1949).

(9) W. E. Shaefer and W. W. Becker, *ibid.*, **25**, 1226 (1953).

(1) (a) The work reported in this paper comprises a part of a program of research on the physical structure and properties of cellulose derivatives supported by the Allegany Ballistics Laboratory, Cumberland, Maryland, an establishment owned by the United States Navy and operated by the Hercules Powder Company under Contract NOrd 10431. (b) This paper was presented before the Division of Polymer Chemistry at the 127th Meeting of the American Chemical Society, Cincinnati, Ohio, April 1955.

(2) R. S. Stein and P. Doty, *J. Am. Chem. Soc.*, **68**, 159 (1946); R. M. Badger and E. H. Blaker, *This Journal*, **63**, 1056 (1949).

(3) S. Newman and P. J. Flory, *J. Polymer Sci.*, **10**, 121 (1953).

(4) A. M. Holtzer, H. Benoit and P. Doty, *This Journal*, **58**, 624 (1954).

(5) P. J. Flory, *J. Chem. Phys.*, **17**, 303 (1949); P. J. Flory and T. G. Fox, Jr., *J. Am. Chem. Soc.*, **73**, 1904 (1951).

(6) L. Mandelkern and P. J. Flory, *J. Chem. Phys.*, **20**, 212 (1952).

(7) (a) T. G. Fox, Jr., and P. J. Flory, *J. Am. Chem. Soc.*, **73**, 1909, 1915 (1951); (b) H. L. Wagner and P. J. Flory, *ibid.*, **74**, 195 (1952); (c) L. Mandelkern and P. J. Flory, *ibid.*, **74**, 2517 (1952); (d) L. Mandelkern, W. R. Krigbaum, H. A. Scheraga and P. J. Flory, *J. Chem. Phys.*, **20**, 1352 (1952).

The monomer molecular weights corresponding to these nitrogen levels are 287 and 286, respectively. Complete nitration to form cellulose trinitrate would correspond to 14.14% N with a monomer molecular weight of 297.

Fractionation.—The procedure for the higher molecular weight material will be described first. With the system acetone-alcohol (5:3) as solvent and a mixture of hydrocarbons, primarily hexane (Skellysolve B) as precipitant, three separate lots of CTN totalling 50 g. were fractionated in essentially parallel fashion into a total of 14 fractions. The initial concentration of polymer in the solvent was 0.36%. Those fractions possessing closely similar intrinsic viscosities were recombined, thereby yielding a total of 7 fractions. Each of these in turn was re-fractionated into four or five fractions with the same solvent-precipitant system but with starting concentrations of 0.2% or less. The final fractions encompassed a range of $\overline{D.P.}$'s from about 200 to 1800, but the end fractions were small in weight. In all instances Skellysolve B was added dropwise to the thermostated solutions with rapid stirring until sufficient turbidity had developed to yield a fraction of reasonable size. The mixture was then warmed 5–10° and allowed to cool slowly to the original temperature over a period of 3–4 hours with stirring. Vigorous stirring was continued overnight before allowing the precipitate to settle out. The supernatant was then decanted or siphoned off and precipitant again added to it to obtain the next fraction. In the first fractionation, and particularly for the early fractions, the precipitate was highly swollen and appeared to be admixed with a large amount of solution. The precipitate was centrifuged, therefore, to compact the highly swollen mass and allow removal of additional solution which was added to the supernatant previously separated. With increasing dilution, and at lower molecular weights, a harder, more compact and readily removable precipitate was obtained.

Fractionation of the lower molecular weight CTN was carried out as a single batch process at an initial concentration of 1% using pure acetone as solvent and hexane as precipitant. The procedure was otherwise the same. Resolution of precipitates was more nearly complete on warming, and greater efficiency of molecular weight separation was achieved on slow cooling, than in the fractionation of polymer H. Precipitates tended to be fine and granular and were separated by decantation from the supernatant with little difficulty. A total of 11 fractions with a range of $\overline{D.P.}$'s from 50 to 500 was thereby obtained.

In both fractionations, all head and tail material was discarded. The precipitates were redissolved in acetone-ethanol (8:2), and their solutions filtered and evaporated to dryness. The final products were wet with alcohol and stored in the dark at 2°.

The semi-rigid character of the precipitate usually encountered when the molecular weight was high indicated that crystallization was at least partially responsible for the phase separation. Equilibrium between phases is difficult to establish under these conditions, with the result that the fractionation may have been inefficient¹⁰ in spite of the low concentrations used here. Re-solution by warming, followed by reprecipitation on slow cooling and continued stirring, was relied upon to effect solution of soluble polymer trapped in the precipitate structure during its formation. Better conditions prevailed for the lower molecular weight fractions and for those removed toward the end of the stepwise fractionation, at which point the concentration of polymer became exceedingly low. The efficiency of fractionation may be assessed by consideration of the ratio of weight to number average molecular weights shown in Table II. A distinct improvement in homogeneity is to be noted as the molecular weight of the fractions decreases.

Stability.—Previous experience with cellulose nitrates¹⁰ prepared in the manner described indicated that their reduced viscosities, η_{sp}/c , in ethyl acetate solutions decrease by less than 1% during a period of one to 13 days following dissolution. Two determinations of the intrinsic viscosity of fraction H-1 made one year apart, the material having been stored as a solid wet with alcohol, gave the same value 15.0.

Solvents.—Butanone was used at first for intrinsic viscosity measurements and osmotic data on some of the fractions. Ethyl acetate was subsequently found to be prefer-

able for light scattering because of greater ease of purification and lower hygroscopicity; viscosity and sedimentation experiments were therefore carried out in this solvent also. Much later, acetone was adopted for the osmotic measurements. The solvents were of reagent grade, further purified by drying over calcium sulfate and distillation in equipment sealed off from the atmosphere with drying tubes.

Determination of Concentrations.—Immediately before use each polymer fraction was vacuum-dried at room temperature to remove the ethyl alcohol. For viscosity, sedimentation and osmotic pressure experiments a stock solution of the fraction was prepared and solutions of lower concentrations were obtained by volumetric dilution of this stock solution. Higher molecular weight fractions were diluted by weighing because of the high viscosity of the stock solutions. Procedures involved in the preparation of samples for light scattering resulted in some loss of solvent by evaporation; in the light scattering experiments it was necessary therefore to determine the concentration of each solution by the method of dry weights. Ethyl alcohol was added during this process to aid in the complete removal of ethyl acetate. The last traces of solvent were removed under vacuum, the samples being pumped until constant weight was attained.

Viscosity.—Intrinsic viscosities, $[\eta]$, were determined at 30° in the usual manner from flow times of the solutions in Ubbelohde type viscometers (shear rate *ca.* 2500 sec.⁻¹). The intrinsic viscosity was determined from combined plots according to the relations, $\eta_{sp}/c = [\eta] + k[\eta]^2c$ and $(\ln \eta_{rel})/c = [\eta] + k'[\eta]^2c$, where *c* is expressed in g./100 cc. Typical curves are shown in Fig. 1 for fraction L-5. The intrinsic viscosity was determined in each case from the best pair of curves having the same intercept and yielding values of *k* and *k'* such that *k* - *k'* = 0.5.

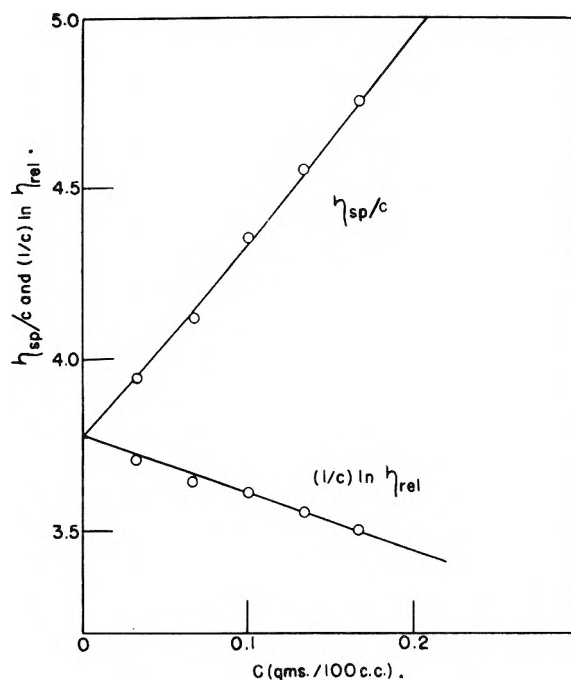


Fig. 1.—Viscosity data for fraction L-5.

For the higher molecular weight fractions a shear correction was applied, measurements being made down to 100 sec.⁻¹ with a special viscometer which has been described elsewhere.¹¹ This correction increased the intrinsic viscosity by 1.0 unit for fraction H-1, and by 0.3 unit for H-2; it was considered to be negligible for the lower molecular weight fractions.

Sedimentation.—Sedimentation velocity experiments were carried out in ethyl acetate at room temperature using a Spinco Model E ultracentrifuge at 44,770 r.p.m. Cells of 12 and 30 mm. optical path length were used to cover a wide range of concentrations.

(10) S. Newman, L. Loeb and C. M. Conrad, *J. Polymer Sci.*, **10**, 463 (1953).

(11) W. R. Krigbaum and P. J. Flory, *ibid.*, **11**, 37 (1953).

The partial specific volume of the polymer, \bar{v} , in ethyl acetate at 25°, as previously determined,¹⁰ is 0.545 cc./g. This value is relatively insensitive to the degree of nitration, concentration and molecular weight. The temperature coefficient of \bar{v} was assumed to be the same as that for the specific volume of fibrous cellulose nitrates, for which data were available.¹² With this assumption the value of \bar{v} at 30° is 0.546 cc./g. No data are available for the pressure dependence of \bar{v} . However, measurements¹³ on similar substances, such as starches and sugars, indicated that the effect of pressure on \bar{v} is negligible at the relatively low hydrostatic pressures in the ultracentrifuge runs.

Sedimentation constants, S , were computed for each of several time intervals during a given run. The dilution effect of the sector-shaped cell was taken into account in computing the mean concentration for each time interval. This procedure was used, rather than the usual plot against the time for the complete run, because of the large concentration dependence of the sedimentation constant. All sedimentation constants were corrected to 30° and 1 atm. in ethyl acetate, the solvent density and viscosity under these conditions being $\rho = 0.8883$ g./cc. and $\eta_0 = 0.004012$ poise, respectively. Data for the dependence of the density¹⁴ and viscosity^{15,16} of ethyl acetate on temperature and pressure were obtained from the literature. The corrected sedimentation constants were plotted as $1/S$ vs. c , expressed in g./100 cc., according to the equation $1/S = 1/S_0 + k_a c + k_b c^2$ which adequately accounts for the curvature exhibited by these plots. The sedimentation constant S_0 at infinite dilution was determined from the best parabola through the experimental points for each fraction using the method of least squares. The frictional coefficient at infinite dilution, f_0 , was computed from S_0 by means of the Svedberg equation, $S_0 = M(1 - \bar{v}\rho)/Nf_0$, where M is the molecular weight and N is Avogadro's number.

Osmotic Pressure.—Osmotic pressure measurements¹⁷ were carried out with Zimm-Myerson type osmometers¹⁷ fitted with membranes of undried cellophane. The performance of the osmometers was checked with solvent initially set at different levels by following the difference in liquid height (Δh) as a function of time. In all cases $\log(\Delta h)$ was found to be linear with time as required. The time taken for (Δh) to decrease its initial height by a factor of one-half was approximately one hour. Values of (Δh) were determined with a cathetometer reading to 0.001 cm. The entire osmometer assembly was enclosed to prevent evaporation of solvent.

The osmotic pressure data were fitted to the equation¹⁸⁻²⁰

$$\pi/c = (\pi/c)_0[1 + \Gamma_2 c + (\Gamma_2 c)^2/4] \quad (1)$$

or

$$(\pi/c)^{1/2} = (\pi/c)_0^{1/2}[1 + \Gamma_2 c/2] \quad (2)$$

i.e., $(\pi/c)^{1/2}$ was plotted against c .

Light Scattering Instrumentation.—Light scattering measurements were made with the modification of an instrument already described.^{21,22} The chromium mirror previously used to reflect the scattered radiation onto the photomultiplier tube was replaced by a totally reflecting glass prism. Corning filters No. 3389 and 5113, isolating the 4358 Å. line from the AH-4 mercury source were located in the incident and scattered beams, respectively, so that errors from fluorescence would be minimized. Provisions were made for insertion of a polaroid (Type HN32) in the scattered beam in two orientations 90° apart. The 1P21 photo-

multiplier tube used in the present work showed only a 1% greater response to horizontally polarized light than to vertically polarized light.

The incident beam was circular in cross-section, somewhat divergent, and measured 5.5 mm. in diameter at the center of the scattering cell. There were two circular apertures in the receiving system—one with 6.5 mm. diameter 35 mm. from the center of the cell, and one with 12 mm. diameter 112 mm. from the center of the cell. To test the effect of increasing the resolution one of the fractions with higher dissymmetry (H-2) was measured with the 12 mm. aperture replaced by a 6 mm. aperture as well as with the regular set-up. The increased resolution led to values of molecular weight and radius of gyration that were not over 3% higher, which is about the limit of precision.

Fluorescein solutions were used for the alignment of the scattering cell with respect to the incident beam and the center of rotation of the receiving system. A suitable cut-off filter arrangement made it possible to absorb scattered radiation and to measure only the fluorescence. Intensities followed the expected $\sin \theta$ relationship within $\pm 0.5\%$ for both vertically polarized and unpolarized light.

Relative intensity of the incident beam and response of the photomultiplier tube were monitored by the scattered radiation from a block of polished poly-(methyl methacrylate) and also by the scattering from a sealed solution of polystyrene in toluene. The use of two monitors provided a means of detecting any sudden changes in the scattering power of one of the materials, a phenomenon that has been suspected of occurring in poly-(methyl methacrylate) blocks, although not observed during the course of this investigation.

The instrument was calibrated with Cornell standard polystyrene in toluene solution (concentration, 0.500 g./100 ml.) at the time each CTN fraction was measured. A value of 208×10^{-6} was taken for the Rayleigh ratio²³ $R(\theta)$ of this standard solution at $\theta = 90^\circ$ and at 4358 Å.²⁴

Light Scattering Solutions.—Vacuum-dried CTN was dissolved in freshly-distilled ethyl acetate; after one day the solution was filtered through a fine sintered-glass filter into stainless steel centrifuge cups (equipped with brass covers) and centrifuged at 20,000 g for six hours. Filtration was not adequate for cleaning CTN solutions although distillation and filtration were found to be satisfactory for the ethyl acetate used for determining solvent scattering.²⁵ By means of viscosity measurements the centrifugation procedure was shown not to remove a significant amount of polymer from solution. The upper two-thirds of the supernatant solution was carefully transferred with a curved-tip pipet to a clean flask. Filtration through an ultra-fine sintered-glass filter into the light scattering cell was the final step in the cleaning procedure. After light scattering measurements had been completed on a given solution an aliquot was removed for refractive increment and dry weight determinations. The remaining solution was transferred to a flask and diluted by adding a measured amount of solvent. This solution was passed through a fresh ultra-fine filter into the light scattering cell and the process repeated until data had been obtained at four or five concentrations. Tests based on light scattering and refractive increment measurements of the solvent indicated that contamination did not occur during these operations.

Light Scattering Measurements.—Light scattering measurements in the angle range 30–135° were made with unpolarized incident light at room temperature (approximately 25°). Since these values were to be compared with intrinsic viscosity and sedimentation constant values at 30° an estimate of the effect of this temperature difference was made by determining the intrinsic viscosity of two of the fractions at both temperatures. These results are indicated in the footnote of Table I.

Depolarization was measured with a polaroid in the scattered beam. A value of 0.01 for ρ_u , the depolarization factor of the solute for unpolarized light, was obtained for all fractions except L-10 for which the value was 0.03. Because of limitations in accuracy, these results indicate merely that the true value of ρ_u for the higher fractions lies between

(23) See ref. 20, p. 290, for the definition of the Rayleigh ratio.

(24) C. I. Carr, Jr., and B. H. Zimm, *J. Chem. Phys.*, **18**, 1616 (1950).

(25) Cf. similar observations of R. H. Blaker, R. M. Badger and T. S. Gilman, *This Journal*, **63**, 794 (1949).

(12) P. Drechsel, private communication.

(13) P. W. Bridgman, *Proc. Am. Acad. Arts Sci.*, **76**, 9 (1945).

(14) "International Critical Tables," Vol. 3, McGraw-Hill Book Co., New York, N. Y., pp. 28, 36.

(15) Ref. 14, Vol. 7, pp. 215, 223.

(16) P. W. Bridgman, *Proc. Am. Acad. Arts Sci.*, **61**, 57 (1926).

(17) B. H. Zimm and I. Myerson, *J. Am. Chem. Soc.*, **68**, 911 (1946).

(18) T. G. Fox, Jr., P. J. Flory and A. M. Bueche, *ibid.*, **73**, 285 (1951).

(19) W. R. Krigbaum and P. J. Flory, *J. Am. Chem. Soc.*, **75**, 1775 (1953).

(20) P. J. Flory, "Principles of Polymer Chemistry," Cornell University Press, Ithaca, N. Y., 1953, p. 279.

(21) S. Newman, W. R. Krigbaum, C. Laugier and P. J. Flory, *J. Polymer Sci.*, **14**, 451 (1954).

(22) Ref. 20, p. 284.

0.00 and 0.02 with a possibly higher value for L-10. Since fluorescence effects would be included in the measured depolarization factor the low value for the latter indicates the absence of appreciable interference from fluorescence. No correction for depolarization was made in the calculation of molecular weights.

Although all fractions except one (H-2) appeared colorless their solutions were found to show some absorption at 4358 Å. This absorption was great enough to be taken into account because of the rather long total path length (10 cm.) of incident and scattered light in the scattering cell. The necessary measurements for this purpose were made with a Beckman Spectrophotometer.

The values of the Rayleigh ratio $R(\theta, c)$ due to the polymer were obtained from the equation

$$R(\theta, c) = \frac{[R(90^\circ)]_{\text{std}}}{[i(90^\circ)]_{\text{std}}/i_m} \left[\frac{1}{T} \frac{i_s}{i_m} - \frac{i_0}{i_m} \right] \left[\frac{\sin \theta}{(1 + \cos^2 \theta)} \right] \left(\frac{n_0}{n_{\text{std}}} \right)^2 \quad (3)$$

where $R(90^\circ)_{\text{std}}$ is the Rayleigh ratio of the calibration standard at 90° (i.e., 208×10^{-6}); $[i(90^\circ)]_{\text{std}}$ is the galvanometer reading for the standard at 90° (corrected for solvent scattering); i_s , i_0 and i_m are the galvanometer readings for the solution, solvent and monitor, respectively; T is the transmission of the solution relative to the solvent. The factor $\sin \theta / (1 + \cos^2 \theta)$ accounts for the dependence of scattering volume and polarization on angle. The quantities n_0 and n_{std} are the refractive indices of ethyl acetate and toluene, respectively; the factor $(n_0/n_{\text{std}})^2$, having the value 0.827, corrects for the refraction of scattered radiation at the surface of the cylindrical wall of the scattering cell.²⁶

Refractive Increment Measurements.—Refractive increments, dn/dc , of the ethyl acetate solutions of CTN were determined with a differential refractometer which has been described previously.²⁷ The instrument was calibrated with aqueous solutions of sucrose using the value 0.144 for the refractive increment of sucrose (with concentration in g./ml.).²⁸ Measurements were made at three or more concentrations for each fraction. The parameter $K = 2\pi^2 n_0^2 (dn/dc)^2 / N\lambda^4$ (see equation 4) was then computed, n_0 being the refractive index of the solvent, λ the wave length of the light *in vacuo*, and N the Avogadro number.

Results

Viscosity.—The viscosity data of Table I were obtained from curves such as those shown in Fig. 1. Shear corrections have been applied to the data for Fractions H-1 and H-2.

TABLE I
INTRINSIC VISCOSITIES^a AND SEDIMENTATION CONSTANTS^b
OF CELLULOSE TRINITRATE FRACTIONS IN ETHYL ACETATE
AT 30°C

Fraction	$[\eta]$	k	$(S_0 \times 10^{13})$ (sec.)	k_s	$-k_s'$	$(f_0/\eta) \times 10^{13}$ (cm.)
L-10	1.07 ^c	0.36 ₅	6.34	0.22 ₈	0.12 ₄	1.39
L-8	2.02 ^c	.39 ₄	7.10	.22 ₇	.06 ₀	2.28
L-5	3.78	.38 ₂	8.65	.35 ₇	.22 ₁	3.15
H-3	5.24	.38 ₁	9.62	.34 ₀	.10 ₃	...
H-2	7.0	.43 ₁	11.13	.47 ₈	.38 ₈	4.75
H-1	15.0	.44 ₀	12.66	.63 ₀	.57 ₀	9.65

^a Concentrations in g./100 cc.; k refers to the data before shear corrections were applied; the errors in $[\eta]$ are estimated as 1% except for fraction H-2 for which the error is estimated as 3%. ^b The errors in S_0 are estimated as 1%. ^c The intrinsic viscosity was also determined at 25° and found to be 1.09₅ and 2.07 for fractions L-10 and L-8, respectively. ^d Computed from the Svedberg equation using the weight average molecular weight given in Table II.

(26) J. J. Hermans and S. Levinson, *J. Optical Soc. Am.*, **41**, 460 (1951).

(27) P. P. Debye, *J. Applied Phys.*, **17**, 332 (1946).

(28) F. J. Bates, National Bureau of Standards Circular C440, "Polarimetry, Saccharimetry and the Sugars," p. 652 (1942).

Sedimentation.—The reciprocals of the corrected sedimentation constants are plotted as functions of concentration in Fig. 2 together with the parabolas computed by the method of least squares. The data are summarized in Table I.

Osmotic Pressure.—The osmotic pressure data are plotted as $(\pi/c)^{1/2}$ vs. c according to equation 2 in Fig. 3, for the solvents indicated, and are summarized in Table II. The osmotic measurements on fraction L-8 were made at 25°, all others at 30°.

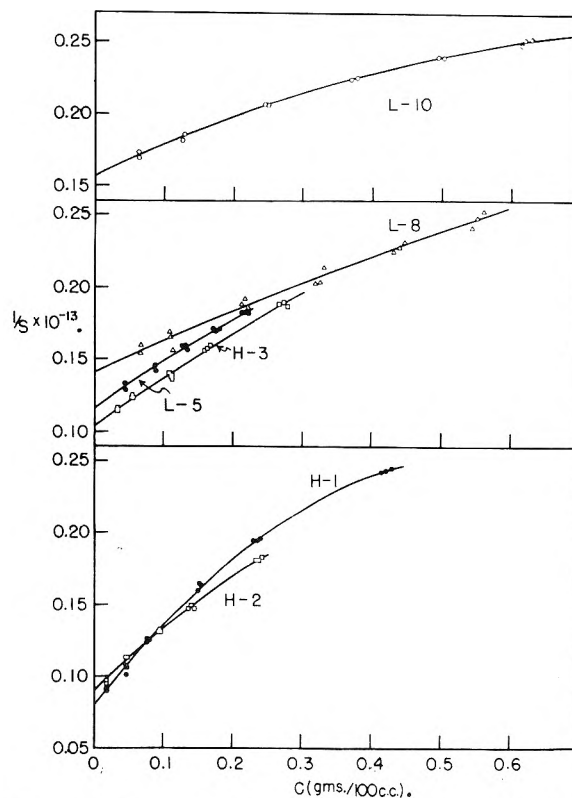


Fig. 2.—Sedimentation data for cellulose trinitrate fractions.

Light Scattering.—The weight average molecular weights, z -average root-mean-square radii of gyration, and second virial coefficients from light scattering measurements at room temperature, ca. 25°, are listed in Table II. The refractive increment dn/dc at 30° used for the evaluation of K was 0.102 cc./g. \pm 0.002. The 10% error in the \bar{M}_w 's includes the precision in $[Kc/R(\theta, c)]_{c=0}$, dn/dc , and instrument calibration. The true error in the root-mean-square radius of gyration will be somewhat larger than the indicated 3% based on the precision in the determination of the $[Kc/R(\theta, c)]_{c=0}$ values, because of the limitations in establishing criteria for the cleanliness of the solutions.

The calculation of the molecular weight, radius of gyration and second virial coefficient from light scattering measurements is not altogether straightforward, particularly in the case of very non-ideal solutions such as those of CTN. For this reason the important details in the treatment of the light scattering data are given below.

The general equation for reduced scattering intensity is²⁹

(29) B. H. Zimm, *J. Chem. Phys.*, **16**, 1093 (1948).

TABLE II
 SUMMARY OF OSMOTIC^a AND LIGHT SCATTERING^b RESULTS

Fraction	$\bar{M}_n \times 10^{-3}$ (osmotic)	Γ_2 , cc./g. (osmotic) ^c	$\bar{M}_w \times 10^{-3}$ (light scat.)	Γ_2 , cc./g. (light scat.) ^c	$(\langle s^2 \rangle_z)^{1/2}$ Å.	\bar{M}_w/\bar{M}_n	η	$\bar{M}_z \times 10^{-3}$ (calcd.)
L-10	34.6	23	41.3	32	144	1.19	5.3	48
L-8	60.6	55	76	55	242	1.25	4.0	91
L-5	89	79	128	77	319	1.45	2.22	169
H-3	110	92
H-2	248	119	507	(2.00) ^d	(1.00) ^d	372
H-1	257	177	573	367	870	2.23	0.81	890

^a The errors in \bar{M}_n are estimated as $\pm 5\%$. ^b The average error in \bar{M}_w is about 10% and that in $(\langle s^2 \rangle_z)^{1/2}$ about 3%. In the case of fraction L-10, having a very small radius of gyration, the uncertainty in the alignment of the light scattering cell increases the uncertainty in $(\langle s^2 \rangle_z)^{1/2}$ to $\pm 12\%$. ^c The Γ_2 from osmotic data apply to solvents as given in Fig. 3. Those from light scattering data are for ethyl acetate. ^d Values assumed.

$$\frac{Kc}{R(\theta, c)} = \frac{1}{MP(\theta)} + 2A_2c + \{3A_3Q(\theta) - 4A_2^2P(\theta)[1 - P(\theta)]\}c^2 + \dots \quad (4)$$

where c is expressed in g./ml., M is the molecular weight (a weight average value for a heterogeneous polymer), A_2 and A_3 are virial coefficients, and $P(\theta)$ and $Q(\theta)$ are functions which depend on θ and on the shape and size of the scattering particle.

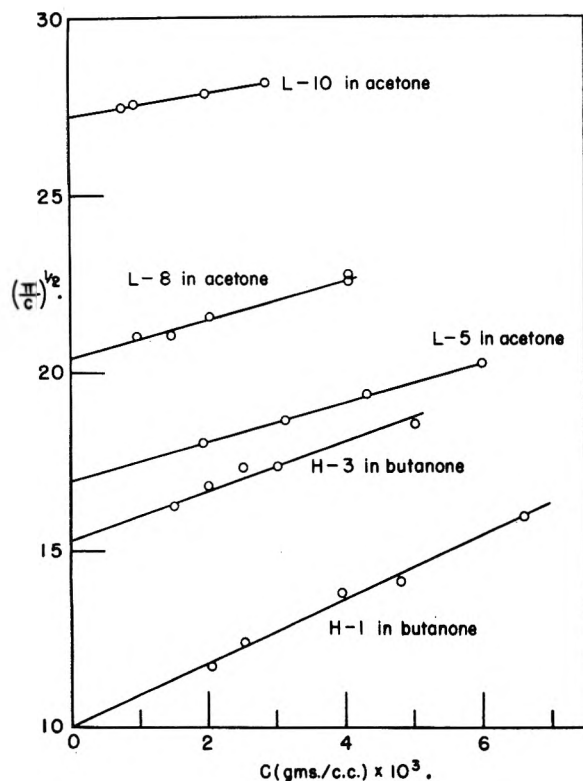


Fig. 3.—Osmotic pressure data plotted according to equation 2.

If $\theta = 0^\circ$ the functions $P(\theta)$ and $Q(\theta)$ reduce to unity and equation 4 becomes

$$Kc/R(0^\circ, c) = (1/M)[1 + 2A_2Mc + 3A_3Mc^2] \quad (5)$$

We therefore consider first the problem of extrapolation to zero angle.

For this purpose the data were plotted as $Kc/R(\theta, c)$ vs. $\sin^2\theta/2$ at each value of c .³⁰ The nature of the extrapolation of such plots to $\theta = 0$ depends both

(30) This procedure²⁹ is valid only at $c = 0$. Despite this, it is customarily used for non-zero values of c because the proper method of extrapolation to $\theta = 0$ is not defined since the function $Q(\theta)$ of equation 4 has not been evaluated.

on the molecular model assumed and on the polymer heterogeneity.^{31,32} If the angular dependence of $R(\theta, c)$ is small, the data obtained in the angular range $\theta \geq 30^\circ$ may be linearly extrapolated to $\theta = 0^\circ$ without ambiguity. However, if the angular dependence of $R(\theta, c)$ is large, the curvature near $\theta = 0^\circ$ is significantly dependent on the heterogeneity and the model. For random coils with a molecular distribution characterized by $\bar{M}_w/\bar{M}_n = 2$, the plot of $Kc/R(\theta, c)$ should extrapolate linearly³¹ to $\theta = 0$. However, for $\bar{M}_w/\bar{M}_n < 2$, such plots will show curvature as θ approaches zero, and the theoretical curve³¹ is required in order to carry out the extrapolation. In such a case the use of a linear extrapolation will conceal the true curvature and lead to an erroneous slope and intercept at $\theta = 0$. The data of Table II were obtained by assuming the random coil model, the calculations being carried out for heterogeneities corresponding to \bar{M}_w/\bar{M}_n equal to 1 and 2, respectively. The heterogeneity most suitable for each particular fraction was determined by comparison of the molecular weights with those from osmotic pressure measurements.³³ Thus, a linear extrapolation of $Kc/R(\theta, c)$ vs. $\sin^2\theta/2$ to $\theta = 0$ was carried out to obtain $Kc/R(0^\circ, c)$ when $\bar{M}_w/\bar{M}_n \cong 2$. The values of $Kc/R(0^\circ, c)$ obtained in this way were then extrapolated to zero concentration, as discussed below. On the other hand, when $\bar{M}_w/\bar{M}_n \cong 1$ the dissymmetry method was used, the values of $Kc/R(\theta, c)$ at $45, 90$ and 135° being extrapolated to zero concentration.³⁴ The value of $Kc/R(0^\circ, 0)$ was then obtained from the product of $Kc/R(90^\circ, 0)$ and $R(90^\circ, 0)/R(0^\circ, 0)$, the latter factor being given by the theory for the scattering from random coils when the dissymmetry ratio $R(45^\circ, 0)/R(135^\circ, 0)$ is known.

We may now consider the problem of extrapolating $Kc/R(0^\circ, c)$ to zero concentration by means of equation 5. Since $A_2 = \Gamma_2/M$ (Γ_2 being the same coefficient as appears in equation 1) and A_3 is approximately equal^{19,35} to $(\Gamma_2^2/M)/4$, equation 5 becomes

(31) B. H. Zimm, *J. Chem. Phys.*, **16**, 1099 (1948).

(32) H. Benoit, *J. Polymer Sci.*, **11**, 507 (1953).

(33) The value of \bar{M}_w for Fraction H-2 would have been 4% lower had it been calculated on the basis of $\bar{M}_w/\bar{M}_n = 1$ instead of the assumed value of $\bar{M}_w/\bar{M}_n = 2$. For the lower molecular weight fractions the \bar{M}_w 's are practically independent of heterogeneity provided $\bar{M}_w/\bar{M}_n \cong 2$.

(34) This procedure has the same limitation mentioned in footnote 30.

(35) W. H. Stockmayer and E. F. Casassa, *J. Chem. Phys.*, **20**, 1560 (1952).

$$Kc/R(0^\circ, c) = [Kc/R(0^\circ, c)]_{c=0} [1 + 2 \Gamma_2 c + 3 \Gamma_2^2 c^2/4] \quad (6)$$

at $\theta = 0^\circ$, or

$$[Kc/R(0^\circ, c)]^{1/2} \sim [Kc/R(0^\circ, c)]^{1/2}_{c=0} [1 + \Gamma_2 c] \quad (7)$$

Equation 6 predicts curvature in plots of $Kc/R(0^\circ, c)$ vs. c which is negligible when $\Gamma_2 c$ is very small, whereas linear plots can be obtained if the data are plotted as $[Kc/R(0^\circ, c)]^{1/2}$ vs. c according to equation 7. The experimental data reported here are not adequate in range of concentration and in precision to demonstrate a superiority of equation 7 over the linear part of equation 6 for the extrapolation to infinite dilution. Somewhat different values are obtained however for the intercept and initial slope, depending on which of these two procedures is used.³⁶ In consideration of the behavior of other systems, we have treated the data according to equation 7, the plots being shown for all of the fractions in Fig. 4. The weight average molecular weights were obtained from the intercepts at $c = 0$ by means of the relation

$$[Kc/R(0^\circ, c)]_{c=0} = 1/\bar{M}_w \quad (8)$$

and the coefficients Γ_2 were evaluated from the initial slopes and intercepts.

The highest concentration used for each fraction has been kept as low as feasible in order to minimize the effect of non-ideality which manifests itself in CTN solutions in all known solvents by a large dependence of $Kc/R(\theta, c)$ on c . The ratio $[Kc/R(0^\circ, c)]_{c=\max}/[Kc/R(0^\circ, c)]_{c=0}$ was 2.9 for the highest molecular weight fraction and approximately 2 for the other fractions. As a consequence of the low concentrations and high virial coefficients, as much as 60% of the observed scattering from the solution was due to the solvent. Nevertheless, adequate precision in the excess scattering due to the polymer was obtained.

The z -average of the mean-square radius of gyration $\langle \bar{s}^2 \rangle_z$ was determined from the angular dependence^{31,32} of the scattered radiation at zero concentration. At $c = 0$ equation 4 reduces to

$$[Kc/R(\theta, c)]_{c=0} = (1/\bar{M}_w) [1 + (4\pi n_0/3\lambda)^2 \langle \bar{s}^2 \rangle_z \sin^2 \theta/2 + \dots] \quad (9)$$

The data were plotted as $[Kc/R(\theta, c)]^{1/2}$ vs. c , at each angle θ , by analogy with equation 7 even though the latter is valid only at $\theta = 0$. The squares of the intercepts of these plots, *i.e.*, $[Kc/R(\theta, c)]_{c=0}$, for each angle were then plotted against $\sin^2 \theta/2$ according to equation 9, the value of $\langle \bar{s}^2 \rangle_z$ being obtained from the slope and intercept.³⁴ The heterogeneity also affects³⁷ the value of $(\langle \bar{s}^2 \rangle_z)^{1/2}$. For the case of $\bar{M}_w/\bar{M}_n \cong 2$, $\langle \bar{s}^2 \rangle_z$ was computed

(36) When the data were plotted as $Kc/R(0^\circ, c)$ vs. c , according to the linear part of equation 6, the much higher values of 43, 75, 93, 148 and 603 were obtained for Γ_2 . On the other hand, the intercept, from which the molecular weight is obtained, is less sensitive to the manner of plotting the data but the effect is still significant. Thus, the use of equation 6 in this manner leads to molecular weights that are higher by 4.5, 6.1, 2.4, 3.2 and 16.0%.

(37) The values recorded for $(\langle \bar{s}^2 \rangle_z)^{1/2}$ for fractions H-1 and H-2 in Table II correspond to $\bar{M}_w/\bar{M}_n = 2$. The assumption of $\bar{M}_w/\bar{M}_n = 1$ would have led to a 10% lower value for fraction H-2. For fraction L-5, the two values assumed for the heterogeneity led to a difference of 5.5% in $(\langle \bar{s}^2 \rangle_z)^{1/2}$, the average of these two values being recorded in Table II. For the lower molecular weight fractions the results were the same for both values of \bar{M}_w/\bar{M}_n .

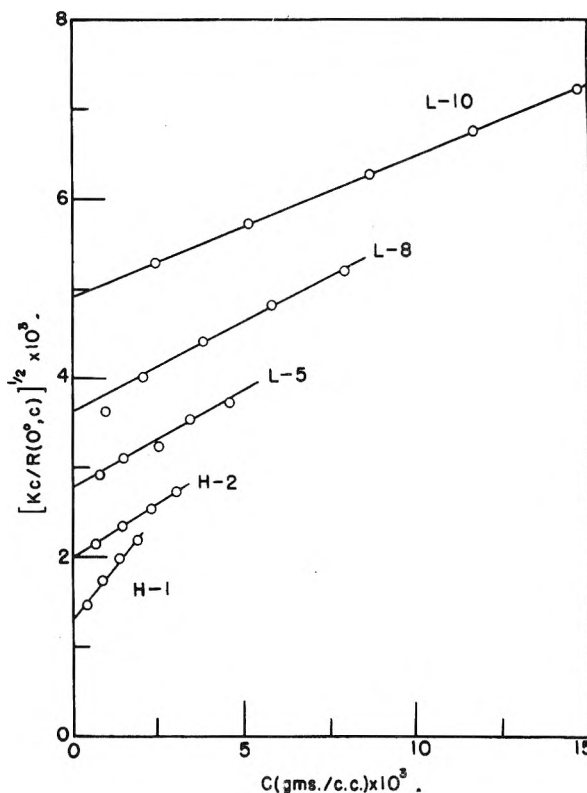


Fig. 4.—Light scattering data at $\theta = 0^\circ$, plotted according to equation 7.

directly from the slope and intercept of the $[Kc/R(\theta, c)]_{c=0}$ vs. $\sin^2 \theta/2$ plot. For the case of $\bar{M}_w/\bar{M}_n \cong 1$, $(\langle \bar{s}^2 \rangle_z)^{1/2}$ was determined from the dissymmetry calculated from the experimental ratio $R(45^\circ, 0)/R(135^\circ, 0)$.

While, in the actual calculations, the data were treated as above for both the angular and concentration extrapolations, for compact illustrative purposes the data for fraction H-2 are shown in Fig. 5 as a Zimm plot.

Molecular Weight Heterogeneity.—Although the fractionations were conducted under exceptionally favorable conditions, it is evident from the values of \bar{M}_w/\bar{M}_n in Table II that the higher fractions are far from homogeneous. It will be assumed for the purpose of introducing suitable corrections for molecular heterogeneity that the fractions possess molecular weight distributions of the Schulz type,^{31,33} namely

$$w_i dM_i = [\lambda^{y+1} M_i^y e^{-\lambda M_i/\Gamma(y+1)}] dM_i \quad (10)$$

where w_i is the weight fraction of polymer having a molecular weight in the range M_i to $M_i + dM_i$, and λ and y are parameters which characterize the average molecular weight and the sharpness of the distribution, respectively. For this distribution $\bar{M}_z:\bar{M}_w:\bar{M}_n = (y+2):(y+1):y$, the values of y and \bar{M}_z calculated directly from \bar{M}_w/\bar{M}_n being given in Table II.

Viscosity-Molecular Weight-Sedimentation Relations.—The molecular weight dependences of the intrinsic viscosity and sedimentation constant are represented graphically in Fig. 6. From these log-

(38) G. V. Schulz, *Z. physik. Chem.*, **B43**, 25 (1939).

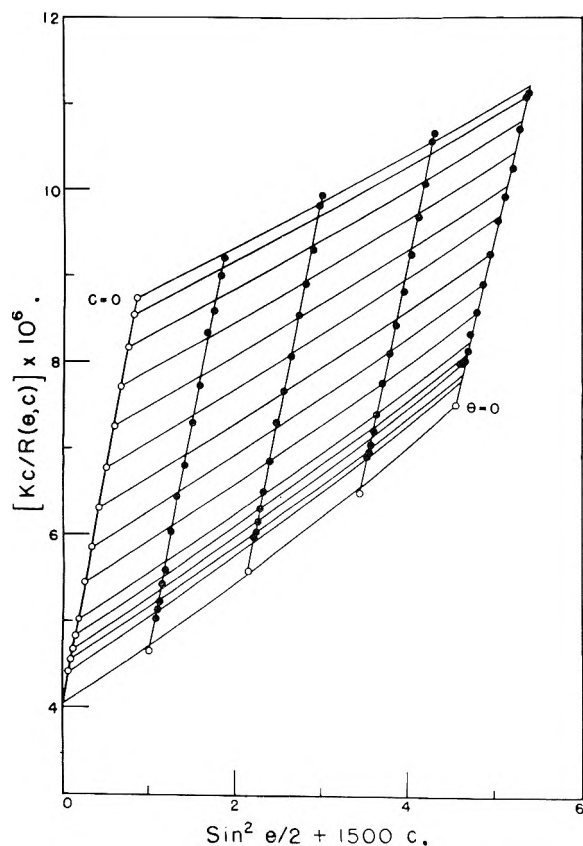


Fig. 5.—Zimm plot of light scattering data for fraction H-2. The units of c are g./cc.

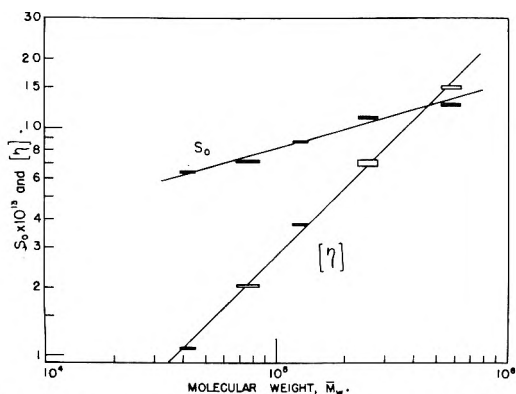


Fig. 6.—Log-log plots giving the molecular weight dependences of the intrinsic viscosity and sedimentation constant.

log plots the following empirical equations were obtained

$$[\eta] = 2.50 \times 10^{-5} \bar{M}_w^{1.01} \quad (11)$$

$$S_0 = 0.304 \times 10^{-13} \bar{M}_w^{0.29} \quad (12)$$

$$S_0 = 6.0 \times 10^{-13} [\eta]^{0.29} \quad (13)$$

The constants in these empirical equations represent average values for the molecular weight region encompassed by the measurements.

Holtzer, Benoit and Doty⁴ found $[\eta] = 1.7 \times 10^{-5} \bar{M}_w^{1.00}$ in acetone, which when converted to intrinsic viscosities in ethyl acetate (according to their data on two samples) yields $[\eta] = 2.35 \times 10^{-5} \bar{M}_w^{1.00}$ for ethyl acetate, with which our results are in excellent agreement. Meyerhoff³⁹ meas-

(39) G. Meyerhoff, *Naturwiss.*, **41**, 13 (1954).

ured sedimentation and diffusion constants on five fractions of CTN ranging from 74 to 593×10^3 in molecular weights. His results lead to an exponent of 0.30 in eq. 12; his value for the proportionality constant is higher, however, by a factor of about 1.5.

Discussion

The empirical relations 11 and 12 differ significantly from those found for flexible polymers.⁷ For the latter the maximum molecular weight dependence of $[\eta]$, attainable in a good solvent,⁴⁰ is $M^{0.8}$. For a flexible polymer obeying this relation, the following equations would also hold: $f_0 \sim M^{0.6}$, $S_0 \sim M^{0.4}$, $(\bar{s}^2)^{1/2} \sim M^{0.6}$. The departures of equations 11 and 12 for CTN from the behavior characteristic of flexible chain molecules could arise because of differences in the configurational statistics, spherical symmetry or from hydrodynamic effects. Each of these factors will now be examined in order to account for the empirical results obtained for CTN in ethyl acetate.

The degree of flexibility of most polymers is such that even at molecular weights as low as 10,000 to 30,000 asymptotic chain statistical behavior may be assumed to hold with satisfactory accuracy. Thus, the ratio of the square of the radius of gyration to the molecular weight remains sensibly constant down to comparatively low degrees of polymerization, except as modified by the so-called "volume effect" due to long range mutual interactions between chain segments.⁵ Expressing the linear deformation of the chain configuration attributable to this effect by α , we may write

$$(\bar{s}^2)^{1/2} = \alpha(\bar{s}_0^2)^{1/2} \quad (14)$$

where $(\bar{s}_0^2)^{1/2}$ is the unperturbed radius of gyration.⁵ Ordinarily \bar{s}_0^2 may be taken to be proportional to M ; in order to ascertain whether this proportionality holds for CTN we must first evaluate the expansion factor α in order to compute \bar{s}_0^2 for each of the fractions.

Estimation of α .—The expansion factor α depends on the average segment density within the domain of the molecule and on the thermodynamic interaction between polymer segments and the solvent. The average segment density for a given chain length is inversely proportional to $(\bar{s}^2)^{3/2}$. The second virial coefficient Γ_2 also depends on $(\bar{s}^2)^{3/2}$ and the thermodynamic interaction; the expansion factor may, in fact, be calculated from Γ_2 with the aid of relations given by the statistical mechanical theory of dilute polymer solutions.⁴¹ While this theory is strictly applicable only to chains with sufficient flexibility to yield an approximately spherical spatial distribution of segments, we shall find that a precise estimate of α is not required, hence deviations due to the inflexibility of the cellulose chains will be inconsequential in this connection.

According to the theory referred to

$$\Gamma_2 = 4(\pi/3)^{3/2} N M^{1/2} (\bar{s}^2/M)^{3/2} X F(X) \quad (15)$$

(40) Ref. 20, p. 622.

(41) (a) P. J. Flory, *J. Chem. Phys.*, **17**, 1347 (1949); (b) P. J. Flory and W. R. Krigbaum, *ibid.*, **18**, 1086 (1950).

TABLE III
CONFIGURATION PARAMETERS

Fraction	$\bar{M}_z \times 10^{-3}$	α	$(\langle s_0^2 \rangle_z)^{1/2}$, Å.	Smoothed values			$\langle r_0^2 \rangle_z^{1/2} / \langle r_{max} \rangle_z$
				$\langle s_0^2 \rangle_z / \bar{M}_z$	$(\langle s_0^2 \rangle_z)^{1/2}$	$\langle s_0^2 \rangle_z / \bar{M}_z$	
L-10	48	1.05	137	0.39	153	0.49	0.39
L-8	91	1.03	235	.61	228	.57	.35
L-5	169	1.04	307	.56	325	.63	.25
H-2	372	1.03	492	.65	497	.66	.18
H-1	890	1.05	829	.77	780	.68	.13

where N is Avogadro's number and

$$X = 2(\alpha^2 - 1) \tag{16}$$

The function $XF(X)$ may be approximated with high accuracy by the expression⁴²

$$XF(X) = (4/\pi^{1/2}) \ln [(\pi^{1/2}/4)X + 1] \tag{17}$$

The values of α given in Table III were calculated from equations 15, 16 and 17 using values of Γ_2 , $\langle s^2 \rangle_z$ and \bar{M}_z given in Table II. Using these values of α and equation 14, the values of $\langle s_0^2 \rangle_z / \bar{M}_z$ given in Table III were obtained.

The stiffness of the chain, and the consequently large s_0^2/M is directly responsible for the nearly negligible expansion, $\alpha - 1$, due to the "volume effect." Although α should increase slowly with M at larger values of M , the change of α with M over the range investigated is quite negligible, and the possible contribution of this change to the exponents in equations 11 and 12 may safely be neglected. (See also Doty, *et al.*⁴) We have, nevertheless, employed the estimated expansion factors to convert the s^2 values observed to the unperturbed s_0^2 , as given in Table III.

The Configuration.—Ratios of the squares of the unperturbed radii of gyration to the molecular weights, given in the fifth column of Table III, are plotted against M in Fig. 7. The decrease in this ratio at molecular weights below 100,000 found by Holtzer, *et al.*,⁴ is here confirmed, but the precision of the experimental results as in their work is insufficient for establishing empirically the dependence of the ratio on M . We therefore resort to the Porod-Kratky⁴³ chain model for the purpose of approximating this dependence. According to this model, the chain direction varies continuously instead of at specified bond junctions. The flexibility of the chain is characterized by a persistence length q , which is defined as the integral of the average projections of chain elements of the infinitely long chain on its initial direction.

Benoit and Doty⁴⁴ have derived the following expression relating the unperturbed radius of gyration to q and the maximum molecular length r_{max} at full extension (contour length)

$$\overline{s_0^2}/q^2 = x/3 - 1 + 2/x - 2[1 - \exp(-x)]/x^2 \tag{18}$$

where x , the number of Porod units per molecule, is defined by

$$x = r_{max}/q \tag{19}$$

Inasmuch as $x > 6$ for our fractions, it will be permissible to drop the exponential term. After taking

(42) T. A. Orofino and P. J. Flory, to be published.

(43) G. Porod, *Monatsh.*, **80**, 251 (1949); O. Kratky and G. Porod, *Rec. trav. chim.*, **68**, 1106 (1949).

(44) H. Benoit and P. Doty, *THIS JOURNAL*, **57**, 958 (1953).

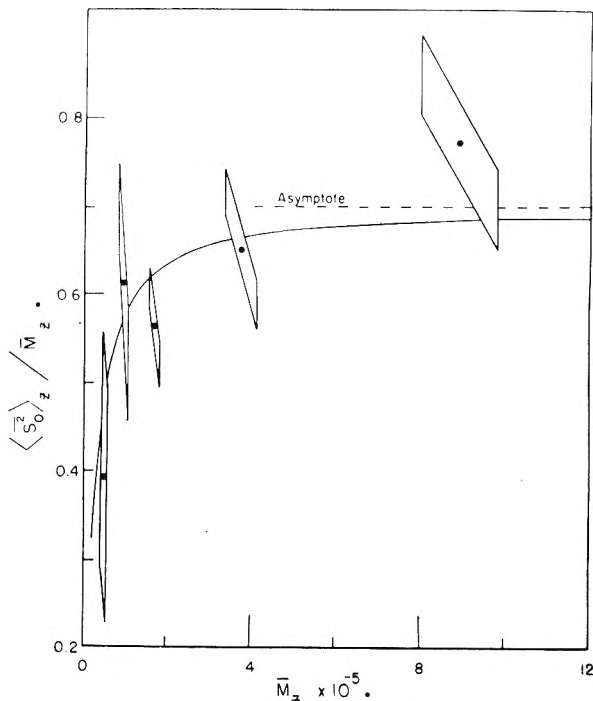


Fig. 7.—Dependence of $\langle s_0^2 \rangle_z / \bar{M}_z$ in Å.²/M on \bar{M}_z . The points were obtained from the experimental data, while the curve is a theoretical one based on equation 18. The shape of the symbols takes into account the average error in $\langle s^2 \rangle_z$ and \bar{M}_z , the latter appearing in both the ordinate and abscissa.

account of molecular heterogeneity⁴⁵ we have in place of equation 18

$$\langle s_0^2 \rangle_z \cong q^2 [\bar{x}_w/3 - 1 + (2/\bar{x}_w)(1 - 1/\bar{x}_w)] \tag{20}$$

In the limit of very large x equations 18 and 20 reduce to $s_0^2/r_{max} = q/3$, which corresponds to constancy of s_0^2/M with M . For smaller x , the additional terms occurring in equation 20 will reduce s_0^2/q , and hence s_0^2/M , below their asymptotic values.

Taking 5.15 Å. for the length of a cellulose unit projected on the axis of the chain at full extension,⁴⁶ we have from equation 19 that

$$x = 5.15M/287q \tag{19'}$$

(45) Since $x \sim M$ we have $\langle s_0^2 \rangle_z = \sum w_i x_i \langle s_0^2 \rangle_i / \sum w_i x_i$. Using this latter relation, equation 18 (with the exponential term dropped) becomes

$$\langle s_0^2 \rangle_z \cong q^2 \left[\frac{1}{3} \frac{\sum w_i x_i^2}{\sum w_i x_i} - 1 + 2 \frac{\sum w_i}{\sum w_i x_i} - 2 \frac{\sum w_i/x_i}{\sum w_i x_i} \right]$$

which reduces to equation 20.

(46) K. H. Meyer, "High Polymers," Vol. IV, Natural and Synthetic High Polymers, 2nd ed., Interscience Publishers, Inc., New York, N. Y., 1950, p. 301.

Substitution of this relation into equation 20, with insertion of the appropriate averages for \bar{M} , yields an expression for $\langle \bar{s}_0^2 \rangle_z$ in terms of \bar{M}_n , \bar{M}_w , \bar{M}_z and the parameter q . Hence, the persistence length q may be calculated from $\langle \bar{s}_0^2 \rangle_z$ (Table III) and the various average molecular weights (Table II). From the data for the three highest fractions $q = 117 (\pm 11) \text{ \AA.}$,⁴⁷ hence the limiting values $(\bar{s}_0^2/r_{\max})_{M=\infty} = 39 (\pm 4) \text{ \AA.}$, and $(\bar{s}_0^2/M)_{M=\infty} = 0.70 (\text{ \AA.}^2/\text{mol. wt.})$. Holtzer, Benoit and Doty found an almost identical value of 0.71 for this latter ratio (as calculated from their $(\bar{r}^2/n)^{1/2} = 35 \text{ \AA.}$, where r is the end-to-end dimension and n is the number of units). The value of $(\bar{s}_0^2/M)_{M=\infty}$ for CTN is much larger than the value of about 0.08 found for several vinyl polymers. Further, in the case of vinyl polymers the asymptotic value is attained at molecular weights below 30,000.

The curve shown in Fig. 7 represents \bar{s}_0^2/M calculated according to equation 18 for homogeneous polymers ($\bar{x}_n = \bar{x}_w = \bar{x}_z$) and $q = 117 \text{ \AA.}$ Holtzer, Benoit and Doty arrived at a similar dependence of \bar{s}_0^2/M on M using a chain model with fixed valence angles and symmetrically hindered bond rotations.⁴⁸ The unavoidably large experimental error in the determination of $\langle \bar{s}^2 \rangle_z$ for the samples of lower molecular weights precludes definite conclusions regarding experimental agreement with the form of the theoretical curve. It is significant nevertheless that the lower fractions occur in a molecular weight region where \bar{s}_0^2/M should be considerably less than its asymptotic value, and the experimental results confirm this expectation. In carrying out this analysis of the configuration we have adopted the Porod-Kratky model, but any other plausible model for such an extended chain should lead to similar conclusions.

Smoothed values of $\langle \bar{s}_0^2 \rangle_z$ calculated from equation 20 using the averaged value of q given above and the values of \bar{x}_n , \bar{x}_w and \bar{x}_z obtained from the corresponding average molecular weights (Table II) with the aid of equation 19', are given for each fraction in the sixth column of Table III. Their ratios to \bar{M}_z are included in the seventh column.

It is of interest also to examine the ratio of the root-mean-square end-to-end length $(\bar{r}_0^2)^{1/2}$ of the chain to its maximum length r_{\max} at full extension. This ratio is given in the last column of Table III, the quantity $\langle \bar{r}_0^2 \rangle_z$ having been obtained by equating $\langle \bar{r}_0^2 \rangle_z$ to $6 \langle \bar{s}_0^2 \rangle_z$ (experimental).⁴⁹ This re-

lation of \bar{r}_0^2 to \bar{s}_0^2 is rigorously true only for a random flight chain. The error arising from failure of the CTN chain to qualify fully under this requirement should not however exceed the experimental error. It will be observed that the mean extension of the fraction of lowest molecular weight approaches half the length at full extension. Use of random flight statistics and assumption of spherical form, as is customary in treating dilute solution properties of polymers, is obviously unjustified in such circumstances.

The quantity $(\bar{r}_0^2/n)^{1/2}$, where n is the number of units in the chain, equals the bond length in the case of a hypothetical freely jointed chain having no restrictions whatever on the angles between successive bonds. The value of this ratio observed for an actual chain has often been designated⁴ as an effective bond length b . Our results, in agreement with those of Holtzer, Benoit and Doty, yield $b = 35 \text{ \AA.}$ for CTN. It has not always been appreciated that this effective bond length refers to the freely jointed chain analog having *the same number of bonds* and hence a much greater contour length (r_{\max}) than that of the actual (stiff) chain. A more appropriate analog is the Kuhn equivalent chain⁵⁰ having *the same contour length* as the actual chain, but a smaller number of bonds as required to yield the same limiting value of \bar{r}_0^2/M or \bar{s}_0^2/M as the actual chain. The segment length for the Kuhn equivalent chain is given by the limiting value of \bar{r}_0^2/r_{\max} , or $6(\bar{s}_0^2/r_{\max})_{M=\infty} = 2q = 234 \text{ \AA.}$ This equivalent chain would consist therefore of rod-like sequences of about 45 anhydroglucose units joined to one another without valence angle restrictions. If the angle between successive rigid sequences in the chain analog is assigned a definitive value (*e.g.*, 110°), but free rotation is assumed to prevail at the junction, the sequence length will be less (*e.g.*, approximately half as great for an angle of 110°).

Although the Porod-Kratky model may be inappropriate for more flexible chains, it is of interest nevertheless to examine values of q calculated in the foregoing manner from \bar{s}_0^2/M for typical vinyl polymers. For polystyrene, polyisobutylene, poly(methyl methacrylate) and poly(vinyl acetate) the q values thus calculated are in the range of 8 to 10 \AA. The lowest and the highest molecular weight fractions of CTN consist of molecules whose weight average lengths correspond to 6.3 and 88 Porod-Kratky units (\bar{x}_w), respectively. For polystyrene corresponding x values (numbers of Porod-Kratky units) are reached at molecular weights of 2,600 and 36,000. These figures indicate the molecular weight range for polystyrene which, from a configurational point of view, should correspond approximately to the range covered by our fractions of cellulose trinitrate. The much greater stiffness of CTN chains compared to that of other polymers is apparent from these comparisons.

Hydrodynamic Considerations.—The intrinsic viscosity $[\eta]$ and the frictional coefficient f_0 may

est for the more heterogeneous samples of higher molecular weight. The values of $(\langle \bar{r}^2 \rangle_n)^{1/2}/\langle r_{\max} \rangle_n$ are 0.46 and 0.24 for the samples of lowest and highest molecular weight, respectively.

(50) Ref. 20, p. 413.

(47) Recently, O. Kratky and H. Sembach, *Makromol. Chem.*, **16**, 115 (1955), estimated the persistence length for CTN (13.1% N) from low angle X-ray scattering by solutions (4 and 8%) in acetone. Their result, 76 \AA. , is somewhat lower than ours. In view of the approximations involved in interpreting the X-ray scattering (G. Porod, *J. Polymer Sci.*, **10**, 157 (1953)), this result is in reasonable agreement with the value obtained by light scattering. Since the X-ray method depends primarily on interferences involving radiation scattered from nearby chain elements, whereas light scattering is predominantly determined by interferences between remote elements, the two results are fundamentally independent.

(48) Holtzer, Benoit and Doty's b^2/b^2 is equivalent, after correction for the "volume effect" expansion (α^2), to the ratio of our \bar{s}_0^2/M to its limiting value at $M = \infty$.

(49) Somewhat larger ratios would have been obtained had number instead of z-average quantities been used, the differences being great-

be related to the chain dimensions in the customary manner^{5,6}

$$[\eta] = \{\Phi'\} (\overline{s_0^2}/M)^{3/2} M^{1/2} \alpha^3 \quad (21)$$

$$f_0/\eta_0 = \{P'\} (\overline{s_0^2}/M)^{1/2} M^{1/2} \alpha \quad (22)$$

Ordinarily $\{\Phi'\}$ and $\{P'\}$ may be assigned constant values which are independent of both the solvent and the polymer, and these are observed to correspond fairly well with those predicted by theory in the limit of high resistance to flow within the domain of the molecule^{51,52} (*i.e.*, low "permeation"⁵³). Owing to the comparatively high extension of the CTN chain, however, it is expedient in this paper to consider that $\{\Phi'\}$ and $\{P'\}$ depend on the molecular weight. They are therefore enclosed in braces to distinguish them from their asymptotically constant values as ordinarily used. Also, the prime is appended to indicate use of the radius of gyration instead of the end-to-end distance in equations 21 and 22.⁵⁴ Similarly, $\overline{s_0^2}/M$ must be regarded as variable with M . The empirical relations (11) and (12), according to which $[\eta]$ and S_0 (and therefore f_0 also) are expressed as proportional to powers of M , suggest the possibility of approximating the individual factors occurring in equation 21 and 22 by setting them proportional to powers of M . From a theoretical point of view, this should be feasible only over limited molecular weight ranges; in fact, the straight lines of Fig. 6, from which equations 11 and 12 are deduced, should be regarded as tangents to curves, the forms of which could be reliably described only from more precise measurements covering a wider range in M .

The contributions of the various factors occurring in equations 21 and 22 to the exponents in the empirical relations (11) and (12) may be treated as follows. Let a_η be the exponent of the molecular weight in the empirical intrinsic viscosity relation (11) and let a_s be the exponent of M in the empirical relation (12) for the sedimentation constant. Then

$$a_\eta = 0.5 + 3a_1 + 1.5a_2 + a_3 \quad (23)$$

and, recalling that the sedimentation constant is proportional to M/f_0

$$a_s = 0.5 - a_1 - 0.5a_2 - a_4 \quad (24)$$

where

$$a_1 = \text{dln } \alpha / \text{dln } M$$

$$a_2 = \text{dln } (\overline{s_0^2}/M) / \text{dln } M$$

$$a_3 = \text{dln } \{\Phi'\} / \text{dln } M$$

$$a_4 = \text{dln } \{P'\} / \text{dln } M$$

The molecular expansion factor α remains very near unity (see Table III) throughout the molecular weight range studied, hence a_1 is negligible for the present system. However, unlike the behavior of vinyl polymers above a molecular weight of 30,000 the values of a_2 , a_3 and a_4 are not zero for CTN.

According to equation 18

(51) J. G. Kirkwood and J. Riseman, *J. Chem. Phys.*, **16**, 565 (1948).

(52) J. G. Kirkwood, R. W. Zwanzig and R. J. Plock, *ibid.*, **23**, 213 (1955).

(53) P. Debye and A. M. Bueche, *ibid.*, **16**, 573 (1948).

(54) The asymptotic value Φ' , equal to $6^{3/2}\Phi$, is 3.2×10^{22} , based on $\Phi = M[\eta]/(\overline{r^2})^{3/2} = 2.2 \times 10^{21}$ as the average of numerous determinations.⁵⁵ Similarly, $P' = 6^{1/2}P$ where $P = (f_0/\eta_0)/(\overline{r^2})^{1/2} = 5.1$.

(55) See ref. 20, pp. 616, 628.

$$a_2 \cong 3(1 - 4/x + 6/x^2)/x(1 - 3/x + 6/x^2 - 6/x^3) \quad (25)$$

The weight average numbers \bar{x}_w of Porod-Kratky segments in our fractions from the lowest to the highest are approximately 6, 12, 20, 38 and 88, respectively. The corresponding a_2 's calculated from equation 25 are 0.4, 0.22, 0.14, 0.08 and 0.03. Since the a_2 's vary with M , the dependence of $\overline{s_0^2}/M$ on M is therefore poorly represented by a power relationship. Our ultimate conclusions will depend, however, merely on the observation that the change in $\overline{s_0^2}/M$ with M accounts for only a minor portion of the deviations of a_η and a_s from one-half over the molecular weight interval of our measurements on CTN. The effective value of a_2 (*i.e.*, the slope of the tangent in the middle of the molecular weight range) should be about 0.10 to 0.15. Taking $a_\eta = 1.01$, $a_s = 0.29$, $a_2 = 0.13$, and $a_1 = 0$, we find from equations 23 and 24 the values $a_3 \cong 0.32$, and $a_4 \cong 0.15$, respectively, which represent the residual molecular weight dependences which may be ascribed to hydrodynamic effects manifested in changes in $\{\Phi'\}$ and $\{P'\}$ with M .

In the Debye-Bueche theory,⁵³ both a_1 and a_2 are considered to equal zero, and departures of a_η (*i.e.*, $0.5 + a_3$, or ϵ in their notation) from 0.5 are attributed solely to a_3 , *i.e.*, to the increase in $\{\Phi'\}$ with M . The frictional coefficient is treated similarly. From the preceding estimates of a_3 and a_4 , therefore, values may be deduced for the Debye-Bueche shielding ratio σ . The results, $\sigma = 3.3$ and $\sigma = 3.2$ from a_3 (viscosity) and a_4 (sedimentation), respectively, are in close agreement. According to the Debye-Bueche theory, our $\{\Phi'\}$ should be proportional to their function $\varphi(\sigma)$. The value of the latter at $\sigma = 3.3$ is 0.68, and in the limit of sufficiently high chain length it reaches 2.50. Hence the average value of $\{\Phi'\}$ within the range investigated here should be about $0.68/2.5 = 0.272$ of its limiting value for infinite M , according to that theory. In a similar fashion their function $\psi(\sigma)$, relating to the frictional coefficient, is found to have the value 0.62 at $\sigma = 3.3$, compared with unity at $M = \infty$.

We may also interpret a_3 and a_4 in terms of the Kirkwood-Riseman theory⁵¹ and deduce, first of all, their parameter x (not to be confused with the previous x used for the number of Porod-Kratky segments) defined by

$$x = (1/6\pi^{3/2})M^{1/2}(\overline{s_0^2}/M)^{-1/2} (\zeta/\eta_0 M_0) \quad (26)$$

where ζ is the frictional coefficient for an element, or "bead," of the polymer chain, M_0 is the molecular weight of one unit and η_0 is the viscosity of the solvent. The expansion factor α is assumed to equal unity. Assigning to the quantity $0.5 + a_3$ (α in the notation of Kirkwood and Riseman) our experimental value 0.82, we obtain from their tabulated calculations $x = 0.77$.

In order to deduce x from a_4 we consider the following relation based on the Kirkwood-Riseman equations

$$\{P'\} = 6\pi^{3/2}x/(1 + 8x/3) \quad (27)$$

It follows from equations 26 and 27 and the defini-

tion of a_4 (see above) that

$$x = (3/16a_4)(1 - 2a_4) \quad (28)$$

Substitution of $a_4 = 0.15$ yields $x = 0.87$, in substantial agreement with the value obtained above from a_3 .

From x and the quantities previously given we may estimate, with the aid of equation 26, a value for the ratio ζ/η_0 per repeating unit ($M_0 = 287$), which should equal 6π times the Stokes' law radius of a unit. The result obtained for the ratio is about 13 Å., which corresponds to an effective radius of less than one Å. unit. This is only about one-fourth the actual mean radius of a structural unit.

The Kirkwood-Riseman theory permits explicit evaluation of $\{\Phi'\}$ according to the relationship

$$\{\Phi'\} = (\pi^{3/2}N/100)xF(x) = 3.35 \times 10^{22}xF(x) \quad (29)$$

where $F(x)$ is a function, tabulated by Kirkwood, Zwanzig and Plock,⁵² of the quantity x defined by equation 26. At $x = 0.8$, $xF(x) = 0.47$, hence the value of $\{\Phi'\}$ predicted by the Kirkwood-Riseman theory from the values assigned to a_3 and a_4 is 1.58×10^{22} . For very large x , the function $xF(x)$ reaches a limit of 1.48, and the theoretical asymptotic value of $\{\Phi'\}$ is therefore $\Phi' = 5.0 \times 10^{22}$. Thus, at $x = 0.8$, $\{\Phi'\}/\Phi' = 0.318$, in fair agreement with the ratio deduced from the Debye-Bueche theory. Experimental results⁵⁵ on various random coiling polymers yield for Φ' the value⁵⁵ 3.2×10^{22} , which is somewhat smaller than the theoretical value; the discrepancy probably is not beyond inaccuracies of the theory, however.

Similarly, from the Kirkwood-Riseman relationship for the frictional coefficient (*i.e.*, equation 27) we find $\{P'\} = 8.5$ at $x = 0.8$. The theoretical asymptotic value at $x = \infty$ is 12.5, and this is in exact agreement with previous experiments⁵⁵ on other systems. The ratio $\{P'\}/P' = 8.5/12.5 = 0.68$ is again in reasonable agreement with the Debye-Bueche theoretical value.

We turn now to the evaluation of $\{P'\}$ and $\{\Phi'\}$ from experimental results using the equations 21 and 22 which define these parameters. Correction factors, q_Φ and q_P (not to be confused with the Porod-Kratky q), respectively, must however be included for the effects of molecular weight heterogeneity. We thus write

$$\{\Phi'\} = q_\Phi[\eta]\bar{M}_w/(\overline{s^2})^{3/2} \quad (30)$$

$$\{P'\} = q_P f_0/\eta_0(\overline{s^2})^{1/2} \quad (31)$$

where $\overline{s^2}$ replaces $\alpha^2 \overline{s_0^2}$. The ratios $[\eta]\bar{M}_w/(\overline{s^2})^{3/2}$ and $f_0/\eta_0(\overline{s^2})^{1/2}$, calculated from results previously presented in Tables I and II, are given in the second and fifth columns of Table IV.

It is shown in the Appendix that

$$q_\Phi = [\Gamma(y + 3 + 2a_1 + a_2)]^{3/2}(y + 1)^{-2} \\ [\Gamma(y + 2)]^{-1/2}[\Gamma(y + 3/2 + 3a_1 + 3a_2/2)]^{-1} \quad (32)$$

and

$$q_P = \Gamma(y + 3/2 - a_1 - a_2/2) \\ [\Gamma(y + 3 + 2a_1 + a_2)]^{1/2}[\Gamma(y + 2)]^{-3/2} \quad (33)$$

These expressions reduce to those given previously^{56,57} when $a_2 = 0$. Values given in Table IV

(56) A. R. Shultz, *J. Am. Chem. Soc.*, **76**, 3422 (1954).

(57) E. V. Gouinlock, P. J. Flory and H. A. Scheraga, *J. Polymer Sci.*, **16**, 383 (1955).

for q_Φ and q_P have been calculated by taking $a_1 = 0$ and assigning to a_2 the values applicable to each fraction as quoted above in the text. The $\{\Phi'\}$ and $\{P'\}$ calculated according to equations 30 and 31 are listed in columns four and seven, respectively, of Table IV. Results of equivalent calculations based on the smoothed values of $(\overline{s^2})^{1/2} = \alpha (\overline{s_0^2})^{1/2}_{\text{smoothed}}$ (see Table III), are given in the last two columns. An increase in both $\{\Phi'\}$ and $\{P'\}$ with molecular weight is indicated. All values of $\{\Phi'\}$ calculated from observed $\overline{s^2}$ are less than the asymptotic $\Phi' = 3.2 \times 10^{22}$ found for more flexible polymers; only the $\{P'\}$ for the highest fraction exceeds the asymptotic $P' = 12.5$. Holtzer, Benoit and Doty, on the other hand, found $\{\Phi\}$ to be independent of M within experimental error,⁵⁸ its value being substantially that of the asymptotic Φ found for other polymers.

For the middle of the molecular weight range ($\bar{M}_w \cong 150,000$) the values of $\{\Phi'\}$ and $\{P'\}$ are approximately 2.3×10^{22} and 11, respectively, as interpolated from columns 9 and 10 of Table IV. These values are greater than those predicted (1.58×10^{22} and 8.5, respectively) from the Kirkwood-Riseman theory on the basis of x values derived from the exponents a_3 and a_4 deduced from analysis of intrinsic viscosity and sedimentation data. Moreover, if their $xF(x)$ function is adopted to account for the variation of $\{\Phi'\}$, the limiting value Φ' approached at very high chain lengths should be approximately $2.3 \times 10^{22}/0.318 = 7.2 \times 10^{22}$, where 0.318 is the ratio of $xF(x)$ at $x = 0.8$ to its value at $x = \infty$ (see above). The result exceeds the theoretical value of Φ' (5.0×10^{22} according to the Kirkwood treatment) and, of greater significance, it is more than twice the value (3.2×10^{22}) found to hold for other polymers. Likewise, $\{P'\} = 11$ would extrapolate according to the Kirkwood-Riseman theory, to $P' = 11/0.68 = 16.2$, which again is too high. Extrapolation to infinite molecular weight according to the Debye-Bueche theory leads to similar inconsistencies.

The quantities $\{\Phi'\}^{1/3} \{P'\}^{-1}$ given in the eighth column of Table IV may be considered to represent, except for a factor of proportionality, ratios of the effective hydrodynamic radii for the frictional coefficient f_0 and for the viscosity. The values given depend only on measured values of $[\eta]$, \bar{M}_w , f_0 (from S_0), and the heterogeneity factors; they are independent of $\overline{s^2}$, the least accurate of the various measured quantities. The values obtained are the same for the different fractions within experimental error, and equal to the value of $\Phi'^{1/3}/P' \equiv \Phi'^{1/3}/P' = 2.5 \times 10^6$ established experimentally for various other polymers.⁵⁵ Thus, the abnormalities in $\{\Phi'\}$ and $\{P'\}$ observed for CTN are mutually related.

Conclusions

The foregoing analysis of the results shows that the portion of the change in $[\eta]/\bar{M}^{1/2}$ or $S_0/\bar{M}^{1/2}$

(58) Holtzer, Benoit and Doty's conclusion that $\{\Phi\}$ is constant is incompatible with their further assertions that \bar{r}^2/n is substantially independent of n for $n > 500$ and that $[\eta]$ is directly proportional to M in the same range. The inconsistency is evident from the definition of $\{\Phi\}$, or of $\{\Phi'\}$. See equation 30.

TABLE IV
HYDRODYNAMIC PARAMETERS FOR CTN IN ETHYL ACETATE AT 30°^a

Fraction	$\frac{[\eta]\bar{M}_w}{(\langle s^2 \rangle_z)^{3/2}} \times 10^{-22}$	$q\Phi$	$\frac{\{\Phi'\}}{\times 10^{-22}}$	$f_0/\eta_0(\langle s^2 \rangle_z)^{1/2}$	qP	$\{P'\}$	Results from smoothed $\langle s^2 \rangle_z$		
							$\frac{\{\Phi'\}^{1/3}/\{P'\}}{\times 10^{-4}}$	$\frac{\{\Phi'\}}{\times 10^{-22}}$	$\{P'\}$
L-10	1.48	1.43	2.1	9.65	1.11	10.7	2.6	1.5	9.6
L-8	1.08	1.46	1.6	9.42	1.10	10.4	2.4	1.7	10.7
L-5	1.49	1.67	2.5	9.87	1.13	11.2	2.6	2.1	10.5
H-2	1.33	2.08	2.8	9.37	1.18	11.1	2.7	2.7	11.0
H-1	1.31	2.14	2.8	11.1	1.18	13.1	2.3	3.3	13.9
Asymptotic values							2.5 ^b	3.2	12.5

^a Intrinsic viscosities are expressed in units of (g./100 cc.)⁻¹, ($\langle s^2 \rangle_z$)^{1/2} in cm., \bar{M}_w in gram molecular weight, and f_0/η_0 in cm. ^b Computed from the asymptotic values Φ' and P' .

with molecular weight not attributable to the increase in $\overline{s_0^2}/M$ with M cannot be reconciled in a satisfactory manner with either of the theories considered. If the parameters σ and x of the Debye-Bueche and the Kirkwood-Riseman theories, respectively, are assigned values as required to account for this change with M (as expressed by the exponents a_3 and a_4), the asymptotic values calculated for the parameters Φ' and P' are untenably large. On the other hand, if the numerical values observed for $\{\Phi'\}$ and $\{P'\}$ had been used to deduce values of x , much larger values would have been obtained, with the consequence that the predicted change in $\{\Phi'\}$ and $\{P'\}$ with M would have been much too small to account for the observed exponents $a_7 = 1.01$ and $a_8 = 0.29$; in other words, the resulting values of a_3 and a_4 would have been too small. Thus, existing theories fail to offer a self-consistent interpretation of the observed decreases in $\{\Phi'\}$ and $\{P'\}$ with decreasing M ; in alternative terms these theories fail to offer a satisfactory explanation for the values of the exponents in the empirical equations 11 and 12.

It may be significant that adoption of a value for the frictional constant ζ for a polymer chain unit predicted from Stokes' law and the radius of a unit would lead, according to the Kirkwood-Riseman theory, to a mean value of $\{\Phi'\}$ which is about two-thirds of Φ' . Such a value would be more or less in agreement with our results. As already indicated, however, the theory applied in this most literal manner would not then account for the observed fall-off in $\{\Phi'\}$. It is natural to postulate in these circumstances that the observed decrease in $\{\Phi'\}$ and $\{P'\}$ (and hence in $[\eta]/M^{1/2}$ and $S_0/M^{1/2}$) with decrease in M is primarily due to causes other than hydrodynamic effects arising merely from the diminished internal frictional resistance at low chain lengths, *i.e.*, to causes other than those considered in the aforementioned theories. Possibly the explanation is to be found in the deviations of the CTN chain at low degrees of polymerization from "random flight" statistical form. Thus the average spatial relationship of one chain element to another deviates considerably from the gaussian representation employed by Kirkwood and Riseman. From the point of view of the Debye-Bueche theory, the form of the molecule deviates considerably from spherical symmetry and hence is poorly approximated by a sphere of uniform density.

Tentatively we suggest that the large exponent (near unity) of equation 11, the small exponent

(near zero) of equation 12, and the associated decreases in $\{\Phi'\}$ and $\{P'\}$ with M arise primarily from severe deviations from random flight statistics and the related deviation from spherical symmetry within the molecular weight range investigated.

Since $\{\Phi'\}$ and $\{P'\}$ for the higher molecular weight fractions are close to the asymptotic values observed for other polymers it seems likely that CTN is not far from asymptotic hydrodynamic behavior. One may venture the prediction that if reliable measurements could be carried out over one additional decade in M , the exponents in equations 11 and 12 would in this range approach values differing from one-half only by the (small) contribution from a_1 . Unfortunately, formidable experimental difficulties in this range remain to be overcome.

Finally, since the observed $\{\Phi'\}$ and $\{P'\}$ are so near their asymptotic values even for such extended chains of moderate degrees of polymerization, the much discussed effect of "permeation" on the hydrodynamic properties of polymers appears to play at most a minor role even in the case of such an extended polymer chain as that of CTN. Its importance in other polymers should be quite negligible, even down to chain lengths where present theories are rendered inapplicable for other reasons. The insignificance of "permeation" for other polymers, in the region where the chains are long enough for "random flight" statistics to apply, has been amply demonstrated.⁷

Appendix

Heterogeneity Corrections for $\{\Phi'\}$ and $\{P'\}$.—

It has been shown previously²¹ that the correct value of Φ' , undistorted by effects of molecular weight heterogeneity, provided it is independent of M over the range of molecular species included, is given by

$$\Phi' = [\eta]\bar{M}_n / \langle (s^2)^{3/2} \rangle_n \tag{A-1}$$

Since, however, \bar{M}_w and $\langle s^2 \rangle_z = \sum w_i M_i \overline{s_i^2} / \sum w_i M_i$ ordinarily are measured by light scattering, we introduce the correction factor

$$q\Phi = \bar{M}_n (\langle s^2 \rangle_z)^{3/2} / \bar{M}_w \langle (s^2)^{3/2} \rangle_n = (\sum w_i M_i \overline{s_i^2})^{3/2} / (\sum w_i M_i)^{3/2} \sum (w_i / M_i) (\overline{s_i^2})^{3/2} \tag{A-2}$$

as required to render equation 30 consistent with A-1. Substituting

$$\overline{s_i^2} = \alpha_i^2 (\overline{s_0^2})_i \sim M_i^{+2a_1 + a_2} \tag{A-3}$$

in equation A-2, we obtain equation 32, after replacing summations by integrals and evaluating

them using the Schulz distribution (equation 10). This result reduces to that obtained previously⁵⁶ for the case of a "Gaussian" chain, *i.e.*, one for which $\overline{s_0^2}/M$ is constant, by substituting $a_2 = 0$.

The analogous correction factor q_p to be used in the calculation of the quantity $\{P'\}$

$$\{P'\} = q_p \left[\frac{1 - \bar{v}_p}{N\eta_0} \right] \left[\frac{\bar{M}_w}{S_{0 < s^2 >_z^{1/2}}} \right] \quad (\text{A-4})$$

has been worked out previously⁵⁷ for $a_2 = 0$ (Gaussian case). When $a_2 \neq 0$ equation A-4 leads to equation 33.

HYDROGEN OVERPOTENTIAL ON SILVER IN SODIUM HYDROXIDE SOLUTIONS

By I. A. AMMAR AND S. A. AWAD

Faculty of Science, Department of Chemistry, Cairo University, Cairo, Egypt

Received March 2, 1956

Hydrogen overpotential, η , has been measured on Ag cathodes in 1.0 to 0.01 *N* aqueous NaOH solutions, in the current density range 3×10^{-8} to 10^{-3} amp./cm.² Measurements have also been carried out at 30, 40, 50 and 60°, and the heat of activation, ΔH^\ddagger , at the reversible potential is calculated. The electron number, λ , is calculated from overpotential measurements at low cathodic polarization, and the values obtained are very near to unity. A slow discharge process from water molecules is established as the rate-determining mechanism for hydrogen evolution on Ag in alkaline solutions. The effect of *pH* on η is also studied and attempts are made toward the explanation of such an effect.

Introduction

Hydrogen overpotential at Ag cathodes in aqueous HCl solutions was studied by Bockris and Conway.¹ They observed two slopes in the linear logarithmic section of the Tafel lines. This was attributed to the specific adsorption of H_3O^+ ions. A slow discharge rate-determining mechanism was suggested by the above authors to account for their overpotential results.

The aim of the present investigation was to study the overpotential characteristics for Ag in aqueous NaOH solutions. Previous work in alkaline solutions² indicated that the discharge from water molecules was rate determining.

Experimental

The experimental technique was essentially the same as that of Bockris and Potter.² The electrodes were sealed under an atmosphere of pure dry hydrogen in fragile glass bulbs. Spectroscopically pure silver wire (1 mm. diameter) was used. The silver wire was spot-welded to platinum before sealing it into glass. The glass bulbs were broken directly before the measurements were started. Pure sodium hydroxide solutions were prepared under an atmosphere of pure hydrogen, followed by preelectrolysis at 1.0×10^{-2} amp./cm.² for 20 hours on a silver preelectrolysis electrode.

All glass parts of the apparatus were made of arsenic-free borosilicate glass, technically known as "Hysil."³ Solution-sealed taps and ground glass joints were used for the construction of the cell. Connections between the various parts of the apparatus were made with the help of movable glass bridges. The apparatus was cleaned with a mixture of "Analar" nitric and sulfuric acids. This was followed by washing with equilibrium water ($K = 2.0 \times 10^{-6}$ mho cm.⁻¹) and the cell was then washed several times by conductance water ($K = 2.0 \times 10^{-7}$ mho cm.⁻¹) prepared by refluxing equilibrium water under an atmosphere of pure hydrogen for 6 hours. Before each run, care was taken to free the previously cleaned cell from oxygen. This was done by filling the cell completely with conductance water, and then replacing this water by pure hydrogen before the NaOH solution was introduced.

Cylinder hydrogen was purified from oxygen, carbon monoxide and other impurities by passing it over hot copper

(450°), then over a mixture of MnO_2 and CuO (technically known as "Hopcalite") to oxidize CO to CO_2 . CO_2 was then removed by soda lime.

A platinized platinum electrode in the same solution and at the same temperature as the test electrode was used as a reference. The direct method of measurements was employed, and Tafel lines were traced between 3×10^{-8} and 10^{-3} amp./cm.² The potential was measured with a valve *pH* meter millivoltmeter, and the current with a multi-range milli-micro-ammeter. At low currents, the current was checked by measuring the *p.d.* across a standard resistance. The temperature was kept constant with the help of an air thermostat controlled to $\pm 0.5^\circ$. The current density was calculated using the apparent surface area.

Results

The Tafel line slope, b , the transfer coefficient, α , and the exchange current, i_0 , for the cathodic hydrogen evolution at Ag in 1.0, 0.2, 0.1, 0.05 and 0.01 *N* aq. NaOH solutions are given in Table I. Figure 1 shows four Tafel lines on Ag in 0.1 *N* aq. NaOH solution at 30, 40, 50 and 60°. At 60° the

TABLE I

Concn. <i>N</i>	Temp., °C.	<i>b</i> (v.)	α	i_0 (amp./cm. ²)
1.0	30	0.120	0.500	3.2×10^{-7}
	40	.120	.517	5.0×10^{-7}
	50	.120	.533	7.1×10^{-7}
	60	.120	.550	1.1×10^{-6}
	0.2	30	0.120	0.500
0.2	40	.120	.517	3.6×10^{-7}
	50	.120	.533	5.6×10^{-7}
	60	.120	.550	8.3×10^{-7}
	0.1	30	0.120	0.500
0.1	40	.120	.517	3.2×10^{-7}
	50	.120	.533	5.0×10^{-7}
	60	.120	.550	8.3×10^{-7}
	0.05	30	0.120	0.500
0.05	40	.120	.517	2.8×10^{-7}
	50	.120	.533	4.5×10^{-7}
	60	.120	.550	7.1×10^{-7}
	0.01	30	0.122	0.492
0.01	40	.122	.508	2.0×10^{-7}
	50	.122	.525	3.2×10^{-7}
	60	.122	.541	4.8×10^{-7}

(1) J. O'M. Bockris and B. Conway, *Trans. Faraday Soc.*, **48**, 724 (1952).

(2) J. O'M. Bockris and E. C. Potter, *J. Chem. Phys.*, **20**, 614 (1952).

(3) Prepared by Chance Bros., Ltd., Birmingham, England.

asymptotic part of the Tafel line is shorter than the corresponding parts at lower temperatures. The transfer coefficient is calculated according to: $b = (2.303RT/\alpha F)$.

The electron number, λ , defined as the number of electrons necessary to complete one act of the rate-determining step,⁴ is calculated using

$$\lambda = -\frac{RT}{i_0 F}(\partial i_c / \partial \eta)_{\eta \rightarrow 0} \quad (1)$$

and

$$\exp(\lambda \eta_a F / RT) = 0.05 \quad (2)$$

η_a is the overpotential at which the Tafel line departs from linearity owing to the appreciable rate of ionization of adsorbed atomic hydrogen. Equation 2 gives approximate values for λ (cf. ref. 4). The values of the electron number, *i.e.*, λ_1 (calculated according to equation 1) and λ_2 (calculated according to equation 2) are given in Table II for 30, 40 and 50°. Values of λ at 60° could not be calculated owing to the fact that only very few measurements of η below 20 mv. can be experimentally obtained (cf. Fig. 1). The relation between η and i_c for small cathodic polarization (below 20 mv.) is shown in Fig. 2 for 0.1 N NaOH solution.

TABLE II

* Values of λ are given to the nearest first decimal figure.

Concn. N	Temp., °C.	$-(\partial \eta / \partial i_c)_{\eta \rightarrow 0}$ v./amp./cm. ²	λ_1	η_a	λ_2
1.0	30	8.0×10^4	1.0	0.070	1.1
	40	5.0×10^4	1.1	0.070	1.2
	50	3.5×10^4	1.1	0.070	1.2
0.2	30	1.2×10^5	1.0	0.065	1.2
	40	8.3×10^4	0.9	0.065	1.2
	50	4.3×10^4	1.2	0.065	1.3
0.1	30	1.2×10^5	1.1	0.070	1.1
	40	8.0×10^4	1.1	0.065	1.2
	50	4.7×10^4	1.2	0.065	1.3
0.05	30	1.5×10^5	1.0	0.075	1.0
	40	8.0×10^4	1.2	0.070	1.2
	50	5.0×10^4	1.2	0.070	1.2
0.01	30	1.7×10^5	1.1	0.075	1.0
	40	1.1×10^5	1.2	0.075	1.1
	50	7.0×10^4	1.2	0.070	1.2

The effect of pH on overpotential at three different current densities (3.2×10^{-6} , 3.2×10^{-5} and 3.2×10^{-4} amp./cm.²) is given in Table III.

TABLE III

Temp., °C.	$(\partial \eta / \partial \text{pH})$ in v. at		
	3.2×10^{-6} amp./cm. ²	3.2×10^{-5} amp./cm. ²	3.2×10^{-4} amp./cm. ²
30	0.025	0.028	0.030
40	.025	.028	.028
50	.025	.025	.025
60	.025	.030	.030

The heat of activation, ΔH_0^* , at the reversible potential is calculated according to the equation

$$i_0 = B \exp(-\Delta H_0^* / RT) \quad (3)$$

where B is the Eyring entropy factor.⁵ The rela-

(4) J. O'M. Bockris and E. C. Potter, *J. Electrochem. Soc.*, **99**, 169 (1952).

(5) S. Glasstone, H. Eyring and K. Laidler, *J. Chem. Phys.*, **7**, 1053 (1939).

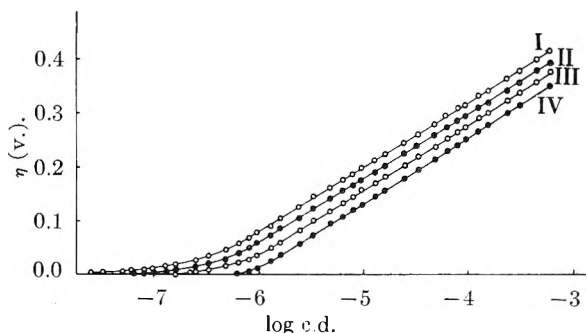


Fig. 1.—Tafel lines for Ag in 0.1 N NaOH solution as a function of temperature: I, 30°; II, 40°; III, 50°; IV, 60°.

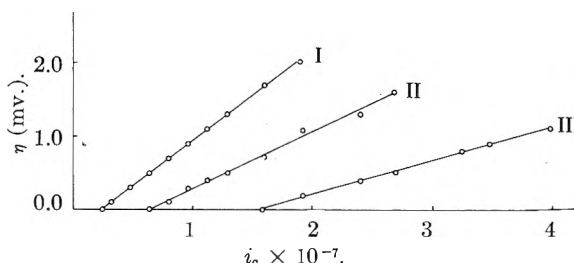


Fig. 2.—Relationship between η (below 20 mv.) and the net cathodic current for Ag in 0.1 N NaOH: I, 30°; II, 40°; III, 50°.

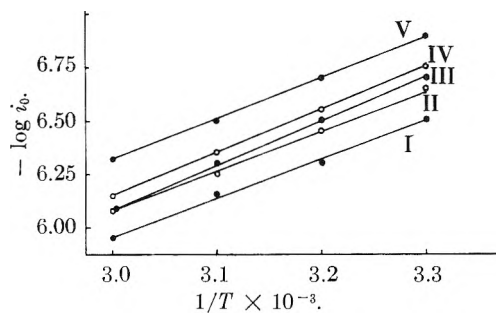


Fig. 3.—Relationship between the logarithm of the exchange current and $(1/T)$: I, 1.0 N; II, 0.2; III, 0.1; IV, 0.05; V, 0.01.

tion between $\log i_0$ and $1/T$ is shown in Fig. 3. Values of ΔH_0^* , thus calculated, are given in Table IV.

TABLE IV

Concn., N	$-[d \log i_0 / d(1/T)]$	ΔH_0^* (kcal.)
1.0	1.81×10^3	8.3
0.2	1.90×10^3	8.8
0.1	2.05×10^3	9.4
0.05	2.00×10^3	9.2
0.01	1.81×10^3	8.3

If ΔH_0^* is assumed to be independent of concentration, a mean value of 8.8 kcal, is obtained from the results given in Table IV. Using this mean value for ΔH_0^* in equation 3, $\log B$ is calculated for the various NaOH solutions studied. The results at 30° are given in Table V. The plot of $\log B$ against the logarithm of the activity of NaOH results in a straight line with a slope of approximately 0.2.

Discussion

The activation overpotential associated with the cathodic hydrogen evolution may be attributed to a slow discharge process, a slow electrochemical de-

TABLE V

Concn., N	$-\log i_0$	$-\log B$
1.0	6.50	0.20
0.2	6.65	.35
.1	6.70	.40
.05	6.75	.45
.01	6.90	.60

sorption or a slow catalytic recombination.⁴ A rate-determining slow discharge process is characterized by a Tafel line slope of 0.120 v. at 30° and by $\lambda = 1$. For a rate-determining electrochemical desorption, the Tafel line exhibits two slopes of 0.040 and 0.120 v. at 30° in the linear logarithmic section, and λ is 2. A rate-determining catalytic mechanism is distinguished by two Tafel line slopes of 0.030 v. at 30° (at the low current density range) and ∞ v. (manifested by the occurrence of a limiting current at high current densities). For this mechanism λ is also 2. From this and the data given in Tables I and II it is evident that the rate of hydrogen evolution at Ag cathodes in NaOH solutions (0.01 to 1.0 N) is controlled by a slow discharge mechanism.

Distinction between the discharge from H_3O^+ ions and the discharge from water molecules can be made with the help of the pH effect on hydrogen overpotential. For the discharge from H_3O^+ ions (cf. ref. 2)

$$\left(\frac{\partial \eta}{\partial \ln a_{H^+}}\right)_{i_c} = \left(\frac{1-\beta}{\beta}\right) \left[\frac{RT}{F} - \left(\frac{\partial \xi}{\partial \ln a_{H^+}}\right)\right] \quad (4)$$

where β is a symmetry factor for the energy barrier of the discharge process, and ξ is the p.d. between the Helmholtz double layer and the bulk of solution. For the condition when $(\partial \xi / \partial \ln a_{H^+}) \approx 0$ and $\beta \approx 0.5$, the pH effect associated with the discharge of H_3O^+ is given by

$$\left(\frac{\partial \eta}{\partial pH}\right)_{i_c} = -(2.303RT/F) \quad (5)$$

thus indicating that η becomes more negative with increase of pH . For the discharge from water molecules (under the same condition as 5), the pH effect is given by

$$\left(\frac{\partial \eta}{\partial pH}\right)_{i_c} = (2.303RT/F) \quad (6)$$

The condition $(\partial \xi / \partial \ln a_{H^+}) \approx 0$ may be applicable when the electrode potential is very near to that of the electrocapillary maximum, whereupon in absence of specific adsorption $\xi \approx 0$. The direction of change of η with pH is thus a good criterion for the distinction between the discharged entities.

It is clear from Table III that $(\partial \eta / \partial pH)_{i_c}$ for the cathodic hydrogen evolution at Ag in NaOH solutions is positive, thus indicating that the discharge takes place from water molecules. Parsons and Bockris⁶ have shown that in alkaline solutions the discharge from water molecules is more probable than the discharge from H_3O^+ ions because the supply of H_3O^+ ions from the bulk of the solution to the electrode would be slow. In such solutions the concentration of water molecules is approximately 10^{14} times the concentration of H_3O^+ ions.

The discharge of hydrogen from water molecules may take the form of a prototropic transfer sug-

gested by Glasstone, Eyring and Laidler.⁵ The value of $\log B$ calculated by the above authors for such a rate-determining mechanism amounts to 1.5. This value is independent of the electrolyte concentration. The factor B is expressed by³

$$B = \lambda FK \frac{kT}{h} a_i \exp\left(\frac{\Delta S_0^*}{R}\right) \quad (7)$$

where K is the transmission coefficient, k is Boltzmann's constant, h is Planck's constant, a_i is the activity of the reactants in the initial state (Helmholtz double layer) and ΔS_0^* is the standard entropy of activation at the reversible potential. It is evident from Table V that the values of $\log B$ calculated for Ag, are different from the value given by Glasstone, Eyring and Laidler. It may thus be concluded that the prototropic transfer is not rate determining, although the discharge takes place from water molecules, for hydrogen evolution on Ag in NaOH solutions.

The pH effect associated with the discharge from water molecules is given by (6) when the cathode potential is very near to that of the electrocapillary maximum. In dilute NaOH solutions, for conditions far from the electrocapillary maximum $(\partial \xi / \partial \ln a_{H^+}) = -(\partial \xi / \partial \ln a_{Na^+}) = -(RT/F)$ and it follows that

$$\left(\frac{\partial \eta}{\partial pH}\right)_{i_c} = 2\left(\frac{2.303RT}{F}\right) \quad (8)$$

In between the above two conditions the pH effect lies between 60 and 120 mv. per unit increase of pH , at 30°. From Table III it is clear that the experimentally observed values of $(\partial \eta / \partial pH)_{i_c}$ are different from the theoretically deduced values given above. The experimental results cannot also be explained on the assumption that hydrogen originates from Na ions and water molecules,⁷ since this mechanism requires that $(\partial \eta / \partial pH)_{i_c} = 2(2.303RT/F)$.

In an attempt to correlate the experimental results, for the pH effect in alkaline solutions with the theory, Bockris and Potter² have suggested the possibility of an increase in the activity of water molecules in the double layer as compared to that in the bulk of solution. This is brought about by the orientation of water molecules under the high field strength near the electrode. Under such conditions the effect of pH on η is given by

$$\left(\frac{\partial \eta}{\partial pH}\right)_{i_c} = \frac{2.303RT}{F} - (\partial \xi / \partial \log a_{H^+}) \left(1 - \frac{4\pi\mu_w Cd}{d\beta F}\right) \quad (9)$$

where $\mu_w = 1.83 \times 10^{-18}$ e.s.u. is the dipole moment of water, Cd is the integral capacity of the diffuse double layer, and $d = 4$ is the dielectric constant in the Helmholtz double layer. The integral capacity, Cd , is calculated according to Grahame.⁸ The pH effect on η for Ag in alkaline solutions is calculated according to (9). Values of $(\partial \xi / \partial \log a_{H^+})$ are calculated¹ taking the potential of the electrocapillary maximum on Ag as 0.05 volt referred to the normal hydrogen electrode. For 0.1 N NaOH, at 30°, the calculated values of $(\partial \eta / \partial pH)_{i_c}$ are:

(6) R. Parsons and J. O'M. Bockris, *Trans. Faraday Soc.*, **47**, 914 (1951).

(7) J. O'M. Bockris and R. G. Watson, *J. chim. phys.*, **49**, 1 (1952).

(8) D. C. Grahame, *Chem. Revs.*, **41**, 441 (1947).

0 mv. at 3.2×10^{-6} amp./cm.², -2 mv. at 3.2×10^{-5} amp./cm.² and -19 mv. at 3.2×10^{-4} amp./cm.². Furthermore, the calculated values of $(\partial\eta/\partial pH)i_c$ are dependent on pH. An alternative explanation for the experimental pH effect on η for Ag in alkaline solutions (Table III) may, thus, be considered.

The net cathodic current, i_c , is related to the exchange current, i_0 , by

$$i_c = i_0 \exp\left(-\frac{\alpha\eta F}{RT}\right) \quad (10)$$

where α is approximately 0.5 at 30° (cf. Table I). From equations 3, 7 and 10

$$i_c = \lambda FK \frac{kT}{h} a_i \exp\left(\frac{\Delta S_0^*}{R}\right) \exp\left(\frac{-\Delta H_0^*}{RT}\right) \exp\left(\frac{-\eta F}{2RT}\right) \quad (11)$$

Taking ΔS_0^* and ΔH_0^* as independent of concentration, equation 11, at constant i_c and temperature reduces to

$$\eta = \text{const.} + (2RT/F) \ln a_i \quad (12)$$

$\log B$ is related to $\log a_{Na}$ by the empirical relation

$$\log B = \text{const.} + 0.2 \log a_{Na} \quad (13)$$

Since the only term in B (cf. equation 7) dependent on concentration is a_i , it follows from (7) and (13) that

$$\log a_i = 0.2 \log a_{Na} \quad (14)$$

Introducing (14) in (12) one gets

$$(\partial\eta/\partial \log a_{Na})i_c = 0.4 \left(\frac{2.303RT}{F}\right) \quad (15)$$

Since $(\partial\eta/\partial \log a_H)i_c = -(\partial\eta/\partial \log a_{Na})i_c$, equation 15, therefore, yields a value of $(\partial\eta/\partial pH)i_c = 0.024$ volt at 30°. The pH effect, thus calculated, is independent of pH and is very close to the experimental values given in Table III.

It must be noted that the validity of the above argument depends on the assumption that ΔS_0^* and ΔH_0^* are independent of concentration, and on the applicability of equations 13 and 14, both of which are based on experiment.

The authors wish to express their thanks to Prof. A. R. Tourky for his interest in the work, and to Prof. J. O'M. Bockris for helpful discussions.

THE RELATIONSHIP OF FORCE CONSTANT AND BOND LENGTH

BY RICHARD P. SMITH

Department of Chemistry, University of Utah, Salt Lake City, Utah

Received March 19, 1956

It is suggested that the force constant is inversely proportional to the square of the equilibrium internuclear distance for groups of molecules A-B where A and B are in the same column of the periodic table (e.g., O₂, SO, S₂, etc.). The relationship also seems to hold for hydrides of elements in the same column. A natural extension would be to suppose that $k_e R_e^2$ is constant for molecules A-B where A is in one particular column and B is in the same or another one, though data are not available to test the more general hypothesis. Our relationship reminds one of a bond length-bond energy correlation of a similar character recently proposed by Pauling.

A number of empirical formulas relating force constant and equilibrium internuclear distance (bond length) have been proposed.¹ Such relationships are useful for predicting unknown constants, for indicating probable errors in existing data, and for pointing the way to more complete bond "models" or otherwise increasing our understanding of the nature of the chemical bond.

It would seem that an empirical relation between molecular constants would be the more likely to be of use in fulfilling any or all of these functions, the simpler it is. Thus the empirical rule that the length of a bond A-B is nearly constant and is usually close to the arithmetic mean of the lengths of A-A and B-B leads at once to a familiar model in which atoms in molecules are represented by spheres of constant radii ("covalent bond radii"). A more complicated rule, though perhaps more accurate, would not lead to this model. Deviations from the expected lengths may then be discussed in terms of the superposition of other effects on the basic model.

Recently Pauling² has suggested the unusually simple rule that in a series of homopolar bonds in-

volving a particular column of the periodic table (e.g., O₂, S₂, Se₂, Te₂) the bond energy is proportional to the reciprocal of the bond length. This relationship is supported by the data for some sequences, but is incompatible with the data for others (e.g., F₂, Cl₂, Br₂, I₂).

It has been noted that $k_e R_e^2$ is nearly constant for the ground states of hydrogen halides.³ (Here R_e is the equilibrium internuclear distance and k_e is the force constant for infinitesimal amplitude, terminology and notation of Herzberg.¹) This is illustrated by the plot of k_e against R_e^{-2} for this series, given in Fig. 1. The data used are indicated in Table I. The least-squares straight line through the origin is drawn in. It is seen that $k_e R_e^2 = \text{constant}$ indeed holds very accurately for this series.

The above correlation suggests that $k_e R_e^2$ may be constant for other groups of this nature. Tests of this hypothesis are indicated in Figs. 1, 2, 3 and 4. The data are mostly taken from Herzberg⁴ and are collected, with literature references, in Table I. In each case, the least-squares lines which pass through the origin are drawn in; the slopes of these lines are given in Table II. For molecules in

(1) G. Herzberg, "Spectra of Diatomic Molecules," 2nd Ed., D. Van Nostrand Company, Inc., New York, N. Y., 1950, pp. 453-459.

(2) L. Pauling, THIS JOURNAL, 58, 662 (1954).

(3) S. Glasstone, "Theoretical Chemistry," D. Van Nostrand Co., Inc., New York, N. Y., 1944, p. 160.

(4) Ref. 1, Appendix.

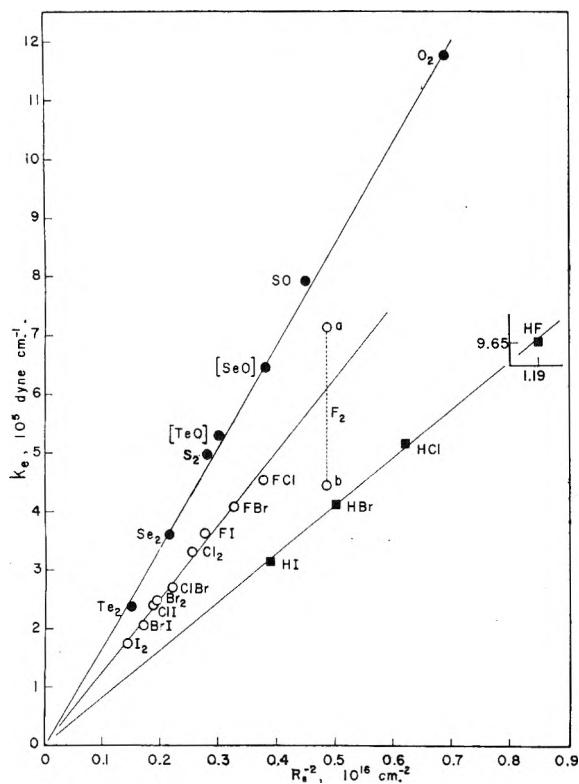


Fig. 1.—Force constants plotted against reciprocal of square of bond length for Group VIA diatomic molecules (filled circles), Group VIIa diatomic molecules (open circles), and H-VIIa molecules (squares).

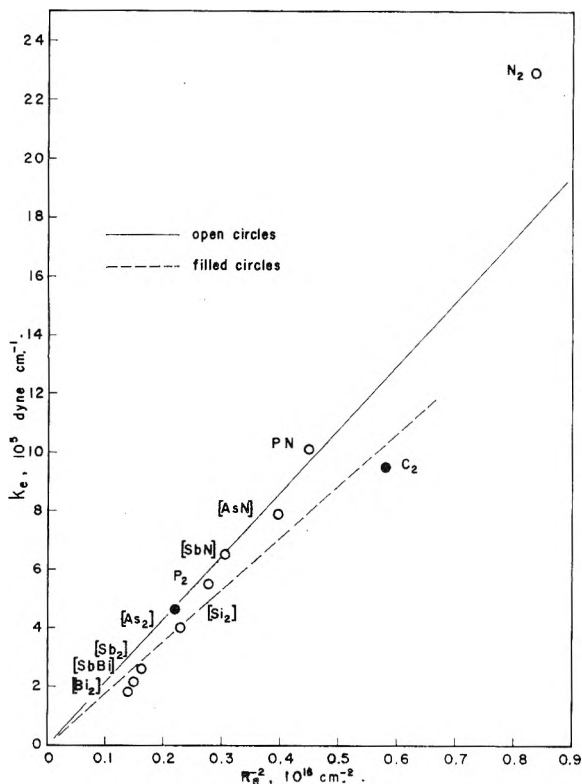


Fig. 2.—Force constants for Group Va (open circles) and Group IVa (filled circles) diatomic molecules plotted against reciprocal of square of bond length.

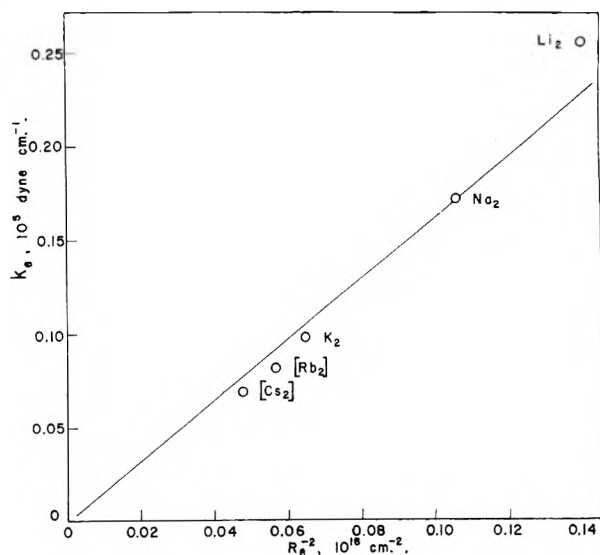


Fig. 3.—Force constants for alkali metal diatomic molecules plotted against reciprocal of square of bond length.

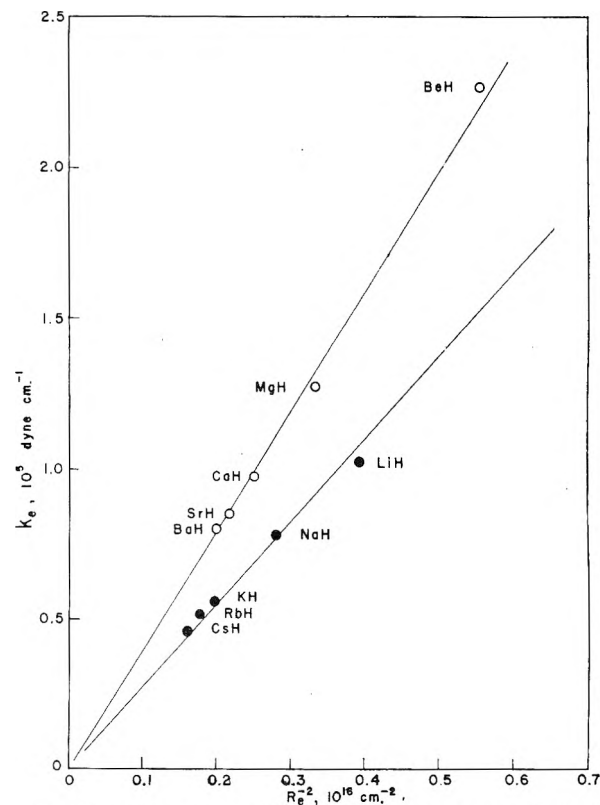


Fig. 4.—Force constants for diatomic hydrides of alkali metals (filled circles) and alkaline earth metals (open circles) plotted against reciprocal square of bond length.

brackets on the graphs, the bond lengths have been estimated from covalent radii, as indicated in Table I.

Our plots include molecules A-B in groups such that atoms A and B are in the same column of the periodic table, and hydrides of elements in particular columns of the periodic table, wherever data are available to allow two or more points to be plotted.

We thus have a relationship which reminds one of Pauling's bond energy-bond length relation.² The two relations are equally simple, and they both ap-

TABLE I

FORCE CONSTANTS AND BOND LENGTHS FOR DIATOMIC MOLECULES

Molecule	$k_e \times 10^5$, dyne/cm.	Ref.	$R_e \times 10^{-8}$, cm.	Ref.
HF	9.655	<i>a</i>	0.9171	<i>a</i>
HCl	5.157	<i>a</i>	1.2746	<i>a</i>
HBr	4.116	<i>a</i>	1.414	<i>a</i>
HI	3.141	<i>a</i>	1.604	<i>a</i>
F ₂	7.145, 4.453	<i>b, a</i>	1.435	<i>a</i>
FCl	4.483, 4.562	<i>c, a</i>	1.6281	<i>a</i>
FBr	4.071, 4.095	<i>a, d</i>	1.7556	<i>a</i>
FI	3.622	<i>d</i>	1.90 ₈	<i>e</i>
Cl ₂	3.286	<i>a</i>	1.988	<i>a</i>
ClBr	2.675, 2.717	<i>a, c</i>	2.138	<i>f</i>
ClI	2.383	<i>a</i>	2.3207	<i>a</i>
Br ₂	2.458	<i>a</i>	2.284	<i>a</i>
BrI	2.064	<i>a</i>	2.434	<i>e</i>
I ₂	1.721	<i>a</i>	2.667	<i>a</i>
O ₂	11.765	<i>a</i>	1.2074	<i>a</i>
SO	7.930	<i>a</i>	1.4933	<i>a</i>
SeO	6.446	<i>a</i>	1.62	<i>g</i>
TeO	5.304	<i>a</i>	1.82	<i>g</i>
S ₂	4.959	<i>a</i>	1.889	<i>a</i>
Se ₂	3.612	<i>a</i>	2.157	<i>a</i>
Te ₂	2.368	<i>a</i>	2.59	<i>a</i>
N ₂	22.962	<i>a</i>	1.094	<i>a</i>
PN	10.157	<i>a</i>	1.4910	<i>a</i>
AsN	7.926	<i>a</i>	1.59	<i>h</i>
SbN	6.564	<i>a</i>	1.79	<i>h</i>
P ₂	5.556	<i>i</i>	1.894	<i>a</i>
As ₂	4.069	<i>i</i>	2.08	<i>i</i>
Sb ₂	2.611	<i>i</i>	2.48	<i>i</i>
SbBi	2.193	<i>i</i>	2.58	<i>h</i>
Bi ₂	1.836	<i>i</i>	2.68	<i>i</i>
C ₂	9.521	<i>i</i>	1.3117	<i>a</i>
Si ₂	4.65 ^k	<i>i</i>	2.14	<i>j</i>
Li ₂	0.255	<i>a</i>	2.673	<i>a</i>
Na ₂	0.172	<i>a</i>	3.079	<i>a</i>
K ₂	0.0985	<i>a</i>	3.923	<i>a</i>
Rb ₂	0.0820	<i>a</i>	4.19	<i>i</i>
Cs ₂	0.0690	<i>a</i>	4.57	<i>i</i>
LiH	1.026	<i>a</i>	1.5954	<i>a</i>
NaH	0.781	<i>a</i>	1.8873	<i>a</i>
KH	0.561	<i>a</i>	2.244	<i>a</i>
RbH	0.515	<i>a</i>	2.367	<i>a</i>
CsH	0.467	<i>a</i>	2.494	<i>a</i>
BeH	2.263	<i>a</i>	1.3431	<i>a</i>
MgH	1.274	<i>a</i>	1.7306	<i>a</i>
CaH	0.977	<i>a</i>	2.0020	<i>a</i>
SrH	0.854	<i>a</i>	2.1455	<i>a</i>
BaH	0.809	<i>a</i>	2.2318	<i>a</i>

^a Ref. 1, Appendix. ^b H. G. Gale and G. S. Monk, *Astrophys. J.*, 69, 77 (1929). ^c L. G. Cole and G. W. Elverum, Jr., *J. Chem. Phys.*, 20, 1543 (1952). ^d R. A. Durie, *Proc. Roy. Soc. (London)*, A207, 388 (1951); R. A. Durie and A. G. Gaydon, *THIS JOURNAL*, 56, 316 (1952). ^e Ref. *c*, estimated by rule of Schomaker and Stevenson. ^f W. Gordy, W. V. Smith and R. F. Trambarulo, "Microwave Spectroscopy," John Wiley and Sons, Inc., New York, N. Y., 1953, Appendix. ^g Estimated using double-bond covalent radii of L. Pauling, "The Nature of the Chemical Bond," 2nd Ed., Cornell University Press, Ithaca, N. Y., 1948, p. 164. ^h Estimated using covalent radii obtained from lengths in corresponding homopolar molecules as estimated by Pauling in ref. 2. ⁱ Ref. 2. ^j Twice Pauling's (ref. *g*) double-bond covalent radius. For C₂ this gives 2(0.665) = 1.33, which is close, and hence this estimate may be satisfactory for Si₂. ^k Uncertain.

TABLE II

LEAST-SQUARE VALUES OF $k_e R_e^2$ FOR GROUPS OF DIATOMIC MOLECULES

Group	$k_e R_e^2$, least squares, erg
H-Halogen	8.194×10^{-11}
Halogen-halogen	12.479 ^a
Group VIa (O ₂ , etc.)	17.217
Group Va (N ₂ , etc.)	21.62
Group IVa (C ₂ , Si ₂)	17.72
Group Ia (Li ₂ , etc.)	1.629
H-Alkali (LiH, etc.)	2.765
H-Alkaline earth (BeH, etc.)	3.970

^a F₂ omitted in calculation.

ply to periodic table columns. Pauling confines his relation to homopolar bonds, whereas our rule is successful for heteropolar bonds involving one column only (*e.g.*, O₂, SO, S₂, etc., fit into one scheme), and for hydrides of elements in one column. It seems remarkable that we have been able to include homopolar and heteropolar molecules in one scheme, whereas one might expect that the relationship would have to be modified for the heteropolar molecules to take polarity into account, as certainly would be necessary in the case of energy-length correlations.

It would seem natural to suppose that $k_e R_e^2$ might be constant for molecules A-B where A is in one column of the periodic table and B is in another column. Thus ClO, BrO, IO, ClS, BrS, etc., might be expected to fit the correlation as a group. But apparently there are not sufficient data to allow a test of the rule for molecules involving two different columns, except for the hydrides which we have considered. The molecules KF, KCl, KBr, KI, NaCl, etc., roughly fit, but there is too much uncertainty in the bond lengths (usually obtained by electron diffraction) to make possible a genuine test.

The nitrogen family and the alkali metals apparently would fit better if the lines were not required to go through the origin, *i.e.*, if an additional arbitrary constant were included. However, this would seem premature, as simplicity would be violated, the data for a number of the molecules in these series are questionable (especially many of the bond lengths, which we have had to estimate), and the other lines could not be improved by extrapolation to a point other than the origin.

(Subsequent to our completion of the above work, our attention has been called to a recent article on the correlation of bond energy, bond length and force constant by Jenkins.⁵ The series Li₂, Na₂, K₂, Rb₂, Cs₂; O₂, Te₂; N₂, P₂, Bi₂; and C-H bonds are considered. The relation $k_e = a/R_e^2 + b$, where *a* and *b* are constants, is applied. As remarked above, we do not believe the data justify use of the additional constant *b*; see particularly our Figs. 1 and 4, which are graphs of the data for which the uncertainty in bond lengths is least. Our work is, of course, more general, as additional series, as F₂, FCl, Cl₂, . . ., are considered, and heteropolar molecules and diatomic hydrides are included.)

Pauling's discussion² of the similarity of certain factors for the ground states of molecules within

groups such as we have considered will of course largely carry over here, and consequently is not repeated.

While we are unable to give a theoretical explanation of our correlation, its simplicity seems to indicate that the search for a "model" which will encompass it may not be fruitless.

We have been unable to find any simple relation of our correlation to others, such as that of Badger.¹

The relation does not hold for the excited states of a molecule, as it is inconsistent with the fairly accurate relation

$$R_e^2 \omega_e = \text{constant}$$

(where ω_e is the equilibrium vibrational frequency) which has been shown by Birge⁶ and by Mecke⁷ to hold in this case.

(6) R. T. Birge, *Phys. Rev.*, **25**, 240 (1925).

(7) R. Mecke, *Z. Physik*, **32**, 823 (1925).

ON THE STOKES-ROBINSON HYDRATION MODEL FOR SOLUTIONS^{1,2}

BY DONALD G. MILLER

Department of Chemistry, Brookhaven National Laboratory, Upton, Long Island, New York

Received March 26, 1956

The Stokes-Robinson hydration model is used to derive the following equation for molal activity coefficients $\log \gamma = \log f' - \log [1 - \{(h - r)mM_1/1000\}]$, which has no solvent activity term. f' is given by the Debye-Hückel expression for electrolytes and is equal to 1 for non-electrolytes. The equation is practical for computation, and fits the data for 2 non-electrolytes and 43 strong electrolytes as well as or better than the original of Stokes-Robinson. The hydration numbers are larger and are in agreement with those determined by various other methods. The choice of an ideality scale is briefly discussed. Further equations which account for both solvation and solute size are derived using a free-volume theory to fix the ideality scale.

Introduction

Recently Stokes and Robinson^{3,4} have focused attention on a useful model for strong electrolyte solutions which formally takes ionic hydration into account. This kind of model had previously been advanced by Bjerrum⁵ and Scatchard^{6,7} for both electrolyte and non-electrolyte solutions, but had received little notice. The basic idea is that instead of consisting of bare particles dissolved in a certain quantity of solvent, the solution really consists of solvated particles dissolved in the remaining "free" solvent. Since the outer surface of the solvated particle consists of solvent molecules, the solvent-solvated solute interactions are essentially reduced to solvent-solvent interactions. Thus the heat of solution of a solvated particle will be practically zero. In the case of an ion, the orienting effects on a polar solvent which would alter the local dielectric constant are now contained in the solvation sphere, and consequently the solvated ion essentially sees only the macroscopic dielectric constant of the solvent. Hence as far as solute-solvent interactions are concerned, the hydrated solute should form practically ideal solutions with the solvent.

With this model and using the Debye-Hückel theory to account for solute-solute interactions, Stokes and Robinson derived an equation for the molality activity coefficients γ of strong electrolytes in terms of the hydration number h and the size of the ions a . With properly chosen values of h and a ,

the agreement between the calculated and observed γ is remarkably good. Their equation, however, contains a term involving the solvent activity. As a result the determination of h and a from experimental data, or the computation of γ once h and a are available, are somewhat difficult.

It is the purpose of this paper to use the same model together with standard thermodynamic methods to derive an equation, similar to Stokes and Robinson's, which is more suited to computation. Equations will also be derived taking into account the effect of different sized particles on the "ideality" scale.

Derivation of the Equation.—The derivation of the new equation will now be sketched. The molality m' of the solvated solute is

$$m' = \frac{m}{1 - \frac{hM_1 m}{1000}} \quad (1)$$

where m is the ordinary molality and M_1 is the molecular weight of the solvent. The mole fraction N_2' of the solvated solute is accordingly

$$N_2' = \frac{rm'}{\frac{1000}{M_1} + rm'} = \frac{rm}{\frac{1000}{M_1} + (r-h)m} \quad (2)$$

where r is the number of ions into which an electrolyte ionizes.⁸ In order to relate the ordinary molal activity coefficient γ to the solvation mole fraction coefficient f' , it is recalled⁹ that no matter what two systems for describing concentration are involved

$$a/a_* = a'/a'_* \quad (3)$$

where a is the activity; and $*$ refers to another composition. When the r th root of (3) is taken, one obtains

(8) The r appears because the sum of ion mole fractions is necessary for considering the electrolyte as a whole. For non-electrolytes $r = 1$.

(9) S. Glasstone, "Thermodynamics for Chemists," D. Van Nostrand, New York, N. Y., 1947, p. 355.

(1) Research carried out under the auspices of the U. S. Atomic Energy Commission.

(2) This paper was presented at the American Chemical Society Meeting, Dallas, Texas, April, 1956.

(3) (a) R. H. Stokes and R. A. Robinson, *J. Am. Chem. Soc.*, **70**, 1870 (1948); (b) R. A. Robinson and R. H. Stokes, *Ann. N. Y. Acad. Sci.*, **51**, 593 (1949).

(4) R. A. Robinson and R. H. Stokes, "Electrolyte Solutions," Butterworth, London, 1955.

(5) N. Bjerrum, *Medd. Vetensk. Nobelinst.*, **5**, 1 (1919).

(6) G. Scatchard, *J. Am. Chem. Soc.*, **43**, 2406 (1921).

(7) G. Scatchard, *ibid.*, **47**, 2098 (1925).

$$\frac{m\gamma}{m_*\gamma_*} = \frac{rmf'}{\frac{1000}{M_1} + (r-h)m} / \frac{rm_*f'_*}{\frac{1000}{M_1} + (r-h)m_*} \quad (4)$$

In this case, the reference state for both activity systems is infinite dilution. Thus in the limit as m_* goes to zero, f'_* and γ_* both go to 1, and (4) can be written as

$$\log \gamma = \log f' - \log \left[1 - \frac{(h-r)mM_1}{1000} \right] \quad (5)$$

This equation is not restricted to electrolyte or aqueous solutions, and h need not be independent of concentration.

Non-electrolytes.—In the non-electrolyte case, the solvated solute should behave ideally, *i.e.*, satisfy Raoult's law. Under these circumstances, $r = 1$ and $f' = 1$. Therefore the molal activity coefficient can be written as

$$\log \gamma = -\log \left[1 - \frac{(h-1)mM_1}{1000} \right] \quad (6)$$

a one parameter equation.

The application of (6) to the data requires a knowledge of h . The procedure is to choose various values of h until the best agreement with observed values is obtained. For aqueous solutions of sucrose and glycerol, the results are listed in Table I, and the fit is seen to be reasonably good. Some of the other non-electrolytes for which data are available would have negative hydration numbers, indicating net repulsive interactions.

Electrolytes.—It is now assumed that the solvated solute would behave ideally when uncharged, that is would obey Raoult's law. Then the deviation from ideality is ascribed to electrostatic interactions resulting from charging up the hydrated ions. These are the fundamental notions used by Debye and Hückel, hence their equation

$$\log f' = \frac{z_+ z_- A \sqrt{\mu'}}{1 + aB \sqrt{\mu'}} \quad (7)$$

may be applied. A and B are numerical constants, z_+ and z_- are the ionic charges with due regard to sign, and μ' is the concentration ionic strength taking into account solvation.

The possibility that Raoult's law is not a proper measure of ideality will be discussed later.

In (7), μ' represents the ionic strength of the hydrated solute. However, it has the same value in terms of moles of unhydrated solute per liter. Moreover, for practical purposes c can be replaced by m in aqueous solutions, and the parameters h and a allowed to take care of the distinction between m and c . Therefore if I is the molal ionic strength, equations 5 and 7 yield

$$\log \gamma = \frac{z_+ z_- A \sqrt{I}}{1 + aB \sqrt{I}} - \log \left[1 - \frac{(h-r)mM_1}{1000} \right] \quad (8)$$

This result is equivalent to the Stokes-Robinson^{3a} equation 9, but without the a_w term.

In order to find the values of h and a which best fit the experimental data, (8) is cast into the following straight line form

$$\frac{z_+ z_- A \sqrt{I}}{\log \gamma [1 - 0.018(h-r)m]} = 1 + aB \sqrt{I} \quad (9)$$

The experimental values of γ and m are inserted in (9) together with some suitable value of h , and the

TABLE I

PARAMETERS OF EQUATIONS 6 AND 8 GIVING THE BEST AGREEMENT WITH EXPERIMENTAL ACTIVITY COEFFICIENTS OF AQUEOUS SOLUTIONS AT 25°

	h	a	i	Range of molality	Av. dev. γ	Max. dev. γ
HCl	13.5	5.03	0.98	0.002-1.4	0.001	0.002
HBr	15.7	5.55	.96	.1 -1.0 ^a	.0005	.001
HI	17.0	7.71	.81	.1 -1.0	.001	.002
HClO ₄	13.6	5.33	1.00	.1 -1.8	.001	.002
LiCl	12.0	4.91	0.95	.1 -1.6	.001	.002
LiBr	13.8	4.75	.99	.1 -1.6	.001	.003
LiI	13.6	8.59	.73	.1 -1.6	.001	.002
LiClO ₄	14.3	6.80	.88	.1 -1.2	.001	.002
NaCl	6.7	3.81	1.05	.1 -5.0	.001	.003
NaBr	7.7	4.47	0.97	.1 -4.0 ^a	.001	.002
NaI	9.1	5.30	0.90	.1 -3.0	.001	.003
NaClO ₄	4.5	3.75	1.06	.1 -6.0 ^a	.001	.003
NaClO ₃	1.99	3.48	1.08	.1 -3.0	.001	.003
NaCNS	6.6	5.66	0.88	.1 -4.0 ^a	.001	.004
NaOH	6.6	5.06	0.82	.1 -2.0	.001	.002
KCl	4.2	3.29	1.07	.001-4.5 ^a	.001	.002
KBr	4.4	3.60	1.04	.1 -5 ^a	.0005	.001
KI	4.8	4.24	1.01	.1 -4	.001	.002
KCNS	2.6	3.69	1.02	.1 -5.0 ^a	.0005	.001
KOH	12.3	4.06	1.08	.1 -1.4	.001	.002
RbCl	4.0	3.01	1.04	.1 -5.0 ^a	.001	.002
RbBr	3.4	3.05	1.04	.1 -5.0 ^a	.0005	.001
RbI	3.7	2.90	1.05	.1 -5.0 ^a	.0005	.001
CsCl	4.2	2.24	1.07	.1 -5.0	.0003	.001
CsBr	4.0	2.15	1.08	.1 -5.0 ^a	.001	.002
CsI	1.6	2.56	1.04	.1 -3.0 ^a	.0005	.002
NH ₄ Cl	3.3	3.72	1.00	.1 -6.0 ^a	.001	.003
MgCl ₂	24.0	5.15	0.97	.1 -1.2	.001	.002
MgBr ₂	29.0	5.88	0.92	.1 -1.0	.002	.003
MgI ₂	34.1	6.25	1.00	.1 -0.7	.001	.002
Mg(ClO ₄) ₂	33.0	7.29	0.89	.1 -0.8	.001	.002
CaCl ₂	20.9	4.82	1.00	.1 -1.4	.001	.002
CaBr ₂	25.0	5.34	0.94	.1 -1.0	.001	.002
CaI ₂	28.4	6.25	.91	.1 -1.0	.001	.002
Ca(ClO ₄) ₂	27.8	6.68	.86	.1 -1.0	.001	.003
SrCl ₂	18.8	4.66	1.00	.1 -1.6	.001	.003
SrBr ₂	22.3	5.03	0.99	.1 -1.2	.0005	.001
SrI ₂	27.4	5.07	1.00	.1 -1.0	.002	.002
Sr(ClO ₄) ₂	27.5	5.42	0.92	.1 -0.9	.001	.003
BaCl ₂	14.0	4.45	1.00	.1 -1.8 ^a	.001	.003
BaBr ₂	18.5	4.85	0.98	.1 -1.4	.001	.002
BaI ₂	24.9	6.19	.82	.2 -1.0	.001	.003
Ba(ClO ₄) ₂	20.9	5.09	.97	.1 -0.9	.001	.002
MnCl ₂	19.0	4.88	.98	.1 -1.4	.0005	.003
FeCl ₂	22.0	4.69	1.01	.1 -1.2	.001	.002
CoCl ₂	22.7	4.88	1.00	.1 -1.2	.001	.002
NiCl ₂	22.7	5.00	0.97	.1 -1.2	.0005	.002
EuCl ₃	33.5	4.94	1.01	.1 -0.9	.001	.002
Sucrose	9.7			.1 -1.6	.001	.002
Glycerol	2.4			.1 -2.0	.001	.003

^a Equation is valid to the limit of the experimental data.

left side is plotted against the \sqrt{I} . If a straight line is not obtained, other values of h are tried. The best value of h will be the one which gives the best straight line, and the slope of this line will also yield the best value of a . Once a sufficiently comprehensive table of $\log [1 - 0.018(h-r)m]$ is available, these computations can be carried out by hand in a reasonable length of time. The computation has also been systematized so that it can be carried out on the laboratory's punched card computer. The data used in the calculations have been taken from previous compilations by Stokes and Robinson.^{4,10,11} Equation 9 can serve rather nicely as a smoothing function once the best straight line is at hand. Slight discrepancies or scattered data show up rather plainly on a suitably large graph.

(10) R. H. Stokes, *Trans. Faraday Soc.*, **44**, 295 (1948).

(11) R. A. Robinson and R. H. Stokes, *ibid.*, **45**, 612 (1949).

In Table I have been collected the results of applying (8) to 48 electrolytes of various valence types in aqueous solution. Included are h , a the intercept¹² i of (9), the range of validity of (8), and the average and maximum deviations of γ . In all but a few cases, comparison of both the fit and the range of validity shows that the present equation is as good as or better than that of Stokes–Robinson. In general, the less highly hydrated salts have a greater region of validity. Quantitatively, equation 8 usually breaks down when $hm \geq 20$ –30, owing to the competition of the ions for each other's water of hydration.

The hydration numbers computed with (8) are in reasonable agreement with those determined by other methods,¹³ namely, entropy,¹⁴ vapor pressure,¹⁵ compressibility,¹⁶ conductance,¹⁷ activity,¹⁸ and dielectric constant,¹⁹ but are uniformly higher than the Stokes–Robinson values.

As with the Stokes–Robinson results, the extent of hydration follows the accepted order with respect to cation charge and size for a given anion. There is in both treatments, however, an anomalous increase in h for some anions with a given cation. On the basis of the present data compilations, it does not seem possible to assign hydration numbers to the individual ions, since, for example, $h_{\text{NaCl}} - h_{\text{LiCl}} \neq h_{\text{NaBr}} - h_{\text{LiBr}}$.²⁰ Consequently mixed electrolytes cannot be treated very well. However the ability of equation 8 to fit the data to such high concentrations and the relative simplicity of numerical work associated with it suggest its use as a practical interpolation formula or smoothing function.

On the Choice of an Ideality Scale.—Previously it was assumed that solvated non-electrolytes and solvated ions (when uncharged) would obey Raoult's law; in other words mole fractions determine ideality. Raoult's law however probably is not the true measure of ideality for this reason.

(12) Theoretically this third parameter i should be 1.00 in equation 9. However, the best fit of (9) to the data leads to various values of i which are usually within a few per cent. of the proper value. This discrepancy is explained by the fact that almost all the data listed in reference 4 were determined by isopiestic methods. In order to transform isopiestic data into activity coefficients, it is necessary to apply the Gibbs–Duhem equation and assign a value to the γ at some given concentration. Usually this assignment is made on the basis of e.m.f. data, etc., at $m = 0.1$. It turns out however that the intercept i is rather sensitive to a small variation in $\gamma_{0.1m}$. Thus a 1/2% error in $\gamma_{0.1m}$ is approximately a 5% error in i . Therefore the major portion of the deviation of i from 1.00 is ascribed to errors in assignment of $\gamma_{0.1m}$ in the Stokes and Robinson tables.⁴ There is of course some smaller variation in i which can arise from a subjective choice of the best straight line. Consideration of the data sources shows that in cases where $\gamma_{0.1m}$ is known well from other measurements, i is only 1 or 2% off. Similarly the cases where i is somewhat further off are those in which $\gamma_{0.1m}$ had to be estimated without the aid of independent measurements. There remain four unexplained discrepancies.

(13) J. O. M. Bockris, *Quart. Rev.*, **3**, 173 (1949).

(14) J. Kielland, *J. Chem. Educ.*, **14**, 412 (1937).

(15) B. H. Van Druyven, *Rec. trav. chim.*, **56**, 1111 (1937).

(16) See reference 4, Table 3.4, p. 60 and references there.

(17) L. D. Tuck, referred to by R. E. Powell, *THIS JOURNAL*, **58**, 523 (1954).

(18) Bourion, *et al.*, *Compt. rend.*, various papers 1933–37.

(19) G. H. Haggis, J. B. Hasted and T. J. Buchanan, *J. Chem. Phys.*, **20**, 1452 (1952).

(20) The hydration number, however, is also affected by errors in the assignment of $\gamma_{0.1m}$; a 1/2% error in $\gamma_{0.1m}$ can change h by as much as 2 units. It is felt that a set of individual ionic hydration numbers could be found if all the $\gamma_{0.1m}$ were properly assigned.

Hydrated solutes must all be bigger than individual solvent molecules. However lattice and other theories of solution have indicated that whenever there is a difference in size among solution components, mole fractions are no longer the proper measure of ideality.

For athermal mixtures, the results of these theories depend not only on the size but the shape and flexibility of the components. For example, with flexible linear chains the ideality scale is based on volume fractions.²¹ However Huggins²² has shown that for spherical components, which the hydrated ions are to the first approximation, the deviation from the mole fraction scale is not large in dilute solution, even when there is a marked disparity in size.²³ There is also some experimental evidence for non-electrolytes²⁴ that Raoult's law is obeyed even if the components are of different sizes. These are the important reasons why mole fraction ideality has been successful in the foregoing. Another contributing factor may be that in hydrogen bonded solvents such as water, the effective solvent size is not that of a single molecule, but is characteristic of larger aggregates of transitory existence. Hence the difference in size of solute and solvent is not as great as would be expected at first thought.

In the following section, a more general ideality scale based on a free volume expression will be considered.

Theory Including Both Hydration and Ion Size.

—Consider the general free volume expression for the ideal entropy of mixing for substances of differing shapes and sizes²⁵

$$\Delta S^M = -R \left[n_o \ln \phi_o + \sum_{j=1}^n n_j \ln \phi_j \right] \quad (10)$$

where o refers to the solvent, n_i are mole numbers, and ϕ_i are *free-volume* fractions.²⁶ We proceed to use this expression to determine an ideality scale as follows.

Let s_i be defined as v_i/v_o , where v_i is the free volume of the i^{th} component. Then the free volume fractions can be written

$$\phi_o = \frac{n_o}{n_o + \sum n_j s_j}, \quad \phi_i = \frac{n_i s_i}{n_o + \sum n_j s_j} \quad (11)$$

Since the solutions are assumed to be athermal, the differentiation of (10) leads to

$$\ln \alpha_i = \frac{\partial(\Delta S^M/R)}{\partial n_i} = \ln \phi_i + \phi_o (1 - s_i) + \sum \phi_j \left(1 - \frac{s_i}{s_j} \right) \quad (12)$$

where α is the activity associated with free volume ideality.

Let us now restrict our considerations to a binary electrolyte in a neutral solvent. If r_1 and r_2

(21) J. A. Hildebrand and R. L. Scott, "Solubility of Non-Electrolytes," Reinhold Publ. Corp., New York, N. Y., 1950, Chapter XX.

(22) M. Huggins, *THIS JOURNAL*, **52**, 248 (1948).

(23) Recently E. Glueckhauf, *Trans. Faraday Soc.*, **51**, 1235 (1955), has taken the volume fraction ideality scale and applied it to the hydration of electrolytes in a slightly different manner than used here. However this scale is more appropriate to flexible chains than the more likely spheres.

(24) J. H. Hildebrand, *J. Chem. Phys.*, **15**, 225 (1947); *Chem. Revs.*, **44**, 37 (1949).

(25) Reference 22, p. 198.

(26) It is clear that from Huggin's results²² that for spheres the free volumes cannot be proportional to the molal volumes.

are the stoichiometric coefficients of the ions upon ionization, then the activity of the electrolyte as a whole is

$$a = a_1^{r_1} a_2^{r_2} = f^r \alpha_1^{r_1} \alpha_2^{r_2} = f^r \alpha_{12} \quad (13)$$

where $r = r_1 + r_2$ and f , the mean activity coefficient, takes into account the possible deviation from free volume ideality. If the free volume fractions are now written in terms of the molality of the hydrated solute and if the average volume ratio of the electrolyte as a whole, $(r_1 s_1 + r_2 s_2)/r$, is denoted by s , then α_{12} is given by

$$\alpha_{12} = \frac{r_1^{r_1} r_2^{r_2} s_1^{r_1} s_2^{r_2} (m'f')^r e^{r\phi_0(1-s)}}{\left(\frac{1000}{M_1} + rm's\right)^r} \quad (14)$$

If one now applies (3), cancels all common terms, substitutes (1), and makes use of the same technique which led to (5), one obtains the desired equation

$$\log \gamma = \log f' + \frac{s(s-1)rmM_1}{1000} - \log \left[1 - \frac{(h-rs)mM_1}{1000} \right] \quad (15)$$

There are some interesting special cases.

If $s = 1$, mole fractions result, and (15) reduces to (5).

For the ideal non-electrolytes, r and f' are both unity and (15) becomes

$$\log \gamma = \frac{s(s-1)mM_1}{1000} - \log \left[1 - \frac{(h-s)mM_1}{1000} \right] \quad (16)$$

If there is no solvation, (16) reduces to equation 9.21 of reference 4. Equation 16 has been fitted to the data for aqueous sacrose from 0.1 to 5*m* with $h = 8.7$, $z = 2.7$. The fit is about as good as that of 9.21⁴ with $h = 0$, $z = 5$. If z were really proportional to the molal volume, it would have been larger than h .

If the Debye-Hückel equation is applied to the solvated ions as before, one obtains for aqueous solutions

$$\log \gamma = \frac{z_+ z_- A \sqrt{I}}{1 + aB \sqrt{I}} + \frac{0.018 s(s-1)rm}{2.303[1 - 0.018(h-rs)m]} - \log [1 - 0.018(h-rs)m] \quad (17)$$

Since at present there is no *a priori* way to determine s , equation 17 remains a three parameter equation.

Acknowledgment.—The author wishes to acknowledge conversations with Professor Joseph E. Mayer and Dr. Edward V. Sayre. He is indebted to Miriam Miller, Lorraine Fischer and Stuart Rideout for very generous aid with the computations.

MECHANISM OF GELATION OF GELATIN. INFLUENCE OF CERTAIN ELECTROLYTES ON THE MELTING POINTS OF GELS OF GELATIN AND CHEMICALLY MODIFIED GELATINS¹

BY JAKE BELLO, HELENE C. A. RIESE AND JEROME R. VINOGRAD

Contribution No. 2090 from the Gates and Crellin Laboratories of Chemistry of the California Institute of Technology, Pasadena California

Received March 26, 1956

The effects of a series of salts and acids on the melting points of gelatin gels have been studied. The effects of ions, of the same or opposite charge, are additive. There is a correlation between the binding of ions, as indicated by pH changes, and their effects on the melting point. However, by the use of amino-acetylated gelatin and a guanidino-nitrated, hydroxyl-sulfated gelatin, it is shown that binding of anions at amino, guanidino or hydroxyl groups is not responsible for melting point changes. By the use of carboxyl-esterified gelatin and hydroxyl-acetylated gelatin, it is shown that binding of cations at carboxyl or hydroxyl groups is not the cause of melting point reduction. Iron (III) ion, at low concentration, raises the melting point by inter- or intramolecular cross-linking through the carboxyl groups. In agreement with previous reports polarizable anions are effective melting point reducers with diiodosalicylate being the most potent observed.

The effects of a variety of additives on the melting points of gelatin gels or setting points of gelatin solutions have been investigated by many workers.²⁻¹¹ Some additives lower the melting or

setting point while others raise it. The most effective melting point reducers heretofore reported are sodium salicylate¹² and sodium acetyltryptophan.¹³ It has been suggested that the effect of additives is due to "attraction"¹² by the gelatin or to some specific interaction.¹⁴ Alternatively, it has

(1) Presented in part before the Division of Colloid Chemistry, 127th Meeting of the American Chemical Society, Cincinnati, Ohio, March-April, 1955.

(2) G. S. d'Alcontres, *Ann. chim. applicata*, **38**, 272 (1948).
 (3) E. H. Büchner and B. Meylink, *Rec. trav. chim.*, **62**, 337 (1943).
 (4) E. H. Büchner, *Kolloid Z.*, **75**, 1 (1936).
 (5) E. H. Büchner, *ibid.*, **78**, 339 (1937).
 (6) J. H. C. Merckel and P. W. Haayman, *ibid.*, **87**, 59 (1939).
 (7) C. Marie and A. Buffat, *Z. physik. Chem.*, **130**, 233 (1927).
 (8) S. R. Trotman and H. S. Ball, *J. Soc. Chem. Ind., Transactions*, **53**, 225 (1934).

(9) G. Grasser, H. Ohoki and Y. Hirakawa, *J. Faculty Agr., Hokkaido Imp. Univ.*, **23**, 165 (1930).

(10) P. C. Nobel, *Rec. trav. chim.*, **70**, 601 (1951).

(11) T. R. Briggs and E. M. C. Hieber, *THIS JOURNAL*, **24**, 74 (1920).

(12) G. A. Feigen and I. L. Trapani, *Arch. Biochem. Biophys.*, **53**, 184 (1954).

(13) R. S. Gordon, Jr., and J. D. Ferry, *Federation Proc.*, **5**, 136 (1946).

(14) J. D. Ferry, "Advances in Protein Chemistry," Vol. IV, (M. L. Anson and J. T. Edsall, editors), Academic Press, Inc., New York, N. Y., 1948, pp. 26-27.

been proposed that the effect is due to changes in the hydrol equilibrium¹⁵⁻¹⁷ or to changes in the distribution of water between the medium and "gelatin micelles."¹⁵

In the present work, we report data on ne w additives bearing on the role of polarizability of additives on gelation, on the effect of acids, on the question of binding of additives and on the effects of additives on chemically modified gelatins.

Experimental

The gelatin used in the work was Wilson Laboratories' U-COP-CO, Special Non-Pyrogenic Gelatin, of isoelectric point 9.2 (by viscosity minimum, turbidity maximum and mixed-bed, ion-exchange resin¹⁸), prepared by acid extraction of pigskins, and having an ash content of 0.5%. Deionized gelatin was prepared by passage through a column of Amberlite MB-3, mixed-bed, ion-exchange resin.¹⁸

Amino-acetylated Gelatin.—This preparation has been described.¹⁹ Van Slyke amino nitrogen determination (modification of Doherty and Ogg²⁰) showed 99.5% acetylation of amino groups.

Esterified Gelatin.—This was prepared by the action of methanol and thionyl chloride. Details of preparation and characterization will be described elsewhere.

Nitrated Gelatin.—Gelatin was simultaneously nitrated and sulfated by treatment with a mixture of concentrated sulfuric acid and 100% nitric acid. Details will be described elsewhere.

Additives.—Unless otherwise noted, the salts were reagent grade chemicals used without further purification. Sodium benzenesulfonate was prepared by neutralization of benzenesulfonic acid and was recrystallized twice from water. The sodium salts of the following acids were prepared by neutralization without further purification: tribromoacetic acid,²¹ diiodoacetic acid, (prepared by Angeli's method²² for triiodoacetic acid; we were not able to prepare triiodoacetic acid following the published directions), dibromoacetic acid (prepared by the method of Petrieff²¹ for tribromoacetic using less bromine), bromoacetic (Eastman Kodak Co., redistilled), trichloroacetic acid (Baker and Adamson, Reagent), trifluoroacetic acid (Minnesota Mining and Manufacturing Co., 100.1% by titration), dichloroacetic acid (Matheson, Coleman and Bell, redistilled through a 12" spiral-packed column) and 2-hydroxy-3,5-diiodosalicylic acid.²³ Thiocyanic acid was prepared from barium thiocyanate and the calculated amount of sulfuric acid followed by removal of the barium sulfate by centrifugation.

Melting Points.—Ten ml. of solution was placed in a 150 × 18 mm. test-tube, which was then stoppered, warmed at 50° for 10 minutes to erase the thermal history of the sample and then placed in a 0 ± 0.01° bath for 20 hours. A Neoprene ball, d_{20}^{25} 1.17, and 6 mm. in diameter, was inserted in the gel below its surface and the tube was warmed at a rate of 5 ± 0.5°/hr. Up to 22 tubes could be measured at one time. The melting point was taken as that temperature at which the ball reached the bottom of the tube. The reproducibility of melting points was about ± 0.2° and a temperature change of 0.1-0.3° occurred between the time the ball was first seen to fall and the time it reached the bottom of the tube. The pH of solutions of gelatin and salts of strong acids was 5-7, and for weaker acids was 8-9. It was found that the melting point of 5% gelatin is independent of pH in this range and careful control of pH was not necessary except to ensure complete ionization of weak acids. When strongly acid or alkaline solutions were used, the 50° heating period was omitted. Since some solutions were too dense to permit the use of

Neoprene balls, glass balls, 4 mm. in diameter, were used in such cases. In the density range in which both glass and Neoprene balls could be used, differences of less than 0.3° in melting point were observed between the two methods.

pH Changes.—The sodium salts and stock solution of deionized gelatin were brought to pH 7.30 ± 0.05. The solutions were mixed and covered. After equilibration at 37 ± 0.1° for ten minutes, the pH was measured with a Beckman Model G pH Meter and glass and calomel electrodes. Measurements were taken periodically during at least ten minutes, although constancy was usually observed in less than five minutes. After each two gelatin-salt solutions were measured, a solution of gelatin alone and of buffer were measured as a check on the meter and electrodes. The standard deviations of 6-8 measurements with each of six salts were 0.03-0.05. Fewer measurements were made with the other salts.

Results and Discussion

In view of the fact that we have used a gelatin of high isoelectric point where other investigators used gelatins of low isoelectric point and that our method of melting point measurement differs from others, it was considered desirable to determine the effects on melting point of a number of additives that have been reported previously. Our results agreed with those of other investigators.

In Table I are shown the melting points of gelatin gels containing various salts. Some of the sodium salts (salicylate, perchlorate, trichloroacetate, benzenesulfonate, thiocyanate, nitrate, chloride) were investigated at concentrations from 0.1-1.0 *M* and the melting point-concentration curves were found to be linear, except for a slight curvature below 0.25 *M*, in agreement with previous work.⁶ Similar effects can be seen in Figs. 2 and 4. Based on this

TABLE I
MELTING POINTS OF 5% GELATIN GELS CONTAINING SALTS

Additive	Concn. moles liter ⁻¹	M. p., °C.
None	..	30.4
Sodium fluoride	1.0	34.5
Sodium methanesulfonate	1.0	31.5
Sodium chloride	1.0	28.0
Sodium bromide	1.0	22.8
Sodium nitrate	1.0	22.3
Sodium thiocyanate	1.0	16.0
Sodium iodide	1.0	16.0
Sodium benzenesulfonate	1.0	15.5
Sodium salicylate	1.0	No gel
Sodium trimethylacetate	1.0	26.5
Sodium chloroacetate	1.0	26.6
Sodium dichloroacetate	1.0	19.6
Sodium trichloroacetate	1.0	12.7
Sodium dibromoacetate	1.0	16.3
Sodium tribromoacetate	1.0	No gel
Sodium diiodoacetate	1.0	12.3
Sodium trifluoroacetate	1.0	24.1
Sodium acetyltryptophan	0.75	13.7
Sodium maleate	0.5	33.7
Sodium succinate	0.25	32.3
Sodium fumarate	0.5	31.5
Sodium acetylenedicarboxylate	0.5	19.4
Lithium chloride	1.0	25.4
Lithium iodide	0.25	26.7
Lithium salicylate	0.25	20.5
Lithium diiodosalicylate	0.23	No gel
Calcium chloride	1.0	16.1
Magnesium chloride	1.0	22.9

(15) E. H. Büchner, *Rec. trav. chim.*, **46**, 439 (1927).

(16) W. D. Bancroft, *This Journal*, **30**, 1194 (1926).

(17) W. D. Bancroft and L. F. Gould, *ibid.*, **38**, 197 (1934).

(18) J. W. Janus, A. W. Kenchington and A. G. Ward, *Research*, **4**, 247 (1951).

(19) J. Bello and J. R. Vinograd, *J. Am. Chem. Soc.*, **78**, 1369 (1956).

(20) A. G. Doherty and C. L. Ogg, *Ind. Eng. Chem., Anal. Ed.*, **15**, 751 (1943).

(21) W. Petrieff, *Ber.*, **8**, 730 (1875).

(22) A. Angeli, *Ber.*, **26**, 595 (1893).

(23) G. H. Woollett and W. W. Johnson, *Org. Syntheses*, **14**, 52 (1934).

linearity, some of the results, where noted, are extrapolated to concentration levels in excess of the solubility limits.

In Fig. 1 is shown the effect of increasing aliphatic chain length on the effect of sodium salts of mono- and dicarboxylic acids on the melting point of gelatin. As the aliphatic chain is increased, there is first an increase of melting point followed by a decrease as the non-polar chain increases toward the detergent range. The effectiveness of melting point reduction by additives with large non-polar groups has been pointed out by Gordon and Ferry.¹³ Ferry¹⁴ has also pointed out that large, polarizable groups make additives effective. Thus, the phenyl-substituted acids, the halogenated acids and the unsaturated acids are more effective melting point reducers than the simple, saturated aliphatic acids. For example disodium succinate raises the melting point 8° per mole while disodium fumarate raises it only 2.3° . Both ions have *trans* configurations. Disodium maleate, which has a *cis* configuration, raises the melting point 6° per mole and disodium acetylenedicarboxylate, which is linear, lowers the melting point by 22° per mole. These results show that both polarizability and structure are important. Among the halogenated acids, the higher

the atomic number of the halogen and the greater the number of halogen atoms, the greater is the melting point reduction. There is no correlation between acid strength and melting point reduction as the acid strength decreases with increasing atomic number and increases with increasing number of halogen atoms.²⁴ The effect is not due to size alone, as trimethylacetate, which is about the same size as tribromoacetate (from Fisher-Hirschfelder-Taylor models), lowers the melting point only one-eighth as much as the latter. The polarizability of the additives is in good correlation with their effectiveness as melting point reducers. The most effective melting point reducer known is lithium 2-hydroxy-3,5-diiodobenzoate (diiodosalicylate) which lowers the melting by 120° per mole; that almost all of the effect is probably due to the diiodosalicylate ion will be shown below.

The effects of some acids are shown in Fig. 2. The large slope of the hydriodic acid curve may be related to the observed partial precipitation of the gelatin which occurs between 0.25 and 0.5 *M* concentration. That the reduction of melting point was not due to extensive degradation was shown by careful neutralization of the hydrochloric acid solutions, followed by determination of the melting point of the neutralized solutions. The data in Fig. 3 show that the melting point reduction is nearly reversible, even at 3 *M*.

(24) H. C. Brown, D. H. McDaniel and O. Häfliger, in "Determination of Organic Structures by Physical Methods" (E. A. Braude and F. C. Nachod, editors) Academic Press, Inc., New York, N. Y., 1955, p. 579.

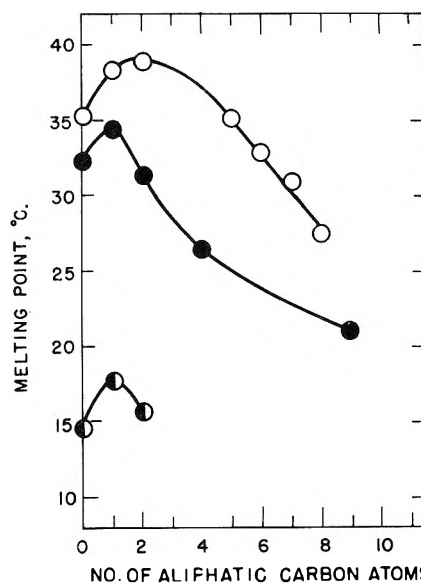


Fig. 1.—Melting point of 5% gelatin containing sodium salts of carboxylic acids; effect of aliphatic chain length: ●, monocarboxylic acids; ○, dicarboxylic acids; ●, phenyl-substituted monocarboxylic acids. Abscissa is number of aliphatic carbon atoms exclusive of carboxyl groups.

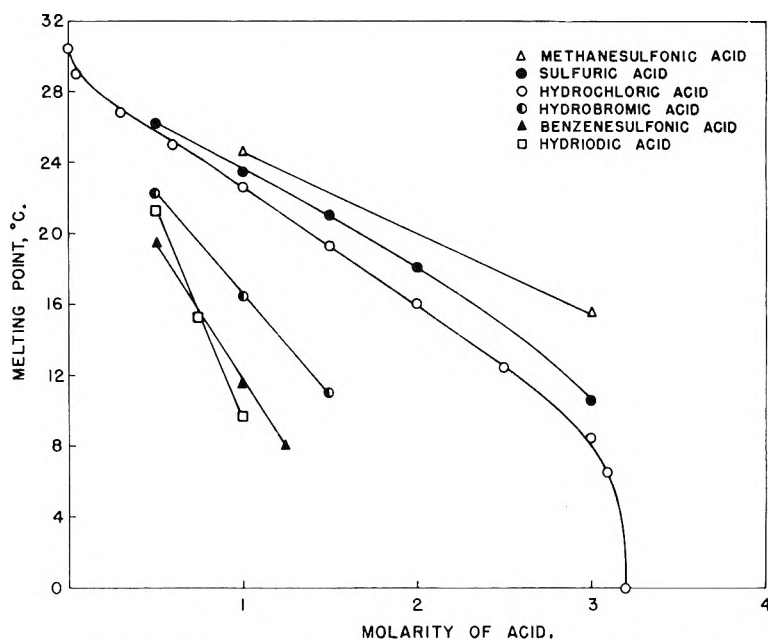


Fig. 2.—Effects of acids on the melting point of 5% gelatin.

In Fig. 4 are shown the effects of urea and some related compounds. Guanidinium chloride is about as effective as hydrochloric acid and both are about twice as effective as urea. Another similarity between hydrogen and guanidinium ions is that guanidinium thiocyanate and thiocyanic acid (but not sodium thiocyanate) precipitate gelatin at about 0.5 *M*, but redissolve the precipitate at 1 *M* concentration. The curve for guanidinium sulfate indicates that the melting point raising effect of sulfate ion becomes greater, per mole, as the concentration increases.

The additives fall into the well-known Hofmeister or lyotropic series and into a series determined

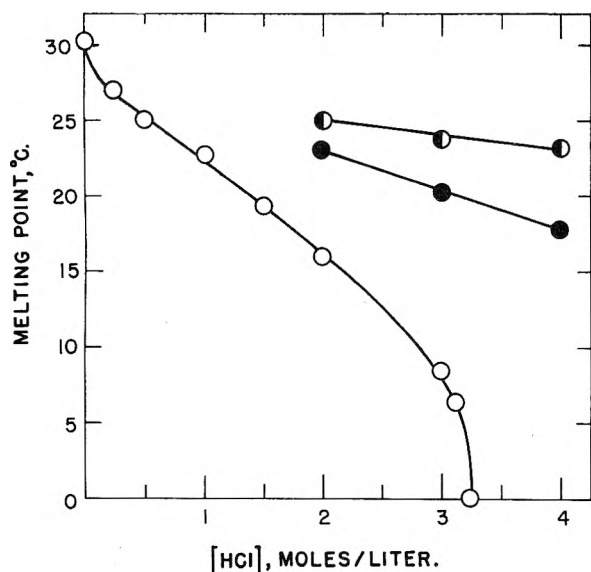


Fig. 3.—Reversibility of melting point reduction by hydrochloric acid: O, hydrochloric acid; ●, after neutralization of O; ○, original gelatin of the same concentration of gelatin and sodium chloride as ●.

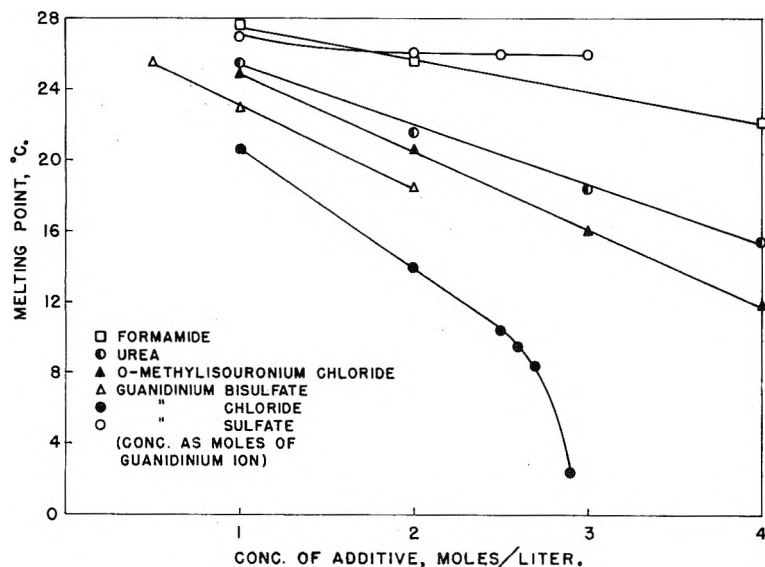


Fig. 4.—Effect of urea and related compounds on the melting point of 5% gelatin gels.

by the effects on the denaturation of proteins, see, for example, Simpson and Kauzmann.²⁵ That is, additives that lower the melting point of gelatin promote the denaturation of proteins and those that raise the melting point of gelatin protect against denaturation. This is particularly notable in the case of sulfate; for while guanidinium chloride is a good melting point reducer and denaturant, guanidinium sulfate has little effect on melting point or denaturation.²⁶

Molar Melting Point Depression.—The fact that the effects of various acids on melting are parallel to, but greater than, the effects of the corresponding sodium salts, suggested that the effects of mixtures might be additive. Since so-

(25) R. B. Simpson and W. Kauzmann, *J. Am. Chem. Soc.*, **75**, 5139 (1953).

(26) N. F. Burke, *THIS JOURNAL*, **47**, 164 (1943).

dium chloride lowered the melting point by about 2°, each of its ions was arbitrarily assigned a value of -1 and from this value and the observed melting point depressions of other salts there was calculated a molar melting point depression, α , for each ion. These have not been tabulated but can be calculated readily from Table I. The additivity of α was tested by comparing the measured melting points of mixtures of salts and of acids with results calculated from the α values. The results are shown in Table II. There is good agreement for all the additives tested except thiocyanic acid and, to a lesser extent, guanidinium thiocyanate. Thiocyanic acid is unstable and turned yellow. The additivity exhibited by the lithium salts makes it probable that the major effect of lithium diiodosalicylate is due to the diiodosalicylate ion.

The Effect of Time on the Melting Point Reduction.—To determine whether the effect of additives is a rate or equilibrium effect, the melting points of gelatin containing various salts was measured after storage at 0° for periods up to 31 days. The results, Fig. 5, show that after the first 2-3 days there is little additional rise in melting point. When 1 M sodium salicylate was used (not shown on the figure) there was no gelation in 31 days. It seems likely from the shapes of the curves that the melting point reductions represent changes in the equilibrium of the gelatin-gelatin or gelatin-solvent interaction.

Effects of Neutral Salts on pH of Gelatin: Binding of Ions.—The possibility that binding of additives may cause the melting point changes was considered. This was first investigated by observing the effects of neutral salts on the pH.²⁷ There have been contradictory reports on the binding of small ions by gelatin. For example, Docking and Heyman²⁸ reported that gelatin binds thiocyanate and chloride, among others, while Williams, *et al.*,²⁹ found no binding of thiocyanate and Carr³⁰ and Carr and Topol³¹ found no binding of chloride.

There have been reports on the effects of salts on the pH of gelatin solutions. Giedroyc and Przylecki³² found that some calcium, magnesium and sodium salts lower the pH, but the concentrations at which they worked were too low (mostly below 0.05 M) to be of significance in regard to melting point effects. Scala³³ found that sodium and calcium chloride cause an increase in pH and that barium chloride produced varying effects at different concentrations.

We have examined the effects of various salts at 1 M concentration on the pH of 5% gelatin solutions.

(27) G. Scatchard and E. Black, *ibid.*, **53**, 88 (1949).

(28) A. R. Docking and E. Heyman, *ibid.*, **43**, 513 (1939).

(29) J. W. Williams, W. M. Saunders and J. S. Cicirelli, *ibid.*, **58**, 774 (1954).

(30) C. W. Carr, *Arch. Biochem. Biophys.*, **46**, 417 (1953).

(31) C. W. Carr and L. Topol, *THIS JOURNAL*, **54**, 176 (1950).

(32) W. Giedroyc and S. J. Przylecki, *Biochem. J.*, **25**, 465 (1931).

(33) A. Scala, *Ann. igiene*, **42**, 313 (1932).

TABLE II
ADDITIVITY OF α VALUES

Additive	M.p. depression, °C.	
	Found	Calcd. from α
0.5 M NaCNS and 0.5 M NaI	15.0	15.2
0.5 M NaCNS and 0.5 M NaBr	10.9	11.7
0.5 M NaCNS and 0.5 M NaCl	9.1	9.2
0.5 M Guanidinium chloride and 0.5 M HCl	10.3	10.2
Benzenesulfonic acid, 1 M	19.0	20.5 ^a
Hydriodic acid, 1 M	20.8	20.0 ^a
Hydrobromic acid, 1 M	14.0	13.6 ^a
Methanesulfonic acid, 1 M	5.5	4.5 ^a
Thiocyanic acid, 1 M	≥ 30.2	20.0
Guanidinium thiocyanate, 1 M	26.4	23.6
LiI, 0.25	15.0	15.2
LiCl, 0.25 M and sodium salicylate 0.25 M	20.5	21.4

^a Calculated from the values for hydrogen ion found for hydrochloric acid.

From the data of Fig. 6 it can be seen that negative ions raise and positive ions lower the pH, the behavior expected if binding occurs. Also, there is a correlation between pH change and melting point change for both melting point reducers and melting point raisers, although only two of the latter were investigated. The pH changes for the amino-acetylated gelatin are smaller than those for the original gelatin as is to be expected if the binding of anions occurs at the positively charged groups³⁴; the acetylated gelatin contains fewer such groups. Somewhat unexpected was the finding that sodium chloride and, to a lesser extent, bromide reduce the pH of the acetylated gelatin while raising that of the non-acetylated gelatin. This suggests that sodium binding occurs. In the case of non-acetylated gelatin, the effect of the sodium binding is swamped by the binding of the anions. The acetylated gelatin has a net negative charge at pH 7, which would promote cation binding while the non-acetylated gelatin has a net positive charge which would have the opposite effect.

Effects of Additives on Chemically Modified Gelatins.—It was considered possible that the correlation between pH change and melting point change was fortuitous and that the bound ions do not affect the melting point. Accordingly, we investigated the effects of a variety of salts on gelatin having one or another of its possible binding sites blocked. The effects of some additives on the melting point of the amino-acetylated gelatin are shown in Table III.

TABLE III

EFFECT OF ADDITIVES ON THE MELTING POINT OF 5% GELS OF AMINO-ACETYLATED GELATIN

Additive	Concn., moles/l. ⁻¹	M.p., °C.	M.p. reduction, °C.
None	..	16.1	..
Sodium bromide	1.0	10.6	5.5
Sodium thiocyanate	1.0	No gel	≥ 16.1
Sodium iodide	1.0	No gel	≥ 16.1
Sodium salicylate	0.5	No gel	≥ 16.1
Lithium diiodosalicylate	0.06	8.8	7.3

(34) I. M. Klotz, *Cold Spring Harbor Symposia on Quantitative Biology*, **14**, 97 (1950).

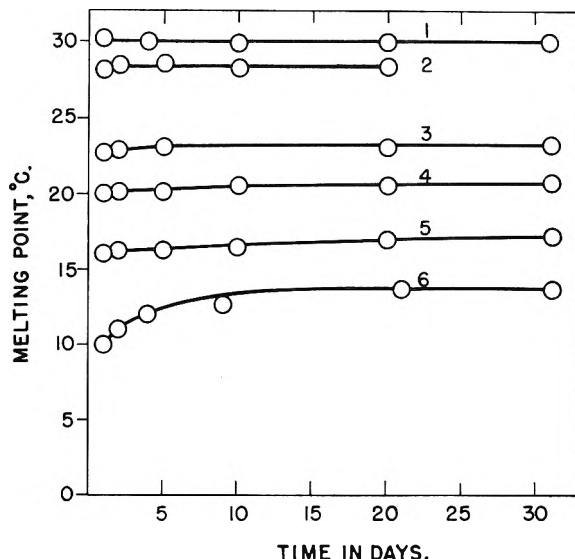


Fig. 5.—Effect of time on melting points of gels containing 1 M salts: 1, no salt; 2, sodium chloride; 3, sodium bromide; 4, guanidinium chloride; 5, sodium thiocyanate; 6, 0.7 M sodium salicylate.

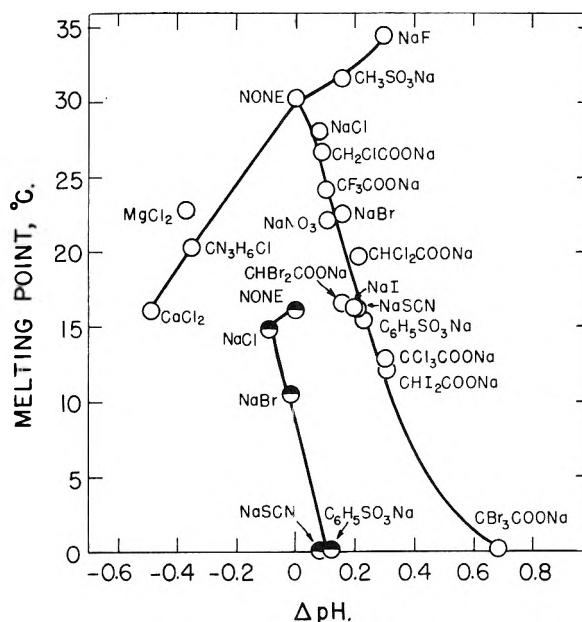


Fig. 6.—Correlation between pH and melting point changes for 1 M salts and 5% gelatin. CN_3H_6Cl is guanidinium chloride; ●, data for amino-acetylated gelatin.

Although sodium bromide has a slightly smaller effect on the melting point of the acetylated gelatin than on that of the original gelatin, the effects of sodium thiocyanate and iodide and of lithium diiodosalicylate on the acetylated gelatin are equal to or greater than on the original gelatin. Lithium diiodosalicylate reduced the melting points of the original and acetylated gelatins by 7.0 and 7.3°, respectively. The data for this salt are especially significant as this salt is the most effective of the melting point reducers and would be expected to be the most strongly bound as, in general, the larger the ion the greater the binding.^{34,35}

(35) J. D. Teresi and J. M. Luck, *J. Biol. Chem.*, **199**, 823 (1952).

The role of binding at amino groups was also investigated by observing the effect on melting point of two additives at pH values high enough to convert most of the charged ammonium groups to uncharged (and, therefore, non-binding) amino groups. At pH 11.7, most of the amino groups are in the uncharged form since the pK values of the ϵ -amino groups of the lysine residues are about 10.5 (see, for example, Tanford and Wagner on lysozyme³⁶), a value in agreement with the titration curve we have obtained on gelatin and that of Ames.³⁷ Also titration in the presence of 1 M sodium thiocyanate did not change the titration curve significantly. This suggests that little or no binding of thiocyanate occurs at high pH. The results, Table IV, show that iodide and benzenesulfonate are as effective at pH 11.7 as at pH 6. From the data of Tables III and IV it is apparent that binding at charged ammonium groups, whether or not it occurs, is not the mechanism by which anions lower the melting point.

TABLE IV

EFFECTS OF SOME SALTS ON THE MELTING POINTS OF 5% GELATIN AT VARIOUS pH VALUES

Additive	Concn., M	pH	M.p., °C.	M.p. reduc- tions ^a
None	..	11.7	29.6	..
Potassium iodide	0.5	11.7	22.4	7.2
Sodium benzenesulfonate	0.5	11.7	22.5	7.1
None	..	6	30.2	..
Potassium iodide	0.5	6	23.0	7.2
Sodium benzenesulfonate	0.5	6	23.2	7.0
Calcium chloride	1	6	16.1	14.1
Guanidium chloride	1	6	22.0	8.2
None	..	2	27.6	..
Calcium chloride	1	2	16.1	11.5
Guanidium chloride	1	2	18.8	8.8

^a Difference between the melting points with and without salt at the same pH.

The possibility of binding of anions at guanidinium groups being responsible for melting point reduction was investigated by observing the effect of lithium diiodosalicylate and sodium thiocyanate on a gelatin having 71% of its guanidinium groups nitrated to uncharged nitroguanidino groups. Simultaneously with the nitration, the hydroxyl groups were sulfated³⁸ by the large excess of sulfuric acid present, resulting in the introduction of 60 sulfate groups per 10^5 g.³⁹ Complete sulfation, in the absence of nitric acid, introduces 150 sulfate groups per 10^5 g.

It was found that lithium diiodosalicylate and sodium thiocyanate were as effective in lowering the melting point of the nitrated gelatin as that of the original gelatin (see Table V). Although the effects of other melting point reducing anions on the nitrated-sulfated gelatin were not investigated, the results obtained show that binding of anions at guanidinium groups or at hydroxyl groups is prob-

(36) C. Tanford and M. L. Wagner, *J. Am. Chem. Soc.*, **76**, 3331 (1954).

(37) W. M. Ames, *J. Sci. Food Agric.*, **3**, 579 (1952).

(38) H. C. Reitz, R. E. Ferrel, H. S. Olcott and H. Fraenkel-Conrat, *J. Am. Chem. Soc.*, **68**, 1024 (1946).

(39) Sulfur analyses by Elek Microanalytical Laboratories, Los Angeles, California.

TABLE V

EFFECTS OF SODIUM SALTS ON THE MELTING POINTS OF GELATIN AND MODIFIED GELATINS^a

Type of gelatin	Salt	Concn. of salt, M	M.p. change, °C.
Original	Thiocyanate	0.5	-7.1
Nitrated	Thiocyanate	0.5	-7.2
Original	Lithium diiodosalicylate	0.06	-7.0
Nitrated	Lithium diiodosalicylate	0.06	-7.0
Original	Acetate	0.25	+1.0
Acetylated	Acetate	0.25	+0.9
Nitrated	Acetate	0.25	+0.9
Original	Succinate ^b	0.25	+1.9
Acetylated	Succinate ^b	0.25	+2.0
Nitrated	Succinate ^b	0.25	+1.6
Original	Dibasic phosphate ^b	0.25	+2.8
Acetylated	Dibasic phosphate ^b	0.25	+2.6
Nitrated	Dibasic phosphate ^b	0.25	+2.8
Original	Fluoride	0.25	+1.1
Acetylated	Fluoride	0.25	+1.3
Nitrated	Fluoride	0.25	+1.4

^a At pH 7 unless otherwise noted. ^b At pH 8.9.

ably not important in melting point reduction, particularly as diiodosalicylate would be expected to be the most strongly bound of the anions investigated.

Similarly, in the case of anions that raise the melting point, the possibility of the effect being due to binding of the anions at cationic sites was investigated with the aid of the acetylated and nitrated-sulfated gelatins. The results are shown in Table V for anions of four different types: inorganic univalent and divalent and organic univalent and divalent. It is apparent that with both the acetylated and nitrated gelatins, the additives are as effective as with the original gelatin, showing that anions that raise the melting point do not do so as a result of being bound at the amino or guanidino groups.

Similarly, the effect of possible binding of cations at the negatively charged carboxylate groups was investigated by determining the melting point reduction by guanidinium chloride and calcium chloride at pH 6 and 2. Binding of guanidinium ion by a low isoelectric gelatin above pH 3 has been reported.⁴⁰ Titration of gelatin with hydrochloric acid, in the presence of 1 M calcium chloride, showed a decrease of 0.6 unit in the pK of the carboxyl groups, indicating that calcium binding occurs. At pH 2 the carboxyl groups are largely in the uncharged state. From Table IV it can be seen that guanidinium chloride is at least as effective at pH 2 as at pH 6, while calcium chloride is 80% as effective at pH 2 as at pH 6. A similar experiment has been reported by Merckel⁴¹ for sodium salts of several acids. However, as sodium ion appears to have little effect on melting point, the data presented here for calcium and guanidinium chlorides are more significant. In addition, the effect of calcium chloride on a gelatin having 70% of its carboxyl groups esterified was determined at pH 1.6 where there are almost no free carboxylate ions. The melting point was reduced by 11.5°, compared

(40) M. D. Grynberg, *Biochem. Z.*, **262**, 272 (1933).

(41) J. H. C. Merckel, *Kolloid Z.*, **78**, 339 (1937).

with 11.5° for normal gelatin at pH 2, and 14.1° for normal gelatin at pH 6. From the foregoing it appears highly unlikely that binding of cations at negative carboxylate groups is very important in melting point reduction, although this may be of some significance in the case of calcium ion.

The possibility that binding of cations to hydroxyl groups may be important in reducing the melting point was tested with calcium chloride and a gelatin having its hydroxyl groups quantitatively and selectively acetylated. The melting point of the hydroxyl-acetylated gelatin was 15.1°; in the presence of 1 *M* calcium chloride there was no gelation. Since the melting point reduction produced by calcium chloride is 14° in the case of normal gelatin, it is evident that binding at hydroxyl groups is not important in gelation.

One cationic melting point raiser has been investigated, namely, iron(III), as the chloride. The effect of iron(III) chloride on the melting point of gelatin gels is a function, at constant gelatin concentration, of the concentration of the iron. Thus, addition of 0.25 *M* iron(III) chloride to a 10% gelatin solution (to obtain final concentrations of 0.13 *M* and 5%, respectively) causes immediate gelation and after the usual storage at 0° for 20 hours, the melting point of the gel is raised by 4°, or 32° per mole of iron chloride. If, however, 1 *M* iron(III) chloride be used, no gelation occurs till cooling, and, after 20 hours at 0°, the melting point is reduced by 8°, compared with the melting point of gelatin alone at the same pH. When a 5% solution of the carboxyl-esterified gelatin is made 0.13 *M* in iron(III) chloride, gelation does not occur till the solution is chilled, and the melting point, after standard treatment, is not raised, but reduced by 1°, or 8° per mole, corresponding to the reduction produced by 1 *M* iron on the original gelatin. The melting point of the esterified gelatin alone is the same as that of the original gelatin, indicating that little degradation occurred in the esterification process. The above observations can be explained by assuming coordination of iron at carboxyl groups. At low concentration of iron, cross-links are formed by coordination of iron with carboxyl groups of two gelatin molecules. Alternatively, intramolecular cross-links may stabilize a structure required for gelation, or both mechanisms may operate. At high concentration of iron, polycoordination of iron is less extensive and the salt acts as a melting point reducer.

Mechanism of Action of Electrolytes on Gelation.

—The foregoing data have shown that, with the exception of iron(III), the effects of ions on the melting points of gelatin gels, are not due to binding at the charged groups or at hydroxyl groups. These conclusions apply only to the small ions we have studied. In the case of polyelectrolytes and micelle forming ions more complex interactions may occur.^{42,43}

Other remaining explanations for the effects of ionic additives are: (1) an effect on the solvent and (2) interactions with parts of the gelatin molecule other than those investigated here. With regard

to the former, the effects of salts on the dielectric constant appear to be an inadequate explanation for the widely varying effects on melting point by the different salts. This has also been found wanting to explain the effects of some salts on the denaturation of ovalbumin.²⁵ The available data do not permit a decision between other possible effects on the solvent, such as the structure-breaking effect⁴⁴ or changes in the degree of the polymerization of water.¹⁷ The last of these was proposed by Bancroft and Gould who made arbitrary assumptions as to the effects of various ions.

The large differences in the effects of various ions on the melting point, both as to direction and magnitude, suggest that the explanation lies in interactions between the ions and the gelatin. (It must be borne in mind, however, that the large changes in melting point may be the result of rather small changes in the configuration of the gelatin molecules.) The only parts of the gelatin molecules not considered above are the non-polar side chains and the peptide groups. Interactions between the non-polar groups and ions such as iodide or calcium are unlikely. Interactions between the non-polar groups and organic ions are possible. In such interactions the relatively non-polar portion of the ion would be oriented toward the gelatin and the charged group toward the water.

The peptide bond remains the most likely site for the action of small ions. These materials then lower the melting point by breaking peptide hydrogen bonds involved in intermolecular cross linking, and, possibly, similar bonds involved in maintaining an intramolecular configuration necessary for gelatin. The formation of segments of gelatin molecules of ordered configuration in the gelation process has been suggested by several authors.^{45,46} The effectiveness of large ions as melting point reducers may be due to their ability to cover the peptide group. That the effectiveness of hydrogen ion may be due to interaction at the peptide bond is suggested by the preparation of 1:1 complexes of amides and hydrohalic acids.⁴⁷⁻⁴⁹ The complexing of anions at peptide bonds is suggested by the finding of Steinhardt and Fugitt⁵⁰ that the rate of acid hydrolysis of the amide and peptide bonds of wool depends on the nature of the anion of the acid, the large polarizable anions having the greatest catalytic effect.

The anions that raise the melting point may do so by protecting the ordered segments of the gelatin from denaturation by water or by cross-linking through interaction at the peptide bonds. The former explanation is supported by the fact that melting point raisers increase the specific rotation of gelatin,⁵¹ as does cooling of a gelatin solution to gelling temperature. Also, melting point raisers protect ovalbumin against urea denaturation.²⁵

If the effects of the additives are due to changing the solvent, then the observed correlation between

(44) H. S. Frank and M. W. Evans, *J. Chem. Phys.*, **13**, 507 (1945).

(45) C. Robinson and M. V. Bott, *Nature*, **168**, 325 (1951).

(46) H. Boedtker and P. Doty, *This Journal*, **58**, 968 (1954).

(47) E. H. White, *J. Am. Chem. Soc.*, **77**, 6215 (1955).

(48) P. Walden, *Chem. Zentr.*, **83**, [1], 122 (1912).

(49) A. Werner, *Ber.*, **36**, 154 (1903).

(50) J. Steinhardt and C. H. Fugitt, *J. Research Natl. Bur. Standards*, **29**, 315 (1942).

(51) E. Stiasny, *Kolloid Z.*, **36**, 353 (1924).

(42) K. G. A. Pankhurst and R. C. M. Smith, *Trans. Faraday Soc.*, **40**, 565 (1944).

(43) M. Joly, *Bull. soc. chim. biol.*, **30**, 398 (1948).

melting point and *pH* change is fortuitous. If the effects on the melting point are due to interactions with the gelatin, such interactions would contribute to the *pH* change, the major part of which is due to binding at the charged groups. It is reasonable to assume that those ions that are most strongly bound at charged groups would also inter-

act most strongly at the polar peptide groups. A precise description of possible complexes between ions and peptide bonds is not possible at present.

Acknowledgment.—This work was supported under Contract No. DA 49-007-MD-298 with the Office of the Surgeon General, Department of the Army, to whom we wish to express our thanks.

OXIDATIVE DEGRADATION OF STYRENE AND α -DEUTEROSTYRENE POLYMERS¹

BY LEO A. WALL, MARY R. HARVEY AND MAX TRYON

National Bureau of Standards, Washington, D. C.

Received March 28, 1956

The oxidation of polystyrene and α -deuterostyrene polymers in the presence of ultraviolet radiation and air at 60° has been investigated. Initially, the deuterated polymer shows an increase in absorption at 340 $m\mu$ of only about $\frac{1}{5}$ that of polystyrene. A post-irradiation effect was observed which disappears upon further irradiation. The reaction occurring during post-irradiation of polystyrene consists of two first-order components with activation energies of 16 and 20–24 kcal. per mole. This may indicate the decomposition of two different hydroperoxide structures during the post-irradiation periods. However, it is suggested that one of these components may result from a *cis-trans* isomerization. It is concluded tentatively that polystyrene oxidizes mainly at the α -position of the monomer unit but that the resulting hydroperoxide, although formed, is extremely labile.

Introduction

In earlier investigations at this Laboratory on the ultraviolet-induced oxidation of polystyrene, the carbonyl and hydroxyl group build-up was followed by infrared spectra^{2a} and the small amounts of volatile components produced were analyzed by mass spectrometry.^{2b} Recently the increase in ultraviolet absorption has been found to be a sensitive indication of degradation.³ Thus ultraviolet spectrometry, which is usually a more convenient and simpler technique to employ than infrared or mass spectrometry, has been used in this work. Often the easily accessible regions in the infrared merely show the presence of certain groups without giving definite further information concerning the specific nature of the structure containing these groups. Mass spectrometry, on the other hand, ordinarily gives analyses of volatile fragments which are, at least at the low extents of reaction so far studied,² invariably contaminated with trace impurities such as solvent and solvent oxidation products. The rate of oxygen consumption would be a more direct quantity to study from a mechanistic viewpoint. We have, however, confined ourselves in this study to the changes in ultraviolet transmission in the region of 280 to 400 $m\mu$, because previous work has shown that decreased transmission occurred in these regions during the early stages of oxidation.³

In the present work the oxidation behavior of α -deuterostyrene polymer was compared with that of polystyrene, the purpose being to establish the site of radical attack. It is well-known that deuterium atoms are abstracted at much lower rates

than protium atoms, and hence such a comparison should enable one to gain basic knowledge of the mechanism of oxidation. If the presence of deuterium atoms alters any of the rate-determining elementary steps of the oxidation process, then the over-all rate will be altered. An analysis of the results in conjunction with other kinetic data will aid in establishing the mechanism in more detail than has hitherto been possible.

Deuterium studies have been used previously to ascertain the site of transfer processes in polymerization reactions^{4,5} and in pyrolytic decomposition of polymers.⁶

Materials and Methods

The polystyrene used in this work was a sample prepared by thermal bulk polymerization at 120° and had an approximate number average molecular weight, as determined from osmotic pressure measurements, of 237,000. This was the same highly purified polystyrene sample used in earlier work.³

The poly- α -deuterostyrene sample was prepared by the bulk polymerization at 70° of α -deuterostyrene. The monomer was synthesized from acetophenone by reduction with lithium aluminum deuteride to give α -deuteromethylphenylcarbinol, which was dehydrated. Mass spectra gave the following analysis: styrene 1.90%, styrene-*d*₁ 97.42%, styrene-*d*₂ 0.54%, styrene-*d*₃ 0.14%.

Both polymer samples were purified of monomer, dimer and similar materials by repeated solution in benzene, followed by precipitation in methanol. The final product was dissolved in benzene, the solution frozen, and the solvent removed by sublimation at reduced pressure. The extent of purification was determined by the ultraviolet absorption of chloroform solutions of these polymers after each cycle of solution and precipitation as recently described.³

Films of these purified polymers were cast from benzene solutions by the method described in references 2a and 3. The film thicknesses used were approximately 0.18 mm.

The films were exposed to ultraviolet radiant energy from a sunlamp in air on a rotating turntable 15 cm. from the lamp. The temperature of the table was 60°. This equipment is described in method No. 6021 of Federal Specifica-

(1) Presented at the 126th Meeting of the American Chemical Society in New York, N. Y., September 12–17, 1954.

(2) (a) B. G. Achhammer, M. J. Reiney and F. W. Reinhart, *J. Research Natl. Bur. Standards*, **47**, 116 (1951); (b) B. G. Achhammer, M. J. Reiney, L. A. Wall and F. W. Reinhart, *J. Polymer Sci.*, **8**, 555 (1952); also Natl. Bur. Standards Circular 525, Polymer Degradation Mechanisms, p. 205 (1953).

(3) M. J. Reiney, M. Tryon and B. G. Achhammer, *J. Research Natl. Bur. Standards*, **51**, 155 (1953).

(4) L. A. Wall and D. W. Brown, *J. Polymer Sci.*, **14**, 513 (1954).

(5) P. D. Bartlett and F. A. Tate, *J. Am. Chem. Soc.*, **75**, 91 (1953).

(6) L. A. Wall, D. W. Brown and V. E. Hart, *J. Polymer Sci.*, **15**, 157 (1955).

tion L-P-406a.⁷ The lamp gives a typical mercury spectrum and peak intensity at 313 $m\mu$.

A Beckman Model DU spectrophotometer with ultraviolet accessories was used, with further accessories for temperature control of the sample compartment.

The comparison of the rates of ultraviolet absorption after exposure to ultraviolet radiation and after storage in the dark at room temperature for both polymers was made as described in earlier work.³

The study of the temperature coefficient at 70, 75 and 80° for the post-radiation reaction in polystyrene was made by removing the sample from the exposure apparatus after a suitable exposure of about 290 hours and immediately placing the sample in the spectrophotometer cell compartment which was controlled at the indicated temperature. The increased absorbance⁸ at 340 $m\mu$ wave length was measured at suitable time intervals.

Results

With purified polystyrene the transmittance progressively decreases on oxidation. In Fig. 1 the full lines represent the results of exposure for the indicated times in hours to ultraviolet in the presence of air at a temperature of about 60°. The dashed lines show the effect of dark storage³ in air at room temperature. This post-effect is removed when the film is briefly exposed again. At 340 $m\mu$ the decrease in transmittance that occurs during the storage period is a maximum.³

The absorption produced in the ultraviolet during these oxidation studies is, as suggested previously, probably due to carbonyl-containing structures. This premise is supported by the fact that plots of the absorbance in the infrared region at 5.78 μ versus the ultraviolet absorbance at 340 $m\mu$, for all samples studied, are essentially linear.

In Fig. 2 there is presented the absorbance of the deuterated polymer and polystyrene as a function of the time of exposure to ultraviolet light in air at 60°. The solid lines represent results obtained by making absorption measurements immediately after the films had been oxidized in the presence of ultraviolet light, while the dashed lines represent the results obtained after an additional storage time of 120 hours. This time was chosen so that a maximum post-effect would be achieved. The difference between the two curves for a given substance is a measure of the total post-effect. Since the curves spread apart, it is seen qualitatively that the post-effect increases with extent of degradation. From this observation it appears that the much smaller post-effect in the poly- α -deuterostyrene may be partly due to the lower extent of apparent degradation. The apparent degradation of the deuterated polymer is markedly less initially, the rate of change in absorbance for this polymer being about a factor of 1/3 that for the polystyrene. This factor is within the range of possible deuterium isotope effects.

It was found that the post-effect developed faster at higher temperatures. In Fig. 3 the absorbance of polystyrene in the ultraviolet is plotted versus time of storage for several temperatures. Higher temperatures produce a much more rapid increase in absorbance.

(7) "Plastics, organic: General specifications, test methods," Federal Specification L-P-406a (Government Printing Office, Washington 25, D. C., Jan. 24, 1944).

(8) Absorbance is defined as $\log 1/T$, where T is the transmittance or the ratio of the transmitted energy to the incident energy.

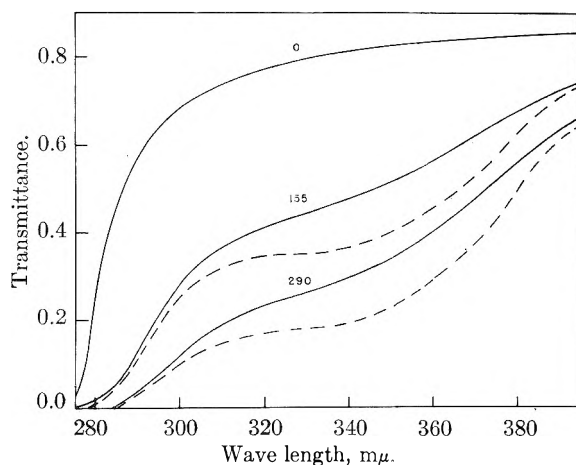


Fig. 1.—Ultraviolet spectra of polystyrene film as progressive oxidation occurs. Hours of exposure indicated: —, after exposure at 60°; ---, after storage for 120 hours at room temperature.

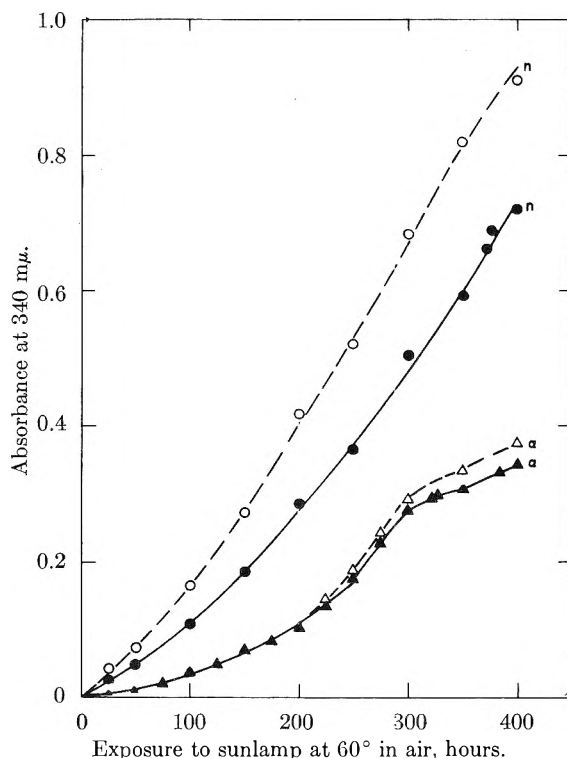


Fig. 2.—Absorbance of oxidized polystyrene films: —, immediately after exposure; ---, after an additional 120 hours of storage in dark at 25°; O, polystyrene; Δ, poly- α -deuterostyrene.

Assuming that the absorbances measured in this work are related to the concentration of products of the degradation reaction, a semi-log plot was made of one minus the fractional increase of absorbance, R , versus time of storage of polystyrene at 70° after ultraviolet irradiation for about 290 hours at 60°. This is shown in Fig. 4 (the curve with open circles) where

$$R = \frac{A_{\infty} - A}{A_{\infty} - A_0}$$

A_{∞} is the limiting absorbance measured during storage, A is the observed absorbance at time t , and A_0 is the initial absorbance before the storage reac-

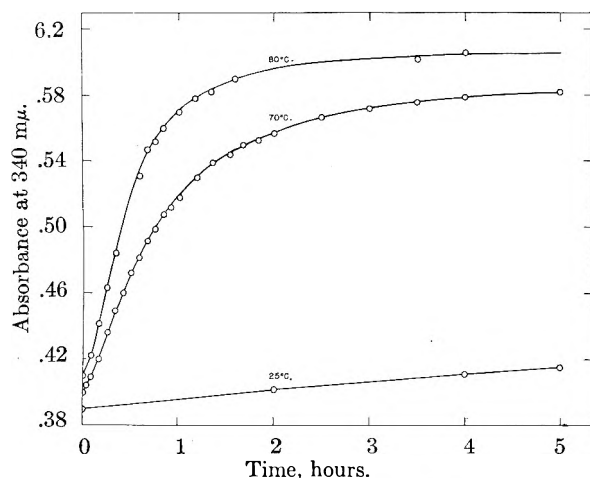


Fig. 3.—Ultraviolet absorbance at 340 $m\mu$ of polystyrene film as a function of time of storage at three temperatures after ultraviolet irradiation for 290 hours at 60°.

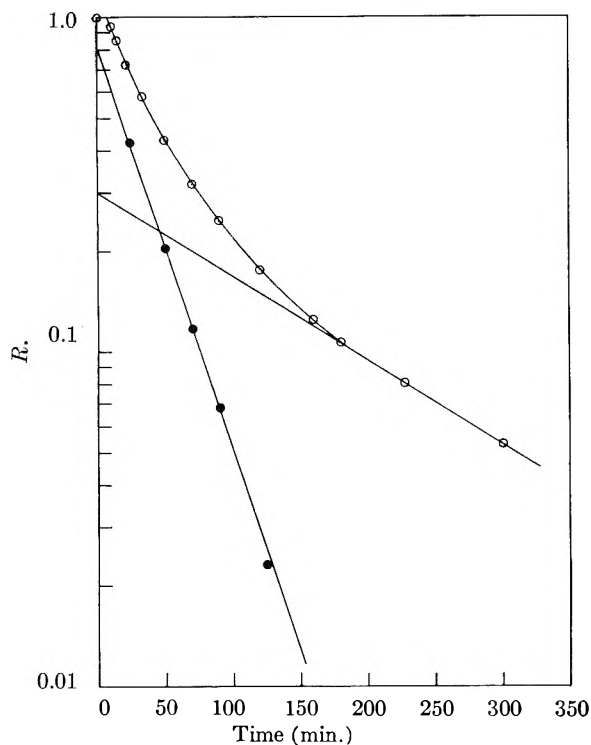


Fig. 4.—Semilog plot of one minus the fractional increase of absorbance, R , versus time; 70° data for post-effect in polystyrene. Straight lines add up to give experimental curve: \circ , experimental points; \bullet , points calculated by difference between experimental curve and extrapolated straight line.

tion begins. Since this plot does not yield a straight line, the storage reaction as measured by ultraviolet absorption is not a first-order reaction. Plotting the same data to test for a second-order reaction also led to curvature. A calculation of the apparent order of reaction from the slope of a plot of $\log dR/dt$ versus $\log R$ gave a value of approximately 1.24.

On the assumption that two simultaneous independent first-order reactions of widely different rates are producing absorbing products and that the faster reaction is complete before the last measurements were made it is possible to estimate the

rates of the two reactions by subtracting the slower from the over-all leaving the faster one. This treatment is common in the case of some radioactive decay problems. In Fig. 4 the over-all reaction is indicated by the curve with open circles and the fast and slow reactions by the straight lines. The closed circles indicate the points calculated by subtracting the slow reaction from the over-all reaction and were used to obtain the straight line for the fast reaction. Thus the experimental results are interpretable as the algebraic sum of two first-order variations in absorbance and thus the data are suggestive of two simultaneous first-order processes. Values of the rate constants obtained from the slopes of these two straight lines at four different temperatures are shown in Table I. Activation energies are obtained from the slopes of the lines in Fig. 5. The fast reaction results in a very good straight line leading to an activation energy of 16 kcal. per mole, while the slow reaction data yield a less well defined straight line indicating an activation energy of the order of 20–25 kcal. The relative error of the estimate of the fast reaction slopes is much smaller than that of the slow reaction slopes since the over-all magnitudes of the fast reaction slopes are so much larger than the slower. It is assumed, of course, that the absolute errors of the two measurements are of the same order of magnitude. Even considering the decreased accuracy inherent in the method for the slow reaction values, it is concluded that its activation energy is somewhat higher than that of the fast reaction. The pre-exponential factors found were 10^{11} sec. $^{-1}$ for the slow reaction and 10^7 sec. $^{-1}$ for the fast reaction. The rate data are given in Table I.

TABLE I

RATE CONSTANTS AS A FUNCTION OF TEMPERATURE FOR THE REACTION THAT FOLLOWS ULTRAVIOLET IRRADIATION OF POLYSTYRENE IN AIR FOR 290 HOURS AT 60°

$$k_{\text{slow}} = 10^{11} \exp -23,500/RT \text{ sec.}^{-1}$$

$$k_{\text{fast}} = 10^7 \exp -16,400/RT \text{ sec.}^{-1}$$

Temp., °C.	Slow reaction k_{slow} , sec. $^{-1}$	Fast reaction k_{fast} , sec. $^{-1}$
25	7.1×10^{-7}	9.9×10^{-6}
70	0.96×10^{-4}	4.54×10^{-4}
75	2.26×10^{-4}	3.82×10^{-4}
80	0.37×10^{-4}	7.19×10^{-4}

Previous work⁹ with γ -ray induced degradation of polystyrene in carbon tetrachloride solution with air present gave a post-effect on the viscosity decrease. Temperature had an accelerating action in this process. It is very likely that both post-effects are due to the decomposition of a hydroperoxide intermediate.

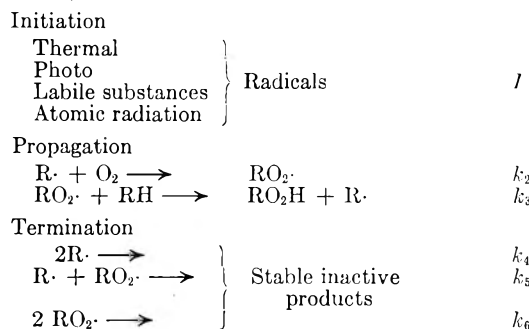
Discussion

As a starting point for a discussion of the oxidation mechanism of polystyrene it is convenient to choose the generally accepted mechanism of oxidation for olefins¹⁰ which is presumably applicable to polydienes. It is our purpose here to ascertain for polystyrene to what degree this mechanism is applicable, and to determine the variations and finer

(9) L. A. Wall and M. Magat, *J. chim. phys.*, **50**, 308 (1953); *Modern Plastics*, **30**, 111 (1953).

(10) L. Bateman, *Quart. Rev.*, **8**, 147 (1954).

details that may be peculiar to this polymer. The mechanism¹⁰ for olefin oxidation, for which a great deal of experimental evidence has been accumulated, is



where I is the over-all rate of initiation and the k 's are the specific rate constants for the indicated reaction. For the system under study in this investigation, photo initiation is evidently the radical producing process. For a long kinetic chain, *i.e.*, propagation occurring much more often than termination, and using the usual steady-state assumption, the following expression¹⁰ is obtained relating the consumption of oxygen to the rate constants and concentrations of reactants

$$\frac{1}{\left(\frac{-d(O_2)}{dt}\right)^2} = \frac{1}{I} \left[\frac{k_4}{k_2^2(O_2)^2} + \frac{2k_5}{k_2k_3(RH)(O_2)} + \frac{k_6}{k_3^2(RH)^2} \right] \quad (1)$$

Fortunately, a limiting case exists for high pressures of oxygen when reaction 2 is much faster than reaction 3, which leads to a much simpler relationship

$$-d(O_2)/dt \text{ High Press } O_2 = (I/k_6)^{1/2} k_3(RH) \quad (2)$$

This equation is only applicable to oxidation at oxygen pressures where the process is independent of oxygen pressure. It is interesting to note the wide variation in behavior of olefins in this respect.¹⁰ In general, rapidly oxidized materials show oxygen dependence up to 800 mm. of oxygen pressure. On the other hand, more difficultly oxidized olefins, for instance hexadecene-1, show no dependence above 1 mm. oxygen pressure at a temperature of 45°. Intuitively, then, one has some basis for assuming that oxidation of polystyrene would be independent of oxygen pressure in the range of conditions used in this study.

If this assumption is valid, then according to equation 2 one should obtain a retarded rate due to the deuterium isotope effect on the rate constant k_3 , provided oxidation normally proceeds through the abstraction of the tertiary hydrogen atom.

Since the oxidation is a photo-induced reaction, it is assumed that no isotope effects would occur in the initiation process. It is more difficult to rule out effects in the termination process except to say that any effects would be expected to be small. Dissociative processes in completely deuterated small molecules, such as ethane, have been observed to be more rapid¹¹ than in completely undeuterated species.

(11) L. A. Wall and W. J. Moore, *J. Am. Chem. Soc.*, **72**, 2840 (1951).

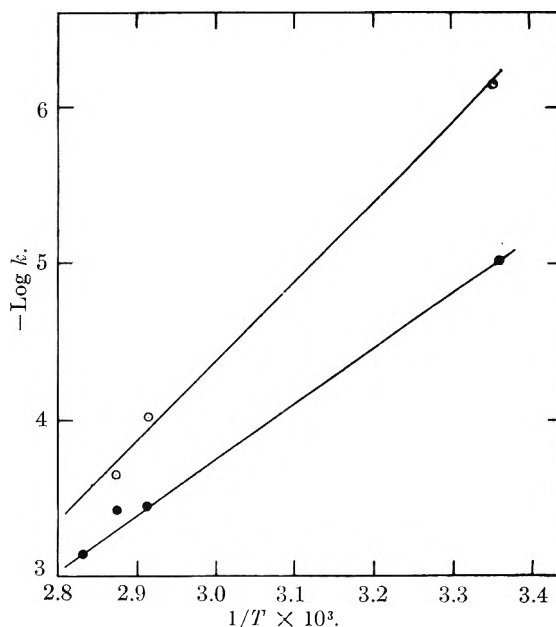


Fig. 5.—Plot of $-\log$ rate constants versus $1/T$: ●, fast reaction; ○, slow reaction.

However, we can conclude tentatively that the over-all oxidation mechanism in polystyrene is similar to that presented above and that at atmospheric oxygen pressure the reaction is independent of oxygen pressure. The post-effect as well as the decreased solubility observed in oxidized polystyrene require further explanation.

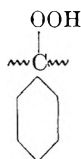
Attempts to detect chemically the hydroperoxide groups assumed to be formed during oxidation of polystyrene have indicated none or very few such structures. Extensive work directed toward the preparation of polystyrene hydroperoxide in appreciable quantity has been unsuccessful, although good yields of hydroperoxide are obtained when the rings in the polystyrene are alkylated with isopropyl groups. These latter results¹² are interpreted as due to either a steric hindrance for the hydrogen abstraction process, k_3 in the above mechanism, or a steric inhibition of resonance in the tertiary radical that is produced by step 3. This would mean a greater activation energy for the abstraction of the tertiary hydrogen atoms along the polystyrene chain compared to that in isopropylbenzene.

Our investigation indicates that there must be small amounts of hydroperoxide structures in the oxidized polymer even though ordinary chemical methods fail to detect them. For instance, a polystyrene powder that was oxidized as a solid for about 48 hours under an ultraviolet lamp catalyzed the polymerization of methyl methacrylate at 47°. The resulting solid was insoluble in benzene indicating a cross-linked material. Also, the post-effect in this study as well as the post-effect on the viscosity of γ -irradiated (in air) carbon tetrachloride solutions of polystyrene⁹ seem most readily explained by a hydroperoxide decomposition. The activation energy for the post-effect herein reported is in the range for peroxide decomposition, although considerably lower than that for peroxides stable at room temperature. It seems therefore reasonable

(12) D. J. Metz and R. B. Mesrobian, *J. Polymer Sci.*, **16**, 345 (1955).

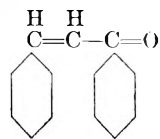
to deduce that such hydroperoxides are produced but that they are quite unstable, presumably due to steric factors, and hence cannot be readily isolated.

The resolution of the over-all post-irradiation phenomenon into two first-order components indicates two independent processes that produce structures highly absorbing in the ultraviolet spectral region. In such a complex system two different hydroperoxide or peroxide decompositions would afford a ready explanation. However, other possibilities exist. For instance, although the fast reaction is likely to be due to a decomposition of a peroxide of the type



the slow reaction, which is actually very slight, may be due to diffusion controlled reactions of relatively long lived free radicals or even thermal oxidation of some intermediate such as an aldehyde structure. There remains also the question of the insolubility of partially oxidized polystyrene. The decomposition of such a hydroperoxide discussed above should lead to chain scission and hence lower molecular weight and greater solubility.

A *cis-trans* isomerization¹³ is another possibility. Some interesting studies^{14,15} of the effect of sunlight on benzalacetophenone



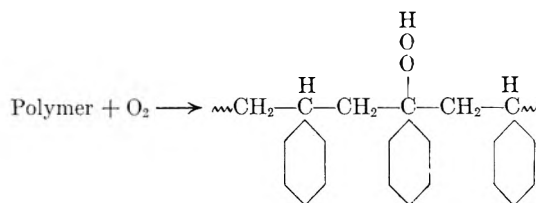
appear to be pertinent to this point. The ultraviolet spectrum of this compound changes drastically when the material is irradiated with sunlight.¹⁴ The absorbance in the region 270 to 350 m μ decreases while in the region 225 to 260 m μ the absorbance increases. The changes are considerably smaller in the latter region. The interpretation of this phenomenon made by the earlier authors¹⁴ is that a dimerization was occurring, destroying the conjugation responsible for the longer wave length absorbance. However, more recently it has been shown to be the result of a photo *trans-cis* isomerization¹⁵ and the *cis*-benzalacetophenone was isolated. This material is thermolabile and bright yellow in color. Several thermal *cis* to *trans* conversions have been reported¹³ having activation energies of 25 kcal. and low frequency factors of about 10⁴. This effect is highly reminiscent of the removal of the post-effect by subsequent irradiation mentioned here and previously.³ It is suggestive that the structure of benzalacetophenone is closely related to that for polystyrene and is a reasonable one to expect from the decomposition of the speculated hydroperoxide of polystyrene. Unfortunately, the absorption of benzalacetophenone is not at a long

enough wave length to account for that produced by the post-effect, although it is estimated that the extinction coefficient is of the correct order of magnitude. Hence, although this structure is probably not correct for the product of the dark reaction, this type of structure is indicated.

The cross-linking of polystyrene that occurs during oxidation may be the result of simple photolytic dissociation producing radicals, which combine, and hydrogen atoms.^{2b} This process would be expected to increase as more absorbing oxygenated groups were formed in the polymer. Such a process would be similar to the cross-linking produced by atomic radiation.¹⁶⁻¹⁸

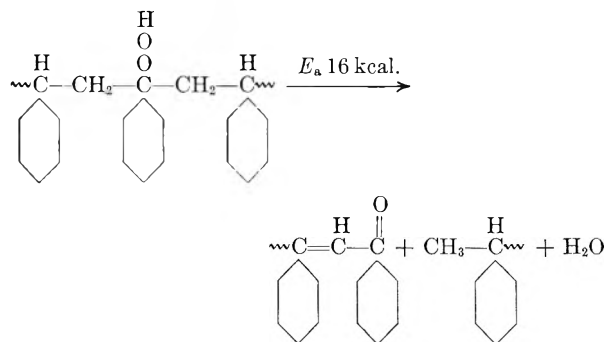
The processes occurring during the photo-induced oxidation of polystyrene appear to involve three different stages, which are presumably taking place simultaneously under the usual oxidation conditions.

Stage 1.—During exposure to light the chain mechanism discussed above is operating, producing hydroperoxide structures in the polymer chain.



The hydroperoxide concentration presumably reaches a small steady value.

Stage 2.—During dark storage the peroxide or peroxides decompose thermally to produce a group highly absorbing in the ultraviolet spectrum.



The conjugated structure shown on the right is probably not correct but is representative of a likely type of group. It is felt that numerous substances or structures are actually present and hence there is difficulty in interpreting the observed spectra. In this respect we have evidence (see Fig. 4) for two processes contributing to the dark reaction. The possibility exists that one of these processes is a thermal *cis-trans* isomerization¹³ and the result of a small concentration of a *cis*-isomer produced during the photo stages of the process.

Stage 3.—Finally, on subsequent exposure of the stored polymer, several different reactions

(13) G. M. Wyman, *Chem. Revs.*, **55**, 625 (1953).

(14) N. H. Cromwell and W. R. Watson, *J. Org. Chem.*, **14**, 411 (1949).

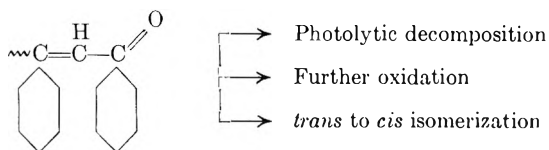
(15) R. E. Lutz and R. H. Jordan, *J. Am. Chem. Soc.*, **72**, 4090 (1950).

(16) M. Dole, C. D. Keeling and D. G. Rose, *J. Am. Chem. Soc.*, **76**, 4304 (1954).

(17) E. J. Lawton, A. M. Bueche and S. J. Balwit, *Nature*, **172**, 76 (1953).

(18) A. Charlesby, *ibid.*, **171**, 167 (1953).

occur to cross-link the polymer and to reduce the absorption in the ultraviolet.



All three processes shown above are quite feasible. Photolytic decomposition could readily remove the absorption and also lead to cross-linking. The structure written would be highly susceptible to

oxidation and by this process the removal of the ultraviolet absorption could occur. Finally, the isomerization process found with benzalacetophenone provides a very facile process that would decrease the ultraviolet absorption.

There are many points, such as the over-all rate of oxygen consumption, that need further investigation. Further work on other deuterated styrenes is now in progress. However, the basic features of the oxidation of polystyrene and associated reactions, although quite complex, seem to be understandable in terms of current mechanisms.

PROTON MAGNETIC RESONANCE STUDIES OF THE HYDROGEN BONDING OF PHENOL, SUBSTITUTED PHENOLS AND ACETIC ACID¹

BY CHARLES M. HUGGINS, GEORGE C. PIMENTEL AND

Department of Chemistry and Chemical Engineering, University of California, Berkeley, California,

JAMES N. SHOOLERY

Varian Associates, Palo Alto, California

Received March 28, 1956

The H-bond shift of the proton magnetic resonance was measured for phenol, *o*-, *m*- and *p*-chlorophenol, *o*-cresol, and acetic acid over the concentration range accessible in CCl₄ solution and, for acetic acid, in acetone solution. The proton resonance behavior can be correlated with the known H-bond properties of these compounds. The effects of steric hindrance, intramolecular H-bonding and H-bonding with the solvent are observed. The correlations among H-bond shifts, infrared frequency changes and H-bond energies, are examined.

Proton magnetic resonance measurements have shown that a significant chemical shift accompanies the formation of a hydrogen bond.^{2,3} (Hereafter this shift will be called an H-bond shift.) Hence nuclear magnetic resonance (NMR) measurements potentially offer a means of detecting and studying hydrogen bond (H-bond) formation. To investigate the relationships between the NMR properties and the deductions based on other physical measurements, we have made proton resonance studies of several substituted phenols: phenol, (I); *o*-cresol, (II); *p*-chlorophenol, (III); *m*-chlorophenol, (IV); and *o*-chlorophenol, (V); and of acetic acid, (VI).

Experimental

The experimental technique and equipment have been described.^{3b} For the phenols, the magnetic field was 9400 oersteds and the precession frequency 40 megacycles except for a few check measurements at 7050 oersteds and 30 megacycles; for acetic acid, the magnetic field was 7050 oersteds. Sample temperature was about 28°. The compounds were each studied in CCl₄ solution from the limit of detectability in dilute solution to the solubility limit. A reference solute, cyclohexane, was included (5% by volume) in the phenol solutions to avoid the necessity for a correction for change of the bulk diamagnetic susceptibility and to nullify instrument drift. Specific solvent effects might, of course, interfere with the use of an internal standard. They are not likely to be present when both solute and standard are present in the same solvent environment and the solvent has high symmetry. Acetic acid was studied in ace-

tone solution as well as in CCl₄. The methyl group proton resonance of acetic acid was used as reference.

All chemicals were of analytical or reagent grade. Their infrared spectra were examined for spurious absorptions.

Results

Phenol Derivatives.—Each solution displayed only one proton resonance which could be attributed to the O-H proton. For each compound the resonance attributed to the O-H proton has a marked concentration dependence. This behavior is that expected from a system in which protons are present in various molecular species which are in rapid equilibrium. The concentration dependence reflects changes in the relative amounts of these molecular species.

The measured resonance shifts, δ , and solution compositions are shown in Figs. 1 and 2. The dimensionless factor δ is defined in accordance with the usage of Gutowsky and Saika.^{3a} This convention differs in algebraic sign from the "shielding" definition, often designated s or σ .

$$\delta = \frac{H_r - H}{H_r} \times 10^6 = \frac{\nu_r - \nu}{\nu_r} \times 10^6$$

H_r = reference proton resonance field (cyclohexane)
 H = proton resonance field of O-H proton

δ is calculated from ν_r , the known resonance frequency (40 or 30 megacycles), and the value of $(\nu_r - \nu)$ obtained by the side-band audio oscillator measurement (see ref. 3b). The accuracy of measurement of δ was limited at high concentrations by interference of the phenyl proton resonance at about $\delta = 5.4$, at low concentrations by the signal-to-noise ratio, and for compound III at all concentrations by an unexplained broadening relative to the other compounds.

(1) This material was submitted in partial satisfaction of the requirements for the Ph.D. degree by C. M. Huggins, University of California, 1955.

(2) U. Liddel and N. F. Ramsey, *J. Chem. Phys.*, **19**, 1608 (1951); J. T. Arnold and M. E. Packard, *ibid.*, **19**, 1608 (1951).

(3) (a) H. S. Gutowsky and A. Saika, *ibid.*, **21**, 1688 (1953); (b) C. M. Huggins, G. C. Pimentel and J. N. Shoolery, *ibid.*, **23**, 1244 (1955).

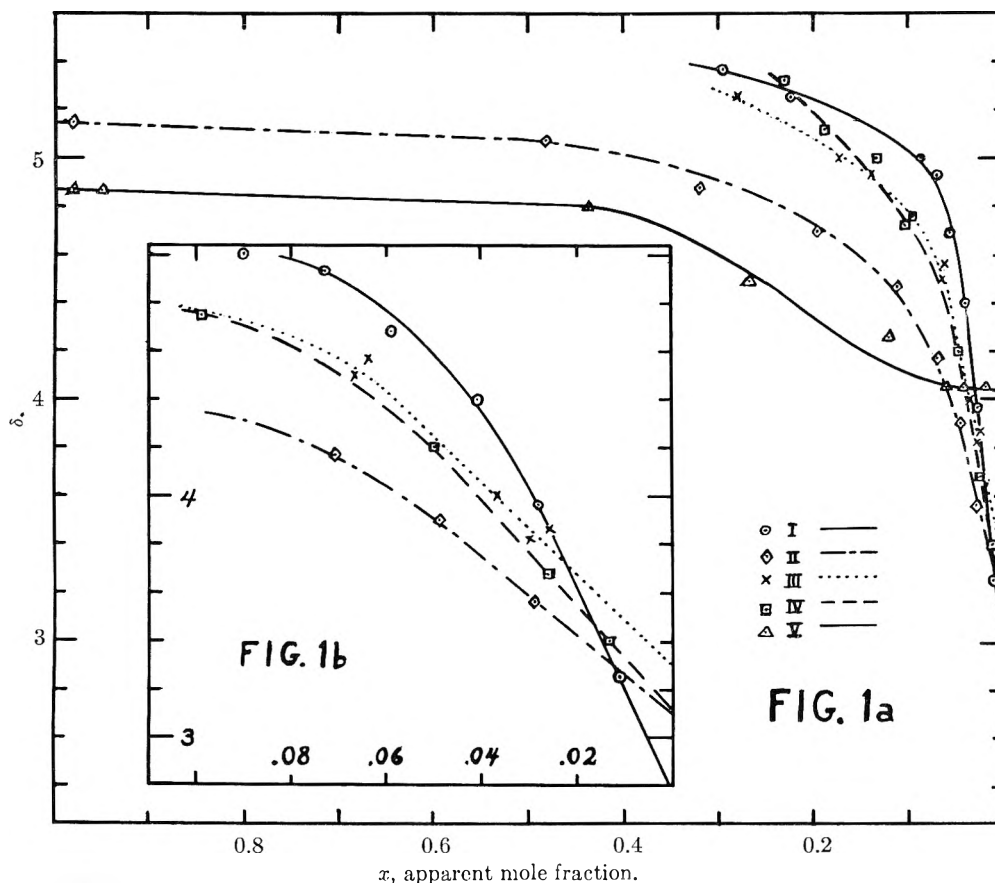


Fig. 1.—O-H proton resonance of phenols in carbon tetrachloride: I, phenol; II, *o*-cresol; III, *p*-chlorophenol; IV, *m*-chlorophenol; V, *o*-chlorophenol.

Figure 1a shows the experimental values of δ for the five phenolic compounds plotted vs. X , the apparent mole fraction of total phenolic material. Figure 1b shows a portion of the same data plotted on an expanded scale to indicate the extrapolation to $X = 0$. Figure 2 shows the data for acetic acid plotted vs. X . Intercepts δ_0 and δ_1 , at $X = 0$ and $X = 1$, respectively, and the slopes at the intercept at $X = 0$, $(d\delta/dX)_0$, are listed in Table I.

Discussion

The most obvious feature of Fig. 1 is the distinc-

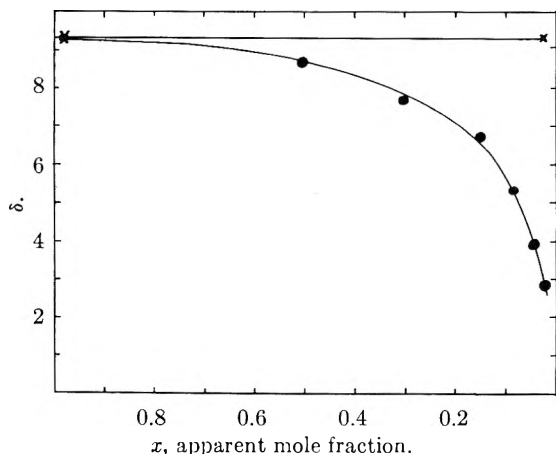


Fig. 2.—O-H proton resonance of acetic acid in carbon tetrachloride and in acetone: x , CCl_4 solvent; \bullet , acetone solvent.

tive curve for compound V. One unique aspect of the data for V is the zero slope at $X = 0$, $(d\delta/dX)_0 \cong 0$. This is certainly caused by the intramolecular H-bonding of monomeric *o*-chlorophenol which stabilizes monomeric V relative to H-bonded polymers of V. Hence at moderate concentrations (at mole fractions as high as 0.06, concentrations near 0.6 M) substantially all of the V is present as monomer. Next we observe that δ_0 for V is significantly higher than for the compounds I-IV. This difference is in the same direction as the shift associated with intermolecular H-bonding and is clearly associated with the presence of intramolecular H-bonding at infinite dilution.

TABLE I

Compound	δ_0	$(d\delta/dX)_0$	δ_1
I Phenol	2.8	42	~ 5.6
II <i>o</i> -Cresol	3.1	16	5.15
III <i>p</i> -Chlorophenol	3.3	20	~ 5.6
IV <i>m</i> -Chlorophenol	3.1	22	~ 5.6
V <i>o</i> -Chlorophenol	4.1	0.0	4.87
VI Acetic acid in CCl_4	9.3
VII Acetic acid in acetone	1.3	..	9.3

Thirdly, the value of δ_1 for V is below the values of δ_1 for I-IV. This could be attributed to the existence of monomeric V at $X = 1$ or to reduced intermolecular H-bonding. The intermolecular H-bonds could be affected either by induction effects of the substituent or by steric hindrance at the *ortho* position. The curves for I and II indicate

the magnitude of the steric effect and verify its importance. Induction effects must be smaller, possibly negligible, as is inferred from the similarity of the curves for I, III and IV. Since the methyl group and the chlorine atom are similar in size, it is reasonable to expect about the same steric effect for II and V. Hence the δ_1 discrepancy between these two compounds suggests some contribution of monomeric species for compound V even at $X = 1$. Thus all of the qualitative differences between the NMR data for *o*-chlorophenol and those for compounds I-IV are understandable and consistent with the properties deduced from other types of studies.

The phenol derivatives II, III and IV have limiting slopes, $(d\delta/dX)_0$, distinctly lower than the limiting slope of phenol itself. This slope can be related to the equilibrium constant for dimerization by making the assumptions: (a) the data extend to sufficiently low values of X to give the true limiting slope where only monomers and dimers are important; (b) the observed δ is the weighted mean of δ_M and δ_D , assumed characteristic values of δ for pure monomer and pure dimer, with weighting factors giving the fractions of the protons in each of the two states. (If the dimer contains two distinct kinds of protons, δ_D is the mean of the characteristic δ 's of the two.)

$$\delta = \frac{m}{x} \delta_M + \frac{1/2(x-m)}{x} (2\delta_D)$$

or

$$\delta = \delta_D - \frac{m}{x} \Delta_D \quad \Delta_D = \delta_D - \delta_M \quad (1)$$

Defining the association equilibrium constant in terms of mole fractions

$$K = X_D/X_M^2 = \frac{(x-m)(2s+x+m)}{4m^2} \quad (2)$$

X_D = mole fraction dimer
 X_M = mole fraction monomer
 x = total moles phenol, all forms
 m = moles monomer at equilibrium
 s = moles solvent

Then in the limit as X approaches zero, we obtain

$$\delta_0 = \delta_M \quad (3)$$

$$(d\delta/dX)_0 = 2K\Delta_D \quad (4)$$

Assumption (b) has been discussed in ref. 3b and seems to be consistent with the data to which it has been applied. Assumption (a) is subject to some doubt since no measurements could be made below $X = 0.01$ (corresponding to a concentration near 0.1 *M*). The equilibrium constants for polymerization of phenol given by Coggeshall and Saier⁴ permit estimates of dimer and trimer concentrations. At $X = 0.01$, the dimer concentration is 4-5 times the trimer concentration and about 77% of the phenol is present as monomer.

The extrapolated δ_0 gives an estimate of δ_M for each compound but no direct estimate of δ_D is available. The extrapolated δ_1 presumably reflects rather heavily the characteristic δ_P of polymers larger than dimers. Presuming that the H-bond shift, Δ , is monotonically related to the H-bond

strength (this assumption is examined in detail later), we may consider $\Delta_P (= \delta_1 - \delta_0)$ to define an upper limit to $\Delta_D (= \delta_D - \delta_M)$. This is in accord with much infrared spectral data indicating that as H-bonded polymers become larger, the H-bonds become stronger.⁵ The pertinent infrared datum is the change in frequency, $\Delta\nu$, of the O-H stretching mode on forming an H-bond and experience indicates that the $\Delta\nu$ for dimer formation is usually at least half as big as $\Delta\nu$ for polymer formation. Thus Kuhn⁶ finds that $\Delta\nu$ for dimeric phenol is 136 cm.^{-1} and for polymer lists 230 cm.^{-1} . This suggests that a reasonable lower limit to Δ_D is $1/4 \Delta_P$.⁷ We are led to an estimate of Δ between Δ_P and $1/4 \Delta_P$ and select $\Delta_D = 1/2 \Delta_P \pm 1/4 \Delta_P$.

With this value of Δ_D , the data of Table I, and equation 4, we can calculate the estimates of K given in Table II. Using infrared measurements,

TABLE II
EQUILIBRIUM CONSTANTS FOR DIMERIZATION OF PHENOL DERIVATIVES

Compound	K		W (kcal./mole)
Phenol	13 ± 7	0.19	4.35
<i>o</i> -Cresol	8 ± 4	0.35	3.8
<i>p</i> -Chlorophenol	9 ± 4	0.28	3.72
<i>m</i> -Chlorophenol	9 ± 4	0.3 ^a	..
<i>o</i> -Chlorophenol	0

^a Estimated from infrared measurements in this Laboratory.

Coggeshall and Saier⁴ estimate the equilibrium constant for dissociation of phenol dimers to be 0.72 using moles/l. concentration units. This corresponds to an association constant of $K \cong 14.5$ in mole fraction units. The infrared measurements are interpreted assuming the equality of the equilibrium constants for formation of trimers and all higher polymers. Of course the agreement is fortuitous in view of the large uncertainty in our measurements. For further comparison there are listed in Table II the fractions of molecules in the monomeric state, f , and the mean association energy of the H-bonded species present, W , at 1.0 moles/l. in CCl_4 at 25° (corresponding to a mole fraction near 0.1). The quantities f and W , taken from a compilation by Mecke,⁸ show a qualitative

(5) R. F. Badger, *J. Chem. Phys.*, **8**, 288 (1940); also see E. R. Lippincott and R. Schroeder, *ibid.*, **23**, 1099 (1955), and references there cited.

(6) L. P. Kuhn, *J. Am. Chem. Soc.*, **74**, 2494 (1952).

(7) It is almost certain that the phenolic dimer is open (not cyclic) and involves one H-bonded proton and one non-H-bonded proton. We can define Δ_P' and Δ_P'' for these two kinds of protons and then our definition of δ_D in equation 1 indicates that $\Delta_D = 1/2(\Delta_P' + \Delta_P'')$. An assumed linear relationship between Δ_P and the characteristic resonance of a proton gives limits on Δ_D' and indicates that Δ_P'' is near zero.

$$\Delta_P > \Delta_D' > 1/2 \Delta_P \\ \Delta_D'' \cong 0$$

Hence our limits are found to be

$$1/2 \Delta_P > \Delta_D > 1/4 \Delta_P$$

However the upper limit must be raised somewhat because it is probable that Δ_P itself includes some weighting from non-H-bonded protons (end groups in short polymers). We estimate

$$\Delta_D = 1/2 \Delta_P \pm 1/4 \Delta_P$$

(8) R. Mecke, *Disc. Faraday Soc.*, **9**, 161 (1950).

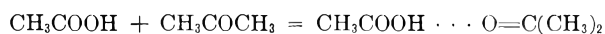
(4) N. D. Coggeshall and E. L. Saier, *J. Am. Chem. Soc.*, **73**, 5414 (1951).

correlation with the equilibrium constants, K , calculated from the NMR data.

Acetic Acid.—Figure 2, presenting the NMR data for acetic acid, suggests at first glance that no H-bond shift occurs on dilution of acetic acid in CCl_4 whereas a large shift occurs on dilution in acetone. Reference to infrared data, however, indicates a more reliable interpretation. Acetic acid in CCl_4 forms only dimeric units and at the lowest concentration studied ($x = 0.02$ or about $0.2 M$) the fraction of molecules present as monomers is very small. Martin⁹ has reported that “. . . carboxylic acids at a concentration in CCl_4 of $M/50$ or higher are almost completely associated.” Consequently the limit of detectability of the proton resonance is at a concentration at which dimers still predominate. In acetone solutions, however, the competition of the solvent as an H-bonding base causes dissociation of the acetic acid dimers at a higher concentration. Of course the extrapolated value δ_0 does not refer to free monomeric acetic acid but rather to the average δ of the equilibrium mixture of monomer, δ_M , and acetic acid-acetone H-bonded complex, δ_x . This limit has been shown to be^{3b}

$$\delta_0 = \frac{1}{1 + K} (K\delta_x + \delta_M) \quad (5)$$

where K refers to the reaction



Correlation with Other Data.—A search for systematics of the proton resonance H-bond shift, Δ , is given in Table III. Also listed are two properties which offer an interesting comparison, the H-bond energy, W , and the infrared frequency change, $\Delta\nu$, of the stretching frequency of the appropriate proton. The Δ of the intramolecular H-bond of V is taken to be the difference between δ_0 of V and the average δ_0 of III and IV. Compounds II-IV are omitted because Δ cannot be estimated without assuming a correlation between Δ and $\Delta\nu$. The value of Δ listed for phenol can be considered to be independently evaluated from the proton resonance provided the equilibrium constant of Coggeshall and Saier is taken as a datum. The uncertainty listed, ± 0.02 , contains no contribution from the uncertainty in K . For acetic acid Δ is estimated from the resonance measurements in acetone solution. The extrapolated value δ_1 in either acetone or CCl_4 gives a reliable estimate of the characteristic reso-

nance of dimer; $\delta_D = 9.3$. The extrapolated value δ_0 lies between δ_x and δ_M . From the measured values of $(\delta_x - \delta_M)$ and K for the chloroform-acetone system (1.0 and 1.8, respectively), reasonable guesses for the acetic acid-acetone system can be made. The required quantities are taken to be $\delta_x - \delta_M = 1.5$ and $K = 3$. Now with equation 5 we calculate $\delta_M = -0.1$, $\delta_x = 1.4$, and $\Delta_D = \delta_D - \delta_M \cong 9$.

TABLE III

Compound	W (kcal./mole)	Δ	$\Delta\nu$ (cm. ⁻¹)
<i>o</i> -Chlorophenol (intramolec.)	1.42 ¹⁰	0.9 \pm 0.2	63 ¹⁰ ; 55 ¹¹
Chloroform-acetone	2.5 ^{3b} 4.0 ¹²	1.0 \pm 0.2 ^{3b}	0 ¹³
Chloroform-triethylamine	4.0 ^{3b}	1.5 \pm 0.2 ^{3b}	\sim 120 ¹³
Phenol	4.35 ⁸	1.5 \pm 0.2	136 ⁶
Acetic acid	6.9 ¹⁵	9 \pm 2	410 ¹⁴

The data in Table III are hardly sufficient to permit deduction of a systematic relationship between Δ and either W or $\Delta\nu$. Still the general qualitative agreement encourages further examination of this type of comparison.

Conclusion

The proton resonance behavior of each of the substances studied can be correlated qualitatively with the known H-bonding properties. Thus NMR measurements will aid in the detection and study of hydrogen bonding. However, it is strikingly clear from Figs. 1 and 2 that an isolated measurement of the proton resonance of a compound which forms H-bonds contains little information. In analogy to the infrared study of H-bonding substances, close attention must be given to the variables which alter the degree of H-bond association and hence the spectrum. The more important variables are temperature, solvent, and concentration. Examination of the proton resonance over the entire concentration range experimentally accessible is essential to a meaningful interpretation.

(10) M. M. Davies, *Trans. Faraday Soc.*, **34**, 1427 (1938).

(11) G. Rossmly, W. Lüttke and R. Mecke, *J. Chem. Phys.*, **21**, 1609 (1953).

(12) E. A. Moelwyn-Hughes and A. Sherman, *J. Chem. Soc.*, 101 (1936).

(13) C. M. Huggins and G. C. Pimentel, *J. Chem. Phys.*, **23**, 896 (1955). The value of $\Delta\nu$ for CDCl_3 in triethylamine, 84 cm.⁻¹, has been used as a basis for the estimate given above, 120 cm.⁻¹.

(14) R. Herman and R. Hofstadter, *ibid.*, **7**, 460 (1939).

(15) R. E. Lundin, F. E. Harris and L. K. Nash, *J. Am. Chem. Soc.*, **74**, 4654 (1952).

(9) A. E. Martin, *Nature*, **166**, 474 (1950).

ISOPROPYL RADICAL REACTIONS. I. PHOTOLYSIS OF DIISOPROPYL KETONE

BY C. A. HELLER AND ALVIN S. GORDON

Chemistry Division, U. S. Naval Ordnance Test Station, China Lake, Calif.

Received March 30, 1956

Diisopropyl ketone has been photolyzed using a medium pressure mercury lamp over the temperature range 100–400°. Pressure has been varied from 40–100 mm. and light intensity varied about tenfold. The kinetics are explained by a primary break of the ketone to give isopropyl radicals. These radicals can disproportionate, combine, or abstract hydrogen from the parent ketone: $\text{iso-C}_3\text{H}_7 + \text{iso-C}_3\text{H}_7 \longrightarrow \text{C}_3\text{H}_8 + \text{C}_3\text{H}_6$ (1); $\text{iso-C}_3\text{H}_7 + \text{iso-C}_3\text{H}_7 \longrightarrow \text{C}_6\text{H}_{14}$ (2); $\text{iso-C}_3\text{H}_7 + \text{RH} \longrightarrow \text{C}_3\text{H}_8 + \text{R}$ (3). The activation energy difference between disproportionation (reaction 1) and combination (reaction 2) is less than one kcal. per mole and the ratio of rate constants $k_1/k_2 = 0.6$ at 200°. The activation energy difference between abstraction and combination $E_3 - 1/2E_2 = 8.5 \pm 0.1$ kcal. per mole (error as standard deviation). Above 200° the ketonyl radicals decompose measurably into C_3H_6 , CO and isopropyl giving a chain reaction. At 350° and above the isopropyl radicals decompose measurably into C_3H_6 and H atoms.

Introduction

Diisopropyl ketone was chosen as a convenient source of isopropyl radicals. The primary step of the photolysis has been previously shown to be a break into radicals with no hydrogen shift such as occurs when a hydrogen on a carbon gamma to the carbonyl group is present.^{1–3} The CO quantum yield is unity from 50 to 150° and over a wide range of wave lengths.³

Isopropyl radicals generated from isobutyraldehyde,⁴ azoisopropane⁵ and diisopropylmercury⁶ have been studied previously. The thermal stability of diisopropyl ketone recommended it for work over a wide temperature range.

Experimental

The diisopropyl ketone (The Matheson Company, Inc., Pract. Grade) was stored over drierite and then distilled through a 30-plate column under 700 mm. of nitrogen. A small portion coming off at 122° was retained. This was vacuum distilled into a bulb at –78° and subjected to evacuation at this temperature. A small methanol impurity was removed by evacuation at –78°. This sample was stored in the dark at –78° since decomposition was shown to occur at room temperature in diffuse sunlight.

The original light source was a Hanovia 2537 lamp, but this produced slight photolysis of the propylene. Therefore, a Hanovia quartz Alpine sun burner, S-100, was used in conjunction with a 2 mm. thick Corning 7910 filter. Light intensity was varied by varying the distance from the lamp to reaction vessel. The cylindrical reaction vessel was 56 mm. i.d. and 66 mm. long with 2.75 mm. thick windows. The reaction vessel was set into an aluminum block furnace with double quartz windows so that the temperature gradient along the vessel was less than 1/2°. At low temperatures and high light intensity the oven changed temperature by a maximum of 1.5° during a run. Temperatures were measured with a chromel–alumel thermocouple.

The vessel was evacuated by an oil diffusion pump. Gold leaf traps further protected the reaction vessel from mercury vapor. Pressure was measured by a spoon type Bourdon gage which was operated against a mercury manometer and measured by a Gaertner micrometer telescope. The glass tubing to the oven was electrically heated by nichrome ribbon.

The products of reaction were Toepler pumped through two Ward-Leroy stills into a sample flask. Four thermal cuts were made with the two stills at –155 and –175°, –78 and –130°, 0 and –45°, and 0 and –20°, respectively.

Gases non-condensable at –175° were measured by a McLeod gage before they were pumped into a sample flask. The volumes of all the fractions were similarly measured, and then analyzed by mass spectrometer (Consolidated 21-103). Each fraction contained contaminants from the others and analysis of each fraction was necessary.¹ Surprisingly, hydrogen was present in the second fraction and occasionally in the third fraction.

The first fraction included H_2 , CO, CH_4 and C_2 hydrocarbons. The second, C_3 and C_4 hydrocarbons, plus small amounts of C_2 and H_2 . The third fraction contained the parent ketone, C_6 , C_5 and C_3 hydrocarbons and isobutyraldehyde. Mass spectra of the C_6 indicated that it was 2,3-dimethylbutane (diisopropyl) to within 5% for all runs. It was specially checked for 2-methylpentane.

Attempts were made to identify peaks due to large molecules other than diisopropyl ketone. A small peak at 156 was found in one case and is attributed to propyl hexyl ketone. A peak at 112 from high temperature runs is probably propyl propenyl ketone, and one at 100, while doubtful, due to mercury peaks interference, may be propyl ethyl ketone. All these higher boiling products were dissolved in the large excess of the parent ketone and even qualitative separation for identification was difficult.

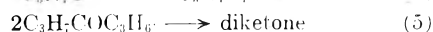
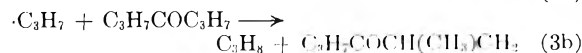
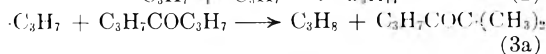
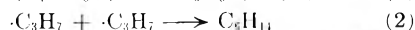
Products.—The following major products were measured: CO, C_3H_8 , C_3H_6 and C_6H_{14} . In addition, H_2 , CH_4 , C_2H_4 and C_2H_6 were present in easily measured quantities in the high temperature runs, and C_2H_2 , ethyl propyl ketone, propyl propenyl ketone, butanes and butenes were present in small quantities in the low temperature runs. A peak at 72 which occurred at all temperatures was assigned to isobutyraldehyde, although it might have been due to pentanes.

Primary Reaction.—The only primary photochemical reaction which occurs in measurable amounts is the split into radicals.



The isobutyryl radical appears to be stable enough to form trace quantities of isobutyraldehyde, but most of it decomposes into CO and isopropyl radicals.

Secondary Reactions.—The following secondary reactions account for most of the products found in the analysis



(1) A. J. C. Nicholson, *Trans. Faraday Soc.*, **50**, 1067 (1954).

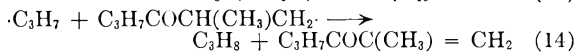
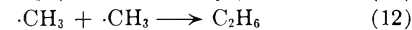
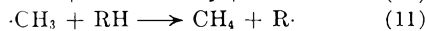
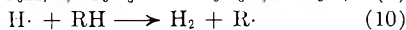
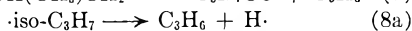
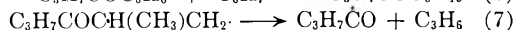
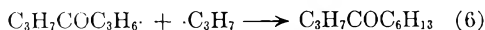
(2) C. R. Masson, *J. Am. Chem. Soc.*, **74**, 4731 (1952).

(3) S. G. Whiteway and C. R. Masson, *ibid.*, **77**, 1508 (1955).

(4) F. E. Blacet and J. G. Calvert, *ibid.*, **73**, 661 (1951).

(5) R. W. Durham and E. W. R. Steacie, *Can. J. Chem.*, **31**, 377 (1953).

(6) H. T. J. Chilton and B. G. Gowenlock, *Trans. Faraday Soc.*, **49**, 1451 (1953).



Low Temperature Mechanism.—The most important reactions at 100° are combination and disproportionation. The ratio of the rate constants for these two reactions is given by

$$k_1/k_2 = \text{C}_3\text{H}_6/\text{C}_6\text{H}_{14} \quad (\text{I})$$

As can be seen in Fig. 1, these reactions have almost equal activation energies. If the activation energy of the combination reaction $E_2 = 0$ then $E_1 = 900$ cal./mole.

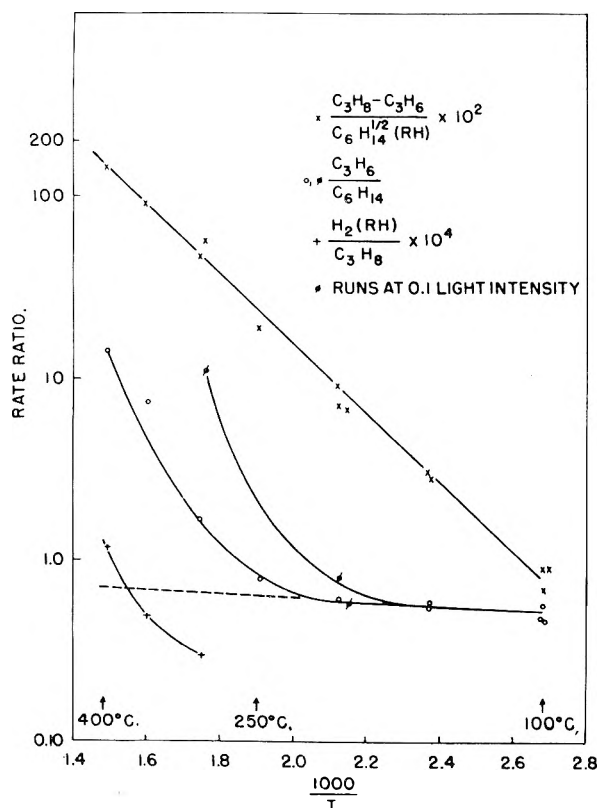


Fig. 1.—Arrhenius plot of the ratio of rate constants for some of the products of the photolysis of diisopropyl ketone.

The k_1/k_2 ratios found in this work disagree with those found using azoisopropane.⁵ In the azoisopropane work the ratio was 0.5 at 30° and 0.37 at 121°. Thus there are unexplained differences in both the values and in the slope of the Arrhenius plot. The values of the ratios from isobutyraldehyde⁴ are scattered and cover the sets of values of both of the above data. In the pyrolysis of diisopropyl mercury⁷ between 228.5 and 441° the ratios were scattered between 0.2 and 0.6 and poor preci-

(7) S. Bywater and E. W. R. Steacie, *J. Chem. Phys.*, **19**, 319 (1951).

sion permitted no measurement of activation energy difference.

The abstraction reaction, which is first order in isopropyl radical concentration can be compared with the combination which is second order in isopropyl radical concentration by the ratio of rate constants

$$k_3/k_2^{1/2} = (\text{C}_3\text{H}_8 - \text{C}_3\text{H}_6)/\text{C}_6\text{H}_{14}^{1/2}[\text{RH}] \quad (\text{II})$$

Lowering the light intensity favors the first-order reaction and permits a more precise measure of the propane formed by abstraction.

The present data do not tell which hydrogen is abstracted from the parent ketone. If reactions 3a and 3b have different activation energies the observed activation energy E_3 , should increase with temperature. To check this two least squares calculations were made: one from 100 to 251° and one from 192 to 398°. The former gave $E_3 = 8.1 \pm$ kcal./mole, and the latter 9.1 ± 0.2 kcal./mole. These two values indicate a change in the relative importance of 3a and 3b but are not the actual values of either 3a or 3b.

It is of interest to calculate the ratio of steric factors of abstraction and combination to see how this compares with that for methyl and ethyl radicals. Using the over-all value of 8.5 kcal./mole gave $P_{33}\sigma^2/P_2^{1/2}\sigma_2$ as 0.78×10^{-10} at 250°. Collision diameters were chosen as $\sigma_3 = 3.0$ Å. and $\sigma_2 = 2.1$ Å. which give $P_3/P_2^{1/2} = 1.8 \times 10^{-3}$. This is similar to the values found for other radicals.⁸

The ketonyl radicals which are formed by the abstraction of hydrogen from the isopropyl ketone appear to be stable at low temperatures. The quantum yield of one for CO yield³ is one indication of stability. Presumably these ketonyl radicals disappear by combination reactions such as reactions 5 and 6.

The production of hydrogen and the lighter hydrocarbons in small amounts at low temperatures is not explained by the mechanism. It is possible that they are due to heterogeneous decomposition of the radicals.

The 72 peak found in trace amounts at low temperatures may be due to isobutyraldehyde which is formed from isobutyryl radicals abstracting hydrogen before they decompose *via* reaction 4.

High Temperature Mechanism.—As the temperature is raised above 100° other reactions become more important although there is always measurable contribution from the combination and disproportionation.

Above 200° there is a rapid increase in the propylene/dimethylbutane ratio and a parallel increase in the CO rate at constant light intensity. This is explained by the decomposition of the ketonyl radical (reaction 7) which gives both propylene and CO as products and which gives an isopropyl radical as a chain carrier. The propylene/dimethylbutane ratio increases at lower light intensity since the dimethylbutane is formed by a second-order reaction while the ketonyl formation and decomposition are both first order in radical concentration.

(8) E. W. R. Steacie, "Atom and Free Radical Reactions," Second Ed., ACS Monograph No. 125, Reinhold Publ. Corp., New York, N. Y., 1954.

SUMMARY OF RUNS—ISOPROPYL KETONE DECOMPOSITION

Run	47	45	49	54	57	58	55	56	63	59	60	65	68 ^a	66	64
Relative light intensity	1.0	1.0	0.1	1.0	0.1	0.1	1.0	0.1	1.0	0.1	1.0	1.0	1.0	1.0	Thermal
T (°C.)	100	100	100	150	150	192	197.5	197.5	251	295	299	353	393	398	401
P ₁ (mm.)	38.4	90.3	92.1	99.3	91.5	41.4	90.9	93.3	89.5	86.4	92.2	93.8	327.4	99.3	88.0
Ket. conc. (m./l.) × 10 ²	0.380	0.388	0.396	0.376	0.347	0.143	0.310	0.318	0.274	0.24	0.260	0.240	0.222	0.237	0.21
t (sec.)	600	600	6000	780	6000	9000	720	6000	600	6000	600	600	420	425	2100
% Decomposition	7.9	7.7	8.0	8.9	7.0	23	8.4	7.4	7.4	17.1	10.1	16.7	12	17	1.64
						Rates (moles l. ⁻¹ sec. ⁻¹) × 10 ⁶									
2,3-Dimethylbutane	37.9	37.6	2.88	23.3	1.80	0.801	17.1	1.028	10.22	0.2056	8.84	3.54		5.71	
Isobutyraldehyde	0.19				1.01	0.018	0.1	0.007	0.006		0.13	0.91		0.15	
Isobutane	0.06		0.012				0.025			0.10					
Butenes ^b							0.05	0.004	0.281	0.073	1.35	1.40		4.06	
Propane	20.10	19.59	2.260	18.56	2.457	1.320	22.01	3.165	24.65	6.38	42.08	43.45		80.01	
Propene	18.49	17.39	1.640	13.06	1.051	0.466	10.43	0.835	8.078	2.33	15.08	26.32		81.04	
Ethane	0.18	0.18		0.32	0.009	0.006	0.07	0.012	0.076	0.091	0.47	0.47		0.50	0.028
Ethene	0.04			0.070	0.010	0.006	0.015	0.012	0.126	0.11	0.73	1.55		6.70	0.182
Carbon monoxide	50.2	50.1	5.25	43.1	4.07	1.96	36.1	3.42	33.70	4.77	43.6	46.7		94.7	1.64
C ₄ + 1/2 C ₃ + 1/2 C ₂ + 1/2 CH ₄ ^c	57.2	56.1	4.83	39.1	3.55	1.69	33.3	3.03	26.5	4.56	37.4	39.3		91.0	
Methane	0.09	0.09	0.001	0.045				0.03		0.06	0.25	1.58		8.03	0.196
Hydrogen	0.16	0.70	0.013	0.16	0.037	0.027	0.27	0.04		0.04	0.43	0.88		3.73	0.168
						Ratios of rates									
I. ΔC ₃ /C ₄ ^{1/2} [RH] × 10 ^{2d}	0.688	0.924	0.922	3.03	3.01	6.67	9.03	7.23	18.9	56.4 ^e	46.4 ^e	90.5 ^e		141 ^g	
II. C ₂ H ₄ /C ₄ H ₁₀	0.49	0.46	0.57	0.56	0.58	0.58	0.61	0.81	0.79	11.3	1.71	7.44		14.2	

^a Propane added, 0.00567 mole l.⁻¹ ^b Calculated as isobutene. ^c Rate of disappearance of ketone calculated on basis of hydrocarbon appearance. ^d ΔC₃ = C₂H₆-C₃H₆; i.e., propane from abstraction. ^e ΔC₃ from calculated C₃H₆, i.e., C₃H₆ ≈ 0.6 C₆H₁₄.

Since there are two kinds of ketonyl radicals possible it would be of interest to see whether they both can decompose *via* reaction 7. For the radical formed in reaction 3a to give propylene there would be required a hydrogen shift during the decomposition, while the ketonyl from reaction 3b decomposes by breaking one carbon-carbon bond with simultaneous formation of a double bond.

The propylene formed by ketonyl decomposition complicates equation II since the quantity to be subtracted from the total propane in equation II is the propane formed by the disproportionation reaction (1). However, the disproportionation propylene can be fairly accurately measured by extrapolating the low temperature range of propylene/dimethylbutane ratios to high temperatures. As may be noted in Fig. 1, the disproportionation propane is only a small proportion of the total propane at high temperature. When the propane is corrected, the Arrhenius plot of $k_3/k_2^{1/2}$ is a straight line over the temperature range studied.

The isopropyl radical apparently is quite stable up to 299° but begins to decompose measurably before 353°. The production of hydrogen gas is presumably *via* reactions 8a and 10. On this basis one can compare reactions 8a and 3a by the following relation

$$k_{8a}/k_{3a} = H_2[\text{DIK}]/C_3H_8 \quad (\text{III})$$

This does not permit an accurate measurement of the activation energy difference as can be seen in Fig. 1.

The data indicate that the rate of formation of ethylene and methane are about equal, and that the rate increases with temperature and with intensity of radiation. It is possible that ethylene and a methyl radical results from the decomposition of an isopropyl radical, since McNesby, *et al.*,⁹ have shown that hydrogen atom transfer along the carbon skeleton can occur at high temperatures. Another possible path is reaction 9 followed by reaction 8b. However, it is difficult to see why the relatively low concentration of product propane should be efficiently converted to *n*-propyl radicals when a much easier hydrogen source is available to the isopropyl radicals from the parent ketone. When propane was added to the ketone prior to reaction (run 68) the rate of formation of hydrogen dropped, while rate of formation of methane and ethylene were almost the same as when no propane was present at the start of the reaction.

There is little possibility that the methane and ethylene could result from an impurity which contains *n*-propyl groups. High resolution mass spectrometer analysis of the diisopropyl ketone and of the α,α'-diisopropyl-d₂ ketone showed that not over 0.6% of the total propyl content was *n*-propyl.

The four-carbon hydrocarbons may be formed by reaction 13 and by addition of methyl to propylene. The 72 peak at high temperature may be due to pentanes formed by addition of propyl to ethylene.

(9) J. R. McNesby and A. S. Gordon, *J. Chem. Phys.*, in press.

Acknowledgment.—The authors wish to acknowledge the mass spectrometer analyses of A. V.

Jensen and the help of S. R. Smith with the interpretation of mass spectrometer records.

THE HEATS OF FORMATION OF TETRAFLUOROETHYLENE, TETRAFLUOROMETHANE AND 1,1-DIFLUOROETHYLENE

BY CONSTANTINE A. NEUGEBAUER AND JOHN L. MARGRAVE

Contribution from the Department of Chemistry of the University of Wisconsin, Madison, Wisconsin

Received April 18, 1956

The standard heats of formation of gaseous tetrafluoroethylene and tetrafluoromethane have been determined by the hydrogenation and decomposition of tetrafluoroethylene in a bomb calorimeter. They are -151.7 ± 1.1 and -217.1 ± 1.2 kcal./mole, respectively. The heat of formation of gaseous 1,1-difluoroethylene was found to be -77.5 ± 0.8 kcal./mole from combustion experiments.

Introduction

The heat of formation of CF_4 by the direct interaction of the elements was reported by v. Wartenberg¹ to be -161 kcal. Later, v. Wartenberg² studied the displacement reaction between CF_4 and K to give KF and carbon, and found -231 kcal. for the heat of formation of CF_4 .

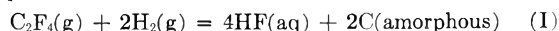
Kirkbride and Davidson,³ using v. Wartenberg's later technique, obtained a value of -218 kcal. for the heat of formation of CF_4 . Jessup, McCosky and Nelson⁴ report -220.4 kcal. for the heat of formation of CF_4 , using the fluorination of methane to give CF_4 and gaseous HF. Later, Scott, Good and Waddington,⁵ by a method involving the heat of combustion of Teflon polymer in the presence of hydrocarbon oils, obtained -218.3 kcal. for CF_4 . Finally, Duus⁶ reports -212.7 kcal. for CF_4 , using the hydrogenation of C_2F_4 to give carbon and gaseous HF, and the decomposition reaction of C_2F_4 to give C and CF_4 . The final state of the carbon was assumed to be graphite in both cases. Corrections for the final state of the HF were estimated. Furthermore, no corrections were made for methane produced in the hydrogenation.

By the method described above, Duus also obtained the heat of formation of gaseous C_2F_4 as -151.3 kcal. On the other hand, both v. Wartenberg,⁷ and Kirkbride and Davidson,⁸ report -162 kcal. for the heat of formation of C_2F_4 .

In general, the literature values for the heats of formation of both compounds show variations and uncertainties large enough to warrant new determinations.

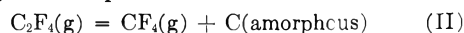
The reactions used to determine the heat of formation of C_2F_4 and CF_4 are similar to those used by Duus. When gaseous C_2F_4 reacts with hydrogen in a calorimetric bomb that initially contains

water, the net reaction may be represented by the equation



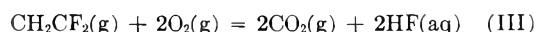
From this reaction, the heat of formation of C_2F_4 can be calculated.

Tetrafluoroethylene decomposes when ignited according to the equation



This reaction, when coupled with the one above, makes possible the determination of the heat of formation of CF_4 . The heat of formation of the amorphous carbon formed in the reactions can be determined by separate combustion experiments.

The heat of formation of 1,1-difluoroethylene has been determined by measuring the heat of the reaction



Experimental

Apparatus and Method.—A conventional isothermal calorimeter of the type described by Dickinson⁹ was employed. The temperature of the water jacket was kept constant at $24.80 \pm 0.002^\circ$ with a vibrating mercury regulator in connection with an electronic relay. The calorimeter cup, of 5-l. capacity, was held in place by three Lucite wedges placed along the upper rim of the calorimeter cover and held firm by the lid of the water jacket. The calorimeter stirrer was driven by a small electric motor at 600 r.p.m. A double valve Parr illium bomb having a volume of 360 ml. was used in all experiments.

The temperature rise in the calorimeter was measured by means of a platinum resistance thermometer, calibrated by the National Bureau of Standards, in connection with a G-2 Mueller resistance bridge, also previously calibrated, and a high sensitivity galvanometer, all supplied by the Leeds and Northrup Co. A change of 0.0001 ohm (0.001°) in the resistance of the thermometer caused a 3 mm. shift in the reflection from the galvanometer mirror on the scale. The galvanometer was used as a null-point instrument, the time at which a predetermined resistance was reached being read from an electric timer. The resistance values were converted to temperature readings by using the method of Werner and Frazer.¹⁰ The corrected temperature rise (in degrees) was calculated by the Dickinson¹¹ method, assuming Newton's law of cooling to hold. The initial temperature was so chosen that the final temperature was about 0.05° above jacket temperature. For convenience in obtaining the appropriate initial tempera-

(1) H. v. Wartenberg and R. Schütte, *Z. anorg. Chem.*, **211**, 222 (1933).

(2) H. v. Wartenberg and G. Riteris, *ibid.*, **268**, 356 (1949).

(3) F. W. Kirkbride and F. G. Davidson, *Nature*, **174**, 79 (1954).

(4) R. S. Jessup, R. E. McCosky and R. A. Nelson, *J. Am. Chem. Soc.*, **77**, 244 (1955).

(5) D. W. Scott, W. D. Good, and Guy Waddington, *J. Am. Chem. Soc.*, *ibid.*, **77**, 245 (1955).

(6) H. C. Duus, *Ind. Eng. Chem.*, **47**, 1445 (1955).

(7) H. v. Wartenberg, *Z. anorg. Chem.*, **278**, 326 (1955).

(8) F. W. Kirkbride and F. G. Davidson, ref. 3.

(9) H. C. Dickinson, *Bull. Natl. Bur. Standards*, **11**, 230 (1914).

(10) F. D. Werner and A. C. Frazer, *Rev. Sci. Instr.*, **23**, 163 (1952).

(11) H. C. Dickinson, ref. 9.

ture, the calorimeter was equipped with a 600-watt heater.

The mass of the calorimeter water was determined to 0.05 g. on an analytical balance of 4-kg. capacity and a sensitivity of 11 mg./div. at a 4-kg. load. In calibration experiments the mass of the benzoic acid samples was determined to 0.01 mg. on a semi-micro analytical balance.

Commercial tank oxygen and hydrogen was used in the combustion and hydrogenation experiments, respectively, and the bomb was flushed 5 times before final filling by admitting the gas to 6 atm. and then reducing to atmospheric pressure.

Calibration.—Benzoic acid, NBS standard sample 39g., having an isothermal heat of combustion at 25° of 26.4338 abs. kj. per g. mass under standard bomb conditions,¹² was used for determining the energy equivalent of the calorimeter. In the experiments 2-g. samples were used in order to achieve about the same temperature rise as is attained in later experiments. The oxygen pressure used in all calibration experiments was 30 atm. Nitric acid, formed by small amounts of nitrogen in the oxygen, was determined by adding 1 ml. of water to the bomb before combustion and titrating the washings with dilute sodium hydroxide solution, using methyl orange as indicator. The value for the heat of formation of nitric acid was taken as 59 kj./mole. The correction from this source never exceeded 12 j. To facilitate ignition, 10 cm. of iron fuse wire, supplied by the Parr Co., were used. Corrections were made for the quantity of wire burned, taking the heat of combustion to be 6.63 kj./g. of wire. This correction was of the order of 70 j.

Twelve combustions of benzoic acid yielded a value of 4695.00 cal./deg. for the energy equivalent of the calorimeter at 25°. The average deviation from the mean for these experiments was 0.066% and the maximum deviation was 0.14%.

Uncertainties and Precision Errors.—The uncertainties in the reported values of the heats of formation were arrived at by taking the square root of the sum of the squares of the uncertainties of the heats of all the reactions which were used to obtain the heat of formation in question, including the uncertainty in the energy equivalent of the calorimeter.

The uncertainty quoted for the heat of a particular reaction is the precision error (twice the standard deviation from the mean), as recommended by Rossini,¹³ and is given by the formula $2\sqrt{\Sigma\Delta^2/n(n-1)}$, where Δ denotes the deviation from the mean, and n the number of trials.

The Hydrogenation of Tetrafluoroethylene.—Compressed tetrafluoroethylene was available in tanks. Most impurities were present to an extent of less than 0.05 mole %, oxygen was present to the extent of 10 p.p.m., and a polymerization inhibitor to the extent of approx. 2900 p.p.m.

The bomb, with 100.0 ml. of water added, was charged with 7 to 8 atm. of C_2F_4 at room temperature. An additional 25 or 36 atm. of hydrogen were then added. This charge was ignited with a 21 mm. long and 1 mm. thick pencil lead carbon rod, wedged between the two electrodes, and brought to incandescence by a current of 6–7 amp. at 9–12 volts. The ignition energy was obtained by observing an ammeter, voltmeter and chronometer simultaneously. The carbon rod can be recovered after the reaction. The HF solution formed in the reaction was about 3 molar.

The analysis for the substances formed in the reaction was a titration of the HF solution with standard 0.1 *N* base to the phenolphthalein end-point. The solution was separated from the carbon by decanting the suspension through a glasswool filter. The residual carbon was washed 3 times with boiling water to liberate any HF absorbed in it and the solution then diluted to a final volume of 2000 ml., from which 100-ml. aliquots were used for titration.

The base was standardized against HCl solution, which in turn was standardized by silver chloride precipitation. In addition, the base was directly standardized against Bureau of Standards benzoic acid sample 39g.

In four of the runs, the product gases were subjected to mass spectrometric analysis. From this the quantity of methane produced in the reaction was calculated and these served as a basis for estimates in those runs where such an analysis was omitted.

The Decomposition of Tetrafluoroethylene.—The tetrafluoroethylene used in the decomposition reactions was from

the same tank as that for the hydrogenations. The bomb was charged with C_2F_4 to a pressure of 9 to 18 atm. The reaction was again initiated with an electrically heated carbon rod. In one of the runs (trial 4), a platinum wire coil, electrically heated to its melting point, was used instead.

To determine the quantity of reactant taking part in the reaction, the carbon produced was quantitatively recovered and determined by chromic acid oxidation to carbon dioxide, which was then absorbed in ascarite towers, according to Scott's¹¹ analytical method. Just weighing the carbon can be shown to give results about 4% high.

Comparison of the mass spectra of tank tetrafluoroethylene and the gaseous decomposition products shows that only CF_4 was produced, since small, miscellaneous peaks appear in both spectra.

There was a pressure increase during the reaction, amounting to about 6 to 8%, probably due to the greater ideality of CF_4 as compared to C_2F_4 .

The Combustion of the Carbon Produced in Reactions I and II.—The heat of combustion of the carbon formed in the two reactions was determined separately. The carbon from the decomposition reactions was procured in blank runs, since the carbon produced in the heat-measurement reactions was used up in the analysis.

The combustion procedure was exactly analogous to the benzoic acid combustions. Before use the carbon was freed from any combustible gases absorbed on it by simultaneously heating it to 100° in a steam-bath and subjecting it to a vacuum for three hours. The carbon, which was quite voluminous when first formed, was then compressed in a conventional pellet press. About one gram was used for each run. Since the weighing of carbon has been shown to be inaccurate, the extent of the reaction was determined by absorbing the CO_2 produced in ascarite towers, which were weighed before and after absorption. Because the Parr bomb leaks at low pressure, the bomb was only bled down to 3 atm., then filled with high purity helium to 15 atm. and bled again. This was repeated seven times.

This procedure was shown to be suitable by first burning samples of spectroscopic graphite powder, which gave a heat of combustion only 0.1% higher than the value of -94.05 kcal./mole, which is the standard heat of formation of CO_2 at 25°.

The Combustion of 1,1-Difluoroethylene.—This gas was supplied to us in tank form by the General Chemical Division of the Allied Chemical and Dye Corp. Mass spectral analysis showed that the only impurities present were O_2 , H_2O and CO_2 . The CO_2 was determined by ascarite absorption and was found to amount to 1.7 mole %.

First 50.0 ml. of water was added to the bomb, which was then filled with 2.5 atm. of CH_2CF_2 . If more of the ethylene is used, the reaction becomes so violent that the bomb might be overstrained. The pressure of O_2 used was 12.5 atm. This charge was ignited with a hot platinum wire; only about 5 cal. were needed for the ignition.

To determine the amount of the ethylene which was oxidized, the product gases were analyzed for CO_2 by absorption on ascarite, as described previously and the correction for the initial CO_2 content of the gas applied. The residual HF solution, about 1 molar, was diluted to 1000 ml., and 50-ml. aliquots were titrated with standard 0.1 *N* base to the phenolphthalein end-point. Mass spectral analysis of the product gases showed virtually complete combustion.

In two cases, when the initial pressure of CH_2CF_2 was too high, a brown precipitate was produced in the reaction. The heat effect was then found to be about 3 kcal. higher than normally. This may have been due to partial polymerization of the ethylene, and these runs were discarded.

When the reaction was run without water being present in the bomb and the bomb opened immediately after the reaction, water was one of the products. This indicates that in the oxidation of CH_2CF_2 one probably obtains some COF_2 initially, which then hydrolyzes according to the equation



to give products in the same thermodynamic state as postulated in reaction III.

(12) NBS certificate accompanying standard sample 39g.

(13) F. D. Rossini, *Chem. Revs.*, **18**, 223 (1936).

(14) W. W. Scott, "Standard Methods of Chemical Analysis," D. Van Nostrand Co., New York, N. Y., 1938, p. 226.

TABLE I
 THE HEAT OF HYDROGENATION OF C₂F₄

Trial	Initial pressure of H ₂ , atm.	1/4 moles HF	Moles CH ₄ ^a	-q _{tot} , cal.	-q _{ign} , cal.	-q _{CH₄} , cal.	-ΔU _B , kcal./mole	q _{cor.} , kcal./mole	-ΔU _c ^o (298°K.), kcal./mole
1	25	0.07875	(0.00253)	11,448	92	44	143.64	0.01	143.63
2	25	.08059	0.00252	11,872	63	44	145.98	.01	145.97
3	25	.07974	(.00253)	11,636	50	44	144.74	.01	144.73
4	25	.08190	(.00253)	12,223	49	44	148.11	.01	148.10
5	36	.06834	.0107	10,184	116	185	144.62	.05	144.57
6	36	.07251	(.0106)	10,860	23	185	146.90	.05	146.85
7	36	.07013	.0104	10,523	33	185	146.94	.05	146.89
8	25	.07935	.00254	11,750	47	44	146.93	.01	146.92

^a () indicate estimates.

Av. 146.0 ± 1.1

 TABLE II
 THE HEAT OF DECOMPOSITION OF C₂F₄

Trial	Initial pressure of C ₂ F ₄ , atm.	Moles of C	-q _{tot} , cal.	-q _{ign} , cal.	-ΔU _B , kcal./mole	-q _{cor.} , kcal./mole	-ΔU _c ^o , kcal./mole
1	10	0.1622	10,395	33	63.88	0.04	63.92
2	9	.1216	8,010	286	63.52	.03	63.55
3	9	.1190	7,680	182	63.01	.03	63.04
4	18	.2699	17,394	200	63.71	.06	63.77

Av. 63.57 ± 0.42

 TABLE III
 THE HEAT OF COMBUSTION OF THE CARBON FORMED IN HYDROGENATION AND DECOMPOSITION OF C₂F₄

Trial	Moles CO ₂	-q _{tot} , cal.	$\frac{-q_{ign} + q_{HNO_3} + q_{fuse}}{wire}$, cal.	-ΔU _B , kcal./mole	-q _{cor.} , kcal./mole	-ΔU _c ^o , kcal./mole
(A) Carbon from reaction I						
1	0.060871	5,839	29	95.45	0.04	95.49
2	.083638	8,019	23	95.60	.04	95.64
Av. 95.56 ± 0.16						
(B) Carbon from reaction II						
1	0.08625	8,303	21	96.02	0.04	96.06
2	.09407	9,043	27	95.85	.04	95.89
3	.12090	11,594	22	95.71	.04	95.75
Av. 95.90 ± 0.18						

 TABLE IV
 THE HEAT OF COMBUSTION OF CH₂CF₂

Trial	1/2 moles HF	1/2 moles CO ₂	-q _{tot} , cal.	-q _{ign} , cal.	-ΔU _B , kcal./mole	-q _{cor.} , kcal./mole	-ΔU _c ^o , kcal./mole
1	0.02632	0.02643	6885.8	1.4	260.97	0.03	261.00
2	.02734	.02739	7165.7	5.7	261.60	.03	261.63
3	.02668	.02578	6898.2	7.9	262.68	.03	262.71
4	.02944	.02912	7627.7	5.0	260.33	.03	260.36
5	.02787	.02745	7251.5	2.2	262.09	.03	262.12

Av. 261.56 ± 0.82

Results and Calculations

All weights were corrected to *in vacuo*. The data refer to a standard temperature of 25°. The atomic weights used were as reported in *J. Am. Chem. Soc.*, 1953. The energy unit is the calorie, defined as equal to 4.1840 abs. joules.

The total heat evolved, q_{tot} , was reduced to the heat of reaction under the conditions of the bomb process, ΔU_B , by making the appropriate corrections for the formation of methane and nitric acid, the burning of fuse wire, and the ignition energy. This value of ΔU_B was then further reduced to ΔU_c^o , the corrected decrease in internal energy with each of the reactants and products in its thermo-

dynamic standard state, by adding q_{cor} . The corrections for hydrogen gas under the mean pressure of the experiment were obtained from the variation of the compressibility coefficient with temperature at constant pressure.¹⁵ Tetrafluoroethylene and 1,1-difluoroethylene were assumed to behave in a manner analogous to carbon dioxide, due to a similarity in critical constants, and were corrected to unit fugacity using the relation $-\Delta U_{CO_2} = 7.0$ cal./mole/atm. Tetrafluoromethane was assumed to behave ideally. Correction to unit fugacity in the combustion of carbon was done in

(15) The NBS-NACA Tables of Thermal Properties of Gases, Table 7.20, Washington, D. C., 1949.

accordance with the Washburn¹⁶ procedure. No corrections were made for the heat of solution of the gas phase in water and acid, but because of the limited solubility of the gases in question these corrections are probably within the experimental error.

Table I gives the results for the hydrogenation experiments on C_2F_4 , according to reaction I. The standard heat of formation of C_2F_4 can be calculated since the heat of formation of $4HF(aq)$, -302.5 kcal., and the heat of formation of $2C$ (amorphous), 3.0 kcal., are accurately known. The ΔnRT correction of -1.8 kcal. gives a value for the heat of hydrogenation at constant pressure of -147.8 kcal./mole. This results in -151.7 ± 1.1 kcal./mole for the standard heat of formation of gaseous tetrafluoroethylene at $298^\circ K$.

Table II gives the results for the decomposition experiments on C_2F_4 , according to reaction II. The standard heat of formation of CF_4 was computed with -151.7 kcal. for the heat of formation of C_2F_4 , and 1.9 kcal. for the heat of formation of the amorphous carbon. The ΔnRT correction of 0.05 kcal./mole gives a value for the heat of decomposition at constant pressure of -63.5 kcal./

(16) E. W. Washburn, *J. Research Natl. Bur. Standards*, **28**, 217 (1933).

mole. This results in -217.1 ± 1.2 kcal./mole for the standard heat of formation of gaseous tetrafluoromethane at $298^\circ K$.

Table III gives the heats of combustion of the amorphous carbon produced in reactions I and II. The standard heats of formation of these carbons at $298^\circ K$. were obtained by subtracting 94.05 kcal. from the average value of $-\Delta U_c^\circ$.

Table IV gives the results for the combustion experiments on 1,1-difluoroethylene, according to reaction III. The standard heat of formation of CH_2CF_2 was calculated with -94.05 kcal. for the heat of formation of CO_2 , and -75.77 kcal./mole for the heat of formation of aqueous HF . The ΔnRT correction of -0.59 kcal./mole gives a value for the heat of combustion at constant pressure of -262.15 kcal./mole. This results in -77.5 ± 0.8 kcal./mole for the standard heat of formation of gaseous 1,1-difluoroethylene at $298^\circ K$.

Acknowledgment.—The authors are grateful to the General Chemical Division of the Allied Chemical and Dye Corporation for supplying the sample of CH_2CF_2 and to the Wisconsin Alumni Research Foundation and the Minnesota Mining and Manufacturing Company for grants supporting this research.

ELECTRIC CONDUCTANCE IN LIQUID LEAD SILICATES AND BORATES

By J. O'M. BOCKRIS AND G. W. MELLORS

University of Pennsylvania, Philadelphia Pa., and National Research Council, Ottawa

Received April 20, 1956

The conductances of $PbO-SiO_2$ and $PbO-B_2O_3$ have been determined over the temperature range liquidus to 1400° . Subsidiary measurements have been made on the density of these systems. The Faradaic yield has been determined. The Faradaic yield is 100%. The specific conductance obeys the Rasch-Hinrichsen equation. Equivalent conductance increases with increase of PbO . A minimum occurs at 8% PbO in the plot of molar volume against composition. The heat of activation for conductance varies with composition and shows characteristic plateaus and inflections. The borates have lower E_A 's. E_A and its variation with composition is interpretable in terms of a discrete silicate ion model over the range (10–20%) up to 66% PbO . Above the orthosilicate and orthoborate composition free O^{2-} ions contribute to the conductance. Pure B_2O_3 has an appreciable intrinsic conductance. A breakdown of the three dimensionally coordinated lattice occurs at about 8% PbO in $PbO-B_2O_3$. Some systems of discrete borate ions are developed; the likely one has the general formula $[B_n O_{3n+2}/2]^{6-}$, and a $-B-O-B-$ angle of 150° . E_A is interpretable as a function of composition in terms of such a structure. In lead glasses, lead cations act as network formers. It can conduct well because ions travel *along* layer planes in the liquid lattice (contrast Ti^{4+} , Al^{3+} , in silicates).

Introduction

Viscosity measurements have led to the suggestion of a model of the liquid silicate network in which at intermediate Si/O ratios discrete silicate ions are postulated.¹ This leads to the questions: (i) What changes in the silicate or borate lattice occur during addition of the first few per cent. of metal oxide (MO)? (ii) What is the structure of the liquid at MO compositions greater than that of the orthosilicate (when oxide ions no longer coordinate to Si)?

Measurements are hence needed on a system which remains liquid at practicable temperatures over the whole composition range. Such measurements have been carried out on the electric conductance of the $PbO-SiO_2$ system from 0–100%

PbO .² Studies on the Faradaic yield during electrolysis in this system and on the conductance of comparable liquid borates are also reported.

Experimental

Conductance

Materials.— SiO_2 was prepared from mineral quartz, cleaned, quenched and ground, heated to redness and stored over silica gel. Hopkin and Williams' "pure" B_2O_3 was dried at 150° and stored in a desiccator. For systems with 0–10% PbO , A.R. boric acid was used as source of B_2O_3 and dehydrated *in situ*. A.R. PbO was dried at 110° and stored in a desiccator. Analyses of typical melts were made after runs; they indicated deviations from intended compositions of less than 1% (by wt.).

Furnace, Electrodes and Conductance Cell.—The furnace resembled that of Bockris, Kitchener and Davies,¹ the main tube being of Mo and acting as heating element. Modifications were: (a) radiation shields were replaced by alumina packing; (b) an atmosphere of forming gas (90% nitrogen—

(1) J. O'M. Bockris, J. W. Kitchener and A. E. Davies, *Trans. Faraday Soc.*, **48**, 536 (1952).

(2) Compositions are in mole per cent. unless otherwise stated.

10% hydrogen) covered the element; (c) an inner refractory tube between the Mo and the crucible allowed control of the atmosphere above the crucible. The electrodes' height was controlled by a rack and pinion mechanism. Forming gas was dried by passage through H_2SO_4 and a column (5 ft.) of P_2O_5 . Pt electrodes, 2 mm. diameter, and Pt crucibles were used. The electrodes were cemented, $3/4$ " apart, in an Al_2O_3 sheath, 1" in diameter, carrying a central tube mounted between the electrodes through which a thermocouple and sheath could pass. The resistance between the electrodes was 4.10^6 ohms at 1500° .

Temperature.—Pt-13% Rh-Pt thermocouples were used. The thermocouples were in closed Al_2O_3 sheaths (covered at the lower end by Pt foil) and dipped 1 cm. into the melt. Each thermocouple was compared with a new one after five runs and rejected when the discrepancy was $\pm 1^\circ$. Temperature-position maps for the inside of the furnace showed that at 1250° a zone 3 cm. long possessed temperature constant to $\pm 2^\circ$. The accuracy of measurement was better than $\pm 3^\circ$.

Electrical Circuit.—The resistance-capacitance bridge utilized a cathode ray oscillograph as indicator. Interference was eliminated by inductance-capacitance filters in the main leads to oscillator and oscilloscope; and by a tuned circuit having a maximum response of 100 cycles sec^{-1} in the amplifier. Pick up from the heating current was eliminated by a 50 cycles sec^{-1} T network. Components were mounted in grounded metal cans with shielded connections.

Cell Constant.—The cell constant was determined for different depths of the liquid in the crucible, the depth of immersion of the electrodes being maintained constant (Fig. 1). Small (0.1–0.2 cm.) changes of the distance between the electrodes gave changes in cell constant of $\pm 0.5\%$. The electrodes were platinized and solutions of 0.1, 0.01 and 0.001 *N* KCl were used.

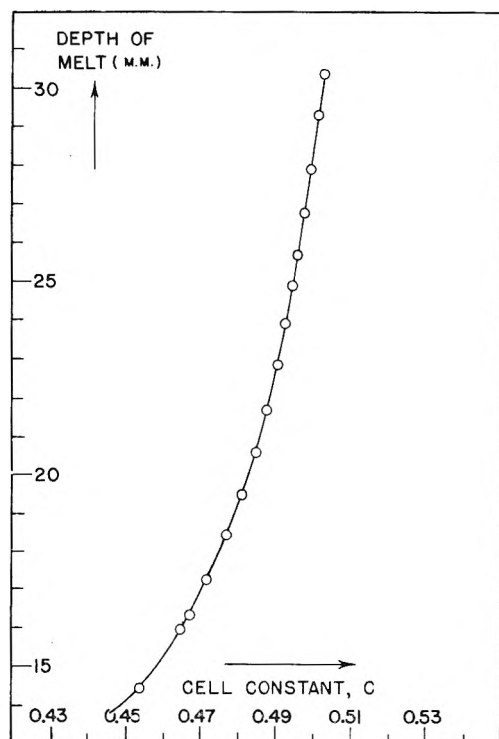


Fig. 1.—Cell constants as a function of depth of immersion.

The cell constants are valid at the temperature of measurement. Changes with temperature were allowed for as follows. (a) In melts of low viscosity the electrodes were raised and reinserted 1 cm. into the melt at each temperature at which a measurement was made. (b) In melts of high viscosity the net expansion of the melt and crucible was found by determining the height at only two different temperatures. The net linear expansion during temperature changes from 1250° to the liquidus of the system had the

order 0.1 cm. Thus, the relevant cell constant at each temperature could be determined. The maximum correction thus arising amounted to 10%.

Polarization.—Measurements were made over the range 500–10,000 cycles sec^{-1} . In this range, conductance was independent of frequency.

Leads and Electrodes.—The resistance of leads and electrodes (R_e) was measured by joining the electrode ends by a Pt rod. R_e varied from 3.7×10^{-2} (19°) to 8.8×10^{-2} ohms (1450° in electrode section).

Volatilization of PbO.—When volatilization was greatest (99.80 wt. % PbO), the change in composition calculated from vapor pressure data³ amounted to 0.6 wt. % for 8 hours heating at 1100° . Analysis after heating under similar conditions showed a change of 0.3 wt. %.

General Procedure.—The PbO and SiO_2 were shaken together for 20 minutes. Sufficient mixture was prepared to give a depth of 2–3 cm. in the crucible after melting. The temperature was raised to 1300° and held there for several hours to give homogeneity. Measurements were made at fall and rise of temperature over the range 1300° to the liquidus.

Reproducibility.—The reproducibility was $\pm 3\%$ for melts containing $>30\%$ PbO except near the solidus where small variations of temperature cause large variations of conductance. For PbL $<30\%$, the reproducibility was $\pm 5\%$ and less near the solidus, due to less accurate cell constant determinations in the viscous melts.

Electrolysis

Materials.—As for conductance work.

Furnace.—The electrode lowering mechanism and top plate of the furnace already described were replaced by a plate with central hole.

Cell and Electrodes.—A molten Pb cathode was used. Crucibles of Al_2O_3 resisted attack over 2–3 hours. The crucible was impervious to molten Pb, and the solubility of Pb in Pb silicates was negligible. The anode was of Pt.

Temperature.—Pt-13% Rh Pt thermocouples were placed $1/8$ " above the melt. Temperatures thus measured were 7° below those of the interior of the melt at 900° .

General Procedure.—A known weight of Pb was melted in the crucible in a reducing atmosphere. The furnace was cooled and the PbO- SiO_2 mixture added. The silicate and Pb were melted under pure N_2 . A Pt anode was inserted and the current (1 amp.) remained constant throughout the experiment (2–3 hours). The crucible was broken up and the Pb reweighed.

Reproducibility₄ was $\pm 2\%$.

Density

Densities are needed to evaluate equivalent conductances. Approximate density values were obtained by determination of the depth of the melt at each temperature and composition. The depth-volume relation for the crucible was known at room temperature and a correction was made from expansivity data for Pt^{4,5} to obtain the volume at the working temperature. Weighed amounts of melt were in the crucible, so that density could be determined. This crude method gave accuracies of better than $\pm 5\%$; however, reproducibility was found to be $\pm 1-2\%$.

Results

In the PbO- SiO_2 system the composition range was 20–100% PbO, owing to the miscibility gap at lower concentrations of PbO.

Figure 2 shows specific conductance as a function of temperature for silicate and borate systems. The usual exponential relation of $\log \kappa$ and $1/T$ applies, $\log \kappa$ increasing regularly with PbO content (Fig. 3). In the silicate, there is a plateau in the E_{A-E}

(3) E. Preston and W. E. S. Turner, *J. Soc. Glass Techn.*, **19**, 296 (1935).

(4) L. Shartsis and S. Spinner, *J. Research Natl. Bur. Standards*, **46**, 175 (1951); "International Critical Tables," Vol. I, McGraw-Hill Book Co., New York, N. Y., p. 46.

(5) Johnson, Matthey and Co., Ltd., "Platinum-Rhodium Thermocouple," London, 1953.

(6) It can be shown that E_A (i.e., $\partial \ln \Lambda / \partial (1/T)$) differs from E_K by less than 1 kcal.

composition plot between 20 and 40% PbO, a rapid decrease from 40% PbO and a minimum at 90%; the borate has similar regions (Fig. 4). Density and molar volume values are in Figs. 5 and 7. Electrolysis results showed 98-102% of the Faradaic yield of Pb for mole fractions PbO from 0.5-1.0.

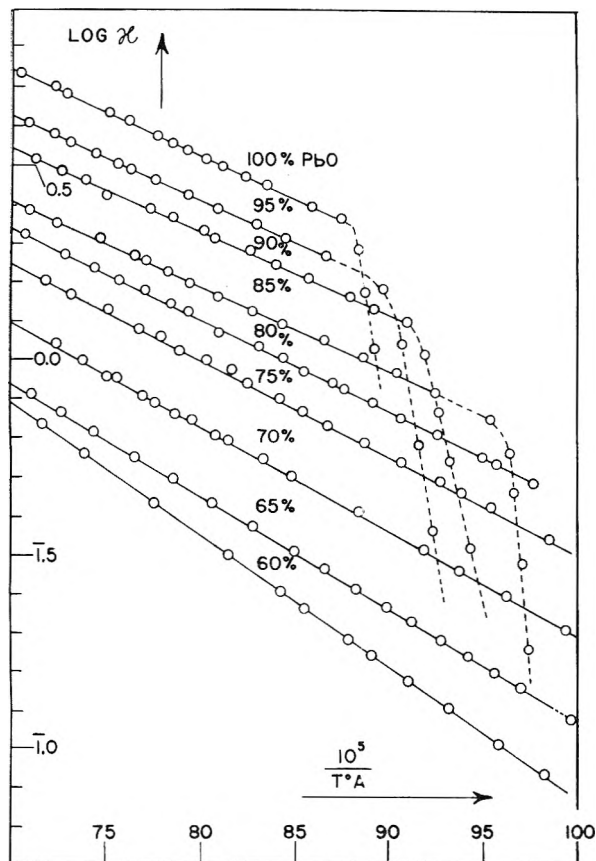


Fig. 2.—Typical log $K/1/T$ lines for PbO-SiO₂ (broken lines = temperatures below the liquidus).

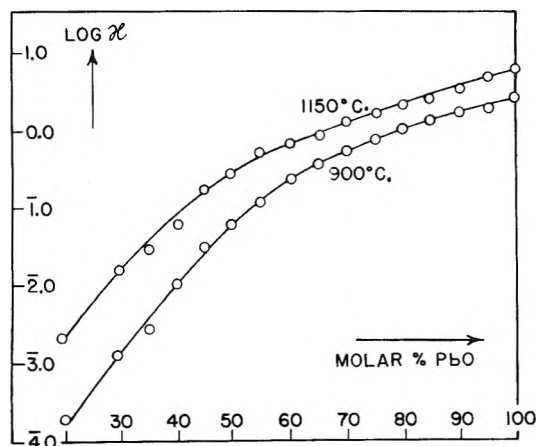


Fig. 3.—Log κ as a function of molar composition for PbO-SiO₂.

Discussion

(A) Comparison with Former Work.—Kheyman and Rybakova⁷ covered part of the range here studied in lead silicates. Their results agree

(7) A. S. Kheyman and L. I. Rybakova, *Invest. Akad. Nauk., Otdel Tech Nauk.*, 1685 (1949).

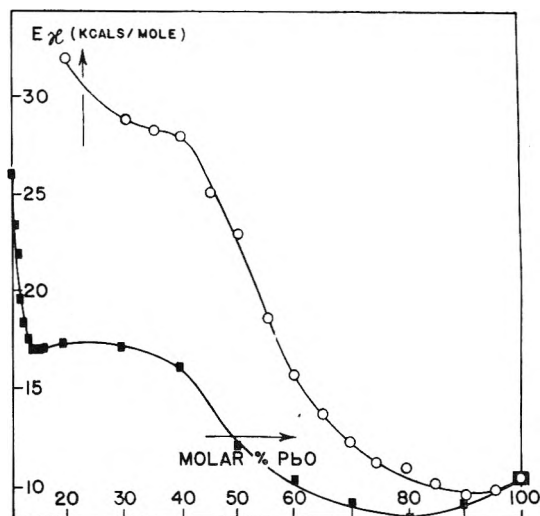


Fig. 4.—Heat of activation as a function of molar composition for PbO-SiO₂ (—○—) and PbO-B₂O₃ (—□—).

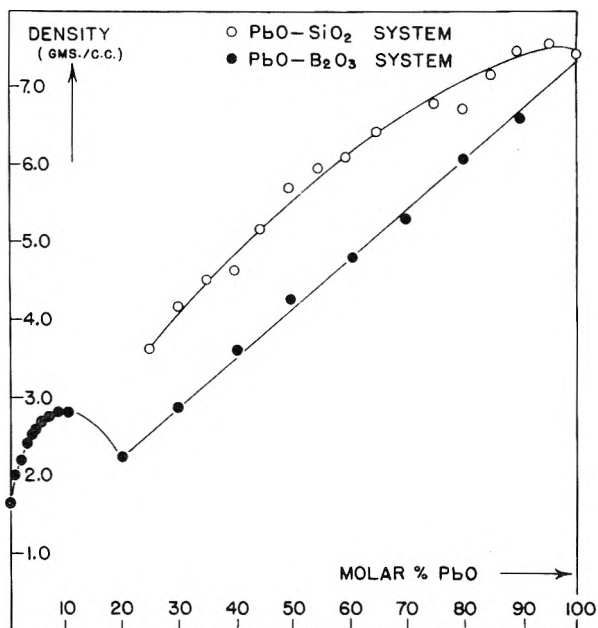


Fig. 5.—Approximate densities at 1050° for PbO-SiO₂ and PbO-B₂O₃ as a function of composition.

with the present fairly well except at compositions low in PbO where discrepancies up to 10% occur. These may have been due to neglect of cell constant variation with temperature by the Russian workers, who inserted electrodes at the high temperature so that melt contraction during temperature fall would introduce error. Schellinger and Olsens⁸ results disagree markedly with the present ones, probably due to the use of silica crucibles which are attacked. Values⁹ for the conductance of B₂O₃ are higher than those reported here for purified B₂O₃ and the discrepancy is hence probably due to impurities.

(B) Conduction Mechanisms.—At compositions richer in PbO than the orthosilicate or orthoborate.

(8) A. K. Schellinger and R. P. Olsen, *J. Metals*, **1**, 984 (1949).

(9) K. Arndt and A. Gessler, *Z. Elektrochem.*, **14**, 662 (1908); S. Kinumaki, and K. Sasaki, *Sci. Rep. Res. Inst., Tokoku Univ.*, **25**, 1318 (1951); L. Shartsis, S. Spinner and W. Capps, *J. Am. Ceram. Soc.*, **38**, 319 (1953).

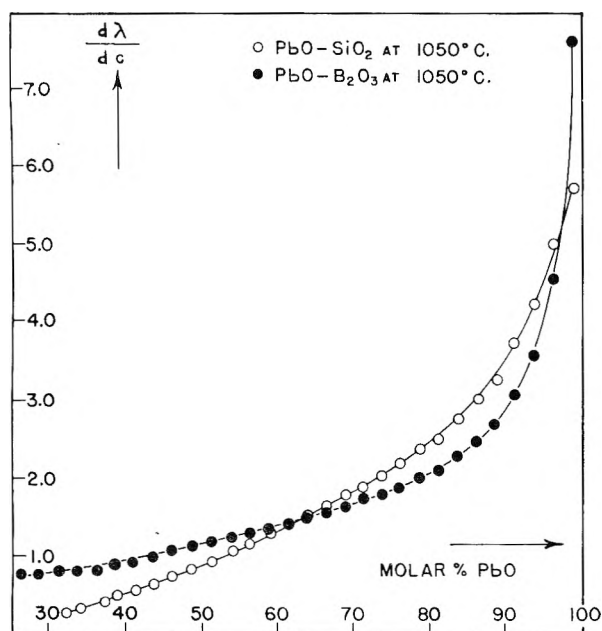


Fig. 6.—Rate of change of conductance as a function of molar composition for PbO-SiO₂ and PbO-B₂O₃ at 1050°.

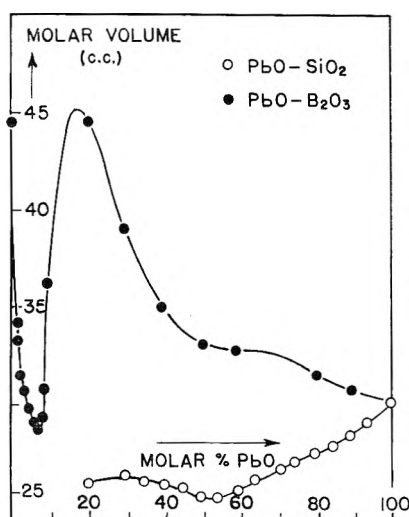


Fig. 7.—Molar volume as a function of composition for PbO-SiO₂ and PbO-B₂O₃ at 1000°.

no further O can coordinate round Si or B atoms. Additional O atoms introduced must therefore form dipoles with Pb⁺⁺ (contributing nothing to conductance), or exist as free O²⁻ ions. In the silicate and borate systems there is increase of compositions richer in PbO than the ortho one (Fig. 6). The formation of non-conducting ionic dipoles is hence improbable.

(C) (i) E_A and Composition (Silicates).—The heat of activation for the Pb⁺⁺ conduction should decrease with increasing PbO content because introduction of PbO causes breaking of -Si-O-Si- bonds, and hence loosening of the lattice. If addition of PbO gave rise to a random breaking of the Si-O bonds, without the formation of particular configurations,¹⁰ there would be a uniform increase in hole formation in the lattice and E should decline

(10) R. W. Douglas, *J. Soc. Glass Tech.*, **31**, 50 (1943).

uniformly with composition. This is inconsistent with the regions of Fig. 4.

If the liquid consists of infinite two-dimensional sheets over the composition range 33–50% PbO,¹¹ the Pb⁺⁺ would exist between the silicate sheets and the distance between the potential energy wells of the Pb⁺⁺ would be constant during change of composition (namely, the distance between two single bonded oxygen ions on the same side of the sheet). However, Fig. 4 shows that the heat of activation commences to decrease at about 40% PbO.

By analogy with the results of Fig. 4 for borates, the heat of activation for transfer of Pb⁺⁺ through the liquid decreases rapidly with initial additions of PbO. This is consistent with ϵ model¹² in which the silicate lattice in these regions of low PbO concentration remains essentially an SiO₂ lattice, in which the addition of PbO produces -O-Pb⁺⁺-O-. The energy for Pb⁺⁺ to jump from one energy well to the next depends on the distance apart of two wells; the closer together these wells, the larger will be the activation energy. At a composition of about 11% PbO the metal ions find themselves in adjacent "cages" consisting entirely of -Si-O-Si- bonding¹³ so that rapid decline in the heat of activation (Fig. 4) should cease at this composition, i.e., each Pb⁺⁺ finds itself next to a potential well into which it may jump. The actual termination is (Fig. 4) at about 20% PbO. This discrepancy between the expected and observed values for composition value for cessation of rapid change in E_A would be understandable if the Pb⁺⁺ ions act as bridges between the discrete silicate ions which (in analogy with the structures in alkali and alkaline earth silicates¹⁴) probably exist above 11% PbO. Thus the Pb⁺⁺-containing silicate lattice would undergo a more gradual breakdown from the continuous 3 dimensionally bonded to the discrete ion lattice, compared with that in alkali metal-containing lattices. The sharpness of the expected change on the E_A -composition plot would be correspondingly less.

The discrete silicate ions expected¹⁴ at compositions above 11% PbO contain O⁻ only at their extremities. As the PbO content increases above 11% PbO, and the silicate ion size decreases, the distance between the O⁻'s on an anion decreases. If the Pb²⁺ ions simply jumped between extremities of silicate anions, E_A would hence decrease regularly with decrease of anion size. However, the silicate anions in the liquid do not pack in a regular array, and this disorder allows Pb²⁺ ions to jump not only between the ends of the same silicate anions, but also between O⁻ ions in different anions. The probability that an O⁻ in one anion exists near to that of another, decreases with increasing length of anion, i.e., decreasing PbO, so that the distance between O⁻ ions is indeed the

(11) K. Endell and H. Hellbrügge, *Naturwiss.*, **30**, 241 (1942); *Glasstech. Ber.*, **20**, 277 (1942).

(12) J. O'M. Bockris and D. C. Lowe, *Proc. Roy. Soc. (London)*, **226A**, 423 (1954).

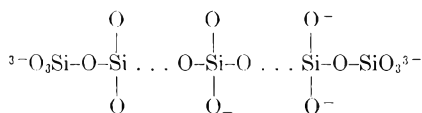
(13) J. O'M. Bockris, J. W. Tomlinson and J. L. White, *Trans. Faraday Soc.*, (March, 1956).

(14) J. O'M. Bockris, J. D. Mackenzie and J. A. Kitchener, *ibid.*, (Dec., 1955).

main (though indirectly operating) factor in reducing E_A during increasing PbO in the 11–33% range (Fig. 4).

In the region between 33 and 50% PbO the anionic structure consists¹³ predominantly of $\text{Si}_6\text{O}_{15}^{6-}$ ions. Little change in heat of activation would be expected on this model at the commencement of this range because the *type* of silicate anion predominant is identical with that in the previous range (11–33%). However, when the single ring structure $\text{Si}_3\text{O}_9^{6-}$ begins to predominate, E_A should decrease, because the jump distance between two energy wells for the Pb^{2+} ion is now decreased, so that the intersection of the Morse curves for the Pb^{2+} ion in the initial and final states of its interstitial jumps occurs at a relatively short distance above that of the initial state. In fact, E_A does begin rapidly to decrease at a composition of about 43% PbO when slightly more than half of the anions are $\text{Si}_3\text{O}_9^{6-}$ (Fig. 4).

To interpret the rapid fall in the E_A in the region 50–66% PbO (Fig. 4), consider E_A during the transition of a Pb^{++} ion held near an O^- on a chain,



to another O^- group. The Morse curves for the Pb^{++} ion before and after transition from one energy well to the next are shown in Fig. 8a and b. In the vicinity of the terminal group in the chain, *i.e.*, the $-\text{SiO}_3^{3-}$ group, the Pb^{2+} ion can be more stable than elsewhere in the chain. Hence, if a Pb^{++} ion jumps from a position near to an O^- ion in the chain to the next O^- ion, the potential energy–distance relation will be as in Fig. 8a. However, if it is possible for a jump to occur from a position near to an O^- ion to one near an SiO_3^{3-} ion, the potential energy–distance plots will be as in Fig. 8b. The heat of activation is hence less in the case b than in the case a. It follows that in the composition range 50–66% PbO, in which the silicate lattice consists only of chains, the heat of activation will become less in as much as the transitions from O^- ions to SiO_3^{3-} ions become more frequently possible. However, it is just with increase of PbO composition that the frequency of juxtaposition of an SiO_3^{3-} group with an O^- group increases, *i.e.*, the heat of activation for the flow of PbO decreases. Transitions of Pb^{2+} ions from one $-\text{SiO}_3^{3-}$ energy well to another could be a comparatively easy process because the minima of the potential energy wells will be comparatively close together and the heat of activation correspondingly small, two SiO_3^{3-} groups being held together coulombically through the divalent Pb^{2+} .

(ii) **Structure at Conditions above the Orthosilicate.**—If O^{--} ions, added above the orthosilicate composition (66% PbO) contributed immediately to conduction $\partial\Lambda/\partial c$ would suffer inflection at 66% PbO, whereas this occurs in fact at 75% (Fig. 6). In Fig. 9 is the stoichiometric concentration of Pb^{++} , SiO_4^{4-} and O^{--} ions calculated on the assumption that above the orthosilicate the melt consists only of these ions. The composition cor-

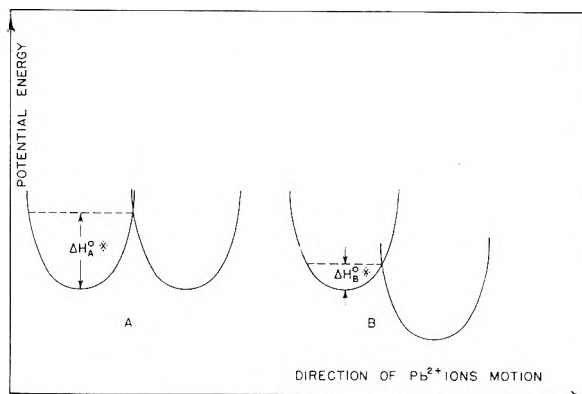


Fig. 8.—Potential energy curves for the transition of Pb^{2+} (a) between two singly charged O^{--} groups; (b) between an O^- ion and an SiO_3^{3-} group.

responding to the inflection on the $\partial\Lambda/\partial c$ –composition curve is (Fig. 9) that at which the smaller and hence better conducting O^{--} ion commences to predominate in the melt, *i.e.*, the composition at which SiO_4^{4-} ions are replaced by the smaller and hence more probably conducting O^{--} ions.

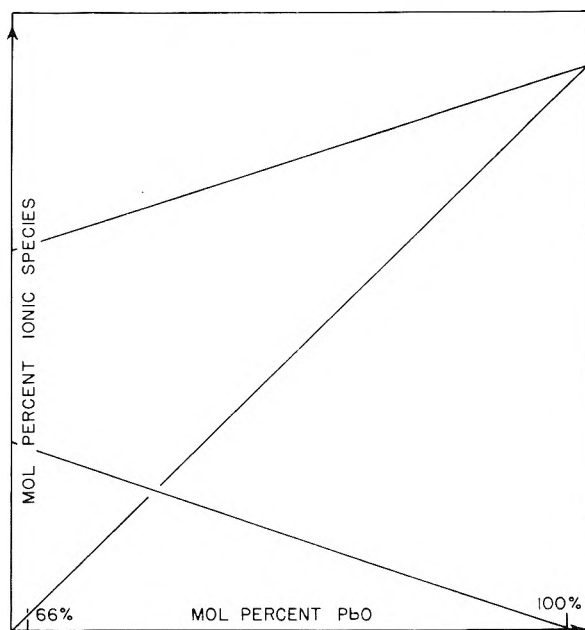


Fig. 9.—Concentration of Pb^{2+} , SiO_4^{4-} and O^{--} ions above the orthosilicate composition.

However, E_A decreases to 90% PbO (silicate) and 80% PbO (borate) and then increases again (Fig. 4). Hence, some of the increase in $\partial\Lambda/\partial c$ observed above 66% PbO arises from this decrease of E_A . The E_A –composition graph can be regarded in terms of two limiting compositions, that of Pb^{++} and O^{--} ions only, and that in which the SiO_4^{4-} lattice predominates. In the latter case, the Pb^{++} ions are subject to relatively small coulombic attraction in their interstitial jumps (relatively large size of the silicate anion) so that E_A is low. However, when the PbO lattice predominates, the smaller O^{--} ion exerts a larger coulombic attraction for Pb^{++} during its interstitial jumping than that exerted by the larger SiO_4^{4-} ion. After 75% PbO, therefore (*cf.* Fig. 9), E_A should commence to

increase. This effect (Fig. 4) evidently is over-compensated by the increasing contribution of the O^- ions to the equivalent conductance which shows a rise through the E_A -composition minima of Fig. 4.

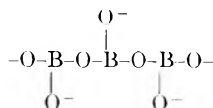
(iii) **Conductance of Pure B_2O_3 .**—Suppose that the κ of pure B_2O_3 at 950° (4.10^{-6} ohms $cm.^{-1}$) is due to residual alkali ions. An order calculation of the necessary concentration of alkali can be made from the free heat of activation for conduction of alkali silicates at 175° which is about 25 kcal. mole $^{-1}$.⁴ Hence $\ln_{2023/\kappa_{1223}} = 25.000/1.98$ ($1/1223 - 1/2023$).

Hence, $\kappa_{1223} = 4.10^{-6} = c_{Alk}^2$ where c_{Alk} is the alkali ion concentration in gram ions $cc.^{-1}$. Thus, $c_{Alk} = 2.10^{-6}$, or 2.10^{-3} g. ions. $l.^{-1}$. The molar volume of B_2O_3 is about 35 $cc. mole^{-1}$ at 950° so that in pure B_2O_3 there are about 28.5 moles $l.^{-1}$ of B_2O_3 . Hence, the necessary alkali impurity = 0.01 mole %. Analysis of the B_2O_3 before purification showed it to contain 0.001 mole % alkali. Conductance of pure B_2O_3 is thus due to self dissociation into ions. The ionic product at 950° is 4×10^{-12} .

(iv) **Borate Structure in the Range 0–20% PbO.**—Figure 7 shows that additions of up to 8% PbO cause a large decrease in molar volume. On introduction, therefore, of PbO to B_2O_3 , the rupture of the $-B-O-B-$ bonds, with the production of O^- 's singly bonded to B, causes a very open vitreous B_2O_3 structure to change to a distorted close packed hexagonal arrangement. This change must be completed at the minimum of the molar volume-composition plot (Fig. 7) and the large increase of molar volume of the melt which occurs on further increase of PbO composition indicates that a considerable loosening of the lattice occurs. There is hence a break up of the continuously bonded borate lattice at about 8% PbO, the resulting lattice consisting, in analogy to the liquid silicates,¹⁴ of discrete borate ions. A more open lattice results, and the molar volume rises.

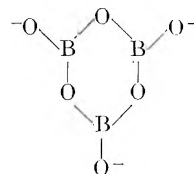
This model is consistent with the E_A -composition relation of Fig. 4 in which a rapid decrease of heat of activation for conductance occurs during addition of the first 8% of the PbO. The $-B-O-B-$ bonds are being broken and the Pb^{++} is presented with a rapidly increasing ease of passage from one interstice to the next. The tendency is complete at 8% PbO when discrete borate ion formation begins.

(v) **E_A and Composition (Borates).** (a) **Model for Liquid Borates.**—The B ion is usually three coordinated,¹⁵ and a model for the structure of liquid borates which is analogous to that recently suggested for the liquid silicates¹² hence follows: At 75% MO the planar discrete BO_3^{3-} ion is the sole anionic constituent of the melt and as B_2O_3 is increased above 25%, the formation of the

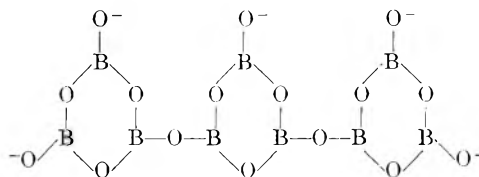


chain begins. The formula for an anion formed

from such a chain would be $(B_nO_{2n+1})^{(n+2)-}$. The formula of the predominant anion for $c_{PbO} < 66\%$ can be obtained by placing the O/B ratio (known from the stoichiometric composition) equal to $(2n+1)/n$. Hence, when $(O)/(Si) = 2$, $n = \infty$, *i.e.*, the chains rapidly increase to very great length near to the composition 50% PbO. When the chain begins this rapid increase in length, it becomes unstable and breaks down to form rings, a tendency toward which arises due to coiling of the chains. Ring systems formable by B and O, are, *e.g.*, three B ring systems

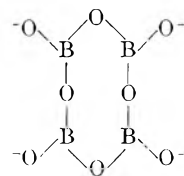


At lower contents of PbO, *i.e.*, at higher O/B ratio, these rings may form a continuous planar system linked through one O atom, namely

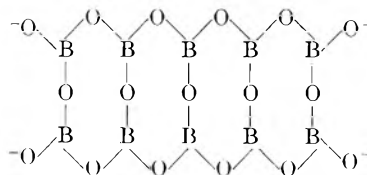


The $-B-O-B-$ angle for such rings is about 120° and the $B_3O_3^{3-}$ ring has been observed in solid metaborates. The general formula is $[B_nO_{(5/3n+1)}]^{(n/3+2)-}$. The O/B ratio is $(5/3n+1)$, and therefore near to the composition $MO \cdot 3B_2O_3$, *i.e.*, 25% PbO, the planar rings become indefinitely large.

A second ring system may be based upon



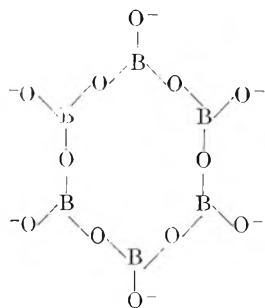
$B_4O_4^{4-}$, the ions for $c_{PbO} < 50\%$ being of the form



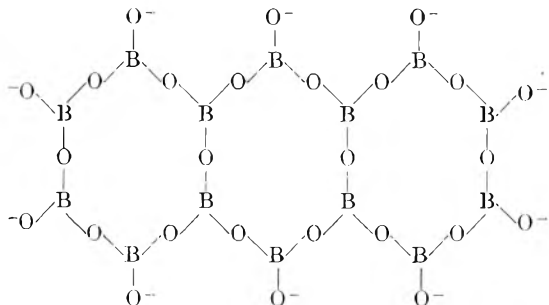
These ions would have a general formula $[B_nO_{3/2n+2}]^{6-}$. The O/B ratio is $(3/2n+2)/n$; hence they have a finite size at any composition. The $-B-O-B-$ angle is 135° . These ions are planar analogs of the discrete ions $[Si_nO_{2n+3}]^{6-}$ which appear to exist in liquid silicates.

Finally a third ring system based upon

(15) For review, see G. J. Mellors, Thesis, London, 1953.

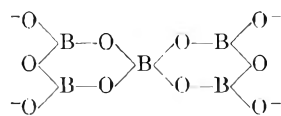


$B_6O_{12}^{6-}$ may be formed, the condensed ions being of the type



with a general formula of $[B_nO_{7/4n+15}]^{(1/2n+3)-}$ becoming "infinite" at a composition of $MO_2 \cdot B_2O_3$ and having a $-B-O-B-$ angle of 150° .

It is also possible to consider ring systems based upon $B_3O_6^{3-}$ rings, and involving condensation around a possible four-valent B, e.g.



Extension to ions at higher B/O ratios is obviously possible.

(b) **Interpretation.**—Between 66 and 50% PbO, the interpretation of the rise of E_A with increase of B_2O_3 concentration (Fig. 4) is similar to that for the silicate (p. 1325). Commencement of the flat portion of the E_A -composition curve at the same composition for borates as for silicates suggests that ring formation is analogous to that for silicates, i.e., the four B ring, $B_4O_8^{4-}$, is formed and the Pb^{2+} ions conduct from positions in energy wells near to the O^- ions of this ion. The E_A -composition curve from 50 to 8% PbO would then be interpreted by a growth in length of the four B rings, that at 8% PbO where the sharp inflection in molar volume occurs, being $(B_{40}O_{62})^{6-}$, an ion containing about 20 rings. This interpretation is better than that in terms of the three B rings because these would involve a $B-O-B$ angle of 120° (135° for 4B rings), whilst the observed $B-O-B$ angle is about 150° .¹⁶ Against the 3B and 6B ring systems is the fact that they reach "infinite" dimensions at 25 and 33% PbO, respectively, whereafter (at higher $c_{B_2O_3}$) a three dimensionally bonded structure would occur. However, the E_A -composition relation is particularly smooth through 25 and 33% B_2O_3 .

(16) A. F. Wells, "Structural Inorganic Chemistry," London, 1945, p. 491.

(D) **Glass Forming Properties of PbO.**—A striking property of PbO is its ability to form glasses with abnormally high metal contents (up to 85.3% PbO with SiO_2 and 83–84% PbO with B_2O_3).¹⁷ At the high PbO contents, the Pb may act as a bridging *central* atom to which O and Si coordinate. The conductance at high PbO contents, however, implies that Pb^{++} and O^{--} are relatively free to conduct. Let the mole per cent. Pb be m . Then, the mole per cent. SiO_2 is $100 - m$, and each SiO_2 requires $2O^{--}$ ions to complete its coordination, so that the mole per cent. of free O^{--} is $m - 2(100 - m)$.

Thus

$$O^{--}/SiO_4^{4-} = (3m - 200)/(100 - m)$$

Suppose $O^{--}/SiO_4^{4-} = 3$, then $m = 83$ (mole)%, i.e., the maximum PbO content for glass formation corresponds approximately to an O^{--}/SiO_4^{4-} ratio of 3. If hexagonal close packing is regarded as the type of arrangement in the melt at the high PbO concentration, i.e., a central Pb atom is in contact with 12 partners, glass formation occurs until less than 4 SiO_4^{4-} groups are in contact with the Pb^{2+} ions, which supports the view that glasses of high PbO content are formed with Pb as a network former.

However, comparison of E_A and the entropy of activation for conductance for $PbO-SiO_2$ and $PbO-B_2O_3$ with those for systems where the cations are network *modifiers*, shows close similarity (free energy of activation = 20–30 kcal. mole⁻¹); whereas values of E_A for conductance¹⁸ in TiO_2 and SiO_2 and $Al_2O_3-SiO_2$, where the cations are network *formers*,¹⁹ are of the order 50–60 kcal. mole⁻¹, and the conductance is correspondingly small. The problem is to explain how the Pb^{2+} ions can escape from their equilibrium positions in the liquid lattice with an energy of activation which appears incompatible with network forming action of Pb^{2+} .

In solid PbO,²⁰ Pb^{2+} has 4 oxygen ions as nearest neighbors, but all four lie on the same side of the Pb at a distance of 2.30 Å. If, as concluded by Fajans and Kreidl,²¹ the structure of lead orthosilicate (of which no X-ray study is available) resembles that of PbO, the above interpretation of the PbO structure would be consistent with a strong tendency to form highly polarized asymmetric groups with the SiO_4^{4-} ions (so long as sufficient are present, *vide supra*) and thus give rise to units which are sufficiently distorted and irregular to prevent a fitting into the rest of the lattice, so that crystallization becomes inhibited.

The relatively low value for the heat of activation for conductance, compared with that for other network formers, follows from the unusual steric relation of Pb^{2+} to the surrounding anions. Whereas in TiO_2-SiO_2 melts, the Ti^{4+} is surrounded sym-

(17) W. J. Moore, Jr., and J. Carey, *J. Soc. Glass. Tech.*, **35**, 43 (1951); A. Klemm and B. Berger, *Glasstech. Ber.*, **5**, 105 (1927–8).

(18) J. O'M. Bockris, J. A. Kitchener, S. Ignatowicz, and J. W. Tomlinson, *Disc. Faraday Soc.*, **4**, 256 (1948); *ibid.*, **48**, 75 (1952).

(19) A. Dietzel, *Z. Elektrochem.*, **48**, 9 (1942).

(20) W. J. Moore, Jr., and L. Pauling, *J. Am. Chem. Soc.*, **63**, 1392 (1941).

(21) K. Fajans and P. Kreidl, *J. Amer. Ceram. Soc.*, **31**, 105 (1948).

metrically by O^{--} ions, the Pb^{2+} , if the group arrangement above the ortho-silicate is similar to that for PbO , has the SiO_4^{4-} and O^{--} groups "on one side".²⁰ It can hence undergo preferential displacement in the direction of the applied field by travelling along the layer plains of the structure, which it can do without passing out of the deep

energy well created in systems in which the cation (e.g., Ti^{4+}) is symmetrically surrounded by O^- . That the Pb^{2+} ions do not have a configuration in the higher glass forming ranges similar to network formers such Ti^{4+} and Al^{3+} is stressed by the increased conductance at high composition of PbO , where the Pb network forming effect commences.

NOTES

THE PHOTOCHEMICAL PROPERTIES OF ZINC OXIDE¹

BY GLENN V. ELMORE AND HOWARD A. TANNER

Charles F. Kettering Foundation, Yellow Springs, Ohio

Received March 5, 1955

Numerous publications describe the darkening produced by the action of light on aqueous zinc oxide suspensions containing silver, copper, mercury or lead compounds.² There are conflicting views, even in the recent literature, as to whether a reduction to free metal occurs, or a dark colored peroxide is formed. Goetz and Inn reported that intimate mixtures of silver oxide with various amphoteric oxides such as ZnO , TiO_2 and SiO_2 form metallic silver in the light.³ Weyl and Forland, however, claim the product is silver peroxide, not metallic silver.⁴

We have studied the photochemical reactions of aqueous ZnO with several metal compounds, with and without organic material added, at 20° . We employed C.P. ZnO which had been heated for 16 hours at 425 to 450° to remove trace organic impurities. Various lots of ZnO vary in their photochemical activity and the one we used was the most active of several tested.⁵ The water used was distilled and passed through an aluminum oxide column. All other chemicals were C.P. grade. The suspensions were irradiated in a closed system using a magnetic stirrer and mercury valves to avoid stopcock grease contamination. The system was carefully degassed before irradiation.

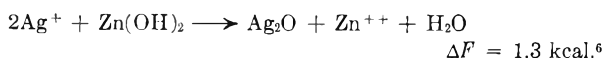
A mixture of Ag_2O and ZnO in aqueous suspension was found to darken quickly before the full light of a Pyrex jacketed General Electric AH-6 high pressure mercury arc. Metallic silver was formed and oxygen was evolved. The amount of silver was always slightly more than one would expect

from the amount of oxygen. Organic impurities could account for this. If oxidizable organic matter is added, the proportion of evolved oxygen is reduced. The results are shown in Fig. 1.

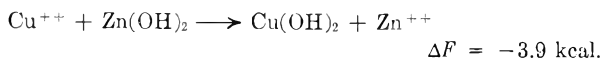
A C-14 labeled formic acid run showed complete oxidation of the formate to carbonate. The data of Fig. 1 indicate that during the 15-minute irradiation period the organic additives were completely oxidized since the stoichiometric amount of metallic silver was always slightly greater than the oxygen equivalent of the additive plus the oxygen evolved. The fourfold greater effect of acetic acid corresponds to its fourfold greater "fuel" value.

Similar results were obtained starting with a ZnO suspension to which $AgNO_3$ solution had been added. We were not able to detect the formation of oxygen if copper or lead was substituted for silver. In the presence of organic matter such as oxalate, however, the formation of metallic copper or lead did occur. All of these results are consistent with the energy changes involved in reactions of the type: $Ag_2O \rightarrow 2Ag + \frac{1}{2}O_2$ and $Ag_2O + H_2O + C_2O_4^{2-} \rightarrow 2Ag + 2HCO_3^-$. If the ZnO is omitted, there is no oxygen evolution from Ag_2O on irradiation. Silver oxalate decomposes in the light in the absence of ZnO but copper and lead do not.

When a yellow filter (Corning no. 3486), which cuts off all wave lengths below 5100 \AA , was interposed between the light source and the reaction vessel a suspension of ZnO in $AgNO_3$ solution turned dark gradually. No oxygen was evolved and only a faint trace of metallic silver could be found. This result can be explained by the formation of a thin film of black Ag_2O over the hydrated surface of the white ZnO particles, the net reaction being



Possibly $AgOH$ is an intermediate but this is unstable and would form the oxide. With copper the corresponding reactions are



(6) All free energy values were taken from W. M. Latimer, "The Oxidation State of the Elements and their Potentials in Aqueous Solutions," Prentice-Hall, New York, N. Y., 1938, Appendix II.

(1) Presented in the division of physical and inorganic chemistry of the 128th National American Chemical Society meeting at Minneapolis, Minn., Sept. 15, 1955.

(2) See for example, G. B. Kistiakowsky, "Photochemical Processes," Chem. Catalog Co., Inc., New York, N. Y., 1928, pp. 155-159, and G. K. Rollefson and M. Burton, "Photochemistry and the Mechanism of Chemical Reactions," Prentice-Hall, Inc., New York, N. Y., 1939, pp. 385-388.

(3) A. Goetz and E. C. Inn, *Rev. Mod. Phys.*, **20**, 131 (1948).

(4) W. A. Weyl and T. Forland, *Ind. Eng. Chem.*, **42**, 257 (1950).

(5) The variation in photochemical activity of ZnO with mode of preparation has been related to the durability of ZnO paints in light. G. Winter, *Nature*, **163**, 326 (1949).

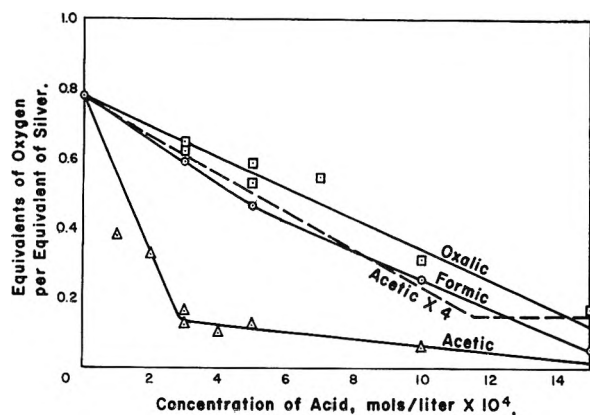


Fig. 1.—Effect of organic acids upon photochemical production of oxygen from silver oxide.

When ZnO was washed with CuSO_4 solution the Cu^{++} ions were removed, almost quantitatively, in the dark, and the ZnO was coated blue, the color of $\text{Cu}(\text{OH})_2$. On warming this turned black due to CuO formation.

With lead the reactions are



When lead nitrate solution was added to ZnO and irradiated in yellow light, there was a change in the apparent texture of the ZnO but no color change. $\text{Pb}(\text{OH})_2$ is white. When the solid was dried and heated it turned yellow, the color of lead oxide. If the irradiation was omitted there was no color formation upon heating.

We conclude that light induces the formation of an insoluble compound on the surface of ZnO from Ag or Pb ions. This has been verified by investigating the effect of light on the concentration of Zn^{++} and Pb^{++} in a suspension of ZnO in $\text{Pb}(\text{NO}_3)_2$ solution. The results are shown in Fig. 2. In the dark the ionic concentrations remained fixed; as soon as the light was turned on the Pb^{++} decreased abruptly and the concentration of Zn^{++} began to increase.

Two other ions, Cd^{++} and Mn^{++} , also precipitate on ZnO upon irradiation but require shorter wave lengths than 5100 Å. Their reactions have larger energy requirements, 3.3 kcal. for $\text{Cd}(\text{OH})_2$ formation and 3.0 kcal. for $\text{Mn}(\text{OH})_2$.

The light induced precipitation reaction of ZnO differs from the light induced oxidation-reduction reactions, such as H_2O_2 formation⁷ and the reduction of Ag^+ , Pb^{++} or Cu^{++} to free metal, in three respects: (a) it does not depend on the crystal structure of ZnO since the same reaction occurs with $\text{Zn}(\text{OH})_2$; (b) the oxidation-reduction reactions require a wave length of 4000 Å. or less, where ZnO absorbs strongly.⁸ It is of interest to note that photoconductivity in ZnO has been observed at 7000 Å.⁸; (c) the precipitation reaction is not dependent on nor affected by the presence of oxidizable organic material.

(7) See for example, J. G. Calvert, K. Theurer, G. T. Rankin and W. M. MacNevin, *J. Am. Chem. Soc.*, **76**, 2575 (1954).

(8) P. H. Miller, Jr., "Semi-Conducting Materials," Butterworths, London, 1951, pp. 176.

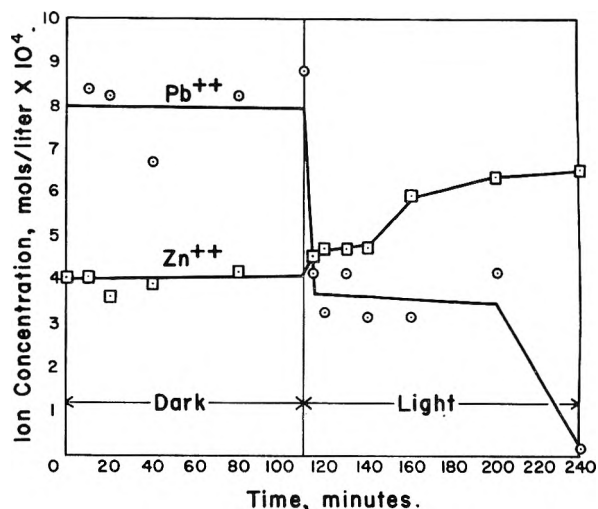


Fig. 2.—Effect of light on a lead nitrate solution in the presence of zinc oxide.

A possible explanation of the precipitation reaction is that light alters the amphoteric character of $\text{Zn}(\text{OH})_2$ in the acid direction. This increases the tendency to form H^+ ions which leaves a negative $-\text{ZnO}^-$ group able to combine with cations such as Ag^+ . The liberated H^+ could then displace Zn^{++} from ZnO or $\text{Zn}(\text{OH})_2$ making the net reaction an exchange of cations.

SOME KINETICS STUDIES WITH PARAHYDROGEN

By G. BOOCOCK AND H. O. PRITCHARD

Chemistry Department, University of Manchester, Manchester 13, England

Received March 6, 1956

Although a large number of hydrogen atom reactions are known, our knowledge of their rates is usually limited to a collision efficiency measured at one temperature only, and even in those cases where an attempt has been made to determine the Arrhenius parameters, *e.g.*, for reactions of the type



the results obtained are far from consistent.^{1,2} The principal difficulty in such experiments is the determination of the stationary hydrogen atom concentration, but in view of some apparently reasonable results obtained by Melville and Robb for reactions of this type, it appeared that the rate of conversion of para-rich hydrogen to normal hydrogen could be satisfactorily used for this purpose. Melville and Robb only report the results of two experiments, one with *n*-hexane and the other with cyclohexane, both carried out at room temperature. Both results appeared reasonable and we decided to study this type of system under varying temperature conditions to try to obtain accurate values for the Arrhenius parameters of a series of abstraction reactions.

(1) E. W. R. Steacie, "Atomic and Free Radical Reactions," Reinhold Publ. Corp., New York, N. Y., 1954.

(2) A. F. Trotman-Dickenson, "Gas Kinetics," Butterworth, New York, N. Y., 1955.

(3) H. W. Melville and J. C. Robb, *Proc. Roy. Soc. (London)*, **A196**, 445 (1949).

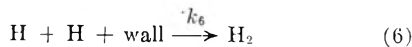
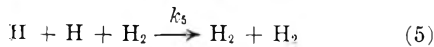
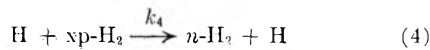
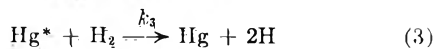
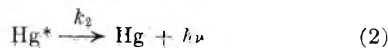
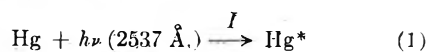
Experimental

Apparatus.—A rectangular quartz cell $15 \times 2 \times 2$ cm. and a low pressure mercury lamp were housed side by side in an electric furnace, the lamp and the cell being separated by a movable shutter. The auxiliary gas-handling system was arranged so that the reactants could be measured out, sampled, and the hydrogen separated off for transference to the micro-thermal conductivity gage, all without coming into contact with a greased tap. (The gage was suspended vertically in a tube containing liquid oxygen which was immersed in a bath of liquid nitrogen: this method of temperature control is far superior to immersion in frozen mercury and avoids the difficulties due to bubble formation which arise if a gage is immersed directly in a refrigerant at its boiling point).

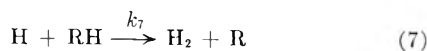
Procedure.—Three types of run were performed, denoted by A, B and C, in which the quantities α , β and γ were determined. α is the value of the absolute conversion rate, *i.e.*, $[H_2] d \log (R_n - R)/dt$, for runs at 1 mm. hydrogen pressure and β and γ the values of the same parameter observed for runs with 100 mm. hydrogen pressure in the absence and in the presence of RH, respectively; R_n denotes the gage resistance for normal hydrogen and R the resistance for samples removed from the reaction vessel after irradiation for a time t . In practice, the basic procedure was to irradiate for a short period of time, say five minutes, and then to remove a sample of gas (freezing out RH in the case of a C run) for transference to the conductivity gage. After thermoconductimetric analysis the sample (remixed with RH in the case of a C run) was returned to the reaction vessel and another irradiation period started.

Results

In the absence of RH, the following reaction scheme accounts satisfactorily for the observed behavior of the system



where Hg^* is $Hg(6^3P)$, I is the intensity of radiation absorbed and $xp-H_2$ represents the excess of para-hydrogen over the normal 25% ($n-H_2$); (the original para-content of the hydrogen was about 70%). In the presence of RH, two other reactions



will operate, the reverse of reaction (7) being neglected because of the low temperatures ($<100^\circ$) being considered.

If reaction 6 is assumed to be diffusion controlled, a consideration of the relative importance of the various reactions 1-7 as $[H_2]$ and $[RH]$ are altered shows that (*cf.* ref. 3)

$$\alpha = I$$

$$\beta = \left[I \left(1 + \frac{k_4 [H_2]}{k_6/[H_2]} \right) \right]$$

$$\gamma = \left[I \left(1 + \frac{k_4 [H_2]}{k_6/[H_2] + k_7 [RH]} \right) \right]$$

whence

$$k_7 = \frac{[H_2]}{[RH]} \frac{k_4 \times \alpha(\beta - \gamma)}{(\gamma - \alpha)(\beta - \alpha)}$$

In the preliminary experiments before any hydrocarbon was introduced into the system, the absolute conversion rate at room temperature fell with decreasing pressure until the pressure range 0.75-1.3 mm. was reached, becoming constant at $\alpha = 2.45 \pm 0.01$ mm. min.⁻¹ $\equiv 8.60 \times 10^{16}$ quanta sec.⁻¹. At 100 mm. pressure, the conversion rate was also perfectly reproducible at $\beta = 35.3 \pm 0.3$ mm. min.⁻¹, indicating a chain length of about 15. But after two C runs using *ca.* 9.5 mm. of *n*-hexane, which gave $\gamma \approx 4.5$ mm. min.⁻¹, values of β became irreproducible, rising successively from 9 to 20 mm. min.⁻¹, although the values of α remained constant: subsequent values of γ lay in the range 3.1-5.6 mm. min.⁻¹ for $[RH] = 10$ mm.

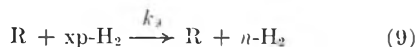
Furthermore, a drift in the values of γ was detected as each individual C run progressed, suggesting that the amount of hydrocarbon undergoing reaction was not negligible. The accumulation of liquid polymer in the reaction cell confirmed this conclusion and suggested a reasonable explanation of the behavior of β values obtained subsequent to a C run. The output of the lamp was reduced to about $1/20$ by masking ($\alpha = 0.136$ mm. min.⁻¹ $\equiv 0.477 \times 10^{16}$ quanta sec.⁻¹); this led to a marked improvement of the linearity of the γ plots but left the relative behavior of the β and γ unchanged.

Since the walls are obviously seriously affected by one C run, it is not feasible to use a clean reaction vessel each time because the effective value of β to be used in the rate expression is changing all the time the C run is in progress. Instead, we used a combined B/C procedure in which one run consisted of a large number of alternate B and C runs of very short duration carried out in rapid succession. In a typical run, the initial reaction mixture of para-rich hydrogen plus hydrocarbon was irradiated for 15 seconds, after which the hydrocarbon was frozen out by passing the gas through a liquid-air trap. A sample of the hydrogen was removed for analysis giving a value of γ and then the whole of the hydrogen was returned to the reaction vessel. A further irradiation for 15 seconds yielded a value of β , after which the whole of the hydrogen sample was re-mixed with the hydrocarbon, returned to the reaction vessel and the process repeated. Thus from the run, after five complete cycles of operation, an average of five values of β and five values of γ was obtained, in which variations in wall condition would approximately cancel out. All subsequent results were obtained in this manner.

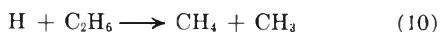
If β were constant and α small (actually $\beta/\alpha \approx 9$), then the rate expression suggests that the quantity $(\beta/\gamma - 1)$ should be approximately proportional to $[RH]$; our observations showed that over a concentration range of $[RH] = 0.080$ mm. to $[RH] = 21.7$ mm., β/γ remained approximately constant (about 2). Or, more precisely, the quantity $\{(\gamma - \alpha)^{-1} - (\beta - \alpha)^{-1}\}$, which should be directly proportional to $[RH]$, actually

increased very rapidly for small [RH], but became roughly independent of it above 10 mm. pressure. Some experiments carried out at 85° showed similar behavior.

Thus, the apparent elimination of wall contamination did not lead to sensible results, and in consequence part of the reason for the failure of the experiment must lie in the inadequacy of the assumed mechanism. A significant omission would appear to be



i.e., the paramagnetic conversion by radicals without reaction, which would vary with the degree of localization of the free electron on the R radical. It was decided to test this by changing the hydrocarbon RH. Methane could not be used because it was not easily separable from hydrogen, and ethane reacted with hydrogen atoms producing methane by



at too great a rate to apply a satisfactory correction. It was considered that propane would give a radical too similar to hexyl radical to produce an observable effect, and in consequence, fluoroform was chosen. The addition of 2 mm. CF₃H did not alter the conversion rate significantly, but 15 mm. increased the conversion rate to $\gamma = 1.12\beta$ (that reaction actually took place was demonstrated by exchange between D₂ and CF₃H upon irradiation). Similar experiments with C₂F₆ also increased the conversion rate to $\gamma = 1.10\beta$. In other words the primary effect was a slight reduction in the rate of diffusion of hydrogen atoms to the walls which was not taken into account in the reaction scheme, but the effect is relatively small and could not account for the observed independence of β/γ and [RH].

The intrusion of reaction 9 can only definitely be confirmed or excluded by studying the parallel system of RH + a mixture of H₂ and D₂ where there is no analogous reaction. However, a number of experiments using *n*-hexane and a 1/1 H₂/D₂ mixture showed that no results of significance were obtainable in the present apparatus because of the relative smallness of the resistance changes and the difficulty of correcting for the introduction of additional hydrogen into the system by exchange with the undeuterated hydrocarbon.

We conclude that the ortho-para conversion method, which has been used in the past³ to measure rate constants of reaction 7, is rendered inaccurate by the adsorption of the hydrocarbon and its decomposition products on the walls of the reaction cell and that, in addition, diffusion effects and some complications in the mechanisms of the individual reactions are also operative in preventing the useful exploitation of this technique.

Acknowledgment.—We are indebted to Dr. A. F. Trotman-Dickenson for suggesting this problem and for his collaboration in the early stages of this work.

RESOLUTION OF TRIS-OXALATO METAL COMPLEXES

By F. P. DWYER AND A. M. SARGESON

Contribution from the Departments of Chemistry, Northwestern, Evanston, Illinois and Sydney Universities, Sydney, Australia

Received February 20, 1956

At various times the resolution of the labile tris-oxalato complexes of aluminum, gallium and iron(III) have been reported, but subsequent attempts at resolution have frequently failed. A summary of the evidence has been presented by Johnson,¹ who himself failed with the iron and aluminum complexes, and Basolo² in a recent review. Since cations, hydroxyl and oxalate ions, have an accelerating influence on the rate of racemization of the tris-oxalato chromate(III) ion³ it was suggested by Basolo⁴ that the conflicting evidence could be due to the presence or absence of extraneous ions during the resolution.

Repetition of the work, using strychnine as the resolving agent for the aluminum^{5,6} and gallium⁷ complexes and *l*- α -phenylethylamine for the iron compound,⁸ in the presence or absence of hydrogen ions and/or oxalate ions, was fruitless. Small levorotations at various times, followed by subsequent loss of the rotation were traced to incomplete elimination and slow precipitation of the strychnine as the iodide. When the resolving agent was removed as the perchlorate no rotation was ever observed. It should be noted, however, that a dextrorotatory specimen of the tris-oxalatoaluminate ion has been claimed⁶ through the use of strychnine. It is also pertinent that addition of calcium chloride to a freshly prepared solution of potassium tris-oxalategallate gave an immediate precipitate of calcium oxalate—an observation also made by Moeller.⁹

When an aqueous alcoholic solution of *l*-tris-1,10-phenanthroline-nickel iodide or chloride (Ni phen₃)-I₂ was added to an aqueous solution of potassium *d,l*-tris-oxalato-cobaltate(III) the sparingly soluble green K-*l*-[Ni phen₃]-*d*-[Co(C₂O₄)₃]-H₂O separated immediately. The green solution remaining, on the addition of alcohol gave *l*-K₃Co(C₂O₄)₃. The dextro form was obtained from the diastereoisomer after elimination of the [Ni phen₃]⁺⁺ cation with potassium iodide and hydrogen peroxide.

This procedure was shown to be a rapid general method of resolution of tris-oxalato metal complexes by the separation of the antipodes of the Cr-(C₂O₄)₃^{'''} and Ru(C₂O₄)₃^{'''} ions. Though diastereoisomers of the same composition were obtained with Al(C₂O₄)₃^{'''} and Fe(C₂O₄)₃^{'''}, (hexahydrate with the iron compound instead of the usual monohydrate), no rotation was ever observed in the potassium salts precipitated with alcohol from the

(1) C. H. Johnson, *Trans. Faraday Soc.*, **31**, 1612 (1935).

(2) F. Basolo, *Chem. Revs.*, **52**, 459 (1952).

(3) D. Beese and C. H. Johnson, *Trans. Faraday Soc.*, **31**, 1632 (1935).

(4) F. Basolo, private communication.

(5) W. Wahl, *Ber.*, **60**, 399 (1927).

(6) G. J. Burrows and K. H. Lander, *J. Am. Chem. Soc.*, **53**, 3600 (1931).

(7) P. Neogi and N. K. Dutt, *J. Indian Chem. Soc.*, **15**, 83 (1938).

(8) W. Thomas, *J. Chem. Soc.*, **121**, 196 (1922).

(9) T. Moeller, private communication.

remaining solution. The operation was performed at 6–8° and not more than a minute elapsed between separation of the diastereoisomer and precipitation of the potassium salt. In one experiment with $K_3Al(C_2O_4)_3$ a slight precipitate of the diastereoisomer separated from the filtrate whilst the filtration was proceeding. This could be due to a slight optical activity being lost through a second-order asymmetric transformation. With both the iron and aluminum complexes, though an excess of resolving agent over the theoretical 1 mole of $[Ni(phen)_3]I_2$ to 2 moles of racemic potassium salt was used, practically all was consumed. This is consistent with failure to effect a resolution being due to optical lability. Similarly no evidence was obtained for the resolution of the tris-oxalato-gallate ion. The diastereoisomer was never obtained pure, and the analytical results suggest contamination with $[Ni(phen)_3]C_2O_4$.

Johnson¹ suggested that the magnetic moment of the tris-oxalatoruthenate should be indicative of whether or not resolution was possible. The moment (2.01 B.M.) indicates possibly covalent bonds. However, since Hund's rule does not necessarily apply to the second and third transitional series, the reliability of the magnetic criterion of bond type is questionable. Attempted resolution by Charonnat¹⁰ through the strychnine and quinine salts and by the method¹¹ of "active racemates" was unsuccessful. Attempts at resolution through the $Ni(phen)_3^{++}$ salt also were fruitless. Rapid racemization could occur through the momentary attainment of a 7- or 8-covalent structure containing aquo groups. This is quite feasible with the higher transitional elements.

Experimental

Specimens of potassium tris-oxalatoaluminum, -ferrate(III), -cobaltate(III) and -chromate(III), kindly supplied by Dr. Basolo, were crystallized from warm aqueous solution by the addition of alcohol and dried over calcium chloride in the dark. Potassium tris-oxalato-gallate and rhodate(III) were prepared as described.^{7,12} *d*- and *l*-tris-1,10-phenanthroline-nickel (II) iodides were obtained as described previously.¹³

Potassium Tris-oxalatoruthenate(III).—The method of Charonnat,¹⁰ operating with potassium pentachloro-aquo-ruthenate(III), was found to yield a product difficult to free from potassium chloride. The substance was best prepared by refluxing a mixture of ammonium pentabromohydroxy-ruthenate(IV) (2.4 g., 1 mole), oxalic acid dihydrate (1.5 g., 3 moles) and 30% formaldehyde (2 ml.) for 0.75 hr. and then adding gradually over a further 0.5 hr. potassium bicarbonate (2.0 g., 5 moles). The refluxing was continued until the color had changed from red to olive green. On protracted heating, the color becomes brown due to the formation of the tris-oxalatoruthenate(II) ion, but this easily reoxidizes in the air. After filtration, the warm solution was precipitated by the addition of alcohol. The green solid was crystallized from warm water containing drops of glacial acetic acid and a little potassium acetate, by the addition of alcohol.

Calcd. for $K_3Ru(C_2O_4)_3 \cdot 3H_2O$: Ru, 18.5. Found: Ru, 18.7.

Potassium *d*- and *l*-Tris-oxalato-cobaltate (III).—*dl*- $K_3Co(C_2O_4)_3$ (0.7 g.) was dissolved in water (14 ml.) with potassium acetate (1 g.) and cooled in ice. An ice-cold solution of *l*- $[Ni(phen)_3]I_2$ (1 g. in 12 ml. H_2O + 12 ml. alcohol) was

added and the sides of the flask scratched to facilitate the deposition of the bright green diastereoisomer.

The solution was quickly filtered and cold alcohol added until the *l*- $K_3Co(C_2O_4)_3$ had precipitated. The diastereoisomer and the active salt were washed with cold absolute alcohol and dried in a vacuum desiccator. The optical isomer may be recrystallized from a little cold water and cold alcohol.

The diastereoisomer was suspended in cold water (20 ml.) and potassium iodide (1 g.), acetic acid (2 drops, 17 *N*) and hydrogen peroxide (2 ml., 3%) added to the suspension and well shaken. The mixture was cooled for 2–3 minutes, filtered and the *d*- $K_3Co(C_2O_4)_3$ precipitated from the filtrate with cold absolute alcohol.

In 0.016% aqueous solution it gave $[\alpha]^{20}_D \pm 4050^\circ$, and in 0.04% solution $[\alpha]^{20}_{5461} \pm 1375^\circ$. These are considerably higher than those reported previously: Delépine,¹¹ $[\alpha]_D^{20}$ 1750°; Jaeger,¹⁴ 250°; Johnson and Mead,¹⁵ <2000°.

Calcd. for $C_{42}H_{26}O_{13}N_6KCoNi$: C, 52.13; H, 3.10; N, 8.58. Found: C, 52.1; H, 3.1; N, 8.6.

Potassium *d* and *l*-Tris-oxalatochromate(III).—The resolution was performed as above with the cobalt complex. The *d*-form was obtained from the diastereoisomer. The specific rotations are higher than previously recorded: $[\alpha]^{20}_D$ 1640, $[\alpha]^{20}_{5461}$ 0.0°; compared with $[\alpha]_D$ 420° (Jaeger¹⁴) and 1170° (Johnson and Mead¹⁵).

Calcd. for $C_{42}H_{26}O_{13}N_6KCrNi$: C, 51.99; H, 2.98; N, 8.66. Found: C, 51.8; H, 3.0; N, 8.6.

Potassium *d* and *l*-Tris-oxalatorhodate(III).—The levorform was obtained from the diastereoisomer. The specific rotations $[\alpha]^{20}_D \pm 85^\circ$ are in good agreement with Delépine's,¹¹ $\alpha_D \pm 87^\circ$.

Calcd. for $C_{42}H_{26}O_{13}N_6KRhNi$: C, 49.31; H, 2.54; N, 8.21. Found: C, 49.1; H, 2.6; N, 8.2.

Unsuccessful Resolutions.—The procedure above gave the required diastereoisomer with the Al, Fe(III) and Ru(III) compounds. The gallium compound was impure. No rotation was observed with the precipitated potassium salt, nor did the diastereoisomer mutarotate in 15 minutes at 15°.

Calcd. for $C_{42}H_{26}O_{13}N_6KAlNi$: C, 52.7; H, 3.1; N, 8.78. Found: C, 53.3; H, 3.0; N, 8.8.

Calcd. for $C_{42}H_{26}O_{13}N_6KFeNi$: C, 47.34; H, 3.4. Found: C, 47.3; H, 3.4.

Calcd. for $C_{42}H_{26}O_{13}N_6KRuNi$: C, 49.33; H, 2.55; N, 8.23. Found: C, 49.2; H, 2.6; N, 8.15.

Calcd. for $C_{42}H_{26}O_{13}N_6KGaNi$: C, 47.58; H, 2.45. Found: C, 53.30; H, 3.68.

(14) F. M. Jaeger, *Rec. trav. chim.*, **38**, 147 (1919).

(15) C. Johnson and A. Mead, *Trans. Faraday Soc.*, **31**, 1621 (1938).

A METHOD FOR DETERMINING RATE EQUATIONS FOR REACTIONS IN WHICH THE CONCENTRATION OF THE REACTANT IS UNKNOWN¹

By JOSEPH H. FLYNN²

National Bureau of Standards, Washington, D. C.

Received March 15, 1956

In the study of reactions of complex substrates cases occur in which the concentration of the reacting species cannot be determined. In these cases it is sometimes difficult to fit experimental kinetic data to an equation using the common "differential" and "integral" methods of kinetic analyses since the expression for the degree of advancement of the reaction is dependent upon knowledge of the initial concentration of reacting

(10) R. Charonnat, *Compt. rend.*, **178**, 96 (1924).

(11) M. Delépine, *Bull. soc. chim.*, **1**, 1256 (1934).

(12) E. Leidie, *Ann. chim.*, [6] **17**, 307 (1913).

(13) F. P. Dwyer and E. C. Gyarfas, *J. Proc. Roy. Soc. N.S.W.*, **83**, 232 (1950).

(1) Presented at the 127th Meeting of the American Chemical Society, Cincinnati, Ohio, March, 1955.

(2) National Bureau of Standards, Washington 25, D. C.

species or the total amount of a product formed at infinite time.

Most chemical reactions may be represented by a first order, first degree differential equation expressing the rate, dx/dt , as a function of x , where x is a linear function of the degree of advancement or extent of reaction. The elimination of x between the differential equation and its integrated form results in an expression for dx/dt as a function of t . Therefore, since the amount of non-reactive product formed in a reaction is ordinarily a linear function of the degree of advancement, experimental determination of the rate of formation of an inactive product permits a test for differential rate equations.

Chemical reactions in which the rate is proportional to a power of the concentration of a single reactant may be represented by the equation

$$\frac{dx}{dt} = k(a - x)^n \quad (1)$$

where k and a are constants that may contain stoichiometric relationships and initial concentrations, and n is defined as the order of the reaction. The rate equations for chemical reactions, in which several reactants contribute to the rate in proportion to powers of their concentrations, may be reduced to equation 1 when contributing reactants are present in stoichiometric amounts. First-order reversible reactions and simultaneous zero and first-order reactions also may be reduced to equation 1.

From the elimination of $(a - x)$ between equation 1 and its integrated form, one obtains

$$\log \frac{dx}{dt} = 0.4343kt + \log ak \quad (n = 1) \quad (2)$$

and

$$\frac{dx^{1-n/n}}{dt} = (n-1)k^{1/n}t + k^{1-n/n}a^{1-n} \quad (n \neq 1) \quad (3)$$

Therefore, if the rate of formation of a product can be determined as a function of time, a straight line relationship between the time and an appropriate function of this rate will constitute a test for a particular order. Values of k and a can be obtained from the slope and intercept of this straight line.

This method may be applied to data obtained from the irradiation of dried purified cellulose in a vacuum with 2537 Å. light.³ The pressure of the evolved hydrogen was measured manometrically in a system which was alternately evacuated and closed off for five-minute periods during the six hours of irradiation. Thus, the hydrogen pressure was kept below 0.03 mm. to avoid a pressure dependent inhibition. Figure 1 indicates a linear relationship between the square of the reciprocal of the rate of hydrogen evolution and the time. Therefore the rate of hydrogen evolution follows the parabolic law, ($n = -1$)

$$\frac{dx^{-2}}{dt} = -\frac{2t}{k} + \frac{a^2}{k^2} \quad (4)$$

For the particular conditions of the experiment $a = -0.300$ mm., $k = -3.80 \times 10^{-5}$ (mm.)²/sec., and equation 1 becomes

(3) Unpublished work of the author.

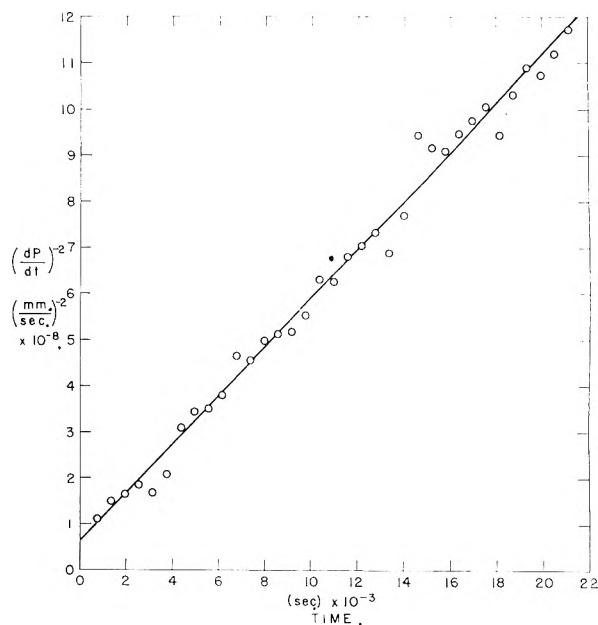


Fig. 1.—(Rate of hydrogen pressure increase)⁻² vs. time of irradiation of cellulose in a vacuum with 2537 Å. light.

$$\frac{dx}{dt} = \frac{3.80 \times 10^{-6}}{0.300 + x} \quad (5)$$

indicating a zero-order rate of hydrogen formation, inhibited by a product of the irradiation.

THE HEATS OF FORMATION OF Na₂O₂, NaO₂ and KO₂^{1,2}

BY PAUL W. GILLES AND JOHN L. MARGRAVE³

Department of Chemistry, University of Kansas, Lawrence, Kansas

Received March 15, 1956

The alkali metals and oxygen form more than the usual variety of compounds. There are M₇O, M₄O, M₃O, M₁O₂ suboxides, M₂O normal oxides, M₂O₂ peroxides, M₂O₃ sesquioxides, MO₂ superoxides and MO₃ ozonides. For an excellent summary of the properties of these compounds and literature citations, reference to the recent review by Brewer⁴ should be made.

The superoxides of potassium, rubidium and cesium are obtained by combustion of the metals or lower oxides, and have been known for many years, but only recently have attempts to prepare NaO₂ been successful.⁵⁻⁷

Because of our proximity to this work, we became interested in the stabilities of the superoxides, their dissociation behavior and the best

(1) Abstracted in part from the thesis by John L. Margrave submitted in partial satisfaction of the requirements for the degree of Doctor of Philosophy at the University of Kansas, December 28, 1950.

(2) Presented before the Division of Physical and Inorganic Chemistry at the 117th Meeting of the American Chemical Society, Detroit, Michigan, April 19, 1950, and at the 118th Meeting of the American Chemical Society, Chicago, Illinois, September 7, 1950.

(3) University of Wisconsin, Madison, Wisconsin.

(4) L. Brewer, *Chem. Revs.*, **52**, 1 (1953).

(5) W. H. Schechter, H. H. Sleser and J. Kleinberg, *J. Am. Chem. Soc.*, **70**, 267 (1948).

(6) W. H. Schechter, J. K. Thompson and J. Kleinberg, *ibid.*, **71**, 1816 (1949).

(7) S. E. Stephanou, W. H. Schechter, W. J. Argersinger, Jr., and J. Kleinberg, *ibid.*, **71**, 1819 (1949).

TABLE I
HEATS OF REACTION OF NaO₂, Na₂O₂ AND KO₂ WITH WATER

Compound	Analyses ^b (wt. %)	cal./g. obsvd.	ΔH reaction, ^c kcal./mole (for pure oxide)	Concn. of final soln., moles H ₂ O/mole MOH
NaO ₂	NaO ₂ = 94%	300.8 ± 1.8 (5 runs)	16.3 ± 0.6	3500
	Na ₂ O ₂ = 6%			
	Na ₂ CO ₃ = not done			
NaO ₂	NaO ₂ = 93.8%	288.4 ± 0.3 (3 runs)	15.6 ± 0.3	3800
	Na ₂ O ₂ = 6.2%			
	Na ₂ CO ₃ = not done			
NaO ₂ ^a	NaO ₂ = 94.0%	302.1 ± 1.2 (2 runs)	16.7 ± 0.3	4800
	Na ₂ O ₂ = 4.4%			
	Na ₂ CO ₃ = 1.6%			
NaO ₂ ^a	NaO ₂ = 92.5%	275.5 ± 1.2 (2 runs)	14.6 ± 0.3	9000
	Na ₂ O ₂ = 6.0%			
	Na ₂ CO ₃ = 1.5%			
NaO ₂ ^a	not done, but same sample as above	294.7 (1 run)	15.9 ± (0.3)	6770
Na ₂ O ₂ (white)	Na ₂ O ₂ = 99.2%	437.9 ± 4.1 (3 runs)	34.0 ± 0.3	3800
	Na ₂ O = 0.8%			
	Na ₂ CO ₃ = not done			
KO ₂	KO ₂ = 92.4%	193.5 ± 0.9 (2 runs)	12.5 ± 0.6	6850
	K ₂ O = 3.2%			
	K ₂ CO ₃ = 2.8%			
	Na ₂ O ₂ = 1.6%			
KO ₂ ^a	KO ₂ = 91.1%	204.1 ± 8.1 (2 runs)	12.8 ± 1.1	13, 100
	K ₂ O = 3.4%			
	K ₂ CO ₃ = 2.2%			
	Na ₂ O ₂ = 3.3%			
KO ₂ ^a	KO ₂ = 93.4%	207.9 ± 8 (1 run)	15.2 ± 0.8	11, 700
	K ₂ CO ₃ = 4.2%			
	Na ₂ O ₂ = 2.4%			

^a Runs made with Berkeley calorimeter. ^b Maximum error in analyses is ±1% except for the first NaO₂ sample used for the first 5 runs where the error in analysis may be ±2%. ^c The maximum limit of error stated for the heat of reaction of the pure compound includes allowance for both the error in the analysis and the error in observing the heat of reaction.

conditions for their preparation. This note presents the results of measurements of the heats of reactions of Na₂O₂, NaO₂ and KO₂ with water. The values are used with available thermochemical data⁸ to calculate the heats of formation.

The samples used in this work were furnished through the courtesy of Drs. C. B. Jackson and W. H. Schechter of the Callery Chemical Company. The KO₂ was prepared by atomizing liquid potassium into an oxygen atmosphere at about 300°; the Na₂O₂ by oxidation of sodium metal; and the superoxide by high pressure oxidation of the peroxide. Prof. Jacob Kleinberg and Dr. Edgar Seyb kindly furnished some NaO₂ samples. Unfortunately, the quality of peroxides and superoxides was not high. There is, as yet, no simple way to determine just what the major contaminants in these materials are, although hydroxides, hydroxide hydrates, carbonates and peroxide hydrates appear likely. The samples were analyzed by (1) measuring the volume of oxygen evolved by a known weight of compound dissolved in water in the presence of MnO₂; (2) titrating the resulting solution to the phenolphthalein and methyl orange points; (3) spectroscopic analysis; (4) X-ray diffraction; and (5) quantitative analysis for metals. Final analyses represent the best set of substances and percentages for agreement with the analytical data.

The materials were received in sealed containers in the form of lumps weighing 5-25 g. or in the form of powder. Different lumps in the same shipment were sometimes different in appearance, and even within the same lump inhomogeneity was often indicated by variations in color. In order to achieve rapid reaction in the calorimeter, the samples were crushed to about 250 mesh. The materials were handled in a dry box in a nitrogen or argon atmosphere.

Nevertheless, the possibility of contamination by atmospheric water or carbon dioxide, and the uncertainty as to the nature of the impurities present make the analysis of these materials the major uncertainty in this work.

Final interpretation of the thermodynamic properties of these substances must wait until highly pure samples are obtained, or until available contaminated samples can be completely analyzed.

The thermal measurements were carried out in two different calorimeters. One was constructed for this investigation. It consisted of a 1.5-l. Dewar flask fitted with a rubber stopper through which the stirrer, breaking mechanism, gas escape tube and electrical leads passed. The copper thermometer and manganin heater were wound between two silver cylinders. Both electrical and chemical calibrations of the calorimeter were made in the usual way. While one of us (JLM) was an AEC postdoctoral fellow, additional measurements were made with the calorimeter in the Department of Chemistry at the University of California at Berkeley, which has been described previously.⁹

In the presence of MnO₂(s) to catalyze the decomposition of peroxides in solution, the substances react with water according to the reactions



The results are given in Table I. The third column gives the values of the heat evolved per gram of sample. The fourth column contains the values of ΔH for the solution reaction as given in one of the two equations above. The value has been corrected for the impurities listed in the

(8) "Selected Values of Chemical Thermodynamic Properties," National Bureau of Standards, Circular 500 (1952).

(9) W. M. Latimer and H. W. Zimmerman, *J. Am. Chem. Soc.*, **61**, 1550 (1939); B. J. Fontana, "NNEs IV-19B," McGraw-Hill Book Co., New York, N. Y., 1950, p. 321.

second column. If other impurities are assumed, different heats will be obtained.

The NaO_2 results show discrepancies among the different groups of runs far beyond the expected experimental error. These arise either because the analytical sample was not the same, in all cases, as the calorimetric sample, or because the calorimetric sample underwent a reaction after the analysis. A reaction with water to form NaOH causes the heat of solution per gram to become smaller. A decomposition to Na_2O_2 causes the heat of solution per gram to increase.

The second and third group of NaO_2 samples were from the same stock. The experiments were separated by a three-month interval. The fourth and fifth groups of samples were sealed into calorimetric bulbs at the same time from the same stock. The experiments were separated by a four-month interval. The results appear to indicate that a slow decomposition to Na_2O_2 may occur and that low heat of solution values should be the most nearly correct. On the other hand, samples stored in sealed containers over long periods showed no great increase in pressure as would result from such decomposition. To obtain the final value, all the results have been averaged. For reaction (2) involving NaO_2 , $\Delta H = -15.9 \pm 0.7$ kcal./mole.

The different groups of samples of KO_2 show wide variation also, attributable to similar causes. The average of the five runs gives $\Delta H = -13.2 \pm 0.8$ kcal./mole for reaction (2) involving KO_2 .

The results have been used together with existing data to calculate the heats of formation given in Table II.

TABLE II
HEATS OF FORMATION AT 298°K. IN KCAL./MOLE

Compound	de Forcrand ^a	Kaule and Roth ^b	Kazarnovskaya and Kazarnovskii ^c	This work
Na_2O_2	-119.3 ^d	-121.2 ^d	...	-122.1 ± 1.2
NaO_2	(-65.0) ^e	-62.1 ± 0.7
KO_2	-66.8 ± 0.8 ^d	...	-67.9	-67.6 ± 0.8

^a R. de Forcrand, *Compt. rend.*, 127, 514 (1898); 158, 843, 991 (1914). ^b H. Kaule and W. Roth, *Z. anorg. Chem.*, 253, 352 (1947); 255, 324 (1948). ^c L. Kazarnovskaya and I. Kazarnovskii, *Zhur. Fiz. Khim.*, 25, 293 (1951). ^d Values recalculated from original experimental data but with heats of formation of aqueous solutions taken from NBS tables. ^e Indicate estimated values.

Through the courtesy of K. K. Kelley of the Pacific Experiment Station of the Bureau of Mines, the low temperature heat capacities of some of these samples have been measured by Todd¹⁰ who reported the entropies at 298°K. In spite of the entropies and the heats of formation that are now available, it does not appear to be possible to establish unequivocally the decomposition behavior of the sodium oxides. The reasons for this situation are (1) high temperature heat capacity data are lacking, and (2) the nature of the solid phases produced by decomposition of the superoxide is not clear. The crystal structure of pure Na_2O_2 is not definitely known, and published lattice con-

stants for $\text{NaO}_2(\text{s})$ indicate a possibility for extensive solid solution.

We are pleased to acknowledge the financial assistance of the Atomic Energy Commission. We are indebted to Drs. Jackson, Schechter, Kleinberg, and Seyb for the samples, and to the late Prof. W. M. Latimer for the use of the University of California calorimeter.

VERIFICATION BY CHROMATOGRAPHY OF THE THERMAL FORMATION OF BARIUM AND LEAD TETRAPOLYPHOSPHATES

BY ROBERT P. LANGGUTH,¹ R. K. OSTERHELD AND E. KARL-KROUPA

Department of Chemistry, Cornell University, Ithaca, N. Y., and Inorganic Chemicals Research Division, Monsanto Chemical Company, Dayton, Ohio

Received March 16, 1956

In an earlier article,² thermal analysis and X-ray diffraction data were used to show that lead tetrapolyphosphate was the only crystalline polyphosphate to form thermally between the lead pyrophosphate and lead tetrametaphosphate compositions. An attempt was made during that study to investigate the reactions occurring in the barium pyrophosphate—barium tetrametaphosphate system. A phase diagram could not be constructed for the system as high temperatures were required which could not be attained with the thermal analysis equipment available. X-Ray diffraction data did show that a barium polyphosphate formed within the system, but the X-ray data were insufficient to identify it.

Recently, chromatographic techniques have been developed which can be used to distinguish the various species of phosphates.³ This method has been used to establish the identity of the barium polyphosphate and to confirm the identity of the lead tetrapolyphosphate.

Experimental

Mixtures of barium monohydrogen and dihydrogen orthophosphate were heated to constant weight at 550°, a temperature above the thermal decomposition temperatures of the individual reactants, but below the temperature of appearance of any liquid phase. The products were ground thoroughly and reheated at 550° for 12 hours to ensure complete reaction.

The sample of lead tetrapolyphosphate was one of the series of samples used to obtain the thermal analysis data reported in the earlier paper.

Samples of the reaction products corresponding in composition to barium tripolyphosphate and tetrapolyphosphate were taken for chromatographic analysis, since these compounds might be expected to form in the barium system in the composition range studied. These samples were converted to the sodium salts in solution by use of the sodium form of Amberlite IR-120 cation-exchange resin. The lead tetrapolyphosphate was converted to the sodium salt by reaction in solution with sodium carbonate.

One- and two-directional paper chromatograms were run on the samples. The developed chromatograms showed

(1) Inorganic Chemicals Division Research, Monsanto Chemical Company, Dayton 7, Ohio.

(2) R. K. Osterheld and R. P. Langguth, *THIS JOURNAL*, 59, 76-80 (1955).

(3) J. P. Ebel, *Bull. soc. chim. France*, 20, 991, 998 (1953); E. Karl-Kroupa, article submitted to *Anal. Chem.* for publication.

(10) S. S. Todd, *J. Am. Chem. Soc.* 75, 1229 (1953).

clearly defined spots. The percentages of the various phosphate species were estimated semi-quantitatively by the aid of reference samples run on the same chromatogram with the sample and are given in Table I.

TABLE I

CHROMATOGRAPHIC ANALYSIS OF POLYPHOSPHATE SAMPLE

Phosphorus as	% of total phosphorus sample corresponding to		
	Ba ₄ (P ₃ O ₁₀) ₂	Ba ₃ P ₄ O ₁₃	Pb ₂ P ₄ O ₁₃
PO ₄ ³⁻	<2	<2	<2
P ₂ O ₇ ⁴⁻	30	10	<5
P ₃ O ₁₀ ⁵⁻	5	<2	<5
P ₄ O ₁₃ ⁶⁻	60	75	85
Long chain (P ₃) _n	<2	10	<2

Discussion

The data in Table I show that in the barium system, barium tetrapolyphosphate is the principal polyphosphate that forms thermally between the barium pyrophosphate and barium tetrametaphosphate compositions. The minor quantities of the other phosphate species can be considered the result of either incomplete thermal reaction or hydrolysis during the conversion to sodium salt with the ion-exchange resin. The 30% of the total phosphorus as pyrophosphate in the sample corresponding to tripolyphosphate is the quantity expected in a sample of that over-all composition. The X-ray diffraction data for the new compound, barium tetrapolyphosphate, and those for barium pyrophosphate and barium tetrametaphosphate are given in Table II.

TABLE II

X-RAY DIFFRACTION DATA FOR BARIUM PHOSPHATES

Ba ₂ P ₂ O ₇		Ba ₃ P ₄ O ₁₃		Ba ₂ (PO ₃) ₄	
d	Int.	d	Int.	d	Int.
3.93	vs	5.10	w	5.16	w
3.58	m	4.66	w	4.24	m
3.37	w	4.19	w	3.76	vw
3.07	w	3.97	w	3.39	vs
2.81	s	3.76	w	3.18	m
2.71	s	3.58	s	3.00	vs
2.32	m	3.44	w	2.70	vw
2.24	w	3.38	w	2.56	vw
2.15	m	3.30	s	2.52	w
2.11	w	2.99	w	2.36	vw
2.03	w	2.93	w	2.25	vs
1.81	w	2.79	m	2.15	w
1.76	w	2.72	w	2.07	w
1.72	w	2.60	w	2.01	w
1.62	w	2.54	w	1.86	w
1.58	w	2.23	m	1.70	w
1.54	w	2.19	w	1.64	w
1.48	w	2.13	vw	1.60	w
1.46	w	2.10	m	1.55	w
1.41	w			1.52	w
1.35	w				

The chromatographic analysis of the lead tetrapolyphosphate sample is in accord with the conclusions reported in the earlier paper based on the phase diagram for the system. The minor quantities of other phosphate species may be attributed to incomplete thermal reaction and hydrolysis during conversion to the sodium salt.

OBVIATION OF SOLUTION DENSITY MEASUREMENTS IN ELECTRIC MOMENT DETERMINATIONS

By GEORGE K. ESTOK

Dept. of Chemistry and Chemical Engineering, Texas Technological College, Lubbock, Texas

Received March 19, 1956

In the determination of electric moments by the dilute solution method considerable time is generally spent in measuring densities. Satisfactory density, d , or specific volume, v , data, however, may be calculated on the assumption of additivity of volumes of solvent and solute as determined from the densities of the pure substances.

Guggenheim¹ has suggested a method which eliminates entirely the need for solution density data, but substitutes in turn the measurement of refractive indices. Treiber and Porod² indicated a method requiring only dielectric constant measurements, assuming additivity of molar volumes of solute and solvent as a substitute for solution density measurements. The working form of their equation for polarization is somewhat inconvenient. In addition, the reliability of the method has not been sufficiently substantiated by comparison with experimental work.

Inasmuch as most workers still report data based on density measurements, it appears that the matter of eliminating such measurements deserves further consideration and simplification.

Subscripts used in the following discussion have their usual significance: *i.e.*, 1, solvent; 2, solute; 12, solution.

Concentrations of solutions are most commonly expressed as mole fraction solute, x_2 , or weight fraction solute, w_2 . The use of w_2 does much to simplify many calculations.

In the Hedestrand method, or its many modifications, values of $\Delta v_{12}/\Delta w_2$, $\Delta d_{12}/\Delta w_2$, $\Delta v_{12}/\Delta x_2$ or $\Delta d_{12}/\Delta x_2$ are used by various authors. The ratio $\Delta v_{12}/\Delta w_2$ is generally the most convenient and will be stressed in the following discussion.

A convenient form of the equation for specific polarization of the solute at infinite dilution is that of Halverstadt and Kumler³

$$p_{2\infty} = \left(\frac{\epsilon_1 - 1}{\epsilon_1 + 2} \right) (v_1 + \beta) + \frac{3v_1\alpha}{(\epsilon_1 + 2)^2} \quad (1)$$

where ϵ_1 = diel. const., solvent; v_1 = spec. vol., solvent

$$\beta = \Delta v_{12}/\Delta w_{2\infty}, \text{ and } \alpha = \Delta \epsilon_{12}/\Delta w_{2\infty}$$

Noting that Δw_2 (from $w_2 = 0$ to some finite value of w_2) is numerically equal to w_2 , and assuming additivity of volumes of solute and solvent, the following equation may be written

$$\Delta v_{12}/\Delta w_{2\infty} = \frac{1}{w_2} \left[\frac{m_1 v_1 + m_2 v_2}{m_{12}} - v_1 \right] \quad (2)$$

where m = weight in grams.

Equation 2 may be reduced algebraically to the form

$$\Delta v_{12}/\Delta w_{2\infty} = v_2 - v_1 \quad (3)$$

(1) E. A. Guggenheim, *Trans. Faraday Soc.*, **47**, 573 (1951).(2) E. Treiber and G. Porod, *Monatsh.*, **80**, 481 (1949).(3) I. F. Halverstadt and W. D. Kumler, *J. Am. Chem. Soc.*, **64**, 2988 (1942).

Where $\Delta d_{12}/\Delta w_{2\infty}$ values are desired the corresponding equation is as

$$\Delta d_{12}/\Delta w_{2\infty} = \frac{1}{w_2} \left[\frac{m_{12}}{m_1 v_1 + m_2 v_2} - d_1 \right] \quad (4)$$

This is not as readily simplified as is eq. 2. However, application of L'Hospital's rule for solving indeterminate forms yields the limiting straight line equation

$$\Delta d_{12}/\Delta w_{2\infty} = - \left(\frac{v_2 - v_1}{v_1^2} \right) = -d_1^2(v_2 - v_1) \quad (5)$$

Changes of v_{12} or d_{12} with respect to x_2 are obtainable from the following relation (valid at infinite dilution)

$$\Delta d_{12}/\Delta x_{2\infty} \text{ (or } \Delta v_{12}/\Delta x_{2\infty}) = \Delta d_{12}/\Delta w_{2\infty} \text{ (or } \Delta v_{12}/\Delta w_{2\infty}) \times \frac{M_2}{M_1}$$

where M is molecular weight.

When the solute is a liquid its density (or specific volume) is normally measured as a physical constant. When the solute is a solid the method is not general, but may be used when a value of v_2 for the substance as a liquid at solution temperature is available. Several ways of obtaining data on solid substances are: (1) measurement of density of the supercooled liquid; (2) extrapolation of densities determined above the melting point; (3) calculation of approximate densities from the densities of certain closely related substances.

Solution data for about fifty compounds were analyzed, and the values of $(v_2 - v_1)$ compared favorably with the $\Delta v_{12}/\Delta w_{2\infty}$ values based on experiment.

Table I includes data on thirty of these compounds in benzene solution, as well as three compounds in dioxane solution. The substances are arranged under three headings for more convenient consideration.

Values of specific volume, v_2 , for compounds in groups (A) and (B) were obtained from published data on liquids or melts at 25°, or extrapolation or interpolation of such data at other temperatures. Data for formamide and propionamide, however, are at 30°.

In group (C) the values of v_2 are based on a density additivity principle analogous to that used to calculate molar refractions from related substances. Although additivity of densities is not a generally valid principle, nevertheless for certain compounds of rigid structure it is useful. Thus, at 25°, the density of aniline (1.0174) plus the density of chlorobenzene (1.1008) less the density of benzene (0.8737) yields 1.2445 as the "contributing density" of *p*-chloroaniline in an ideal solution. The case of sulfanilamide illustrates an interesting example. Benzenesulfonamide itself is a solid. However, from published data of β (*i.e.*, $\Delta v_{12}/\Delta w_{2\infty}$) in dioxane solution by Kumler and Halverstadt,⁴ and eq. 3, it is possible to obtain a density value for benzenesulfonamide for use in calculating the density, and hence v_2 , for sulfanilamide.

Agreement between $(v_2 - v_1)$ and $\Delta v_{12}/\Delta w_{2\infty}$ values based on measurements is quite good, particularly

(4) W. D. Kumler and I. F. Halverstadt, *J. Am. Chem. Soc.*, **63**, 2183 (1941).

TABLE I

COMPARISON OF CALCULATED AND OBSERVED VALUES OF $\Delta v_{12}/\Delta w_{2\infty}$ IN BENZENE SOLUTION AT 25°^a
Benzene $v_1 = 1.145$ (25°), 1.152 (30°); dioxane $v_1 = 0.973$ (25°)

Compound	v_2	$v_2 - v_1$	$\Delta v_{12}/\Delta w_{2\infty}$ obsd.
(A) "Normal" Liquids			
<i>o</i> -Bromoanisole	0.665	-0.480	-0.473 ^t
Bromobenzene	.672	-.473	-.481 ^c
Ethyl dichloroacetate	.783	-.362	-.362 ^d
4-Chloropyridine	.833	-.312	-.301 ^e
Ethyl chloroacetate	.867	-.278	-.268 ^f
Triethyl phosphate	.940	-.205	-.209 ^f
Benzylideneacetone	.973	-.172	-.178 ^g
<i>p</i> -Tolualdehyde	.985	-.160	-.160 ^g
Tri- <i>n</i> -butyl thiophosphate	1.019	-.126	-.127 ^f
Ethyl methyl ketone	1.244	0.099	0.100 ^h
(B) "Associative" types			
Trichloroacetic acid	0.612	-0.533	-0.529 ^d
Dichloroacetic acid	.643	-.502	-.494 ^d
Benzoic acid	.853	-.292	-.280 ⁱ
Phenol	.934	-.211	-.209 ⁱ
Acetic acid	.958	-.187	-.141 ^d
<i>n</i> -Butyric acid	1.050	-.095	-.081 ^d
<i>n</i> -Caproic acid	1.083	-.062	-.049 ^d
Ethyl alcohol	1.274	0.129	0.150 ^j
<i>n</i> -Butylamine	1.366	.221	.235
Formamide (30°)	(0.889)	(-0.263)	(-0.304) ^k
Propionamide (30°)	(1.006)	(-.146)	(-.145) ^k
Benzoic acid (dioxane)	(0.853)	(-.120)	(-.130) ^l
(C) Solid disubstituted benzenes			
<i>p</i> -Dinitrobenzene	0.656	-0.489	-0.477 ^m
<i>p</i> -Nitroaniline	.744	-.401	-.425
<i>p</i> -Chloroaniline	.802	-.343	-.337
Ethyl <i>p</i> -aminobenzoate	.843	-.302	-.279
<i>p</i> -Aminoacetophenone	.856	-.289	-.290
<i>p</i> -Aminobenzonitrile	.874	-.271	-.285
<i>p</i> -Methoxycinnamonnitrile	.877	-.268	-.240
<i>p</i> -Dimethylaminobenzaldehyde	.893	-.252	-.244
<i>p</i> -Methoxybenzonnitrile	.896	-.249	-.244
<i>p</i> -Aminobenzoic acid (dioxane)	(0.760)	(-0.213)	(-0.238) ⁿ
Sulfanilamide (dioxane)	(0.637)	(-.336)	(-.337) ⁿ

^a Unless otherwise indicated; also all values without superior letter are from: C. Curran and G. K. Estok, *J. Am. Chem. Soc.*, **72**, 4575 (1950); ^b W. F. Anzilotti and B. C. Curran, *ibid.*, **65**, 607 (1943); ^c M. M. Otto and H. H. Wenzke, *Ind. Eng. Chem., Anal. Ed.*, **6**, 187 (1934); ^d R. J. W. LeFevre and H. Vine, *J. Chem. Soc.*, 1799 (1938); ^e D. G. Leis and B. C. Curran, *J. Am. Chem. Soc.*, **67**, 79 (1945); ^f G. K. Estok and W. W. Wendlandt, *ibid.*, **77**, 4767 (1955); ^g G. K. Estok and J. S. Dehn, *ibid.*, **77**, 4768 (1955); ^h G. K. Estok and J. H. Sikes, *ibid.*, **75**, 2745 (1953); ⁱ J. W. Williams, and R. J. Allgeier, *ibid.*, **49**, 2416 (1927); ^j F. E. Hoecker, *J. Chem. Phys.*, **4**, 431 (1936); ^k W. W. Bates and M. E. Hobbs, *J. Am. Chem. Soc.*, **73**, 2151 (1951); ^l C. J. Wilson and H. H. Wenzke, *ibid.*, **57**, 1265 (1935); ^m C. G. LeFevre and R. J. W. LeFevre, *J. Chem. Soc.*, 957 (1935); ⁿ G. K. Estok, unpublished data.

with respect to the group (A) compounds. In group (B) only acetic acid and formamide have deviations over 0.04. The higher molecular weight

molecules in this group exhibit quite satisfactory behavior. Deviations of 0.02–0.03 are not uncommon in group (C). This is not unexpected in view of the approximate nature of v_2 for these solids. It should be realized that in many cases considerable doubt also attaches to the experimentally extrapolated values.

In order to test the influence of the deviations on the moments, several have been calculated using both data. In all cases where the moment is not too small the effect is negligible (less than 0.01 D). In the following Table II are given moment values from the conventional method, and $\Delta\mu$, caused by using ($v_2 - v_1$).

TABLE II
MOMENT DEVIATIONS CAUSED BY USE OF ($v_2 - v_1$)

Compound	μ_{obsd}	$\frac{\Delta\mu}{D}$
<i>p</i> -Dinitrobenzene	~0.5 D	-0.03
4-Chloropyridine	.84	-.01
<i>n</i> -Butylamine	1.32	-.008
Benzoic acid (dioxane)	1.71	.004
Ethyl <i>p</i> -aminobenzoate	3.30	-.009
Formamide	3.37	.004
<i>p</i> -Aminobenzonitrile	5.96	.002
<i>p</i> -Nitroaniline	6.31	.005

The published values of about 0.5 and 0.84 D for *p*-dinitrobenzene and 4-chloropyridine, respectively, are much more doubtful than the values of $\Delta\mu$ indicated for them. For the other moments above 1.00 D , the deviations are negligible.

From the foregoing it is seen that solution density measurements are unnecessary when a value for v_2 , the specific volume of the solute (as a liquid), is available. Furthermore, it is actually unnecessary to calculate a value for ($v_2 - v_1$) since eq. 1 in this method reduces to the simpler form

$$p_{2\infty} = \left(\frac{\epsilon_1 - 1}{\epsilon_1 + 2} \right) v_2 + \frac{3v_1\alpha}{(\epsilon_1 + 2)^2} \quad (6)$$

and v_1 is eliminated entirely from the first term. Electric moments determined using eq. 6 should be just as reliable as those determined by the conventional method. In addition, this method would lead to a degree of standardization in the calculations of various workers.

SOME ADSORPTION DATA ON ACETYLENE BLACK

By MAX J. KATZ

Signal Corps Engineering Laboratories, Fort Monmouth, N. J.

Received March 27, 1956

A considerable literature has evolved on the adsorptive properties of many types of carbon black but very little has been reported on acetylene black.^{1,2} This material has unique properties in a LeClanche cell and it was considered of interest to study some of its surface characteristics. For this purpose a series of blacks was obtained by graph-

itizing a sample of Shawinigan acetylene black at successively higher temperatures up to 3000°. The process was monitored by electron microscopy and X-ray diffractometry. Specific surface areas were calculated from BET plots of nitrogen adsorption data and calorimetric heats of adsorption were determined for the two end members of the series.

Experimental.—A conventional adsorption apparatus was used for this work. The calorimeter and measuring techniques were essentially similar to those described by Beebe and his co-workers.⁴ The thermocouple output was fed to Liston-Becker d.c. amplifier and the data recorded as a time-temperature curve. Planimeter integration of the curve and determination of the cooling rate gave the heat change corresponding to each adsorption increment. The estimated accuracy of the measurement was $\pm 5\%$. "Research grade" gases from Airco were used without further purification. All samples were outgassed to 10^{-6} mm. at room temperature. Flushing out with nitrogen and repeating the outgassing procedure gave reproducible isotherms.

Results and Discussion.—The BET surface area was found, in general, to decrease with temperature of graphitization, ranging from 58 square meters per gram for the starting sample, L2463, to 40 for the sample graphitized at 3000°, L2817 (Table I). This is in agreement with a similar trend noted by Polley, *et al.*, on their series of graphitized blacks.⁵

TABLE I

Sample	Graphitization temp., °C.	Specific surface area, sq. m./g.
L2463	---	58
L2815	1000	65
L2816	2000	48
L2817	3000	40

The high value for L2815 is evidently due to chemical clean up. For temperatures above 1000° physical changes predominate. None of the isotherms showed hysteresis to indicate any measurable porosity (in the Kelvin sense). Since the electron-micrograms showed no significant change in particle size, the reduction of surface evidently results from the elimination of minute cracks or micropores.

High interaction energies for low coverage have been attributed to the presence of such imperfections.⁶ This is consistent with the calorimetric data for nitrogen at 78°K. (Fig. 1). Here, for L2817 the initial heats are several hundred cal./mole less than for corresponding coverages for L2463. The surface of L2463 is especially interesting because of its unusual degree of energetic homogeneity. The long plateau up to $V/V_m = 0.9$, as well as the low initial heats compared to those reported for heterogeneous carbon surfaces, indicates considerable surface order before graphitization.

It has been pointed out⁷ that the degree of graphitization is limited by the initial particle size of the black and in general, increases as the particle size increases. A comparison of the crystallite dimen-

(3) The samples were supplied through the courtesy of Godfrey L. Cabot, Inc., Cambridge, Mass.

(4) R. A. Beebe, J. Biscoe, W. R. Smith and C. B. Wendell, *J. Am. Chem. Soc.*, **69**, 95 (1947).

(5) M. H. Polley, W. D. Schaeffer and W. R. Smith, *THIS JOURNAL*, **57**, 469 (1953).

(6) R. A. Beebe and D. M. Young, *ibid.*, **58**, 93 (1954).

(7) H. T. Pinnick, *Phys. Rev.*, **86**, 817 (1952).

(1) Heats of immersion of acetylene black in water and methanol are given by G. Kraus, *THIS JOURNAL*, **59**, 343 (1955).

(2) R. E. Dobbins and R. P. Rossman, discuss the effect of ball milling on an acetylene black surface, *Ind. Eng. Chem.*, **38**, 1145 (1946).

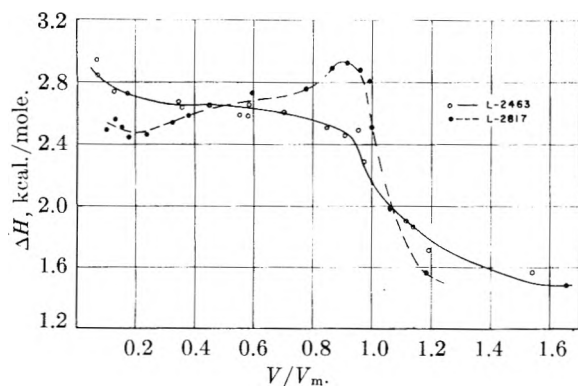


Fig. 1.—Heats of adsorption on acetylene black.

sions and particle diameters (Table II) indicates that L-2817 has attained a higher degree of internal ordering than Graphon. One might expect a corresponding increase in surface homogeneity. This indeed is the conclusion that may be drawn from the heat curve for L2817. The general shape of the curve is similar to that reported for Graphon. However, the maximum associated with intermolecular attraction of adsorbate molecules, has been displaced from approximately $V/V_m = 0.6$ in the case of Graphon to $V/V_m = 0.9$ in the present example. Thus, in L2817 there is a much sharper distinction between the region of monolayer completion and subsequent adsorption.

TABLE II

	Parent blacks		Graphitized end products	
	Spheron 6	L2463 All values in Ångströms	Graphon	L-2817
Particle Size	250	500		
L_a^a		51	76	92
L_c^b		23	46	74

^a L_a = crystallite dimension parallel to carbon layers within crystal. ^b L_c = crystallite dimension perpendicular to parallel layer groups.

A comparison⁶ has been made between the height of the maximum in the heat curve for argon on Graphon with the theoretical interaction energy for an argon molecule on a graphite surface. It was suggested that the experimentally observed maxima may be lower than expected because of residual disorder on the graphon surface. It is interesting that the maxima for nitrogen on graphon and L-2817 both occur at about 3 kcal./mole in spite of differences in degree of graphitization.

Acknowledgment.—The author is indebted to Prof. R. A. Beebe for helpful discussions and suggestions on calorimetric technique.

STUDIES WITH RANEY COBALT CATALYST

BY ANDREW J. CHADWELL, JR., AND HILTON A. SMITH

Department of Chemistry, The University of Tennessee, Knoxville, Tennessee

Received March 29, 1956

In a recent article¹ studies dealing with certain characteristics of Raney nickel catalyst were reported. Raney cobalt alloy is now commercially available, and studies dealing with similar char-

(1) H. A. Smith, A. J. Chadwell, Jr., and S. S. Kirslis, *THIS JOURNAL*, **59**, 820 (1955).

acteristics of Raney cobalt catalyst have been made and are reported here.

Experimental

Raney cobalt catalyst was prepared in a manner similar to that used for nickel. Fifty grams of the alloy² containing 40% cobalt and 60% aluminum was dissolved in a solution of 200 g. of sodium hydroxide in 1 l. of distilled water at 50°. The digestion time with stirring was one hour. The catalyst was washed in a continuous-type washer with 8 l. of distilled water which had had hydrogen bubbled through it for 15 minutes prior to use and also during the washing. The catalyst was then washed with 1 l. of 95% ethanol in the washer. The catalyst was removed and washed five times by centrifugation and decantation with 100% ethanol. The ethanol washings were cloudy. The catalyst was stored in the refrigerator.

It is interesting to note that the Raney cobalt is easier to wash free of alkali than is the Raney nickel. The wash solution was neutral to phenolphthalein after 1 l. of water had passed through the washer, whereas 10 to 12 l. is sometimes required with the nickel.

The palmitic acid was Eastman Kodak Company white label grade. The behenic acid was a sample which had been prepared by hydrogenation of erucic acid and subsequent recrystallization. Fatty acid adsorption studies were made as previously described.³ Inconclusive results were obtained with palmitic acid. A cobalt compound, which is slightly soluble in the benzene, is formed during the shaking. As a result, evaporations of the supernatant benzene solutions are contaminated, giving erroneous readings. This benzene-soluble compound may be a cobalt palmitate formed when oxygen in the adsorption tube oxidizes a small amount of the cobalt, allowing a salt to form. Several adsorption measurements were carried out with the benzene-acid solutions covered with argon instead of nitrogen and oxygen from the air. The blue coloration was present in the benzene solution at the completion of the shaking, although the intensity of the color was decreased somewhat. A smooth adsorption isotherm was not obtained using palmitic acid as the adsorbate.

Behenic acid, $\text{CH}_3-(\text{CH}_2)_{20}-\text{COOH}$, was substituted for palmitic acid in an attempt to reduce the solubility of the cobalt salt. Behenic acid is less soluble than palmitic acid in benzene. Also, the oxygen was swept out of the adsorption tube with argon saturated with benzene prior to shaking. In contrast to the results obtained with palmitic acid, little blue coloration was observed in the behenic acid-benzene solution following the adsorption. As in the case of palmitic acid, the color was most intense in the strongest acid solutions. The results of the adsorption studies are shown in Fig. 1.

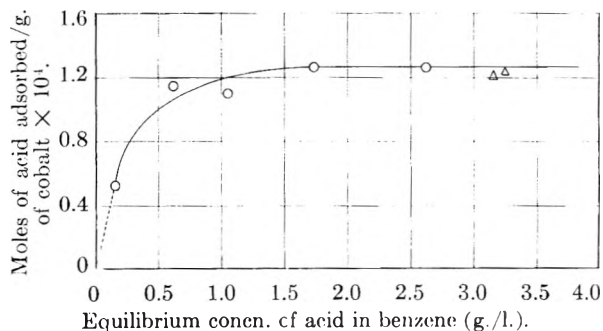


Fig. 1.—Adsorption of long-chain fatty acids on Raney cobalt as a function of the concentration of the acid in benzene, 25°: O, behenic acid; Δ, palmitic acid.

Total aluminum determinations were made by the method of Willard and Tang.⁴ Hydrogen content determinations and catalytic activity toward hydrogenation of benzene were determined in the same manner as for Raney nickel.¹

(2) The alloy was obtained from the Raney Catalyst Company, Chattanooga, Tennessee.

(3) H. A. Smith and J. F. Fuzek, *J. Am. Chem. Soc.*, **68**, 229 (1946).

(4) H. H. Willard and N. K. Tang, *Ind. Eng. Chem., Anal. Ed.*, **357** (1937).

Experimental Results and Discussion

As seen from Fig. 1, fatty acids are adsorbed on Raney cobalt in a manner somewhat similar to that found for nickel, although a higher concentration is necessary to form a monolayer. The number of moles of behenic (C_{22}) acid adsorbed per unit weight of nickel is the same within experimental error as that for palmitic acid (C_{16}). Experiments with fatty acids of shorter chain length were even more subject to errors due to formation of soluble cobalt soaps than were those with palmitic acid. The surface area of the cobalt catalyst calculated by assuming a cross section of 20.5 \AA^2 for the adsorbed acid is 15.6 square meters per gram, which is a little less than the value usually obtained for Raney nickel.

The total aluminum content of the cobalt catalyst was found to vary between 3.3 and 2.7% depending on whether a single batch of alkali was employed or whether the aluminum was removed from the alloy by treatment with several fresh batches of alkali at 10-minute intervals. Raney nickel prepared under similar conditions analyzed around 11% total aluminum.

Hydrogen content studies with Raney cobalt indicated that hydrogen was present in the freshly prepared catalyst, but not to the extent found in Raney nickel. Values obtained on several samples ranged from 40 to 70 standard milliliters of hydrogen per gram of cobalt. The hydrogen is held rather tightly by the cobalt. Pumping at room temperature for 0.5 hour removed only about 6% of the total hydrogen. Upon flaming the decomposition bulb with a Bunsen flame, the remaining hydrogen was given off. A rapid explosion was not obtained as in the case with Raney nickel. Residual hydrogen determinations showed that 99% of the total hydrogen was removed in this manner.

The hydrogenation of benzene over freshly prepared Raney cobalt was found to proceed slowly at 120° with the rate becoming fairly rapid at 150° or above. The rate was found to be first order in hydrogen pressure and independent of the quantity of benzene placed in the bomb. Plots of the logarithm of hydrogen pressure against time gave good straight lines with the exception of slight curvature during the first minute or two of the reaction when freshly prepared catalyst was employed. As the catalyst aged, the kinetic behavior deviated from strictly first-order behavior. The activation energy was found to be approximately 23 kcal. per mole in the range $155\text{--}180^\circ$. At 160° , $k_{1.0} = 4.65 \times 10^{-5} \text{ sec.}^{-1}$ for 1 l. hydrogen volume and 1 g. of catalyst.

A Comparison of Raney Nickel and Raney Cobalt Catalysts.—Raney cobalt is somewhat easier to prepare than Raney nickel in that the removal of alkali by washing can be accomplished rather quickly with the cobalt while a lengthy washing procedure is required for nickel. The aluminum content is some 10–12% for nickel but only around 3% for cobalt. The surface area as measured by fatty acid adsorption is somewhat smaller than for nickel; the acid is more strongly held in the nickel, while benzene-soluble compounds are formed with the cobalt. This difficulty can be fairly well overcome

by the use of very long chain acids. The hydrogen content of the cobalt is less than for nickel, but the hydrogen appears to be more strongly bound. The hydrogenation activity of the cobalt catalyst as measured by its ability to effect the addition of hydrogen to benzene is less than that of nickel. However, the activation energy is greater for the cobalt so that the differences in activity become less as the temperature increases. The lower activity of the cobalt may well be caused by the firmer bonding of hydrogen to the cobalt. As the temperature is raised, the hydrogen becomes more readily available, and hence the activity is increased.

Acknowledgment.—The authors are grateful to the Office of Ordnance Research, United States Army, for the sponsorship of this research.

THE KINETICS OF THE DECOMPOSITION OF MALONIC ACID IN AROMATIC AMINES

BY LOUIS WATTS CLARK

Contribution from the Department of Chemistry, Saint Joseph College
Emmitsburg, Maryland

Received March 30, 1956

Kinetic studies have been reported on the decarboxylation of malonic acid in aqueous solution,¹ as well as in several non-aqueous solvents including glycerol,² dimethyl sulfoxide,² triethyl phosphate,³ quinoline⁴ and aniline.⁵ Apparently, no kinetic study of the decomposition of malonic acid in pyridine has been reported. Preliminary experiments in this Laboratory having revealed that malonic acid is smoothly decarboxylated in pyridine solution at temperatures near 100° , the kinetics of the reaction were carefully investigated for the sake of comparison with other aromatic amines.

Since the decomposition of malonic acid in aniline proceeds quite slowly at 80 and 100° (the temperatures at which the experiments reported⁵ were performed), further studies were made at higher temperatures. Results of these investigations are reported herein.

Experimental

Reagents.—The reagents used were (1) reagent grade malonic acid; (2) reagent grade aniline, boiling range $183\text{--}186^\circ$; (3) reagent grade pyridine, boiling range $114\text{--}116^\circ$.

Apparatus and Technique.—The apparatus and technique in this study were the same as those used in studying the decomposition of malonic acid in triethyl phosphate.³

The Decomposition of Malonic Acid in Pyridine and Aniline.—At the beginning of each experiment 100 ml. of the amine (saturated with dry CO_2 gas) was placed in the reaction flask in the thermostat oil-bath. A sample of malonic acid weighing either 0.1764 g. in the case of pyridine or 0.1810 g. in the case of aniline (the amount required to produce 38.0 and 39.0 ml. of CO_2 , respectively, on complete reaction) was placed in a thin glass capsule and introduced at the proper moment into the solvent in the usual manner. The rapidly rotating mercury sealed stirrer immediately crushed the capsule, the contents dissolved and mixed in the solvent, and reaction began. The course of the reaction was followed in the usual manner.

(1) G. A. Hall, Jr., *J. Am. Chem. Soc.*, **71**, 2691 (1949).

(2) L. W. Clark, *This Journal*, **60**, 825 (1956).

(3) L. W. Clark, *ibid.*, **60**, 1150 (1956).

(4) P. E. Yankwich and R. L. Belford, *J. Am. Chem. Soc.*, **75**, 4178 (1953).

(5) Y. Ogata and R. Oda, *Bull. Inst. Phys. Chem. Res. (Tokyo)*, *Chem. Ed.*, **23**, 217 (1944); *C. A.*, **43**, 7904 (1949).

TABLE I
DECOMPOSITION OF MALONIC ACID IN AROMATIC AMINES, KINETIC DATA

System	E^* (cal.)	A (sec.^{-1})	Temp. coeff.	ΔH^\ddagger (cal.)	ΔS^\ddagger (e.u.)	ΔF_{140}^\ddagger (cal.)	$k_{(140^\circ)}$ (sec.^{-1})
1. Malonic acid	34,500	1.8×10^{14}	2.72	33,000	+ 4.5	31,100	0.00024
2. Malonic acid plus quinoline	18,500	2.57×10^7	1.78	17,800	-27.0	24,300	.00364
3. Malonic acid plus aniline	22,850	6.32×10^9	2.01	22,800	-14.3	28,700	.0050
4. Malonic acid plus pyridine	26,600	1.59×10^{12}	2.75	26,000	+ 7.2	23,000	.0126

The above procedure was repeated at five different temperatures between 98–114° in the case of pyridine, and at six different temperatures between 126–144° in the case of aniline. The total volume of carbon dioxide obtained in each experiment was 100% of the theoretical yield within the limits of error of the experiment. Duplicate and triplicate runs at each temperature gave reproducible results.

Results and Discussion

A plot of $\log(a - x)$ vs. t in the case of each amine at each temperature studied gave excellent straight lines, indicating that the decomposition of malonic acid in pyridine and in aniline is a first-order reaction. From the slopes of the lines thus obtained the specific reaction velocity constants for the reaction in the two solvents at the various temperatures studied were calculated. For the case of the decomposition of malonic acid in pyridine the temperatures studied and the corresponding specific reaction velocity constants obtained in sec.^{-1} were as follows: 98.2°, 0.000335; 102.3°, 0.000496; 107.0°, 0.000764; 110.9°, 0.00111; 113.5°, 0.00141. Results for the case of the decomposition of malonic acid in aniline were as follows: 126.6°, 0.00184; 131.8°, 0.002735; 135.7°, 0.00358; 138.6°, 0.00437; 141.8°, 0.00550; 144.1°, 0.00640.

A straight line was obtained in each case when $\log k$ was plotted against $1/T$ according to the Arrhenius equation. From the slopes of the lines thus obtained the activation energy and the frequency factor for the reaction in each solvent were calculated. On the basis of the Eyring equation the enthalpy of activation, entropy of activation and free energy of activation at 140° for the reaction in each solvent were calculated. The kinetic data for the reactions studied are summarized in Table I which includes also for comparison data for molten malonic acid⁶ and for malonic acid in quinoline.⁴

Some insight into the role of the solvent may be gained by considering the data in Table I. A comparison of the data in lines 1 and 2 shows that quinoline effects a very large lowering of the enthalpy of activation as well as a large decrease in the entropy of activation of the reaction with respect to molten malonic acid. This results in a lowering of the free energy of activation, so that, at this temperature (140°), malonic acid decomposes 15 times as fast in quinoline as it does alone. A comparison of lines 1 and 3 reveals that aniline lowers the enthalpy of activation by a large amount and also lowers the entropy of activation considerably, resulting in a small decrease in the free energy of activation at 140° with respect to molten malonic acid. Malonic acid decomposes 21 times as fast in aniline at

140° as it does alone. A comparison of lines 1 and 4 reveals that pyridine lowers the enthalpy of activation less than does aniline and *increases* the entropy of activation, so that the probability of the formation of the activated state of malonic acid is greater in pyridine than in the molten state. The free energy of activation is lower in pyridine than in any other solvent shown. At 140° malonic acid decomposes 52 times as fast in pyridine as in the molten state.

This order of increasing efficacy of the amines follows the order of increasing basicity as well as the order of decreasing molecular complexity of the solvent.

Studies on the decarboxylation of acetonedicarboxylic acid in aniline⁷ have been explained on the basis of the formation of an intermediate unstable compound between reactant and solvent molecules. The decomposition of malonic acid in non-aqueous solvents has been explained on the basis of decarboxylation of the undissociated form of the acid.⁵ Results reported herein strongly suggest the possibility that intermediate compound formation may be involved in the case of the decomposition of malonic acid in aromatic amines. The active methylene hydrogen atoms could attach to the unshared electrons on nitrogen. The greater the availability of the electrons the greater would be the probability of the formation of the activated state, other factors being equal. The electron structure of the molecule being thus distorted decarboxylation could occur at either carboxyl group. Results obtained in non-nitrogenous, non-aqueous, basic type solvents^{2,3} are in harmony with this view.

Further work on this problem is contemplated.

(7) E. O. Wigg, *THIS JOURNAL*, **32**, 961 (1928).

THE PROTONATION OF N-METHYLACETAMIDE

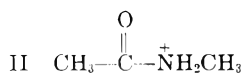
BY JAKE BELLO

Contribution No. 2094 from the Gates and Crellin Laboratories of
Chemistry, California Institute of Technology, Pasadena, California
Received April 9, 1956

Mizushima, *et al.*,¹ have reported that N-methylacetamide (I) in aqueous hydrochloric acid has an absorption peak at 2695 Å., which is not present in the absence of acid. This new absorption was attributed to the formation of the ion II, since

(1) S. Mizushima, T. Simanouni, S. Nakagura, K. Kuratani, M. Tsuboi, H. Baba and O. Fujioka, *J. Am. Chem. Soc.*, **72**, 3490 (1950); S. Mizushima, *Adv. Prot. Chem.*, **9**, 299 (1954); S. Mizushima, "Structure of Molecules and Internal Rotation," Academic Press, Inc., New York, N. Y., 1954, p. 118.

(6) C. N. Hinshelwood, *J. Chem. Soc.*, **117**, 156 (1920).



it occurred near the 2650 Å. band of acetone. On the assumption that the intensity of absorption of II and of acetone are similar, it was concluded that in a solution 2 *M* in I and 5 *M* in hydrochloric acid about 5% of I was converted to II, to give a concentration 0.1 *M* in II. From such data there were also calculated an equilibrium constant for the dissociation of II and a value for the resonance energy of the "peptide" bond in I.

We have had occasion to investigate the spectra of solutions of I in acid preliminary to a study of protein-acid systems. We have found for 2 or 4 *M* I in 5 or 10 *M* hydrochloric acid *no* absorption at 2695 Å., or, indeed, at any wave length above the beginning of 2050 Å. band at about 2400 Å. According to Mizushima, *et al.*, a 2 *M* solution of I in 5 *M* hydrochloric acid has an optical density about equal to that of 0.1 *M* acetone. The optical density of 0.1 *M* acetone in water is about 1.6 and we could have detected readily an effect equal to 3% of the above. In addition, no absorption at 2695 Å. was detected in concentrated sulfuric acid; that extensive solvolysis did not occur in this solvent was shown by dilution with water, resulting in an optical density at 2050 Å. equal (within 10%) to that of original I at the same concentration. Acetic acid, which could be formed on solvolysis, absorbs weakly at 2050 Å.² In addition, no absorption above 2400 Å. was observed with 2 *M* acetamide or *N-n*-butylacetamide in 5 *M* hydrochloric acid.

We conclude, therefore, that the reported absorption band at 2395 Å. does not exist, that there is no evidence for the formation of II and that the calculated resonance energy is not valid. We have confirmed the report² that in acid solution the 2050 Å. absorption peak of I is reduced.

Experimental

Freezing points are corrected.

Materials.—Two samples of *N*-methylacetamide were used. One was White Label Grade purchased from the Eastman Kodak Co. and was purified by fractional distillation through a 12" Widmer column, b.p. 70–71° at 2.5–3 mm., followed by two fractional crystallizations from the melt; yield 25%, f.p. 30.0° (reported f.p. 28.80°; m.p. 28°). The m.p. of the original amide is given by the seller as 27.5–29°.

The second specimen was prepared by the dropwise addition of 2.2 moles of acetyl chloride to 6 moles of methylamine (Matheson, 96.5%) in 700 ml. of anhydrous ethyl ether cooled with Dry Ice. After filtration of the methylamine hydrochloride, the filtrate was distilled through the Widmer column. The fraction boiling at 79–81° at 4.5–5 mm. was collected for use; yield 82%, f.p. 29.8°.

Anal. Calcd. for C₃H₇NO: N, 19.2. Found (Kjeldahl): N, 18.9.

Both specimens gave identical infrared and ultraviolet spectra.

Acetamide (Merck, Reagent) was used without additional purification; *N-n*-butylacetamide was White Label (Eastman Kodak Co.) grade and was distilled *in vacuo* through the Widmer column, b.p. 106° at 4 mm. (reported 103.5 at 3.5 mm.²).

Acetone, Merck, Reagent, "suitable for spectrophotometric use" was used.

(2) A. R. Goldfarb, A. Mele and N. Gutstein, *J. Am. Chem. Soc.*, **77**, 6194 (1955).

(3) K. W. F. Kehlrausch and R. Seka, *Z. physik. Chem.*, **B43**, 355 (1939).

Spectra.—Spectra were determined with a Cary Model 11 recording spectrophotometer. The spectrum of 2 *M* I in 5 *M* hydrochloric acid was also measured with a Beckman Model DU spectrophotometer. Both instruments gave identical results. The reference solution in every case was identical to the solution being investigated except for the absence of amide.

Acknowledgments.—We wish to thank the Office of the Surgeon General, Department of the Army, for financial support under Contract No. 49-007-MD-298, and Miss Helene Riese for technical assistance.

DIFFUSION OF ISOIONIC, SALT-FREE BOVINE SERUM ALBUMIN¹

BY IGNACIO TINOCO, JR.,² AND P. A. LYONS

Contribution #1371 from the Sterling Chemistry Laboratory
Yale University, New Haven, Connecticut

Received May 18, 1966

As part of a study of the thermodynamic properties of isoionic protein solutions,^{3–5} diffusion measurements have been made on aqueous solutions of isoionic, salt-free bovine serum albumin. The concentration dependence is quite different from that normally found for the diffusion of proteins in salt solutions.⁶ This is to be anticipated since in salt-free solutions the diffusing protein component is a weak electrolyte for which the degree of dissociation changes with concentration.

The isoionic, salt-free protein solutions were prepared by an ion-exchange technique described previously.⁴ Concentrations were determined from dry weight measurements. Diffusion coefficients were measured at 25° using the Gouy interferometric technique.^{7,8}

The values reported were obtained from the lower fringes in the Gouy patterns corresponding to the central part of the index of refraction gradient. Viscosity data which were required for the work were measured with an Ostwald viscosimeter.

The diffusion data are listed in Table I and are plotted in Fig. 1. The concentration dependence of the diffusion coefficient is quite pronounced; in the concentration region studied the diffusion coefficient more than doubles. Since the molecular weight of the protein molecule is constant under the same conditions,⁴ its frictional coefficient would be expected to be nearly unchanged. In the isoionic *pH* region (*pH* 5–6) the protein component may be considered to be a weak electrolyte ionizing to give hydrogen ions and charged protein ions.

(1) This work was supported in part by NONR contract 659(00) and in part by A.E.C. contract (30-1)-1375.

(2) Public Health Service Research Fellow of the National Cancer Institute.

(3) J. G. Kirkwood and J. B. Shumaker, *Proc. Natl. Acad. Sci. U. S.*, **38**, 863 (1952).

(4) S. N. Timasheff, H. M. Dintzis, J. G. Kirkwood and B. D. Coleman, *ibid.*, **41**, 710 (1955).

(5) S. N. Timasheff and I. Tinoco, Jr., *Arch. Biochem. Biophys.*, submitted.

(6) J. M. Creeth, *Biochem. J.*, **51**, 10 (1952).

(7) L. G. Longworth, *ibid.*, **69**, 2510 (1947).

(8) G. Kegeles and I. J. Gosting, *ibid.*, **69**, 2516 (1947).

The expression for the diffusion coefficient in these solutions may be shown to be

$$D = D_p^\circ (\eta_0/\eta) (1 + [\bar{Z}]) \left(1 + c \frac{d \ln y}{dc}\right) \quad (1)$$

In this expression D_p° is the hypothetical diffusion coefficient of the un-ionized protein molecule at infinite dilution; it is assumed to be the same for the ionized protein species. η_0 and η are the viscosities of water and solution, respectively. The absolute value of the average charge on the protein molecule is $|\bar{Z}|$ and $(1 + c \frac{d \ln y}{dc})$ is the usual thermodynamic correction. Analogous expressions may be derived for weak electrolytes for which all the species in equilibrium have different mobilities.⁷

TABLE I

\bar{W}_{BSA}^a	C_{BSA}^b	D^c	$\frac{D\eta/\eta_0}{1 + c \left(\frac{d \ln y}{dc}\right)}$	$ \bar{Z} ^d$
9.92	14.37	6.18	8.31	0.1
3.96	5.74	6.68	7.83	.05
2.88	4.03	6.80	7.76	.04
1.90	2.75	7.15	7.95	.06
1.05	1.52	7.87	8.48	.1
0.99	1.43	9.07	9.75	.3
.80	1.16	8.95	9.65	.3
.52	0.75	11.05	11.60	.6
.26	0.38	13.7	14.1	.9

^a Average concentration of bovine serum albumin (BSA) in g./l. ^b Average concentration of BSA in mole/l. $\times 10^5$. ^c Diffusion coefficient in cm.²/sec. $\times 10^7$. ^d Absolute value of average charge on BSA in protonic units.

The value of \bar{Z} would be expected to change markedly with concentration since the degree of ionization would increase with decreasing concentration giving rise to a progressively higher average charge on the protein.

Figure 1 demonstrates the change in D due to the change in \bar{Z} . The filled circles represent a plot of $(D \eta/\eta_0)/(1 + c \frac{d \ln y}{dc})$. The thermodynamic term was obtained from light scattering measurements on the same system.⁴ Using Creeth's value⁶ of $D_p^\circ = 7.46 \times 10^{-7}$ cm.²/sec., obtained for bovine serum albumin in buffered solution, values of $|\bar{Z}|$ may be computed ranging from about 0.1 at the highest concentration to about 0.9 at the lowest concentration. These values are listed in Table I.

A value of $D_p^\circ = 7.5_3 \times 10^{-7}$ cm.²/sec. could have been obtained directly from our experiments by extrapolation of the diffusion data at high concentrations as shown in Fig. 1. Although this figure is in good agreement with Creeth's determination, his definitive value was used in the calculations because of the slight residual ionization of the protein even at the highest concentration measured. With more extensive and more precise data a preferable way to compute \bar{Z} would be to

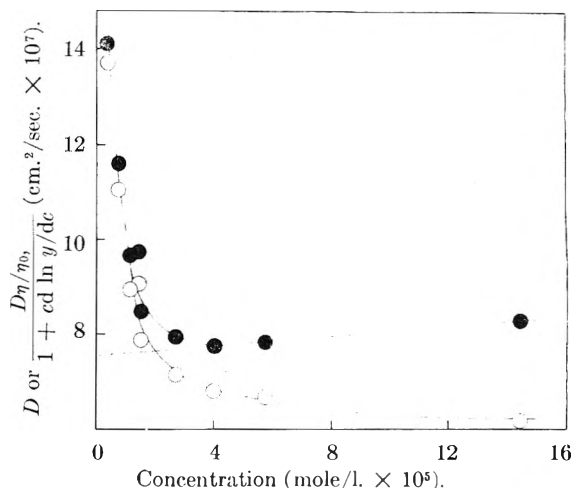


Fig. 1.—O, the diffusion coefficient D plotted vs. concentration c in mole/l. (mol. wt. 69,000); ●, $1 + \frac{D\eta/\eta_0}{c \frac{d \ln y}{dc}}$ vs. c .

substitute for D_p° in equation 1 the value of $D/(1 + c \frac{d \ln y}{dc})(\eta_0/\eta)$ which could be estimated from an extrapolation of a plot of this quantity against \bar{c} from concentrations where ionization is negligible to Creeth's limiting value. This estimate would be a better measure of the mobility of B.S.A. molecules and anions at finite concentrations.⁹ Neglecting this refinement results in high values of \bar{Z} at \bar{c} greater than 4×10^{-5} . Our present interest is in the values of $|\bar{Z}|$ in solutions for which the degree of ionization is appreciable and these would remain essentially unchanged if this refinement were adopted.

In principle, values of \bar{Z} may be obtained from pH or conductance measurements. However the difficulty of measuring the pH or the conductance of a salt-free protein solution (particularly at concentrations below 1 g./l. or about 10^{-5} mole/l.) makes direct comparisons rather unconvincing. It can be shown qualitatively that at pH 5 a 10 g./l. solution of bovine serum albumin should have a charge of about 0.1 which is consistent with the diffusion data.

This diffusion study did not have as a purpose the rigorous determination of the concentration dependence of the charge on bovine serum albumin molecules. An attempt has merely been made to indicate the effects that do occur and to outline the information to be obtained from these results when the protein is treated in the same manner as a simple weak electrolyte.

Acknowledgments.—We wish to thank Professor J. G. Kirkwood for indicating the derivation of eq. 1. To him, as well as to Dr. S. N. Timasheff, we are also indebted for several illuminating discussions of this general problem.

(9) V. Vitagliano and P. A. Lyons, *J. Am. Chem. Soc.*, **78**, 1549 (1956).

COMMUNICATIONS TO THE EDITOR

EXTRAPOLATION OF COOLING CURVES IN MEASUREMENTS OF HEAT CAPACITY

Sir:

During measurement of the heat of fusion of phosphoric acid hemihydrate, $2\text{H}_3\text{PO}_4 \cdot \text{H}_2\text{O}$ (m.p. 29.32°) in an adiabatic calorimeter, a fairly common situation arose in which the approach to temperature equilibrium was so slow as to require analytical or graphical estimation of the equilibrium temperature. The method of treatment cited most often seems to be one reported by Barieau and Giauque.² The data for three such points are treated here by three methods.

In method 1,² values of $-\ln(dT/dt)$, where T represents temperature and t time, were plotted against time, and a linear equation was fitted to the data

$$-\ln(dT/dt) = A - Bt$$

This equation was integrated to give

$$\ln B(T_t - T_\infty) = A - Bt$$

and the value of the integral was added to a value of T at a selected time, t .

In method 2, the cooling curve was taken as a section of a hyperbola of the form

$$T = T_k - (t - t_k)/(A + Bt)$$

where T_k and t_k represent temperature at a selected time. The equation was solved for large values of t , to extend the equation to the asymptote, and the value of T so obtained was taken as the equilibrium temperature.

In method 3, T was plotted against $1/t$ and a straight line was drawn through the points to intercept the T axis at $t = \infty$.

Table I shows the results for the first and last measured points in each series. The values of T at infinite time are in good agreement for such a long extrapolation.

The particular preparation of phosphoric acid hemihydrate for which part of the measurements are reported here was found to be not sufficiently

pure. A new batch has been prepared, and the results of the measurements will be reported later.

The present treatment of cooling curves is an extension of the method proposed by Barieau and Giauque.²

TABLE I
EXTRAPOLATION OF COOLING CURVES

Time after heat off, min.	Temperature, ° K.		
	Point 118	Point 119	Point 120
14	302.3258		302.6133
24		302.3264	
92		302.3118	
95	302.3080		
219			302.3086
$t = \infty$			
Method 1	302.3016	302.3038	302.2967
Method 2	302.3012	302.3030	302.2973
Method 3	302.2982	302.3038	302.3032

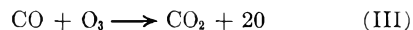
DIVISION OF CHEMICAL DEVELOPMENT
TENNESSEE VALLEY AUTHORITY EDWARD P. EGAN, JR.
WILSON DAM, ALABAMA

RECEIVED JULY 2, 1956

SECOND EXPLOSION LIMITS OF CARBON MONOXIDE-OXYGEN MIXTURES

Sir:

In our recent criticism¹ of a paper by von Elbe, Lewis and Roth,² one of our points concerned the derivation of their equation 2. In our derivation of the explosion condition, we neglected to consider their reaction



We wish to point out that when equation (III) is included, their equation 2, in which k_3 does not explicitly appear, is correctly derived.

CHEMISTRY DIVISION ALVIN S. GORDON
U. S. NAVAL ORDNANCE TEST STATION R. H. KNIFE
CHINA LAKE, CALIFORNIA

RECEIVED AUGUST 10, 1956

(1) A. S. Gordon and R. H. Knipe, *THIS JOURNAL*, **60**, 1023 (1956).

(2) G. von Elbe, B. Lewis and W. Roth, "Fifth Symposium on Combustion," Reinhold Publishing Co., New York, N. Y., 1955, p. 610.

(1) W. H. Ross and R. M. Jones, *THIS JOURNAL*, **47**, 2165 (1925).

(2) R. E. Barieau and W. F. Giauque, *ibid.*, **72**, 5676 (1950).

▲ ▲

NEW REPRINTS

American Chemical Society:

Journal—

Ready March 1956

Vols. 26, 27, 1904-1905

Single volumes, paper bound \$35.00 each
(about 1,600 pp. per vol.)

Previously published:

Vols. 1-25

(Proceedings 2 vols., Journal Vols. 1-25,
1879-1903; General Index to Vols. 1-20)
Cloth bound in 37 vols. 650.00

Chemical Abstracts—

Vol. 4, 1910, paper bound in 5 parts 75.00

Vol. 5, 1911, paper bound in 5 parts 75.00

*These reprints are being undertaken by
arrangement with the American Chemical Society.
Please address orders and inquiries to*

**JOHNSON REPRINT
CORPORATION**

125 East 23 Street
New York 10, New York

▲ ▲

CHEMIST, PHYSICAL, Ph.D.

Advanced Work in HIGH TEMPERATURE and RELATED FIELDS

●

As part of its work on advanced missile weapons systems, the Special Defense Projects Department of GE is doing advanced work on:

- Kinetics of the upper atmosphere
- Radiation and collision processes
- Emission and absorption characteristics of gases
- High temperature radiation
- Gas composition at high temperature
- Molecular characteristics of vaporized materials
- Transport properties of dilute gases at high temperature
- Equilibrium properties of gases
- Surface kinetics
- Gas kinetics at high temperature
- Hypersonic inviscid flow

If you have several years experience in the field and are interested in work in these areas, write in confidence (not necessary to name present employer) to:

Mr. W. Billingsley

Special Defense Projects Department

GENERAL  ELECTRIC

3198 Chestnut Street, Room 105-A
Philadelphia 4, Pa.

*Follow
the
newest*

field... **NON-METALLICS**

HUGHES RESEARCH AND DEVELOPMENT LABORATORIES HAVE SEVERAL OPENINGS FOR CHEMICAL AND OTHER ENGINEERS IN DEVELOPMENT LEADING TO PRODUCTION OF NEW APPLICATIONS FOR NON-METALLIC MATERIALS.

**ENGINEERS
AND
PHYSICISTS**

Hughes Laboratories are engaged in a highly advanced research, development and production program involving wide use of non-metallic materials in missile and radar components. The need is for men with experience in these materials to investigate the electrical, physical, and heat-resistant properties of plastics and other non-metallics.

**ENGINEERS
OR APPLIED
PHYSICISTS**

These men are required to plan, coordinate, and conduct special laboratory and field test programs on missile components. Experience is required in materials development, laboratory instrumentation, and design of test fixtures.

**RESEARCH
CHEMIST**

The Plastics Department has need for an individual with a Ph.D. Degree, or equivalent experience in organic or physical chemistry, to investigate the basic properties of plastics. Work involves research into the properties of flow, mechanisms of cure, vapor transmission, and electrical and physical characteristics of plastics.

*Scientific
Staff
Relations*

HUGHES RESEARCH & DEVELOPMENT LABORATORIES

*Culver City,
Los Angeles County, California*

